Oxidative Stress, Inflammation, and Atherosclerosis-Related Diseases
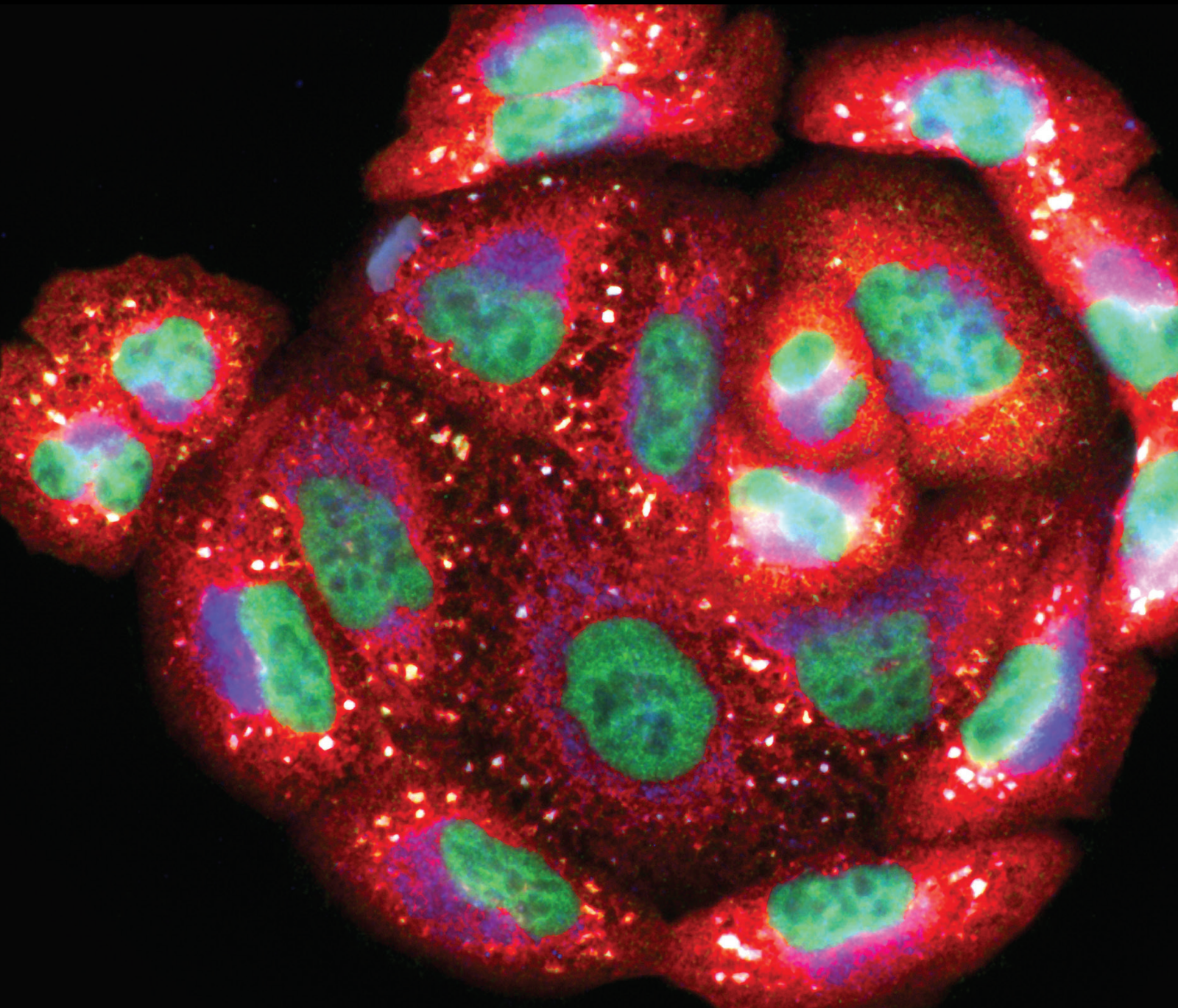
Lead Guest Editor: Jianlei Cao
Guest Editors: Hui Chen, Mark Slevin, and Lei Yu

Oxidative Stress, Inflammation, and Atherosclerosis-Related Diseases

Oxidative Stress, Inflammation, and Atherosclerosis-Related Diseases

Lead Guest Editor: Jianlei Cao
Guest Editors: Hui Chen, Mark Slevin, and Lei Yu

Tim Hofer, Norway
John D. Horowitz, Australia
Silvana Hrelia, Italy
Dragan Hrncic, Serbia
Zebo Huang, China
Zhao Huang, China
Tarique Hussain, Pakistan
Stephan Immenschuh, Germany
Norsharina Ismail, Malaysia
Franco J. L, Brazil
Sedat Kacar, USA
Andleeb Khan, Saudi Arabia
Kum Kum Khanna, Australia
Neelam Khaper, Canada
Ramoji Kosuru, USA
Demetrios Kouretas, Greece
Andrey V. Kozlov, Austria
Chan-Yen Kuo, Taiwan
Gaocai Li, China
Guoping Li, USA
Jin-Long Li, China
Qiangqiang Li, China
Xin-Feng Li, China
Jialiang Liang, China
Adam Lightfoot, United Kingdom
Christopher Horst Lillig, Germany
Paloma B. Liton, USA
Ana Lloret, Spain
Lorenzo Loffredo, Italy
Camilo López-Alarcón, Chile
Daniel Lopez-Malo, Spain
Massimo Lucarini, Italy
Hai-Chun Ma, China
Nageswara Madamanchi, USA
Kenneth Maiese, USA
Marco Malaguti, Italy
Steven McAnulty, USA
Antonio Desmond McCarthy, Argentina
Sonia Medina-Escudero, Spain
Pedro Mena, Italy
Víctor M. Mendoza-Núñez, Mexico
Lidija Milkovic, Croatia
Alexandra Miller, USA
Sara Missaglia, Italy

Premysl Mladenka, Czech Republic
Sandra Moreno, Italy
Trevor A. Mori, Australia
Fabiana Morroni, Italy
Ange Mouithys-Mickalad, Belgium
Iordanis Mourouzis, Greece
Ryoji Nagai, Japan
Amit Kumar Nayak, India
Abderrahim Nemmar, United Arab
Emirates
Xing Niu, China
Cristina Nocella, Italy
Susana Novella, Spain
Hassan Obied, Australia
Pál Pacher, USA
Pasquale Pagliaro, Italy
Dilipkumar Pal, India
Valentina Pallottini, Italy
Swapnil Pandey, USA
Mayur Parmar, USA
Vassilis Paschalis, Greece
Keshav Raj Paudel, Australia
Ilaria Peluso, Italy
Tiziana Persichini, Italy
Shazib Pervaiz, Singapore
Abdul Rehman Phull, Republic of Korea
Vincent Pialoux, France
Alessandro Poggi, Italy
Zsolt Radak, Hungary
Dario C. Ramirez, Argentina
Erika Ramos-Tovar, Mexico
Sid D. Ray, USA
Muneeb Rehman, Saudi Arabia
Hamid Reza Rezvani, France
Alessandra Ricelli, Italy
Francisco J. Romero, Spain
Joan Roselló-Catafau, Spain
Subhadeep Roy, India
Josep V. Rubert, The Netherlands
Sumbal Saba, Brazil
Kunihiro Sakuma, Japan
Gabriele Saretzki, United Kingdom
Luciano Saso, Italy
Nadja Schroder, Brazil

Anwen Shao (iD), China
Iman Sherif, Egypt
Salah A Sheweita, Saudi Arabia
Xiaolei Shi, China
Manjari Singh, India
Giulia Sita (iD), Italy
Ramachandran Srinivasan (iD), India
Adrian Sturza (iD), Romania
Kuo-hui Su (iD), United Kingdom
Eisa Tahmasbpour Marzouni (iD), Iran
Hailiang Tang, China
Carla Tatone (iD), Italy
Shane Thomas (iD), Australia
Carlo Gabriele Tocchetti (iD), Italy
Angela Trovato Salinaro, Italy
Rosa Tundis (iD), Italy
Kai Wang (iD), China
Min-qi Wang (iD), China
Natalie Ward (iD), Australia
Grzegorz Wegrzyn, Poland
Philip Wenzel (iD), Germany
Guangzhen Wu (iD), China
Jianbo Xiao (iD), Spain
Qiongming Xu (iD), China
Liang-Jun Yan (iD), USA
Guillermo Zalba (iD), Spain
Jia Zhang (iD), China
Junmin Zhang (iD), China
Junli Zhao (iD), USA
Chen-he Zhou (iD), China
Yong Zhou (iD), China
Mario Zoratti (iD), Italy

Contents

Contents

Contents

Retraction

Retracted: Capsaicin Alleviates Vascular Endothelial Dysfunction and Cardiomyopathy via TRPV1/eNOS Pathway in Diabetic Rats

Oxidative Medicine and Cellular Longevity

This article has been retracted by Hindawi, as publisher, following an investigation undertaken by the publisher [1]. This investigation has uncovered evidence of systematic manipulation of the publication and peer-review process. We cannot, therefore, vouch for the reliability or integrity of this article.

Please note that this notice is intended solely to alert readers that the peer-review process of this article has been compromised.

Wiley and Hindawi regret that the usual quality checks did not identify these issues before publication and have since put additional measures in place to safeguard research integrity.

We wish to credit our Research Integrity and Research Publishing teams and anonymous and named external researchers and research integrity experts for contributing to this investigation.

The corresponding author, as the representative of all authors, has been given the opportunity to register their agreement or disagreement to this retraction. We have kept a record of any response received.

References

[1] Q. Wang, C. Zhang, C. Yang, Y. Sun, K. Chen, and Y. Lu, "Capsaicin Alleviates Vascular Endothelial Dysfunction and Cardiomyopathy via TRPV1/eNOS Pathway in Diabetic Rats," *Oxidative Medicine and Cellular Longevity*, vol. 2022, Article ID 6482363, 11 pages, 2022.

Retraction

Retracted: Macrophage Rmp Ameliorates Myocardial Infarction by Modulating Macrophage Polarization in Mice

Oxidative Medicine and Cellular Longevity

This article has been retracted by Hindawi, as publisher, following an investigation undertaken by the publisher [1]. This investigation has uncovered evidence of systematic manipulation of the publication and peer-review process. We cannot, therefore, vouch for the reliability or integrity of this article.

Please note that this notice is intended solely to alert readers that the peer-review process of this article has been compromised.

Wiley and Hindawi regret that the usual quality checks did not identify these issues before publication and have since put additional measures in place to safeguard research integrity.

We wish to credit our Research Integrity and Research Publishing teams and anonymous and named external researchers and research integrity experts for contributing to this investigation.

The corresponding author, as the representative of all authors, has been given the opportunity to register their agreement or disagreement to this retraction. We have kept a record of any response received.

References

[1] J. Zhang, Z. Yin, L. Yu et al., "Macrophage Rmp Ameliorates Myocardial Infarction by Modulating Macrophage Polarization in Mice," *Oxidative Medicine and Cellular Longevity*, vol. 2022, Article ID 6248779, 12 pages, 2022.

Retraction

Retracted: Hemodynamic and Geometric Risk Factors for In-Stent Restenosis in Patients with Intracranial Atherosclerotic Stenosis

Oxidative Medicine and Cellular Longevity

This article has been retracted by Hindawi following an investigation undertaken by the publisher [1]. This investigation has uncovered evidence of one or more of the following indicators of systematic manipulation of the publication process:

(1) Discrepancies in scope
(2) Discrepancies in the description of the research reported
(3) Discrepancies between the availability of data and the research described
(4) Inappropriate citations
(5) Incoherent, meaningless and/or irrelevant content included in the article
(6) Manipulated or compromised peer review

The presence of these indicators undermines our confidence in the integrity of the article's content and we cannot, therefore, vouch for its reliability. Please note that this notice is intended solely to alert readers that the content of this article is unreliable. We have not investigated whether authors were aware of or involved in the systematic manipulation of the publication process.

Wiley and Hindawi regrets that the usual quality checks did not identify these issues before publication and have since put additional measures in place to safeguard research integrity.

We wish to credit our own Research Integrity and Research Publishing teams and anonymous and named external researchers and research integrity experts for contributing to this investigation.

The corresponding author, as the representative of all authors, has been given the opportunity to register their agreement or disagreement to this retraction. We have kept a record of any response received.

References

[1] X. Song, H. Qiu, S. Wang, Y. Cao, and J. Zhao, "Hemodynamic and Geometric Risk Factors for In-Stent Restenosis in Patients with Intracranial Atherosclerotic Stenosis," *Oxidative Medicine and Cellular Longevity*, vol. 2022, Article ID 6951302, 14 pages, 2022.

Retraction

Retracted: The Effects of Statin Therapy on Oxidized LDL and Its Antibodies: A Systematic Review and Meta-Analysis

Oxidative Medicine and Cellular Longevity

This article has been retracted by Hindawi, as publisher, following an investigation undertaken by the publisher [1]. This investigation has uncovered evidence of systematic manipulation of the publication and peer-review process. We cannot, therefore, vouch for the reliability or integrity of this article.

Please note that this notice is intended solely to alert readers that the peer-review process of this article has been compromised.

Wiley and Hindawi regret that the usual quality checks did not identify these issues before publication and have since put additional measures in place to safeguard research integrity.

We wish to credit our Research Integrity and Research Publishing teams and anonymous and named external researchers and research integrity experts for contributing to this investigation.

The corresponding author, as the representative of all authors, has been given the opportunity to register their agreement or disagreement to this retraction. We have kept a record of any response received.

References

[1] T. Jamialahmadi, F. Baratzadeh, Ž. Reiner et al., "The Effects of Statin Therapy on Oxidized LDL and Its Antibodies: A Systematic Review and Meta-Analysis," *Oxidative Medicine and Cellular Longevity*, vol. 2022, Article ID 7850659, 15 pages, 2022.

Retraction

Retracted: Genetic Analysis Reveals Different Mechanisms of IL-5 Involved in the Development of CAD in a Chinese Han Population

Oxidative Medicine and Cellular Longevity

This article has been retracted by Hindawi, as publisher, following an investigation undertaken by the publisher [1]. This investigation has uncovered evidence of systematic manipulation of the publication and peer-review process. We cannot, therefore, vouch for the reliability or integrity of this article.

Please note that this notice is intended solely to alert readers that the peer-review process of this article has been compromised.

Wiley and Hindawi regret that the usual quality checks did not identify these issues before publication and have since put additional measures in place to safeguard research integrity.

We wish to credit our Research Integrity and Research Publishing teams and anonymous and named external researchers and research integrity experts for contributing to this investigation.

The corresponding author, as the representative of all authors, has been given the opportunity to register their agreement or disagreement to this retraction. We have kept a record of any response received.

References

[1] W. Zhang, J. He, M. Liu et al., "Genetic Analysis Reveals Different Mechanisms of IL-5 Involved in the Development of CAD in a Chinese Han Population," *Oxidative Medicine and Cellular Longevity*, vol. 2023, Article ID 1700857, 10 pages, 2023.

Retraction

Retracted: Sirtuin 1 Induces Choroidal Neovascularization and Triggers Age-Related Macular Degeneration by Promoting LCN2 through SOX9 Deacetylation

Oxidative Medicine and Cellular Longevity

This article has been retracted by Hindawi, as publisher, following an investigation undertaken by the publisher [1]. This investigation has uncovered evidence of systematic manipulation of the publication and peer-review process. We cannot, therefore, vouch for the reliability or integrity of this article.

Please note that this notice is intended solely to alert readers that the peer-review process of this article has been compromised.

Wiley and Hindawi regret that the usual quality checks did not identify these issues before publication and have since put additional measures in place to safeguard research integrity.

We wish to credit our Research Integrity and Research Publishing teams and anonymous and named external researchers and research integrity experts for contributing to this investigation.

The corresponding author, as the representative of all authors, has been given the opportunity to register their agreement or disagreement to this retraction. We have kept a record of any response received.

References

[1] S. Zhao, Z. Huang, H. Jiang et al., "Sirtuin 1 Induces Choroidal Neovascularization and Triggers Age-Related Macular Degeneration by Promoting LCN2 through SOX9 Deacetylation," *Oxidative Medicine and Cellular Longevity*, vol. 2022, Article ID 1671438, 16 pages, 2022.

Hindawi

Retraction

Retracted: Combined Association of Low-Density Lipoprotein Cholesterol Levels and Systolic Blood Pressure to the Outcome of Intracerebral Hemorrhage: Data from the China Stroke Center Alliance

Oxidative Medicine and Cellular Longevity

This article has been retracted by Hindawi following an investigation undertaken by the publisher [1]. This investigation has uncovered evidence of one or more of the following indicators of systematic manipulation of the publication process:

(1) Discrepancies in scope

(2) Discrepancies in the description of the research reported

(3) Discrepancies between the availability of data and the research described

(4) Inappropriate citations

(5) Incoherent, meaningless and/or irrelevant content included in the article

(6) Manipulated or compromised peer review

The presence of these indicators undermines our confidence in the integrity of the article's content and we cannot, therefore, vouch for its reliability. Please note that this notice is intended solely to alert readers that the content of this article is unreliable. We have not investigated whether authors were aware of or involved in the systematic manipulation of the publication process.

In addition, our investigation has also shown that one or more of the following human-subject reporting requirements has not been met in this article: ethical approval by an Institutional Review Board (IRB) committee or equivalent, patient/participant consent to participate, and/or agreement to publish patient/participant details (where relevant).

Wiley and Hindawi regrets that the usual quality checks did not identify these issues before publication and have since put additional measures in place to safeguard research integrity.

We wish to credit our own Research Integrity and Research Publishing teams and anonymous and named external researchers and research integrity experts for contributing to this investigation.

The corresponding author, as the representative of all authors, has been given the opportunity to register their agreement or disagreement to this retraction. We have kept a record of any response received.

References

[1] Y. Ding, Y. Wang, L. Liu et al., "Combined Association of Low-Density Lipoprotein Cholesterol Levels and Systolic Blood Pressure to the Outcome of Intracerebral Hemorrhage: Data from the China Stroke Center Alliance," *Oxidative Medicine and Cellular Longevity*, vol. 2022, Article ID 6206315, 8 pages, 2022.

Retraction

Retracted: Association between Oxidative Burden and Restenosis: A Case-Control Study

Oxidative Medicine and Cellular Longevity

This article has been retracted by Hindawi, as publisher, following an investigation undertaken by the publisher [1]. This investigation has uncovered evidence of systematic manipulation of the publication and peer-review process. We cannot, therefore, vouch for the reliability or integrity of this article.

Please note that this notice is intended solely to alert readers that the peer-review process of this article has been compromised.

Wiley and Hindawi regret that the usual quality checks did not identify these issues before publication and have since put additional measures in place to safeguard research integrity.

We wish to credit our Research Integrity and Research Publishing teams and anonymous and named external researchers and research integrity experts for contributing to this investigation.

The corresponding author, as the representative of all authors, has been given the opportunity to register their agreement or disagreement to this retraction. We have kept a record of any response received.

References

[1] S. Ganjali, A. Mansouri, M. Abbasifard, S. A. Moallem, Z. Tayarani-Najaran, and A. Sahebkar, "Association between Oxidative Burden and Restenosis: A Case-Control Study," *Oxidative Medicine and Cellular Longevity*, vol. 2022, Article ID 3577761, 10 pages, 2022.

Retraction

Retracted: Provisional Decision-Making for Perioperative Blood Pressure Management: A Narrative Review

Oxidative Medicine and Cellular Longevity

This article has been retracted by Hindawi following an investigation undertaken by the publisher [1]. This investigation has uncovered evidence of one or more of the following indicators of systematic manipulation of the publication process:

(1) Discrepancies in scope

(2) Discrepancies in the description of the research reported

(3) Discrepancies between the availability of data and the research described

(4) Inappropriate citations

(5) Incoherent, meaningless and/or irrelevant content included in the article

(6) Manipulated or compromised peer review

The presence of these indicators undermines our confidence in the integrity of the article's content and we cannot, therefore, vouch for its reliability. Please note that this notice is intended solely to alert readers that the content of this article is unreliable. We have not investigated whether authors were aware of or involved in the systematic manipulation of the publication process.

Wiley and Hindawi regrets that the usual quality checks did not identify these issues before publication and have since put additional measures in place to safeguard research integrity.

We wish to credit our own Research Integrity and Research Publishing teams and anonymous and named external researchers and research integrity experts for contributing to this investigation.

The corresponding author, as the representative of all authors, has been given the opportunity to register their agreement or disagreement to this retraction. We have kept a record of any response received.

References

[1] Q. Song, J. Li, and Z. Jiang, "Provisional Decision-Making for Perioperative Blood Pressure Management: A Narrative Review," *Oxidative Medicine and Cellular Longevity*, vol. 2022, Article ID 5916040, 17 pages, 2022.

Retraction

Retracted: The Therapeutic Roles of Cinnamaldehyde against Cardiovascular Diseases

Oxidative Medicine and Cellular Longevity

This article has been retracted by Hindawi, as publisher, following an investigation undertaken by the publisher [1]. This investigation has uncovered evidence of systematic manipulation of the publication and peer-review process. We cannot, therefore, vouch for the reliability or integrity of this article.

Please note that this notice is intended solely to alert readers that the peer-review process of this article has been compromised.

Wiley and Hindawi regret that the usual quality checks did not identify these issues before publication and have since put additional measures in place to safeguard research integrity.

We wish to credit our Research Integrity and Research Publishing teams and anonymous and named external researchers and research integrity experts for contributing to this investigation.

The corresponding author, as the representative of all authors, has been given the opportunity to register their agreement or disagreement to this retraction. We have kept a record of any response received.

References

[1] L. Lu, Y. Xiong, J. Zhou, G. Wang, B. Mi, and G. Liu, "The Therapeutic Roles of Cinnamaldehyde against Cardiovascular Diseases," *Oxidative Medicine and Cellular Longevity*, vol. 2022, Article ID 9177108, 23 pages, 2022.

Retraction

Retracted: A Pharmacological Review of Tanshinones, Naturally Occurring Monomers from Salvia miltiorrhiza for the Treatment of Cardiovascular Diseases

Oxidative Medicine and Cellular Longevity

This article has been retracted by Hindawi, as publisher, following an investigation undertaken by the publisher [1]. This investigation has uncovered evidence of systematic manipulation of the publication and peer-review process. We cannot, therefore, vouch for the reliability or integrity of this article.

Please note that this notice is intended solely to alert readers that the peer-review process of this article has been compromised.

Wiley and Hindawi regret that the usual quality checks did not identify these issues before publication and have since put additional measures in place to safeguard research integrity.

We wish to credit our Research Integrity and Research Publishing teams and anonymous and named external researchers and research integrity experts for contributing to this investigation.

The corresponding author, as the representative of all authors, has been given the opportunity to register their agreement or disagreement to this retraction. We have kept a record of any response received.

References

[1] Y. Yang, M. Shao, W. Cheng et al., "A Pharmacological Review of Tanshinones, Naturally Occurring Monomers from Salvia miltiorrhiza for the Treatment of Cardiovascular Diseases," *Oxidative Medicine and Cellular Longevity*, vol. 2023, Article ID 3801908, 24 pages, 2023.

Retraction

Retracted: Marine-Derived Piericidin Diglycoside S18 Alleviates Inflammatory Responses in the Aortic Valve via Interaction with Interleukin 37

Oxidative Medicine and Cellular Longevity

This article has been retracted by Hindawi, as publisher, following an investigation undertaken by the publisher [1]. This investigation has uncovered evidence of systematic manipulation of the publication and peer-review process. We cannot, therefore, vouch for the reliability or integrity of this article.

Please note that this notice is intended solely to alert readers that the peer-review process of this article has been compromised.

Wiley and Hindawi regret that the usual quality checks did not identify these issues before publication and have since put additional measures in place to safeguard research integrity.

We wish to credit our Research Integrity and Research Publishing teams and anonymous and named external researchers and research integrity experts for contributing to this investigation.

The corresponding author, as the representative of all authors, has been given the opportunity to register their agreement or disagreement to this retraction. We have kept a record of any response received.

References

[1] S. Li, J. She, J. Zeng et al., "Marine-Derived Piericidin Diglycoside S18 Alleviates Inflammatory Responses in the Aortic Valve via Interaction with Interleukin 37," *Oxidative Medicine and Cellular Longevity*, vol. 2022, Article ID 6776050, 18 pages, 2022.

Retraction

Retracted: Inhibition of Oxidative Stress: An Important Molecular Mechanism of Chinese Herbal Medicine (Astragalus membranaceus, Carthamus tinctorius L., Radix Salvia Miltiorrhizae, etc.) in the Treatment of Ischemic Stroke by Regulating the Antioxidant System

Oxidative Medicine and Cellular Longevity

This article has been retracted by Hindawi, as publisher, following an investigation undertaken by the publisher [1]. This investigation has uncovered evidence of systematic manipulation of the publication and peer-review process. We cannot, therefore, vouch for the reliability or integrity of this article.

Please note that this notice is intended solely to alert readers that the peer-review process of this article has been compromised.

Wiley and Hindawi regret that the usual quality checks did not identify these issues before publication and have since put additional measures in place to safeguard research integrity.

We wish to credit our Research Integrity and Research Publishing teams and anonymous and named external researchers and research integrity experts for contributing to this investigation.

The corresponding author, as the representative of all authors, has been given the opportunity to register their agreement or disagreement to this retraction. We have kept a record of any response received.

References

[1] X. Zhao, Y. He, Y. Zhang, H. Wan, H. Wan, and J. Yang, "Inhibition of Oxidative Stress: An Important Molecular Mechanism of Chinese Herbal Medicine (Astragalus membranaceus, Carthamus tinctorius L., Radix Salvia Miltiorrhizae, etc.) in the Treatment of Ischemic Stroke by Regulating the Antioxidant System," *Oxidative Medicine and Cellular Longevity*, vol. 2022, Article ID 1425369, 10 pages, 2022.

Retraction

Retracted: Mitochondrial Dysfunction and Cardiovascular Disease: Pathophysiology and Emerging Therapies

Oxidative Medicine and Cellular Longevity

This article has been retracted by Hindawi, as publisher, following an investigation undertaken by the publisher [1]. This investigation has uncovered evidence of systematic manipulation of the publication and peer-review process. We cannot, therefore, vouch for the reliability or integrity of this article.

Please note that this notice is intended solely to alert readers that the peer-review process of this article has been compromised.

Wiley and Hindawi regret that the usual quality checks did not identify these issues before publication and have since put additional measures in place to safeguard research integrity.

We wish to credit our Research Integrity and Research Publishing teams and anonymous and named external researchers and research integrity experts for contributing to this investigation.

The corresponding author, as the representative of all authors, has been given the opportunity to register their agreement or disagreement to this retraction. We have kept a record of any response received.

References

[1] C. A. Stamerra, P. Di Giosia, P. Giorgini, C. Ferri, V. N. Sukhorukov, and A. Sahebkar, "Mitochondrial Dysfunction and Cardiovascular Disease: Pathophysiology and Emerging Therapies," *Oxidative Medicine and Cellular Longevity*, vol. 2022, Article ID 9530007, 16 pages, 2022.

Retraction

Retracted: Intermittent Hypoxia and Atherosclerosis: From Molecular Mechanisms to the Therapeutic Treatment

Oxidative Medicine and Cellular Longevity

This article has been retracted by Hindawi, as publisher, following an investigation undertaken by the publisher [1]. This investigation has uncovered evidence of systematic manipulation of the publication and peer-review process. We cannot, therefore, vouch for the reliability or integrity of this article.

Please note that this notice is intended solely to alert readers that the peer-review process of this article has been compromised.

Wiley and Hindawi regret that the usual quality checks did not identify these issues before publication and have since put additional measures in place to safeguard research integrity.

We wish to credit our Research Integrity and Research Publishing teams and anonymous and named external researchers and research integrity experts for contributing to this investigation.

The corresponding author, as the representative of all authors, has been given the opportunity to register their agreement or disagreement to this retraction. We have kept a record of any response received.

References

[1] B. Luo, Y. Li, M. Zhu, J. Cui, Y. Liu, and Y. Liu, "Intermittent Hypoxia and Atherosclerosis: From Molecular Mechanisms to the Therapeutic Treatment," *Oxidative Medicine and Cellular Longevity*, vol. 2022, Article ID 1438470, 16 pages, 2022.

Retraction

Retracted: Colostomy Delays Cell Loss in the Brain and Improves Juvenile Survival in a Neonatal Rat Model of Hirschsprung's Disease

Oxidative Medicine and Cellular Longevity

This article has been retracted by Hindawi following an investigation undertaken by the publisher [1]. This investigation has uncovered evidence of one or more of the following indicators of systematic manipulation of the publication process:

(1) Discrepancies in scope

(2) Discrepancies in the description of the research reported

(3) Discrepancies between the availability of data and the research described

(4) Inappropriate citations

(5) Incoherent, meaningless and/or irrelevant content included in the article

(6) Peer-review manipulation

The presence of these indicators undermines our confidence in the integrity of the article's content and we cannot, therefore, vouch for its reliability. Please note that this notice is intended solely to alert readers that the content of this article is unreliable. We have not investigated whether authors were aware of or involved in the systematic manipulation of the publication process.

Wiley and Hindawi regrets that the usual quality checks did not identify these issues before publication and have since put additional measures in place to safeguard research integrity.

We wish to credit our own Research Integrity and Research Publishing teams and anonymous and named external researchers and research integrity experts for contributing to this investigation.

The corresponding author, as the representative of all authors, has been given the opportunity to register their agreement or disagreement to this retraction. We have kept a record of any response received.

References

[1] D. Xie, Y. Du, Y. Wang, G. D. H. Croaker, Z. Z. Wei, and Z.-M. Song, "Colostomy Delays Cell Loss in the Brain and Improves Juvenile Survival in a Neonatal Rat Model of Hirschsprung's Disease," *Oxidative Medicine and Cellular Longevity*, vol. 2022, Article ID 3792798, 7 pages, 2022.

Hindawi

Retraction

Retracted: The RPL4P4 Pseudogene Is a Prognostic Biomarker and Is Associated with Immune Infiltration in Glioma

Oxidative Medicine and Cellular Longevity

This article has been retracted by Hindawi following an investigation undertaken by the publisher [1]. This investigation has uncovered evidence of one or more of the following indicators of systematic manipulation of the publication process:

(1) Discrepancies in scope

(2) Discrepancies in the description of the research reported

(3) Discrepancies between the availability of data and the research described

(4) Inappropriate citations

(5) Incoherent, meaningless and/or irrelevant content included in the article

(6) Peer-review manipulation

The presence of these indicators undermines our confidence in the integrity of the article's content and we cannot, therefore, vouch for its reliability. Please note that this notice is intended solely to alert readers that the content of this article is unreliable. We have not investigated whether authors were aware of or involved in the systematic manipulation of the publication process.

Wiley and Hindawi regrets that the usual quality checks did not identify these issues before publication and have since put additional measures in place to safeguard research integrity.

We wish to credit our own Research Integrity and Research Publishing teams and anonymous and named external researchers and research integrity experts for contributing to this investigation.

The corresponding author, as the representative of all authors, has been given the opportunity to register their agreement or disagreement to this retraction. We have kept a record of any response received.

References

[1] Z. Wang, Y. Aili, Y. Wang et al., "The RPL4P4 Pseudogene Is a Prognostic Biomarker and Is Associated with Immune Infiltration in Glioma," *Oxidative Medicine and Cellular Longevity*, vol. 2022, Article ID 7967722, 28 pages, 2022.

Retraction

Retracted: Conservative Therapy vs. Endovascular Approach for Intracranial Vertebrobasilar Artery Trunk Large Aneurysms: A Prospective Multicenter Cohort Study

Oxidative Medicine and Cellular Longevity

This article has been retracted by Hindawi following an investigation undertaken by the publisher [1]. This investigation has uncovered evidence of one or more of the following indicators of systematic manipulation of the publication process:

(1) Discrepancies in scope

(2) Discrepancies in the description of the research reported

(3) Discrepancies between the availability of data and the research described

(4) Inappropriate citations

(5) Incoherent, meaningless and/or irrelevant content included in the article

(6) Peer-review manipulation

The presence of these indicators undermines our confidence in the integrity of the article's content and we cannot, therefore, vouch for its reliability. Please note that this notice is intended solely to alert readers that the content of this article is unreliable. We have not investigated whether authors were aware of or involved in the systematic manipulation of the publication process.

In addition, our investigation has also shown that one or more of the following human-subject reporting requirements has not been met in this article: ethical approval by an Institutional Review Board (IRB) committee or equivalent, patient/participant consent to participate, and/or agreement to publish patient/ participant details (where relevant).

Wiley and Hindawi regrets that the usual quality checks did not identify these issues before publication and have since put additional measures in place to safeguard research integrity.

We wish to credit our own Research Integrity and Research Publishing teams and anonymous and named external researchers and research integrity experts for contributing to this investigation.

The corresponding author, as the representative of all authors, has been given the opportunity to register their agreement or disagreement to this retraction. We have kept a record of any response received.

References

[1] Q. Wu, T. Li, W. Jiang, J. A. Hernesniemi, L. Li, and Y. He, "Conservative Therapy vs. Endovascular Approach for Intracranial Vertebrobasilar Artery Trunk Large Aneurysms: A Prospective Multicenter Cohort Study," *Oxidative Medicine and Cellular Longevity*, vol. 2022, Article ID 9682507, 10 pages, 2022.

Retraction

Retracted: A Pharmacological Review of Tanshinones, Naturally Occurring Monomers from Salvia miltiorrhiza for the Treatment of Cardiovascular Diseases

Oxidative Medicine and Cellular Longevity

This article has been retracted by Hindawi, as publisher, following an investigation undertaken by the publisher [1]. This investigation has uncovered evidence of systematic manipulation of the publication and peer-review process. We cannot, therefore, vouch for the reliability or integrity of this article.

Please note that this notice is intended solely to alert readers that the peer-review process of this article has been compromised.

Wiley and Hindawi regret that the usual quality checks did not identify these issues before publication and have since put additional measures in place to safeguard research integrity.

We wish to credit our Research Integrity and Research Publishing teams and anonymous and named external researchers and research integrity experts for contributing to this investigation.

The corresponding author, as the representative of all authors, has been given the opportunity to register their agreement or disagreement to this retraction. We have kept a record of any response received.

References

[1] Y. Yang, M. Shao, W. Cheng et al., "A Pharmacological Review of Tanshinones, Naturally Occurring Monomers from Salvia miltiorrhiza for the Treatment of Cardiovascular Diseases," *Oxidative Medicine and Cellular Longevity*, vol. 2023, Article ID 3801908, 24 pages, 2023.

Review Article

A Pharmacological Review of Tanshinones, Naturally Occurring Monomers from *Salvia miltiorrhiza* for the Treatment of Cardiovascular Diseases

Ye Yang [iD],[1,2] **Mingyan Shao,**[2,3] **Wenkun Cheng,**[2,3] **Junkai Yao,**[1,2] **Lin Ma,**[2,4] **Yong Wang** [iD],[2,3] **and Wei Wang** [iD][2,5]

[1]*Dongzhimen Hospital, Beijing University of Chinese Medicine, Beijing, China*
[2]*Key Laboratory of TCM Syndrome and Formula (Beijing University of Chinese Medicine), Ministry of Education, Beijing, China*
[3]*School of Chinese Medicine, Beijing University of Chinese Medicine, Beijing 100029, China*
[4]*School of Life Sciences, Beijing University of Chinese Medicine, Beijing, China*
[5]*Guangzhou University of Chinese Medicine, Guangzhou, China*

Correspondence should be addressed to Yong Wang; wangyong@bucm.edu.cn and Wei Wang; wangwei26960@126.com

Cardiovascular diseases (CVDs) are a set of heart and blood vessel disorders that include coronary heart disease (CHD), rheumatic heart disease, and other conditions. Traditional Chinese Medicine (TCM) has definite effects on CVDs due to its multitarget and multicomponent properties, which are gradually gaining national attention. Tanshinones, the major active chemical compounds extracted from *Salvia miltiorrhiza*, exhibit beneficial improvement on multiple diseases, especially CVDs. At the level of biological activities, they play significant roles, including anti-inflammation, anti-oxidation, anti-apoptosis and anti-necroptosis, anti-hypertrophy, vasodilation, angiogenesis, combat against proliferation and migration of smooth muscle cells (SMCs), as well as anti-myocardial fibrosis and ventricular remodeling, which are all effective strategies in preventing and treating CVDs. Additionally, at the cellular level, Tanshinones produce marked effects on cardiomyocytes, macrophages, endothelia, SMCs, and fibroblasts in myocardia. In this review, we have summarized a brief overview of the chemical structures and pharmacological effects of Tanshinones as a CVD treatment to expound on different pharmacological properties in various cell types in myocardia.

1. Introduction

Cardiovascular diseases (CVDs), such as myocardial infarction (MI), heart failure (HF), and myocardial ischemia/reperfusion (I/R) injury, are the most prevalent noncommunicable disease and the leading cause of mortality with an estimated 17.9 million lives being taken annually worldwide [1]. The mortality ratio of coronary heart disease (CHD), including MI and its ultimate trigger of HF, is considered to be the highest among deaths caused by CVDs, primarily due to a blockage that prevents blood from reaching the heart [2]. CVDs have imposed a substantial economic burden on healthcare systems [3]. Currently, the main drug regimens in Western medicine against CHDs include β-receptor blockers, angiotensin-converting enzyme inhibitors (ACEIs), angiotensin receptor blockers (ARBs), and lipid-lowering therapy presented by Statins, which are associated with many severe disadvantages. For instance, there is a strict prohibition on β-receptor blockers due to the harmful effects of their early use at high dosages and their use in high-risk MI patients who have HF or cardiogenic shock [4]. ACEIs are not indicated for patients with systolic blood pressure (SBP) $< 90\sim100$ mmHg, shock, acute kidney injury, and renal failure [5]. At the same time, Statins may cause adverse effects including rhabdomyolysis [6]. In summary, the current treatments are associated with numerous side effects and high costs. In this view, it is essential to focus on traditional and alternative medicine [7].

Chinese herbal medicines (CHMs) have been carried over for more than 2500 years for various clinical usages of different diseases and symptoms in China. Before the introduction of modern Western medicine, CHMs were the only method of healthcare in China [8]. Currently, accumulated scientific evidence has shown that abundant monomers naturally occurring from CHMs have achieved good efficacies in treating CVDs [9–11]. *Salvia miltiorrhiza* (*S. miltiorrhiza*) is a perennial plant belonging to the family *Labiatae*, genus *Salvia*, and a shade-growing herb. The dried root and rhizome of *S. miltiorrhiza* are often referred to as *Danshen* in China [12]. As the top-grade Chinese herb, *S. miltiorrhiza* promotes blood circulation, removes blood stasis, and invigorates qi. Therefore, *S. miltiorrhiza* and the Chinese medicine formulas majorly composed of it have been clinically prescribed for treating CVDs, especially the blood stasis symptom type. For example, the study has found *Danshen* Decoction, comprising *S. miltiorrhiza*, *Santalum album*, and *Amomum villosum*, as a potential therapeutic reagent, exerting a remarkable cardioprotective function against acute ischemic myocardial injury in rats, possibly through its anti-inflammatory and anti-oxidative properties [13]. Compound *Danshen* Dripping Pills containing *S. miltiorrhiza*, *Panax notoginseng*, and *Bornes camphor* have displayed therapeutic effects of ameliorating myocardial ischemia, reversing the metabolic reprogramming, as well as normalizing the level of myocardial substrates and the genes/enzymes responsible for metabolic changes in isoproterenol (ISO)-induced rats [14].

The anti-CVD activity of *S. miltiorrhiza* is due to its bioactive constituent, i.e., salvianolic acids and Tanshinones. Prior to phenolic acids, the liposoluble compounds in *S. miltiorrhiza* known Tanshinones were isolated and examined [15]. Many drug delivery systems and chemical modifications of Tanshinones have also been designed to enhance pharmacological activities [16, 17]. Therefore, we focused on the medicinal research of Tanshinones in this review to summarize their anti-CVD influence. In recent years, Tanshinones, the primary active chemical compounds in *S. miltiorrhiza*, have attracted extensive attention on treating CVDs [18–20]. Many pharmacological studies have documented that Tanshinones exhibit antiatherosclerosis (AS), antihypertension, antimyocardial fibrosis, and anti-I/R injury, all effective strategies for preventing and treating CVDs [18–20]. In recent years, various Tanshinone-based formulations with practical therapeutic benefits have developed. Among them, Tanshinone injection, sodium Tan IIA sulfonate (STS), is mainly used in the adjuvant treatment of CHDs [21]. It has been shown that STS had positive effects when combined with conventional Western medicine treatment, intending to systematically evaluate the efficacy and safety of STS in the treatment of CHDs and provide the basis for its clinical application [22]. This review has summarized the primary active chemical constituents of *S. miltiorrhiza*, the pharmacological effects of Tanshinones, and their underlying mechanisms for alleviating CVDs. The Graphical Summary is provided in the Supplementary Materials (available here).

2. Properties of Tanshinones

The chemical components of *S. miltiorrhiza* were identified in the 1930s when Japanese scholars first isolated two liposoluble components, i.e., Tanshinone I and II. After that, Chinese scholars demonstrated that Tanshinone II was a mixture of two components comprising Tanshinone IIA and IIB [15]. After that, many new compounds have been isolated from *S. miltiorrhiza*, and their chemical structures have been extensively elucidated [15]. Chemical components of *S. miltiorrhiza* can be categorized primarily as hydrosoluble or liposoluble compounds, representing the predominant secondary metabolites. Chemical and pharmacological studies have validated these metabolites as the primary bioactive constituents of *S. miltiorrhiza* [23]. Among them, the fat-soluble Tanshinones majorly belong to diterpenoid quinones, represented by Tanshinone I (Tan I), Tanshinone IIA (Tan IIA), Tanshinone IIB (Tan IIB), Cryptotanshinone (CTS), and 15,16-dihydrotanshinone I (DHT) [24]. A series of liposoluble compounds has been developed into preparations for clinical application [25, 26]. Furthermore, each Tanshinone product has a specific biological activity [27]. The chemical and physical properties of representative Tanshinones are shown in Table S1.

Tanshinones are abietane diterpenes, most of which have ortho-quinone or para-quinone structures with three or four carbon rings on the skeleton. Tanshinones have poor stability because of their active double bond, making them susceptible to heat-induced reduction and decomposition reactions [24]. The chemical structure of Tan IIA was modified to create STS, an important derivative with dramatically more water solubility than Tan IIA, to address this resistance to druggability [28]. Among them, the chemical structures of representative Tanshinone compounds are shown in Figure 1.

3. Pharmacological Activities of Tanshinones on CVDs

According to recently reported studies, Tanshinones possess numerous cardiac effects involving multiple cell types and pathological links, including anti-inflammation, anti-oxidative stress, anti-apoptosis, anti-necroptosis, anti-hypertrophy, vasodilation, angiogenesis, combat against proliferation and migration of smooth muscle cells (SMCs), as well as anti-myocardial fibrosis and ventricular remodeling, in myocardial tissues and cardiomyocytes, macrophages, endothelial cells, SMCs, and fibroblasts. Therefore, Tanshinones can be used as a promising candidate for the treatment of CVDs. This review summarizes the primary pharmacological effects and their underlying mechanisms of representative Tanshinones to determine their prospective protein targets.

3.1. The Pharmacological Mechanism of Tanshinones for Protecting Myocardia and Cardiomyocytes against CVDs

3.1.1. Antioxidative Effect of Tanshinones on Myocardia and Cardiomyocytes. Oxidative stress is involved in the occurrence and progression of various CVDs. The rapid production and
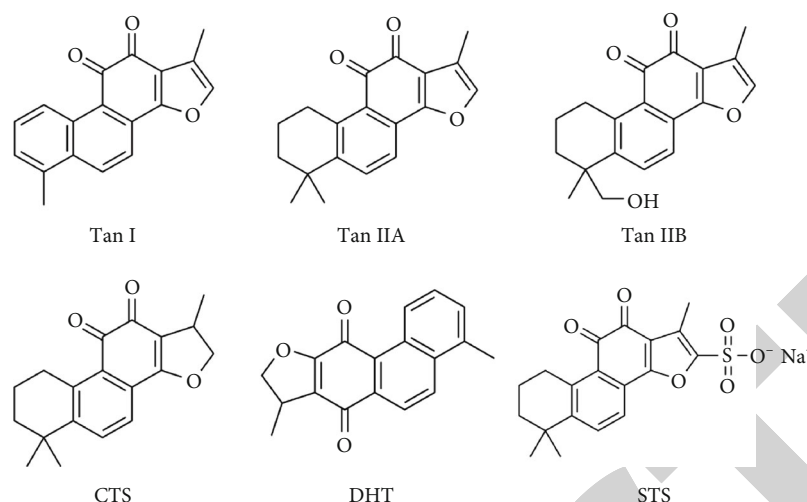
Figure 1: Chemical structures of representative Tanshinones.

accumulation of free radicals and their oxidation products can react with various cell components, such as membrane phospholipids, proteins, and nucleic acids, resulting in structural cell damage and functional metabolic disorders [29, 30]. Under physiological conditions, cells' reactive oxygen species (ROS) benefit their biological activities. When the balance between ROS production and antioxidative defense is disturbed, oxidative stress-related pathology is followed by altered intracellular homeostasis [31, 32]. Given this fact, antioxidative stress is a therapeutic target in various CVDs.

The transcription factor NFE2L2/Nrf2 (nuclear factor erythroid-derived 2-like 2) promotes the expression of anti-oxidants and detoxification enzymes to combat ROS and toxic metabolites, such as heme oxygenase-1 (HO-1) and NAD(P)H-quinone oxidoreductase-1 (NQO-1) [33]. The study suggested that Tan I could dose-dependently promote the protein content and trans-localization of Nrf2 from the cytoplasm into the nucleus. Surface plasma resonance (SPR) detection confirmed that Tan I directly targeted Nrf2 and might serve as a potential agonist of Nrf2. Through positive regulation of the Nrf2 pathway, Tan I promoted the expression of anti-oxidation-related protein downstream while inhibiting the protein contents of the mitogen-activated protein kinase (MAPK) family via the Nrf2/MAPK pathway to protect oxidative stress-insulted myocardial tissues and H9c2 cardiomyocytes both *in vivo* and *in vitro* [34]. However, it has been demonstrated that the MAPK protein family member phosphorylated- (p-) extracellular signal-regulated kinase 1/2 (ERK1/2) can facilitate Nrf2's nuclear translocation to promote the transcription of anti-oxidant enzymes [35, 36]. Tan I was thought to have an anti-oxidative function that was quite distinct from the ERK1/2-Nrf2 pathway by activating Nrf2 and inhibiting MAPKs. During myocardial I/R injury, mitochondrial respiratory chain (MRC) complex I is suppressed, followed by transient ROS production. According to the research, the expression of hypoxia-inducible factor 1α (HIF-1α) could be stabilized by pre-administration of DHT due to transient accumulation of ROS through reversible inhibition of the

MRC complex I. However, HIF-1α acting as a transcription factor promotes *Nrf2* transcription and activates the expression of downstream anti-oxidative enzymes. Therefore, DHT could exert a protective effect against cardiac I/R damage, as demonstrated by reduced infarct sizes and enhanced cardiac function in I/R rats and hydrogen peroxide (H₂O₂)-induced H9c2 cardiomyocytes [37]. Furthermore, protein kinase C (PKC), which is Nrf2's upstream kinase, can phosphorylate Nrf2 to turn it on and translocate it from the cytoplasm to the nucleus [38, 39]. In contrast, another upstream pathway of Nrf2 is the glycogen synthase kinase 3β (GSK-3β)/Fyn pathway playing the opposite role. Intranuclear accumulation of Fyn can promote Nrf2 to trans-localize from the nucleus to the cytoplasm, leading to the inactivated Nrf2 as a transcription factor. However, protein kinase B (PKB/Akt) can phosphorylate GSK-3β to inhibit the nuclear translocation of Fyn. The research has confirmed that DHT could restrain Nrf2 degradation and enhance its nuclear import by upregulating the PKC/Nrf2 pathway. DHT has also been shown to inhibit Nrf2 nuclear export by enhancing the PKB activation to downregulate the GSK-3β/Fyn pathway [40]. In addition to DHT, it has been confirmed that Tan I could also promote nuclear Nrf2 protein to increase the expression of related enzymes to combat oxidative stress by the Akt/Nrf2 pathway upregulation [41]. The classical pathway, phosphatidylinositol-3 kinase (PI3K)/Akt, is essential to regulate various biological processes such as oxidative stress and cellular apoptosis [42, 43]. Tan IIA was reported to activate the PI3K/Akt pathway, followed by the upregulation of its downstream mammalian target of rapamycin (mTOR) and endothelial nitric oxide synthase (eNOS) to prevent cellular oxidative stress and apoptosis [44]. Moreover, the excessive opening of mitochondrial permeability transition pores (mPTPs) often occurs during cardiac I/R lesion, causing the release of ROS and cytochrome C (cyt c). It has been reported that Tan IIA could elevate the expression level of the apoptotic regulatory factor, i.e., 14-3-3η, to increase B cell lymphoma-2 (BCL-2) translocation to the mitochondrial outer membrane. Tan IIA enhanced

the cell survival of anoxia/reoxygenation (A/R)-stimulated H9c2 cardiomyocytes by inhibiting mPTP opening, ROS production, and cyt c delivery as a result of its interaction with BCL-2 and voltage-dependent anion-selective channel 1 (VDAC-1). Table 1 and Figure 2 summarize the antioxidant activity of Tanshinones in protecting the myocardia and cardiomyocytes against CVDs [45].

3.1.2. Antiapoptosis and Antinecroptosis Effects of Tanshinones on Myocardia and Cardiomyocytes. When myocardial ischemia occurs, persistent oxygen deficit leads to membrane integrity damage, triggering irreversible cell death. Since cardiomyocytes lack regenerative capacity, cardiomyocyte apoptosis results in progressive loss of cardiomyocytes and left ventricular dilation after MI [46, 47]. Apoptosis belongs to programmed cell death and involves genetically determined cell elimination [48]. As an end consequence of cellular damage during CVDs, cardiomyocyte apoptosis is the ultimate target of Tanshinone compounds.

During the progression of MI, it is one of the main pathological mechanisms of oxidative stress and cellular apoptosis that the cardiomyocyte damage induced by endoplasmic reticulum stress (ERS). Among them, several major proteins play essential roles. Inositol-requiring enzyme 1 (IRE1) activates and promotes the expression of C/EBP homologous protein (CHOP) under the ERS stimulation. In addition to IRE1, activating transcription factor 4 (ATF4) is also one of the upstream regulatory proteins of CHOP. Glucose regulatory protein (GRP78) and CHOP are both ERS-associated molecules that jointly promote the activation of kinases in the apoptosis pathway [49, 50]. According to the reported studies, Tan IIA could alleviate the apoptotic state of myocardial tissues and their isolated cardiomyocytes in MI rats via downregulating protein levels in the IRE1 and ATF4 pathways [51]. Tan IIA was also shown to reduce acute ethanol-induced cardiomyocyte apoptosis by reversing the upregulation of programmed cell death protein 4 (PDCD4), following the promotion of the PI3K/Akt signaling pathway in acute ethanol-treated mice *in vivo* and H9c2 cells *in vitro* [52]. As an antitumor drug widely used, the cardiotoxic side effects of Doxorubicin (DOX) may produce severe cellular stress to trigger endogenous apoptosis [53]. During this process, p53 is considered an essential proapoptotic protein [54]. As the downstream proteins of p53 transcription factor, p53 upregulated modulator of apoptosis (Puma) and BCL-2 interacting mediator of cell death (Bim) also produce a marked effect on promoting apoptosis [55]. Moreover, the forkhead box O1 transcription factor (Foxo1) is also the upstream transcription factor of *Puma* and *Bax* [56–58]. CTS has been reported to upregulate the expression of the antiapoptotic factor BCL-2 while suppressing the genetic transcription of the proapoptotic factors, i.e., *Puma* and *Bim*, via downregulating p53. Concurrently, CTS has been validated that it might not only inhibit the activity of Foxo1 and its downstream genetic transcription of *Puma* and *Bax* but also restrain the translocation of BAX to mitochondria via weakening its combination with 14-3-3σ, jointly regulated by the advanced PI3K/Akt pathway and the subsequent inhibition of c-Jun N-terminal kinase

(JNK/SAPK) phosphorylation. The afore-mentioned routes are all potential targets for CTS's anti-DOX strategy in the cardiac injury model [59]. STS was also reported in a comparable study to suppress *Bim* transcription via Akt-dependent phosphorylation and inactivation of Foxo3a by its phosphorylation and nuclear-to-cytoplasmic translocation. However, no obvious regulatory effect on Foxo1 and Foxo4 in the Foxo family by STS was reported [60]. Furthermore, Tan IIA could elevate the expression level of miRNA-133 and phosphorylate serine (Ser) 473 site in Akt, through which the PI3K/Akt pathway was stimulated. By means of the above process, apoptosis induced by mitochondrial oxidative stress and ERS could be restrained using Tan IIA [50, 61, 62]. Arachidonic acid (AA), a type of polyunsaturated fatty acid, is also a precursor that can be metabolized by different enzymes into biological eicosenoic acids. It is considered the essential proapoptotic participant in myocardial I/R injury that the hydroxylated metabolite, 20-hydroxyeicosatetraenoic acid (20-HETE) of AA [63, 64]. The data suggested that DHT might inhibit AA by decreasing the formation of 20-HETE and alleviating cardiomyocyte apoptosis [65].

Autophagy is primarily responsible for degrading long-lived proteins or whole organelle substrates and maintaining intracellular homeostasis. Autophagy typically crosses with elevated oxidative stress and cellar apoptosis [66–68]. The important subtype, macroautophagy, develops double-membrane autophagosomes sequestering abandoned or recyclable substrates and then extends to autolysosomes by fusing with acidic lysosomes that mediate constituents to be degraded under the regulation of lysosomal-associated membrane proteins 1/2 (LAMP1/2) [69–71]. During this process, protein 1 light chain 3-II (LC3-II) and Sequestosome-1 (p62/SQSTM1) are essential autophagy biomarkers engaging in segregating cargoes [72, 73]. As the classical pathway responsible for autophagy, mTOR kinase is a negative regulator of UNC-51-like kinase 1 (ULK1)-Beclin1 (ATG6) pathway that stimulates autophagosome formation [74, 75] and transcription factor EB (TFEB) that regulates the transcriptions of genes relevant to lysosomal biogenesis and degradation [76, 77]. The study has demonstrated that Tan IIA could reduce DOX-induced cardiotoxicity without compromising antitumor activity by decreasing p-ULK1 to activate the Beclin1 pathway, and sequestration of TFEB in the nucleus, via inhibiting the phosphorylation of mTOR from inactivating autophagy and impairing autophagic flux [78].

Programmed necrosis (necroptosis) is a form of cell necrosis. Contrary to apoptosis, its process results in plasma membrane rupture and cell content overflow, triggering the immune system and inflammatory response [79]. Necroptosis is mainly mediated by the complex formed by receptor interacting protein kinase 1 (RIP1), receptor interacting protein kinase 3 (RIP3), and mixed lineage kinase domain-like protein (MLKL) [80, 81]. Another study has revealed that Tan I alleviated the excretion of inflammatory factors by suppressing necroptosis in cardiomyocytes induced by cardiac I/R injury that is positively regulated by the RIP1/RIP3/MLKL pathway [41]. The antiapoptosis and antinecroptosis effects of Tanshinones on protecting myocardia

Table 1: The antioxidative effect of Tanshinones on protecting myocardia and cardiomyocytes against CVDs.

Tanshinones	In vivo/in vitro	Models	Effective doses	Related mechanisms	Refs.
Tan I	In vivo/in vitro	*In vivo:* Mice received intraperitoneal injection of ISO to establish an oxidative stress-induced myocardial damage model; *In vitro:* H9c2 cardiomyocytes treated with tert-butyl hydroperoxide (t-BHP) to establish an oxidative stress-induced cellular damage model	*In vivo:* 10 mg/kg; *In vitro:* 0.625, 1.25, 2.5 μM	*In vivo:* ↓ Myocardial injury, the heart weight/body weight (HW/BW) ratio, collagen deposition, BCL-2-associated X protein (BAX), caspase3, the MAPK pathway; ↑ Cardiac function, BCL-2, the Nrf2 pathway; *In vitro:* ↓ BAX, malondialdehyde (MDA), the MAPK pathway; ↑ BCL-2, superoxide dismutase (SOD), the Nrf2 pathway	[34]
DHT	In vivo/in vitro	*In vivo:* I/R-induced myocardial damage in rats; *In vitro:* H_2O_2-induced cellular damage in H9c2 cardiomyocytes	*In vivo:* 0.1 mg/kg; *In vitro:* 0.5, 1, 2 μM	*In vivo:* ↓ Infarct size, myocardial injury markers; ↑ Cardiac function; *In vitro:* ↓ Apoptosis rate, lactate dehydrogenase (LDH), MRC complex I; ↑ Cell viability, HIF-1α, the Nrf2 pathway, HO-1, NQO-1, SOD, catalase (CAT)	[37]
Tan IIA	In vitro	A/R-induced cellular damage in H9c2 cardiomyocytes	2, 8, 32 μM	↓ Apoptosis rate, LDH, MDA, ROS, cyt c, caspase-3, mPTP opening; ↑ Cell viability, SOD, 14-3-3η, mitochondrial colocalization of 14-3-3η, BCL-2, and VDAC-1	[45]
Tan IIA	In vivo/in vitro	*In vivo:* I/R-induced myocardial damage in rats; *In vitro:* A/R-induced cellular damage in neonatal rat ventricular myocytes (NRVMs)	*In vivo:* 20 mg/kg; *In vitro:* 1 μM	*In vivo:* ↓ Creatine kinase isoenzyme (CK-MB), LDH, MDA, H_2O_2; ↑ SOD, sorbitol dehydrogenase (SDH), cytochrome c oxidase, the PI3K/Akt pathway, p-mTOR, p-eNOS; *In vitro:* ↓ Apoptosis rate, CK-MB, LDH; ↑ Cell viability, p-mTOR, p-eNOS	[44]
DHT	In vivo/in vitro	*In vivo:* I/R-induced myocardial damage in mice; *In vitro:* A/R-induced cellular damage in HL-1 cardiomyocytes	*In vivo:* 5 mg/kg; *In vitro:* 0.1, 1, 5 μM	*In vivo:* ↓ Infarct size, surface area of cells, 8-hydroxy-20-deoxyguanosine (8-OHDG), apoptosis rate, LDH, MDA; ↑ Cardiac function, the Nrf2 pathway, HO-1, NQO-1; *In vitro:* ↓ Apoptosis rate, LDH, cyto-Nrf2, the GSK-3β/Fyn pathway; ↑ p-Nrf2, the PKC/Nrf2 pathway, PKB, HO-1, NQO-1	[40]
Tan I	In vivo/in vitro	*In vivo:* I/R-induced myocardial damage in rats; *In vitro:* H9c2 cardiomyocytes treated with t-BHP to establish an oxidative stress-induced cellular damage model	*In vivo:* 10, 20 mg/kg; *In vitro:* 0.125, 0.25, 0.5, 1, 2 μM	*In vivo:* ↓ Pathological injury of myocardial tissues, MDA; ↑ SOD; *In vitro:* ↓ LDH, ROS; ↑ Cell viability, mitochondrial membrane potential, p-Akt, Nrf2, HO-1, NQO-1	[41]
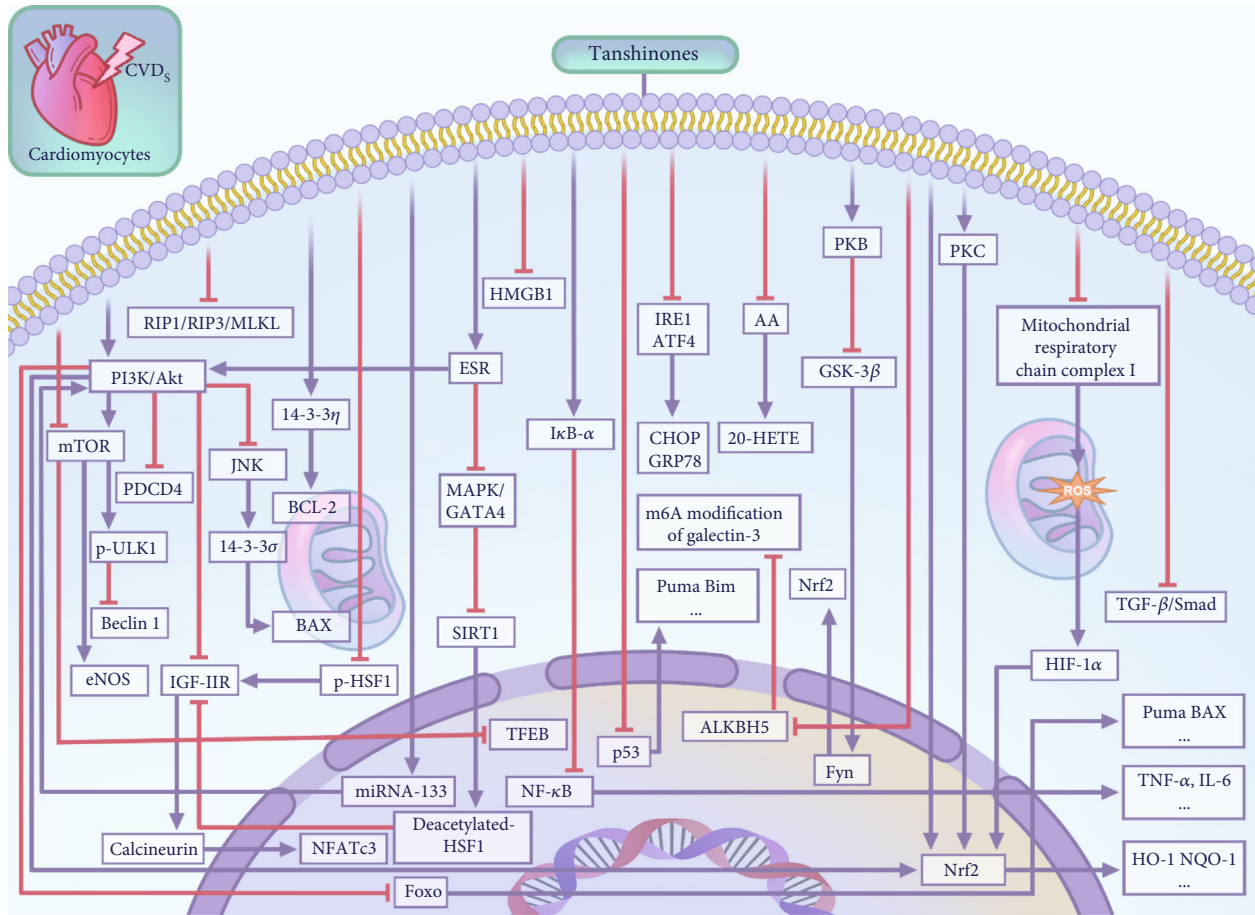
FIGURE 2: The pharmacological mechanism of Tanshinones for protecting myocardia and cardiomyocytes against CVDs.

and cardiomyocytes against CVDs have been summarized in Table 2 and Figure 2.

3.1.3. Anti-inflammatory Effect of Tanshinones on Myocardia and Cardiomyocytes.
Inflammation can cause severe mitochondrial damage and microenvironment disruption [82]. Tanshinone compounds can also exert an anti-inflammatory effect on CVDs. Under conditions of cellular stress, cellular inflammation is initiated by proinflammatory factors such as tumor necrosis factor-α (TNF-α), interleukin-6 (IL-6), and inducible nitric oxide synthase (iNOS) [83, 84].

Some studies have revealed that the release of multiple pro-inflammatory factors could be held up through down-regulating high mobility group box-B1 (HMGB1) expression, one of the damage-associated molecular patterns (DAMPs), in I/R-insulted myocardial tissues of rats by Tan IIA [85] or STS [86]. The nuclear factor kappa-B (NF-κB) pathway, a classical inflammatory response pathway, transcribes several pro-inflammatory factors following the nuclear import of NF-κB, which can be inhibited by the cytoplasmic NF-κB inhibitor (IκB) [87, 88]. Research has demonstrated that STS exhibits the efficacy of suppressing inflammatory factors via deactivating the NF-κB pathway in I/R-damaged cardiac tissues of rats [89]. The anti-inflammatory effect of Tanshinones on protecting myocar-

dia and cardiomyocytes against CVDs is summarized in Table 3 and Figure 2.

3.1.4. Antihypertrophic Effect of Tanshinones on Myocardia and Cardiomyocytes.
As the cardiac response to increased hemodynamic load, cardiac hypertrophy is characterized by growing cardiac mass and cardiomyocyte hypertrophy. Cardiac hypertrophy is the compensatory process that keeps the heart muscle's ability to contract and lower the stress on ventricle walls. Pathological myocardial hypertrophy is one of the leading causes of CVD-associated morbidities and mortalities. It is one of the most significant sequelae following MI and is closely associated with the onset of chronic heart failure (CHF) [90].

Angiotensin II (Ang II) upregulates the MAPK and GATA binding protein 4 (GATA4) pathways, as well as the expression of insulin-like growth factor II (IGF-II) and its receptor (IGF-IIR). This helps promote the transcription of hypertrophy-related genes [91–93]. While estrogen receptor (ESR) plays a protective role against cardiomyocyte hypertrophy, usually being activated to reverse the changes of adverse factors mentioned above [94]. The study has shown that Tan IIA might activate ESR to inhibit the MAPK/GATA4 pathway. This would activate the NAD-dependent deacetylase Sirtuin-1 (SIRT1)/deacetylated heat

TABLE 2: The antiapoptosis and necroptosis effects of Tanshinones on protecting myocardia and cardiomyocytes against CVDs.

Tanshinones	In vivo/in vitro	Models	Effective doses	Related mechanisms	Refs.
Tan IIA	In vivo/in vitro	In vivo: MI rats established by left anterior descending branch (LAD) ligation; In vitro: H_2O_2-induced cellular damage in isolated cardiomyocytes of LAD-induced MI rats	In vivo: 10 mg/kg; In vitro: 10, 20, 30, 40 μM	In vivo: ↓ Infarct size, apoptosis rate, caspase 3, cyt c, apoptotic protease activating factor-1 (Apaf-1), BAX; ↑ Cardiac function, BCL-2; In vitro: ↓ Apoptosis rate, caspase 3, cyt c, Apaf-1, BAX, ROS, thiobarbituric acid reactive substances (TBARS), ATF4, IRE1α; ↑ Cell viability, BCL-2	[51]
Tan IIA	In vivo/in vitro	In vivo: Acute ethanol-induced myocardial damage in mice; In vitro: Acute ethanol-induced H9c2 cardiomyocyte injury	In vivo: 5, 10 mg/kg; In vitro: 3, 10 μM	In vivo: ↓ Apoptosis rate, PDCD4; ↑ Cardiac function, the PI3K/Akt pathway; In vitro: ↓ Apoptosis rate, PDCD4; ↑ The PI3K/Akt pathway	[52]
CTS	In vivo/in vitro	In vivo: DOX-induced myocardial damage in rats; In vitro: DOX-induced H9c2 cardiomyocyte injury	In vivo: 50 mg/kg; In vitro: 2, 5, 10 μM	In vivo: ↓ Collagen deposition, apoptosis rate, MDA, ROS, 14-3-3σ, p-JNK, BAX, Bim, Puma, cleaved-caspase 3/9, p53, nuclear-Foxo1; ↑ Cardiac function, surface area of cells, SOD, CAT, glutathione peroxidase (GSH-px), mitochondrial membrane potential, BCL-2, the PI3K/Akt pathway; In vitro: ↓ Apoptosis rate, ROS; ↑ Cell viability, surface area of cells, mitochondrial membrane potential	[59]
STS	In vivo/in vitro	In vivo: I/R-induced myocardial damage in rats; In vitro: H_2O_2-induced cellular damage in isolated cardiomyocytes of neonatal rats after administration	In vivo: 20 mg/kg; In vitro: Isolated cardiomyocytes of neonatal rats after administration	In vivo: ↓ Infarct size, apoptosis rate, DNA fragmentation, cyt c, ROS, caspase 3, Bim; ↑ Cardiac function, p-Akt, p-Foxo3a; In vitro: ↓ Apoptosis rate, Bim, caspase 3; ↑ p-Akt, p-Foxo3a	[60]
Tan IIA	In vitro	H_2O_2-induced H9c2 cardiomyocyte damage	0.3, 1, 3, 10 μM	↑ Cell viability, BCL-2, miRNA-133, the PI3K/Akt pathway	[61]
Tan IIA	In vitro	H_2O_2/DOX-induced H9c2 cardiomyocyte damage	5, 10, 15, 20, 25, 30 μM	↓ Apoptosis rate, cleaved-caspase 3/9; ↑ Cell viability, miRNA-133	[62]
Tan IIA	In vitro	ERS-induced apoptosis model in NRVMs established by Tunicamycin (Tm)	0.1 μM	↓ Apoptosis rate, caspase 3/12, GRP78, CHOP; ↑ miRNA-133	[50]
DHT	In vivo	I/R-induced myocardial damage in rats	1, 2, 4 mg/kg	↓ Infarct size, pathological injury of myocardial tissues, apoptosis rate, CK-MB, LDH, BAX, cleaved-caspase 3/9, 20-HETE, CHOP, GRP78; ↑ Cardiac function, BCL-2	[65]

TABLE 2: Continued.

Tanshinones	In vivo/in vitro	Models	Effective doses	Related mechanisms	Refs.
Tan I	In vivo/in vitro	*In vivo:* I/R-induced myocardial damage in rats *In vitro:* H9c2 cardiomyocytes treated with t-BHP to establish an oxidative stress-induced cellular damage model	*In vivo:* 10, 20 mg/kg *In vitro:* 0.125, 0.25, 0.5, 1, 2 μM	*In vivo:* ↓ Pathological injury of myocardial tissues, tumor necrosis factor-α (TNF-α), interleukin-6 (IL-6), p-RIP1, p-RIP3, p-MLKL *In vitro:* ↓ LDH, p-RIP1, p-RIP3, p-MLKL ↑ Cell viability	[41]
Tan IIA	In vivo/in vitro	*In vivo:* DOX-induced myocardial damage in mice *In vitro:* DOX-induced H9c2 cardiomyocyte damage	*In vivo:* 10 mg/kg *In vitro:* 0.5, 1 μM	*In vivo:* ↓ Pathological injury of myocardial tissues, apoptotic ratio, CK-MB, LDH, BAX, autophagosome and autolysosome accumulation, LC3-II, p62, p-mTOR, p-ULK1 ↑ Cardiac function, BCL-2, Cathepsin B, Beclin 1, LAMP1, nuclear-TFEB *In vitro:* ↓ Apoptotic rate, autophagosome and autolysosome accumulation, LC3-II, p62, p-mTOR, p-ULK1 ↑ Cell viability, Cathepsin B, Beclin 1, LAMP1, nuclear-TFEB	[78]

Table 3: The anti-inflammatory and antihypertrophic effects of Tanshinones on protecting myocardia and cardiomyocytes against CVDs.

Tanshinones	In vivo/in vitro	Models	Effective doses	Related mechanisms	Refs.
Tan IIA	In vivo	I/R-induced myocardial damage in rats	10, 20, 40 mg/kg	↓ Creatine kinase (CK), aspartate transaminase (AST), TNF-α, IL-6, iNOS, HMGB1	[85]
STS	In vivo	I/R-induced myocardial damage in rats	8 mg/kg	↓ Infarct size, CK-MB, LDH, AST, MDA, the NF-κB pathway ↑ Cardiac function, SOD, GSH-px, HO-1, IκB-α	[89]
STS	In vivo	MI rats established by LAD ligation	20.8 mg/kg	↓ Collagen deposition, pathological injury of myocardial tissues, HMGB1, TNF-α, interleukin-1β (IL-1β) ↑ Cardiac function	[86]
Tan IIA	In vitro	Ang II-induced hypertrophy in H9c2 cardiomyocyte	40 μM	↓ Atrial natriuretic peptide (ANP), brain natriuretic peptide (BNP), interleukin-8 (IL-8), calcineurin, NFATc3, Gαq, PKC-α, CaMKII, TNF-α, the NF-κB pathway, IGF-IIR, p-HSF1, GATA4, the MAPK pathway ↑ ESR, SIRT1	[95]
Tan IIA	In vitro	Ang II-induced hypertrophy in H9c2 cardiomyocyte	40 μM	↓ Apoptosis rate, cleaved-caspase 3/9, BAX, cyt c, matrix metalloprotein-9/2 (MMP-9/2), β-catenin, p-GATA4, NFATc3, IGF-IR, IGF-IIR, the MAPK pathway ↑ Tissue inhibitor of metalloproteinase (TIMP 1/2), ESR, the PI3K/Akt pathway	[96]
Tan IIA	In vivo	TAC-induced myocardial hypertrophy in rats	15 mg/kg	↓ Left ventricular posterior wall thickness (LVPWT), interventricular septal thickness (IVST), HW/BW, ratio of left ventricular weight/body weight (LVW/HW), apoptosis rate, caspase-3, MDA, TNF-α, IL-6, BAX ↑ SOD, BCL-2, SIRT1	[98]
Tan IIA	In vitro	Leu27 IGF-II-induced hypertrophy in H9c2 cardiomyocyte	10, 100 μM	↓ Surface area of cells, ANP, BNP, calcineurin, NFAT3 ↑ ESR, the PI3K/Akt pathway	[100]
Tan IIA	In vivo/in vitro	In vivo: TAC-induced myocardial hypertrophy in rats In vitro: Ang II-induced hypertrophy in H9c2 cardiomyocyte	In vivo: 2, 5, 10 mg/kg In vitro: 25, 50, 100 μM	In vivo: ↓ Pathological injury of myocardial tissues, LVPWT, IVST, HW/BW, LVW/HW, galectin-3 ↑ Cardiac function In vitro: ↓ Surface area of cells, ANP, BNP, β-MHC, ALKBH5, galectin-3 ↑ Cell viability, m6A, m6A modification of galectin-3	[102]
Tan IIA	In vitro	ISO-induced hypertrophy in NRVMs	10, 30, 100 μM	↓ Surface area of cells, ANP, BNP, β-MHC, calcineurin, NFATc3	[99]

Table 4: The anti-oxidative and anti-inflammatory effects of Tanshinones on macrophages against CVDs.

Tanshinones	In vivo/in vitro	Models	Effective doses	Related mechanisms	Refs.
Extracts of S. *miltiorrhiza* (Tan I, Tan IIA, DHT, CPT)	In vitro	H$_2$O$_2$-stimulated murine macrophage cell line RAW 264.7	1, 10, 50 μg/mL	↓ ROS ↑ Cell viability, HO-1, the Nrf2 pathway	[104]
DHT	In vitro	LPS-induced murine macrophage cell line RAW 264.7	20 μM	↓ NO, TNF-α, IL-6, iNOS, COX-2, ROS, the NF-κB pathway, the MAPKs (JNK1/2, p38 MAPK, ERK1/2) pathway, TLR4, p-IKK-α/β, p-IκB-α	[112]
CTS	In vivo/in vitro	In vivo: D-GalN-sensitized mice challenged by LPS In vitro: LPS-induced murine macrophage cell line RAW 264.7	In vivo: 20, 40 mg/kg In vitro: 12.5, 25, 50, 100 μM	In vivo: ↑ Survival rate In vitro: ↓ NO, iNOS, COX-2, the MAPK pathway, the NF-κB pathway, TLR4, CD14, TAK1 ↑ Cell viability	[113]
CTS	In vitro	LPS-induced murine macrophage cell line RAW 264.7	2.5, 5, 10 μM	↓ TNF-α, IL-6, the MAPKs (ERK1/2, p38 MAPK, JNK1/2) pathway, the NF-κB pathway ↑ Cell viability, IκB-α	[114]
DHT	In vivo/in vitro	In vivo: AS model established by HCD fed ApoE$^{-/-}$ mice In vitro: LPS-induced murine macrophage cell line RAW 264.7	In vivo: 25 mg/kg In vitro: 0.1, 0.5 μM	In vivo: ↓ Necrotic core area, plaque size, collagen/plaque area, ROS, MDA, RIP3, CD68 ↑ Plaque stability, SOD, GSH In vitro: ↓ COX2, iNOS, TNF-α, IL-6, p-PERK, CHOP, intracellular Ca^{2+} level, ROS, the RIP1/RIP3/MLKL pathway, TLR4, MyD88 ↑ Adenosine triphosphate (ATP), SOD	[109]
Tan IIA	In vivo	AS model established by HCD fed ApoE$^{-/-}$ mice	30 mg/kg	↓ Atherosclerotic lesion size, VCAM-1, ICAM-1, MMP-2/3/9, MCP-1, galectin-3, CD68, the RAGE pathway, the NF-κB pathway, p-IκB-α, the MAPKs (JNK1/2, ERK1/2, p38 MAPK) pathway ↑ Collagen content, macrophage content, SMC content, IκB-α	[111]
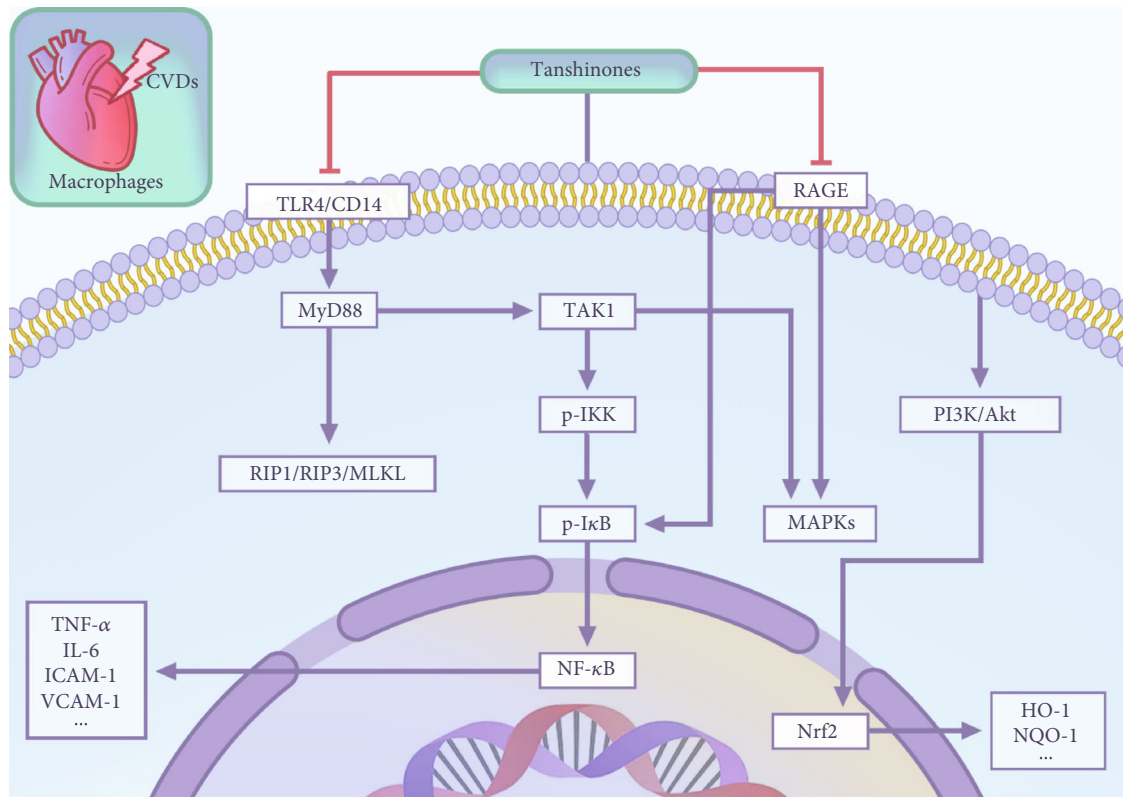
FIGURE 3: The pharmacological mechanism of Tanshinones on macrophages against CVDs.

shock factor-1 (deacetylated-HSF1) and decrease the phosphorylation modification of HSF1. Moreover, this would also inhibit HSF1 from binding to the promoter region to restrain the transcription of *IGF-IIR* [95, 96]. The reduction of *IGF-IIR* expression monitors the restrained contents of cardiac hypertrophy-associated hallmark proteins, such as calcineurin, Gαq, PKC-α, Ca^{2+}/calmodulin-dependent protein kinases II (CaMKII), and the nuclear translocation of nuclear factor of activated T cells (NFATc3), subsequently [95, 96]. Furthermore, ESR enhances the PI3K/Akt pathway, while Tan IIA might indirectly heighten the signal transduction of the PI3K/Akt pathway via upregulating ESR expression and then bring down the activation of calcineurin and NFATc3 induced by IGF-IIR [96]. Additionally, the transforming growth factor beta (TGF-β)/Smad pathway is a classical way of contributing to cardiomyocyte hypertrophy [97]. Tan IIA has been shown to inactivate the TGF-β/Smad pathway, resulting in remiss cardiomyocyte hypertrophy [96]. Exclusive of the Ang II-stimulated models *in vitro* mentioned above, similar effects of Tan IIA have been reported on cardiomyocytes stimulated by the analog of IGF-IIR that Leu27 IGF-II, or ISO [98–100]. For the *in vivo* experiment, the study used transverse aortic constriction (TAC) to induce myocardial remodeling in rats. The obtained results have demonstrated that Tan IIA could also repress cardiomyocyte hypertrophy by SIRT1 upregulation *in vivo*, consistent with the findings *in vitro* [98]. In addition, the pathological changes of cardiac hypertrophy can also be modulated by RNA methylation of N6-methyladenosine (m6A), which is involved in this pathway together with

RNA demethylase ALKBH5 (ALKBH5) [101]. Tan IIA was found to elevate intracellular m6A content and the m6A-modified form of galectin-3 in cardiomyocytes, which was realized by inhibiting ALKBH5 activation. Galectin-3 which had undergone the m6A modification and lost its initial stability exhibited lower expression, eventually inhibiting cardiac hypertrophy [102]. The antihypertrophic effect of Tanshinones on protecting myocardia and cardiomyocytes against CVDs is summarized in Table 3 and Figure 2.

3.2. The Pharmacological Mechanism of Tanshinones on Macrophages against CVDs

3.2.1. Antioxidative Effect of Tanshinones on Macrophages.
Oxidative stress in macrophages plays a crucial function in AS. Foam cells originating from macrophages trigger the AS process in response to various stimuli, including oxidation resulting from the accumulation and modification of lipoproteins in artery walls [103]. The study has found that the extracts from *S. miltiorrhiza* containing Tan I, Tan IIA, CPT, and DHT presented an upregulated function of the PI3K/Akt-mitogen-activated protein kinase kinase 1 (MEK1)-Nrf2 pathway, which transcribes a variety of antioxidative enzymes [104]. The antioxidative effect of Tanshinones on macrophages against CVDs is summarized in Table 4 and Figure 3.

3.2.2. Anti-inflammatory Effect of Tanshinones on Macrophages.
Accumulating evidence has demonstrated that inflammation exerts a vital function on lesion, destabilization, and rupture

Table 5: The antioxidative, anti-inflammatory, and angiogenic effects of Tanshinones on protecting endothelia against CVDs.

Tanshinones	In vivo/in vitro	Models	Effective doses	Related mechanisms	Refs.
Tan IIA	In vitro	HCAECs stimulated by ferroptosis inducers (Erastin or RSL3)	50 nM	↓ Cell death rate, LDH, ROS ↑ SOD1, NQO1, GSH, FTH1, Nrf2, SLC7A11	[117]
Tan IIA	In vitro	HUVECs subjected to cyclic strain	1, 3, 10 μM	↓ IL-8 ↑ HO-1, the PI3K/Akt pathway, the Nrf2 pathway	[118]
Tan IIA	In vitro	Oxidative endothelial cell injury induced by Acrolein	20, 30, 40 μg/mL	↓ Apoptosis rate, ROS, carbonylation, -SOH, p-p38 ↑ Cell viability, free sulfhydryl (-SH) activity, CSE, H_2S, p-VASP, p-CREB, Cx43	[123]
DHT	In vivo/in vitro	*In vivo:* AS model established by HCD fed ApoE$^{-/-}$ mice; *In vitro:* LPS-stimulated HUVECs	*In vivo:* 10, 25 mg/kg; *In vitro:* 10 nM	*In vivo:* ↓ Atherosclerotic plaque, necrotic core areas, total cholesterol (TC), triglyceride (TG), low-density lipoprotein cholesterol (LDL-C), MDA, LOX-1, NOX4, the NF-κB pathway; ↑ SOD, GSH; *In vitro:* ↓ ROS, H_2O_2, superoxide anion ($O_2^{\bullet-}$), ox-LDL endocytosis, human monocyte cell line (THP-1) adhesion to endothelial cells, LOX-1, NOX4, TLR4, MyD88, the NF-κB pathway	[126]
CTS	In vitro	ox-LDL-induced HUVECs	0.01, 0.05, 0.1, 0.5, 1 μM	↓ ICAM-1, VCAM-1, E-selectin, ROS, p-eNOS, THP-1 adhesion to endothelial cells, p-IKKβ, p-IκBα, the NF-κB pathway; ↑ Cell viability	[129]
Tan IIA	In vitro	TNF-α-stimulated HUVECs	1, 5, 10, 20 μM	↓ LDH, THP-1 adhesion to endothelial cells, VCAM-1, ICAM-1, E-selectin, fractalkine/CX3CL1, p-IκB-α, p-IKK-α/β, the NF-κB pathway	[127]
Tan IIA	In vitro	TNF-α-stimulated HUVECs	0.1, 1, 5, 10 μM	↓ THP-1 adhesion to endothelial cells, PTX3, VCAM-1, ICAM-1, THP-1, the NF-κB pathway, the MAPKs (p38 MAPK, ERK1/2, JNK1/2) pathway; ↑ Cell viability, IκB-α	[128]
CTS	In vitro	TNF-α-stimulated HUVECs	1, 2.5, 5, 10, 20 μM	↓ Endothelial permeability, THP-1 adhesion to endothelial cells, VCAM-1, ICAM-1, MCP-1; ↑ NO	[130]
Tan IIA	In vivo/in vitro	*In vivo:* MI mice established by LAD ligation; *In vitro:* HUVECs	*In vivo:* 50 mg/kg; *In vitro:* Not mentioned	*In vivo:* ↓ Infarction size, pathological injury of myocardial tissues, left ventricular end-systolic diameter (LVESD), left ventricular end-diastolic diameter (LVEDD); ↑ Cardiac function, VEGF, Ang-I; *In vitro:* ↓ miR-499-5p; ↑ PTEN	[135]
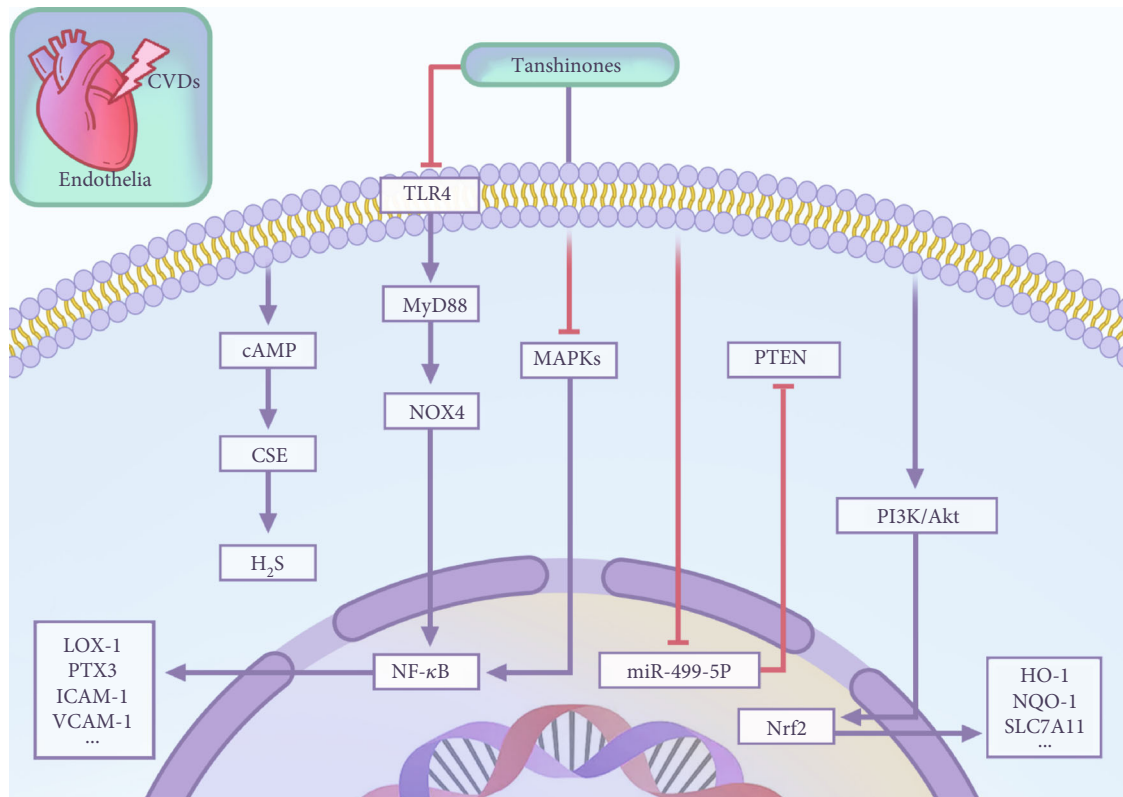
FIGURE 4: The pharmacological mechanism of Tanshinones for protecting endothelia against CVDs.

of atherosclerotic plaques composed of a lipid-rich necrotic core covered by a thin fibrous cap, predominantly involving SMCs, macrophages, structural collagen, and plaques infiltrated with inflammatory cells [105]. During the AS process, the release of many inflammatory cytokines, such as vascular cellular adhesion molecule-1 (VCAM-1), intercellular adhesion molecule-1 (ICAM-1), monocyte chemotactic protein-1 (MCP-1), and matrix metalloproteinase-2/3/9 (MMP-2/3/9), promotes the progression of plaque vulnerability [106, 107]. Inflammation has also been confirmed to play a crucial role in injury pathogenesis secondary to ischemia [108].

The NF-κB pathway regulates the release of inflammatory mediators such as NO, iNOS, TNF-α, IL-6, and cyclo-oxygenase (COX-2). The study found that DHT could significantly reduce these mediators by inactivating the NF-κB pathway, in an AS model of apolipoprotein-E-deficient (ApoE$^{-/-}$) mice fed a high cholesterol/high-fat diet (HCD/HFD) or lipopolysaccharide (LPS)-induced murine macrophage cell line RAW 264.7. As the upstream of NF-κB, DHT has been revealed that it could suppress Toll-like receptor 4 (TLR4) and myeloid differentiation factor 88 (MyD88). The downstream of the TLR4/MyD88 also contains the RIP1/RIP3/MLKL phosphorylation attributing to necroptosis, considered a highly proinflammatory pattern of cell death. Through deactivating the RIP1 pathway, DHT could relieve ERS performed as decreased pancreatic endoplasmic reticulum kinase (PERK), CHOP, and intracellular Ca^{2+} level, as well as mitigate oxidative stress [109]. Additionally, the receptor of advanced glycation end products (RAGE) pathway plays a critical role in the generation

of chemokines and adhesion molecules mentioned above, serving a pivotal role in the MAPKs and NF-κB pathway activation [106, 110]. The study has displayed that Tan IIA could restrain the RAGE pathway and its downstream pathways, the MAPK and NF-κB, to alleviate the erosion and thinning fibrous caps responsible for plaque instability [111]. Furthermore, DHT [112] and CTS [113, 114] could significantly suppress inflammatory mediators and ROS generation in LPS-induced macrophages *in vitro* or D-galactosamine- (D-GalN-) sensitized mice challenged by LPS *in vivo*. The mechanism has been found that DHT [112] and CTS [113, 114] inhibited TLR4 dimerization and CD14 expression that have the capacity of initiating the LPS-induced signaling cascades including TGF-β-activated kinase 1 (TAK1) phosphorylation. Downstream of TAK1, DHT [112] and CTS [113, 114] could also reduce phosphorylated IκB kinase (IKK)-α/β, phosphorylated IκB-α, NF-κB phosphorylation, and its nuclear translocation, as well as interrupt JNK1/2, ERK1/2, and p38 mitogen-activated protein kinase (p38 MAPK) phosphorylation. The anti-inflammatory effect of Tanshinones on macrophages against CVDs is summarized in Table 4 and Figure 3.

3.3. The Pharmacological Mechanism of Tanshinones for Protecting Endothelia against CVDs

3.3.1. Antioxidative Effect of Tanshinones on Endothelia.
It is widely accepted that endothelial dysfunction is a crucial risk factor for CVDs, including AS. The accumulation of reactive oxygen species (ROS) due to oxidative stress in the form of

TABLE 6: The vasodilative, antiproliferative, and antimigration effects of Tanshinones on SMCs against CVDs.

Tanshinones	In vivo/in vitro	Models	Effective doses	Related mechanisms	Refs.
Tan IIA	In vivo/ex vivo/in vitro	In vivo: SHRs Ex vivo: Aortic rings isolated from SHR, followed by precontracted with PE or KCl In vitro: A7r5 line of rat aortic SMCs precontracted with PE or KCl	In vivo: 20, 40, 60 mg/kg Ex vivo: 0.1, 1, 10 μM In vitro: 0.1, 1, 10 μM	In vivo: ↓ Systolic blood pressure (SBP) Ex vivo: ↓ Contraction force In vitro: ↓ [Ca^{2+}]i	[138]
Tan IIA	In vivo/in vitro	In vivo: Intimal hyperplasia model established by the right common carotid artery damaged by balloon dilatation in rats In vitro: Vascular SMCs in rat aorta cultured with 10% fetal bovine serum (FBS)	In vivo: 13.3, 40, 120 mg/kg In vitro: 0.1, 0.25, 0.5, 1 μg/mL	In vivo: ↓ Intimal thickening, intimal area, intimal cell proliferation ↑ Cell cycle in G$_0$/G$_1$ phase In vitro: ↓ Cell proliferation, p-ERK1/2, c-fos ↑ Cell cycle in G$_0$/G$_1$ phase	[140]
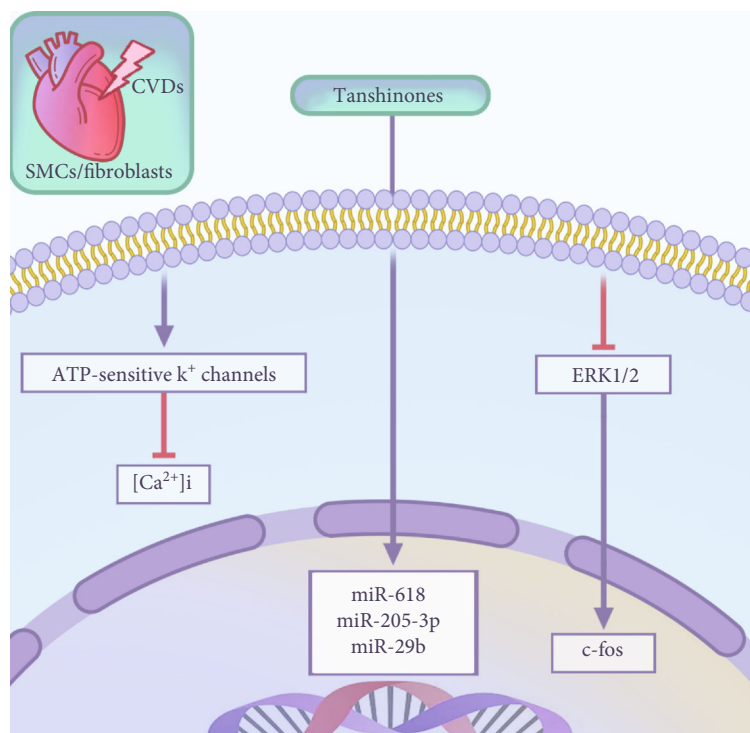
Figure 5: The pharmacological mechanism of Tanshinones on SMCs and fibroblasts against CVDs.

lipid peroxidation is the primary causative factor in endothelial dysfunction [115].

Lipid peroxidation-induced ferroptosis, characterized as the accumulation of iron and ROS, is closely related to endothelial cell injury and is involved in the pathogenesis and progression of AS [115, 116]. The report has approved that Tan IIA could enhance Nrf2 expression and its nuclear translocation to upregulate various antioxidative proteins including NQO-1 and solute carrier family 7 member 11 (SLC7A11). In this view, Tan IIA promoted ferritin heavy chain 1 (FTH1) expression as one of the components of the ferritin complex to preserve iron homeostasis and combat ferroptosis in human coronary artery endothelial cells (HCAECs) stimulated by ferroptosis inducers [117]. Besides, in human umbilical vein endothelial cells (HUVECs) subjected to cyclic strain, Tan IIA has also been reported that it could advance the Nrf2 pathway through the excitation of the PI3K/Akt pathway [118]. Additionally, endogenous hydrogen sulfide (H_2S), an essential gaseous mediator and potent antioxidant synthesized by H_2S-synthesizing enzymes, i.e., cystathionine γ-lyase (CSE), has beneficial effects such as vasodilation, cardioprotection, anti-inflammation, and antioxidation [119–122]. The study has confirmed that Tan IIA could promote the cyclic adenosine monophosphate (cAMP) pathway comprised of the phosphorylated level of protein kinase A (PKA) substrates, vasodilator-stimulated phosphoprotein (VASP), and cAMP-responsive element-binding protein (CREB), and CREB-controlled gene product, Cx43. By activating the CSE-H_2S pathway upregulated by the cAMP pathway, Tan IIA could overcome oxidative stress-induced damage, as demonstrated by decreased protein carbonylation

and sulfonic acid (SOH) production [123]. The antioxidative effect of Tanshinones on protecting endothelia against CVDs is summarized in Table 5 and Figure 4.

3.3.2. Anti-inflammatory Effect of Tanshinones on Endothelia. The structural and biochemical changes caused by an inflammatory response directed at the injury site can lead to severe cardiac remodeling and dysfunction, which can manifest clinically as HF [124]. Therefore, resisting excessive inflammation responses emerges as a critical strategy for cardioprotection. Proinflammatory cytokines are also the crucial pathogenic element bringing about endothelial dysfunction, which contributes to the initiation of AS [115, 125].

DHT has been shown to have impacts on the NF-κB pathway, thus inhibiting the expression of the lectin-like ox-LDL receptor-1 (LOX-1), oxidized-low-density lipoprotein (ox-LDL) endocytosis, and monocyte adhesion via weakening the TLR4/MyD88/NADPH oxidase 4 (NOX4) pathway [126]. Additionally, Tan IIA [127, 128] and CTS [129, 130] have also been recognized as inhibitors of the MAPKs (p38 MAPK, ERK1/2, and JNK1/2) and NF-κB pathway to abate the release of pentraxin 3 (PTX3) associated with endothelial dysfunction, chemokines represented by MCP-1, and adhesion molecules such as VCAM-1, ICAM-1, and fractalkine/CX3CL1, which urge monocyte adhesion to endothelial cells. The anti-inflammatory effect of Tanshinones on protecting endothelia against CVDs is summarized in Table 5 and Figure 4.

3.3.3. Angiogenic Effect of Tanshinones on Endothelia. Microvascular perfusion including angiogenesis in the infarction

TABLE 7: The antifibrotic effect of Tanshinones on fibroblasts against CVDs.

Tanshinones	In vivo/in vitro	Models	Effective doses	Related mechanisms	Refs.
Tan IIA	In vitro	TGF-β1-stimulated rat primary CFs after cultivated in serum-free DMEM	10 μM	↑ miR-205-3p ↓ Col1a1, Col3a1	[145]
Tan IIA	In vivo/in vitro	In vivo: HF rats induced by LAD ligation In vitro: Ang II-treated CFs	In vivo: 1.5 mg/kg In vitro: 10 μM	In vivo: ↓ LVESD, LVEDD, MDA, Col1, Col3, TGF-β, α-SMA, MMP2/9, NOX ↑ Cardiac function, left ventricular (LV) systolic pressure and the maximum of the first differentiation of LV pressure (LV ± dp/dt$_{max}$), SOD In vitro: ↓ MDA, Col1, Col3, TGF-β, α-SMA, MMP2/9, NOX ↑ SOD	[148]
Tan IIA	In vivo/in vitro	In vivo: AMI rats induced by LAD ligation In vitro: TGF-β1-induced CFs	In vivo: 5, 10, 15 mg/kg In vitro: 1, 10, 50 μM	In vivo: ↓ TGF-β1, Col1, Col3, α-SMA ↑ miR-29b In vitro: ↓ TGF-β1, Col1, Col3, α-SMA ↑ miR-29b	[146]
Tan IIA	In vivo/in vitro	In vivo: MI rats induced by LAD ligation In vitro: Ang II-treated CFs	In vivo: 5, 10, 15 mg/kg In vitro: 1, 10, 50 μM	In vivo: ↓ TGF-β1, Col1, Col3, α-SMA ↑ miR-618 In vitro: ↓ TGF-β1, Col1, Col3, α-SMA ↑ miR-618	[147]
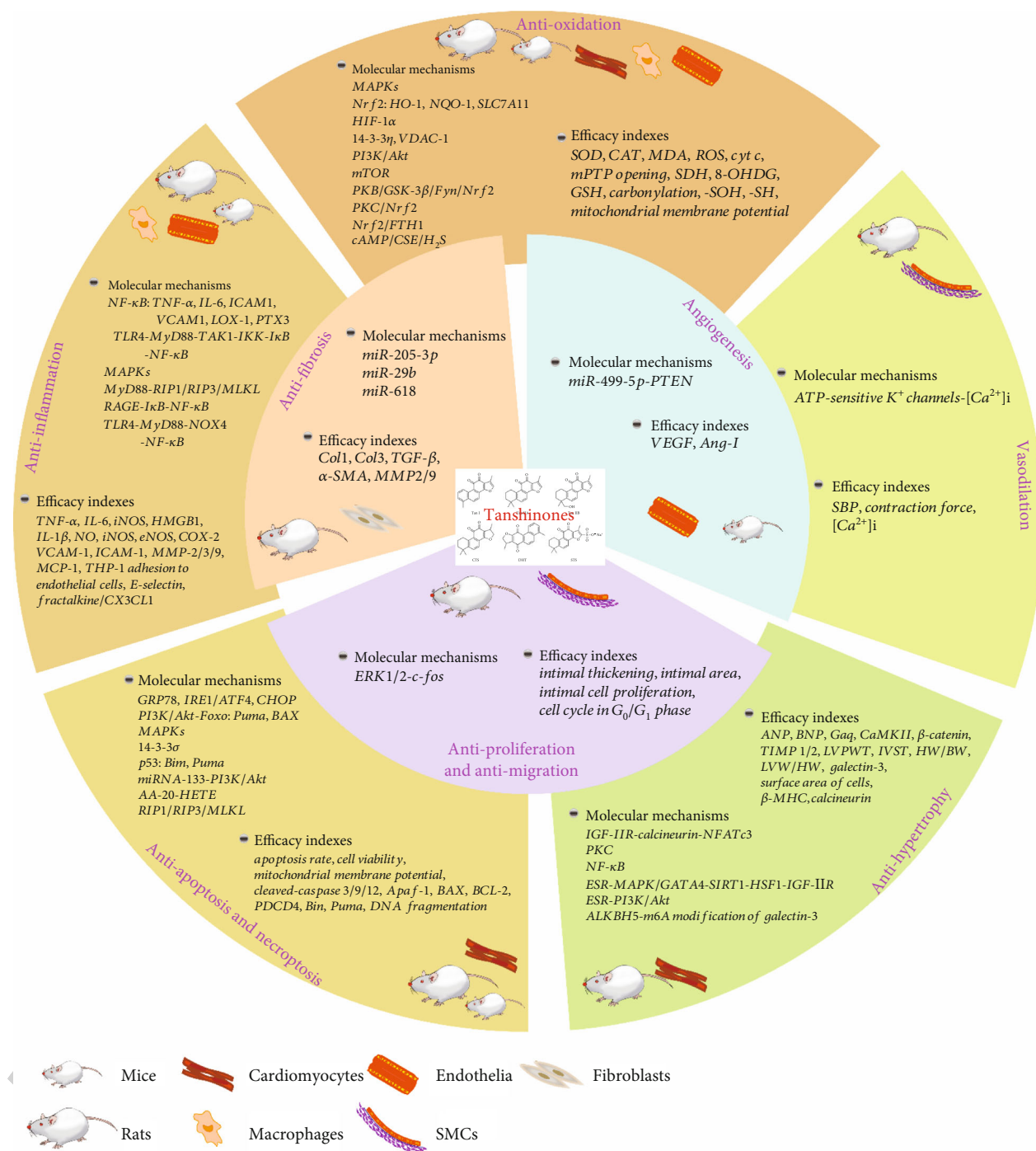
Figure 6: The summarized pharmacological activities and the underlying mechanisms of Tanshinones.

zone plays a vital role in the repair and regeneration of myocardia, after late-stage MI or cardiac I/R [131]. Angiogenesis, forming new blood vessels from preexisting vascular networks, is regulated by multiple stimulators and inhibitors [132]. After being stimulated by proangiogenic factors, including vascular endothelial growth factor (VEGF), endothelia play a crucial role in sprouting angiogenesis, along with the tightly controlled processes of cell migration and proliferation, sprout fusion, and lumen development [133, 134]. The

literature has reported that Tan IIA could upregulate phosphatase and tensin homolog (PTEN), the critical protein directing cell growth, survival, and proliferation, through downregulating miR-499-5p. This way, Tan IIA could reach the goal of revascularization in the infarct zone, attributed to its responsibility for the miR-499-5p/PTEN pathway [135]. The angiogenic effect of Tanshinones on protecting endothelia against CVDs is summarized in Table 5 and Figure 4.

3.4. The Pharmacological Mechanism of Tanshinones on SMCs against CVDs

3.4.1. Vasodilative Effect of Tanshinones on SMCs. Vascular SMCs constitute the majority of vascular wall tissues and maintain vascular tension. In a hypertensive state, the increased sensitivity of adenosine triphosphate (ATP)-sensitive K$^+$ channels results in an augmented relaxation as one of the compensatory mechanisms to maintain vasodilation when the endothelial function is undergoing a disordered condition. Activation of K$^+$ channels during the change in membrane potential leads to vasorelaxation and lowers the amount of intracellular calcium ([Ca^{2+}]i). The blockage of Ca^{2+} channels elicits vasodilatation, as the most common way to exert antihypertensive or vasodilative efficacies [136, 137]. The study has confirmed that Tan IIA could display vasodilative activity presented by decreasing contraction in phenylephrine (PE) or potassium chloride (KCl)-precontracted spontaneously hypertensive rats (SHRs), its aortic rings isolated from SHRs, or A7r5 line of rat aortic SMCs. The related mechanism enhanced ATP-sensitive K$^+$ channels and lowered [Ca^{2+}]i to stimulate vasodilatation [138]. The vasodilative effect of Tanshinones on SMCs against CVDs is summarized in Table 6 and Figure 5.

3.4.2. Antiproliferative and Antimigration Effects of Tanshinones on SMCs. Blood vessel performance is impacted by alterations in the size and function of vascular SMCs, which serve as the pathological basis for multiple CVDs. The proliferation and migration of vascular SMCs induced by growth factors such as platelet-derived growth factor (PDGF) and basic fibroblast growth factor (bFGF) are considered to play the central role in the development of intimal hyperplasia, the critical event in AS and restenosis after percutaneous coronary intervention (PCI) [139]. Tan IIA was found to be capable of suppressing vascular SMC proliferation and migration, manifested as a cell cycle block in the G$_0$/G$_1$ phase, by inhibiting ERK1/2 phosphorylation and c-fos expression both *in vivo* and *in vitro* [140]. The antiproliferative and antimigration effects of Tanshinones on SMCs against CVDs are summarized in Table 6 and Figure 5.

3.5. The Pharmacological Mechanism of Tanshinones on Fibroblasts against CVDs

3.5.1. Antifibrotic Effect of Tanshinones on Fibroblasts. The most significant consequence of MI is irreversible ventricular remodeling bound up with cardiomyocyte loss and invasion of fibrotic scar tissues in patients. Cardiac fibrosis can lead to HF and affect the patient's prognosis and quality of life [141, 142]. Active fibroblasts or myofibroblasts are the central cellular effectors in cardiac fibrosis, serving as the primary origin of matrix proteins [143]. As the vital regulator in the development of cardiac fibrosis, TGF-β1 displays a crucial function in enhancing extracellular matrix (ECM) deposition [143, 144]. Furthermore, Tan IIA has been suggested to reverse increased levels of collagen type 1 (Col1) and collagen type 3 (Col3), and growing α-smooth muscle actin (α-SMA) in TGF-β1 stimulated cardiac fibroblasts

(CFs) and acute myocardial infarction (AMI) or HF rats induced by ligating left anterior descending branch (LAD) of the coronary artery through upregulating miR-205-3p [145], miR-29b [146], or miR-618 [147]. It has also been found that Tan IIA was also able to mitigate oxidative stress in HF rats and Ang II-treated CFs to downregulate Col1/Col3, α-SMA, and MMP2/9 [148]. The antifibrotic effect of Tanshinones on fibroblasts against CVDs is summarized in Table 7 and Figure 5.

The pharmacological activities of Tanshinones are summarized in Figure 6.

4. Conclusion

Substantial studies have confirmed Tanshinones' potential therapeutic effects, particularly in CVDs, for their numerous pharmacological activities and clinical application. Researches have verified that Tanshinones exhibit extensive activities in multiple pathological links on various myocardial cell types. The therapeutic effects of Tanshinones against CVDs include anti-inflammation, antioxidative stress, antiapoptosis, antinecroptosis, antihypertrophy, vasodilation, angiogenesis, combat against proliferation and migration of SMCs, as well as antimyocardial fibrosis and ventricular remodeling, in myocardial tissues and cardiomyocytes, macrophages, endothelial cells, SMCs, and fibroblasts. However, the mechanism by which Tanshinones exert their therapeutic influence on CVDs is complicated, and some therapeutic effects that may involve a combination of multiple pathways are still unclear. In this view, further studies are needed to determine the extensive mechanisms through which Tanshinones exert their therapeutic properties on CVDs.

Data Availability

The data used to support the findings of this study are included within the supplementary information file.

Conflicts of Interest

The authors declare that they have no conflict of interest.

Authors' Contributions

Ye Yang, Mingyan Shao, and Wenkun Cheng performed literature searches and article writing. Junkai Yao and Lin Ma conducted the data sorting and supervision. Yong Wang and Wei Wang designed and funded the research. All authors agree to be accountable for the content of the work. Ye Yang, Mingyan Shao, and Wenkun Cheng contributed equally to this manuscript.

Acknowledgments

Supplementary Materials

Supplementary 1. Graphical summary. The pharmacological effects of Tanshinones and their underlying mechanisms for alleviating CVDs. Supplementary 2. Table S1. The chemical and physical properties of representative Tanshinones. (*Supplementary Materials*)

References

[1] C. W. Tsao, A. W. Aday, Z. I. Almarzooq et al., "Heart Disease and Stroke Statistics-2022 Update: a report from the American Heart Association," *Circulation*, vol. 145, no. 8, pp. e153–e639, 2022.

[2] K. G. Hayman, D. Sharma, R. D. Wardlow, and S. Singh, "Burden of cardiovascular morbidity and mortality following humanitarian emergencies: a systematic literature review," *Prehospital and Disaster Medicine*, vol. 30, no. 1, pp. 80–88, 2015.

[3] I. Hetherington and H. Totary Jain, "Anti-atherosclerotic therapies: milestones, challenges, and emerging innovations," *Molecular Therapy : the Journal of the American Society of Gene Therapy*, vol. 30, no. 10, pp. 3106–3117, 2022.

[4] P. Ponikowski, A. A. Voors, S. D. Anker et al., "2016 ESC Guidelines for the diagnosis and treatment of acute and chronic heart failure: the task force for the diagnosis and treatment of acute and chronic heart failure of the European Society of Cardiology (ESC)developed with the special contribution of the Heart Failure Association (HFA) of the ESC," *European Heart Journal*, vol. 37, no. 27, pp. 2129–2200, 2016.

[5] L. Køber, C. Torp-Pedersen, J. E. Carlsen et al., "A clinical trial of the angiotensin-converting-enzyme inhibitor trandolapril in patients with left ventricular dysfunction after myocardial Infarction," *The New England Journal of Medicine*, vol. 333, no. 25, pp. 1670–1676, 1995.

[6] R. Collins, C. Reith, J. Emberson et al., "Interpretation of the evidence for the efficacy and safety of statin therapy," *The Lancet*, vol. 388, no. 10059, pp. 2532–2561, 2016.

[7] Y. Wang, H. Zhang, Z. Wang et al., "Blocking the death checkpoint protein TRAIL improves cardiac function after myocardial infarction in monkeys, pigs, and rats," *Science Translational Medicine*, vol. 12, no. 540, 2020.

[8] N. Raja Khan, E. Stener Victorin, X. K. Wu, and R. S. Legro, "The physiological basis of complementary and alternative medicines for polycystic ovary syndrome," *American Journal of Physiology Endocrinology and Metabolism*, vol. 301, no. 1, pp. E1–E10, 2011.

[9] Q. Zhang, J. Liu, H. Duan, R. Li, W. Peng, and C. Wu, "Activation of Nrf2/HO-1 signaling: An important molecular mechanism of herbal medicine in the treatment of atherosclerosis *via* the protection of vascular endothelial cells from oxidative stress," *Journal of Advanced Research*, vol. 34, pp. 43–63, 2021.

[10] Y. Long, D. Li, S. Yu et al., "Natural essential oils: A promising strategy for treating cardio- cerebrovascular diseases," *Journal of Ethnopharmacology*, vol. 297, article 115421, 2022.

[11] X. Li, L. Li, W. Lei et al., "Traditional Chinese medicine as a therapeutic option for cardiac fibrosis: Pharmacology and mechanisms," *Biomedicine & Pharmacotherapy*, vol. 142, article 111979, 2021.

[12] Q. Jia, R. Zhu, Y. Tian et al., "*Salvia miltiorrhiza* in diabetes: A review of its pharmacology, phytochemistry, and safety," *Phytomedicine: International Journal of Phytotherapy and Phytopharmacology*, vol. 58, article 152871, 2019.

[13] K. P. Yan, Y. Guo, Z. Xing et al., "Dan-Shen-Yin protects the heart against inflammation and oxidative stress induced by acute ischemic myocardial injury in rats," *Experimental and Therapeutic Medicine*, vol. 3, no. 2, pp. 314–318, 2012.

[14] N. Aa, J. H. Guo, B. Cao et al., "Compound danshen dripping pills normalize a reprogrammed metabolism of myocardial ischemia rats to interpret its time-dependent efficacy in clinic trials: a metabolomic study," *Metabolomics: Official Journal of the Metabolomic Society*, vol. 15, no. 10, p. 128, 2019.

[15] S. Gao, Z. Liu, H. Li, P. J. Little, P. Liu, and S. Xu, "Cardiovascular actions and therapeutic potential of tanshinone IIA," *Atherosclerosis*, vol. 220, no. 1, pp. 3–10, 2012.

[16] Y. Zhang, P. Jiang, M. Ye, S.-H. Kim, C. Jiang, and J. Lü, "Tanshinones: sources, pharmacokinetics and anti-cancer activities," *International Journal of Molecular Sciences*, vol. 13, no. 12, pp. 13621–13666, 2012.

[17] Y. Cai, W. Zhang, Z. Chen, Z. Shi, C. He, and M. Chen, "Recent insights into the biological activities and drug delivery systems of tanshinones," *International Journal of Nanomedicine*, vol. 11, pp. 121–130, 2016.

[18] T. O. Cheng, "Danshen: a popular chinese cardiac herbal drug," *Journal of the American College of Cardiology*, vol. 47, no. 7, 2006.

[19] X. X. Zhang, Y. F. Cao, L. X. Wang, X. L. Yuan, and Z. Z. Fang, "Inhibitory effects of tanshinones towards the catalytic activity of UDP-glucuronosyltransferases (UGTs)," *Pharmaceutical Biology*, vol. 55, no. 1, pp. 1703–1709, 2017.

[20] X. H. Ma, Y. Ma, J. F. Tang et al., "The biosynthetic pathways of tanshinones and phenolic acids in Salvia miltiorrhiza," *Molecules*, vol. 20, no. 9, pp. 16235–16254, 2015.

[21] X. Li, Y. Lou, J. J. Shang, H. X. Liu, J. P. Chen, and H. W. Zhou, "Traditional Chinese medicine injections with activating blood circulation, equivalent effect of anticoagulation or antiplatelet, for acute myocardial infarction," *Medicine*, vol. 101, no. 24, article e29089, 2022.

[22] M. L. Yu, S. M. Li, X. Gao, J. G. Li, H. Xu, and K. J. Chen, "Sodium tanshinone II A sulfonate for coronary heart disease: a systematic review of randomized controlled trials," *Chinese Journal of Integrative Medicine*, vol. 26, no. 3, pp. 219–226, 2020.

[23] Z. M. Li, S. W. Xu, and P. Q. Liu, "*Salvia miltiorrhiza* Burge (Danshen): a golden herbal medicine in cardiovascular therapeutics," *Acta Pharmacologica Sinica*, vol. 39, no. 5, pp. 802–824, 2018.

[24] X.-D. MEIm, C. Yan-Feng, C. Yan-Yun et al., "Danshen: a phytochemical and pharmacological overview," *Chinese Journal of Natural Medicines*, vol. 17, no. 1, pp. 59–80, 2019.

[25] Y. Lu, Y. Yan, and X. Liu, "Effects of alprostadil combined with tanshinone IIa injection on microcirculation disorder, outcomes, and cardiac function in AMI patients after PCI," *Annals of Palliative Medicine*, vol. 10, no. 1, 2021.

[26] S. Mao, L. Wang, X. Zhao et al., "Efficacy of sodium tanshinone IIA sulfonate in patients with non-ST elevation acute coronary syndrome undergoing percutaneous coronary intervention: results from a multicentre, controlled, randomized trial," *Cardiovascular Drugs and Therapy*, vol. 35, no. 2, pp. 321–329, 2021.

[27] S. Kim, J. Chen, T. Cheng et al., "PubChem in 2021: new data content and improved web interfaces," *Nucleic Acids Research*, vol. 49, no. D1, pp. D1388–D1395, 2021.

[28] X. H. Tian and J. H. Wu, "Tanshinone derivatives: a patent review (January 2006- September 2012)," *Expert Opinion On Therapeutic Patents*, vol. 23, no. 1, pp. 19–29, 2013.

[29] C. Y. Su, Q. L. Ming, K. Rahman, T. Han, and L. P. Qin, "*Salvia miltiorrhiza* : Traditional medicinal uses, chemistry, and pharmacology," *Chinese Journal of Natural Medicines*, vol. 13, no. 3, pp. 163–182, 2015.

[30] K. Chen and J. F. Keaney, "Evolving concepts of oxidative stress and reactive oxygen species in cardiovascular disease," *Current Atherosclerosis Reports*, vol. 14, no. 5, pp. 476–483, 2012.

[31] K. Raedschelders, D. M. Ansley, and D. D. Y. Chen, "The cellular and molecular origin of reactive oxygen species generation during myocardial ischemia and reperfusion," *Pharmacology & Therapeutics*, vol. 133, no. 2, pp. 230–255, 2012.

[32] J. Fujii, T. Homma, and T. Osaki, "Superoxide radicals in the execution of cell death," *Antioxidants*, vol. 11, no. 3, 2022.

[33] Q. M. Chen, "Nrf2 for cardiac protection: pharmacological options against oxidative stress," *Trends In Pharmacological Sciences*, vol. 42, no. 9, pp. 729–744, 2021.

[34] Y. T. Wu, L. P. Xie, Y. Hua et al., "Tanshinone I inhibits oxidative stress-induced cardiomyocyte injury by modulating Nrf2 signaling," *Frontiers In Pharmacology*, vol. 12, article 644116, 2021.

[35] Y. Tan, T. Ichikawa, J. Li et al., "Diabetic downregulation of Nrf2 activity via ERK contributes to oxidative stress-induced insulin resistance in cardiac cells in vitro and in vivo," *Diabetes*, vol. 60, no. 2, pp. 625–633, 2011.

[36] A. K. Verma, A. Yadav, J. Dewangan et al., "Isoniazid prevents Nrf2 translocation by inhibiting ERK1 phosphorylation and induces oxidative stress and apoptosis," *Redox Biology*, vol. 6, pp. 80–92, 2015.

[37] L. Jiang, H. Zeng, L. Ni et al., "HIF-1α preconditioning potentiates antioxidant activity in ischemic injury: the role of sequential administration of dihydrotanshinone I and protocatechuic aldehyde in cardioprotection," *Antioxidants & Redox Signaling*, vol. 31, no. 3, pp. 227–242, 2019.

[38] N. C. Weber, O. Toma, J. I. Wolter et al., "The noble gas xenon induces pharmacological preconditioning in the rat heart in vivo via induction of PKC-epsilon and p38 MAPK," *British Journal of Pharmacology*, vol. 144, no. 1, pp. 123–132, 2005.

[39] H. Konishi, E. Yamauchi, H. Taniguchi et al., "Phosphorylation sites of protein kinase C delta in H2O2-treated cells and its activation by tyrosine kinase in vitro," *Proceedings of the National Academy of Sciences of the United States of America*, vol. 98, no. 12, pp. 6587–6592, 2001.

[40] H. Zeng, L. Wang, J. Zhang et al., "Activated PKB/GSK-3β synergizes with PKC- δ signaling in attenuating myocardial ischemia/reperfusion injury *via* potentiation of NRF2 activity: Therapeutic efficacy of dihydrotanshinone-I," *Acta Pharmaceutica Sinica B*, vol. 11, no. 1, pp. 71–88, 2021.

[41] Y. Zhuo, R. Yuan, X. Chen et al., "Tanshinone I exerts cardiovascular protective effects in vivo and in vitro through inhibiting necroptosis via Akt/Nrf2 signaling pathway," *Chinese Medicine*, vol. 16, no. 1, p. 48, 2021.

[42] C. Gu, Q. Zhang, Y. Li et al., "The PI3K/AKT pathway-the potential key mechanisms of traditional Chinese medicine for stroke," *Frontiers in Medicine*, vol. 9, article 900809, 2022.

[43] Y. Zhang, L. Wei, D. Sun et al., "Tanshinone IIA pretreatment protects myocardium against ischaemia/reperfusion injury through the phosphatidylinositol 3-kinase/Akt-dependent pathway in diabetic rats," *Diabetes, Obesity & Metabolism*, vol. 12, no. 4, pp. 316–322, 2010.

[44] Q. Li, L. Shen, Z. Wang, H. P. Jiang, and L. X. Liu, "Tanshinone IIA protects against myocardial ischemia reperfusion injury by activating the PI3K/Akt/mTOR signaling pathway," *Biomedicine & Pharmacotherapy*, vol. 84, pp. 106–114, 2016.

[45] Z. Zhang, H. He, Y. Qiao et al., "Tanshinone IIA pretreatment protects H9c2 cells against anoxia/reoxygenation injury: involvement of the translocation of Bcl-2 to mitochondria mediated by 14-3-3η," *Oxidative Medicine and Cellular Longevity*, vol. 2018, Article ID 3583921, 13 pages, 2018.

[46] C. Niermann, S. Gorressen, M. Klier et al., "Oligophrenin1 protects mice against myocardial ischemia and reperfusion injury by modulating inflammation and myocardial apoptosis," *Cellular Signalling*, vol. 28, no. 8, pp. 967–978, 2016.

[47] C. X. Guo, X. Jiang, X. J. Zeng et al., "Soluble receptor for advanced glycation end-products protects against ischemia/reperfusion-induced myocardial apoptosis via regulating the ubiquitin proteasome system," *Free Radical Biology & Medicine*, vol. 94, pp. 17–26, 2016.

[48] S. Elmore, "Apoptosis: a review of programmed cell death," *Toxicologic Pathology*, vol. 35, no. 4, pp. 495–516, 2007.

[49] H. Hu, M. Tian, C. Ding, and S. Yu, "The C/EBP homologous protein (CHOP) transcription factor functions in endoplasmic reticulum stress-induced apoptosis and microbial infection," *Frontiers in Immunology*, vol. 9, p. 3083, 2019.

[50] J. Feng, S. Li, and H. Chen, "Tanshinone IIA ameliorates apoptosis of cardiomyocytes induced by endoplasmic reticulum stress," *Experimental Biology and Medicine*, vol. 241, no. 18, pp. 2042–2048, 2016.

[51] Y. Fang, C. Duan, S. Chen et al., "Tanshinone-IIA inhibits myocardial infarct via decreasing of the mitochondrial apoptotic signaling pathway in myocardiocytes," *International Journal of Molecular Medicine*, vol. 48, no. 2, 2021.

[52] H. Deng, B. Yu, and Y. Li, "Tanshinone IIA alleviates acute ethanol-induced myocardial apoptosis mainly through inhibiting the expression of PDCD4 and activating the PI3K/Akt pathway," *Phytotherapy Research: PTR*, vol. 35, no. 8, pp. 4309–4323, 2021.

[53] S. Fulda and K. M. Debatin, "Extrinsic versus intrinsic apoptosis pathways in anticancer chemotherapy," *Oncogene*, vol. 25, no. 34, pp. 4798–4811, 2006.

[54] K. H. Khoo, K. K. Hoe, C. S. Verma, and D. P. Lane, "Drugging the p53 pathway: understanding the route to clinical efficacy," *Nature Reviews Drug Discovery*, vol. 13, no. 3, pp. 217–236, 2014.

[55] K. Nakano and K. H. Vousden, "*PUMA*, a Novel Proapoptotic Gene, Is Induced by p53," *Molecular Cell*, vol. 7, no. 3, pp. 683–694, 2001.

[56] P. Wang, Y. C. Lu, J. Wang et al., "Type 2 diabetes promotes cell centrosome amplification via AKT-ROS-dependent signalling of ROCK1 and 14-3-3σ," *Cellular Physiology and Biochemistry: International Journal of Experimental Cellular Physiology, Biochemistry, and Pharmacology*, vol. 47, no. 1, pp. 356–367, 2018.

[57] J. Fan, G. Xu, D. J. Nagel, Z. Hua, N. Zhang, and G. Yin, "A model of ischemia and reperfusion increases JNK activity, inhibits the association of BAD and 14-3-3, and induces apoptosis of rabbit spinal neurocytes," *Neuroscience Letters*, vol. 473, no. 3, pp. 196–201, 2010.

[58] B. Y. Li, Y. Y. Guo, G. Xiao, L. Guo, and Q. Q. Tang, "SERPINA3C ameliorates adipose tissue inflammation through the Cathepsin G/Integrin/AKT pathway," *Molecular Metabolism*, vol. 61, article 101500, 2022.

[59] L. Li, B. Wu, Q. Zhao et al., "Attenuation of doxorubicin-induced cardiotoxicity by cryptotanshinone detected through association analysis of transcriptomic profiling and KEGG pathway," *Aging*, vol. 12, no. 10, pp. 9585–9603, 2020.

[60] M. Q. Zhang, Y. L. Zheng, H. Chen et al., "Sodium tanshinone IIA sulfonate protects rat myocardium against ischemia-reperfusion injury via activation of PI3K/Akt/FOXO3A/Bim pathway," *Acta Pharmacologica Sinica*, vol. 34, no. 11, pp. 1386–1396, 2013.

[61] Y. Gu, Z. Liang, H. Wang et al., "Tanshinone IIA protects H9c2 cells from oxidative stress-induced cell death via microRNA-133 upregulation and Akt activation," *Experimental and Therapeutic Medicine*, vol. 12, no. 2, pp. 1147–1152, 2016.

[62] T. Song, Y. Yao, T. Wang, H. Huang, and H. Xia, "Tanshinone IIA ameliorates apoptosis of myocardiocytes by up-regulation of miR-133 and suppression of Caspase-9," *European Journal of Pharmacology*, vol. 815, pp. 343–350, 2017.

[63] M. Sato, U. Yokoyama, T. Fujita, S. Okumura, and Y. Ishikawa, "The roles of cytochrome p450 in ischemic heart disease," *Current Drug Metabolism*, vol. 12, no. 6, pp. 526–532, 2011.

[64] V. Nilakantan, C. Maenpaa, G. Jia, R. J. Roman, and F. Park, "20-HETE-mediated cytotoxicity and apoptosis in ischemic kidney epithelial cells," *American Journal of Physiology Renal Physiology*, vol. 294, no. 3, pp. F562–F570, 2008.

[65] Y. Wei, M. Xu, Y. Ren et al., "The cardioprotection of dihydrotanshinone I against myocardial ischemia-reperfusion injury via inhibition of arachidonic acid ω-hydroxylase," *Canadian Journal of Physiology and Pharmacology*, vol. 94, no. 12, pp. 1267–1275, 2016.

[66] G. He, Y. Ma, Y. Zhu et al., "Cross talk between autophagy and apoptosis contributes to ZnO nanoparticle-induced human osteosarcoma cell death," *Advanced Healthcare Materials*, vol. 7, no. 17, article e1800332, 2018.

[67] J. Liu, Z.-N. Guo, X.-L. Yan et al., "Crosstalk between autophagy and ferroptosis and its putative role in ischemic stroke," *Frontiers In Cellular Neuroscience*, vol. 14, article 577403, 2020.

[68] C. Kraft, M. Peter, and K. Hofmann, "Selective autophagy: ubiquitin-mediated recognition and beyond," *Nature Cell Biology*, vol. 12, no. 9, pp. 836–841, 2010.

[69] T. D. Evans, I. Sergin, X. Zhang, and B. Razani, "Target acquired: selective autophagy in cardiometabolic disease," *Science Signaling*, vol. 10, no. 468, 2017.

[70] J. J. Bartlett, P. C. Trivedi, and T. Pulinilkunnil, "Autophagic dysregulation in doxorubicin cardiomyopathy," *Journal of Molecular and Cellular Cardiology*, vol. 104, pp. 1–8, 2017.

[71] D. L. Li, Z. V. Wang, G. Ding et al., "Doxorubicin blocks cardiomyocyte autophagic flux by inhibiting lysosome acidification," *Circulation*, vol. 133, no. 17, pp. 1668–1687, 2016.

[72] X. Liu, Y. Li, X. Wang et al., "The BEACH-containing protein WDR81 coordinates p62 and LC3C to promote aggrephagy," *The Journal of Cell Biology*, vol. 216, no. 5, pp. 1301–1320, 2017.

[73] V. Rogov, V. Dötsch, T. Johansen, and V. Kirkin, "Interactions between autophagy receptors and ubiquitin-like proteins form the molecular basis for selective autophagy," *Molecular Cell*, vol. 53, no. 2, pp. 167–178, 2014.

[74] A. U. Gurkar, K. Chu, L. Raj et al., "Identification of ROCK1 kinase as a critical regulator of Beclin1-mediated autophagy during metabolic stress," *Nature Communications*, vol. 4, no. 1, p. 2189, 2013.

[75] A. M. Orogo and Å. B. Gustafsson, "Therapeutic targeting of autophagy: potential and concerns in treating cardiovascular disease," *Circulation Research*, vol. 116, no. 3, pp. 489–503, 2015.

[76] J. A. Martina, Y. Chen, M. Gucek, and R. Puertollano, "MTORC1 functions as a transcriptional regulator of autophagy by preventing nuclear transport of TFEB," *Autophagy*, vol. 8, no. 6, pp. 903–914, 2012.

[77] J. F. Moruno-Manchon, N.-E. Uzor, S. R. Kesler et al., "TFEB ameliorates the impairment of the autophagy-lysosome pathway in neurons induced by doxorubicin," *Aging*, vol. 8, no. 12, pp. 3507–3519, 2016.

[78] X. Wang, C. Li, Q. Wang et al., "Tanshinone IIA restores dynamic balance of autophagosome/autolysosome in doxorubicin-induced cardiotoxicity via targeting Beclin1/LAMP1," *Cancers*, vol. 11, no. 7, p. 910, 2019.

[79] Z. Wang, P. Zhang, Q. Wang et al., "Protective effects of Ginkgo Biloba dropping pills against liver ischemia/reperfusion injury in mice," *Chinese Medicine*, vol. 15, no. 1, p. 122, 2020.

[80] J. Yang, F. Zhang, H. Shi et al., "Neutrophil-derived advanced glycation end products-Nε-(carboxymethyl) lysine promotes RIP3-mediated myocardial necroptosis via RAGE and exacerbates myocardial ischemia/reperfusion injury," *FASEB Journal*, vol. 33, no. 12, pp. 14410–14422, 2019.

[81] J. Zhang, P. Yu, F. Hua et al., "Sevoflurane postconditioning reduces myocardial ischemia reperfusion injury-induced necroptosis by up-regulation of OGT-mediated O-GlcNAcylated RIPK3," *Aging*, vol. 12, no. 24, pp. 25452–25468, 2020.

[82] A. C. Manetti, A. Maiese, M. D. Paolo et al., "MicroRNAs and sepsis-induced cardiac dysfunction: a systematic review," *International Journal of Molecular Sciences*, vol. 22, no. 1, p. 321, 2021.

[83] M. Magna and D. S. Pisetsky, "The role of HMGB1 in the pathogenesis of inflammatory and autoimmune diseases," *Molecular Medicine*, vol. 20, no. 1, pp. 138–146, 2014.

[84] D. Ghosh, A. Singh, A. Kumar, and N. Sinha, "Regulation of inducible gene expression by the transcription factor NF-κB," *Immunologic Research*, vol. 19, no. 2-3, pp. 183–190, 1999.

[85] H. Hu, C. Zhai, G. Qian et al., "Protective effects of tanshinone IIA on myocardial ischemia reperfusion injury by reducing oxidative stress, HMGB1 expression, and inflammatory reaction," *Pharmaceutical Biology*, vol. 53, no. 12, pp. 1752–1758, 2015.

[86] B. Zhang, P. Yu, E. Su et al., "Sodium tanshinone IIA sulfonate improves adverse ventricular remodeling post-MI by reducing myocardial necrosis, modulating inflammation,

and promoting angiogenesis," *Current Pharmaceutical Design*, vol. 28, no. 9, pp. 751–759, 2022.

[87] Z. Luo, M. Tian, G. Yang et al., "Hypoxia signaling in human health and diseases: implications and prospects for therapeutics," *Signal Transduction and Targeted Therapy*, vol. 7, no. 1, p. 218, 2022.

[88] S. Shahbazi and T. Zakerali, "The inhibitory role of benzodioxole-piperamide on the phosphorylation process as an NF-Kappa B silencer," *Biomedicine & Pharmacotherapy*, vol. 145, article 112471, 2022.

[89] B. Wei, W. W. Li, J. Ji, Q. H. Hu, and H. Ji, "The cardioprotective effect of sodium tanshinone IIA sulfonate and the optimizing of therapeutic time window in myocardial ischemia/reperfusion injury in rats," *Atherosclerosis*, vol. 235, no. 2, pp. 318–327, 2014.

[90] J. Silva and P. A. da Costa Martins, "Non-coding RNAs in the therapeutic landscape of pathological cardiac hypertrophy," *Cells*, vol. 11, no. 11, p. 1805, 2022.

[91] H. Zhou, Y. Yuan, Y. Liu et al., "Icariin attenuates angiotensin II-induced hypertrophy and apoptosis in H9c2 cardiomyocytes by inhibiting reactive oxygen species-dependent JNK and p38 pathways," *Experimental and Therapeutic Medicine*, vol. 7, no. 5, pp. 1116–1122, 2014.

[92] J. H. van Berlo, M. Maillet, and J. D. Molkentin, "Signaling effectors underlying pathologic growth and remodeling of the heart," *The Journal of Clinical Investigation*, vol. 123, no. 1, pp. 37–45, 2013.

[93] C. H. Chu, B. S. Tzang, L. M. Chen et al., "IGF-II/mannose-6-phosphate receptor signaling induced cell hypertrophy and atrial natriuretic peptide/BNP expression via Galphaq interaction and protein kinase C-alpha/CaMKII activation in H9c2 cardiomyoblast cells," *The Journal of Endocrinology*, vol. 197, no. 2, pp. 381–390, 2008.

[94] C. J. Liu, J. F. Lo, C. H. Kuo et al., "Akt mediates 17beta-estradiol and/or estrogen receptor-alpha inhibition of LPS-induced tumor necresis factor-alpha expression and myocardial cell apoptosis by suppressing the JNK1/2-NFkappaB pathway," *Journal of Cellular and Molecular Medicine*, vol. 13, no. 9B, pp. 3655–3667, 2009.

[95] Y. F. Chen, N. H. Lee, P. Y. Pai et al., "Tanshinone-induced ERs suppresses IGFII activation to alleviate Ang II-mediated cardiac hypertrophy," *Journal of Receptor and Signal Transduction Research*, vol. 37, no. 5, pp. 493–499, 2017.

[96] Y. F. Chen, C. H. Day, N. H. Lee et al., "Tanshinone IIA inhibits β-catenin nuclear translocation and IGF-2R activation via estrogen receptors to suppress angiotensin II-induced H9c2 cardiomyoblast cell apoptosis," *International Journal of Medical Sciences*, vol. 14, no. 12, pp. 1284–1291, 2017.

[97] Y. Li, K. Aase, H. Li, G. von Euler, and U. Eriksson, "Isoform-specific expression of VEGF-B in normal tissues and tumors," *Growth Factors*, vol. 19, no. 1, pp. 49–59, 2001.

[98] J. Feng, S. Li, and H. Chen, "Tanshinone IIA inhibits myocardial remodeling induced by pressure overload via suppressing oxidative stress and inflammation: possible role of silent information regulator 1," *European Journal of Pharmacology*, vol. 791, pp. 632–639, 2016.

[99] X. Tan, J. Li, X. Wang et al., "Tanshinone IIA protects against cardiac hypertrophy via inhibiting calcineurin/NFATc3 pathway," *International Journal of Biological Sciences*, vol. 7, no. 3, pp. 383–389, 2011.

[100] Y. S. Weng, H. F. Wang, P. Y. Pai et al., "Tanshinone IIA Prevents Leu27IGF-II-Induced Cardiomyocyte Hypertrophy Mediated by Estrogen Receptor and Subsequent Akt Activation," *The American Journal of Chinese Medicine*, vol. 43, no. 8, pp. 1567–1591, 2015.

[101] Y. Qin, L. Li, E. Luo et al., "Role of m6A RNA methylation in cardiovascular disease (review)," *International Journal of Molecular Medicine*, vol. 46, no. 6, pp. 1958–1972, 2020.

[102] M. Zhang, Y. Chen, H. Chen et al., "Tanshinone IIA alleviates cardiac hypertrophy through m6A modification of galectin-3," *Bioengineered*, vol. 13, no. 2, pp. 4260–4270, 2022.

[103] A. C. Li and C. K. Glass, "The macrophage foam cell as a target for therapeutic intervention," *Nature Medicine*, vol. 8, no. 11, pp. 1235–1242, 2002.

[104] S. E. Lee, S. I. Jeong, H. Yang et al., "Extract of *Salvia miltiorrhiza* (Danshen) induces Nrf2-mediated heme oxygenase-1 expression as a cytoprotective action in RAW 264.7 macrophages," *Journal of Ethnopharmacology*, vol. 139, no. 2, pp. 541–548, 2012.

[105] A. P. Burke, F. D. Kolodgie, A. Farb, D. Weber, and R. Virmani, "Morphological predictors of arterial remodeling in coronary atherosclerosis," *Circulation*, vol. 105, no. 3, pp. 297–303, 2002.

[106] L. Sun, T. Ishida, T. Yasuda et al., "RAGE mediates oxidized LDL-induced pro-inflammatory effects and atherosclerosis in non-diabetic LDL receptor-deficient mice," *Cardiovascular Research*, vol. 82, no. 2, pp. 371–381, 2008.

[107] G. Stoll and M. Bendszus, "Inflammation and Atherosclerosis," *Stroke*, vol. 37, no. 7, pp. 1923–1932, 2006.

[108] D. Tousoulis, E. Oikonomou, E. K. Economou, F. Crea, and J. C. Kaski, "Inflammatory cytokines in atherosclerosis: current therapeutic approaches," *European Heart Journal*, vol. 37, no. 22, pp. 1723–1732, 2016.

[109] W. Zhao, C. Li, H. Zhang et al., "Dihydrotanshinone I attenuates plaque vulnerability in apolipoprotein E-deficient mice: role of receptor-interacting protein 3," *Antioxidants & Redox Signaling*, vol. 34, no. 5, pp. 351–363, 2021.

[110] E. Harja, D. X. Bu, B. I. Hudson et al., "Vascular and inflammatory stresses mediate atherosclerosis via RAGE and its ligands in apoE$^{-/-}$ mice," *The Journal of Clinical Investigation*, vol. 118, no. 1, pp. 183–194, 2008.

[111] D. Zhao, L. Tong, L. Zhang, H. Li, Y. Wan, and T. Zhang, "Tanshinone II A stabilizes vulnerable plaques by suppressing RAGE signaling and NF-κB activation in apolipoprotein-E-deficient mice," *Molecular Medicine Reports*, vol. 14, no. 6, pp. 4983–4990, 2016.

[112] X. Wu, H. Gao, Y. Hou et al., "Dihydronortanshinone, a natural product, alleviates LPS-induced inflammatory response through NF-κB, mitochondrial ROS, and MAPK pathways," *Toxicology and Applied Pharmacology*, vol. 355, pp. 1–8, 2018.

[113] X. Li, L. H. Lian, T. Bai et al., "Cryptotanshinone inhibits LPS-induced proinflammatory mediators via TLR4 and TAK1 signaling pathway," *International Immunopharmacology*, vol. 11, no. 11, pp. 1871–1876, 2011.

[114] S. Tang, X. Y. Shen, H. Q. Huang et al., "Cryptotanshinone suppressed inflammatory cytokines secretion in RAW264.7 macrophages through inhibition of the NF-κB and MAPK signaling pathways," *Inflammation*, vol. 34, no. 2, pp. 111–118, 2011.

[115] T. Bai, M. Li, Y. Liu, Z. Qiao, and Z. Wang, "Inhibition of ferroptosis alleviates atherosclerosis through attenuating lipid peroxidation and endothelial dysfunction in mouse aortic endothelial cell," *Free Radical Biology & Medicine*, vol. 160, pp. 92–102, 2020.

[116] S. J. Dixon, K. M. Lemberg, M. R. Lamprecht et al., "Ferroptosis: an iron-dependent form of nonapoptotic cell death," *Cell*, vol. 149, no. 5, pp. 1060–1072, 2012.

[117] L. He, Y.-Y. Liu, K. Wang et al., "Tanshinone IIA protects human coronary artery endothelial cells from ferroptosis by activating the NRF2 pathway," *Biochemical and Biophysical Research Communications*, vol. 575, pp. 1–7, 2021.

[118] S. W. Zhuang, T. H. Cheng, N. L. Shih et al., "Tanshinone IIA Induces Heme Oxygenase 1 Expression and Inhibits Cyclic Strain-Induced Interleukin 8 Expression in Vascular Endothelial Cells," *The American Journal of Chinese Medicine*, vol. 44, no. 2, pp. 377–388, 2016.

[119] B. Lv, S. Chen, C. Tang, H. Jin, J. Du, and Y. Huang, "Hydrogen sulfide and vascular regulation - an update," *Journal of Advanced Research*, vol. 27, pp. 85–97, 2021.

[120] V. Citi, A. Martelli, E. Gorica, S. Brogi, L. Testai, and V. Calderone, "Role of hydrogen sulfide in endothelial dysfunction: pathophysiology and therapeutic approaches," *Journal of Advanced Research*, vol. 27, pp. 99–113, 2021.

[121] Y. Kimura, Y. I. Goto, and H. Kimura, "Hydrogen sulfide increases glutathione production and suppresses oxidative stress in mitochondria," *Antioxidants & Redox Signaling*, vol. 12, no. 1, pp. 1–13, 2010.

[122] Z. Zhang, X. Fang, X. Yang et al., "Hydrogen sulfide donor NaHS alters antibody structure and function via sulfhydration," *International Immunopharmacology*, vol. 73, pp. 491–501, 2019.

[123] Q. Yan, Z. Mao, J. Hong et al., "Tanshinone IIA stimulates cystathionine γ-lyase expression and protects endothelial cells from oxidative injury," *Antioxidants*, vol. 10, no. 7, p. 1007, 2021.

[124] M. G. Del Buono, F. Moroni, R. A. Montone, L. Azzalini, T. Sanna, and A. Abbate, "Ischemic cardiomyopathy and heart failure after acute myocardial infarction," *Current Cardiology Reports*, vol. 24, no. 10, pp. 1505–1515, 2022.

[125] S. Paone, A. A. Baxter, M. D. Hulett, and I. K. H. Poon, "Endothelial cell apoptosis and the role of endothelial cell-derived extracellular vesicles in the progression of atherosclerosis," *Cellular and Molecular Life Sciences*, vol. 76, no. 6, pp. 1093–1106, 2019.

[126] W. Zhao, C. Li, H. Gao, Q. Wu, J. Shi, and X. Chen, "Dihydrotanshinone I attenuates atherosclerosis in ApoE-deficient mice: role of NOX4/NF-κB mediated lectin-like oxidized LDL receptor-1 (LOX-1) of the endothelium," *Frontiers in Pharmacology*, vol. 7, p. 418, 2016.

[127] C. C. Chang, C. F. Chu, C. N. Wang et al., "The anti-atherosclerotic effect of tanshinone IIA is associated with the inhibition of TNF-α-induced VCAM-1, ICAM-1 and CX3CL1 expression," *Phytomedicine: International Journal of Phytotherapy and Pharmacopharmacology*, vol. 21, no. 3, pp. 207–216, 2014.

[128] J. Fang, Q. Chen, B. He et al., "Tanshinone IIA attenuates TNF-α induced PTX3 expression and monocyte adhesion to endothelial cells through the p38/NF-κB pathway," *Food and Chemical Toxicology*, vol. 121, pp. 622–630, 2018.

[129] W. Zhao, C. Wu, and X. Chen, "Cryptotanshinone inhibits oxidized LDL-induced adhesion molecule expression via ROS dependent NF-κB pathways," *Cell Adhesion & Migration*, vol. 10, no. 3, pp. 248–258, 2016.

[130] Z. Ahmad, C. T. Ng, L. Y. Fong et al., "Cryptotanshinone inhibits TNF-α-induced early atherogenic events in vitro," *The Journal of Physiological Sciences*, vol. 66, no. 3, pp. 213–220, 2016.

[131] L. Badimon and M. Borrell, "Microvasculature recovery by angiogenesis after myocardial infarction," *Current Pharmaceutical Design*, vol. 24, no. 25, pp. 2967–2973, 2018.

[132] P. Carmeliet, "Angiogenesis in health and disease," *Nature Medicine*, vol. 9, no. 6, pp. 653–660, 2003.

[133] C. A. Franco, S. Liebner, and H. Gerhardt, "Vascular morphogenesis: a Wnt for every vessel?," *Current Opinion In Genetics & Development*, vol. 19, no. 5, pp. 476–483, 2009.

[134] J. Li, R. Li, X. Wu et al., "An update on the potential application of herbal medicine in promoting angiogenesis," *Frontiers in Pharmacology*, vol. 13, article 928817, 2022.

[135] X. Wang and C. Wu, "Tanshinone IIA improves cardiac function via regulating miR-499-5p dependent angiogenesis in myocardial ischemic mice," *Microvascular Research*, vol. 143, article 104399, 2022.

[136] S. Sonkusare, P. T. Palade, J. D. Marsh, S. Telemaque, A. Pesic, and N. J. Rusch, "Vascular calcium channels and high blood pressure: Pathophysiology and therapeutic implications," *Vascular Pharmacology*, vol. 44, no. 3, pp. 131–142, 2006.

[137] T. P. Flagg, D. Enkvetchakul, J. C. Koster, and C. G. Nichols, "Muscle KATP channels: recent insights to energy sensing and myoprotection," *Physiological Reviews*, vol. 90, no. 3, pp. 799–829, 2010.

[138] P. Chan, I. M. Liu, Y.-X. Li, W.-J. Yu, and J.-T. Cheng, "Antihypertension Induced by Tanshinone IIA Isolated from the Roots of *Salvia miltiorrhiza*," *Evidence-based Complementary and Alternative Medicine*, vol. 2011, Article ID 392627, 8 pages, 2011.

[139] T. Li, B. Wang, H. Ding et al., "Effect of extracellular vesicles from multiple cells on vascular smooth muscle cells in atherosclerosis," *Frontiers in Pharmacology*, vol. 13, article 857331, 2022.

[140] X. Li, J. R. Du, Y. Yu, B. Bai, and X. Y. Zheng, "Tanshinone IIA inhibits smooth muscle proliferation and intimal hyperplasia in the rat carotid balloon-injured model through inhibition of MAPK signaling pathway," *Journal of Ethnopharmacology*, vol. 129, no. 2, pp. 273–279, 2010.

[141] S. N. Ricketts and L. Qian, "The heart of cardiac reprogramming: the cardiac fibroblasts," *Journal of Molecular and Cellular Cardiology*, vol. 172, pp. 90–99, 2022.

[142] Y. Ma, G. V. Halade, and M. L. Lindsey, "Extracellular matrix and fibroblast communication following myocardial infarction," *Journal of Cardiovascular Translational Research*, vol. 5, no. 6, pp. 848–857, 2012.

[143] N. G. Frangogiannis, "Cardiac fibrosis," *Cardiovascular Research*, vol. 117, no. 6, pp. 1450–1488, 2021.

[144] P. Stawowy, C. Margeta, H. Kallisch et al., "Regulation of matrix metalloproteinase MT1-MMP/MMP-2 in cardiac fibroblasts by TGF-beta1 involves furin-convertase," *Cardiovascular Research*, vol. 63, no. 1, pp. 87–97, 2004.

[145] P. Qiao, J. Xu, X. Liu, and X. Li, "Tanshinone IIA improves ventricular remodeling following cardiac infarction by regulating miR-205-3p," *Disease Markers*, vol. 2021, Article ID 8740831, 6 pages, 2021.

Retraction

Retracted: Genetic Analysis Reveals Different Mechanisms of IL-5 Involved in the Development of CAD in a Chinese Han Population

Oxidative Medicine and Cellular Longevity

This article has been retracted by Hindawi, as publisher, following an investigation undertaken by the publisher [1]. This investigation has uncovered evidence of systematic manipulation of the publication and peer-review process. We cannot, therefore, vouch for the reliability or integrity of this article.

Please note that this notice is intended solely to alert readers that the peer-review process of this article has been compromised.

Wiley and Hindawi regret that the usual quality checks did not identify these issues before publication and have since put additional measures in place to safeguard research integrity.

We wish to credit our Research Integrity and Research Publishing teams and anonymous and named external researchers and research integrity experts for contributing to this investigation.

The corresponding author, as the representative of all authors, has been given the opportunity to register their agreement or disagreement to this retraction. We have kept a record of any response received.

References

[1] W. Zhang, J. He, M. Liu et al., "Genetic Analysis Reveals Different Mechanisms of IL-5 Involved in the Development of CAD in a Chinese Han Population," *Oxidative Medicine and Cellular Longevity*, vol. 2023, Article ID 1700857, 10 pages, 2023.

Hindawi

Research Article

Genetic Analysis Reveals Different Mechanisms of IL-5 Involved in the Development of CAD in a Chinese Han Population

Wenjuan Zhang,[1,2,3,4] Junyi He,[1,2,3] Meilin Liu,[1,2,3] Mingkai Huang,[1,2,3] Qianwen Chen,[1,2,3,5] Jiangtao Dong,[1,2,3,6] Hongsong Zhang,[1,2,3,7] Tian Xie,[1,2,3] Jing Yuan [1,2,3] and Lingfeng Zha [1,2,3]

[1]Department of Cardiology, Union Hospital, Tongji Medical College, Huazhong University of Science and Technology, China
[2]Hubei Key Laboratory of Biological Targeted Therapy, Union Hospital, Tongji Medical College,
 Huazhong University of Science and Technology, China
[3]Hubei Provincial Engineering Research Center of Immunological Diagnosis and Therapy for Cardiovascular Diseases,
 Union Hospital, Tongji Medical College, Huazhong University of Science and Technology, Wuhan 430022, China
[4]Department of Geriatrics, The Central Hospital of Wuhan, Tongji Medical College, Huazhong University of Science
 and Technology, Wuhan 430022, China
[5]Hubei Maternal and Child Health Hospital, Wuhan 430070, China
[6]Department of Cardiovascular Surgery, Union Hospital, Tongji Medical College, Huazhong University of Science and Technology,
 Wuhan 430022, China
[7]Department of Cardiology, Nanjing First Hospital, Nanjing Medical University, Nanjing, China

Correspondence should be addressed to Jing Yuan; yhelen13@163.com and Lingfeng Zha; 1009229908@qq.com

Background. Coronary artery disease (CAD) is a complex disease and the leading cause of death worldwide. It is caused by genetic and environmental factors or their interactions. Candidate gene association studies are an important genetic strategy for the study of complex diseases, and multiple variants of inflammatory cytokines have been found to be associated with CAD using this method. Interleukin-5 (IL-5) is an important inflammatory immune response factor that plays a role in a various inflammatory disease. Clinical tests and animal experiments indicated that IL-5 is involved in CAD development, but the exact mechanisms are unclear. This study investigated the genetic relationship between the single nucleotide polymorphisms (SNPs) in *IL5* and CAD. *Materials and Methods.* Based on the Chinese Han population, we collected 1,824 patients with CAD and 1,920 control subjects and performed a two-stage case-control association analysis for three SNPs in *IL5* (rs2057687, rs78546665, and rs2069812) using the high resolution melt (HRM) technology. Logistic regression analyses were applied to adjust for traditional risk factors for CAD and to perform haplotype and gene interaction analyses. Multiple linear regression analyses were used to study relationships between the selected SNPs and serum lipid levels. *Results.* In this study, two-stage case-control association analysis revealed that the allele and genotype frequency distributions of the three *IL5* SNPs were not statistically significant between the case and control groups. In addition, none of the *IL5* haplotypes were associated with CAD. Further stratified analyses were conducted by sex, age, hypertension, and disease status, respectively, and the results revealed that the rs2057687 and rs2069812 of *IL5* were associated with CAD in the male group ($p_{adj} = 0.025$, OR, 0.77 (95% CI, 0.62-0.97); $p_{adj} = 0.016$, OR, 0.82 (95% CI, 0.70-0.97), respectively); the rs2057687 and rs78546665 of *IL5* were associated with late-onset CAD ($p_{adj} = 0.039$, OR, 0.78 (95% CI, 0.62-0.99); $p_{adj} = 0.036$, OR, 1.46 (95% CI, 1.02-1.53), respectively); the rs2069812 of *IL5* was associated with CAD in the hypertension group ($p_{adj} = 0.036$, OR, 0.84 (95% CI, 0.71-0.99)); and none of the SNPs in *IL5* were associated with different CAD states (anatomical CAD and clinical CAD). In addition, the association between SNPs and the

serum lipid levels indicated that rs78546665 was positively correlated with triglyceride levels ($p = 0.012$). Finally, SNP-SNP interaction analyses revealed that interactions of rs2057687 and rs2069812 were associated with CAD ($p_{adj} = 0.046$, OR, 0.77 (95% CI, 0.13-4.68)). *Conclusion.* This study suggested that the common variants of *IL5* might play a role in CAD by affecting the risk factors for CAD and through SNP-SNP interactions, which provides a new target for specific treatment of CAD patients and a theoretical basis for personalized medicine.

1. Introduction

Coronary artery disease (CAD) is a complex cardiovascular disease (CVD) caused by the combined action of genetic and environmental factors. Its pathological basis is coronary atherosclerosis (AS) and/or coronary artery spasm [1, 2]. CAD is one of the leading causes of death worldwide, causing huge economic and medical burdens on society [3]. Currently, the number of patients with CAD in China has reached 11 million [4]. Epidemiological investigations, twin studies, and relative risk studies have shown that there is a significant genetic predisposition to CAD. Compared to people without CAD, relatives of CAD patients have a 2-3.9-fold higher chance of developing CAD [5, 6]. Although genetic studies such as genome wide association studies (GWASs) have found numerous CAD susceptibility genes, these can explain only approximately 28% of the heritability of CAD, which is estimated to be between 40% and 60% [1, 7]. In addition, the specific pathogenic mechanisms underlying a considerable number of CAD susceptibility genes have not been clarified, and researchers still need to determine the genetic basis of CAD using a variety of strategies [8].

Interleukin-5 (IL-5) is a multieffector inflammatory cytokine that plays a role in various diseases by regulating a variety of cells, such as Th2 cells, NK cells, mast cells, B cells, and eosinophils [9]. IL-5 also plays a key role in the development of CVDs. Research has shown that IL-5 can promote the secretion of T15/EO6 IgM antibody and prevent macrophages from absorbing oxidized low-density lipoprotein (ox-LDL) [10], which may explain why selective macrophage overexpression of IL-5 can prevent atherosclerosis from progressing [11]. Sampi et al. tested plasma IL-5 and ox-LDL concentrations in 1,100 middle-aged Finnish individuals in 2008, as well as the human carotid artery intima-media thickness (cIMT) by ultrasound [12]. The results revealed a positive correlation between IL-5 levels and LDL concentrations, while serum IL-5 levels were negatively correlated with cIMT [12]. This is consistent with another study that found a negative correlation between IL-5 and cIMT changes in the common carotid arteries in females [13]. In addition, IL-33 significantly increased IL-5 expression and antioxidant LDL antibodies, whereas administration of IL-5 monoclonal antibody and IL-33 prevented the reduction of atherosclerotic plaque area and the reduction in IL-33-induced ox-LDL antibodies. These findings imply that IL-33 induces IL-5 and LDL antibodies, which may act as a preventive mechanism against atherosclerosis [14].

Single nucleotide polymorphisms (SNPs) of *IL5* have been found to be related to many diseases: for example, rs2069812 on *IL5* was found to be associated with gastric cancer susceptibility in the Polish population [15]. Although existing evidence suggests that IL-5 is involved in atherosclerosis, the genetic relationship between *IL5* and CAD remains unclear. This study investigated the relationship between SNPs of *IL5* and CAD in a Chinese Han population to explore the genetic role of the *IL5* in CAD, so as to gain insight into the role of IL-5 in the development of CAD. To the best of our knowledge, this genetic perspective study is the first to be conducted in a Chinese Han population, providing a theoretical basis for the clinical treatment of CAD.

2. Materials and Methods

2.1. Study Population. UnionID is a growing database of DNA samples based on the Chinese Han population and is dedicated to explore the molecular genetic mechanisms of various CVDs. At present, the samples in this sample bank are mainly from the Wuhan Union Hospital in the central region of China. All individuals selected for the sample bank signed informed consent forms. The research involved in the sample bank met the requirements of the World Medical Association Declaration of Helsinki and was approved by the local ethics committee of Union Hospital (Wuhan, Hubei) (No. 0157-01). CAD samples and control samples from UnionID were included in our study. The inclusion criteria for CAD samples were [16–18] as follows: (1) coronary angiography of the patient confirmed that at least one main vessel (left main artery, anterior descending branch, circumflex branch, or right coronary artery) was more than 70% narrowed; (2) the patient's history suggested that they had undergone percutaneous coronary intervention (PCI) or coronary artery bypass grafting (CABG); and (3) the patient had a history of myocardial infarction (MI), and the criteria for MI were chest pain for more than half an hour, dynamic ECG changes, and enzymatic changes in levels of creatine kinase isoenzyme (CKMB) and troponin (TNI). Patients with coronary spasm, juvenile hypertension, type 1 diabetes, or congenital heart disease (CHD) were excluded. The inclusion criteria for the control group were as follows: all of whom were over 35 years old without CAD, MI, juvenile hypertension, type 1 diabetes, CHD, rheumatic immune diseases, neoplastic diseases, and stroke. The discovery population comprised 768 CAD samples and 768 control samples. The validation population included 1,056 CAD samples and 1,152 control samples. The combined population consisted of 1,824 CAD samples and 1,920 control samples. Traditional risk factors for CAD include age, sex, body mass index (BMI), hypertension, diabetes mellitus (DM), smoking history, total cholesterol (Tch), triglyceride (TG), high-density lipoprotein cholesterol (HDL-c), and low-density lipoprotein cholesterol (LDL-c),

which were all recorded in detail for each participant. The flow chart of the association analysis between IL-5 and CAD is shown in Figure 1.

2.2. Tag SNP Selection. LD block maps of the Chinese population covering *IL5* and its upstream and downstream 5 kbp regions were found in the online databases: SNPinfo Web Server (https://snpinfo.niehs.nih.gov/), Ensembl database (http://www.ensembl.org/), and dbSNP (http://www.ncbi.nlm.nih.gov/projects/SNP/). A tag SNP on *IL5* was selected according to the following selection principles: (1) MAF > 0.05 and $r^2 > 0.8$, (2) preferentially selected SNPs that have been reported to be associated with inflammation in the literature, and (3) preferentially selected SNPs located in the gene promoter and exon regions. Finally, three tag SNPs in *IL5* gene were included in this study: rs2069812, rs78546665, and rs2057687 (Supplementary Table S1).

2.3. DNA Extraction and Genotyping. Human peripheral blood genomic DNA was extracted following the instructions of the BloodGen Mini Kit blood gene column small amount extraction Kit (CW 2087). DNA was PCR amplified in a 25 μL reaction system containing 2.5 μL 10x PCR buffer, 0.5 μL dNTPs, 0.5 μL forward and reverse primers (Supplementary Table S2), 1 μL DNA, 1 μL Taq DNA polymerase, 0.5 μL SYTO 9, and 19 μL double-distilled water with TAKARA-TP600 PCR amplifier (Takara, Japan) and genotyped using a Rotor-Gene 6000 High Resolution Melt (HRM) system (Corbett Life Science, Australia). PCR amplification involved preheating at 94°C for 5 minutes, then denaturation at 94°C for 10 seconds, annealing at the optimum temperature for each SNP (59°C for rs2069812, 56°C for rs78546665, and 55°C for rs2057687) for 10 seconds, and extension at 72°C for 15 seconds for 35 cycles. After holding the sample at 72°C for 5 minutes, the endpoint temperature was maintained at 22°C. For HRM genotyping, the peak of allele detection for rs2069812 was 79-83°C, for rs78546665 was 74-78°C, and for rs2057687 was 82-87°C (Supplementary Table S2).

2.4. Statistical Analysis. The Hardy-Weinberg equilibrium (HWE) was tested using PLINK software (v.1.07) in the control population. Allelic and genotypic association analyses were conducted using 2×2 and 2×3 Pearson's chi-squared contingency tables, respectively. Odds ratio (OR) and 95% confidence interval (CI) were calculated using SPSS (v.23.0). Multiple logistic regression was used to adjust for traditional risk factors for CAD, while multiple linear regression was used to assess the effects of SNP genotypes on serum lipid levels (SPSS, v.23.0). Haplotype reconstruction and analysis were performed using Haploview or multiple logistic regression (SPSS, v.23.0). Statistical power analysis and sample size estimation were performed using the Power and Sample Size Calculations program (PS, v.3.0). The statistical power for all SNPs selected in this study was more than 90% with an effect size of 1.3 (HapMap CHB + JPT data), type I error rate alpha was 0.05, and the MAF for rs2057687 is 0.121, for rs78546665 is 0.155, and for rs2069812 is 0.296. The sample size ratio between the control and case groups was 1.

3. Results

3.1. Population Characteristics. The clinical characteristics of the CAD patients were compared with those of the control group individuals in the discovery, validation, and combined populations (Table 1). The discovery population comprised 768 CAD and 768 control samples. The validation population included 1,056 CAD samples and 1,152 control samples. The combined population consisted of 1,824 CAD samples and 1,920 control samples. The statistical results showed that the trend of each clinical data point in the discovery, validation, and combined groups was consistent. In the combined population, the CAD group's average age, average BMI, proportion of males, and smoking population were significantly higher than those of the control group with p value $< 1 \times 10^{-6}$. Moreover, the proportion of patients with diabetes and hypertension in the CAD group was significantly higher than that in the control with p value $< 1 \times 10^{-6}$. Tch, TG, and LDL-c levels in the CAD group were significantly higher than those in the control group with p value $< 1 \times 10^{-6}$, respectively. The average density of HDL-c in the CAD group was significantly lower than that in the control group with p value $< 1 \times 10^{-6}$.

3.2. Allelic and Genotypic Association Analyses of SNPs in the IL5 Gene with CAD. None of the three SNPs in *IL5* deviated from the HWE test in the control population ($p > 0.001$). However, in the first phase of the discovery population, the mutant allele frequencies of rs2057687-T, rs78546665-T, and rs2069812-G in the control population were higher than those in the CAD population (in the control population, MAF for rs2057687-T is 0.134, MAF for rs78546665-T is 0.166, and MAF for rs2069812-G is 0.313, while in the CAD population, MAF for rs2057687-T is 0.087, MAF for rs78546665-T is 0.148, and MAF for rs2069812-G is 0.285). rs2057687 was significantly correlated with CAD before correction for traditional risk factors, and the observed p value was 7×10^{-5}. The other two SNPs, rs78546665 and rs2069812, did not correlate with CAD before correction. After correcting for traditional risk factors, rs2057687 was still significantly correlated with CAD ($p_{adj} = 0.035$, OR, 0.68 (95% CI, 0.47-0.97)), but the adjusted p values of the other two SNPs were >0.05 (Table 2). In the second-stage validation and combined populations, the three SNPs were not significant after traditional risk factor correction ($p_{adj} > 0.05$) (Table 2).

For genotypic association analysis, in the first phase of the discovery population, rs2057687 was significantly correlated with CAD in both additive (TT/CT/CC) ($p_{obs} = 3.61 \times 10^{-4}$) and dominant modes (TT+CT/CC) ($p_{obs} = 7.40 \times 10^{-5}$). After adjusting for traditional risk factors, rs2057687 was significantly correlated with CAD in both additive (TT/CT/CC) ($p_{adj} = 0.032$, OR, 0.67 (95% CI, 0.46-0.97)) and dominant modes (TT+CT/CC) ($p_{adj} = 0.034$, OR, 0.65 (95% CI, 0.44-0.97)). In the second-stage validation and combined population, the three SNPs were not significant in the three analysis
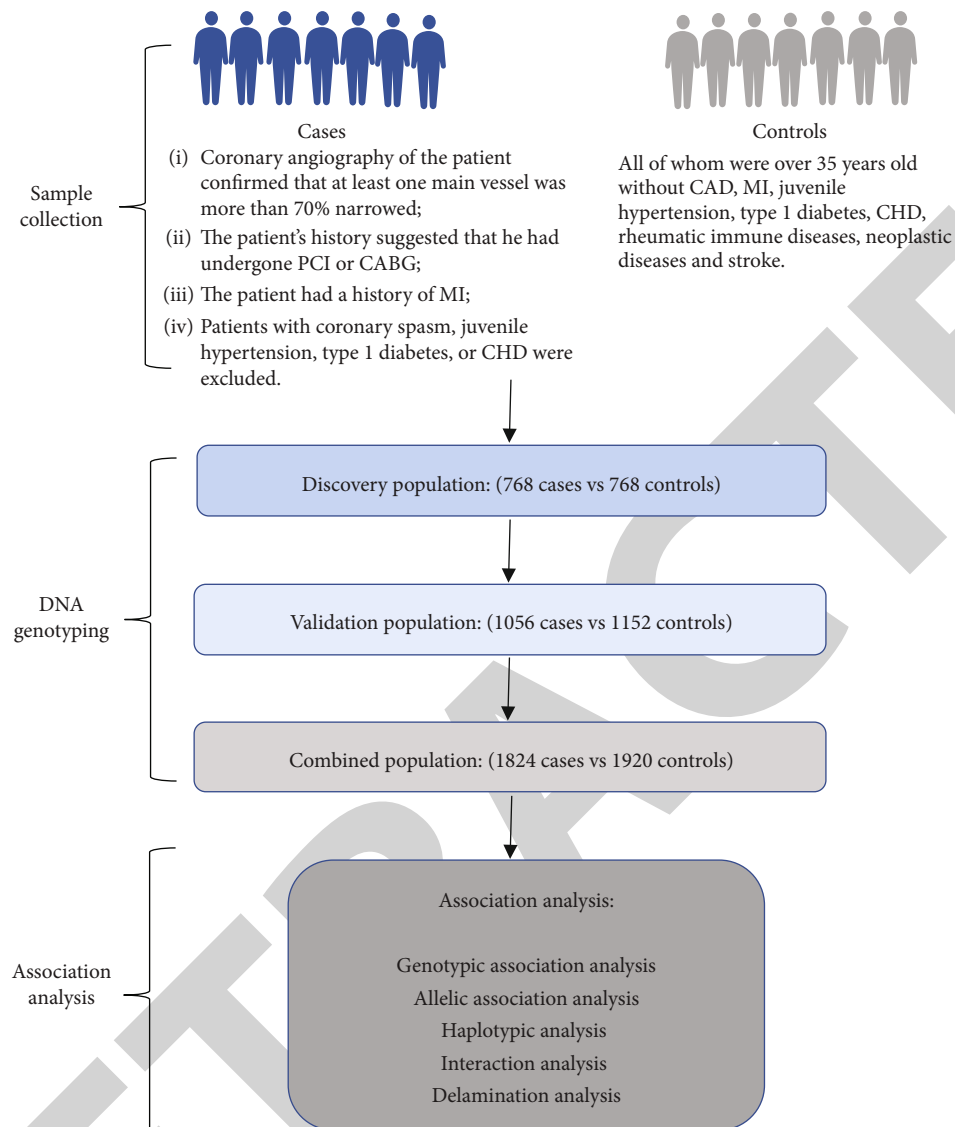
FIGURE 1: Flow chart of the association analysis between IL-5 and CAD.

modes either before or after risk factor correction, with p values > 0.05 (Supplementary Table S3).

3.3. Haplotypic and Interaction Analyses between SNPs in the IL5 Gene and CAD.

Haplotype analysis of multiple SNPs is an effective method for association analysis. Haplotype association analysis can provide better insight into the role of a gene in a given disease, with a combination of alleles from all tested SNPs within the gene region. The IL5 haplotype was constructed using three IL5 SNPs, and haplotype association analysis was performed in the combined population (Supplementary Figure S1). In our population, eight haplotypes (CGA, CGG, CTA, CTG, TGA, TGG, TTA, and TTG in the order of rs2057687-rs78546665-rs2069812) were detected, in which the CGA haplotype accounted for over 50% of the total haplotypes in the CAD and control populations. The frequency of the TGG haplotype was 9.2% in the control population, higher than 7.6% in the CAD population. Logistic regression analysis indicated that this haplotype was related to

CAD before traditional risk factors were corrected, and the observed p value was 0.017. The frequency of another haplotype, TGA, was also higher in the control population than in the CAD population, with an observed p value of 0.068 as a fair association. However, after the correction for traditional risk factors by multiple logistic regression analysis, none of the eight haplotypes were associated with CAD, and the lowest p value was 0.087 (Table 3).

Pairwise interaction analysis of the three SNPs on IL5 revealed three interactions, one of which was significant. There were eight genotypic combinations in the combined population for which the interaction of rs2057687-TT/ rs2069812-AG was correlated with CAD ($p_{adj} = 0.046$, OR, 0.77 (95% CI, 0.13-4.68)) (Table 4). The results for the other two interactions are not presented as no significant results were found.

3.4. Delamination Analysis for the Association of SNPs in the IL5 Gene with CAD Subgroups.

Considering that age, sex,

TABLE 1: The characteristics of the study population.

Characteristics	Discovery cohort			Validation-cohort			Combined cohort		
	CAD ($n = 768$)	Control ($n = 768$)	p	CAD ($n = 1056$)	Control ($n = 1152$)	p	CAD ($n = 1824$)	Control ($n = 1920$)	p
Age (years)	63.3 ± 11.1	51.6 ± 12.3	$<10^{-6}$	61.7 ± 11.3	57.9 ± 11.8	$<10^{-6}$	62.4 ± 11.2	55.4 ± 12.4	$<10^{-6}$
Male (%)	71.5	59.2	$<10^{-6}$	73.7	50.8	$<10^{-6}$	72.8	54.2	$<10^{-6}$
Smoking (%)	46.5	20.2	$<10^{-6}$	44.6	24.5	$<10^{-6}$	45.4	22.8	$<10^{-6}$
BMI (kg/m^2)	24.2 ± 1.54	23.7 ± 1.41	$<10^{-6}$	24.4 ± 1.61	23.7 ± 1.41	$<10^{-6}$	24.3 ± 1.58	23.7 ± 1.41	$<10^{-6}$
Hypertension (%)	68.6	14.7	$<10^{-6}$	67.0	44.5	$<10^{-6}$	67.7	32.6	$<10^{-6}$
DM (%)	34.8	4.3	$<10^{-6}$	30.3	13.0	$<10^{-6}$	32.2	9.5	$<10^{-6}$
Tch (mmol/L)	5.09 ± 1.18	4.53 ± 0.90	$<10^{-6}$	5.16 ± 1.16	4.99 ± 1.22	$<10^{-6}$	5.13 ± 1.17	4.81 ± 1.13	$<10^{-6}$
TG (mmol/L)	1.79 ± 1.16	1.45 ± 0.87	$<10^{-6}$	1.82 ± 1.31	1.52 ± 1.01	$<10^{-6}$	1.81 ± 1.25	1.49 ± 0.96	$<10^{-6}$
HDL-c (mmol/L)	1.12 ± 0.29	1.28 ± 0.31	$<10^{-6}$	1.10 ± 0.28	1.30 ± 0.33	$<10^{-6}$	1.11 ± 0.29	1.29 ± 0.32	$<10^{-6}$
LDL-c (mmol/L)	2.98 ± 1.02	2.54 ± 0.72	$<10^{-6}$	3.06 ± 1.08	2.81 ± 0.92	$<10^{-6}$	3.03 ± 1.05	2.70 ± 0.86	$<10^{-6}$

The data are shown as mean ± SD. Categorical data, including gender, smoking status, and other data, were tested using chi-square tests, and measurement data, such as BMI, age, and blood lipid level, were tested using t-tests between the cases and controls in each population; CAD: coronary artery disease; DM: diabetes mellitus; BMI: body mass index; Tch: total cholesterol; TG: triglyceride; HDL-c: high-density lipoprotein cholesterol; LDL-c: low-density lipoprotein cholesterol. Age for the case group is the age at diagnosis; age for the control group is the age at enrollment.

TABLE 2: Allelic association analysis between *IL5* and CAD.

Population	SNP allele	N		MAF		p_{hwe}	p_{obs}	p_{adj}	OR (95% CI)
		Case	Control	Case	Control				
Discovery	rs2057687^T	667	729	0.087	0.134	0.793	7×10^{-5}	0.035	0.68 (0.47-0.97)
	rs78546665^T	619	692	0.148	0.166	0.259	0.197	0.173	0.81 (0.59-1.10)
	rs2069812^G	742	745	0.285	0.313	0.224	0.099	0.519	0.93 (0.73-1.07)
Validation	rs2057687^T	993	1023	0.123	0.119	0.050	0.690	0.661	1.05 (0.84-1.31)
	rs78546665^T	907	972	0.182	0.165	0.201	0.161	0.157	1.16 (0.95-1.41)
	rs2069812^G	1039	1017	0.302	0.301	0.020	0.953	0.860	0.99 (0.84-1.15)
Combined	rs2057687^T	1660	1752	0.108	0.125	0.102	0.030	0.225	0.89 (0.74-1.07)
	rs78546665^T	1526	1664	0.168	0.166	0.806	0.760	0.674	1.04 (0.88-1.22)
	rs2069812^G	1781	1762	0.295	0.306	0.011	0.307	0.336	0.94 (0.83-1.07)

SNP: single nucleotide polymorphism; CAD: coronary artery disease; MAF: minor allele frequency; p_{obs}: observed p value; p_{adj}, p value adjusted by the covariates; age, sex, BMI, hypertension, diabetes mellitus, smoking history, Tch, TG, HDL-c, and LDL-c were adjusted; OR: odds ratio after adjustment; p_{hwe}: p value from the Hardy–Weinberg equilibrium tests.

and hypertension may have different effects on CAD, the combined population was divided into different subgroups. Patients with CAD were divided into early-onset CAD and late-onset CAD according to the age at onset: early-onset CAD was defined as the age of first onset in males ≤ 55 years and in females ≤ 65 years, while the late-onset CAD was defined as the age of first onset in males > 55 years and in females > 65 years. The study population was divided into hypertensive and nonhypertensive individuals based on whether they had hypertension. Patients with CAD were divided into clinical CAD and anatomical CAD according to the state of the disease: clinical CAD was defined as the occurrence of MI, PCI, CABG, and other surgical treatment, while the anatomical CAD was defined as severe coronary artery stenosis, with coronary angiography indicating that a stenosis degree of at least one main vessel was greater than 70%, regardless of whether MI occurred or whether PCI, CABG, and other surgical treatments were performed. Asso-

ciation analysis was conducted in different subgroups to explore the relationship between SNPs in *IL5* and CAD in these subgroups.

Allelic association analysis showed that rs2057687 and rs2069812 were significantly correlated with CAD in males ($p_{adj} = 0.025$, OR, 0.77 (95% CI, 0.62-0.97); $p_{adj} = 0.016$, OR, 0.82 (95% CI, 0.70-0.97), respectively). The results from the genotypic association analysis showed that rs2057687 was correlated with CAD in males in a dominant mode (TT+CT/CC) ($p_{adj} = 0.027$, OR, 0.76 (95% CI, 0.59-0.97)) and additive mode (TT/CT/CC) ($p_{adj} = 0.025$, OR, 0.77 (95% CI, 0.62-0.97)). rs2069812 was correlated with CAD in males in the additive mode (GG/AG/AA) ($p_{adj} = 0.018$, OR, 0.83 (95% CI, 0.71-0.97)) and recessive mode (GG/AG +AA) ($p_{adj} = 0.021$, OR, 0.67 (95% CI, 0.48-0.94)). rs78546665 was not associated with CAD in males in either allelic or genotypic association analyses. In addition, no

TABLE 3: Haplotype association analysis between *IL5* and CAD.

| | Haplotype | N | | p_{obs} | p_{adj} | OR (95% CI) |
		Case (%)	Control (%)			
	C-G-A	1702 (59.3)	1677 (56.7)	—	—	1
	C-G-G	446 (15.6)	484 (16.4)	0.193	0.087	0.85 (0.71-1.02)
	C-T-A	333 (11.6)	332 (11.2)	0.889	0.681	1.05 (0.85-1.29)
IL5 gene (rs2057687$^{T/C}$-rs78546665$^{T/G}$-rs2069812$^{G/A}$)	C-T-G	87 (3.0)	98 (3.3)	0.736	0.980	1.00 (0.69-1.44)
	T-G-A	16 (0.6)	28 (0.9)	0.068	0.191	0.61 (0.29-1.28)
	T-G-G	218 (7.6)	271 (9.2)	0.017	0.184	0.85 (0.67-1.75)
	T-T-A	4 (0.1)	9 (0.3)	0.170	0.361	0.50 (0.12-2.19)
	T-T-G	62 (2.2)	59 (2.0)	0.851	0.872	0.96 (0.61-1.52)

p_{obs}: observed p value; p_{adj}, p value adjusted by the covariates; age, sex, BMI, hypertension, diabetes mellitus, smoking history, Tch, TG, HDL-c, and LDL-c were adjusted; OR: odds ratio after adjustment.

TABLE 4: Interaction analysis between rs2057687 and rs2069812 in *IL5* and CAD under the genotypic model.

| Gene/SNP (*n*, case/control) | Types | N (%) | | p_{adj} | OR (95% CI) |
		Case	Control		
	TT/GG	16 (1.0)	22 (1.4)	0.125	1.25 (0.53-2.94)
	TT/AG	4 (0.2)	5 (0.3)	0.046	0.77 (0.13-4.68)
	CT/GG	68 (4.1)	61 (3.7)	0.684	1.13 (0.73-1.77)
IL5-rs2057687^{T}/*IL5*-rs2069812^{G} (1640/1628)	CT/AG	226 (13.8)	252 (15.5)	0.177	1.12 (0.86-1.44)
	CT/AA	19 (1.2)	31 (1.9)	0.344	1.49 (0.74-3.01)
	CC/GG	67 (4.1)	93 (5.7)	0.794	1.56 (1.05-2.33)
	CC/AG	416 (25.4)	391 (24.0)	0.499	1.01 (0.81-1.24)
	CC/AA	824 (50.2)	773 (47.5)	—	1

p_{adj}: p value adjusted by the covariates; age, sex, BMI, hypertension, diabetes mellitus, smoking history, Tch, TG, HDL-c, and LDL-c were adjusted; OR: odds ratio after adjustment.

SNPs were found to be associated with CAD in females (Table 5).

Allelic association analysis showed that no SNPs were correlated with anatomical CAD or clinical CAD, and the p values were not significant either before or after correction ($p > 0.05$) (Table 6). rs2057687 and rs78546665 were associated with late-onset CAD ($p_{adj} = 0.039$, OR, 0.78 (95% CI, 0.62-0.99); $p_{adj} = 0.036$, OR, 1.46 (95% CI, 1.02-1.53), respectively) (Table 7). rs2069812 was correlated with CAD-with-hypertension after correcting for traditional risk factors ($p_{adj} = 0.036$, OR, 0.84 (95% CI, 0.71-0.99)) (Table 7).

3.5. Associations between SNPs in the IL5 Gene and of Serum Lipid Concentrations. Lipids, as independent risk factors for CAD, play a key role in the occurrence and development of CAD. We further explored the relationship between SNPs in *IL5* and serum lipid levels (Tch, TG, HDL-c, and LDL-c). The link between SNPs in *IL5* and serum lipid levels was calculated using a multiple linear regression model in additive, recessive, and dominant modes. However, only in the recessive mode (TT/TG+GG) was rs78546665 positively correlated with triglyceride levels, with a p value of 0.012 and a β value of 0.282 after correction (Table 8).

4. Discussion

This study explored the genetic involvement of IL-5 in CAD by examining the association between SNPs in *IL5* and CAD in a Chinese Han population. We found that the rs2057687 and rs2069812 were associated with CAD in the male group, rs2057687 and rs78546665 were associated with late-onset CAD, rs2069812 was associated with CAD in the hypertension group, and rs78546665 was positively correlated with triglyceride levels. In addition, interactions between rs2057687 and rs2069812 were associated with CAD.

IL-5 is a multifunctional cytokine that stimulates the proliferation, differentiation, and activation of eosinophils and can also induce the differentiation of B and T cells. Previous studies have shown that a variety of inflammatory cells, including macrophages and T lymphocytes, but also mast cells, NK cells, and eosinophils, release IL-5. IL-5 overexpression significantly reduces macrophage and CD4^{+} T lymphocyte infiltration in a mouse acute aortic dissection (AAD) model. Additionally, IL-5 overexpression reduces the levels of IL-1, IL-6, IL-18, and TNF-a in the body [19]. Zhao et al. found that IL-5 overexpression in macrophages reduces AS in LDLR$^{-/-}$ mice [11]. Increased IL-5 levels are found in the plasma of patients with AS, unstable angina,

TABLE 5: Allelic and genotypic association analyses of *IL5* with CAD in gender subgroups.

SNP allele	Model	Male			Female		
		p_{obs}	p_{adj}	OR (95% CI)	p_{obs}	p_{adj}	OR (95% CI)
rs2057687[T]	ALLE	0.007	0.025	0.77 (0.62-0.97)	0.703	0.264	1.20 (0.87-1.65)
	DOM	0.014	0.027	0.76 (0.59-0.97)	0.729	0.279	1.22 (0.85-1.73)
	REC	0.079	0.373	0.68 (0.29-1.60)	0.820	0.630	1.33 (0.42-4.22)
	ADD	0.024	0.025	0.77 (0.62-0.97)	0.932	0.269	1.20 (0.87-1.64)
rs78546665[T]	ALLE	0.619	0.281	1.12 (0.91-1.38)	0.983	0.490	0.91 (0.69-1.20)
	DOM	0.798	0.385	1.11 (0.88-1.40)	0.974	0.663	0.93 (0.67-1.29)
	REC	0.376	0.290	1.46 (0.73-2.91)	0.986	0.376	0.70 (0.31-1.56)
	ADD	0.675	0.278	1.12 (0.91-1.38)	0.999	0.502	0.91 (0.69-1.20)
rs2069812[G]	ALLE	0.040	0.016	0.82 (0.70-0.97)	0.378	0.132	1.18 (0.95-1.45)
	DOM	0.108	0.081	0.83 (0.68-1.02)	0.470	0.137	1.23 (0.94-1.62)
	REC	0.073	0.021	0.67 (0.48-0.94)	0.497	0.454	1.18 (0.76-1.83)
	ADD	0.112	0.018	0.83 (0.71-0.97)	0.695	0.149	1.16 (0.95-1.42)

p_{obs}: observed p value; p_{adj}: p value adjusted by the covariates; OR: odds ratio after adjustment; ADD: additive mode, rs2057687_TT/CT/CC, rs78546665_TT/GT/GG, and rs2069812_GG/AG/AA; DOM: dominant mode, rs2057687_TT+CT/CC, rs78546665_TT+GT/GG, and rs2069812_GG+AG/AA; REC: recessive model, rs2057687_TT/CT+CC, rs78546665_TT/GT+GG, and rs2069812_GG/AG+AA.

TABLE 6: Allelic association analysis of *IL5* with CAD in different disease state subgroups.

SNP allele	CAD-anatomical				CAD-clinical			
	N (case/control)	p_{obs}	p_{adj}	OR (95% CI)	N (case/control)	p_{obs}	p_{adj}	OR (95% CI)
rs2057687[T]	1198/1752	0.107	0.361	0.91 (0.74-1.11)	1445/1752	0.026	0.255	0.89 (0.74-1.08)
rs78546665[T]	1096/1664	0.423	0.333	1.09 (0.91-1.30)	1321/1664	0.520	0.467	1.07 (0.90-1.26)
rs2069812[G]	1282/1762	0.237	0.396	0.94 (0.82-1.08)	1544/1762	0.337	0.394	0.94 (0.83-1.08)

CAD-anatomical: CAD subjects with severe coronary stenosis; CAD-clinical: CAD subjects with MI or revascularization; p_{obs}: observed p value; p_{adj}: p value adjusted by the covariates; OR: odds ratio after adjustment.

TABLE 7: Allelic association analysis of *IL5* with CAD in the onset age subgroups and the CAD with hypertension subgroups.

SNP allele	CAD-early-onset		CAD-late-onset		CAD-with-HP		CAD-without-HP	
	p_{adj}	OR (95% CI)	p_{adj}	OR (95% CI)	p_{adj}	OR (95% CI)	p_{adj}	OR (95% CI)
rs2057687[T]	0.745	1.04 (0.81-1.34)	0.039	0.78 (0.62-0.99)	0.679	0.95 (0.74-1.23)	0.193	0.83 (0.62-1.10)
rs78546665[T]	0.105	0.83 (0.65-1.04)	0.036	1.46 (1.02-1.53)	0.879	1.02 (0.82-1.27)	0.564	1.08 (0.84-1.39)
rs2069812[G]	0.461	0.94 (0.79-1.11)	0.310	0.92 (0.78-1.08)	0.036	0.84 (0.71-0.99)	0.343	1.10 (0.91-1.33)

CAD-with-HP: CAD with hypertension; CAD-without-HP: CAD without hypertension; p_{adj}: p value adjusted by the covariates; OR: odds ratio after adjustment.

and AMI [20, 21]. IL-5 protein is two times more abundant in the blood of ApoE^{-/-} mice than in ApoE^{+/+} mice [22]. A recent study found no correlation between baseline IL-5 levels and the risk of coronary artery events or stroke after 15.7 ± 6.3 years of follow-up. However, the presence of carotid bifurcation plaques was related to lower IL-5 levels, and a lack of IL-5 promoted plaque growth at the oscillating blood flow site in ApoE^{-/-} mice [23]. Additionally, the anti-atherosclerotic effects of valsartan were reduced by anti-IL-5 monoclonal antibody (mAb) therapy, and macrophage infiltration was higher in the anti-IL-5 mAb group than that in the control group [24]. Valsartan treatment reduced the antiatherosclerotic effects without raising blood pressure,

indicating that at least in part, valsartan reduced atherosclerosis through enhancing the Th2 immune response [24].

LDL is oxidized during atherogenesis, and new specific epitopes of oxidization arise that can be recognized and responded to by adaptive T cell-dependent (TD) and innate T cell-independent innate type 2 (TI-2) immune cells. The TD immune response produces a large number of TH2 cells, which suppress atherosclerosis by secreting IL-5. In addition, IL-5 stimulates the production and secretion of T15/EO6 IgM via the TI-2 immune response of innate B-1 cells, and T15/EO6 IgM can inhibit the uptake of ox-LDL by macrophages, thus playing a protective role in the development of atherosclerosis [12, 25]. When IL-5 is lacking, the

TABLE 8: Genotypic association between *IL5* and serum lipid levels.

	Dominant			Recessive			Additive		
	β	SE	p_{adj}	β	SE	p_{adj}	β	SE	p_{adj}
rs2057687[T]									
Tch	-0.016	0.048	0.741	-0.140	0.154	0.365	-0.023	0.043	0.584
TG	-0.054	0.045	0.230	-0.215	0.145	0.138	-0.060	0.040	0.137
HDL-c	0.019	0.013	0.142	0.016	0.041	0.685	0.016	0.011	0.154
LDL-c	-0.004	0.036	0.906	-0.060	0.130	0.645	0.001	0.040	0.992
rs78546665[T]									
Tch	-0.020	0.044	0.655	0.154	0.120	0.200	0.001	0.038	0.983
TG	0.070	0.036	0.051	0.282	0.113	0.012	0.055	0.041	0.184
HDL-c	-0.011	0.012	0.338	-0.024	0.032	0.456	-0.011	0.010	0.285
LDL-c	0.008	0.032	0.794	0.110	0.102	0.253	-0.004	0.037	0.905
rs2069812[G]									
Tch	-0.017	0.038	0.660	0.030	0.064	0.634	-0.004	0.028	0.897
TG	-0.023	0.037	0.535	0.046	0.062	0.455	-0.004	0.028	0.897
HDL-c	-0.002	0.010	0.809	-0.012	0.017	0.468	-0.004	0.008	0.609
LDL-c	-0.002	0.033	0.949	0.013	0.054	0.807	0.002	0.024	0.950

Tch: total cholesterol; TG: triglyceride; HDL-c: high-density lipoprotein cholesterol; LDL-c: low-density lipoprotein cholesterol; ADD: additive mode, rs2057687_TT/CT/CC, rs78546665_TT/GT/GG, and rs2069812_GG/AG/AA; DOM: dominant mode, rs2057687_TT+CT/CC, rs78546665_TT+GT/GG, and rs2069812_GG+AG/AA; REC: recessive model, rs2057687_TT/CT+CC, rs78546665_TT/GT+GG, and rs2069812_GG/AG+AA.

production of T15/EO6 IgM is reduced, leading to accelerated development of atherosclerosis [10]. It was also found that IL-5 levels were negatively correlated with carotid intimal thickness and significantly positively correlated with IgM levels. Plasma IL-5 levels are associated with plasma levels of ox-LDL-binding antibodies and with a reduction in subclinical atherosclerosis in humans [12]. Zhao et al. found that plasma T15/EO6 IgM in mice with specific IL-5 overexpression in macrophages of LDLR$^{-/-}$ mice increased by 58%, and the aortic plaque area and volume decreased by 43% and 2.4 times compared with the control group after 12 weeks of feeding a high-fat diet [11].

Type 2 innate lymphoid cells (ILC2s) are a population of innate cells of lymphoid origin that drive strong type 2 immunity [26]. Mice lacking ILC2 effector cytokines exhibit increased atherosclerosis, and activation of ILC2s is associated with a lower atherosclerotic burden [27]. ILC2s are a potent source of IL-5[28] and ILC2-derived IL-5 is required to reduce atherosclerosis [27]. As a major source of type 2 cytokines, selective genetic deletion of *ILC2* in LDLR$^{-/-}$ mice accelerates the onset of atherosclerosis, which is avoided by reconstitution with wild type but not IL5$^{-/-}$ ILC2 [28]. ILC2s improve recovery of heart function after MI in mice by promoting cardiac repair. Low doses of IL-2 in patients with ACS activated circulating ILC2s and significantly increased circulating IL-5 levels. IL-2 supplementation in mice increases ILC2 activation and enhances IL-5 secretion, ultimately improving recovery. The protective effect of ILC2s after MI may be due to the production of IL-5 [29].

These findings indicate that IL-5 can inhibit the occurrence of atherosclerosis, and genetic studies have shown that there are CAD susceptibility sites near the *IL5* gene [30]. In our study, the relationship between SNPs of the *IL5* gene and CAD was investigated from a genetic perspective to elucidate its molecular mechanism. We selected three SNPs on *IL5* gene and conducted a two-stage, large sample association analysis in the CAD and control populations of the Han Chinese population and found that these three SNPs were not independently associated with CAD. A previous CAD GWAS meta-analysis from the CARDIoGRAMplusC4D Consortium indicated that rs2057687 and rs2069812 in *IL5* are not associated with CAD of European ancestry [31]. Considering the differences between different disease states, we divided the CAD population into anatomical and clinical CAD populations and found no association between the SNPs and CAD in these two populations. However, when age and sex factors were considered in the analysis, we found that rs2069812 and rs2057687 in *IL5* were associated with CAD in males. It is well known that the incidence of CAD in males is generally higher than that in women, which is most likely related to the presence of more CAD susceptibility sites in males. Recently, sex-specific GWASs displayed a male-specific effect of *IL5* on the mean area of detected carotid plaques [32]. Silveira et al. analyzed plasma IL-5 and its effect on cIMT and found a protective effect of IL-5 in females. In female cervical sections, there is an increasing and substantial negative connection between IL-5 and cIMT [13], and serum IL-5 levels are also associated with other risk factors, such as LDL-c, serum creatinine, fasting plasma glucose, sex, and age [33]. rs2069812 and rs78546665 in *IL5* were associated with late-onset CAD, which is a chronic inflammatory disease in which inflammatory factors play an important role. At different stages of the disease, inflammatory cells selectively secrete cytokines, so the activity of cytokines is a dynamic process. IL-5 may be activated at a later stage and participate in disease development. In addition, in many cases, the mutation does not act directly on the disease, but on the risk factors for the disease, and occurs only when the risk factors are continuously

exposed. We further conducted association analysis on two important independent risk factors for CAD and found that rs2069812 was associated with CAD in the hypertensive population, indicating that this SNP was involved in CAD by influencing hypertension. Compared to females with normal blood pressure, females with both hypertensive conditions (gestational hypertension and preeclampsia) exhibited an atherogenic lipid profile at early gestation. However, only those later developing gestational hypertension showed observably elevated serum IL-5 levels [34]. In an association analysis with the lipid profiles, rs78546665 was found to be correlated with total serum cholesterol, indicating that there is a complex and close correlation between the SNPs in *IL5* and blood lipids, which are also involved in the occurrence and development of CAD. Recent studies have found that IL-5 is involved in the lipid metabolism of immune cells and that IL-5 stimulates ABCA1 expression and cholesterol efflux via the miR-211/ JAK2/STAT3 signaling pathway in THP-1-derived macrophages [35]. In addition, moderate alcohol consumption decreases serum IL-5 concentrations (~14%) [36]. In conclusion, the role of a single SNP in *IL5* may lead to CAD by acting on the traditional risk factors for CAD in many ways.

Haplotype analysis can be used to effectively assess the relationship between a group of linked SNPs and diseases or traits. To evaluate the role of *IL5* in CAD, we constructed a haplotype of *IL5* and conducted a haplotype association analysis, but no correlations were found between the *IL5* haplotype and CAD. Furthermore, gene-gene interaction analysis is an effective method for analyzing the effects of interactions between two loci or two genes on traits or diseases. When a trait is controlled by two loci or genes, one locus can mask or increase the effect of the other locus. We further analyzed the influence of the interaction between SNPs of *IL5* on CAD. Through interaction analysis, rs2057687 and rs2069812 were found to be correlated with CAD, while our previous single SNP analysis showed no correlation between a single SNP and CAD, indicating that a single SNP has only a weak effect on CAD. In complex gene regulation networks, association analysis of a single locus may miss the locus truly related to CAD or ignore the influence of gene interactions on disease. Interaction analysis involving multiple loci can provide an understanding of the role of gene regulatory pathways in diseases.

Our study investigated the genetic relationship between *IL5* and CAD in a Chinese Han population. The results showed that the SNPs in *IL5* might play a role in CAD by affecting the traditional risk factors for CAD and through SNP-SNP interactions, providing a new target for the specific treatment of CAD and a theoretical basis for personalized medicine. However, there are still certain limitations to this study. Populations from different areas may be inconsistent due to geographical and living environments, which results in some differences in genetic background and disease susceptibility. However, in this study, our samples, for the most part, were from the Chinese Han population from central China. Studies in North China or other populations should be validated, and more SNPs should be included in further studies. In addition, our study only found the susceptibility SNPs and possible pathogenesis of CAD through statistical methods from the perspective of genetics, which needs further verification by functional experiments.

Data Availability

All data used to support the findings of this study are available from the corresponding author upon request.

Consent

All participants wrote the informed consent.

Conflicts of Interest

No conflict of interests exist in this work.

Authors' Contributions

L.F.Z., W.J.Z., and M.L.L. conceived and designed the experiments. H.S.Z., Q.W.C., J.T.D., T.X., and M.K.H. performed the experiments and analyzed the data. W.J.Z., M.L.L., and M.K.H. contributed reagents/materials/analysis tools. L.F.Z and J.Y.H. wrote the paper. J. Y and J.Y.H. revised the paper. All authors reviewed the manuscript. Wenjuan Zhang, Junyi He, Meilin Liu, and Mingkai Huang contributed equally to this work.

Acknowledgments

Supplementary Materials

Table S1: information for selected tag SNPs of *IL5*. Table S2: primer sequences for PCR and temperature for PCR and genotyping. Table S3: genotypic association analysis between *IL5* and CAD. Figure S1: LD block of *IL5*. (*Supplementary Materials*)

References

[1] M. E. Marenberg, N. Risch, L. F. Berkman, B. Floderus, and U. de Faire, "Genetic susceptibility to death from coronary heart disease in a study of twins," *The New England Journal of Medicine*, vol. 330, no. 15, pp. 1041–1046, 1994.

[2] P. Libby and P. Theroux, "Pathophysiology of coronary artery disease," *Circulation*, vol. 111, no. 25, pp. 3481–3488, 2005.

[3] G. B. D. Disease, I. Injury, and C. Prevalence, "Global, regional, and national incidence, prevalence, and years lived with disability for 354 diseases and injuries for 195 countries and territories, 1990-2017: a systematic analysis for the Global Burden of Disease Study 2017," *Lancet*, vol. 392, no. 10159, pp. 1789–1858, 2018.

[4] M. Zhou, H. Wang, X. Zeng et al., "Mortality, morbidity, and risk factors in China and its provinces, 1990-2017: a systematic analysis for the Global Burden of Disease Study 2017," *Lancet*, vol. 394, no. 10204, pp. 1145–1158, 2019.

Retraction

Retracted: The Therapeutic Roles of Cinnamaldehyde against Cardiovascular Diseases

Oxidative Medicine and Cellular Longevity

This article has been retracted by Hindawi, as publisher, following an investigation undertaken by the publisher [1]. This investigation has uncovered evidence of systematic manipulation of the publication and peer-review process. We cannot, therefore, vouch for the reliability or integrity of this article.

Please note that this notice is intended solely to alert readers that the peer-review process of this article has been compromised.

Wiley and Hindawi regret that the usual quality checks did not identify these issues before publication and have since put additional measures in place to safeguard research integrity.

We wish to credit our Research Integrity and Research Publishing teams and anonymous and named external researchers and research integrity experts for contributing to this investigation.

The corresponding author, as the representative of all authors, has been given the opportunity to register their agreement or disagreement to this retraction. We have kept a record of any response received.

References

[1] L. Lu, Y. Xiong, J. Zhou, G. Wang, B. Mi, and G. Liu, "The Therapeutic Roles of Cinnamaldehyde against Cardiovascular Diseases," *Oxidative Medicine and Cellular Longevity*, vol. 2022, Article ID 9177108, 23 pages, 2022.

Review Article

The Therapeutic Roles of Cinnamaldehyde against Cardiovascular Diseases

Li Lu [ID],[1] Yuan Xiong [ID],[1] Juan Zhou [ID],[2] Guangji Wang,[3] Bobin Mi [ID],[1] and Guohui Liu [ID][1]

[1]*Department of Orthopaedics, Union Hospital, Tongji Medical College, Huazhong University of Science and Technology, Wuhan 430022, China*
[2]*Department of Cardiology, Hubei Provincial Hospital of Traditional Chinese Medicine, Wuhan 430073, China*
[3]*Department of Cardiology, The Central Hospital of Wuhan, Tongji Medical College, Huazhong University of Science and Technology, Wuhan 430014, China*

Correspondence should be addressed to Bobin Mi; mibobin@hust.edu.cn and Guohui Liu; liuguohui@hust.edu.cn

Evidence from epidemiological studies has demonstrated that the incidence and mortality of cardiovascular diseases (CVDs) increase year by year, which pose a great threat on social economy and human health worldwide. Due to limited therapeutic benefits and associated adverse effects of current medications, there is an urgent need to uncover novel agents with favorable safety and efficacy. Cinnamaldehyde (CA) is a bioactive phytochemical isolated from the stem bark of Chinese herbal medicine Cinnamon and has been suggested to possess curative roles against the development of CVDs. This integrated review intends to summarize the physicochemical and pharmacokinetic features of CA and discuss the recent advances in underlying mechanisms and potential targets responsible for anti-CVD properties of CA. The CA-related cardiovascular protective mechanisms could be attributed to the inhibition of inflammation and oxidative stress, improvement of lipid and glucose metabolism, regulation of cell proliferation and apoptosis, suppression of cardiac fibrosis, and platelet aggregation and promotion of vasodilation and angiogenesis. Furthermore, CA is likely to inhibit CVD progression via affecting other possible processes including autophagy and ER stress regulation, gut microbiota and immune homeostasis, ion metabolism, ncRNA expression, and TRPA1 activation. Collectively, experiments reported previously highlight the therapeutic effects of CA and clinical trials are advocated to offer scientific basis for the compound future applied in clinical practice for CVD prophylaxis and treatment.

1. Introduction

In the past decade, cardiovascular diseases (CVDs) contributed the most to mortality and disability across the world, accounting for an estimated 18 million fatalities annually. According to the WHO statistics, more than 500 million people were suffering from CVDs in 2019, which is approximately double that in 2009 [1–3]. The number of CVDs patients has rapidly increased recently mostly because of the lack of physical exercise, consumption of high calorie diet, air pollution, and other factors [1, 4]. As numerous pathogenic events, such as inflammatory response and oxidative stress, as well as highly prevalent predisposing threats,

such as diabetes and obesity, are associated with CVDs, the effects of currently available drugs on the prevention and treatment of CVDs are unsatisfactory, despite the advancements in basic research and improvements of clinical therapies [5–8]. This fact, along with the side effects associated with long-term use of synthetic anti-CVD medicines, such as aspirin, statins, and diuretics, implies a tremendous unmet need for exploring complementary and alternative approaches with high safety and efficacy for CVD management [9].

There is growing interest in naturally occurring products because of their easy availability, low toxicity, and favorable efficiency in reducing the incidence and severity of many

health issues [10, 11]. Cinnamon, a popular spice and a type of traditional herbal medicine, has been widely applied to alleviate illness and improve health in Asian countries [12]. Historically, cinnamaldehyde (CA) has been a major active ingredient of the essential oil extracted from the stem bark of cinnamon. In addition to its use as a spice and a flavoring additive in foodstuff and perfumes, CA has been reported to exhibit protective roles against several diseases, including endotoxemia, sepsis, diabetes, ulcerative colitis, and arthritis [13–17]. Accumulating evidence demonstrates that CA can potentially inhibit the initiation and progression of CVDs, and the therapeutic potential of CA is brought by its pleiotropic pharmacological properties involving anti-inflammatory, antiapoptotic, antioxidative, vasodilatory, hypolipidemic, and proangiogenic activities [18–23]. For instance, oral gavage of CA alleviated the progression of plaque lesions via inhibiting the systemic inflammation and regulating blood lipid profiles [22]. Another study reported that the severity of cardiac fibrosis was evidently ameliorated after CA administration in fructose-fed rats [19]. This integrated review summarized and evaluated the current knowledge about the cardiovascular protective actions and relevant molecular mechanisms of CA, with the hope to facilitate future development of discovering new anti-CVD candidates with real-world applications.

2. Progress in the Pharmacological Characteristics of CA

2.1. Chemical Composition of Cinnamon. The genus Cinnamomum, which belongs to the Lauraceae family, consists of nearly 250 species mostly cultured in the East and South Asia. As a generic term, cinnamon mainly contains two plant species Cinnamomum verum and Cinnamomum cassia Blume. Cinnamon is broadly used as a fragrance additive in daily chemical and dietary supplement industries [13, 14]. Of note, cinnamon has obtained a lot of attention in recent years, due to its stated health benefits [12, 24]. It is documented that the volatile essential oils, the major source of CA, are mainly isolated from the dried stem bark of cinnamon, owing that this segment contains the highest content of oils in the plant, up to 2.5% of bark weight [14, 25]. CA, a yellow and viscous aldehyde liquid constituting nearly 90% of the essential oils, was first purified by Dumas and Péligot via steam distillation and then was synthesized by Chiozza in 1850s [15]. With the development of isolation technique and biosynthetic method, it is convenient to obtain CA and its bioactive derivatives possessing excellent cardiovascular protective properties have been found, including 2-methoxycinnamaldehyde, 2-benzoyloxycinnamaldehyde, 2-hydroxycinnamaldehyde, α-bromo-4-chlorocinnamaldehyde, and cinnamic acid [26–30]. The chemical structures of CA and the derivatives are presented in Figure 1.

2.2. Physicochemical and Pharmacokinetic Profiles of CA. Extensive research has been conducted to investigate the physicochemical features of CA. Laboratory data has revealed that CA, which naturally exists in *trans*-CA form, is poorly dissolved in water but possesses superior solubility in organic solvents such as ethyl alcohol, acetic acid, and propylene glycol [15, 31]. Furthermore, CA is volatile and can be easily oxidized to cinnamic acid when exposed to an oxygen-owning environment, which makes it unstable in the bloodstream [32]. With a molecular formula of C_9H_8O weighing 132.2, CA (or 3-phenyl-2-propenal) displays a relatively low melting point of -7.5°C and a high boiling point of 248°C, determining its liquid form in the daily application [14, 31]. Considering that the pharmacokinetic parameters of medications are vital for the apprehension of functional mechanisms and the guidance of further clinical practice, several scholars have analyzed the pharmacokinetics of CA through multiple detection techniques [31–39] (Table 1). Based on the results of gas chromatography-mass spectrometry, intravenous administration was a preferable mode of bioavailability for CA when compared to the oral route, as reflected by the low AUC_{0-t}, short $T_{1/2}$ and T_{max}, and high C_{max} in the group that adopted intravenous delivery [35]. Another study explored CA distribution in vivo and discovered that CA was rapidly absorbed and distributed in tissues such as the heart, liver, spleen, lung, kidney, brain, stomach, and intestine, reaching the peak levels in most tissues within 6 h after oral gavage of CA. The spleen was reported to be the major tissue possessing relatively high CA concentration, expect for the digestive tract, implicating the regulatory roles of CA in inflammatory responses and immune functions [40]. In terms of metabolic transformations, the stomach, intestine, and liver are the principal parts required for the biological conversion of CA, which is possibly be related to the low bioavailability of oral administration [40, 41]. With a structure of α, β-unsaturated aldehyde, CA is more prone to oxidization via enzymatic catalysis, followed by degradation to benzoic acid, and ultimately, getting excreted through urine mainly in the form of hippuric acid [42, 43]. Additionally, concentrations of CA and its metabolites in vivo are difficult to determine after 24 h, which indicates CA's properties of rapid elimination from the body without any long-term accumulation [40].

2.3. Drug Carriers of CA. Although CA has been approved as a generally safe compound by the Food and Drug Administration (FDA) in America and Europe, the low aqueous dissolvability, high volatility, and instability of CA weaken its effectiveness and thereby limit its utilization to some extent [13, 14]. Experimental data has revealed that ≥80% of CA was metabolized when it entered the body [42]. From the perspective of the beneficial pharmacological effects of CA, interests in developing drug encapsulation carriers incorporated with CA are gaining great popularity in enhancing the bioavailability and efficacy of CA. For this purpose, vehicle substrates of the delivery system are incorporated into a matrix to produce small capsules that can protect the active compounds from external factors. This approach elevates the water solubility, stability, and circulatory half-life of the entrapped agents in vivo [44]. Some materials with preferred biodegradability, biocompatibility, and nontoxicity have been used as vectors of CA, which include microemulsion, nanoparticle, polymeric micelle, liposome, nanofiber, and liquid crystal gel [45–65] (Table 2). Zhao et al. suggested that CA encapsulated in submicrometer emulsions exhibited
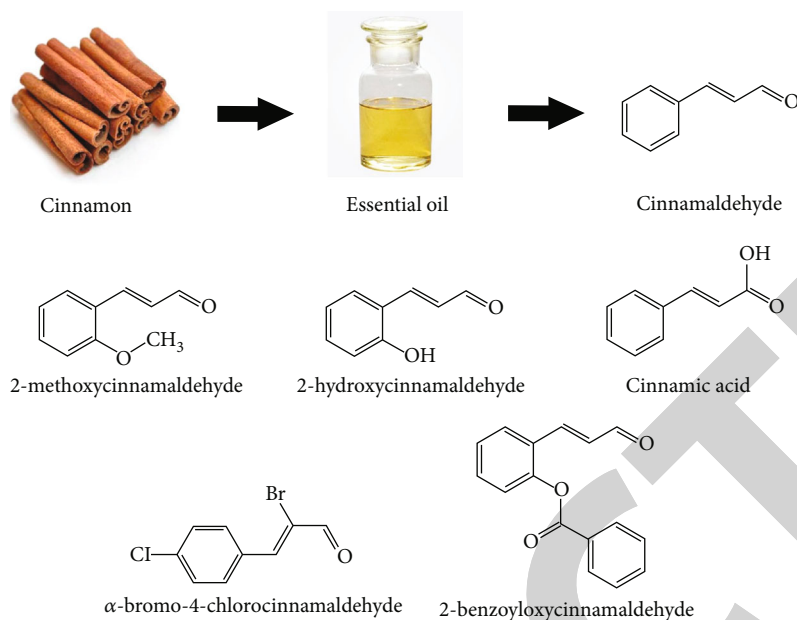
Figure 1: The chemical structures of CA and its derivatives.

higher plasma concentration, faster tissue distribution, and better antitumor effects in rats when compared to CA alone [32]. Similarly, Dong et al. reported that nanogel packaging of CA enabled the controlled release and oxidation inhibition of drug and oxidation inhibition, which consequently increased CA's bioavailability and more effectively promoted cancer cell apoptosis [53]. With the advancement in molecular biology, a large number of bioactive substances, including dextran, silica, chitosan, cyclodextrin, and hyaluronic acid, have been found to synthesize carriers for improving the therapeutic efficacy of CA [46, 48, 51, 53, 60]. Furthermore, other agents such as suberin, polysorbate 80, and egg yolk lecithin have been reported to be effective in increasing the stability of delivery systems [59, 63]. Recently, some studies indicated that the submicron emulsion loading of CA potently alleviated the development of idiopathic pulmonary fibrosis by inhibiting inflammation and oxidative stress [66]. On the other hand, another study demonstrated that cinnamon essential oil entrapped in emulsions exhibited eminent hypolipidemic, hypoglycemic, and antioxidant effects in diabetic rats [67]. Owing to the impellent effects of inflammation, oxidative injury, and lipid and glucose metabolism disorder on CVD progression, these vehicles might also compliment the roles of CA in the treatment of CVDs; however, these notions remain to be established.

3. Protective Activities of CA in the Management of CVDs

3.1. Amelioration of Inflammatory Response. Inflammation is recognized as a necessary physiological process of the host in response to pathogen invasion or tissue damage, which ultimately results in restoration of internal hemostasis. Nonetheless, inappropriate inflammation persistence is an obnoxious pathological phenomenon that might stimulate

the production of plentiful inflammatory cytokines and then induce tissue destruction and organ dysfunction, eventually leading to severe disorders [68, 69]. Chronic inflammation acts as the key threat in the pathogenesis of CVDs. It is already known that inflammation involves the reactions of different types of cells, among which the macrophages exert principal accelerative roles. On activation by diverse proinflammatory stimuli, macrophages generate an excess amount of cytokines and enzymes by driving intracellular inflammation-associated signaling transduction and inactivating and degrading IκB, followed by the activation of NF-κB which translocate into the nucleus and transcribes a mass of proinflammatory genes [11, 70, 71]. CA was reported to reduce the contents of iNOS and COX-2 in RAW264.7 macrophages and the concentrations of TNF-α, NO, and PGE$_2$ in a culture media by suppressing LPS-evoked activation of NF-κB [72, 73]. Schink et al. reported a reduction in the level of IL-8 by LPS-stimulated THP-1 cells after pretreatment with *trans*-CA, and the potential mechanism behind this action was possibly due to the drug-induced restraint of TLR4 oligomerization and the subsequent inflammation signal flow, followed by phosphorylation inhibition of Akt and IκB, which retained NF-κB in the cytoplasm in an inactive form [74, 75]. In addition to prohibiting the translocation of NF-κB into the nucleus, *trans*-CA was demonstrated to exhibit inhibitory roles against the DNA-binding activities of NF-κB under the stimulation of inflammation factors [76]. Via inducing the maturation and the release of IL-1β, NLRP3 inflammasome serves as a fundamental inflammation-promoting regulator. There was evidence that CA intervention delayed NLRP3/IL-1β signal pathway by blocking the succinate/HIF-1α axis in macrophages [17]. Moreover, Kim et al. reported that *trans*-CA could mitigate LPS-provoked activation of ERK1/2, JNK, and p38, accompanied by reduction of contents of iNOS, IL-1β, IL-6, and TNF-α in RAW264.7 cells [77].

TABLE 1: The in vivo pharmacokinetic features of CA.

Formulation	Sample	Dosage of contained CA	Delivery route	Detection method	Parameters					Ref.
					T_{max}	C_{max}	AUC0-t	$T_{1/2}$	MRT	
CA	Male F344 rat plasma	250 mg/kg	Oral	HPLC	0.4 ± 0.1 h	1.3 ± 0.2 µg/mL	10.5 ± 1.2 µg·h/mL	—	—	[33]
		500 mg/kg			4.1 ± 0.9 h	2.4 ± 0.4 µg/mL	35.2 ± 1.4 µg·h/mL	11.0 ± 0.6 h	—	
ME-CA		250 mg/kg			1.9 ± 0.5 h	1.2 ± 0.1 µg/mL	14.7 ± 2.0 µg·h/mL	—	—	
		500 mg/kg			2.7 ± 0.8 h	1.8 ± 0.1 µg/mL	36.2 ± 4.2 µg·h/mL	12.0 ± 1.2 h	—	
CA	Male SD rat plasma	20 mg/kg	Intravenous	GC-MS	0.04 ± 0.02 h	547 ± 142 ng/mL	375 ± 83.5 ng/L	3.26 ± 2.82 h	0.96 ± 0.21 h	[32]
SME-CA		20 mg/kg			0.04 ± 0.02 h	1052 ± 184 ng/mL	589 ± 59.2 ng/L	2.17 ± 0.96 h	0.84 ± 0.14 h	
Guizhi-gancao decoction	Male rat plasma	47 mg/kg	Oral	UPLC-MS/MS	0.2 ± 0.1 h	1.1 ± 0.5 ng/mL	2.1 ± 0.2 ng·h/mL	1.5 ± 0.3 h	—	[34]
CA	Male SD rat plasma	50 mg/kg	Oral	HPLC	0.33 ± 0.05 h	301.6 ± 67.9 mg/L	447.1 ± 3.8 mg·h/L	—	—	[31]
CA-SME		50 mg/kg			1.00 ± 0.13 h	1063.4 ± 165.4 mg/L	1802.2 ± 80.8 mg·h/L	—	—	
CA	Male SD rat plasma	125 mg/kg	Oral	GC-MS	1.8 ± 0.4 h	82 ± 15 ng/mL	677 ± 127 ng·h/mL	6.8 ± 2.6 h	5.8 ± 1.3 h	[35]
		250 mg/kg			2 ± 0.7 h	121 ± 14 ng/mL	1141 ± 265 ng·h/mL	6.2 ± 1.5 h	7.1 ± 1.6 h	
		500 mg/kg			1.6 ± 0.5 h	249 ± 36 ng/mL	1984 ± 531 ng·h/mL	6.7 ± 1.5 h	7.6 ± 0.6 h	
		20 mg/kg	Intravenous		0.03 h	547 ± 142 ng/mL	355 ± 53 ng·h/mL	1.70 ± 0.32 h	0.8 ± 0.2 h	
TCA gel	Male Wistar rat plasma	100 mg/kg	Percutaneous	UPLC	1.83 ± 1.07 h	9.71 ± 5.92 µg/mL	58.4 ± 25.4 mg·h/mL	—	4.52 ± 1.05 h	[36]
TCA V2 phase		100 mg/kg			7.33 ± 3.59 h	8.09 ± 2.16 µg/mL	42.9 ± 29.6 mg·h/mL	—	10.7 ± 2.9 h	
TCA H2 phase		100 mg/kg			1.20 ± 0.46 h	11.33 ± 1.90 µg/mL	94.1 ± 10.9 mg·h/mL	—	6.34 ± 1.34 h	
CA	Male SD rat plasma	250 mg/kg	Oral	HPLC	0.31 ± 0.07 h	70.40 ± 23.91 µg/mL	—	—	2.9 ± 0.71 h	[37]
CA-SEDDS		250 mg/kg			0.92 ± 0.20 h	182.0 ± 29.2 µg/mL	—	—	1.76 ± 0.20 h	
CRO	Male rat plasma	12.52 mg/kg	Oral	UHPLC-MS/MS	1.0 ± 0.0 h	22.7 ± 3.2 ng/mL	131 ± 6.7 ng·h/mL	8.7 ± 0.7 h	—	[38]
SBP	Male SD rat plasma	15.73 mg/kg	Oral	HS-SPDE-GC-MS/MS	0.50 ± 0.23 h	18.76 ± 2.11 ng/mL	262.2 ± 63.9 ng·h/mL	13.3 ± 5.8 h	9.80 ± 0.66 h	[39]

ME-CA: microencapsulated CA; SME-CA: submicrometer emulsion of CA; CA-SME: CA submicron emulsion; TCA: *trans*-CA; TCA V2 phase: TCA V2 phase: a compound contains phytantriol, water, and *trans*-CA; TCA H2 phase: a compound contains phytantriol, triglyceride, water, and *trans*-CA; CA-SEDDS: CA with self-emulsifying drug delivery systems; CRO: *Cinnamoni Ramulus*; SBP: Shexiang Baoxin Pill; T_{max}: the time to reach C_{max}; C_{max}: the maximum plasma concentration; AUC$_{0-t}$: area under the curve to termination time; $T_{1/2}$: half-life; MRT: mean residence time; HPLC: high-performance liquid chromatography; GC-MS: gas chromatography-mass spectrometry; UPLC-MS/MS: ultraperformance liquid chromatography-tandem mass spectrometry; UPLC: ultraperformance liquid chromatography; UHPLC-MS/MS: ultrahigh-performance liquid chromatography-tandem mass spectrometry; HS-SPME-GC-MS: headspace solid-phase microextraction coupled to gas chromatography-mass spectrometry.

TABLE 2: The parameters of drug delivery vehicles loading CA.

Formulation	Carrier	Average diameter	Polymer dispersion index	Zeta potential	Entrapment efficiency	Application	Ref.
Nanoparticle	P-SS-D	125 nm	0.16	—	—	Antitumor	[45]
Nanoparticle	Dextran, 10-hydroxy camptothecin	182.3 nm	0.225	-3.86 mV	57.6%	Antitumor	[46]
Nanoparticle	PLGA	130.4 nm	0.512	-3.54 ~ -3.86 mV	—	Antifungal	[47]
Inclusion complex	β-Cyclodextrin	2-4 μm	—	—	45.39%	Antioxidant	[48]
Liposome	DSPE-PEG2000-PMB	150~200 nm	0.1 ~ 0.2	0 ~ 10 mV	31.93 ± 0.6%	Antibacteria	[49]
Liposome	Egg yolk lecithin, tween 80, chitosan	550~650 nm	—	60~80 mV	50~60%	Antibacteria	[50]
Nanocapsule	Chitosan	165 ± 6 nm	0.18	42 ± 5 mV	78 ± 3%	Antibacteria	[51]
Nanoparticle	Chitosan	254.66 nm	0.28	15.26 mV	77.3%	Antitumor	[52]
Nanoparticle	MSN@GO-HA	115.59 ± 13.98 nm	0.25 ± 0.02	−27.53 ± 4.56 mV	84.36 ± 3.52%	Antitumor	[53]
Submicrometer emulsion	Soybean oil, egg lecithin, glceriunm	130 ± 5.92 nm	—	−25.7 ± 6.0 mV	99.5 ± 0.25%	Antitumor	[32]
Nanovesicle	Hyaluronic acid, ethanol	250~350 nm	—	-25 ~ -30 mV	75~ 85%	Antiulcerative colitis	[54]
Liposome	DODAB:MO	545 ± 17 nm	0.46 ± 0.06	48.2 ± 2.1 mV	44.1 ± 2.7%	Antifungal	[55]
Nanoparticle	GNP	326 ± 48 nm	—	−45 ± 1 mV	—	Antibacteria	[56]
Microsphere	PHBV/MBGN	7.2 ± 1.5 μm	0.4 ± 0.1	−21.3 ± 0.5 mV	99.96 ± 0.01%	Antiosteomyelitis	[57]
Nanoparticle	PSCI	123.4 nm	—	-11.4 mV	41.4%	Antitumor	[58]
Liposome	Egg yolk lecithin, tween 80, ethanol	75~ 92 nm	<0.3	—	30~ 40%	Antibacteria	[59]
Nanosphere	SiO$_2$, hydrogel	200~ 250 nm	—	5 ~ 15 mV	—	Antiwound infection	[60]
Nanogel	PssNCT	200 nm	0.155 ± 0.016	-25~ 0 mV	86.3%	Antitumor	[61]
Nanoparticle	Hyaluronic acid, mesoporous silica	100 nm	—	12.3 mV	—	Antibacteria	[62]
Nanoparticle	Suberin	80~ 110 nm	0.16~ 0.23	-30 mV	—	Antibacteria, antitumor	[63]
Nanocapsule	LNC	99 ± 6 nm	0.120 ± 0.024	−17.7 ± 2.12 mV	—	Antibacteria	[64]
Nanoparticle	Hyaluronic acid	166.0 ± 9.5 nm	0.198 ± 0.005	—	—	Antitumor	[65]

P-SS-D: an amphiphilic polymer skeletal containing 1,3-dimercapto-2-propanol, 1,3-dimercaptopropane, N,N′-carbonyldiimidazole, DOPA, triethylamine; PLGA: DL-lactide-co-glycolide; DSPE-PEG2000-PMB: a liposomal system containing N-hydroxy succinimide, polymyxin B, 1-(3-dimethylaminopropyl)-3-ethylcarbodiimide, DSPE-PEG2000-COOH; MSN@GO-HA: graphene oxide wrapped mesoporous silica nanoparticles modified with hyaluronic acid; DODAB:MO: a system of dioctadecyldimethylammonium bromide and monoolein; GNP: gold nanoparticles; PHBV/MBGN: polyhydroxybutyrate-co-hydroxyvalerate with mesoporous bioactive glass nanoparticles; PSCI: platelet membrane-coated mesoporous silica nanoparticles; PssNCT: N-isopropylacrylamide-co-CA-co-D-α-tocopheryl polyethylene glycol 1000 succinate; LNC: a lipid nanocapsule containing polyxyl 15 hydroxystearate, hydrogenated lecithin, triglycerides.

Considering that MAPK cascades involving ERK1/2, JNK, and p38 axis are well-established contributors to the development of inflammation, this agent possibly displays anti-inflammatory effects by weakening the activities of MAPKs signaling molecules (Figure 2(a)). Apart from encumbering the production of proinflammatory elements such as TNF-α, IL-6, IL-8, NLRP3, and COX-2, CA had been demonstrated to increase the generation of anti-inflammatory cytokines IL-10 and TGF-β, partly owing to the facilitation of

macrophage polarization toward M2 phenotype and the suppression of M1-related proteins production, although the precise mechanisms remained elusive [78, 79].

In the pathological niche, proinflammatory mediators induce vascular endothelial cells (ECs) to elaborate many bioactive substances, such as interleukins, prostaglandins, and adhesion molecules. These inflammatory constituents trigger the disorders of biological properties of ECs, which is termed as endothelial dysfunction, an important
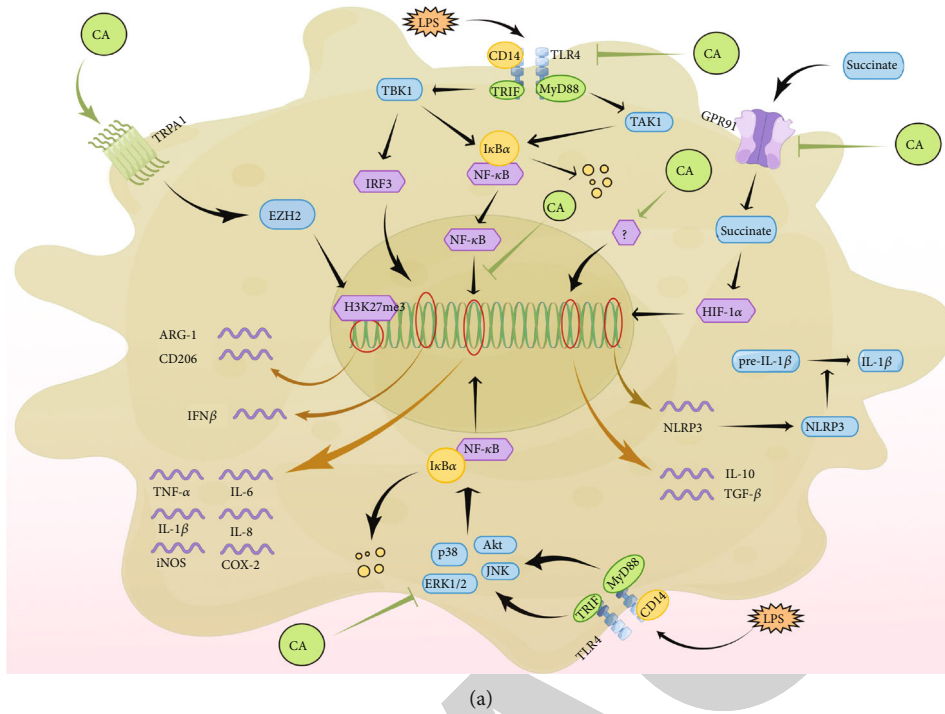
(a)
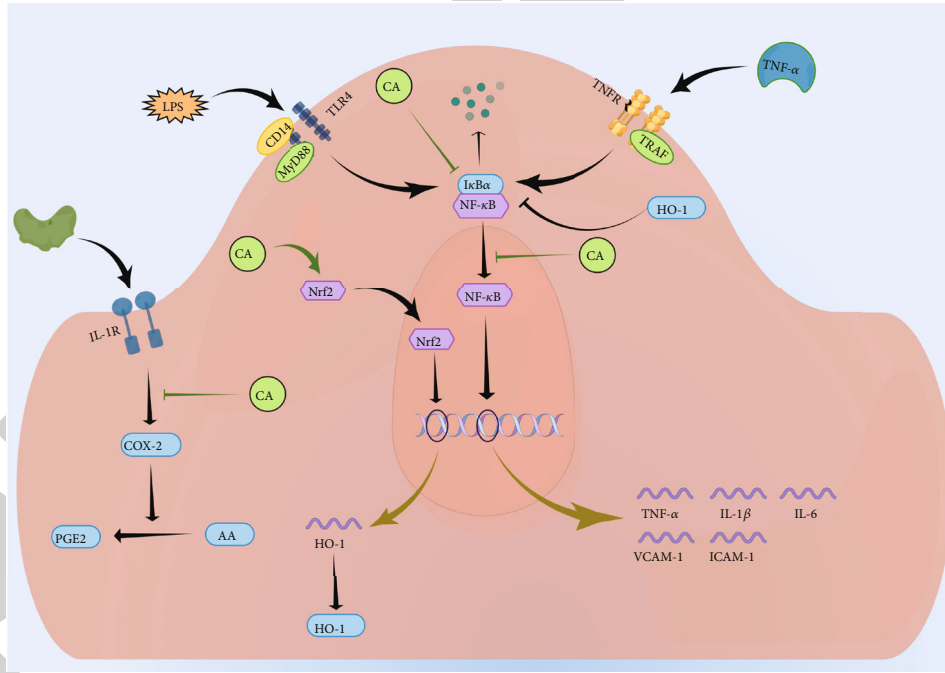
(b)

FIGURE 2: (a) The potential signal cascades regulated by CA for affecting inflammation development in macrophages. CA inhibits the expression of proinflammatory factors via suppressing the activities of NF-κB and HIF-1α and facilitates M2 phenotype transformation via regulating EZH2 activity. LPS: lipopolysaccharide; TLR4: Toll-like receptor 4; MyD88: myeloid differentiation primary response 88; TRIF: Toll/IL-1R domain-containing adaptor-inducing IFN-β; TAK1: TGF-β-activated kinase 1; TBK1: tank binding kinase 1; NF-κB: nuclear factor of κB; IRF3: interferon regulatory factor 3; GPR91: G-protein-coupled receptor 91; EZH2: enhancer of zeste homolog 2; TRPA1: transient receptor potential ankyrin-1; HIF-1α: hypoxia-inducible factor-1α; H3K27me3: histone H3 lysine 27 trimethylation; ARG-1: arginase-1; NLRP3: NOD-like receptor family pyrin domain containing 3; IL-1β: interleukin-1β; TGF-β: transforming growth factor-β; JNK: c-Jun N-terminal kinase; ERK1/2: extracellular signal-regulated kinase 1/2; Akt: protein kinase B; iNOS: inducible nitric oxide synthase; COX-2: cyclooxygenase-2; TNF-α: tumor necrosis factor α; IFNβ: interferon β. (b) CA exerts beneficial roles against inflammation response in ECs induced by cytokines. NF-κB is regarded as the main target involved in the anti-inflammatory effects of CA. HO-1: heme oxygenase-1; VCAM-1: vascular cell adhesion molecule-1; ICAM-1: intercellular adhesion molecule-1; Nrf2: nuclear factor erythroid-2-related factor 2; AA: arachidonic acid; PGE2: prostaglandin E2.

predisposing risk event contributing to CVD development [80, 81]. Results from Liu et al. demonstrated that the increment of LPS-evoked mRNA and protein contents of IL-1β, IL-6, and TNF-α in ECs was reversed by preincubation of CA in a dose- and time-dependent manner. The authors further analyzed the mechanisms and found that the transduction blockade of the TLR4/NF-κB pathway was implicated in anti-inflammatory actions of CA [82]. Moreover, CA had been reported to prevent the rise in the concentration of PGE$_2$ in IL-1β-insulted ECs by decreasing the activity of COX-2 [83]. Moreover, the upregulation of adhesion molecules on ECs leads to excessive recruitment of circulating leukocytes on the endothelial layer and then facilitates their infiltration across the tunica intima and into the subendothelium, where the leukocytes release excessive inflammation effectors that aggravate the vasculature damage [80]. An experiment performed by Liao et al. claimed that the exposure of ECs to CA led to a time-dependent increment in the IκB protein level, followed by the abrogation of NF-κB activation and the expression of inflammatory genes VCAM-1 and ICAM-1, resulting in the disruption of TNF-α-initiated monocytes adhesion to the EC monolayer [84] (Figure 2(b)). Interestingly, another scholar uncovered that CA administration could potently suppress VCAM-1 generation by disrupting NF-κB nuclear translocation in umbilical vein ECs insulted by TNF-α, without affecting the production of ICAM-1 and the phosphorylation of NF-κB [85]. The discrepancies observed between these two studies might be explained by the differences in the cell types, dosage, and intervention duration of CA and the participating anti-inflammatory signaling cascades.

Increasing investigations have placed a focus on the involvement of vascular smooth muscle cells (VSMCs) in the development of vascular inflammatory diseases, as there is proof that activated VSMCs display contributing roles to the vessel disorder through producing vast proinflammatory factors [86]. It was clarified that CA had the capacity of antagonizing ox-LDL-elicited inflammation response in VSMCs, as seen by contents decrement of TNF-α, IL-6, MCP-1, and NO, which was attributed to CA-induced inhibition of inflammatory signaling pathways containing JNK, p38, and NF-κB [87].

With respect to the anti-inflammatory functions of CA in vivo, several studies were conducted to explore this trait using different animal models. Using ApoE$^{-/-}$ mice with high fat diet (HFD) for 12 weeks to induce atherosclerotic model, Li et al. showed that supplement with CA for consecutive 8 weeks significantly reduced the size of atheroma plaques in the aorta. Furthermore, they observed that CA treatment caused inflammation alleviation in mice, as indicated by phosphorylation reduction of aortic IκB and NF-κB as well as levels decrement of blood IL-6, MCP-1, TNF-α, and NO [22]. It is speculated that the antiatherosclerotic actions of CA could be explained by the inflammation suppression at least in part, by the fact that the inflammatory reaction has been illustrated to present indispensable effects in each stage of plaque lesion development. Accumulating statistics manifest that viral infection-triggered inflammation in myocarditis could collapse homeostasis of myocardial cells and

arrangement integrity of myocardial tissues, leading to irreversible cardiac injury. It was revealed that intraperitoneal administration of CA to BALB/c mice infected with coxsackie virus B3 obviously reduced the severity of myocarditis, as indicated by abatement of necrosis, calcification, and fibrosis in the heart tissue, which was associated with the amelioration of myocardial inflammation infiltration resulting from CA-elicited inhibition of TLR4/NF-κB cascade transduction and expressions diminishment of target inflammatory molecules including TNF-α, iNOS, IL-1β, and IL-6 [29, 88]. These in vitro and in vivo studies suggest that the CA's effectiveness in delaying inflammation mainly derives from its abilities in interrupting proinflammatory gene expression via suppressing upstream NF-κB activation.

3.2. Improvement of Oxidative Stress. Accumulating evidences support that occurrence of oxidative stress is either due to the overproduction of reactive oxygen species (ROS) or impairment of the antioxidant defense system, which leads to an imbalance between oxidants and ROS scavengers tilting toward an oxidative status. These free radicals, including superoxide anion, hydrogen peroxide, and hydroxyl radical, could directly induce lipid peroxidation, protein oxidation, and DNA damage, which, in turn, results in abnormalities in the cellular structure and functions, including loss of membrane integrity, disarrangement of the cytoskeleton, alterations in energy metabolism, and cascade signal flow, as well as the onset of apoptosis-related events, thereby giving rise to the vascular and myocardial injury [11, 89]. It was reported that the protective effects of CA could, to some extent, be interpreted by its repressive actions on oxidative stress, as reflected by content decrement of oxidation damage biomarker malondialdehyde (MDA) in the circulation of HFD-fed mice with plaque regression following CA administration [22]. This observation was confirmed by another independent study implemented by Nour et al., wherein oral gavage of CA to rabbits fed with a high-cholesterol diet for 4 weeks inhibited the development of atherosclerosis. Meanwhile, they showed that CA treatment could effectively lead to a significant decrease in the levels of MDA and myeloperoxidase (MPO) and an increase in the activities of enzymatic antioxidants superoxide dismutase (SOD) and catalase (CAT) in the aortic tissues, respectively [90]. Concerning the regulatory roles in the redox condition of vascular cells, CA could normalize the contents of ROS and MDA in ox-LDL-stimulated ECs by enhancing the level of SOD via activating nuclear factor erythroid-2-related factor 2 (Nrf2), an important transcriptional factor responsible for the expression of antioxidative genes, as reported by Li and colleagues [91]. In agreement, evidence from in vitro experiments attributed antioxidative abilities of CA to its contributing roles in facilitating the transduction of the p38 pathway and the activation of Nrf2, accompanied by generation of antioxidant defense enzyme heme oxygenase (HO-1) in ECs irritated by H$_2$O$_2$ [85].

Previous studies have indicated that one essential reason why hyperglycemia is believed to be implicated in the etiology of CVDs is accounted for its inducible capacity in favoring oxidative stress. Advanced glycation end products

(AGEs), formed by nonenzymatic reactions of glycolysis intermediates with proteins and/or lipids, are capable of increasing intracellular ROS level by interacting with the receptors (RAGE) which, in turn, activate NADPH oxidase (NOX), the primary enzyme responsible for ROS biosynthesis [92, 93]. Some scholars certified that CA produced inhibitory roles in the transduction of AGEs/RAGE/NOX cascade and sequentially improved the ROS overload in a hyperglycemic environment [94]. Moreover, through elevating the expression of antioxidant substances including HO-1, NADPH dehydrogenase quinone 1 (NQO1), CAT, and glutathione peroxidase 1 (GPX1) via strengthening the activity of the Nrf2 signaling pathway, CA alleviated high glucose-induced oxidative damage on ECs and vascular walls, apart from reducing the activities of NOX p22 and p47, as demonstrated by arterial relaxation and remodeling alleviation [95, 96].

After the treatment through reperfusion strategies like stent angioplasty and intravascular thrombolysis, oxygen and other nutrients in the blood swarm into the myocardium previously supplied by an obstructed artery, which elicits an enormous burst in the ROS activity that exceeds the defensive capacity and then cause an undue formation of ROS that ultimately results in cell death, known as cardiac ischemia/reperfusion (I/R) injury [97, 98]. Results from Sedighi et al. showed that the serum activities of SOD, CAT, and GPX were increased and that the concentrations of MDA and lactate dehydrogenase (LDH) were decreased in the presence of CA, followed by a reduction of the infarct size, cTnI level, and duration of arrhythmias in rats suffering from myocardial I/R damage [99]. Further investigations on the potential mechanisms uncovered that CA might mitigate oxidative stress-induced I/R injury by activating Nrf2/HO-1 and Akt/PPARα axis that were responsible for ROS scavenging and suppressing TLR4/NOX4 cascade participating in ROS generation, respectively, thereby lowering ROS-induced NF-κB activation and expression of downstream cytokines participating in cardiomyocyte impairment [18, 95, 96]. In the animal models of cardiac injury evoked by isoproterenol, LPS, and fructose, the therapeutic actions of CA were focused on improving the oxidative status by restraining the ROS producers NOX and xanthine oxidase (XOD) and increasing the levels of antioxidant enzymes SOD, GSH, and CAT, which, in turn, hampered the signal flow of inflammation-related pathways involving JNK, ERK1/2, p38, and TLR4/6-IRAK4/1 axis, eventually causing expression decline of cytotoxic target effectors, such as TNF-α, IL-6, NLRP3, and IL-1β [18, 19, 100] (Figure 3). An increasing number of studies document that ROS functions as an agonist of inflammation-associated signaling pathways and that antioxidants are highly efficient in retarding the inflammatory response. Accordingly, CA is likely to interfere with oxidative stress-provoked cardiovascular injury via regulating distal inflammation signaling cascades.

3.3. Regulation of Blood Lipid and Glucose Metabolism. The perspective that atherosclerosis is regarded as a dyslipidemia-related illness has garnered concern because lipid metabolism dysfunction manifests indispensable effects in each stage of plaque lesions and strategies, therefore extenuating dysfunction of lipid metabolism is effective for the treatment of atherosclerosis

[80]. It was indicated that CA repressed the increase in the levels of TG, TC, and LDL-C in HFD-induced ApoE⁻/⁻ mice, accompanied by a reduction of the atherosclerotic lesion size, which might be due to CA-evoked inhibition of lipid deposition and resultant foam cell formation in the subendothelium. This result conformed to those obtained from other studies involving atherosclerotic animal models demonstrating that CA-elicited protective effects were at least partly linked to the actions of improvements in the lipid profiles [22, 90]. Moreover, another mechanism underlying CA-induced delayed generation of foam cells was that CA weakened activation of the ox-LDL-induced NF-κB pathway and downstream expression of LOX-1 required for devouring oxidized lipoproteins [87]. As is already known, hyperlipidemia results from an imbalance between lipid generation and elimination, and AMPK, a serine/threonine protein kinase, serves as an indispensable cellular energy sensor responsible for multiple metabolic processes including lipid anabolism and catabolism [101]. It had been documented that CA administration induced fatty acid oxidation and halted its synthesis in 3T3-L1 adipocytes via activating AMPK, followed by the inhibition of SREBP1c-FAS/SCD-1/GPAT and phosphorylation of ACC [102]. In terms of other relevant bioactive proteins, the increase in the levels of HSL, DGAT2, and PNPLA2 promoting lipolysis and the reduction in the contents of PLIN, FGF21, aP2, and GPD preventing lipolysis were seen in mature adipocytes treated with CA [103, 104]. Moreover, there was evidence uncovering that CA was capable of enhancing the PKA/p38 MAPK pathway activity to facilitate fat consumption and diminishing the PPAR-γ and C/EBPα expression to reduce fat accumulation in adipocytes [102, 105]. In addition to mediating the metabolic events of adipose cells, CA was found to directly regulate the functions of signal molecules implicated in lipid metabolism in hepatocytes, as reflected by content elevation of phosphorylated AMPK and level decrement of SREBP1c/ACC, whereas the SREBP2 axis, an AMPK target pathway, and its downstream effectors, including HMG-CoA associated with cholesterol production and LDLR implicated in cholesterol ejection, displayed no alteration in the expression levels of CA-fed rat hepatocytes [106]. Considering that the liver acts as the main organ responsible for energy substance metabolism, CA probably exerts cholesterol-lowering roles via affecting the signaling networks in hepatic cells, and elucidating the inner mechanisms is beneficial for paving the way for clinical usage of CA in the management of hypercholesterolemia-triggered CVDs.

A considerable amount of data exists indicating that hyperglycemia as a critical contributor to the pathogenesis of several CVDs such as atherosclerosis, myocardial infarction, hypertension, and cardiomyopathy. Primarily, by means of favoring inflammation reaction and oxidative stress, high blood glucose causes structural and functional damage to diverse cell types such as vascular ECs, VSMCs, circulating monocytes, and myocardial cells, ultimately leading to disorders of the cardiovascular system [107, 108]. Considering the antihyperglycemic potential of CA as previously reported, the glucose-modulating effects of CA were likely to account for its protective roles against CVDs to some extent. With respect to the hypoglycemic mechanisms, CA was found to boost cellular uptake of glucose and
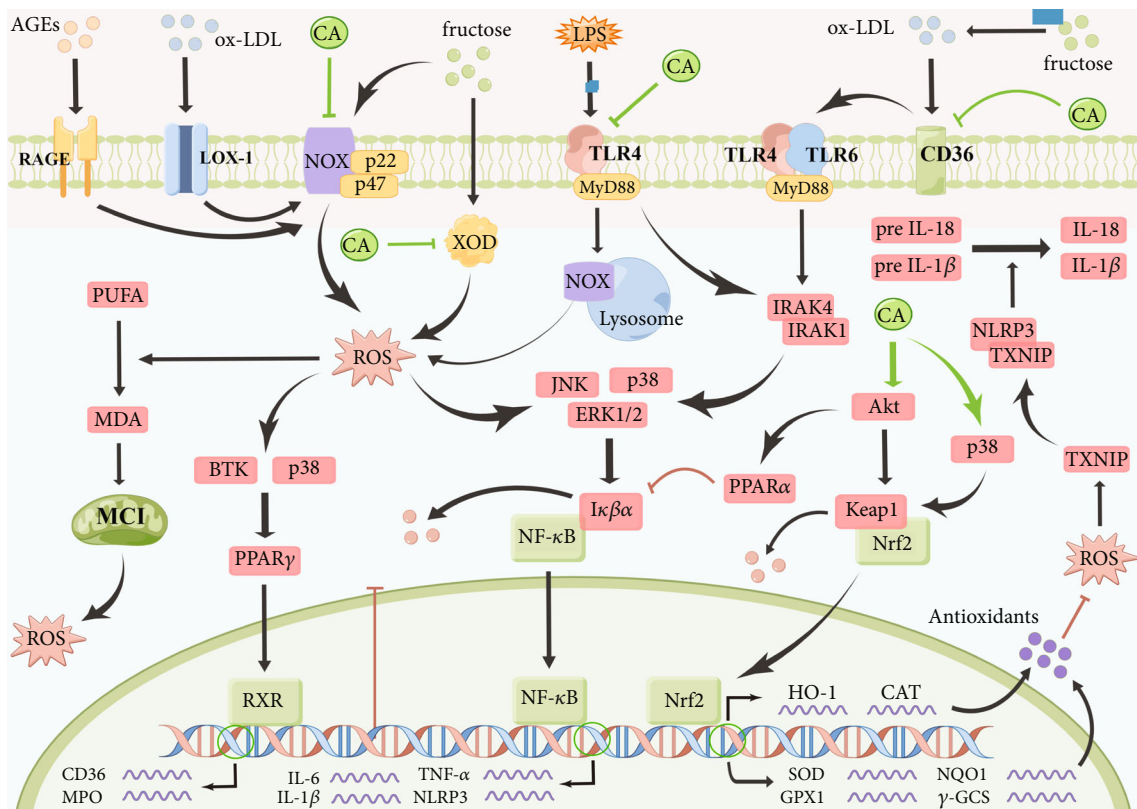
Figure 3: The schematic description of signaling pathways responsible for the actions of CA to alleviate oxidative stress. Activation of multiple membrane receptors increase the activity of NOX which is the main producer of intracellular ROS. Excessive ROS triggers cellular damage by accelerating lipid peroxidation and enhancing signals transduction of inflammatory pathways. CA is capable of improving the imbalance of redox through decreasing the activities of NOX and XOD and increasing the activation of Nrf2 axis. PUFA: polyunsaturated fatty acids; MCI: mitochondrial respiratory chain complex I; TXNIP: thioredoxin-interacting protein; AGEs: advanced glycation end products; RAGE: receptor of AGEs; ox-LDL: oxidized low-density lipoprotein; LOX-1: lectin-like oxidized low-density lipoprotein receptor-1; NOX: NADPH oxidase; XOD: xanthine oxidase; IRAK1: interleukin receptor-associated kinase 1; ROS: reactive oxygen species; MDA: malondialdehyde; PPARα: peroxisome proliferator-activated receptor-α; BTK: Bruton's tyrosine kinase; Keap1: Kelch-like ECH-associated protein 1; RXR: retinoid X receptor; MPO: myeloperoxidase; CAT: catalase; SOD: superoxide dismutase; NQO1: NADPH dehydrogenase quinone 1; GPX1: glutathione peroxidase 1; γ-GCS: γ-glutamyl cysteine synthetase.

glycogen biosynthesis and improve insulin resistance and dysfunction of pancreatic islets [15, 109]. Specifically, via controlling the upstream signaling cascades including PPARs/RXRs, IRS-1/PI3K/Akt, AMPK, retinol binding protein 4, and PGC-1α/MEF2 which were implicated in GLUT4 expression and membrane translocation, the treatment with CA overtly enhanced glucose ingestion and insulin sensitivity in adipose and muscle tissues, thereby leading to the decrement of blood glucose content and HOMA-IR index [94, 110–112]. Considering the excessive gluconeogenesis and insufficient glycogen synthase occurred in the liver of diabetic subjects, CA had been reported to ameliorate glucose metabolism via reversing this disorder through reducing PEPCK and G6Pase activities and strengthening the GYS-2 and PK activities [103, 113] (Figure 4).

3.4. Inhibition of VSMC Proliferation and Migration. Currently, there has been growing attention paid to immoderate proliferation and migration of VSMCs due to their inducible roles in the development of CVDs. Exposed to varying stimuli, VSMCs with a quiescent pattern acquire activated properties

which are characterized by undue growth and movement to target regions to exacerbate tissue hypertrophy, extracellular matrix (ECM) degradation, and remodeling, thereby accelerating the occurrence of several CVDs like restenosis after angioplasty, pulmonary arterial hypertension (PAH), and aortic dissection [86, 114]. By reducing the content of proliferating cell nuclear antigen (PCNA) related to the S phase of cell cycle transition, CA suppressed VSMC proliferation triggered by ox-LDL, by the fact that valid progression of cell cycle was fundamental for the proliferative process [87] (Figure 5). With regard to CA-driven antiproliferative mechanisms, Kwon et al. illustrated that cinnamon extracts containing CA and its derivations probably disrupted the activities of mitosis-related signal molecules including PLCγ1, AKT, JNK, and p38 MAPK to cause cell cycle arrest at G0/G1 and S phase in growth factor-stimulated VSMCs, as indicated by decreased expressions of cyclin D1/E and CDK2/4 and increased levels of p21 and p27 [115]. It is declared that matrix metalloproteinases (MMPs) belong to a group of endopeptidases cleaving ECM constituents and facilitating VSMC mobilization. The reduced migratory abilities were seen in ox-LDL-elicited VSMCs after
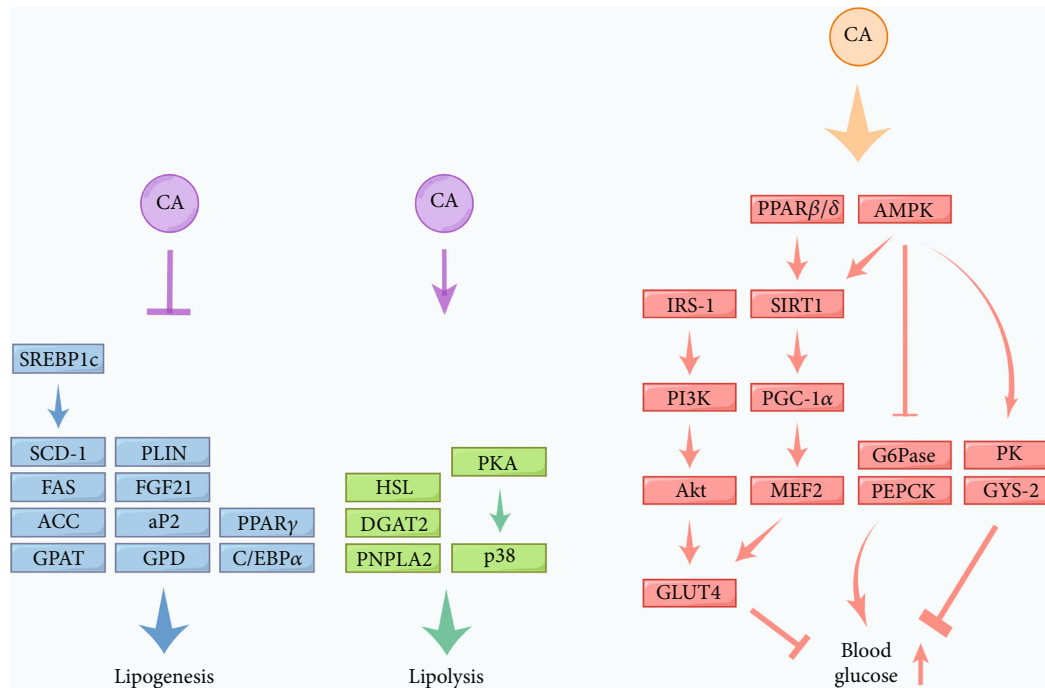
FIGURE 4: CA reduces the concentrations of circulating lipid and glucose by promoting energy catabolism and weakening its anabolism. SREBP1c: sterol regulatory element-binding protein 1c; FAS: fatty acid synthase; SCD-1: stearoyl-CoA desaturase-1; GPAT: glycerol phosphate acyltransferase; ACC: acetyl-CoA carboxylase; PKA: protein kinase A; C/EBPα: CCAAT enhancer-binding protein α; PLIN: perilipin; FGF21: fibroblast growth factor-21; GPD: glyceraldehyde-3-phosphate dehydrogenase; PPARγ: peroxisome proliferator-activated receptor γ; HSL: hormone-sensitive lipase; DGAT2: diacylglycerol O-acyltransferase 2; PNPLA2: patatin-like phospholipase domain containing 2; AMPK: AMP-activated protein kinase; SIRT: sirtuin; PI3K: phosphatidylinositol-4,5-bisphosphate 3-kinase; IRS-1: insulin receptor substrate-1; PGC-1α: peroxisome proliferator-activated receptor-gamma coactivator-1α; GLUT4: glucose transporter 4; MEF2: myocyte enhancer factor 2; G6Pase: glucose-6-phosphatase; PK: pyruvate kinase; PEPCK: phosphoenolpyruvate carboxykinase; GYS-2: glycogen synthase 2.

intervention with CA, which was attributed to drug-induced MMP-2 level diminution by abating p38, JNK, and NF-κB pathway transduction [87]. Meanwhile, a decrease in MMP-2 content and NF-κB activation within aortic tissues was observed in the atherosclerotic mice upon CA gavage [22]. Another study revealed that CA was beneficial for improving the neointimal hyperplasia after balloon injury in diabetic rodent models by activating Nrf2 axis, accompanied by inhibition of VSMC proliferation and migration, which further confirmed the protective effects of CA against VSMCs-driven disorders [116]. Moreover, monocrotaline was reported to trigger PAH, augment myofibril stiffness, and cause an elevation in right ventricular (RV) pressure overload, while CA was capable of inhibiting the monocrotaline-induced increase in RV systolic pressure via ameliorating the RV fibrosis [117]. However, whether CA attenuated the PAH development to improve RV pressure overload was unknown. Considering that uncontrolled growth and mobilization of VSMCs are highly implicated in the progression of PAH, exploring the regulatory roles of CA in pathological processes of this disease might be of great value for the management of PAH.

3.5. Alleviation of Myocardial Fibrosis.
In response to cytokines or ROS-evoked injury, cardiac fibroblasts undergo a programmed conversion into myofibroblasts which release numerous endogenous substances, particularly collagen fibrils, resulting in redundant ECM recruitment and deposi-tion, a process termed myocardial fibrosis. Interest in cardiac fibrosis has increased since the discovery of its contributing properties in deteriorating the reduction of myofiber compliance and exacerbating the dysfunction of heart contraction and dilation [118]. Several studies have ascertained that a variety of biomacromolecule-mediated signals participate in the pathophysiological course of myocardial fibrosis, among which TGF-β is a crucial initiator [119]. Kang and collaborators, by Masson trichrome staining, determined that fructose-induced cardiac fibrosis was markedly improved by CA. They further stated that the antifibrotic capacities of CA might be linked to the blockade of the ROS-CD36 axis, followed by TLR4/6-IRAK4/1-NLRP3 cascade retardation and subsequent inactivation of TGF-β-mediated Smad2/3 and Smad4 pathways [19]. Moreover, the potential of CA to directly encumber the proliferation and activation of TGF-β-induced myocardial fibroblasts was verified by a prominent reduction in the expression of Ki-67 and α-SMA. Further amelioration in the level and accumulation of collagen-I/III in the ventricle was observed. The inner mechanistic analysis manifested that calcitonin gene-related peptide- (CGRP-) dependent restraint of the TGF-β/NF-κB signaling pathway might account for CA-elicited fibrosis-inhibiting actions [117]. Owing to the involvement of MAPKs in the pathogenesis of myocardial fibrosis and hypertrophy, CA application showed inhibitory
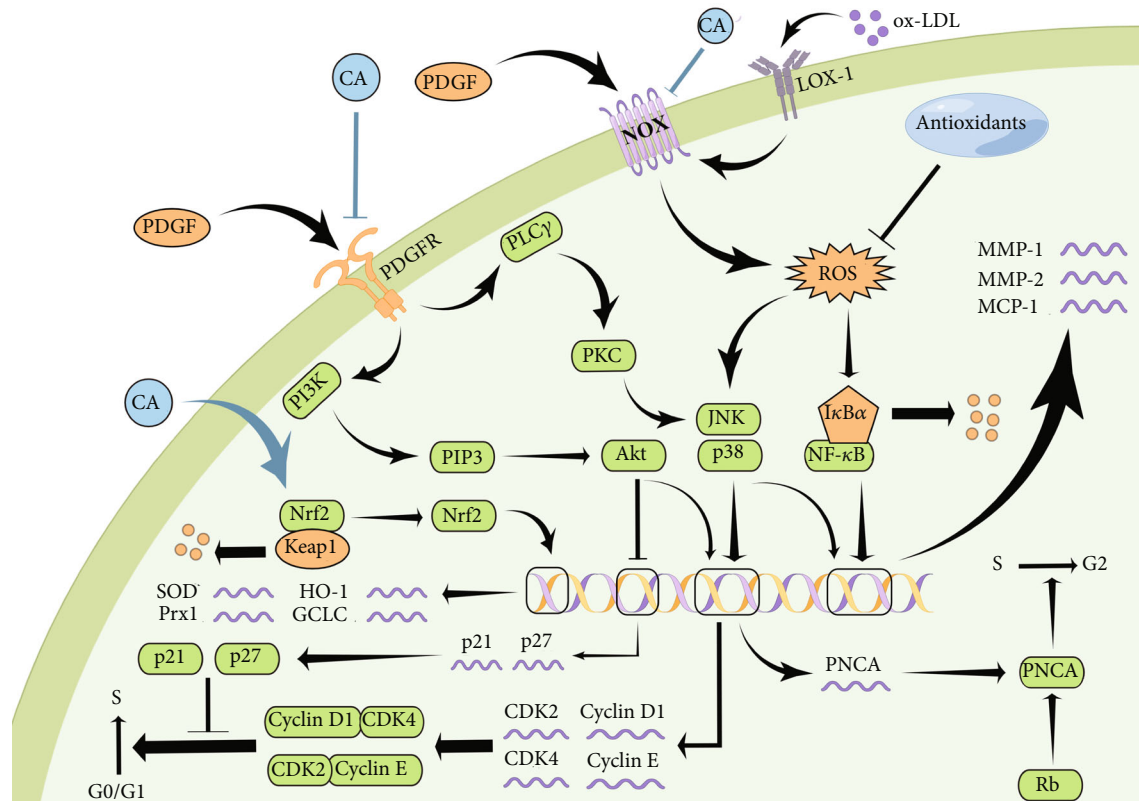
FIGURE 5: The possible targets mediated by CA to suppress VSMC proliferation and migration. PDGF-PDGFR signaling and oxidative stress induce activation of downstream pathways associated with the expression of cell cycle proteins, CDKs, and MMPs. The protective mechanisms of CA are attributed to the blockade of PDGFR activation and decrease of ROS level. PDGF: platelet-derived growth factor; PDGFR: PDGF receptor; NOX: NADPH oxidase; LOX-1: LOX-1: lectin-like oxidized low-density lipoprotein receptor-1; PLCγ: phospholipase C γ; PKC: protein kinase C; MMP: metalloproteinase; MCP-1: monocyte chemoattractant protein-1; Akt: protein kinase B; PI3K: phosphatidylinositol-4,5-bisphosphate 3-kinase; PIP3: phosphatidylinositol (3,4,5)-triphosphate; JNK: c-Jun N-terminal kinase; Keap1: Kelch-like ECH-associated protein 1; Nrf2: nuclear factor erythroid-2-related factor 2; PNCA: proliferating cell nuclear antigen; Rb: retinoblastoma tumor suppressor protein; CDK: cyclin-dependent kinase; Prx1: peroxiredoxin; GCLC: glutamate-cysteine ligase catalytic subunit; SOD: superoxide dismutase; HO-1: heme oxygenase-1.

effects on cardiomyocyte enlargement, myocardial fibroblasts growth, and collagen secretion, partly by weakening the MEK1/2-ERK1/2 signal pathway [120–122]. During the development of cardiac fibrosis, stromal cells arise from the transdifferentiation of vascular ECs are considered to play contributing roles via favoring profibrotic factors production and ECM accumulation. By the suppression of the TGF-β/Smads pathway, the treatment of CA potently increased the contents of CD31 and CD34 and vessel density and decreased the levels of α-SMA and vimentin in the heart tissue of mice irritated by pressure overload, suggesting the CA-evoked antagonistic effects on ECs transdifferentiation to stromal cells [123]. It is noteworthy that at the early stage of postmyocardial infarction, moderate cardiac fibrosis is profitable for improving patient prognosis via maintaining structural integrity and compensating for the functional deficiency of the heart. CA had been proved to accelerate myofibroblast formation in cardiac tissues upon MI injury and activation of the Ca2+ influx-CaN-NFAT pathway was likely to be implicated in this fibrotic actions [124]. Thus, it could be inferred that the regulatory roles of CA in myocardial fibrosis vary according to the specific conditions of

the diseases, ultimately improving the process of blood pumping, which implies that CA displays a good prospect in the prevention and treatment of cardiac failure.

3.6. Promotion of Vascular Dilation. Temporary vascular contraction is a common physiological reaction seen in strengthening body vigilance and adaptability under stress stimulation. However, persistent vasoconstriction is detrimental to the functioning of internal biological networks, since it induces blood pressure elevation or vasospasm-related tissues ischemia. A series of research findings have identified VSMCs as the chief executors controlling vessel contraction and relaxation. With exposure to both exogenous and endogenous irritants, the myosin and actin in VSMCs undergo conformational changes that modulate the performance of myofilament sliding essential for the process of vasomotion [114, 125]. In vitro, CA was found to induce the relaxant response in vasculatures of different areas including coronary artery, thoracic aorta, and mesenteric artery [21, 93, 126]. This was further verified by in vivo studies suggesting that increased blood pressure evoked by hyperglycemia in rats was recovered via CA

intervention [127, 128]. In light of the eminent vasorelaxant actions of CA, several researches were conducted to disclose relevant potential mechanisms, which showed that the activation of Nrf2 and eNOS in ECs played important roles. It was elucidated that excessive ROS triggered the degradation of NO, and the enhanced activity of Nrf2 was capable of mediating the production of antioxidant genes HO-1, NQO1, and CAT and then preventing NO depletion [95]. Since eNOS served as the main NO-producing enzyme, upregulation of Nrf2 and eNOS was profitable for preserving the NO level, thereby favoring this factor diffusion into adjacent VSMCs where NO activated sGC/cGMP/PKG axis associated with phosphorylation of functional proteins promoting vasorelaxation [11, 93, 129]. As for other mechanisms underlying vasodilator properties of CA, blockade of Ca2+ influx and intracellular Ca2+ release and improvement of K+ channels functionality in VSMCs were involved [21, 130, 131] (Figure 6). However, evidence had also suggested that ROS exerted positive roles in facilitating CA-mediated cerebral arterial dilation, as vindicated by transduction suppression of CGRP-PKA and NO-PKG cascade located in the interface between neurons and VSMCs under antioxidant administration [132, 133]. A possible explanation for such a finding might be that CA produced vasorelaxant functions varying according to the surroundings. Furthermore, moderate oxidative stress was beneficial to increase blood supply in the brain tissue for avoiding damage in response to ischemic events. This, together with the recent data that *trans*-CA alleviated cardiac hypertrophy by improving tubulin detyrosination via regulating the SOCE signaling pathway and STIM1/Orai1 translocation, indicated that there were probably unknown mechanisms by which CA elicited epigenetic changes within the contractile proteins to display vasodilator abilities [134].

3.7. Suppression of Platelet Activation and Aggregation. Compelling evidence has highlighted the paramount hazardous characteristics of thromboembolic diseases to human health, due to their close relationship with disability and mortality worldwide. During the process of thrombosis, platelet activation and aggregation are identified as the initiating steps contributing to the development of this pathological disorder, emphasizing antiplatelet medications as the key means for minimizing the risk of these ischemic and anoxic events [135, 136]. In view of the prothrombotic actions of ADP, collagen, arachidonic acid, thrombin, TXA$_2$, and TXB$_2$, CA was discovered to weaken platelet activation and aggregation induced by the above mentioned cytokines, which was partly attributed to the drug-evoked effects on synthesis inhibition and receptor antagonism of these bioactive substances [137–140]. Moreover, the activation of the eNOS/NO pathway in ECs and the amelioration of phospholipase C/Ca^{2+} influx signaling axis in platelets might be other mechanisms underlying CA's aggregation-abrogating capacities in the bloodstream, owing that the elevation of NO derived from proximal vascular ECs and the decrement of Ca^{2+} content uptake in the platelet triggered the activation of factors like cGMP possessing antiaggregative behaviors and lowered the activity of enzymes including

MLCK favoring the onset of aggregation, respectively [93, 95, 141]. Additionally, cinnamic acid treatment was found to abate the generation of TNF-α-stimulated tissue factors in ECs through disrupting the NF-κB signal pathway [30]. As cinnamic acid acts as the primary metabolite of CA and the tissue factor is a vital protein implicated in the process of intrinsic hemostasis pathway, there is a possibility that CA plays anti-inflammatory actions to prohibit tissue factor-irritated activation of platelet (Figure 7). From the perspective of thrombolysis in vivo, CA intervention obviously decreased the rate of acute pulmonary thromboembolic death and reduced thrombus weight in the arteriovenous shunt thrombosis model, further demonstrating the safety and efficacy of CA [137, 138].

3.8. Modulation of Cellular Apoptosis. Statistics from laboratory investigations endorse the notion that cellular senescence and programmed apoptosis are crucial for an organism to sustain internal homeostasis; yet, excessive apoptosis of ECs and cardiomyocytes have been intimately related to the pathogenesis of CVDs [80, 81, 142]. In detail, ECs, forming the lining of blood vessels, produce and release diverse active mediators to maintain vasculature tension and integrity, regulate platelet adhesion, balance oxidative stress, and prohibit inflammation response. Cardiomyocytes, acting as the "core engine," exhibit irreplaceable effects on life activities by pumping blood throughout the body. When these cells are subjected to continuous proapoptotic stimuli, their structure and functions get injured, leading to the development of atherosclerosis, thrombosis, and heart failure [11, 18]. It had been unveiled that CA offered protective roles against EC apoptosis under the environment of oxidative stress and the inner mechanisms were associated with CA-triggered activation of the Nrf2 signaling axis and restraint of NAPDH activity, accompanied by a decline in the intracellular ROS level, restoration of the mitochondrial membrane potential, and alleviation of cytochrome c leakage into the cytosol. These events, in turn, caused transduction blockade of the caspase-related cascade promoting apoptotic cell death [85, 95, 96]. Moreover, given that the ratio of Bax/Bcl-2 participating in the activation of caspase-9/-3 was upregulated by the TLR4/NF-κB pathway and downstream PARP acting as apoptosis executor was decreased by eNOS/NO signaling separately, CA-induced suppression of TLR4/NF-κB and enhancement of eNOS/NO might further confirm its potent prosurvival behaviors against the intrinsic apoptotic pathway in ECs [82, 143]. There was evidence that LPS-evoked cardiac damage was improved by CA treatment, which, to some extent, ascribed to the disruption of proapoptotic signal flow provoked by oxidative stress and inflammatory factors, as seen by activity inhibition of the TLR4/NOX4 and MAPKs/NF-κB pathway in cardiomyocytes [18]. Furthermore, Zheng et al. proved that CA preconditioning protected myocardial cells from ischemia/hypoxia-induced apoptosis via decreasing the expression of Bax and caspase-3 and elevating Bcl-2 level in a PI3K/Akt axis activation-dependent way [20] (Figure 8). It was worth noting that CA conveys motivated functions in favoring apoptosis of tumorous cells through modulating certain molecular pathways such as Wnt/β-catenin, PERK/CHOP, and AMPK/mTOR [144–146]. Although past studies on
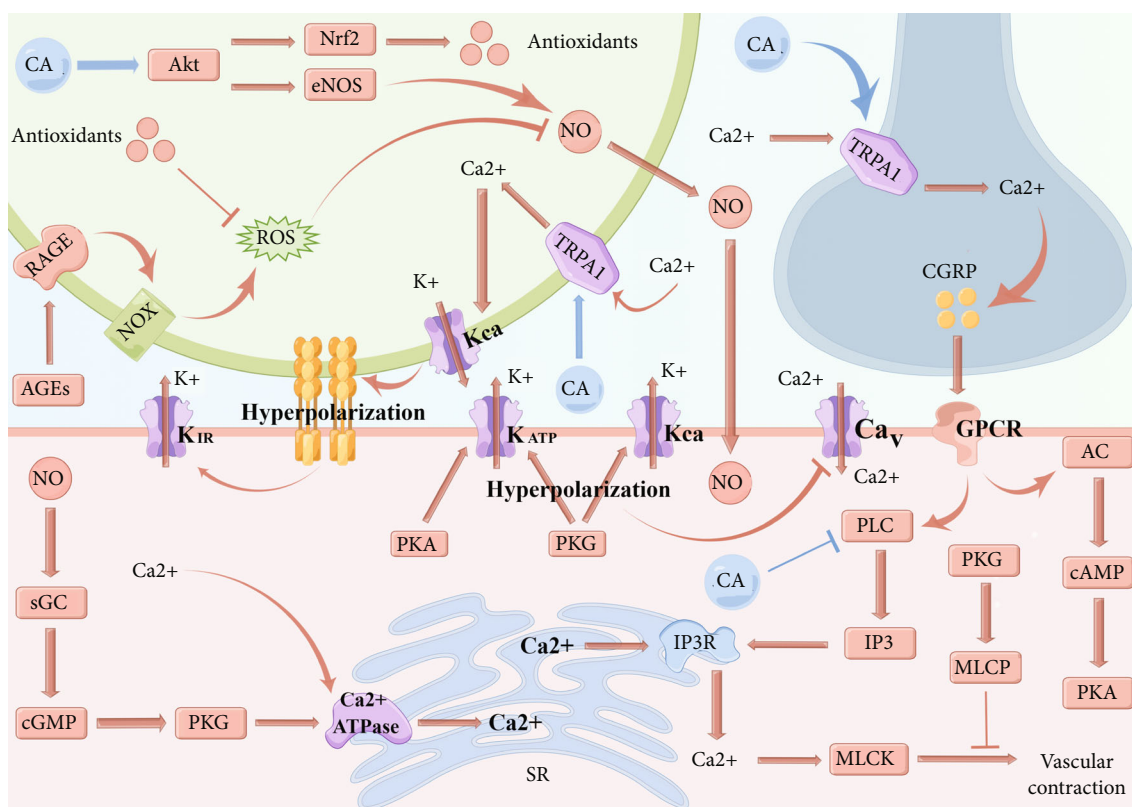
FIGURE 6: CA modulates the transfer of messenger molecules to decrease Ca2+ content in VSMCs and then induce the occurrence of vascular dilation. NO and CGRP derived from ECs and neurons enter into adjacent VSMCs for opening specific potassium channel which facilitates outflow of potassium and thus causing the hyperpolarization of membrane, which inhibit the open of voltage gated calcium channel and the influx of calcium. The activation of Ca2+-ATPase and inactivation of IP3R in SR is capable of accelerating Ca2+ in the cytoplasm entry into the SR. CGRP: calcitonin gene-related peptide; SR: sarcoplasmic reticulum; MLCK: myosin light-chain kinase; MLCP: myosin light-chain phosphatase; Akt: protein kinase B; Nrf2: nuclear factor erythroid-2-related factor 2; ROS: reactive oxygen species; eNOS: endothelial nitric oxide synthase; NO: nitric oxide; TRPA1: transient receptor potential ankyrin-1; AGEs: advanced glycation end products; RAGE: receptor of AGEs; NOX: NADPH oxidase; GPCR: G protein-coupled receptor; PLC: phospholipase C; IP3: inositol triphosphate; IP3R: IP3 receptor; PKA: protein kinase A; cAMP: cyclic adenosine monophosphate; AC: adenylyl cyclase; PKG: protein kinase G; cGMP: cyclic guanosine monophosphate; sGC: soluble guanylate cyclase.

CA-induced double-faced impacts on apoptosis regulation are scarce, it could be supposed that drug dosage and application time, genetic phenotype, redox balance, and signal network mediation are likely to be responsible for CA-related vascular protective and antineoplastic effects. These results, in accordance with the findings that CA was capable of accelerating angiogenesis in noncancerous tissues compensating for ischemic injury while hindering angiogenesis in cancerous tissues aggravating malignant metastasis, indicate that CA has considerable potentials to present as the alternative and adjuvant avenue for improving cardiovascular damage evoked by chemotherapy [23, 146, 147].

4. Other Recent Advances in the Mechanisms of CA against CVDs

With the in-depth understanding of pathogenic courses of CVDs, several molecular actions are newly deemed to be implicated in the regulation of disease development, such as organelle autophagy, endoplasmic reticulum stress, gut microbiota mediation, and ion metabolism [148–151]. Cur-

rently, there is a continuing rise in these activities as the promising targets of CA applicable to the cardiovascular system protection upon harmful irritants.

It is revealed that autophagy, featured by a catabolic process degrading intracellular components in a lysosomal dependent manner, is essential for cellular homeostasis and survival [148]. Zhao and colleagues reported that CA repressed hyperactive autophagic actions caused by oxidative stress and inflammation reaction to mitigate organelle overdigestion and maintain cellular integrity, then delaying occurrence of myocardial death stimulated by LPS [18]. Another study showed that obesity-induced autophagy depression in hepatocytes was enhanced by CA gavage, followed by the amplification of hepatic lipid-lowering capacities and the improvement of dyslipidemia in the circulation [106].

When the cells are subjected to adverse threats, numerous unfolded and misfolded proteins assemble in the endoplasmic reticulum (ER) to initiate a series of molecular reactions toward restoring the normal functions of ER, which is defined as ER stress [149]. CA had been reported to alleviate the activation of agonists involved in lipid synthesis by weakening the
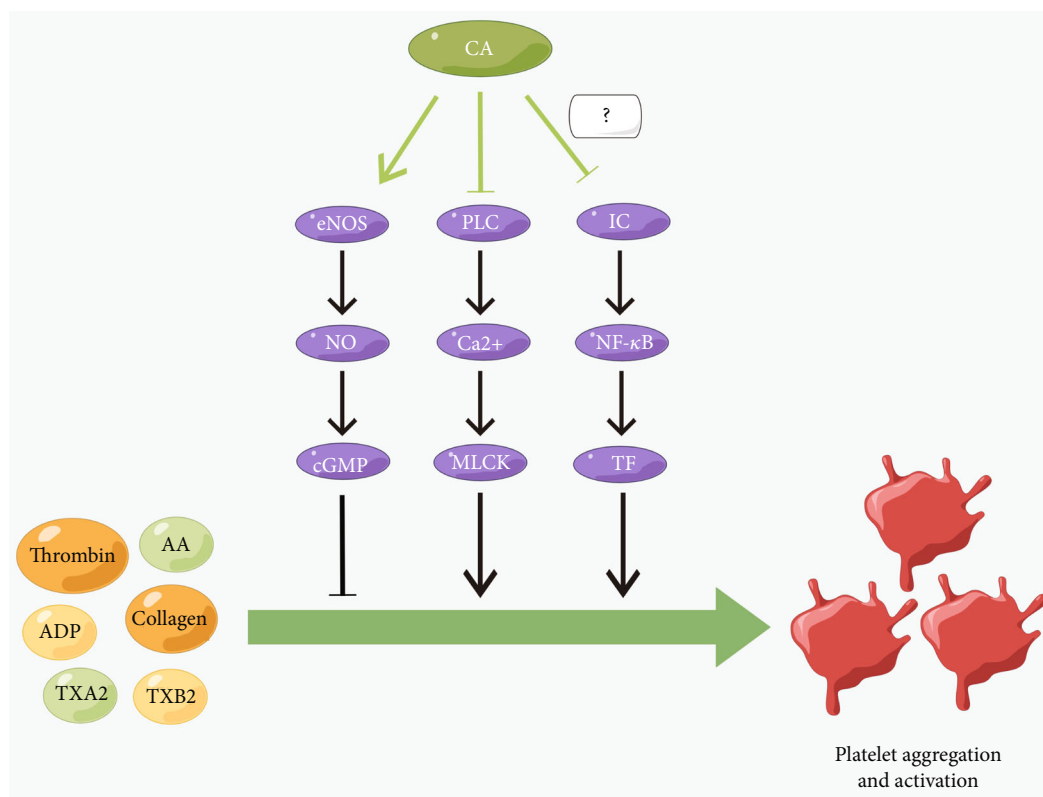
Figure 7: The regulatory effects of CA on the suppression of platelet activation and aggregation. NO synthesized by eNOS of vascular endothelium diffuses into circulating platelet and further induces the production of cGMP which prohibits the aggregative ability. PLC activation triggers level increase of intracellular calcium and then elevates the activity of MLCK responsible for the activation and aggregation of platelets. IC: inflammatory cytokines; TF: tissue factor; eNOS: endothelial nitric oxide synthase; NO: nitric oxide; cGMP: cyclic guanosine monophosphate; PLC: phospholipase C; MLCK: myosin light-chain kinase; NF-κB: nuclear factor of κB; AA: arachidonic acid; ADP: adenosine diphosphate; TXA2: thromboxane A2; TXB2: thromboxane A2.

ER stress in the liver [106]. Additionally, because of the pivotal roles of ER stress in apoptosis progression, the antiapoptotic mechanisms in ECs and cardiomyocytes exerted by CA might be relying on ER stress modulation to some extent, which warrants further investigation [145].

The immunoreaction acts as the defensive and adaptive conduct for eliminating exogenous and endogenous stimuli in vivo by cooperation of multiple cells and cytokines. Statistics have emerged that exorbitance and misrecognition of the immune system is associated with the development of atherosclerosis and myocarditis [80, 152]. Given that CA possesses immunoregulatory effects including influencing T-cell differentiation and proliferation, regulating monocyte phenotype transformation, and affecting expression of surface antigens, costimulatory molecules, pattern recognition receptors, and complement receptors, figuring out the implication of immunomodulation in CA-elicited cardiovascular protection is worthy [153–156].

As previously portrayed, dysfunction of the gut microbiota is detrimental for the normal operation of physiological processes in vivo, leading to energy metabolism disorder, arterial wall malfunction, myocardial fibrosis, and so on [157]. Results from Zhao et al. indicated that CA intervention reversed level increase of blood glucose in mice under the hyperglycemic condition, through ameliorating imbalance of intestinal flora

[158]. It is also plausible that one of the cardioprotective mechanisms of CA might be linked to mitigation of gut microbiota alteration; hence, the forward exploration is needed.

Recently, interest in trace elements has elevated since their abilities to induce a multitude of microcosmic events affecting cell fate, particularly ferroptosis, an iron-dependent mediated form of cell death [151]. Bioinformatic data predicted that CA probably alleviated intracellular iron shortage to inhibit pulmonary vascular remodeling and reduce pulmonary artery pressure, then postponing the deterioration of PAH [159]. As the contribution of ferroptosis regulation to the pharmacological benefits of CA is largely unknown, detailed basic researches are rewarding to be employed for determining whether CA diminishes vascular injury by improving the activation of ferroptosis.

Noncoding (nc) RNAs, comprising microRNAs, long noncoding (lnc) RNAs and circular RNAs, are a group of bioactive factors regulating gene expression at the post-transcriptional level to cause translational enhancement or repression, without clear potentials to encode polypeptides [160]. Administration of CA dramatically restrained inflammatory responses in mice suffering from ulcerative colitis through regulating the expression of miR-21, miR-155, and lncRNA H19 and MIAT, as proved by contents reduction of TNF-α, IL-1β, IL-6, COX-2, and NLRP3 [16, 161]. It is
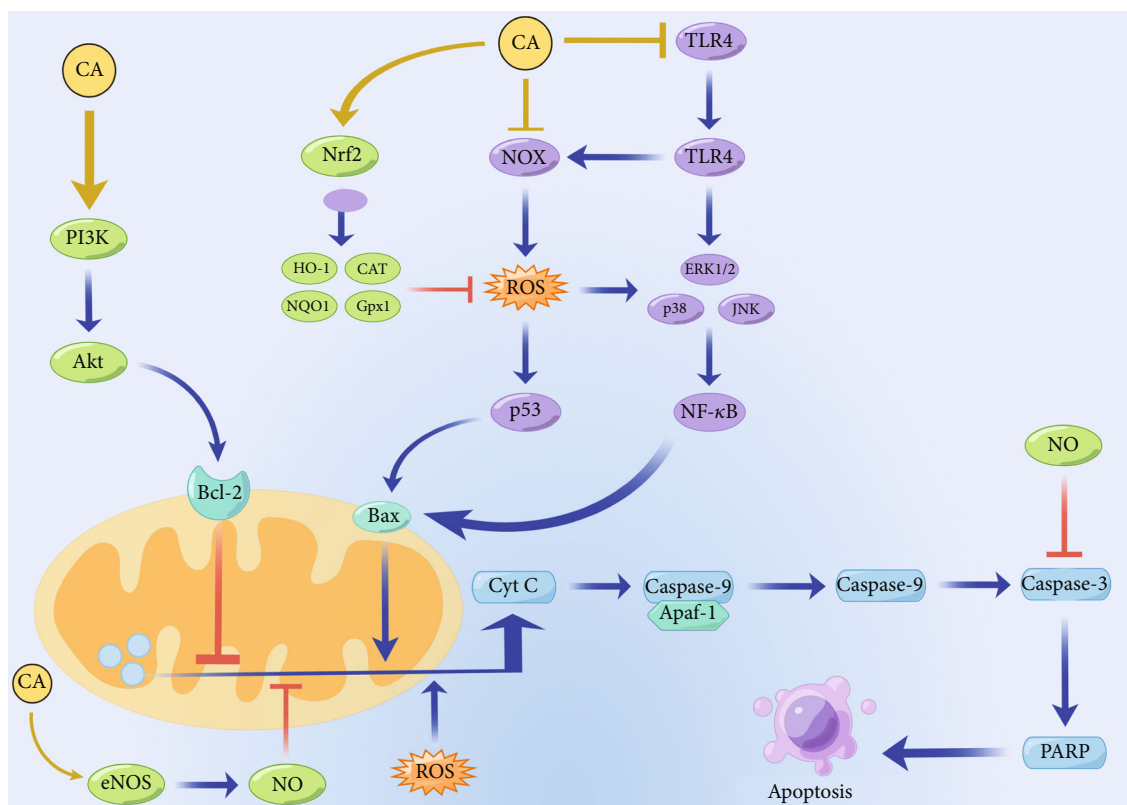
FIGURE 8: CA displays inhibitory roles in cellular death via suppressing the mitochondrial-dependent apoptotic pathway. Oxidative stress and inflammatory cascades induce activities increase of p53 and NF-κB, both of which contribute to level elevation of Bax. While PI3K/Akt and Nrf2 signaling axis induce content increase of Bcl-2 and level reduction of Bax on the membrane, which weaken Cyt C release into the cytosol and then disrupt the activation of caspase-9 and caspase-3. PI3K: phosphatidylinositol-4,5-bisphosphate 3-kinase; Akt: protein kinase B; NOX: NADPH oxidase; Nrf2: nuclear factor erythroid-2-related factor 2; HO-1: heme oxygenase-1; CAT: catalase; GPX1: glutathione peroxidase 1; TLR4: Toll-like receptor 4; JNK: c-Jun N-terminal kinase; ERK1/2: extracellular signal-regulated kinase 1/2; NQO1: NADPH dehydrogenase quinone 1; NF-κB: nuclear factor of κB; eNOS: endothelial nitric oxide synthase; NO: nitric oxide; Bcl-2: B-cell lymphoma 2; PARP: poly (ADP-ribose) polymerase; Cyt C: cytochrome C; Apaf-1: apoptosis protease activating factor-1.

suggested that above miRNAs and lncRNAs play crucial roles in the inflammation development of cardiovascular tissues, implying that controlling their levels has great possibility to be another target for CA to the management of inflammation-related CVDs [162–165].

Distributed in multifarious organs including the brain, skin, vasculature, and heart, transient receptor potential ankyrin-1 (TRPA1) is expressed as a six-transmembrane nonselective cation channel with a high calcium permeability and considered to be a signal-carrying messenger activated by physical and chemical products, among which CA serves as an important external agonist [166]. Emerging attention is paid to the signaling network containing TRPA1 because diverse therapeutic effects following CA-triggered TRPA1 activation have been established, such as vasodilation promotion, inflammation restraint, apoptosis abolishment, and immune regulation [79, 133, 143, 154]. It remains obscure whether CA interferes with diseases development predominately or solely depending on mediating TRPA1 activity, illuminating this confusion would provide a feasible direction for thoroughly recognizing the cardiovascular protective mechanisms of CA and lay the theoretical foundation for the compound applied in CVDs prophylaxis and treatment.

5. Potential Risks of CA

However, the current knowledge on the safety, stability, and bioavailability of CA is limited. Although herb medications have been widely applied in disease treatment for a long time, the appearance of side effects such as hepatic and renal damage are not rare. Thus, investigating whether CA exhibits excellent safety in clinical application is of high priority. According to the FDA of multiple countries, CA is proved as no safety concerns at doses of not exceeding daily acceptable consumption, whereas higher and nonnutritional intake of CA is prone to the appearance of genetic alteration and hepatotoxicity [15]. It is deciphered that CA administration in cellular and animal studies conducted at a specific period of time determines its absence of toxicity and carcinogenicity, the possible effects of this compound regarding long-term duration and other delivery routes are still vague [167, 168]. The results of previous animal studies indicate that CA has a wide spectrum of efficacious dosage against CVDs, ranging from 5 mg/kg to 200 mg/kg. In terms of the upper tolerant level, CA is reported to possess an oral lethal dose scope from a low of 600 mg/kg body weight to a high of 3400 mg/kg body weight in diverse individuals. For instance, the
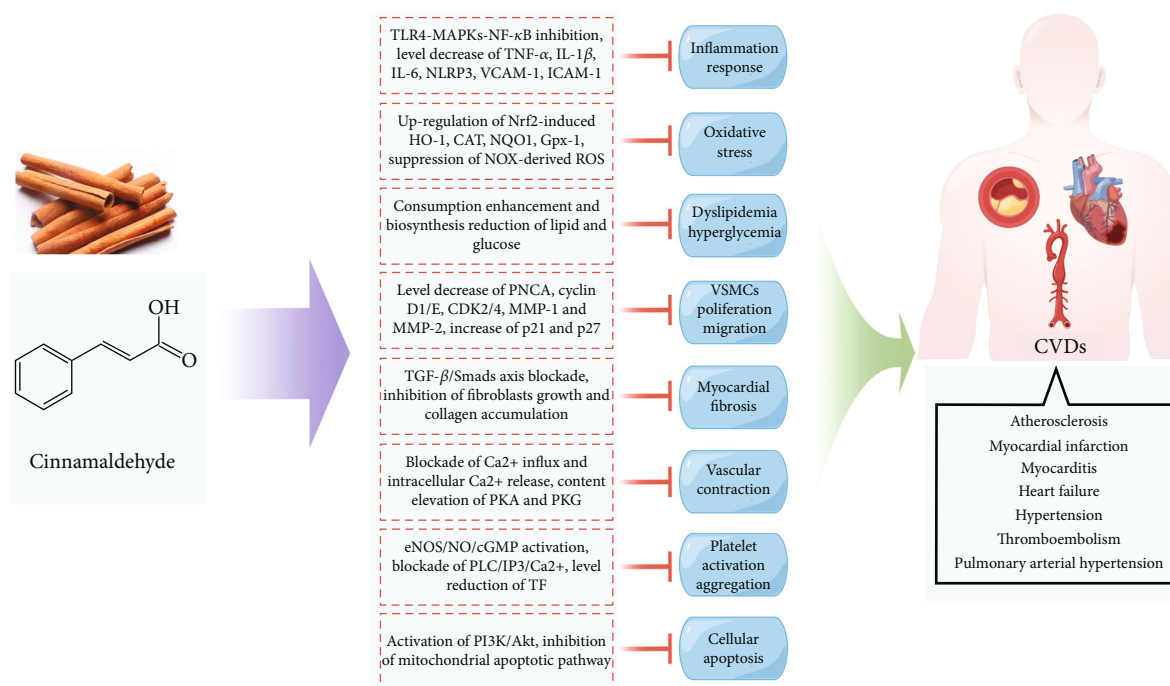
FIGURE 9: The schematic diagram of CA against the pathogenic factors involved in the development of CVDs.

occurrence of hepatotoxicity of CA uptake dosage in rats and mice is 1100 mg/kg/body weight and 850 mg/kg/body weight, respectively [15]. Moreover, it has been reported that CA has a high volatility, indicating the instability of this drug during the process of isolation and delivery. Considering the hydrophobic property of CA, exposure of this agent to aqueous solutions usually lead to a poor bioavailability (approximately 20%). Despite that CA easily dissolve in organic solvents, the toxicity of which is a major concern. It has been demonstrated that several bio-materials including liposomes, nanoparticles, and hydro-gels possess favorable biocompatibility, biodegradability, and low immunogenicity properties and are found to encapsulate drugs to act as delivery carriers. By loading in biomaterials, the bioactive compounds could overcome own shortcomings including poor water solubility, low retention, burst release, and rapid clearance, accompanied by acquisition of desirable stability and bioavailability [44]. There is evidence that CA encapsulated in certain nanocarriers obtains decreased cytotoxicity and increased bioavailability, yet whether these constituents possess san-ative roles in inhibiting CVDs development is outside the scope of existing investigations [31, 32]. As such, further in vivo experiments should be undertaken for purpose of optimizing the pharmacodynamics and pharmacokinetics associated with curative potentials of CA. In addition, growing clinical trials are advocated to offer scientific basis for the safe and effective use of CA in the management of CVDs.

6. Conclusion

Multiple lines of evidence support that CVDs, with compli-cated etiology and upward trend in the incidence year by year, are a cluster of pathological factors that impair the

power source and mobile carrier of blood flow and seriously harm the physical and mental health of mankind [1, 2]. A nonnegligible reason for this situation is the limitation of therapy and the undesirable adverse effects of drugs used in the clinical practice. Nowadays, much emphasis has been placed on herbal products and dietary ingredients due to the valuable effects of constituents derived from them on disease management. CA, commonly used as a flavoring and fragrance agent, is a naturally occurring phytochemical and has been documented to possess wide spectrum of anti-CVD properties over the past decades [9, 11, 15]. In this review, we summarize and evaluate CA-elicited therapeutic roles against cardiovascular disorders via diverse pharmaco-logical activities, among which inhibition of inflammation and oxidative stress, improvement of lipid and glucose metabolism, regulation of cell proliferation and apoptosis, suppression of cardiac fibrosis, and platelet aggregation and promotion of vasodilation and angiogenesis are involved (Figure 9). Moreover, a phenomenon that a few molecular actions induced by CA lead to dissimilar out-comes between two types of disease models is discussed, dif-ferences in cell type and phenotype, compound dosage and duration, and signaling transduction regulation might be the plausible interpretation, which deserve intensive labora-tory probe. Meanwhile, in-depth analyses so far have dem-onstrated that CA is likely to produce cardiovascular benefits through several equivocal mechanisms including mediating autophagy and ER stress, improving gut microbi-ota and immune homeostasis and affecting ion metabolism, ncRNA expression, and TRPA1 activation, ascertaining their reliability is of vital importance for providing novel insights into the protective effects exerted by CA on alleviating the CVD development.

Abbreviations

CVDs: Cardiovascular diseases
CA: Cinnamaldehyde
FDA: Food and Drug Administration
NF-κB: Nuclear factor-kappa B
iNOS: Inducible nitric oxide synthase
COX-2: Cyclooxygenase-2
TNF-α: Tumor necrosis factor α
NO: Nitric oxide
PGE$_2$: Prostaglandin E2
LPS: Lipopolysaccharide
IL-8: Interleukin-8
TLR4: Toll-like receptor 4
Akt: Protein kinase B
PI3K: Phosphatidylinositol-4,5-bisphosphate 3-kinase
IL-1β: Interleukin-1β
NLRP3: NOD-like receptor family pyrin domain containing 3
HIF-1α: Hypoxia-inducible factor-1α
ERK1/2: Extracellular signal-regulated kinase 1/2
JNK: c-Jun N-terminal kinase
IL-6: Interleukin-6
MAPKs: Mitogen-activated protein kinases
IL-10: Interleukin-10
TGF-β: Transforming growth factor-β
ECs: Endothelial cells
VCAM-1: Vascular cell adhesion molecule-1
ICAM-1: Intercellular adhesion molecule-1
VSMCs: Vascular smooth muscle cells
ox-LDL: Oxidized low-density lipoprotein
MCP-1: Monocyte chemoattractant protein-1
ApoE: Apolipoprotein E
HFD: High-fat diet
ROS: Reactive oxygen species
MDA: Malondialdehyde
MPO: Myeloperoxidase
SOD: Superoxide dismutase
CAT: Catalase
Nrf2: Nuclear factor erythroid-2-related factor 2
HO-1: Heme oxygenase-1
H2O2: Hydrogen peroxide
AGEs: Advanced glycation end products
NOX: NADPH oxidase
NQO1: NADPH dehydrogenase quinone 1
GPX1: Glutathione peroxidase 1
I/R: Ischemia/reperfusion
LDH: Lactate dehydrogenase
cTnI: Cardiac troponin I
PPARα: Peroxisome proliferator-activated receptor-α
XOD: Xanthine oxidase
IRAK: Interleukin-1 receptor-associated kinase
TG: Triglyceride
TC: Total cholesterol
LDL-C: Low-density lipoprotein cholesterol
LOX-1: Lectin-like oxidized low-density lipoprotein receptor-1
AMPK: AMP-activated protein kinase
SREBP: Sterol regulatory element-binding protein
FAS: Fatty acid synthase
SCD-1: Stearoyl-CoA desaturase-1
GPAT: Glycerol phosphate acyltransferase
ACC: Acetyl-CoA carboxylase
PKA: Protein kinase A
C/EBPα: CCAAT enhancer-binding protein α
LDLR: Low-density lipoprotein receptor
IRS-1: Insulin receptor substrate-1
PGC-1α: Peroxisome proliferator-activated receptor-gamma coactivator-1α
GLUT4: Glucose transporter 4
ECM: Extracellular matrix
PAH: Pulmonary arterial hypertension
PCNA: Proliferating cell nuclear antigen
PLCγ1: Phospholipase C γ1
CDK: Cyclin-dependent kinase
MMPs: Metalloproteinases
CGRP: Calcitonin gene-related peptide
eNOS: Endothelial nitric oxide synthase
sGC: Soluble guanylate cyclase
PKG: Protein kinase G
TXA$_2$: Thromboxane A2
MLCK: Myosin light chain kinase
PARP: Poly(ADP-ribose) polymerase
ER: Endoplasmic reticulum
TRPA1: Transient receptor potential ankyrin-1.

Conflicts of Interest

The authors declare that there is no conflict of interest regarding the publication of this paper.

Authors' Contributions

Li Lu and Yuan Xiong contributed equally to this work.

Acknowledgments

References

[1] G. A. Roth, G. A. Mensah, C. O. Johnson et al., "Global burden of cardiovascular diseases and risk factors, 1990-2019: update from the GBD 2019 study," *Journal of the American College of Cardiology*, vol. 76, no. 25, pp. 2982–3021, 2020.

[2] S. Safiri, N. Karamzad, K. Singh et al., "Burden of ischemic heart disease and its attributable risk factors in 204 countries

and territories, 1990-2019," *European Journal of Preventive Cardiology*, vol. 29, no. 2, pp. 420–431, 2022.

[3] W. M. Schultz, H. M. Kelli, J. C. Lisko et al., "Socioeconomic status and cardiovascular outcomes: challenges and interventions," *Circulation*, vol. 137, no. 20, pp. 2166–2178, 2018.

[4] D. P. Leong, P. G. Joseph, M. McKee et al., "Reducing the global burden of cardiovascular disease, part 2: prevention and treatment of cardiovascular disease," *Circulation Research*, vol. 121, no. 6, pp. 695–710, 2017.

[5] S. Wu, S. Zhang, X. Wu, and X. Zhou, "m⁶A RNA Methylation in Cardiovascular Diseases," *Molecular therapy: the journal of the American Society of Gene Therapy*, vol. 28, no. 10, pp. 2111–2119, 2020.

[6] J. A. Leopold and J. Loscalzo, "Emerging role of precision medicine in cardiovascular disease," *Circulation Research*, vol. 122, no. 9, pp. 1302–1315, 2018.

[7] A. Hafiane and S. S. Daskalopoulou, "Targeting the residual cardiovascular risk by specific anti-inflammatory interventions as a therapeutic strategy in atherosclerosis," *Pharmacological Research*, vol. 178, article 106157, 2022.

[8] S. Zhao, C. K. Cheng, C. L. Zhang, and Y. Huang, "Interplay between oxidative stress, cyclooxygenases, and prostanoids in cardiovascular diseases," *Antioxidants & Redox Signaling*, vol. 34, no. 10, pp. 784–799, 2021.

[9] R. Liperoti, D. L. Vetrano, R. Bernabei, and G. Onder, "Herbal medications in cardiovascular medicine," *Journal of the American College of Cardiology*, vol. 69, no. 9, pp. 1188–1199, 2017.

[10] C. Zhao, S. Li, J. Zhang et al., "Current state and future perspective of cardiovascular medicines derived from natural products," *Pharmacology & Therapeutics*, vol. 216, article 107698, 2020.

[11] C. Yu and J. Xiao, "The Keap1-Nrf2 system: a mediator between oxidative stress and aging," *Oxidative Medicine and Cellular Longevity*, vol. 2021, Article ID 6635460, 16 pages, 2021.

[12] M. Dorri, S. Hashemitabar, and H. Hosseinzadeh, "Cinnamon (Cinnamomum zeylanicum) as an antidote or a protective agent against natural or chemical toxicities: a review," *Drug and Chemical Toxicology*, vol. 41, no. 3, pp. 338–351, 2018.

[13] A. A. Doyle and J. C. Stephens, "A review of cinnamaldehyde and its derivatives as antibacterial agents," *Fitoterapia*, vol. 139, article 104405, 2019.

[14] M. Friedman, "Chemistry, antimicrobial mechanisms, and antibiotic activities of cinnamaldehyde against pathogenic bacteria in animal feeds and human foods," *Journal of Agricultural and Food Chemistry*, vol. 65, no. 48, pp. 10406–10423, 2017.

[15] R. Zhu, H. Liu, C. Liu et al., "Cinnamaldehyde in diabetes: a review of pharmacology, pharmacokinetics and safety," *Pharmacological Research*, vol. 122, pp. 78–89, 2017.

[16] S. L. Qu, L. Chen, X. S. Wen et al., "Suppression of Th17 cell differentiation via sphingosine-1-phosphate receptor 2 by cinnamaldehyde can ameliorate ulcerative colitis," *Biomedicine & Pharmacotherapy*, vol. 134, article 111116, 2021.

[17] P. Liu, J. Wang, W. Wen et al., "Cinnamaldehyde suppresses NLRP3 derived IL-1β via activating succinate/HIF-1 in rheumatoid arthritis rats," *International Immunopharmacology*, vol. 84, article 106570, 2020.

[18] H. Zhao, M. Zhang, F. Zhou et al., "Cinnamaldehyde ameliorates LPS-induced cardiac dysfunction via TLR4-NOX4 pathway: the regulation of autophagy and ROS production," *Journal of Molecular and Cellular Cardiology*, vol. 101, pp. 11–24, 2016.

[19] L. L. Kang, D. M. Zhang, C. H. Ma et al., "Cinnamaldehyde and allopurinol reduce fructose-induced cardiac inflammation and fibrosis by attenuating CD36-mediated TLR4/6-IRAK4/1 signaling to suppress NLRP3 inflammasome activation," *Scientific Reports*, vol. 6, no. 1, article 27460, 2016.

[20] B. Zheng, J. Qi, Y. Yang et al., ">Mechanisms of cinnamic aldehyde against myocardial ischemia/hypoxia injury in vivo and in vitro: involvement of regulating PI3K/AKT signaling pathway," *Biomedicine & Pharmacotherapy*, vol. 147, article 112674, 2022.

[21] G. Raffai, B. Kim, S. Park, G. Khang, D. Lee, and P. M. Vanhoutte, "Cinnamaldehyde and cinnamaldehyde-containing micelles induce relaxation of isolated porcine coronary arteries: role of nitric oxide and calcium," *International Journal of Nanomedicine*, vol. 9, pp. 2557–2566, 2014.

[22] W. Li, W. Zhi, J. Zhao et al., "Cinnamaldehyde attenuates atherosclerosisviatargeting the IκB/NF-κB signaling pathway in high fat diet-induced ApoE−/−mice," *Food & Function*, vol. 10, no. 7, pp. 4001–4009, 2019.

[23] X. Yuan, L. Han, P. Fu et al., "Cinnamaldehyde accelerates wound healing by promoting angiogenesis via up- regulation of PI3K and MAPK signaling pathways," *Laboratory investigation; a journal of technical methods and pathology*, vol. 98, no. 6, pp. 783–798, 2018.

[24] S. Momtaz, S. Hassani, F. Khan, M. Ziaee, and M. Abdollahi, "Cinnamon, a promising prospect towards Alzheimer's disease," *Pharmacological Research*, vol. 130, pp. 241–258, 2018.

[25] S. Shreaz, W. A. Wani, J. M. Behbehani et al., "Cinnamaldehyde and its derivatives, a novel class of antifungal agents," *Fitoterapia*, vol. 112, pp. 116–131, 2016.

[26] J. S. Hwa, Y. C. Jin, Y. S. Lee et al., "2-Methoxycinnamaldehyde from Cinnamomum cassia reduces rat myocardial ischemia and reperfusion injury *in vivo* due to HO-1 induction," *Journal of Ethnopharmacology*, vol. 139, no. 2, pp. 605–615, 2012.

[27] J. Y. Kwon, S. H. Hong, S. D. Park et al., "2'-Benzoyloxycinnamaldehyde inhibits nitric oxide production in lipopolysaccharide-stimulated RAW 264.7 cells *via* regulation of AP-1 pathway," *European Journal of Pharmacology*, vol. 696, no. 1-3, pp. 179–186, 2012.

[28] S. H. Lee, S. Y. Lee, D. J. Son et al., "Inhibitory effect of 2'-hydroxycinnamaldehyde on nitric oxide production through inhibition of NF-κB activation in RAW 264.7 cells," *Biochemical Pharmacology*, vol. 69, no. 5, pp. 791–799, 2005.

[29] Y. Zhang, W. Cao, Y. H. Xie et al., "The comparison of α-bromo-4-chlorocinnamaldehyde and cinnamaldehyde on coxsackie virus B3-induced myocarditis and their mechanisms," *International Immunopharmacology*, vol. 14, no. 1, pp. 107–113, 2012.

[30] X. Li, Z. Wen, X. He, and S. He, "Effects of cinnamic acid on expression of tissue factor induced by TNFα in endothelial cells and its mechanisms," *Journal of the Chinese Medical Association*, vol. 69, no. 5, pp. 207–212, 2006.

[31] Z. Yong, W. Xingqi, H. Jie, H. Rongfeng, and C. Xiaoqin, "Formulation, production, *in vitro* release and *in vivo* pharmacokinetics of cinnamaldehyde sub-micron emulsions,"

Pharmaceutical Development and Technology, vol. 25, no. 6, pp. 676–685, 2020.

[32] H. Zhao, J. Yuan, Q. Yang, Y. Xie, W. Cao, and S. Wang, "Cinnamaldehyde in a novel intravenous submicrometer emulsion: pharmacokinetics, tissue distribution, antitumor efficacy, and toxicity," *Journal of Agricultural and Food Chemistry*, vol. 63, no. 28, pp. 6386–6392, 2015.

[33] J. Yuan, M. P. Dieter, J. R. Bucher, and C. W. Jameson, "Application of microencapsulation for toxicology studies. III. Bioavailability of microencapsulated cinnamaldehyde," *Fundamental and Applied Toxicology*, vol. 20, no. 1, pp. 83–87, 1993.

[34] B. Ji, L. Zhuo, B. Yang et al., "Development and validation of a sensitive and fast UPLC-MS/MS method for simultaneous determination of seven bioactive compounds in rat plasma after oral administration of Guizhi-gancao decoction," *Journal of Pharmaceutical and Biomedical Analysis*, vol. 137, pp. 23–32, 2017.

[35] H. Zhao, Y. Xie, Q. Yang et al., "Pharmacokinetic study of cinnamaldehyde in rats by GC-MS after oral and intravenous administration," *Journal of Pharmaceutical and Biomedical Analysis*, vol. 89, pp. 150–157, 2014.

[36] J. Wan, S. M. Wang, Z. P. Gui et al., "Phytantriol-based lyotropic liquid crystal as a transdermal delivery system," *European Journal of Pharmaceutical Sciences*, vol. 125, pp. 93–101, 2018.

[37] Y. Cai, L. Liu, M. Xia et al., "SEDDS facilitate cinnamaldehyde crossing the mucus barrier: the perspective of mucus and Caco-2/HT29 co-culture models," *International Journal of Pharmaceutics*, vol. 614, article 121461, 2022.

[38] B. Ji, Y. Zhao, Q. Zhang et al., "Simultaneous determination of cinnamaldehyde, cinnamic acid, and 2-methoxy cinnamic acid in rat whole blood after oral administration of volatile oil of Cinnamoni Ramulus by UHPLC-MS/MS: an application for a pharmacokinetic study," *Journal of chromatography. B: Analytical technologies in the biomedical and life sciences*, vol. 1001, pp. 107–113, 2015.

[39] W. Chang, L. Han, H. Huang et al., "Simultaneous determination of four volatile compounds in rat plasma after oral administration of Shexiang Baoxin Pill (SBP) by HS-SPDE-GC-MS/MS and its application to pharmacokinetic studies," *Journal of chromatography. B: Analytical technologies in the biomedical and life sciences*, vol. 963, pp. 47–53, 2014.

[40] H. Zhao, Q. Yang, Y. Xie et al., "Simultaneous determination of cinnamaldehyde and its metabolite in rat tissues by gas chromatography-mass spectrometry," *Biomedical chromatography : BMC*, vol. 29, no. 2, pp. 182–187, 2015.

[41] H. Devaraj, S. Niranjali, and M. Raveendran, "Effect of food flavor cinnamaldehyde on liver microsomal cytochrome P-450 in rats," *Bulletin of Environmental Contamination and Toxicology*, vol. 49, no. 2, pp. 306–311, 1992.

[42] Y. Chen, Y. Ma, and W. Ma, "Pharmacokinetics and bioavailability of cinnamic acid after oral administration of Ramulus Cinnamomi in rats," *European Journal of Drug Metabolism and Pharmacokinetics*, vol. 34, no. 1, pp. 51–56, 2009.

[43] J. Yuan, J. R. Bucher, T. J. Goehl, M. P. Dieter, and C. W. Jameson, "Quantitation of cinnamaldehyde and cinnamic acid in blood by HPLC," *Journal of Analytical Toxicology*, vol. 16, no. 6, pp. 359–362, 1992.

[44] B. Muhoza, B. Qi, J. D. Harindintwali, M. Y. F. Koko, S. Zhang, and Y. Li, "Encapsulation of cinnamaldehyde: an insight on delivery systems and food applications," *Critical reviews in food science and nutrition*, pp. 1–23, 2021.

[45] S. Luo, D. Ma, R. Wei et al., "A tumor microenvironment responsive nanoplatform with oxidative stress amplification for effective MRI-based visual tumor ferroptosis," *Acta Biomaterialia*, vol. 138, pp. 518–527, 2022.

[46] C. Zhao, W. Cao, H. Zheng et al., "Acid-responsive nanoparticles as a novel oxidative stress-inducing anticancer therapeutic agent for colon cancer," *International Journal of Nanomedicine*, vol. 14, pp. 1597–1618, 2019.

[47] B. Y. Gursu, I. Dag, and G. Dikmen, "Antifungal and antibiofilm efficacy of cinnamaldehyde-loaded poly(DL-lactide-co-glycolide) (PLGA) nanoparticles against Candida albicans," *International microbiology : the official journal of the Spanish Society for Microbiology*, vol. 5, no. 2, pp. 245–258, 2022.

[48] Y. J. Jo, H. S. Cho, and J. Y. Chun, "Antioxidant activity of β-cyclodextrin inclusion complexes containing *trans*-cinnamaldehyde by DPPH, ABTS and FRAP," *Food Science and Biotechnology*, vol. 30, no. 6, pp. 807–814, 2021.

[49] N. Sang, L. Jiang, Z. Wang et al., "Bacteria-targeting liposomes for enhanced delivery of cinnamaldehyde and infection management," *International Journal of Pharmaceutics*, vol. 612, article 121356, 2022.

[50] X. Wang, F. Cheng, X. Wang, T. Feng, S. Xia, and X. Zhang, "Chitosan decoration improves the rapid and long-term antibacterial activities of cinnamaldehyde-loaded liposomes," *International Journal of Biological Macromolecules*, vol. 168, pp. 59–66, 2021.

[51] X. Qin, T. Kraft, and F. M. Goycoolea, "Chitosan encapsulation modulates the effect of trans-cinnamaldehyde on AHL-regulated quorum sensing activity," *Colloids and Surfaces B: Biointerfaces*, vol. 169, pp. 453–461, 2018.

[52] K. M. Kamel, I. A. Khalil, M. E. Rateb, H. Elgendy, and S. Elhawary, "Chitosan-coated cinnamon/oregano-loaded solid lipid nanoparticles to augment 5-fluorouracil cytotoxicity for colorectal cancer: extract standardization, nanoparticle optimization, and cytotoxicity evaluation," *Journal of Agricultural and Food Chemistry*, vol. 65, no. 36, pp. 7966–7981, 2017.

[53] K. Dong, Z. Z. Zhao, J. Kang et al., "Cinnamaldehyde and doxorubicin co-loaded graphene oxide wrapped mesoporous silica nanoparticles for enhanced MCF-7 cell apoptosis," *International Journal of Nanomedicine*, vol. Volume 15, pp. 10285–10304, 2020.

[54] Y. Zhang, H. Zhang, K. Zhang et al., "Co-hybridized composite nanovesicles for enhanced transdermal eugenol and cinnamaldehyde delivery and their potential efficacy in ulcerative colitis," *Nanomedicine : nanotechnology, biology, and medicine*, vol. 28, article 102212, 2020.

[55] K. Miranda-Cadena, M. Dias, A. Costa-Barbosa et al., "Development and characterization of monoolein-based liposomes of carvacrol, cinnamaldehyde, citral, or thymol with Anti-*Candida* activities," *Antimicrobial agents and chemotherapy*, vol. 65, no. 4, 2021.

[56] M. Ramasamy, J. H. Lee, and J. Lee, "Development of gold nanoparticles coated with silica containing the antibiofilm drug cinnamaldehyde and their effects on pathogenic bacteria," *International Journal of Nanomedicine*, vol. 12, pp. 2813–2828, 2017.

[57] K. Chotchindakun, J. Pekkoh, J. Ruangsuriya et al., "Fabrication and characterization of cinnamaldehyde-loaded mesoporous bioactive glass nanoparticles/PHBV-based microspheres for preventing bacterial infection and promoting bone tissue regeneration," *Polymers*, vol. 13, no. 11, pp. 1–18, 2021.

[58] C. Huang, S. Ding, W. Jiang, and F. B. Wang, "Glutathione-depleting nanoplatelets for enhanced sonodynamic cancer therapy," *Nanoscale*, vol. 13, no. 8, pp. 4512–4518, 2021.

[59] W. Chen, F. Cheng, C. J. Swing, S. Xia, and X. Zhang, "Modulation effect of core-wall ratio on the stability and antibacterial activity of cinnamaldehyde liposomes," *Chemistry and Physics of Lipids*, vol. 223, article 104790, 2019.

[60] L. Li, X. Sun, M. Dong et al., "NIR-regulated dual-functional silica nanoplatform for infected-wound therapy *via* synergistic sterilization and anti-oxidation," *Colloids and surfaces B: Biointerfaces*, vol. 213, article 112414, 2022.

[61] K. Dong, Q. Lei, R. Guo et al., "Regulating intracellular ROS signal by a dual pH/reducing-responsive nanogels system promotes tumor cell apoptosis," *International Journal of Nanomedicine*, vol. 14, pp. 5713–5728, 2019.

[62] B. B. Wang, L. X. Yan, L. J. Chen, X. Zhao, and X. P. Yan, "Responsive nanoplatform for persistent luminescence "turn-on" imaging and "on-demand" synergistic therapy of bacterial infection," *Journal of Colloid and Interface Science*, vol. 610, pp. 687–697, 2022.

[63] I. L. Liakos, C. Menager, N. Guigo et al., "Suberin/*trans*-cinnamaldehyde oil nanoparticles with antimicrobial activity and anticancer properties when loaded with paclitaxel," *ACS Applied Bio Materials*, vol. 2, no. 8, pp. 3484–3497, 2019.

[64] C. Valcourt, P. Saulnier, A. Umerska et al., "Synergistic interactions between doxycycline and terpenic components of essential oils encapsulated within lipid nanocapsules against gram negative bacteria," *International Journal of Pharmaceutics*, vol. 498, no. 1-2, pp. 23–31, 2016.

[65] Q. Liu, X. Ding, X. Xu et al., "Tumor-targeted hyaluronic acid-based oxidative stress nanoamplifier with ROS generation and GSH depletion for antitumor therapy," *International Journal of Biological Macromolecules*, vol. 207, pp. 771–783, 2022.

[66] L. Yan, F. Song, H. Li et al., "Submicron emulsion of cinnamaldehyde ameliorates bleomycin-induced idiopathic pulmonary fibrosis via inhibition of inflammation, oxidative stress and epithelial-mesenchymal transition," *Biomedicine & Pharmacotherapy*, vol. 102, pp. 765–771, 2018.

[67] K. A. A. Mohammed, H. M. S. Ahmed, H. A. Sharaf et al., "Encapsulation of cinnamon oil in whey protein counteracts the disturbances in biochemical parameters, gene expression, and histological picture of the liver and pancreas of diabetic rats," *Environmental Science and Pollution Research International*, vol. 27, no. 3, pp. 2829–2843, 2020.

[68] N. N. Besednova, B. G. Andryukov, T. S. Zaporozhets et al., "Molecular targets of brown algae phlorotannins for the therapy of inflammatory processes of various origins," *Marine Drugs*, vol. 20, no. 4, pp. 1–27, 2022.

[69] M. E. Colling, B. E. Tourdot, and Y. Kanthi, "Inflammation, infection and venous thromboembolism," *Circulation Research*, vol. 128, no. 12, pp. 2017–2036, 2021.

[70] A. Hussain and C. M. Ballantyne, "New approaches for the prevention and treatment of cardiovascular disease: focus on lipoproteins and inflammation," *Annual Review of Medicine*, vol. 72, no. 1, pp. 431–446, 2021.

[71] Y. Tong, L. Cai, S. Yang, S. Liu, Z. Wang, and J. Cheng, "The research progress of vascular macrophages and atherosclerosis," *Oxidative Medicine and Cellular Longevity*, vol. 2020, Article ID 7308736, 4 pages, 2020.

[72] J. C. Liao, J. S. Deng, C. S. Chiu et al., "Anti-Inflammatory Activities of *Cinnamomum cassia* Constituents *In Vitro* and *In Vivo*," *Evidence-based Complementary and Alternative Medicine*, vol. 2012, Article ID 429320, 12 pages, 2012.

[73] E. G. Gulec Peker and K. Kaltalioglu, "Cinnamaldehyde and eugenol protect against LPS-stimulated oxidative stress and inflammation in raw 264.7 cells," *Journal of Food Biochemistry*, vol. 45, no. 12, article e13980, 2021.

[74] A. Schink, K. Naumoska, Z. Kitanovski et al., "Anti-inflammatory effects of cinnamon extract and identification of active compounds influencing the TLR2 and TLR4 signaling pathways," *Food & Function*, vol. 9, no. 11, pp. 5950–5964, 2018.

[75] H. S. Youn, J. K. Lee, Y. J. Choi et al., "Cinnamaldehyde suppresses toll-like receptor 4 activation mediated through the inhibition of receptor oligomerization," *Biochemical Pharmacology*, vol. 75, no. 2, pp. 494–502, 2008.

[76] A. M. Reddy, J. H. Seo, S. Y. Ryu et al., "Cinnamaldehyde and 2-methoxycinnamaldehyde as NF-kappaB inhibitors from *Cinnamomum cassia*," *Planta Medica*, vol. 70, no. 9, pp. 823–827, 2004.

[77] M. E. Kim, J. Y. Na, and J. S. Lee, "Anti-inflammatory effects of trans-cinnamaldehyde on lipopolysaccharide-stimulated macrophage activation via MAPKs pathway regulation," *Immunopharmacology and Immunotoxicology*, vol. 40, no. 3, pp. 219–224, 2018.

[78] C. Pannee, I. Chandhanee, and L. Wacharee, "Antiinflammatory effects of essential oil from the leaves of *Cinnamomum cassia* and cinnamaldehyde on lipopolysaccharide-stimulated J774A.1 cells," *Journal of Advanced Pharmaceutical Technology & Research*, vol. 5, no. 4, pp. 164–170, 2014.

[79] Q. Wang, K. Chen, F. Zhang et al., "TRPA1 regulates macrophages phenotype plasticity and atherosclerosis progression," *Atherosclerosis*, vol. 301, pp. 44–53, 2020.

[80] P. Libby, "The changing landscape of atherosclerosis," *Nature*, vol. 592, no. 7855, pp. 524–533, 2021.

[81] T. C. Lu, Y. H. Wu, W. Y. Chen, and Y. C. Hung, "Targeting oxidative stress and endothelial dysfunction using tanshinone IIA for the treatment of tissue inflammation and fibrosis," *Oxidative Medicine and Cellular Longevity*, vol. 2022, Article ID 2811789, 20 pages, 2022.

[82] Y. Liu, L. Li, L. Gao, C. Liang, and H. Yang, "Cinnamaldehyde attenuates lipopolysaccharide induced inflammation and apoptosis in human umbilical vein endothelial cells," *Zhonghua xin xue Guan Bing za zhi*, vol. 47, no. 6, pp. 465–470, 2019.

[83] J. Y. Guo, H. R. Huo, B. S. Zhao et al., "Cinnamaldehyde reduces IL-1β-induced cyclooxygenase-2 activity in rat cerebral microvascular endothelial cells," *European Journal of Pharmacology*, vol. 537, no. 1-3, pp. 174–180, 2006.

[84] B. C. Liao, C. W. Hsieh, Y. C. Liu, T. T. Tzeng, Y. W. Sun, and B. S. Wung, "Cinnamaldehyde inhibits the tumor necrosis factor-α-induced expression of cell adhesion molecules in endothelial cells by suppressing NF-κB activation: effects upon IκB and Nrf2," *Toxicology and Applied Pharmacology*, vol. 229, no. 2, pp. 161–171, 2008.

[85] N. Y. Kim, N. T. Trinh, S. G. Ahn, and S. A. Kim, "Cinnamaldehyde protects against oxidative stress and inhibits the TNF-α-induced inflammatory response in human umbilical vein endothelial cells," *International Journal of Molecular Medicine*, vol. 46, no. 1, pp. 449–457, 2020.

[86] J. M. Miano, E. A. Fisher, and M. W. Majesky, "Fate and state of vascular smooth muscle cells in atherosclerosis," *Circulation*, vol. 143, no. 21, pp. 2110–2116, 2021.

[87] W. Li, W. Zhi, J. Zhao, Q. Yao, F. Liu, and X. Niu, "Cinnamaldehyde protects VSMCs against ox-LDL-induced proliferation and migration through S arrest and inhibition of p38, JNK/MAPKs and NF-κB," *Vascular Pharmacology*, vol. 108, pp. 57–66, 2018.

[88] Y. Ding, L. Qiu, G. Zhao, J. Xu, and S. Wang, "Influence of cinnamaldehyde on viral myocarditis in mice," *The American Journal of the Medical Sciences*, vol. 340, no. 2, pp. 114–120, 2010.

[89] A. Daiber, O. Hahad, I. Andreadou, S. Steven, S. Daub, and T. Münzel, "Redox-related biomarkers in human cardiovascular disease - classical footprints and beyond," *Redox Biology*, vol. 42, article 101875, 2021.

[90] O. A. A. Nour, G. S. G. Shehatou, M. A. Rahim, M. S. El-Awady, and G. M. Suddek, "Cinnamaldehyde exerts vasculoprotective effects in hypercholestrolemic rabbits," *Naunyn-Schmiedeberg's Archives of Pharmacology*, vol. 391, no. 11, pp. 1203–1219, 2018.

[91] X. D. Li, L. W. Gu, Q. S. Ran et al., "Protective effects of three phenylallyl compounds from Guizhi decoction ox-LDL-induced oxidative stress injury of human brain microvascular endothelial cells," *Zhongguo Zhong yao za zhi= Zhongguo Zhongyao Zazhi= China Journal of Chinese Materia Medica*, vol. 41, no. 12, pp. 2315–2320, 2016.

[92] M. Khalid, G. Petroianu, and A. Adem, "Advanced glycation end products and diabetes mellitus: mechanisms and perspectives," *Biomolecules*, vol. 12, no. 4, p. 542, 2022.

[93] M. M. Tarkhan, K. S. Balamsh, and H. M. El-Bassossy, "Cinnamaldehyde protects from methylglyoxal-induced vascular damage: effect on nitric oxide and advanced glycation end products," *Journal of Food Biochemistry*, vol. 43, no. 7, article e12907, 2019.

[94] M. E. Abdelmageed, G. S. Shehatou, R. A. Abdelsalam, G. M. Suddek, and H. A. Salem, "Cinnamaldehyde ameliorates STZ-induced rat diabetes through modulation of IRS1/PI3K/AKT2 pathway and AGEs/RAGE interaction," *Naunyn-Schmiedeberg's Archives of Pharmacology*, vol. 392, no. 2, pp. 243–258, 2019.

[95] F. Wang, C. Pu, P. Zhou et al., "Cinnamaldehyde prevents endothelial dysfunction induced by high glucose by activating Nrf2," *Cellular Physiology and Biochemistry*, vol. 36, no. 1, pp. 315–324, 2015.

[96] P. Wang, Y. Yang, D. Wang et al., "Cinnamaldehyde ameliorates vascular dysfunction in diabetic mice by activating Nrf2," *American Journal of Hypertension*, vol. 33, no. 7, pp. 610–619, 2020.

[97] W. Zhao, Y. Zhou, T. Xu, and Q. Wu, "Ferroptosis: opportunities and challenges in myocardial ischemia-reperfusion injury," *Oxidative Medicine and Cellular Longevity*, vol. 2021, Article ID 9929687, 12 pages, 2021.

[98] W. Á. Trujillo-Rangel, L. García-Valdés, M. M.-d. Villar, R. Castañeda-Arellano, S. E. Totsuka-Sutto, and L. García-Benavides, "Therapeutic Targets for Regulating Oxidative Damage Induced by Ischemia- Reperfusion Injury: A Study from a Pharmacological Perspective," *Oxidative medicine and cellular longevity*, vol. 2022, Article ID 8624318, 25 pages, 2022.

[99] M. Sedighi, A. Nazari, M. Faghihi et al., "Protective effects of cinnamon bark extract against ischemia–reperfusion injury

and arrhythmias in rat," *Phytotherapy research : PTR*, vol. 32, no. 10, pp. 1983–1991, 2018.

[100] F. Song, H. Li, J. Sun, and S. Wang, "Protective effects of cinnamic acid and cinnamic aldehyde on isoproterenol- induced acute myocardial ischemia in rats," *Journal of Ethnopharmacology*, vol. 150, no. 1, pp. 125–130, 2013.

[101] Q. Wang, J. Sun, M. Liu, Y. Zhou, L. Zhang, and Y. Li, "The new role of AMP-activated protein kinase in regulating fat metabolism and energy expenditure in adipose tissue," *Biomolecules*, vol. 11, no. 12, p. 1757, 2021.

[102] B. Huang, H. D. Yuan, D. Y. Kim, H. Y. Quan, and S. H. Chung, "Cinnamaldehyde prevents adipocyte differentiation and adipogenesis via regulation of peroxisome proliferator-activated receptor-γ (PPARγ) and AMP-activated protein kinase (AMPK) pathways," *Journal of Agricultural and Food Chemistry*, vol. 59, no. 8, pp. 3666–3673, 2011.

[103] P. Khare, S. Jagtap, Y. Jain et al., "Cinnamaldehyde supplementation prevents fasting-induced hyperphagia, lipid accumulation, and inflammation in high-fat diet-fed mice," *BioFactors*, vol. 42, no. 2, pp. 201–211, 2016.

[104] J. G. Neto, S. K. Boechat, J. S. Romão, L. R. Kuhnert, C. C. Pazos-Moura, and K. J. Oliveira, "Cinnamaldehyde treatment during adolescence improves white and brown adipose tissue metabolism in a male rat model of early obesity," *Food & Function*, vol. 13, no. 6, pp. 3405–3418, 2022.

[105] J. Jiang, M. P. Emont, H. Jun et al., "Cinnamaldehyde induces fat cell-autonomous thermogenesis and metabolic reprogramming," *Metabolism: clinical and experimental*, vol. 77, pp. 58–64, 2017.

[106] J. G. O. Neto, S. K. Boechat, J. S. Romao, C. C. Pazos-Moura, and K. J. Oliveira, "Treatment with cinnamaldehyde reduces the visceral adiposity and regulates lipid metabolism, autophagy and endoplasmic reticulum stress in the liver of a rat model of early obesity," *The Journal of Nutritional Biochemistry*, vol. 77, article 108321, 2020.

[107] P. Yang, J. Feng, Q. Peng, X. Liu, and Z. Fan, "Advanced glycation end products: potential mechanism and therapeutic target in cardiovascular complications under diabetes," *Oxidative Medicine and Cellular Longevity*, vol. 2019, Article ID 9570616, 12 pages, 2019.

[108] S. A. Amiel, P. Aschner, B. Childs et al., "Hypoglycaemia, cardiovascular disease, and mortality in diabetes: epidemiology, pathogenesis, and management," *The Lancet Diabetes and Endocrinology*, vol. 7, no. 5, pp. 385–396, 2019.

[109] Z. Ataie, M. Dastjerdi, K. Farrokhfall, and Z. Ghiravani, "The effect of cinnamaldehyde on iNOS activity and NO-induced islet insulin secretion in high-fat-diet rats," *Evidence-based Complementary and Alternative Medicine*, vol. 2021, Article ID 9970678, 8 pages, 2021.

[110] W. Zhang, Y. Xu, F. Guo, Y. Meng, and M. Li, "Anti-diabetic effects of cinnamaldehyde and berberine and their impacts on retinol-binding protein 4 expression in rats with type 2 diabetes mellitus," *Chinese Medical Journal*, vol. 121, no. 21, pp. 2124–2128, 2008.

[111] J. E. Li, K. Futawaka, H. Yamamoto et al., "Cinnamaldehyde contributes to insulin sensitivity by activating PPARδ, PPARγ, and RXR," *The American Journal of Chinese Medicine*, vol. 43, no. 5, pp. 879–892, 2015.

[112] N. P. Gannon, J. K. Schnuck, C. M. Mermier, C. A. Conn, and R. A. Vaughan, "*trans-Cinnamaldehyde* stimulates mitochondrial biogenesis through PGC-1 α and PPARβ/δ leading

to enhanced GLUT4 expression," *Biochimie*, vol. 119, pp. 45–51, 2015.

[113] P. Anand, K. Y. Murali, V. Tandon, P. S. Murthy, and R. Chandra, "Insulinotropic effect of cinnamaldehyde on transcriptional regulation of pyruvate kinase, phosphoenolpyruvate carboxykinase, and GLUT4 translocation in experimental diabetic rats," *Chemico-Biological Interactions*, vol. 186, no. 1, pp. 72–81, 2010.

[114] J. Shi, Y. Yang, A. Cheng, G. Xu, and F. He, "Metabolism of vascular smooth muscle cells in vascular diseases," *American Journal of Physiology. Heart and Circulatory Physiology*, vol. 319, no. 3, pp. H613–H631, 2020.

[115] H. Kwon, J. J. Lee, J. H. Lee et al., "Cinnamon and its components suppress vascular smooth muscle cell proliferation by up-regulating cyclin-dependent kinase inhibitors," *The American Journal of Chinese Medicine*, vol. 43, no. 4, pp. 621–636, 2015.

[116] N. E. Buglak, W. Jiang, and E. S. M. Bahnson, "Cinnamic aldehyde inhibits vascular smooth muscle cell proliferation and neointimal hyperplasia in zucker diabetic fatty rats," *Redox Biology*, vol. 19, pp. 166–178, 2018.

[117] W. Li, Z. Zhang, X. Li et al., "CGRP derived from cardiac fibroblasts is an endogenous suppressor of cardiac fibrosis," *Cardiovascular Research*, vol. 116, no. 7, pp. 1335–1348, 2020.

[118] M. Liu, B. L. de Juan Abad, and K. Cheng, "Cardiac fibrosis: myofibroblast-mediated pathological regulation and drug delivery strategies," *Advanced Drug Delivery Reviews*, vol. 173, pp. 504–519, 2021.

[119] N. G. Frangogiannis, "Transforming growth factor-β in myocardial disease," *Nature Reviews Cardiology*, vol. 19, no. 7, pp. 435–455, 2022.

[120] L. Yang, Q. Wu, Y. Liu, Z. F. Hu, Z. Y. Bian, and Q. Z. Tang, "Cinnamaldehyde attenuates pressure overload-induced cardiac hypertrophy," *International Journal of Clinical and Experimental Pathology*, vol. 8, no. 11, pp. 14345–14354, 2015.

[121] J. Huang, J. Huang, Q. Yang, and L. He, "Effects and mechanisms of cinnamaldehyde on proliferation and collagen synthesis induced by high glucose in cardiac fibroblasts," *Chinese Journal of Diabetes*, vol. 24, no. 9, pp. 836–839, 2016.

[122] D. Qian, J. Tian, S. Wang et al., "Trans-cinnamaldehyde protects against phenylephrine-induced cardiomyocyte hypertrophy through the CaMKII/ERK pathway," *BMC complementary medicine and therapies*, vol. 22, no. 1, p. 115, 2022.

[123] Y. Xiao, Q. Wu, X. Jiang, and Q. Tang, "Cinnamaldehyde attenuates pressure overload-induced cardiac fibrosis via inhibition of endothelial mesenchymal transition," *Zhonghua yi xue za zhi*, vol. 97, no. 11, pp. 869–873, 2017.

[124] S. Li, X. Sun, H. Wu et al., "TRPA1 promotes cardiac myofibroblast transdifferentiation after myocardial infarction injury via the Calcineurin-NFAT-DYRK1A signaling pathway," *Oxidative Medicine and Cellular Longevity*, vol. 2019, Article ID 6408352, 17 pages, 2019.

[125] Y. Zhu, J. Qu, L. He et al., "Calcium in vascular smooth muscle cell elasticity and adhesion: novel insights into the mechanism of action," *Frontiers in Physiology*, vol. 10, p. 852, 2019.

[126] G. Pozsgai, J. V. Bodkin, R. Graepel, S. Bevan, D. A. Andersson, and S. D. Brain, "Evidence for the pathophysiological relevance of TRPA1 receptors in the cardiovascular system *in vivo*," *Cardiovascular Research*, vol. 87, no. 4, pp. 760–768, 2010.

[127] H. M. El-Bassossy, A. Fahmy, and D. Badawy, "Cinnamaldehyde protects from the hypertension associated with diabetes," *Food and Chemical Toxicology*, vol. 49, no. 11, pp. 3007–3012, 2011.

[128] A. Singh, S. A. Khan, R. Choudhary, and S. H. Bodakhe, "Cinnamaldehyde attenuates cataractogenesis via restoration of hypertension and oxidative stress in fructose-fed hypertensive rats," *Journal of pharmacopuncture*, vol. 19, no. 2, pp. 137–144, 2016.

[129] A. V. Araújo, F. A. Andrade, M. Paulo et al., "NO donors induce vascular relaxation by different cellular mechanisms in hypertensive and normotensive rats," *Nitric Oxide*, vol. 86, pp. 12–20, 2019.

[130] J. Alvarez-Collazo, L. Alonso-Carbajo, A. I. López-Medina et al., "Cinnamaldehyde inhibits L-type calcium channels in mouse ventricular cardiomyocytes and vascular smooth muscle cells," *Pflugers Archiv : European journal of physiology*, vol. 466, no. 11, pp. 2089–2099, 2014.

[131] Y. L. Xue, H. X. Shi, F. Murad, and K. Bian, "Vasodilatory effects of cinnamaldehyde and its mechanism of action in the rat aorta," *Vascular Health and Risk Management*, vol. 7, pp. 273–280, 2011.

[132] P. W. Pires and S. Earley, "Neuroprotective effects of TRPA1 channels in the cerebral endothelium following ischemic stroke," *eLife*, vol. 7, article e35316, 2018.

[133] A. A. Aubdool, X. Kodji, N. Abdul-Kader et al., "TRPA1 activation leads to neurogenic vasodilatation: involvement of reactive oxygen nitrogen species in addition to CGRP and NO," *British Journal of Pharmacology*, vol. 173, no. 15, pp. 2419–2433, 2016.

[134] J. Tian, X. L. Shan, S. N. Wang et al., "trans-Cinnamaldehyde suppresses microtubule detyrosination and alleviates cardiac hypertrophy," *European Journal of Pharmacology*, vol. 914, article 174687, 2022.

[135] F. Violi, D. Pastori, P. Pignatelli, and R. Carnevale, "Nutrition, thrombosis, and cardiovascular disease," *Circulation Research*, vol. 126, no. 10, pp. 1415–1442, 2020.

[136] S. Navarrete, C. Solar, R. Tapia, J. Pereira, E. Fuentes, and I. Palomo, "Pathophysiology of deep vein thrombosis," *Clinical and Experimental Medicine*, 2022.

[137] V. Ballabeni, M. Tognolini, S. Bertoni et al., "Antiplatelet and antithrombotic activities of essential oil from wild *Ocotea quixos* (Lam.) Kosterm. (Lauraceae) calices from Amazonian Ecuador," *Pharmacological Research*, vol. 55, no. 1, pp. 23–30, 2007.

[138] J. Huang, S. Wang, X. Luo, Y. Xie, and X. Shi, "Cinnamaldehyde reduction of platelet aggregation and thrombosis in rodents," *Thrombosis Research*, vol. 119, no. 3, pp. 337–342, 2007.

[139] S. Y. Kim, Y. K. Koo, J. Y. Koo et al., "Platelet anti-aggregation activities of compounds from *Cinnamomum cassia*," *Journal of Medicinal Food*, vol. 13, no. 5, pp. 1069–1074, 2010.

[140] R. H. Raghavendra and K. A. Naidu, "Spice active principles as the inhibitors of human platelet aggregation and thromboxane biosynthesis," *Prostaglandins, Leukotrienes, and Essential Fatty Acids*, vol. 81, no. 1, pp. 73–78, 2009.

[141] K. Y. Kim, S. Bang, S. Han et al., "TRP-independent inhibition of the phospholipase C pathway by natural sensory ligands," *Biochemical and Biophysical Research Communications*, vol. 370, no. 2, pp. 295–300, 2008.

[142] F. Guo, Y. Wang, J. Wang et al., "Choline protects the heart from doxorubicin-induced cardiotoxicity through vagal activation and Nrf2/HO-1 pathway," *Oxidative Medicine and*

Hindawi

Retraction

Retracted: Colostomy Delays Cell Loss in the Brain and Improves Juvenile Survival in a Neonatal Rat Model of Hirschsprung's Disease

Oxidative Medicine and Cellular Longevity

This article has been retracted by Hindawi following an investigation undertaken by the publisher [1]. This investigation has uncovered evidence of one or more of the following indicators of systematic manipulation of the publication process:

(1) Discrepancies in scope

(2) Discrepancies in the description of the research reported

(3) Discrepancies between the availability of data and the research described

(4) Inappropriate citations

(5) Incoherent, meaningless and/or irrelevant content included in the article

(6) Peer-review manipulation

The presence of these indicators undermines our confidence in the integrity of the article's content and we cannot, therefore, vouch for its reliability. Please note that this notice is intended solely to alert readers that the content of this article is unreliable. We have not investigated whether authors were aware of or involved in the systematic manipulation of the publication process.

Wiley and Hindawi regrets that the usual quality checks did not identify these issues before publication and have since put additional measures in place to safeguard research integrity.

We wish to credit our own Research Integrity and Research Publishing teams and anonymous and named external researchers and research integrity experts for contributing to this investigation.

The corresponding author, as the representative of all authors, has been given the opportunity to register their agreement or disagreement to this retraction. We have kept a record of any response received.

References

[1] D. Xie, Y. Du, Y. Wang, G. D. H. Croaker, Z. Z. Wei, and Z.-M. Song, "Colostomy Delays Cell Loss in the Brain and Improves Juvenile Survival in a Neonatal Rat Model of Hirschsprung's Disease," *Oxidative Medicine and Cellular Longevity*, vol. 2022, Article ID 3792798, 7 pages, 2022.

Research Article

Colostomy Delays Cell Loss in the Brain and Improves Juvenile Survival in a Neonatal Rat Model of Hirschsprung's Disease

Dan Xie,[1,2] **Yitong Du,**[1] **Yutao Wang,**[3] **Geoffrey David Hain Croaker,**[4] **Zheng Zachory Wei** [iD],[1,3] **and Zan-Min Song** [iD][2]

[1]*Department of Neurology, Beijing Friendship Hospital Center for Neurological Disorders, Neuroscience Institute, National Clinical Research Center for Digestive Diseases, Beijing, China*

[2]*The Eccles Institute of Neuroscience, The John Curtin School of Medical Research and Medical School, Australian National University, Canberra, ACT, Australia*

[3]*Department of Clinical Medicine, School of Basic Medical Sciences, Capital Medical University, Beijing, China*

[4]*Paediatric Surgery, The Canberra Hospital, Canberra, ACT, Australia*

Correspondence should be addressed to Zheng Zachory Wei; weizz@ctrlyin.org and Zan-Min Song; z.song@griffith.edu.au

Hirschsprung's disease is a congenital malformation characterized by the absence of enteric ganglia in the distal intestine and gut obstruction. Our previous study indicates the brain pathology during the disease progression. A subpopulation of Hirschsprung's disease patients is also associated with anomalies of the central nervous system. In the investigation, we studied a rat model of Hirschsprung's disease, known as spotting lethal (*sl/sl*) $ET_B^{-/-}$ rats, which carries a spontaneous deletion in endothelin receptor B (human gene name: *EDNRB*) and manifests a similar phenotype as humans with Hirschsprung's disease. Homozygous mutant *sl/sl* rats were successfully rescued from premature death by performing colostomy and dramatically survived to their juvenile age. By the body weight measured, their body growth was not revealed to be significantly different between $ET_B^{-/-}$ and wildtype $ET_B^{+/+}$ or heterozygous (+/*sl*) $ET_B^{+/-}$ groups while all underwent the same colostomy. Cell loss was investigated in several brain regions by using terminal deoxynucleotidyl transferase-mediated dUTP nick end-labeling assay (TUNEL) in $ET_B^{+/+}$, $ET_B^{-/-}$, and $ET_B^{+/-}$ rats. Number of TUNEL-positive cells in the cerebellum and the hippocampus of $ET_B^{-/-}$ rats was significantly increased compared with that of the $ET_B^{+/+}$ and $ET_B^{+/-}$ rats. TUNEL-positive cells were observed in the molecular layer and granular cell layers of the cerebellum. In contrast, no significant difference in the density of TUNEL-positive cells was revealed in the cerebral cortex. These results suggest that either endothelin receptor B *sl* mutation or colostomy has predominant lasting effects on the cell survival/loss in the cerebellum and hippocampus of adult $ET_B^{-/-}$ rats. Our findings provide the information on cellular changes in the brains of patients with Hirschsprung's disease due to congenital *EDNRB* mutation as well as clinically relevant interventions.

1. Introduction

The major functions of the intestine are controlled by the enteric nervous system located within the wall of the gut tissue [1]. The absence of enteric neurons can cause a serious medical condition called Hirschsprung's disease [2, 3]. It is a congenital malformation due to a failure of neural crest-derived precursors to colonize intestine during fetal period. The serious consequences include from severe intestinal obstruction to death. Although surgical removal of the blocked intestine saves the lives of Hirschsprung's disease patients, some are complicated with a whole variety of neurological deficits [4]. This indicates that the malformation in Hirschsprung's disease is not limited to the gut but also involves abnormalities in the central nervous system. Our previous reports include a dramatic increase in TUNEL-positive cells in the cerebellum at an early neonatal day 3 of age in rats [5]. The pathological changes are strictly different from neurotropic factor pathways (e.g., BDNF or GDNF). We have previously tested a surgical procedure for

prolonging the life of the spotting lethal $ET_B^{-/-}$ rat [6]. That allows us to further study the long-term neural mechanisms in the developing brain model of Hirschsprung's disease.

The mutation of the gene for endothelin receptor B (human gene name: *EDNRB*) is known to cause both sporadic and familial Hirschsprung's disease in genetically isolated population of Old Order Mennonite [2, 3]. *EDNRB* is the major receptor subtype with the roles in neural cell differentiation, neuronal migration, proliferation, or survival during development [7]. However, little piece of evidence is known about the cellular changes in the brains from Hirschsprung's disease patients. Study of the animal model is useful for the understanding of cellular changes and the potential interventions.

The current study utilizes a strain, known as spotting lethal (*sl/sl*) $ET_B^{-/-}$ rat, which carries a spontaneous deletion of 301 bp within *EDNRB* gene, and manifests a similar phenotype as in humans with Hirschsprung's disease [8, 9]. The $ET_B^{-/-}$ rats demonstrate a significant decrease in cellular proliferation and an increase in cell death in the cerebellum and the hippocampus/dentate gyrus. *EDNRB*role is critical not only for its effect on the development of the enteric nervous system but also an effect on the development of the brain. Studies on the American MENSA family of Hirschsprung's disease have shown an epilepsy and mental retardation. This phenotype behind an *EDNRB* function remains to be determined [10]. Additionally, due to the genetic lethality of *EDNRB* gene defects, investigation was not focused on the effect of *EDNRB*neural development and the CNS. Our observations based on rat model of enterocutaneous stoma included the effect of *EDNRB* in the developing brain. We curiously tested *EDNRB* deficiency in the rats that led to increased neuronal apoptosis and decreased proliferation in the cerebellum and hippocampus. It was confirmed that *EDNRB* promoted neuronal proliferation and inhibited apoptosis during the development of the nervous system.

However, it was not known whether some of the effects observed in neonatal rats persist into adult life due to inevitable premature death of $ET_B^{-/-}$ rats. To study the changes in juvenile rats, we performed colostomy on 7-day-old $ET_B^{-/-}$ rats as previously reported by our group [6]. This surgical operation allowed the contents of the large bowel to be discharged directly through the abdominal wall. The $ET_B^{-/-}$ rat could live to a juvenile age for our research. In this morphological study, we focused on the effects of *EDNRB* deficiency on cell death in different brain regions of the juvenile $ET_B^{-/-}$ rat, by comparing with their wild type (+/+) $ET_B^{+/+}$ or heterozygous (+/sl) $ET_B^{+/-}$ littermates.

2. Material and Methods

2.1. Experimental Design. Genotyping was done at an earlier age of the rats, for surgical design and grouping during postnatal day 5 (P5) to day 7 (P7). The grouping was randomly performed for colostomy or sham operations after considering genotyping results [8]. The research protocol was modified from our previous article [11], with changes in the surgical conditions considering the study design and the homozygous rats, which usually had poorer nutrition, slower growth, and lighter weight. Compared to the previous protocol, this updated result suggested a much lower mortality rate, consistently showing improved postoperative survival rate. Consequently, it was conducive to any postoperative observation, with extended animal growth to no shorter than postnatal 28 days under surgery. Otherwise, that gene with a fatal mutation was related to the loss of intestine peristaltic function and to the megacolon unable to defecate, leading to water and electrolytes disorder around their P7 to P10 when they barely survived. Our design included colostomy surgeries on the homozygotes to allow the excretion of feces from the stomas throught the abdominal wall. The operated rats survived till skin pigment changes into small black patches and the stomach distention, bowel obstruction and megacolon were relieved.

2.2. Animals. Experiments were performed on the Wistar-Imamichi, congenital aganglionosis rat strain that was shown to lack a functional *EDNRB* due to a spontaneous 301 base pair deletion in *EDNRB* gene [9]. Littermates of $ET_B^{+/+}$, $ET_B^{+/-}$, and $ET_B^{-/-}$ rats were generated by heterozygous mating originally from an established colony at the Australian National University animal facilities. The neonatal phenotype for homozygote includes small spotting skin due to reduced cutaneous pigmentation. During P5 to P7, the pups were genotyped as previously performed [8]. All treatment and subsequent operations on rats were approved by the animal ethics committee of the Australian National University.

2.3. Colostomy Surgery. Procedures of colostomy in neonatal rats were followed with slight modifications [6]. Briefly, a total of 22 rats of different genotypes at the age of P7 were anesthetized with 2% isoflurane carried in O_2 at 300 ml/min through an inhalation mask. Abdominal skin was cleaned with chlorhexidine and cetrimide solution (Pfizer Australia) and 70% ethanol. A midline incision was made to minimise faecal soiling and subsequent inflammation of the hind limbs. The proximal colon adjacent to the caecum was pulled through the incision on the abdominal wall. Four sutures along the circumference of the colon wall were anchored to abdominal muscle at the rostral end of incision using absorbable 8-0 braided coated Vicryl (Ethicon Inc.). At about 0.5 cm distal to this sutured region, another segment was similarly sutured to the caudal end of the incision. The bowel was severed in between to perform two colostomies. Both were further fixed to the skin using the 6-0 nonabsorbable polypropylene monofilament suture (Ethicon Inc.). The skin between the two colostomies was closed using 6-0 suture. Wound was applied with Wound-Gard (Virbac Pty Ltd., Australia), a bitter tasting antiseptic cream, to prevent the mother from licking the wound and cannibalism, which occurred for eight rats without the cream application. After regaining consciousness, the pups were wiped thoroughly with the mother's bedding and faecal pellets before being returned to the mother, together with unoperated pups in the same cage. Postoperated rats were then monitored on a daily basis. Warm saline-soaked cotton tips were used to remove dried faecal matter blocking the stoma. All operated

pups were weaned at P21 after birth and fed with normal rat chow for additionally one week. Body weights were recorded at P28 and brain tissue was collected according to our previous study [11]. We were able to collect data from fourteen rats with colostomy (four $ET_B^{+/+}$ rats, six $ET_B^{+/-}$ rats, and four $ET_B^{-/-}$ rats).

Sham operations were performed in additional five $ET_B^{+/+}$ rats, which entailed incising abdominal wall, followed by gently handling the intestine and suturing the wounds. Those rats were handled in the same way with the others receiving the colostomy. With our surgical interventions, the survival rate of the animals detected at P28 was around 66.7%.

2.4. Tissue Preparation and TUNEL Assay. The effect of *EDNRB* deficiency on cell death in the juvenile rat brain was assessed using terminal deoxynucleotidyl transferase-mediated dUTP nick end-labeling (TUNEL). Four to six rats for each genotype and operations ($ET_B^{+/+}$ with colostomy, $ET_B^{+/-}$ with colostomy, and $ET_B^{-/-}$ with colostomy) were examined at the age of P28 (three weeks after colostomy). Rats were sacrificed after i.p. injection of pentobarbital at 100 mg/kg and transcardial perfusion-fixed with 4% paraformaldehyde. Brains were dissected and postfixed and coronal sections were made at 12 μm on a cryostat. Three to four random sections from each region of the rat were processed for TUNEL with recombinant terminal transferase (Roche Diagnostics, Cat. 03333574001) combined with biotinylated dUTP (Roche, Cat. 11093070910), followed with streptavidin conjugated Alexa Fluor 594 (Invitrogen, Cat. S32356). Sections were counterstained with DAPI (300 nM in PBS).

2.5. Image Analysis. Fluorescence images of TUNEL-stained sections were examined under Nikon A1 confocal microscope system with appropriate filter sets. Images were collected from three to four random sections in each region for cell counting using ImageJ (1.46r; W. Rasband, NIH, USA) within the cerebellum, the hippocampus/dentate gyrus, and the cerebral cortex. All cell counting was carried out by experimenters blinded to the genotype.

2.6. Cell Culture and Western Blot Analysis. Human SH-SY5Y cell line was applied to confirm the roles of the *EDNRB* mutations in the neural-like cells. The culture conditions were used according to protocols with slight modification [12]. Cells were maintained in RPMI-1640 medium (Life Technologies, USA), supplemented with 10% fetal bovine serum (Hyclone, USA) and 100 U/ml penicillin/streptomycin (ABAM Life Technologies, California, USA) at 5% CO_2, 37°C with humidified air in an incubator. Transfection was performed and plasmid provided by Dr. Jinling Huang (Peking University; Hechuang Biotech, Guangzhou, China) with human cell line *EDNRB* gene nucleotide deletion of GTGCCTAAAGGAGACAGGACGGCAGGATCTC CGCCACGCACCATCTCCCCTCCCCCGTGCCAAGGAC CCATCGAGATCAAGGAGACTTTCAAATACATCAACA CGGTTGTGTCCTGCCTTGTGTTCGTGCTGGGGATCA TCGGGAACTCCACACTTCTGAGAATTATCTACAAGA ACAAGTGCATGCGAAACGGTCCCAATATCTTGATCG

CCAGCTTGGCTCTGGGAGACCTGCTGCACATCGTCA TTGACATCCCTATCAATGTCTACAAG according to matching of the rat gene nucleotide sequence reported [9]. The *EDNRB* gene was mutated via the transfection using Lipofectamine 3000 kit. After medium change, the cells were then supplemented with 100 μg/ml G418 (Life Technologies).

The protein sample was collected from control cell lines or *EDNRB* mutation cell lines. We performed the experiments according to our previous publication with minor modifications [13]. The cells were scratched and lysed on ice in RIPA buffer (20 mM pH 7.5 Tris-HCl, 150 mM NaCl, 1 mM Na_2EDTA, 1 mM EGTA, 1% Triton, 2.5 mM sodium pyrophosphate, 1 mM beta-glycerophosphate, 1 mM Na_3VO_4, 1 μg/ml leupeptin, and 1 mM phenylmethylsulfonyl fluoride). With 30 min incubation in EP tubes, the cell lysates were centrifuged at 12,000 × g for 30 min at 4°C. Supernatant was then collected. Protein concentration in the solution was determined using a Coomassie Brilliant Blue protein assay kit (Bio-Rad). Western blot was carried out and AEP antibody 6E3 as previously described [14].

2.7. Statistical Analysis. Results of body weight and number of dead cells (e.g., TUNEL-positive cells per mm^2) were presented as the mean ± SEM. For statistical analysis of data from different genotypes, one-way analysis of variance (ANOVA) was used followed by a Tukey's multiple comparison test (Prism 5, GraphPad, CA, USA) unless otherwise specified. Differences were considered significant at $P < 0.05$.

3. Results

3.1. The Effect of Colostomy on the Body Growth of Rats. Our previous study showed that colostomy was able to rescue $ET_B^{-/-}$ rats that would otherwise die early due to gut blockage and subsequent malnutrition [6]. We performed colostomy surgery on the P7 rats (Figure 1). The weight gain of four groups of rats was compared at 28 days old (three weeks after colostomy). In rats that received colostomy, the averaged body weight in $ET_B^{-/-}$ rats was lower than that in $ET_B^{+/+}$ rats or $ET_B^{+/-}$ rats, although it did not reach a statistically significant level (Figure 2). However, colostomy operation per se did affect body weight, since the weight of $ET_B^{+/+}$ group with sham operations was significantly higher than $ET_B^{+/+}$ rats with colostomy. The human cell culture experiments further suggested that there were not dependent on either BDNF or GDNF ($P > 0.05$, Figure S1) in the cells with mutated *EDNRB*, consistent with our previous reports in the animal model. We assumed that colostomy operation compromised body growth, probably due to decreased fluid and electrolyte absorption and accelerated gastric emptying but showed protection of the brain.

3.2. Significant Cell Loss in the Cerebellum in $ET_B^{-/-}$ Rats. To evaluate the detrimental cell death effect of the mutated *EDNRB*, TUNEL-positive nuclei were stained and compared among four groups of juvenile rats: $ET_B^{+/+}$ with colostomy, $ET_B^{+/-}$ with colostomy, and $ET_B^{-/-}$ with colostomy under genotyping (Figure S2). The Purkinje cell nuclei with DAPI
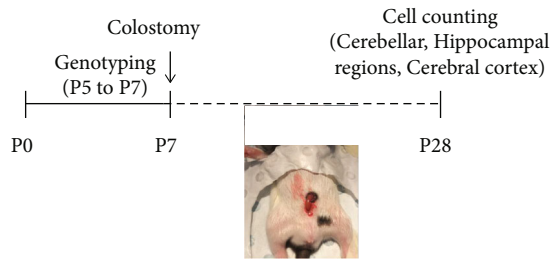
Figure 1: The surgery procedure and experimental design. P0/5/7/28: postnatal day 0/5/7/28.
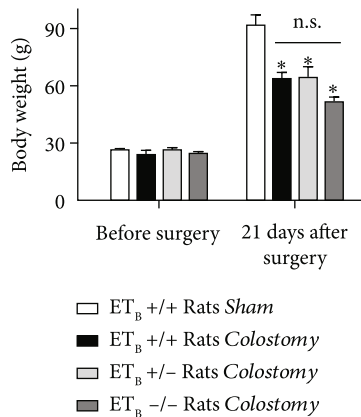
Figure 2: Body weight after colostomy surgery. Comparison of the body weight of $ET_B^{+/+}$ rats without colostomy (sham operated) and $ET_B^{+/+}$ rats, $ET_B^{+/-}$ rats, or $ET_B^{-/-}$ rats with colostomy. The colostomy surgeries were performed at P7 and the body weights were measured at an age of 28 days. All rats with colostomy had comparable body weights regardless of their genotypes. We observed a slight lighter in all the operated rats than the $ET_B^{+/+}$ rats without colostomy. Importantly, colostomy saved $ET_B^{-/-}$ rats till at least 28 days after birth, compared to a barely survival rate among $ET_B^{-/-}$ rats without colostomy (data not shown).

labeling were located between the molecular layer and the granular cell layer. TUNEL-positive nuclei were found in the cerebellum of $ET_B^{+/+}$ rats (Figures 3(a)–3(f)). Significantly higher number of TUNEL-positive nuclei per section was revealed in the same region of $ET_B^{-/-}$ rats with colostomy (Figures 3(e) and 3(f)).

By examining the four layers of the juvenile cerebellum (Figure 3), the largest proportion of TUNEL-positive cells in $ET_B^{-/-}$ rats were located in the molecular layer, followed by the granular cell layer. The white matter and Purkinje cell layer had occasional TUNEL-positive cells. It might be interesting to notice that the proportion remained similar across different genotypes and no statistically significant difference was found in any layers between each of the four genotypes (data not shown). Those results indicated that *EDNRB* mutation could be consistently/broadly involved in apoptosis in the cerebellum of juvenile $ET_B^{-/-}$ rats.

3.3. Significant Cell Loss in the Hippocampus/Dentate Gyrus in $ET_B^{-/-}$ Rats.
The cerebral cortex, the dentate gyrus, and the hippocampus were examined among normal, $ET_B^{+/-}$

and $ET_B^{-/-}$ genotypes littermates. TUNEL-positive nuclei were found in CA1 to CA3 regions of the hippocampus and the dentate gyrus of $ET_B^{+/+}$ rats (Figure S3). In contrast, density of TUNEL-positive nuclei in the hippocampus/dentate gyrus was significantly higher in $ET_B^{-/-}$ rats than in $ET_B^{+/+}$ rats with colostomy. Little difference in the hippocampus was seen between $ET_B^{+/+}$ and $ET_B^{+/-}$ or between $ET_B^{+/-}$ and $ET_B^{-/-}$ groups of juvenile rats. Interestingly, pursuing our previous design, there was no increased level of BDNF or GDNF (data not shown), two growth factors that contribute to brain development and repair greatly.

3.4. Cell Loss in the Cerebral Cortex.
Few TUNEL-positive cells were found in the cerebral cortex of juvenile rats (Figure 3(g)). There was no significant change between each of the groups and $ET_B^{-/-}$ animals received colostomy. These results indicated that the loss of functional *EDNRB* had little relation with the cell death in the cerebral cortex of juvenile rats. Consistently, the animal survival was dramatically improved (Figure 4).

4. Discussion

In Hirschsprung's disease (or congenital aganglionic megacolon), it occurs with abnormal development of intestinal neurons (ganglion cells) and delayed progression of stool through the intestines. Following surgical procedures in clinic, it is commonly observed for children with Hirschsprung's disease to have few problems [15]. Based on evidences from abdominal x-ray, contrast enema, and rectal biopsy, the pathological gut segment can be removed by the surgery. There are usually few follow-up interventions although neurodevelopmental issues of the children are documented [16]. The clinical follow-up studies have limitations. Understanding the disease progression in central nervous system research is useful for the further exploration of neurodevelopment mechanisms and treatment [17].

Our previous collaborational study has shown that $ET_B^{-/-}$ rats can be rescued from premature death when colostomy is performed at the neonatal period [6]. This operation enables us to keep $ET_B^{-/-}$ rats survive up to four to six weeks when they are sacrificed. The present study confirms that $ET_B^{-/-}$ rats (which would otherwise die) have similar weight gain as their $ET_B^{+/+}$ and $ET_B^{+/-}$ littermates that receive the same colostomy surgery. This indicates that the effects on cell death in the brain are unlikely related to malnutrition. However, rats with colostomy have significantly lower body weight than sham-operated $ET_B^{+/+}$ rats, which suggests that colostomy per se compromises body growth. The mechanisms are related to decreased fluid and electrolyte absorption and accelerate gastric emptying as in human with colostomy. Therefore, the comparison of brain development has to be between different genotypes with colostomy. There was no difference in behaviors as well as the general body size of the rats.

The effect of null mutation of *EDNRB* was further examined for cell death in the cerebellum, the cerebral cortex, the dentate gyrus, and the hippocampus by comparing $ET_B^{-/-}$,

(a)   (b)   (c)

(d)   (e)

(f)   (g)
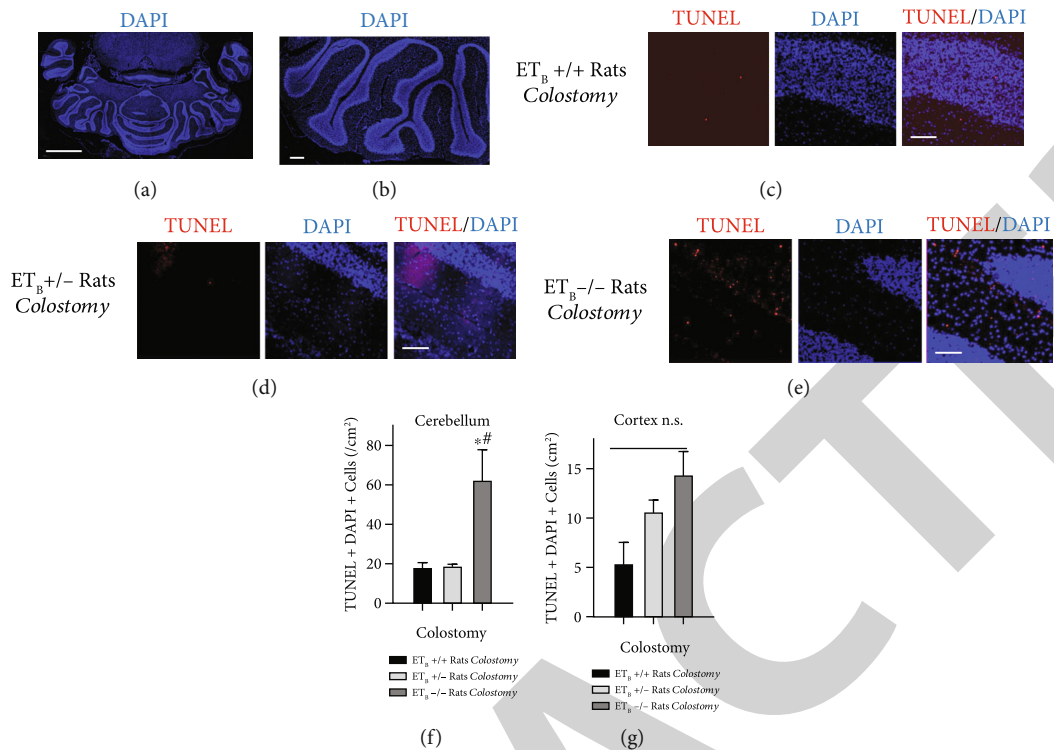
FIGURE 3: Cell death analysis in the brain regions. Representative confocal images of transverse sections of the cerebellum of the juvenile rats indicated the brain regions showing TUNEL-positive nuclei (red) with DAPI counterstaining (blue). The structure of juvenile cerebellum was revealed with DAPI staining, where molecular layer, granular cell layer, and white matter were clearly recognizable. (a) Lower magnification view of a section from sham-operated $ET_B^{+/+}$ rat showing folia. (b) Higher magnification view of the same section showing the molecular layer, granular cell layer, white matter, and Purkinje cell layer. (c and d) Occasional TUNEL-positive nuclei are found in granular cell layer and the molecular layer in $ET_B^{+/+}$ rats and in $ET_B^{+/-}$ rats with colostomy. (e) Substantially higher density of TUNEL-positive nuclei were located in the molecular layer of the $ET_B^{-/-}$ rats but very few in granular and Purkinje cell layers. Scale bar, 200 μm (a) and 20 μm (b–e). Summary data on the density of TUNEL-positive nuclei in the cerebellum (f) and cerebral cortex (g) of rats from different genotypes. Averages from 4-6 rats in each genotype were compared with one-way ANOVA, specifically Kruskal-Wallis test with Dunn's multiple comparisons test (for (g)), where $*$ denotes $P < 0.01$.
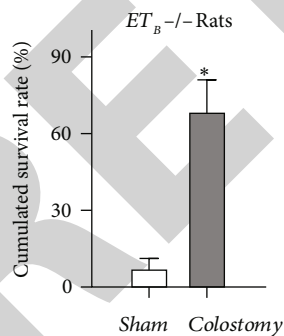
FIGURE 4: Survival rates after colostomy surgery.

$ET_B^{+/-}$, and $ET_B^{+/+}$ littermates that received colostomy. The deficiency of EDNRB substantially increased cell death in the cerebellum, hippocampus, and dentate gyrus of juvenile $ET_B^{-/-}$ rats, compared with $ET_B^{+/+}$ littermates. However, no such change was observed in the cerebral cortex.

EDNRB receptor expression is differentially regulated during early and later brain development. In embryos, EDNRB is abundantly expressed in cells lining the ventricles, but its expression is substantially decreased in the cortex and subventricular zones at P14 [18]. In contrast, the expression of EDNRB in the cerebellum and hippocampus persists in juvenile rats [19]. EDNRB is generally related to the development of neural crest lineage. Growing evidence shows its regulatory effects on a number of regions of the brain, including the cerebellum, hippocampus, and early cerebral cortex. This study further shows pathological cell death persisting in juvenile $ET_B^{-/-}$ rat cerebellum and hippocampus where EDNRB is normally expressed at this age [20]. We have not observed a significant increase in cell death of the cerebral cortex, which is consistent with significant decrease in the EDNRB expression within the first two weeks following birth [21]. Taken together, the mutated EDNRB effects in different regions of the brain further support a receptor mediated event during development. Variants have been identified in the RET/EDNRB pathways, accounting for 30% of any sporadic Hirschsprung's disease cases [22]. Unfortunately, our study may not provide direct targets for clinical applications. The signaling pathways are followed and the research will be reported in our further paper.

Hirschsprung's disease is associated with a variety of congenital abnormalities in the CNS, including microcephaly, agenesis of the corpus callosum, asymmetry of lateral

ventricles, central hypoventilation, sensorineural deafness, seizures, mental retardation, and autonomic nervous abnormalities [23–25]. Although Hirschsprung's disease in humans is polygenic, the *EDNRB* mutation causes a substantial proportion of sporadic and familial cases [26–28]. The currently reported brain structural changes have not been studied in human brains with Hirschsprung's disease. Our results in $ET_B^{-/-}$ rats may allow us to extrapolate that the major effects on human Hirschsprung's disease with congenital *EDNRB* mutation are associated with early development and an increased cell death within the cerebellum and the hippocampus. In addition, cerebral cortical cell protection may be critically important to the juvenile survival in the disease, which are explored further by our group.

5. Conclusion

The *sl/sl* $ET_B^{-/-}$ rats were rescued from premature death by performing colostomy. Cell loss significantly occurred in the cerebellum and hippocampal formation of juvenile $ET_B^{-/-}$ rats. ENDRB mutation could possess long lasting effects on the cell death in the cerebellum and hippocampus. Our findings would help improve the understanding of cellular changes in the brains of Hirschsprung's disease patients with congenital *EDNRB* mutation as well as clinically relevant interventions.

Data Availability

The datasets used and/or analysed during the current study are available from the corresponding author on reasonable request. The morphological and biochemical data used to support the findings of this study were supplied by D.X. and Z.S. under license and so cannot be made freely available. Requests for access to these data should be made to Z.S. at z.song@griffith.edu.au.

Additional Points

Highlights. (i) Colostomy rescued rats with Hirschsprung's disease (spotting lethal rats) from premature death. (ii) Cell loss significantly occurred in the cerebellar and hippocampal regions of juvenile spotting lethal rats. (iii) Colostomy with endothelin receptor B *sl* mutation in the rat could be associated with protection of cerebral cortical cells.

Disclosure

A preprint has previously been published (https://www .researchsquare.com/article/rs-1537125/v1) [29]. The authors declared all sources of funding received for the research. The funder was not involved in the study design, collection, analysis, interpretation of data, the writing of this article, or the decision to submit it for publication.

Conflicts of Interest

The authors declare no conflict of interest related to this paper.

Authors' Contributions

D.X., Y.D., and Y.W. contributed to investigation, data curation, formal analysis, review, and editing. G.D.H.C. and Z.Z.W. conceptualized the study and contributed to funding acquisition and supervision. Z.S. contributed to conceptualization, funding acquisition, methodology, formal analysis, and writing original draft and editing. Dan Xie and Yitong Du contributed equally to this work.

Supplementary Materials

Supplementary 1. Figure S1: protein level analysis of human cell line with *EDNRB* deletion mutation. The relative protein levels were compared based on the protein samples of human SH-SY5Y cell lyses. The *EDNRB mut* experiments indicated the deletion mutation in the cells, in which *EDNRB* protein expression was detected significantly low (A). Neither BDNF (B) nor GDNF (C) was changed.

Supplementary 2. Figure S2: representative images showing related phenotype of the $ET_B^{-/-}$ rat. In the rats with congenital *EDNRB* gene defects, we recorded the consequences due to the intestinal obstruction with malnutrition and electrolyte disorders, or peritoneal infections. Mostly, the neonatal rats with homozygous mutations could die within one week of birth. We first applied colostomies to the *EDNRB* gene defective neonatal rats after genetic testing of the newborn ones. It was allowed to observe the cellular apoptosis and proliferation as well as the animal survival of $ET_B^{-/-}$ rats for the body growth and nervous system development. With the surgical interventions, $ET_B^{-/-}$ neonatal rats survived to adulthood. Importantly, with/without the operation on the rats with congenital *EDNRB* gene defects, there were both changes in hair melanin pigmentation (A and B). Typically, there were 200 bp and 500 bp gene fragments for $ET_B^{+/-}$, the bp alone for $ET_B^{+/+}$, and the 500 bp alone for $ET_B^{-/-}$ rats (as shown in C).

Supplementary 3. Figure S3: representative images of the hippocampus of a juvenile $ET_B^{-/-}$ rat with colostomy showing the distribution of TUNEL-positive nuclei (red) with DAPI counterstaining. (A–C) Low magnification view of the hippocampus (including CA1 and CA3) and dentate gyrus. (D-I) TUNEL-positive nuclei were visible in all the three brain regions of $ET_B^{-/-}$ rats. Scale bar: 50 μm for (C) and 20 μm for (F) and (I). (J) Summary data comparing the density of TUNEL-positive nuclei in the hippocampus

Retraction

Retracted: Macrophage Rmp Ameliorates Myocardial Infarction by Modulating Macrophage Polarization in Mice

Oxidative Medicine and Cellular Longevity

This article has been retracted by Hindawi, as publisher, following an investigation undertaken by the publisher [1]. This investigation has uncovered evidence of systematic manipulation of the publication and peer-review process. We cannot, therefore, vouch for the reliability or integrity of this article.

Please note that this notice is intended solely to alert readers that the peer-review process of this article has been compromised.

Wiley and Hindawi regret that the usual quality checks did not identify these issues before publication and have since put additional measures in place to safeguard research integrity.

We wish to credit our Research Integrity and Research Publishing teams and anonymous and named external researchers and research integrity experts for contributing to this investigation.

The corresponding author, as the representative of all authors, has been given the opportunity to register their agreement or disagreement to this retraction. We have kept a record of any response received.

References

[1] J. Zhang, Z. Yin, L. Yu et al., "Macrophage Rmp Ameliorates Myocardial Infarction by Modulating Macrophage Polarization in Mice," *Oxidative Medicine and Cellular Longevity*, vol. 2022, Article ID 6248779, 12 pages, 2022.

Hindawi

Research Article

Macrophage Rmp Ameliorates Myocardial Infarction by Modulating Macrophage Polarization in Mice

Jian Zhang [iD],[1] **Zongtao Yin,**[1] **Liming Yu,**[1] **Zhishang Wang,**[1] **Yu Liu,**[1] **Xiaoru Huang,**[2] **Song Wan** [iD],[3] **Hui-yao Lan** [iD],[2] **and Huishan Wang** [iD][1]

[1]*Department of Cardiovascular Surgery, General Hospital of Northern Theater Command, No. 83, Wenhua Road, Shenhe District, Shenyang, Liaoning, China*
[2]*Department of Medicine & Therapeutics, and Li Ka Shing Institute of Health Sciences, The Chinese University of Hong Kong, Shatin, NT, Hong Kong*
[3]*Division of Cardiothoracic Surgery, Department of Surgery, The Chinese University of Hong Kong, Prince of Wales Hospital, Shatin, NT, Hong Kong*

Correspondence should be addressed to Song Wan; swan@surgery.cuhk.edu.hk, Hui-yao Lan; hylan@cuhk.edu.hk, and Huishan Wang; huishanw@126.com

Background. Inflammation plays important roles during myocardial infarction (MI). Macrophage polarization is a major factor that drives the inflammatory process. Our previous study found that RNA polymerase II subunit 5-mediating protein (RMP) knockout in cardiomyocytes caused heart failure by impairing mitochondrial structure and function. However, whether macrophage RMP plays a role in MI has not been investigated. *Methods.* Macrophage RMP-knockout in combination with a mouse model of MI was used to study the function of macrophage RMP in MI. Next, we modified bone marrow-derived macrophages (BMDMs) by plasmid transfection, and the BMDMs were administered to LysM-Cre/DTR mice by tail vein injection. Immunoblotting and immunofluorescence were used to detect macrophage polarization, fibrosis, angiogenesis, and the p38 signaling pathway in each group. *Results.* Macrophage RMP deficiency aggravates cardiac dysfunction, promotes M1 polarization, and inhibits angiogenesis after MI. However, RMP overexpression in macrophages promotes M2 polarization and angiogenesis after MI. Mechanistically, we found that RMP regulates macrophage polarization through the heat shock protein 90– (HSP90–) p38 signaling pathway. *Conclusions.* Macrophage RMP plays a significant role in MI, likely by regulating macrophage polarization via the HSP90–p38 signaling pathway.

1. Introduction

Myocardial infarction (MI) is a serious ischemic heart disease caused by atherosclerosis and is associated with high morbidity and mortality rates [1]. Following infarction, cardiomyocyte death and acute inflammation are induced [2]. Inflammation plays important roles during MI [3, 4]. Macrophage polarization is considered to be a major factor that drives the inflammatory process [3]. Macrophages are generally divided into two groups: the classically activated (M1) macrophages and the alternatively activated (M2) macrophages [5, 6]. M1 macrophages could degrade the extracellular matrix and get rid of cell debris; in contrast,

M2 macrophages promote the production of anti-inflammatory cytokines, angiogenesis, and collagen deposition [7]. Therefore, targeting macrophage-mediated inflammatory reactions may be an attractive approach to ameliorate MI.

RNA polymerase II subunit 5-mediating protein (RMP), also known as unconventional prefoldin RPB5 interactor, is widely studied in several types of malignant tumors [8–13]. Some studies showed that RMP could interact with heat shock protein 90 (HSP90) and the R2TP/prefoldin-like complex, which assembles RNA polymerase II before its nuclear translocation [14]. We previously showed that RMP levels are significantly decreased in the cardiomyocytes of patients

(a)

(b)
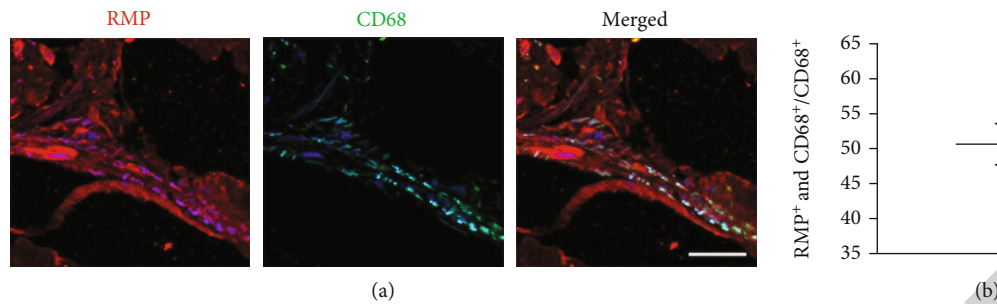
FIGURE 1: RMP expression is upregulated in human macrophages after myocardial infarction. (a) Representative immunofluorescence staining of RNA polymerase II subunit 5-mediating protein (RMP, red) and CD68 (green) from patients with advanced ischemic heart failure. Scale bar = 100 μm. (b) Quantification of both RMP- and CD68-positive cells.

with heart failure compared with their levels in normal cardiac tissues [15]. Mechanistically, RMP-knockout in cardiomyocytes causes heart failure by impairing mitochondrial structure and function [15]. However, whether macrophage RMP plays a role in MI and how RMP affects macrophage phenotypes have not been investigated.

2. Materials and Methods

This research fully complied with ethics guidelines. All animal experiments were performed following the NIH guidelines (*Guide for the Care and Use of Laboratory Animals*) and the ARRIVE guidelines. All experiments were conducted in accordance with the protocols approved by the Institutional Animal Care and Use Committee of the General Hospital of the Northern Theater Command (No. 2015023).

2.1. Human Heart Tissue. Ischemic failure hearts from patients who underwent heart transplantation were collected from the General Hospital of the Northern Theater Command, Shenyang, China. This study was approved by the Ethics Committee of the General Hospital of the Northern Theater Command (No. 2015103). All participants provided written informed consent.

2.2. MI Mouse Model. MI was induced by ligation of the left main descending coronary artery as described previously [16]. Briefly, mice were anesthetized with ketamine (50 mg/kg) and xylazine (50 mg/kg). The operation was performed under artificial ventilation with respirator support. The left descending coronary artery was ligated using a 6-0 silk suture. Mice in the sham group underwent the same procedure without the ligation step.

2.3. Animals

2.3.1. Control and Macrophage-Specific Rmp-Knockout Mice. $RMP^{flox/flox}$ mice were generated as described previously [15]. Macrophage-specific *Rmp*-knockout (MRKO) and littermate control (LC) mice were generated by mating $RMP^{flox/flox}$ mice with transgenic mice expressing Cre recombinase under the control of the lysozyme M (LysM) promoter. The MRKO and LC mice had a C57BL6 background. Two-month-old age- and weight-matched male LC and MRKO mice were used for the experiments.

In the macrophage depletion study, macrophages were conditionally deleted from LysM-Cre/diphtheria toxin receptor (DTR) mice by intraperitoneal injection of diphtheria toxin as described previously [16].

2.4. Bone Marrow-Derived Macrophage Transplantation. Bone marrow cells were isolated from mice with a C57BL/6J background as described previously [16]. Briefly, bone marrow cells were obtained by flushing the femur and tibia with Dulbecco's modified Eagle's medium/F12 medium. Cell suspensions were collected the next day and further differentiated into macrophages by 5 days of stimulation in Dulbecco's modified Eagle's medium/F12 containing 10% fetal bovine serum and 10 ng/mL macrophage colony-stimulating factor. The bone marrow-derived macrophages (BMDMs) were then transfected with plasmids expressing a short hairpin RNA targeting *Rmp* (shRmp) or *Rmp* according to the manufacturer's protocol. Plasmids expressing shRmp were purchased from GeneChem Co., Ltd. (Shanghai, China), and the plasmid-expressing mouse *Rmp* was kindly provided by Dr. Liwei Dong (International Cooperation Laboratory on Signal Transduction, Eastern Hepatobiliary Surgery Institute, the Second Military Medical University, Shanghai, China). After 24 h of transfection, cell suspensions (1×10^6 cells) were prepared and administered to the LysM-Cre/DTR mice by tail vein injection, 5 days after intraperitoneal injection of diphtheria toxin. Diphtheria toxin was given until cardiac tissues were harvested.

2.5. Echocardiography. Transthoracic echocardiography was performed using a Vevo770 high-resolution ultrasound imaging system (VisualSonics, Toronto, Canada) with an RMV 707B scan head (30 MHz, VisualSonics) 1 week after surgery. Mice were anesthetized with ketamine (50 mg/kg) and xylazine (50 mg/kg) on a warming plate to maintain body temperature. Left ventricular internal diameters at end-diastole and end-systole were obtained using M-mode recording. The left ventricular ejection fraction (LVEF) and left ventricular end-diastolic volume (LVEDV) were calculated according to the guidelines of the Vevo770 system (VisualSonics).

2.6. Histology. Cardiac tissue sections were prepared and fixed in 4% paraformaldehyde to obtain paraffin-embedded coronal sections for Masson's trichrome staining and immunohistochemical analysis [15]. Masson's trichrome staining

(a)

(b)

(c)

(d)

(e)

(f)

(g)

(h)
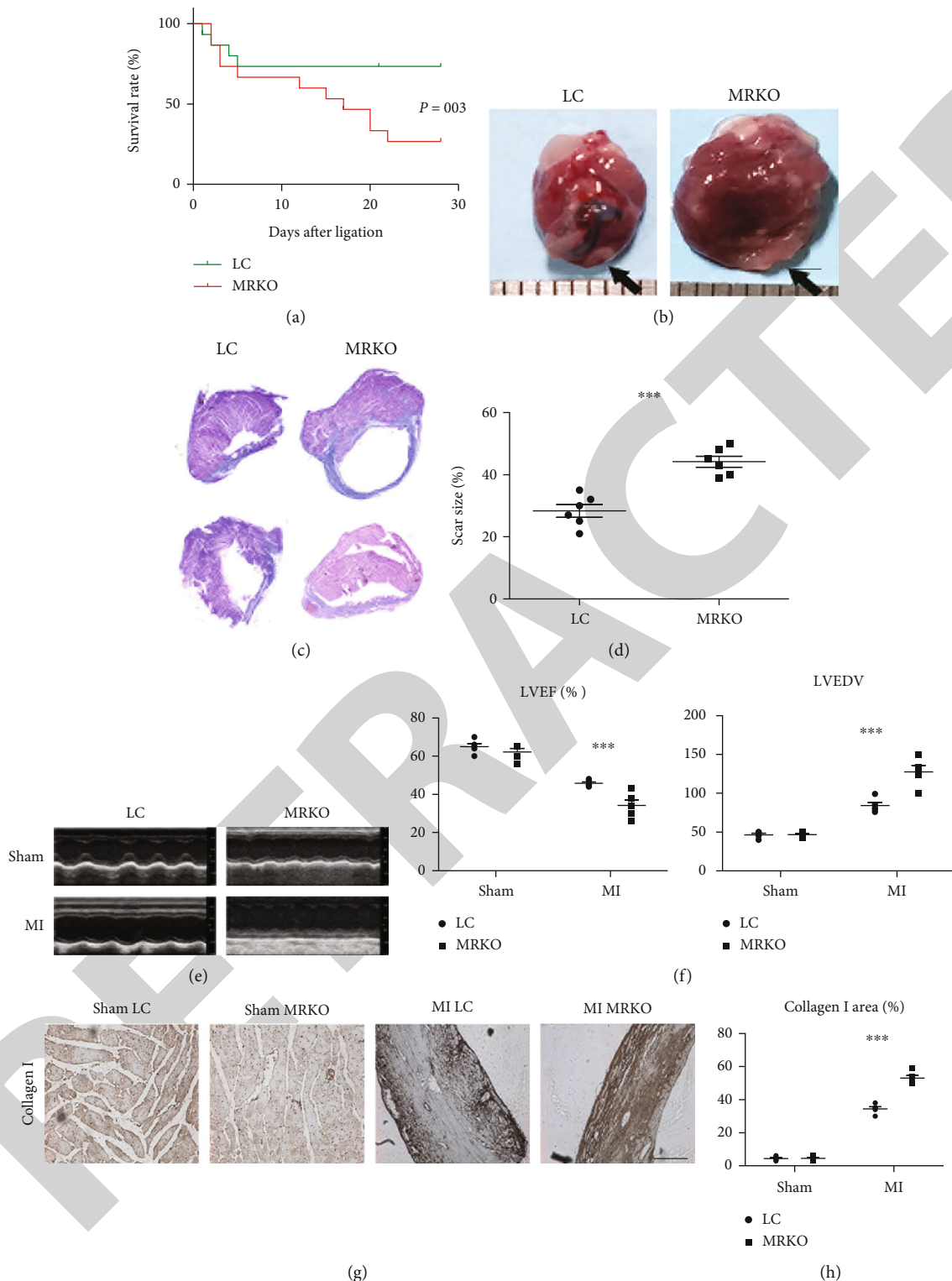
FIGURE 2: Macrophage Rmp deficiency aggravates cardiac dysfunction after myocardial infarction. (a) Survival curves for macrophage-specific Rmp-knockout (MRKO) and littermate control (LC) mice. ***$P < 0.001$. $N = 15$ mice per group. (b) Representative images of the hearts from LC and MRKO mice collected 7 days after myocardial infarction (MI). Scale bar = 2 mm. (c) Representative images of infarct size after Masson's trichrome staining of the hearts collected 7 days after the induction of MI. (d) Quantification of fibrosis as a percentage of total myocardial tissue area. Values are mean ± SEM of $n = 6$ per group. Student's t test, *$P < 0.05$. (e) Representative echocardiography (M-mode) and left ventricular function 7 days after the induction of MI. (f) Echocardiographic analysis of LVEF and LVEDV ($n = 5$; Student's t test, ***$P < 0.001$). (g) Immunohistochemical staining of collagen I accumulation at the infarct site 7 days after the induction of MI. Scale bar = 200 μm. (h) Quantitative analysis of collagen I ($n = 5$; Student's t test, ***$P < 0.001$).

(a)

(b)

(c)

(d)

(e)

(f)

(g)

(h)
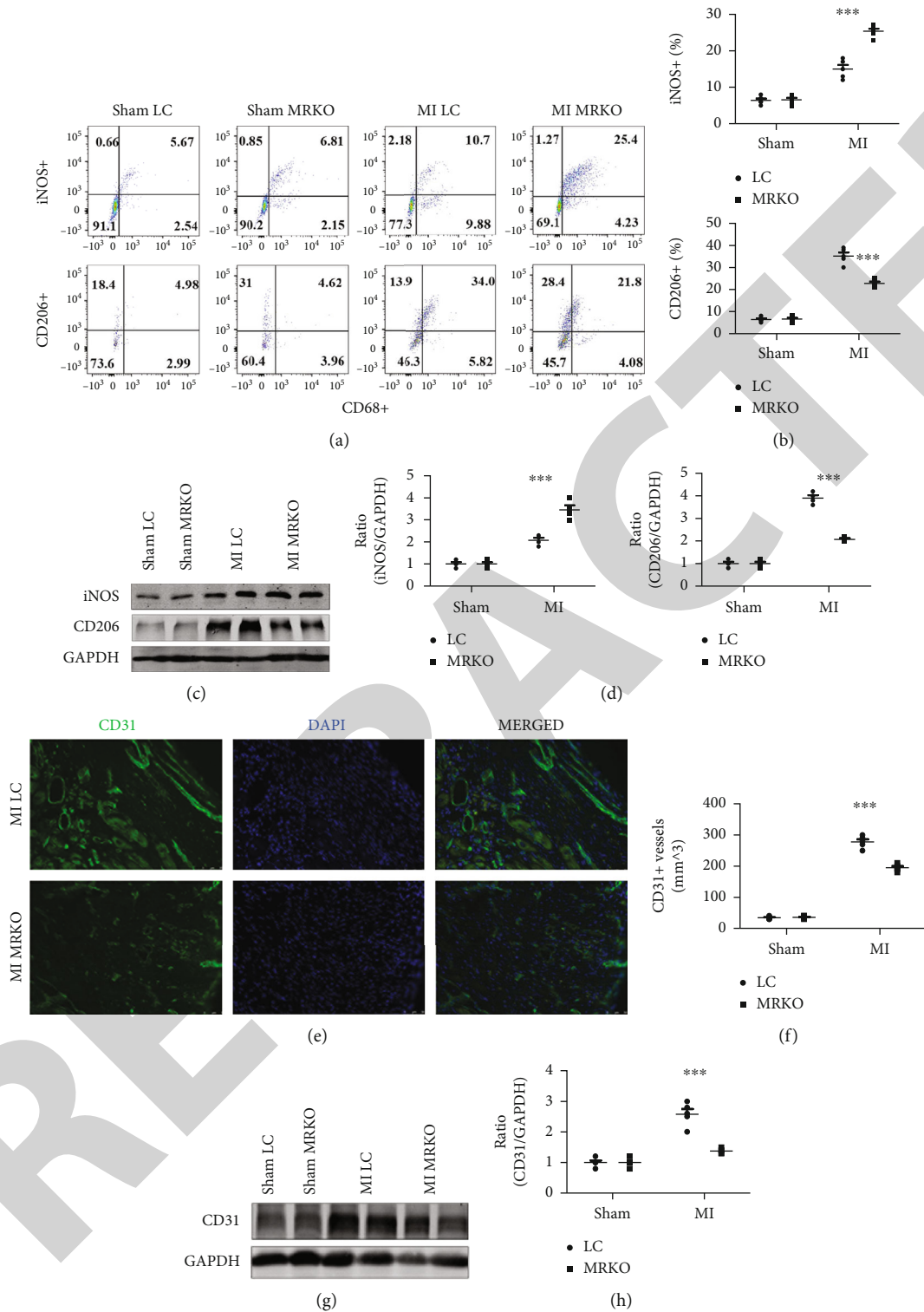
FIGURE 3: Macrophage Rmp deficiency promotes M1 polarization and inhibits angiogenesis after myocardial infarction. (a) Three-color flow cytometry shows the M1 (CD68+/iNOS+) and M2 (CD68+/CD206+) macrophages at the infarct site 7 days after myocardial infarction (MI). (b) Quantitative analysis of M1 and M2 macrophages ($n = 5$; Student's t test, ***$P < 0.001$). (c) Representative images of CD206 and iNOS by western blotting 7 days after MI. (d) Corresponding densitometric quantification of the immunoreactive bands. Values are mean ± SEM of $n = 5$ per group. ***$P < 0.001$ versus LC by unpaired Student's. (e) Two-color immunofluorescence shows CD31 in LC and MRKO mice 7 days after MI. (f) Quantitative analysis of CD31. Values are mean ± SEM of $n = 5$ per group. ***$P < 0.001$ versus LC by unpaired Student's. (g) Representative images of CD31 in the infarct area of LC and MRKO mice by western blotting 7 days after MI. (h) Quantitative analysis of CD31. Values are mean ± SEM of $n = 5$ per group. ***$P < 0.001$ versus LC by unpaired Student's.
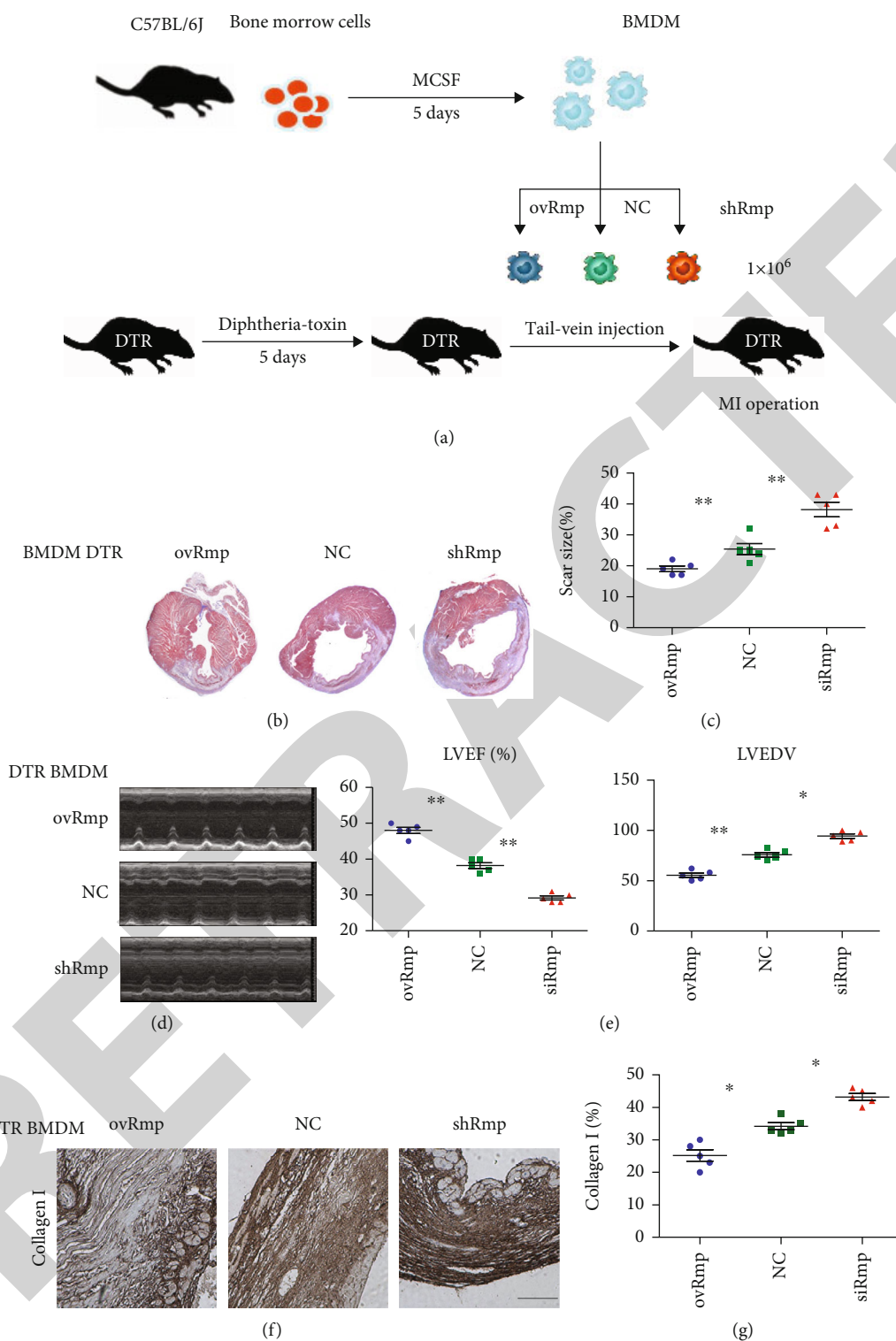
FIGURE 4: Macrophage Rmp protects against myocardial infarction. (a) Study design of bone marrow transplantation experiments, in which the mice were induced MI. (b) Representative images of infarct size by Masson's trichrome staining 7 days after MI. (c) Quantitative analysis of fibrosis as a percentage of total myocardial tissue area. $n = 4 – 6$ per group. Values are mean ± SEM. Student's t test, $^{**}P < 0.01$. (d) Representative echocardiography (M-mode) 7 days after MI. (e) Echocardiographic analysis of LVEF and LVEDV ($n = 5$; Student's t test, $^{*}P < 0.05$ and $^{**}P < 0.01$). (f) Immunohistochemical staining of collagen I accumulation at the infarct site 7 days after MI. Scale bar = 200 μm. (g) Quantitative analysis of collagen I ($n = 5$; Student's t test, $^{*}P < 0.05$).

(a)

(b)

(c)

(d)

(e)

(f)
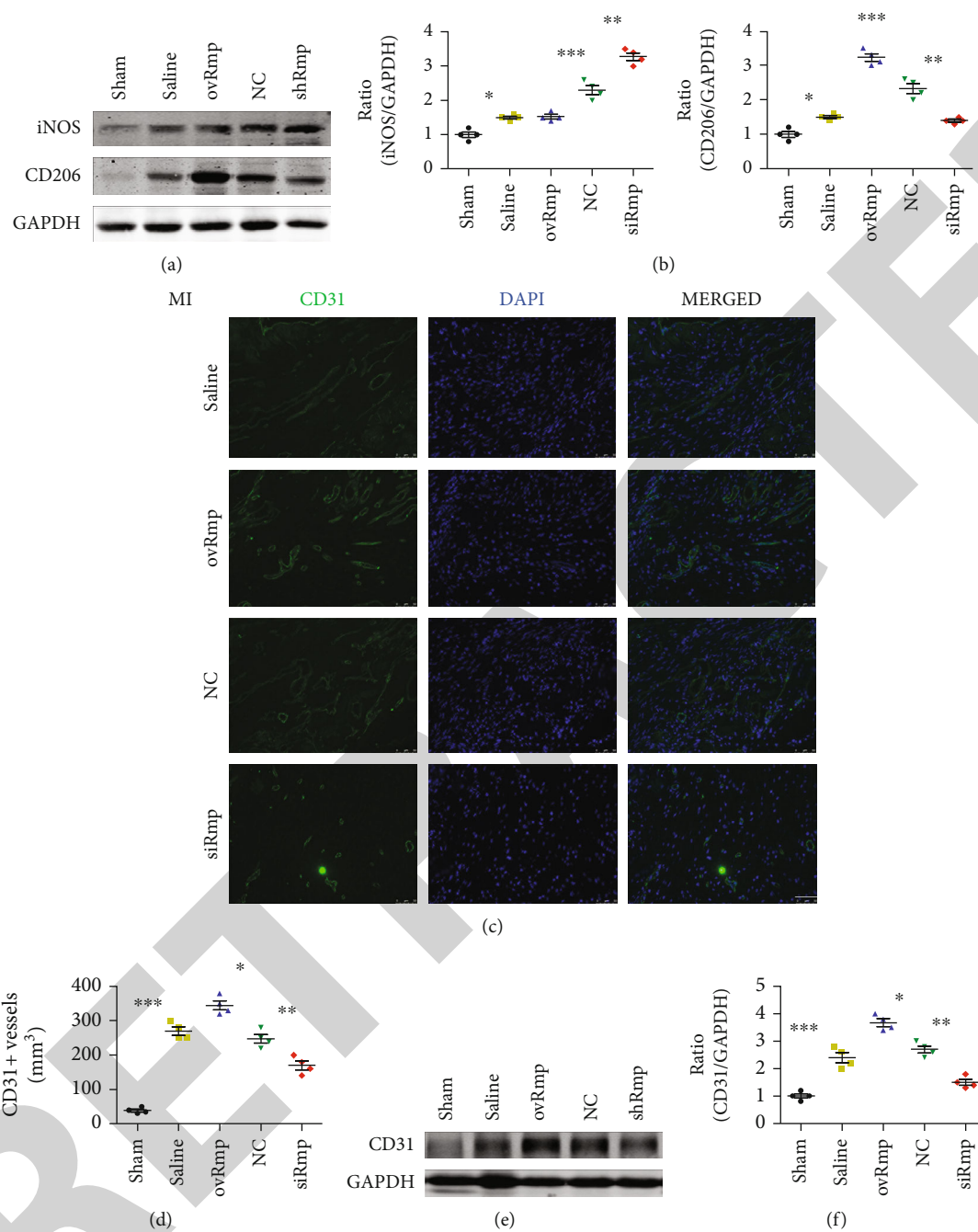
Figure 5: Macrophage Rmp promotes macrophage M2 polarization and angiogenesis after myocardial infarction. (a) Representative images of CD206 and iNOS by western blotting 7 days after myocardial infarction (MI). (b) Corresponding densitometric quantification of the immunoreactive bands. Values are mean ± SEM of $n = 4 - 6$ per group. $^{*}P < 0.05$, $^{**}P < 0.01$, and $^{***}P < 0.001$ by unpaired Student's. (c) Two-color immunofluorescence analysis shows CD31 in mice receiving the indicated bone marrow-derived macrophages (BMDMs) 7 days after MI. (d) Quantitative analysis of CD31. Values are mean ± SEM of $n = 5$ per group. $^{*}P < 0.05$, $^{**}P < 0.01$, and $^{***}P < 0.001$ by unpaired Student's. (e) Representative image analysis of CD31 in the infarct area of mice receiving the indicated BMDMs by western blotting 7 days after MI. (f) Quantitative analysis of CD31. Values are mean ± SEM of $n = 5$ per group. $^{*}P < 0.05$, $^{**}P < 0.01$, and $^{***}P < 0.001$ by unpaired Student's.

(BA4079A; Baso Diagnostics, Zhuhai, China) was performed following the manufacturer's instructions. Immunohisto-chemical staining was performed using antibodies against RMP (11277-1-AP, 1 : 50; Proteintech, Wuhan, China) and collagen I (1310-01, 1 : 100; Southern Tech, Ardmore, OK, USA). The scar area, intimal area, and medial area were

measured using Image-Pro Plus software (Media Cybernetics, Bethesda, MD, USA) [17].

2.7. Immunofluorescence. Periodate–lysine–paraformalde-hyde-fixed cardiac tissue was used to prepare frozen sections. RMP was labeled with an anti-RMP antibody (11277-1-AP,

(a)

(b)

(c)

(d)

(e)

(f)

Figure 6: Continued.

(g)
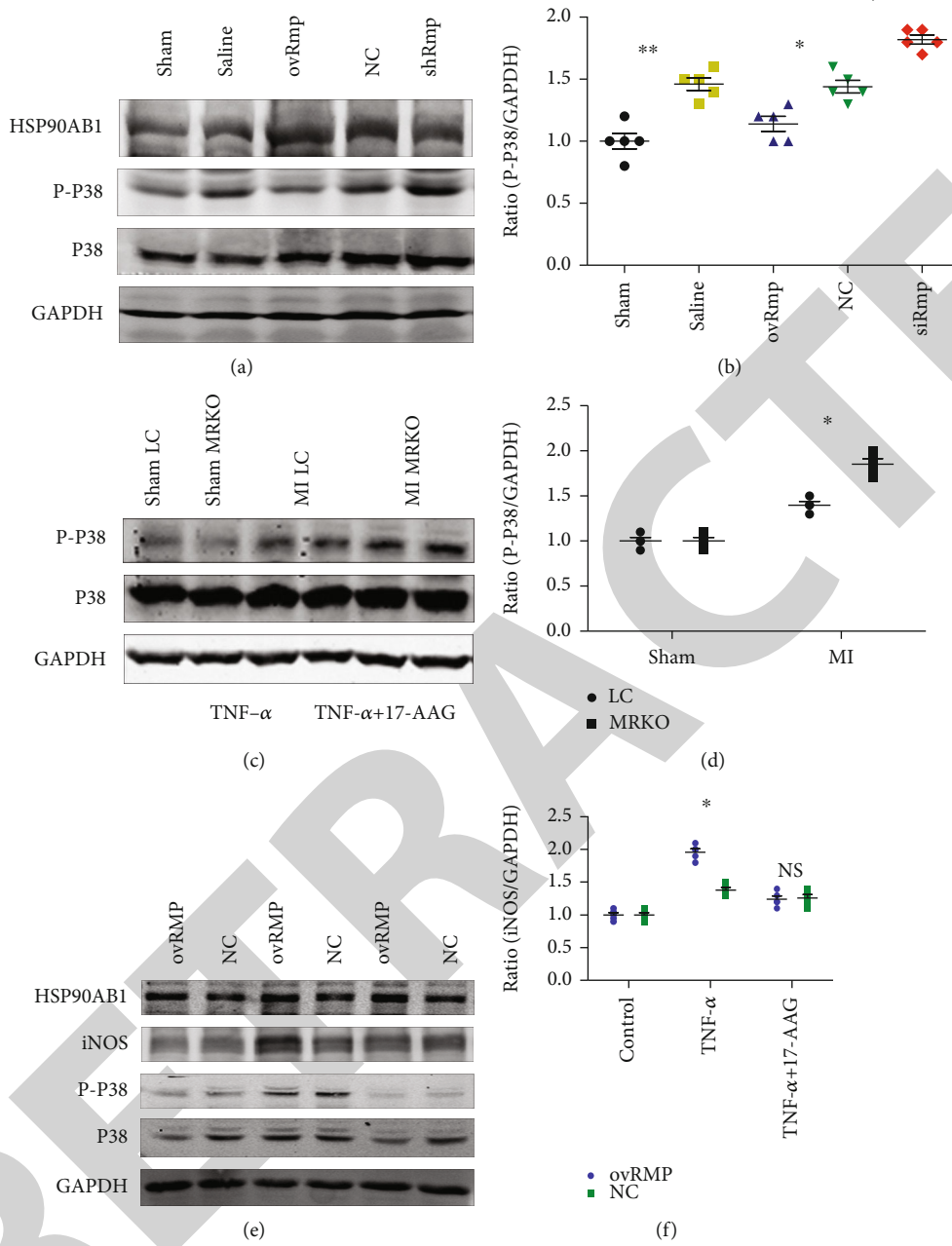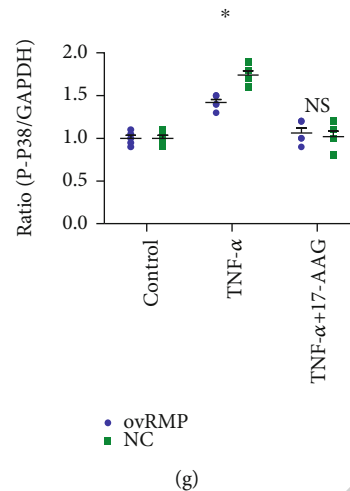
Figure 6: Rmp regulates macrophage polarization through heat shock protein 90-dependent mechanisms. (a) Representative image and quantitative analysis of phosphorylated (p-) p38 and nonphosphorylated p38 in the infarct area of mice by western blotting 7 days after myocardial infarction (MI). (b) Corresponding densitometric quantification of the immunoreactive bands. Values are mean ± SEM of $n = 4 - 6$ per group. $^{*}P < 0.05$ and $^{**}P < 0.01$, by unpaired Student's. (c) Representative image analysis of p-p38 and p38 in the infarct area of littermate control (LC) and macrophage-specific Rmp-knockout (MRKO) mice by western blotting 7 days after MI. (d) Quantitative analysis of p-p38. Values are mean ± SEM of $n = 5$ per group. $^{*}P < 0.05$, by unpaired Student's. (e) Representative images analysis of p-p38 and p38 in bone marrow-derived macrophages by western blotting. (f and g) Quantitative analysis of iNOS and p-p38. Values are mean ± SEM of $n = 5$ per group. $^{*}P < 0.05$; ns, $P > 0.05$ by unpaired Student's.

1 : 50, Proteintech). Macrophages in human cardiac tissues were labeled with an anti-CD68 antibody (NB100-683; Novus, Centennial, CO, USA). Nuclei were counterstained with $4'$,6-diamidino-2-phenylindole.

2.8. Quantitative Reverse Transcription PCR. Total RNA isolation and real-time PCR were performed as described previously [14, 15]. The *Rmp* primer sequences were as follows: forward, $5'$-TGCCAAGAGAAAATCCAGCAT-$3'$; reverse, $5'$-AGGTCCTCAGCCTCTCTTGAA-$3'$.

2.9. Western Blot Analysis. Western blot analysis was performed as described previously [15]. Nitrocellulose membranes were incubated overnight at 4°C with diluted antibodies against inducible nitric oxide synthase (iNOS; ab178945; Abcam, Cambridge, UK), cluster of differentiation (CD) 206 (sc-58986; Santa Cruz Biotechnology, Dallas, TX, USA), RMP (11277-1-AP, 1 : 1,000, Proteintech), CD31 (92841; Cell Signaling Technology, Danvers, MA, USA), HSP90AB1 (5087, Cell Signaling Technology), phosphorylated p38 (4511 s, Cell Signaling Technology), or total p38 (8690 s, Cell Signaling Technology). BMDMs were treated with 200 nM 17-allylamino-17-demethoxygeldanamycin (17-AAG; S1141; Selleck, Houston, TX, United States).

2.10. Statistical Analysis. The data are presented as mean ± standard error of the mean. Data between groups were compared with an unpaired two-tailed Student's t test using Prism 5 (GraphPad Software, La Jolla, CA, USA). Values of $P < 0.05$ were considered statistically significant. Cumulative mortality was analyzed using Kaplan-Meier curves, and a log-rank test was used to assess statistical significance ($P < 0.05$).

3. Results

3.1. RMP Expression Is Upregulated in Human Macrophages after MI. We first evaluated RMP levels in heart tissue samples from patients with advanced ischemic heart failure who underwent heart transplantation (Table S1). In contrast to the RMP expression level in cardiomyocytes, immunofluorescence showed a significant increase in macrophages of the infarct zone compared with remote areas (Figures 1(a) and 1(b)).

3.2. Macrophage RMP Deficiency Aggravates Cardiac Dysfunction after MI. To study the role of macrophage RMP in MI, we generated MRKO mice using the Cre–lox system. BMDMs isolated from LC and MRKO mice were analyzed to assess knockdown efficiency. Owing to the lack of a commercial antibody against mouse RMP [15], *Rmp* mRNA levels were used to validate the knockout model (Figure S1A).

Next, we induced MI by ligating the left anterior descending artery in LC and MRKO mice. MRKO mice showed a significantly higher mortality rate than LC mice (Figure 2(a)). The hearts of MRKO mice were more dilated than those of LC mice 7 days after MI (Figure 2(b)). Furthermore, the scars were markedly larger in MRKO mice than in LC mice (Figures 2(c) and 2(d)). Echocardiography demonstrated a significant decrease in the LVEF and a significant increase in the LVEDV of MRKO mouse hearts compared with LC mouse hearts (Figures 2(e) and 2(f)). Immunohistochemical

analysis also showed that the loss of RMP in macrophages resulted in more severe cardiac fibrosis, as indicated by increased collagen I accumulation at the infarct site in MRKO mice (Figures 2(g) and 2(h)).

3.3. Macrophage RMP Deficiency Promotes M1 Polarization and Inhibits Angiogenesis after MI.

Studies have shown that macrophage polarization affects infarct healing after MI [3]. Flow cytometry was performed to assess macrophage polarization. The results showed that the expression levels of iNOS (an M1 macrophage marker) were upregulated, while those of CD206 (an M2 macrophage marker) were downregulated in MRKO mice compared with LC mice (Figures 3(a) and 3(b)), suggesting that the deletion of RMP in macrophages promoted M1 macrophage polarization. Western blot analysis confirmed the increase in iNOS expression levels and the decrease in CD206 expression levels in MRKO mice (Figures 3(c) and 3(d)). Angiogenesis is crucial for maintaining cardiac function following MI. We found that the deletion of RMP in macrophages decreased the number of CD31-expressing cells at the infarct site (Figures 3(e) and 3(f)). Moreover, macrophage-specific deletion of RMP downregulated total cardiac expression of CD31 (Figures 3(g) and 3(h)).

3.4. RMP in Macrophages Protects against MI.

To further assess the role of RMP in macrophages, we used LysM-Cre/DTR mice to delete macrophages. Furthermore, we modified the macrophages by overexpressing or knocking down RMP. The modified macrophages were then administered to LysM-Cre/DTR mice (Figure 4(a)), and the expression of RMP in modified macrophages was detected (Figure S1B). To test this model, we administered BMDMs from Cre-dependent tdTomato reporter transgenic mice [17] to LysM-Cre/DTR mice. Immunofluorescence analysis indicated that most macrophages present were those that were administered (Figure S1C). Mice receiving BMDMs overexpressing RMP (ovRmp BMDMs) showed a clear trend of reduced infarct size compared with mice receiving negative control BMDMs (NC BMDMs) (Figures 4(b) and 4(c)). In contrast, mice receiving RMP knockdown BMDMs (shRmp BMDMs) showed an increased infarct size (Figures 4(b) and 4(c)). RMP overexpression in macrophages improved the LVEF and attenuated dilation (LVEDV, Figures 4(d) and 4(e)). Furthermore, mice with macrophage-specific overexpression of RMP developed mild cardiac fibrosis, as evidenced by a decrease in collagen I accumulation compared with mice receiving NC BMDMs (Figures 4(f) and 4(g)).

3.5. Macrophage RMP Promotes Macrophage M2 Polarization and Angiogenesis after MI.

Treatment with ovRmp BMDMs suppressed MI-induced iNOS expression but promoted CD206 expression (Figures 5(a) and 5(b)). Moreover, mice receiving ovRmp BMDMs showed more CD31-positive cells at the infarct site compared with mice receiving NC BMDMs (Figures 5(c) and 5(d)). Furthermore, western blotting analysis also showed that macrophage-specific overexpression of RMP promoted angiogenesis (Figures 5(e) and 5(f)).

3.6. RMP Regulates Macrophage Polarization through HSP90-Dependent Mechanisms.

Previously, we used label-free mass spectrometry to identify the possible binding proteins of RMP in the AC16 cell line (Table S2). We found that HSP90AB1 is a protein that binds to RMP. This was confirmed by immunofluorescence and co-immunoprecipitation analyses (Figure S1D and E). Several groups have reported that HSP90AB1, along with HSP90AA, modulates macrophage polarization through the p38 mitogen-activated protein kinase (MAPK) pathway [16, 18, 19]. In our mouse model, we also showed that phosphorylated p38 levels were decreased in mice receiving ovRmp BMDMs compared with mice receiving NC BMDMs (Figures 6(a) and 6(b)). In MRKO mice, phosphorylated p38 was upregulated 7 days after MI (Figures 6(c) and 6(d)). Next, we used 17-AAG, a potent HSP90 ATPase inhibitor, to block the effects of HSP90. In vitro, RMP overexpression was induced by tumor necrosis factor alpha (TNF-α) in BMDMs. We also found that RMP inhibited TNF-α-induced iNOS expression and p38 activation, and these effects were blocked by 17-AAG (Figures 6(e)–6(g)).

4. Discussion

In this study, we demonstrated that the deletion of RMP in macrophages significantly aggravated myocardial healing after MI in mice. Our findings showed that mice lacking RMP developed more severe MI and showed impaired angiogenesis. Importantly, we also found that RMP overexpression in macrophages improved post-MI cardiac physiology and increased cardiac M2 macrophage polarization.

Our data identified macrophage RMP as a promising new target for treating MI. Following MI, the death of cardiomyocytes causes an immune response that leads to further tissue destruction [5]. Macrophages have been recognized as important regulators of and participants in inflammation and fibrosis following MI. In the initial stage of MI, the injured heart is dominated by proinflammatory (M1) macrophages, whereas several days later, macrophages with an anti-inflammatory phenotype (M2) become predominant. Several studies have indicated that M2-like macrophages are beneficial for cardiac tissue repair [20]. Therefore, therapeutic strategies that promote M2 polarization of MI macrophages may also promote myocardial repair. Macrophage RMP deficiency has been shown to aggravate MI, especially because the effects of RMP are cardioprotective, by shifting proinflammatory cardiac M1 macrophages to the reparative M2 phenotype. Indeed, macrophage RMP exerts its inhibitory effect on macrophage activation via the p38 MAPK signaling pathway. Understanding this mechanism may help us develop novel treatment strategies for ischemic heart disease. However, effective and safe ways to deliver inhibitors or purified protein to the infarction area are still lacking. Percutaneous

coronary intervention may be the optimal way to deliver drugs, inhibitors, or purified protein for treating MI.

As an oncogene, *Rmp* is amplified and overexpressed in many malignancies, such as ovarian cancer [21], hepatocellular carcinoma [9, 12], prostate cancer [22], cholangiocarcinoma [13], and colorectal cancer [23]. Our previous study found that cardiomyocyte-specific knockout of *Rmp* results in contractile dysfunction, cardiac dilatation, and fibrosis owing to impaired mitochondrial structure and function through the regulation of peroxisome proliferator-activated receptor-gamma coactivator alpha-dependent mitochondrial function via a transforming growth factor-beta/mothers against the decapentaplegic homolog 3-dependent mechanism [15]. RMP is a transcription-mediating protein that binds with RNA polymerase II subunit 5 [9]. Mass spectrometry results showed that HSP90AB1 is a potential RMP-binding protein. Moreover, co-immunoprecipitation analysis confirmed the binding between RMP and HSP90AB1. In line with our findings, RMP, as part of a protein complex known as the R2TP/prefoldin-like complex, along with HSP90, has been shown to be responsible for the cytoplasmic assembly of RNA polymerase II [14, 24]. HSP90 proteins constitute a family of highly conserved molecular chaperones that modulate the biological activities of their client proteins. It has been reported that HSP90 participates in macrophage activation [25]. In intervertebral disc degeneration, the HSP90 inhibitor 17-AAG attenuates the proinflammatory activity of M1 macrophages by inhibiting the p38 MAPK pathway. HSP90 has been reported to be essential for iNOS (M1 marker) gene transactivation [26]. Here, we found that RMP overexpression inhibited iNOS expression in BMDMs, but HSP90 inhibition with 17-AAG upregulated the iNOS expression inhibited by RMP. We found that the p38 MAPK pathway was the possible signaling pathway modulating the effects of RMP on macrophage polarization.

As an oncogene, *Rmp* has been reported to promote venous invasion and vascularization [9, 10]. However, angiogenesis benefits cardiac tissue repair after MI. Our data showed that RMP in macrophages promotes angiogenesis after MI. This finding is consistent with the proangiogenic effect of RMP in many malignancies. Furthermore, RMP, along with HSP90AB1 and HSP90AA, may be involved in regulating protein expression. Hypoxia-inducible factor- (HIF-) 1α is a master transcriptional factor for angiogenesis during cardiac repair, and Hsp90 has been reported to stabilize HIF-1α [27, 28]. The binding between RMP and HSP90 observed in our study may also indicate that RMP participates in the regulation of HIF-1α expression after MI. However, the underlying mechanism whereby macrophage RMP promotes angiogenesis was not fully elucidated.

5. Conclusion

In summary, macrophage RMP plays a significant role in MI, likely by regulating macrophage polarization via the HSP90–p38 signaling pathway. These results have uncovered a novel function of macrophage RMP in MI, and they support the selective targeting of RMP in macrophages as an effective novel strategy to treat MI.

Abbreviations

MI: Myocardial infarction
RMP: RNA polymerase II subunit 5-mediating protein
BMDM: Bone marrow-derived macrophage
Hsp90: Heat shock protein 90
MRKO: Macrophage-specific *Rmp*-knockout
LC: Littermate control
LysM: Lysozyme M
DTR: Diphtheria toxin receptor
LVEF: Left ventricular ejection fraction
LVEDV: Left ventricular end-diastolic volume
MAPK: Mitogen-activated protein kinase
TNF-α: Tumor necrosis factor alpha.

Data Availability

The data used to support the findings of this study are available from the corresponding author upon request.

Consent

All authors gave their consent for publication.

Conflicts of Interest

The authors have declared that no conflict of interest exists.

Authors' Contributions

JZ, ZY, and HW designed research studies, conducted experiments, acquired and analyzed data, and contributed to writing the manuscript. JZ, ZW, LY, LY, and XL conducted experiments and acquired and analyzed data. SW and HL designed research studies, analyzed data, and contributed to writing the manuscript. HW designed research studies, analyzed data, and contributed to writing the manuscript. Jian Zhang and Zongtao Yin contributed equally to this work.

Supplementary Materials

Supplementary 1. Figure S1: (A) relative expression of Rmp in BMDM from LC and MRKO mice. (B) Relative expression of Rmp in modified BMDM. (C) Representative immunofluorescence staining of F4/80 (green) and Tomato from

DTR mice receiving BMDM of Cre-dependent tdTomato. (D) Representative immunofluorescence staining of RMP (green) and HSP90AB1 (red) in AC16 cell. (E) AC16 cells were harvested. Whole-cell lysates were immunoprecipitated with RMP or HSP90AB1 antibody respective or control immunoglobulin G and analyzed by western blotting. Cell lysates were also subjected to immunoblotting. (F) Relative expression of TNF-α and IL-6 in BMDM from LC and MRKO mice under the treatment of LPS (upper). Relative expression of TNF-α and IL-6 in overexpressed Rmp BMDM (lower).

Supplementary 2. Table S1: clinical characteristics pertaining to patients with ischemic heart failure.

Supplementary 3. Table S2: label-free mass spectrometry identified the possible binding proteins of RMP in the AC16 cell line.

References

[1] T. Jernberg, P. Hasvold, M. Henriksson, H. Hjelm, M. Thuresson, and M. Janzon, "Cardiovascular risk in post-myocardial infarction patients: nationwide real world data demonstrate the importance of a long-term perspective," *European Heart Journal*, vol. 36, no. 19, pp. 1163–1170, 2015.

[2] N. G. Frangogiannis, "*Pathophysiology of Myocardial Infarction,*" *Physiology*, vol. 5, pp. 1841–1875, 2015.

[3] Z. Li, M. Nie, L. Yu et al., "Blockade of the notch signaling pathway promotes M2 macrophage polarization to suppress cardiac fibrosis remodeling in mice with myocardial infarction," *Frontiers in Cardiovascular Medicine*, vol. 8, article 639476, 2022.

[4] J. Zhang, L. Yu, Y. Xu et al., "Long noncoding RNA upregulated in hypothermia treated cardiomyocytes protects against myocardial infarction through improving mitochondrial function," *International Journal of Cardiology*, vol. 266, pp. 213–217, 2018.

[5] Y. Kim, S. Nurakhayev, A. Nurkesh, Z. Zharkinbekov, and A. Saparov, "Macrophage polarization in cardiac tissue repair following myocardial infarction," *International Journal of Molecular Sciences*, vol. 22, no. 5, p. 2715, 2021.

[6] Y. Xue, D. Nie, L. J. Wang et al., "Microglial polarization: novel therapeutic strategy against ischemic stroke," *Aging and Disease*, vol. 12, no. 2, pp. 466–479, 2021.

[7] R. Gentek and G. Hoeffel, "The innate immune response in myocardial infarction, repair, and regeneration," *Advances in Experimental Medicine and Biology*, vol. 1003, pp. 251–272, 2017.

[8] Y. Feng, K. Chen, L. Pan et al., "RPB5-mediating protein promotes the progression of non-small cell lung cancer by regulating the proliferation and invasion," *Journal of Thoracic Disease*, vol. 13, no. 1, pp. 299–311, 2021.

[9] J. Zhang, Y. F. Pan, Z. W. Ding et al., "RMP promotes venous metastases of hepatocellular carcinoma through promoting IL-6 transcription," *Oncogene*, vol. 34, no. 12, pp. 1575–1583, 2015.

[10] J. Zhang, T. Y. Jiang, B. G. Jiang et al., "RMP predicts survival and adjuvant TACE response in hepatocellular carcinoma," *Oncotarget*, vol. 6, no. 5, pp. 3432–3442, 2015.

[11] J. L. Fan, J. Zhang, L. W. Dong et al., "URI regulates tumorigenicity and chemotherapeutic resistance of multiple myeloma by modulating IL-6 transcription," *Cell Death & Disease*, vol. 5, no. 3, article e1126, 2014.

[12] K. S. Tummala, A. L. Gomes, M. Yilmaz et al., "Inhibition of De Novo NAD$^+$ Synthesis by Oncogenic URI Causes Liver Tumorigenesis through DNA Damage," *Cancer Cell*, vol. 26, no. 6, pp. 826–839, 2014.

[13] Z. H. Wan, T. Y. Jiang, Y. Y. Shi et al., "RPB5-mediating protein promotes cholangiocarcinoma tumorigenesis and drug resistance by competing with NRF2 for KEAP1 binding," *Hepatology*, vol. 71, no. 6, pp. 2005–2022, 2020.

[14] P. Mita, J. N. Savas, S. Ha, N. Djouder, J. R. Yates, and S. K. Logan, "Analysis of URI nuclear interaction with RPB5 and components of the R2TP/prefoldin-like complex," *PLoS One*, vol. 8, no. 5, article e63879, 2013.

[15] J. Zhang, J. Sheng, L. Dong et al., "Cardiomyocyte-specific loss of RNA polymerase II subunit 5-mediating protein causes myocardial dysfunction and heart failure," *Cardiovascular Research*, vol. 115, no. 11, pp. 1617–1628, 2019.

[16] Y. Y. Qin, X. R. Huang, J. Zhang et al., "Neuropeptide Y attenuates cardiac remodeling and deterioration of function following myocardial infarction," *Molecular Therapy: The Journal of the American Society of Gene Therapy*, vol. 30, no. 2, pp. 881–897, 2022.

[17] P. C. Tang, J. Y. Chung, V. W. Xue et al., "Smad3 promotes cancer-associated fibroblasts generation via macrophage-myofibroblast transition," *Advanced Science*, vol. 9, no. 1, article e2101235, 2022.

[18] K. Fujita, T. Otsuka, T. Kawabata et al., "HSP90 limits thrombin-stimulated IL-6 synthesis in osteoblast-like MC3T3-E1 cells: regulation of p38 MAPK," *International Journal of Molecular Medicine*, vol. 42, no. 4, pp. 2185–2192, 2018.

[19] J. Szyller and I. Bil-Lula, "Heat shock proteins in oxidative stress and ischemia/reperfusion injury and benefits from physical exercises: a review to the current knowledge," *Oxidative Medicine and Cellular Longevity*, vol. 2021, Article ID 6678457, 12 pages, 2021.

[20] Y. Cheng and J. Rong, "Macrophage polarization as a therapeutic target in myocardial infarction," *Current Drug Targets*, vol. 19, no. 6, pp. 651–662, 2018.

[21] J. P. Theurillat, S. C. Metzler, N. Henzi et al., "URI is an oncogene amplified in ovarian cancer cells and is required for their survival," *Cancer Cell*, vol. 19, no. 3, pp. 317–332, 2011.

[22] P. Mita, J. N. Savas, E. M. Briggs et al., "URI Regulates KAP1 Phosphorylation and Transcriptional Repression via PP2A Phosphatase in Prostate Cancer Cells," *The Journal of Biological Chemistry*, vol. 291, no. 49, pp. 25516–25528, 2016.

[23] K. A. Lipinski, C. Britschgi, K. Schrader, Y. Christinat, L. Frischknecht, and W. Krek, "Colorectal cancer cells display chaperone dependency for the unconventional prefoldin URI1," *Oncotarget*, vol. 7, no. 20, pp. 29635–29647, 2016.

[24] S. Boulon, B. Pradet-Balade, C. Verheggen et al., "HSP90 and its R2TP/Prefoldin-like cochaperone are involved in the cytoplasmic assembly of RNA polymerase II," *Molecular Cell*, vol. 39, no. 6, pp. 912–924, 2010.

[25] B. Saha, F. Momen-Heravi, I. Furi et al., "Extracellular vesicles from mice with alcoholic liver disease carry a distinct protein cargo and induce macrophage activation through heat shock protein 90," *Hepatology*, vol. 67, no. 5, pp. 1986–2000, 2018.

[26] S. Luo, T. Wang, H. Qin, H. Lei, and Y. Xia, "Obligatory role of heat shock protein 90 in iNOS induction," *American Journal of*

Retraction

Retracted: Marine-Derived Piericidin Diglycoside S18 Alleviates Inflammatory Responses in the Aortic Valve via Interaction with Interleukin 37

Oxidative Medicine and Cellular Longevity

This article has been retracted by Hindawi, as publisher, following an investigation undertaken by the publisher [1]. This investigation has uncovered evidence of systematic manipulation of the publication and peer-review process. We cannot, therefore, vouch for the reliability or integrity of this article.

Please note that this notice is intended solely to alert readers that the peer-review process of this article has been compromised.

Wiley and Hindawi regret that the usual quality checks did not identify these issues before publication and have since put additional measures in place to safeguard research integrity.

We wish to credit our Research Integrity and Research Publishing teams and anonymous and named external researchers and research integrity experts for contributing to this investigation.

The corresponding author, as the representative of all authors, has been given the opportunity to register their agreement or disagreement to this retraction. We have kept a record of any response received.

References

[1] S. Li, J. She, J. Zeng et al., "Marine-Derived Piericidin Diglycoside S18 Alleviates Inflammatory Responses in the Aortic Valve via Interaction with Interleukin 37," *Oxidative Medicine and Cellular Longevity*, vol. 2022, Article ID 6776050, 18 pages, 2022.

Research Article

Marine-Derived Piericidin Diglycoside S18 Alleviates Inflammatory Responses in the Aortic Valve via Interaction with Interleukin 37

Shunyi Li [iD],[1] **Jianglian She** [iD],[2,3] **Jingxin Zeng**,[1,4] **Kaiji Xie**,[1,4] **Zichao Luo** [iD],[1,4]
Shuwen Su [iD],[1,4] **Jun Chen**,[1,4] **Gaopeng Xian** [iD],[1,4,5] **Zhendong Cheng** [iD],[1,4] **Jing Zhao**,[6]
Shaoping Li [iD],[6] **Xingbo Xu** [iD],[7] **Dingli Xu** [iD],[1,4] **Lan Tang** [iD],[3] **Xuefeng Zhou** [iD],[2]
and Qingchun Zeng [iD][1,4,5]

[1]*State Key Laboratory of Organ Failure Research, Department of Cardiology, Nanfang Hospital, Southern Medical University,
Guangzhou 510515, China*
[2]*CAS Key Laboratory of Tropical Marine Bio-resources and Ecology, Guangdong Key Laboratory of Marine Materia Medica,
South China Sea Institute of Oceanology, Chinese Academy of Sciences, Guangzhou 510301, China*
[3]*NMPA Key Laboratory for Research and Evaluation of Drug Metabolism, Guangdong Provincial Key Laboratory of New
Drug Screening, School of Pharmaceutical Sciences, Southern Medical University, Guangzhou 510515, China*
[4]*Guangdong Provincial Key Laboratory of Shock and Microcirculation, Southern Medical University, Guangzhou 510515, China*
[5]*Bioland Laboratory (Guangzhou Regenerative Medicine and Health Guangdong Laboratory), Guangzhou 510005, China*
[6]*State Key Laboratory of Quality Research in Chinese Medicine, Institute of Chinese Medical Sciences, University of Macau,
Macau, China*
[7]*Department of Cardiology and Pneumology, University Medical Center of Göttingen, Georg-August-University,
Göttingen, Germany*

Correspondence should be addressed to Dingli Xu; dinglixu@smu.edu.cn, Lan Tang; tl405@smu.edu.cn,
Xuefeng Zhou; xfzhou@scsio.ac.cn, and Qingchun Zeng; qingchunzeng@smu.edu.cn

Shunyi Li and Jianglian She contributed equally to this work.

Calcific aortic valve disease (CAVD) is a valvular disease frequently in the elderly individuals that can lead to the valve dysfunction. Osteoblastic differentiation of human aortic valve interstitial cells (HAVICs) induced by inflammation play a crucial role in CAVD pathophysiological processes. To date, no effective drugs for CAVD have been established, and new agents are urgently needed. Piericidin glycosides, obtained from a marine-derived *Streptomyces* strain, were revealed to have regulatory effects on mitochondria in previous studies. Here, we discovered that 13-hydroxypiericidin A 10-O-α-D-glucose $(1\rightarrow6)$-β-D-glucoside (S18), a specific piericidin diglycoside, suppresses lipopolysaccharide- (LPS) induced inflammatory responses of HAVICs by alleviating mitochondrial stress in an interleukin (IL)-37-dependent manner. Knockdown of IL-37 by siRNA not only exaggerated LPS-induced HAVIC inflammation and mitochondrial stress but also abrogated the anti-inflammatory effect of S18 on HAVICs. Moreover, S18 alleviated aortic valve lesions in IL-37 transgenic mice of CAVD model. Microscale thermophoresis (MST) and docking analysis of five piericidin analogues suggested that diglycosides, but not monoglycosides, exert obvious IL-37-binding activity. These results indicate that S18 directly binds to IL-37 to alleviate inflammatory responses in HAVICs and aortic valve lesions in mice. Piericidin diglycoside S18 is a potential therapeutic agent to prevent the development of CAVD.

1. Introduction

Calcific aortic valve disease (CAVD) is the leading cause of cardiac valvular disorder in developed countries, with the estimated prevalence of 12.6 million cases and more than 2% of the population over 75 years old in 2017 [1]. Calcific aortic valvular, implicated as valvular stenosis, results in progressive left ventricular hypertrophy or obstruction and ultimately ischaemic injury to the heart [2, 3]. However, there is no effective pharmacological treatment to delay CAVD progression other than valve replacement with a mechanical or bioprosthetic valve for late-stage patients with CAVD. Thus, more effective anti-CAVD agents are urgently needed to improve clinical outcomes and to decrease the need for valve replacement in patients.

The pathogenesis of CAVD is complex and multifactorial, with spatiotemporal heterogeneity. Lipoprotein deposition, haemodynamic stress, inflammation, and immune reactions are implicated in the initial and propagated period of CAVD [4]. It is well established from a variety of studies that the inflammation in valve is a characteristic hallmark in the progression of CAVD [5–9]. In previous searches on Meng et al. lipopolysaccharide (LPS), a Toll-like receptor 4 (TLR4) agonist, was found to be an important proinflammatory factor in human aortic valve interstitial cells (HAVICs) and resulted in activation of NF-κB signal pathway and subsequent induction of inflammation in HAVICs [10, 11]. Thus, these findings related to the proinflammatory signal pathway responsible for the anti-inflammatory mechanism in CAVD provide significant insights for the development of therapies.

Increasing evidence suggests that reactive oxygen species (ROS) are overproduced, and antioxidant levels are decreased both in animal models of CAVD and in the calcified aortic valve of patients with CAVD [12, 13]. Mitochondria are the main sources of intracellular ROS, the overproduction of which is responsible for multiple cellular processes involved in cardiovascular diseases, including inflammation, apoptosis, and ossification [14]. Furthermore, the alerts of mitochondria masses and mitochondrial dysfunction result in ROS overexpression to trigger oxidative stress and inflammation [15]. Valerio et al. found that the GSSG-GSH ratio was higher in CAVD patients, which suggests oxidative stress may play a vital role in the development of CAVD [16]. Our previous studies also found that mitochondrial stress is activated in calcified aortic valve and inhibition of mitochondrial stress with N-acetyl-L-cysteine (NAC) treatment attenuates osteogenic responses in HAVICs. In addition, the NF-κB p65 phosphorylation induced by mitochondrial stress is attenuated by NAC treatment [17]. These results indicate that mitochondrial quality control has a prominent effect on maintaining normal aortic valve function. However, the underlying mechanism of mitochondrial stress in HAVICs remains elusive.

Interleukin (IL)-37, a member of the IL-1 family, is known to inhibit innate and acquired immune responses [18]. IL-37 is known to be expressed in human heamatopoietic cells, epithelial cells, breast carcinoma cells, HAVICs, and other cells [18, 19]. Previous research has established that IL-37 has powerful protective effects on inflammatory diseases, autoimmune diseases, and cancers [18, 20, 21]. Additionally, intracellular IL-37 modulates adaptive antitumour immunity through multiple signal pathways, such as the NF-κB pathway, and subsequently suppresses tumour growth [20]. Our previous studies have revealed that IL-37 suppresses LPS-induced inflammatory and osteogenic responses in HAVICs [22]. Thus, IL-37 plays a vital role in the pathobiological process associated with CAVD. Specifically, our data revealed that the expression of IL-37 is decreased in calcified aortic valve compared with those from patients with non-CAVD. These findings suggest that the discovery of anti-inflammatory agents interacting with IL-37 provides an up-to-date strategy for the prevention of CAVD.

Marine-derived microorganisms have an unrivalled potential for drug development and the production of highly potent natural compounds. The piericidin family is an important kind of active microbial metabolite that features a 4-pyridinol core linked with a methylated polyketide side chain [23]. Accumulating evidence suggests that natural piericidins obtained from marine-derived *Streptomyces* have received considerable attention in recent years because of their important medicinal activities [23, 24]. Our group has previously obtained 43 natural piericidins from two strains of marine-derived *Streptomyces*, including 29 new compounds [25–27], and found that the main piericidin metabolites, including piericidin A (PA) and glucopiericidin A (GPA), have the potential to be developed as potential anti-renal carcinoma drugs. Mechanistic studies have shown that these piericidins, whether aglycones or glycosides, could reduce ROS levels and regulate oxidative stress, as inhibitors of mitochondrial respiratory chain complex I. Piericidins can inhibit NF-κB activation by forcing the antioxidative protein peroxiredoxin 1 (PRDX1) into the nucleus [25]. The pharmaceutical potential of natural piericidins, especially the antioxidant and anti-inflammatory effects of special glycosides, is still worth further study. In our research, to discover new agents with anti-inflammatory and mitochondrial regulatory effects, the piericidin glycoside GPA and a special piericidin diglycoside, 13-hydroxypiericidin A 10-O-α-D-glucose (1→6)-β-D-glucoside (S18), were screened and studied. The piericidin diglycoside S18 showed potent anti-inflammatory effects in HAVICs. The potential ability of S18 to act as an anti-CAVD agent is worthy of further study. Here, we investigated the effect of piericidin diglycoside S18 in the development of CAVD in vivo and in vitro. A novel anti-CAVD candidate was observed and confirmed in the present study.

2. Methods and Materials

2.1. Fermentation and Isolation of S18 and GPA. The strain *Streptomyces psammoticus* SCSIO NS126, derived from a mangrove sediment sample collected from the Pearl River estuary of the South China Sea, was fermented in a volume of 100 L, according to a previously described method [25]. The culture broth was extracted with ethyl acetate three times and then concentrated under a vacuum. The extract (75.0 g) underwent chromatography on silica gel to give eight fractions (Frs. 1~8). With the guidance of high-

performance liquid chromatography (HPLC) analysis, Frs. 7 was purified with silica gel again to give six subfractions (Frs. 7-1~7-6). Frs. 7-2 was purified by semipreparative HPLC to obtain compound GPA (358 mg), while S18 (58 mg) was obtained and purified by repeated semipreparative HPLC isolation. The obtained compound was determined to be ≥95% purity by analytical HPLC. The structures of the obtained compounds were determined to be GPA and S18 by comparison of high-resolution mass spectrometry (HRMS) and nuclear magnetic resonance (NMR) data (Figures S1-S6) with the literature data [25]. The compounds were stored at -20°C until use and dissolved in DMSO to a stock concentration of 10 mM.

2.2. Human Aortic Valves.

Human calcified aortic valves were collected from five patients with CAVD who underwent aortic valve replacement in 2020-2021. The clinical features of patients are shown in Supplementary Table S1. Control noncalcified aortic valves were intraoperatively collected from four patients who underwent aortic valve replacement due to acute aortic dissections. The exclusion criteria included infective endocarditis, congenital valve disease, and rheumatic heart disease. CAVD was diagnosed when the leaflet thickness was ≥3 mm, the peak AV velocity was ≥1.5 m/s, and there was increased echogenicity (aortic root echogenicity was the control) [28]. Written informed consent was obtained from all patients in this study. The protocol of this study was conducted in accordance with the Declaration of Helsinki and was approved by the Nanfang Hospital, Southern Medical University.

2.3. Cell Culture and Treatment.

HAVICs were isolated and cultured as previously reported [17]. In brief, valve leaflets were subjected to digestion with collagenase, and cells were collected by centrifugation. The cells were cultured in M199 growth medium (Gibco, C11150500BT) containing penicillin G, streptomycin, and 10% fetal bovine serum. Cells from passages 3-6 that reached 80-90% confluence were used for this study.

To determine the influence of S18 on the inflammatory responses in LPS-stimulated HAVICs, HAVICs were treated with LPS (200 ng/mL, Sigma, L4391) in the absence or presence of S18 (0.5 μM) for 24 hours.

To evaluate the role of NF-κB in the suppression of HAVIC inflammation by S18, HAVICs were treated with LPS (200 ng/mL) in the absence or presence of S18 (0.5 μM) for 4 hours.

To determine whether mitochondrial stress is involved in the LPS-induced HAVIC inflammatory responses, HAVICs were treated with NAC (1 mM, Beyotime, S0077) for 1 hour prior to LPS stimulation.

To evaluate the role of IL-37 in mediating the effect of S18 on HAVICs, HAVICs were treated with IL-37 siRNA (50 nM, OBiO) for 8 hours followed by stimulation with LPS with or without S18 (0.5 μM).

To determine the role of IL-37 in attenuating the mitochondrial stress in HAVICs, HAVICs were preincubated with recombinant IL-37 (0.1 ng/mL, MCE, HY-P70455) for 1 hour followed by LPS (200 ng/mL) stimulation.

2.4. Experimental Mouse Model.

All animal experiments were performed according to the guidelines from Directive 2010/63/EU of the European Parliament on the protection of animals used for scientific purposes. The study was approved by the Ethics Committee for Animal Experiments of Southern Medical University. IL-37-Tg mice were constructed in the Shanghai Model Organisms Center. IL-37-Tg mice were constructed via PiggyBAC transposase system. Briefly, PiggyBAC mRNA was obtained by transcription in vitro. PiggyBAC mRNA and the vector containing the target insert were microinjected into the fertilized eggs of C57BL/6J mice.

Mice (8-week-old males) were separated into three groups. Mice were injected intraperitoneally with saline and fed a normal diet ($n = 5$), or mice were injected intraperitoneally with S18 (0.8 mg/kg) and fed an adenine diet ($n = 5$). As reported previously [29], 1.48×10^{-2} mol/kg adenine (Sigma-Aldrich, A8626) was added to the diet for 21 days. Thereafter, renal function was evaluated by examining serum BUN and creatinine levels (Mindray, China). Then, 2.27×10^{-5} mol/kg vitamin D (Sigma-Aldrich, C9756) dissolved in olive oil (Sigma-Aldrich, O1514) was injected intraperitoneally on 10 consecutive days. After an additional 4 days, the mice were anaesthetized by intraperitoneal injection with sodium pentobarbital, and tissue was harvested. The heart was perfused with 10 mL of normal saline under physiological pressure before tissue collection. The heart tissues were embedded in paraffin and dissected into 5 μm sections. The sections were fixed in 4% paraformaldehyde for haematoxylin and eosin (H&E) staining, Von Kossa staining, and immunofluorescence staining.

2.5. Microscale Thermophoresis (MST).

The ability of piericidin diglycosides to bind with potential ligands was analysed using MST. The IL-37 protein (MCE, HY-P70455) was labelled with Monolith NT™ Protein Labelling Kit Blue (Nano Temper Technologies, MO-L002) according to the manufacturer's protocol. The compounds were diluted in 16 dilution steps covering the range of appropriate concentrations. After 15 minutes of incubation at room temperature, the samples were loaded into capillaries, and thermophoresis was measured on Monolith NT.115 instrument (Nano Temper Technologies, Germany). The K_d values were calculated using NT Analysis software (Nano Temper Technologies, Germany).

2.6. Molecular docking.

The Schrödinger 2017-1 suite (Schrödinger Inc., New York, NY) was employed to perform the docking analysis. The IL-37 structure was retrieved from the available crystal structures (PDB: 6NCU) and constructed following the protein Preparation Wizard workflow in the Maestro package. The binding site was selected using the Grid Generation procedure. The prepared ligand was flexibly docked into the receptor using Glide (XP mode) with default parameters.

2.7. Statistical Analysis.

Data are presented as the mean ± SEM. Statistical analyses were performed using GraphPad Prism 7.0. Comparisons between multiple groups were analysed using one-way analysis of variance (ANOVA) with a

post hoc Bonferroni/Dunn test, two-group comparisons were analysed using a *t*-test, and differences were determined by the Mann–Whitney *U* test. $p \leq 0.05$ was considered to statistical significance.

3. Results

3.1. Effects of Marine-Derived Natural Products S18 and GPA on Cell Viability. The piericidin diglycoside S18 and piericidin monoglycoside GPA were discovered in the culture broth of *Streptomyces pasmmoticus* SCSIO NS126, an actinomycete strain derived from a mangrove sediment samples that were obtained from the Pearl River estuary of the South China Sea. S18 and GPA were identified as 13-hydroxypiericidin A 10-O-α-D-glucose (1$\rightarrow$6)-β-D-glucoside and glucopiericidin A through HRMS and NMR analyses (Figures S3 and S5), respectively, as previously reported [25]. S18, as a specific piericidin diglycoside, is a relatively rare and novel natural piericidin [23]. The chemical structures of S18 and GPA are shown in Figures 1(a) and 1(b).

HAVICs, the principal cell type of the aortic valve, exert a prominent effect on CAVD by undergoing myofibroblastic differentiation and depositing fibrotic matrix [30]. To assess the toxic effects of S18 and GPA on the proliferation of HAVICs, we treated HAVICs with different concentrations of S18 and GPA for 2 days and assessed cell viability with a Cell Counting Kit-8 (CCK-8) assay. After treatment with a series of concentrations of S18 from 0 to 4μM for 2 days, the results showed no difference in cell viability (Figures 1(c) and 1(d)). Thus, S18 has no obvious toxicity on HAVICs. However, GPA at a concentration above 0.5μM showed toxic effects on HAVICs (Figures 1(d)–1(f)).

3.2. S18 Suppresses LPS-Mediated Inflammatory Responses in HAVICs. To determine the role of S18 in HAVICs, we exposed cells to LPS (200 ng/mL) with increasing concentrations of S18 (0.5, 1, or 2μM) for 24 hours. Figure 2(a) shows that S18 reduced the expression of intercellular cell adhesion molecule-1 (ICAM-1) in LPS-treated HAVICs in a dose-dependent fashion, while GPA had no effect on the level of ICAM-1 in HAVICs at the tested concentrations (Figure 2(b)). Notably, the LPS-induced increases in ICAM-1 level in HAVICs was significantly reduced by 25% with 0.5μM S18. Simultaneously, 0.5μM S18 reduced the expression of interleukin IL-8 and monocyte chemoattractant protein-1 (MCP-1) by 31% and 40%, respectively (Figures 2(c) and 2(d)). The levels of ICAM-1, IL-8, and MCP-1 genes in HAVICs were also reduced by S18 treatment (Figure 2(e)). These results demonstrate that S18 negatively regulates HAVIC inflammatory responses to LPS.

3.3. S18 Protects against LPS-Induced Mitochondrial Stress. Recent evidence has suggested that mitochondrial activity has a potential role in the development of cardiovascular calcification. Next, the role of S18 in mitochondrial function was explored. As expected, we found that the ROS production was upregulated 2.1 folds in LPS-treated HAVICs, while S18 treatment markedly reduced LPS-induced ROS production by over 25% (Figure 3(a)). Next, fluorescence images of

JC-1 and tetramethylrhodamine, methyl ester (TMRM) staining revealed that the mitochondrial membrane potential (MMP) was upregulated by over 40% in HAVICs treated with LPS and S18, compared with that in HAVICs treated with LPS alone (Figures 3(b) and 3(c)), suggesting that S18 attenuates mitochondrial stress. Moreover, the mitochondrial quantity was determined with Mito-Tracker Green. LPS-exposed cells showed reduction in mitochondrial mass, which was indicated by the downregulation of the Mito-Tracker Green fluorescence signals. On the contrary, the LPS-induced mitochondrial dysfunction was significantly restored (approximately 40%) by S18 therapy (Figure 3(d)). Taken together, these observations reveal that LPS elicits mitochondrial dysfunction in HAVICs, which is attenuated by S18.

3.4. S18 Suppresses Inflammation through the NF-κB p65-Dependent Pathway in HAVICs. To date, it has been well established through a variety of studies that the NF-κB pathway plays an essential role in many cardiovascular diseases including CAVD, cardiac hypertrophy, and heart failure [31]. Cytokines, including ICAM-1, IL-8, and MCP-1, converge in the downstream activation of the NF-κB pathway in CAVD. To investigate the mechanism by which inflammatory responses to LPS are mitigated by S18 in HAVICs, we evaluated the effect of S18 on NF-κB, as it is crucial to mediate HAVIC inflammation. Figure 4(a) shows that the induction of NF-κB phosphorylation (approximately 4 folds) by LPS in HAVICs was suppressed by over 40% with S18. The immunofluorescence staining images in Figure 4(b) confirmed the inhibitory effect of S18 on LPS-induced nuclear translocation of NF-κB p65 (Figure 4(b)). NAC, a classical antioxidant, has been used to scavenge ROS and prevent mitochondrial stress [32]. Next, we tested the hypothesis that the increased ROS levels induced by mitochondrial stress account for NF-κB activation in HAVICs exposed to LPS. As expected, NAC treatment suppressed LPS-induced NF-κB p65 phosphorylation by 25% and nuclear translocation (Figures 4(c) and 4(d)). Thus, these results suggest that S18 functions as a potent inhibitor of NF-κB p65 to restrain LPS-induced inflammatory responses in HAVICs.

3.5. IL-37 Is Involved in the S18-Mediated Attenuation of HAVIC Inflammatory Responses to LPS. Our previous studies found that recombinant IL-37 exerts potent protective effects on CAVD and that recombinant IL-37 alleviates MyD88-mediated inflammatory mediator production after stimulating TLR2/4 in HAVICs [33]. Five patients with CAVD and four patients with non-CAVD were recruited in this study (Figure 5(a)). We also found that the level of IL-37 protein in calcified aortic valve was notably lower, compared with that in non-CAVD patients (Figures 5(a) and 5(b)). To elucidate the molecular mechanisms of S18 in HAVICs, we explored the role of IL-37 on the effect of S18-mediated attenuation of inflammatory cytokines in HAVICs. The Western blotting results showed that IL-37 was upregulated by approximately 35% in HAVICs after S18 treatment (Figure 5(c)). We also detected the expression

(a)

(b)

(c)

Concentration of S18 (μM)	Cell viability mean ± SEM	p Value
0	1	-
0.25	0.91 ± 0.05	0.766
0.5	1.01 ± 0.04	0.999
1	0.93 ± 0.05	0.928
2	1.09 ± 0.06	0.793
4	1.08 ± 0.06	0.870

(d)

(e)

Concentration of GPA (μM)	Cell viability mean ± SEM	p Value
0	1	-
0.025	0.89 ± 0.02	0.927
0.05	0.92 ± 0.08	0.981
0.1	0.84 ± 0.4	0.639
0.5	0.81 ± 0.04	0.414
1	0.647 ± 0.09	0.017
2	0.53 ± 0.01	0.001
4	0.32 ± 0.08	< 0.001

(f)
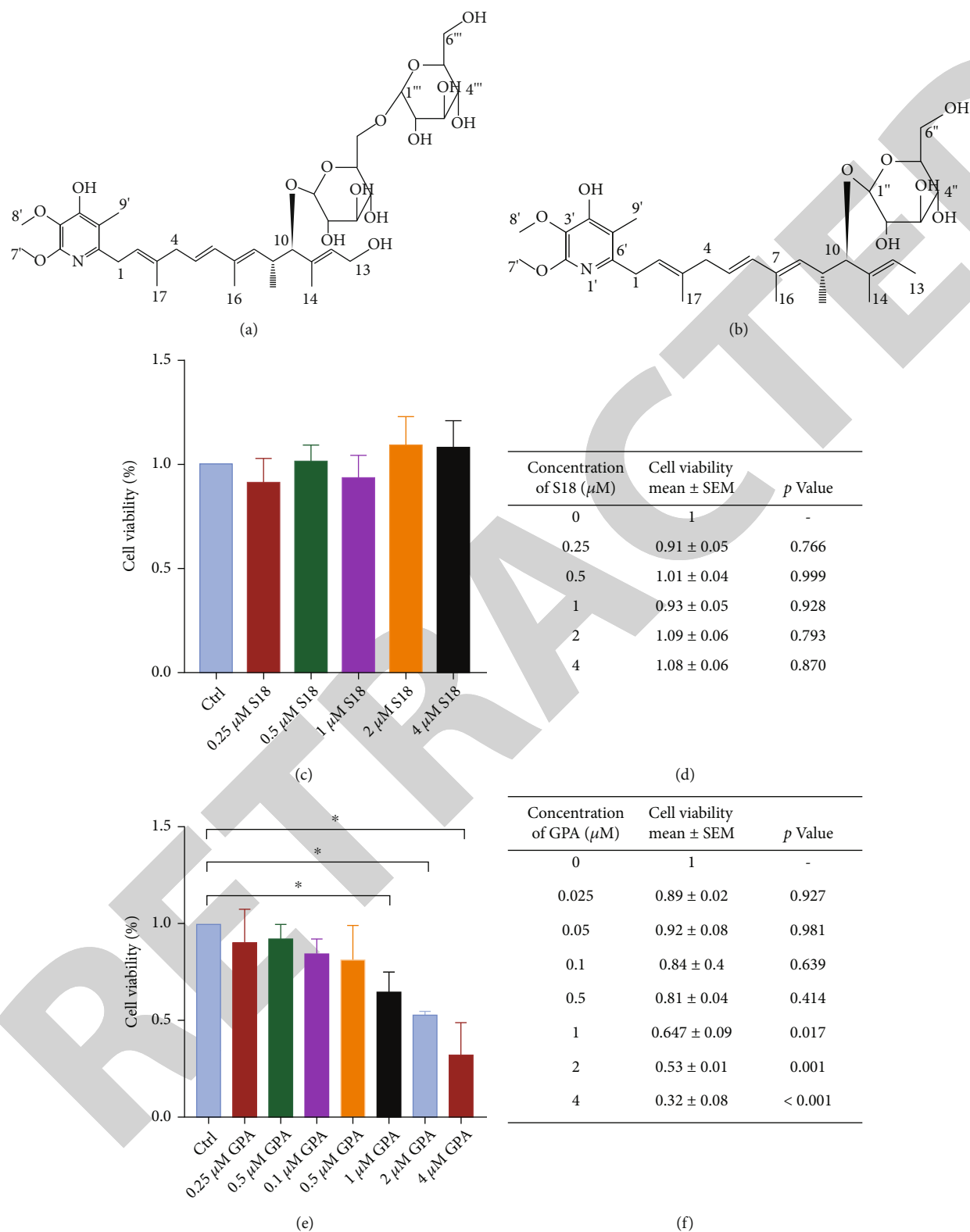
FIGURE 1: Viability of HAVICs following S18 and GPA treatment. (a, b) The structure of S18 and GPA. (c–f) Cell viability with or without S18 or GPA treatment for 2 days, $n = 5$. $^*p < 0.05$ compared with the control.

of IL-37 in GPA-treated HAVICs. However, GPA failed to induce IL-37 expression (Figure S7). Subsequently, knockdown experiments were performed in HAVICs. As shown in Figure 5(d), the IL-37 level in HAVICs was effectively knocked down by siRNA but not by the scrambled siRNA. Moreover, the expression of ICAM-1 and IL-8 was downregulated by 25% and 20% in LPS-treated HAVICs, respectively. Thus, IL-37 knockdown significantly

(a)

(b)

(c)

(d)

Figure 2: Continued.

(e)
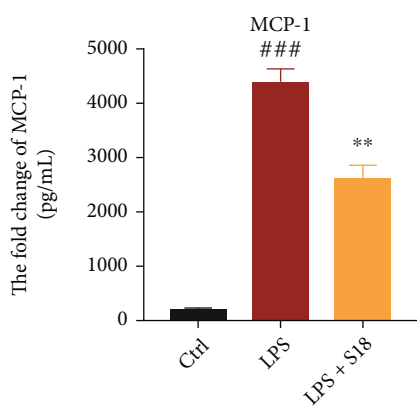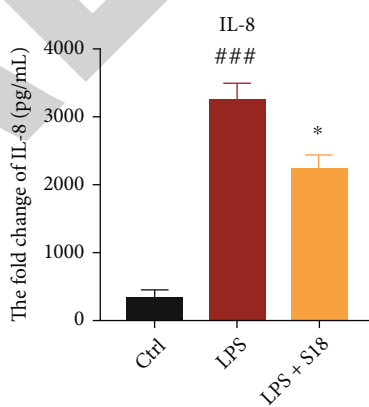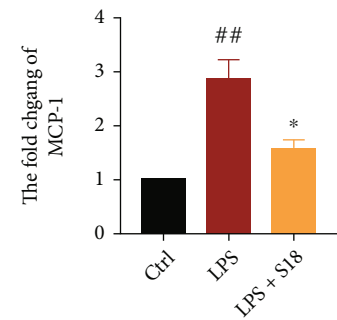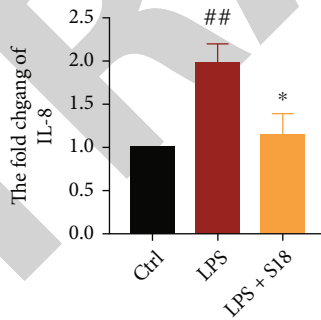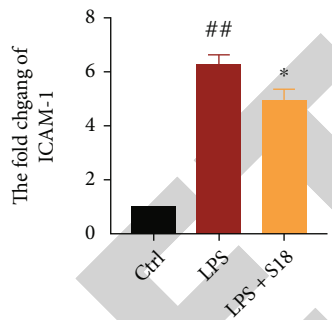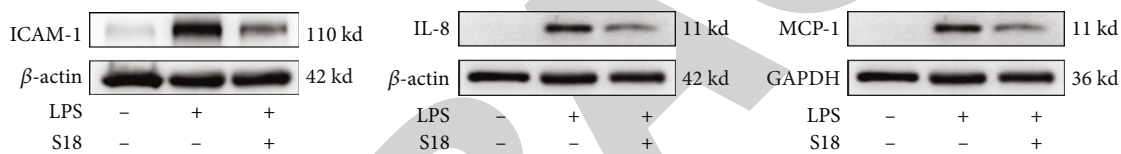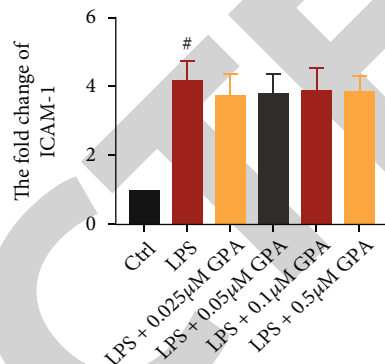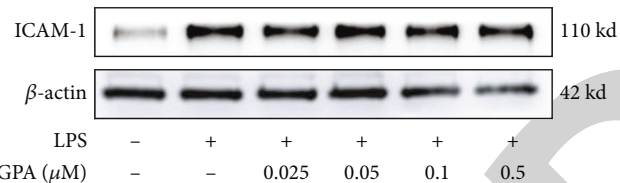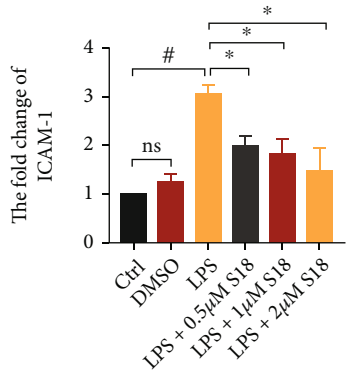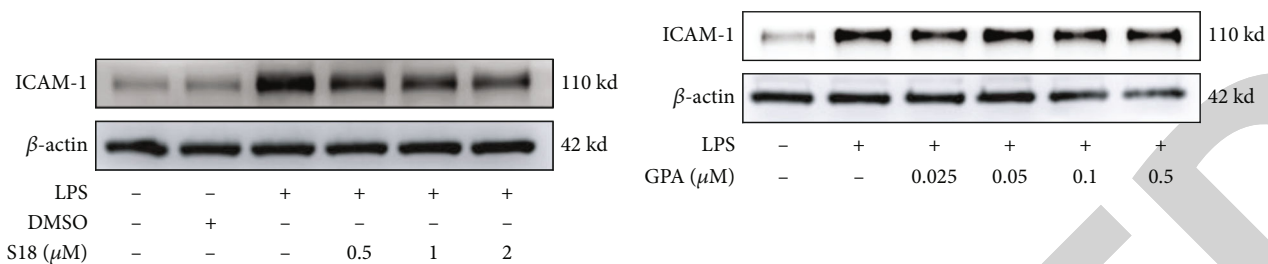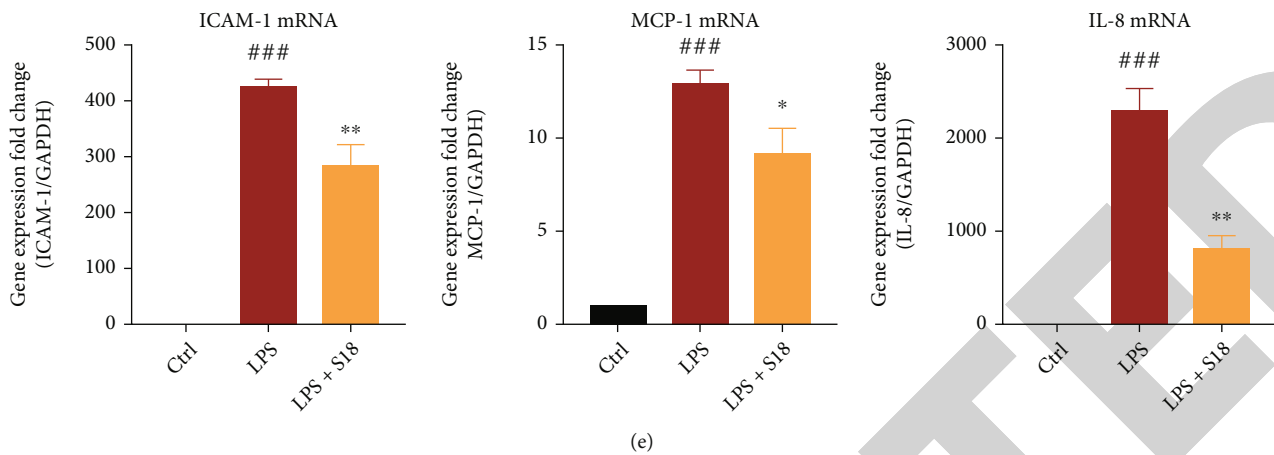
Figure 2: S18 ameliorates inflammatory responses in vitro. (a, b) Cells were stimulated with 200 ng/mL LPS and then treated or not treated with S18 and GPA for 24 hours. Immunoblotting results show the expression of ICAM-1 in HAVICs, $n = 4$. (c) The expression of ICAM-1, IL-8, and MCP-1 was determined via Western blotting and quantification analysis after 24 hours of treatment with S18 (0.5 μM), $n = 5$. (d) The levels of IL-8 and MCP-1 in the culture medium of cells from valves were tested by enzyme-linked immunosorbent assay (ELISA), $n = 5$. (e) The mRNA levels of ICAM-1, IL-8, and MCP-1 were determined by quantitative real-time polymerase chain reaction (qRT-PCR), $n = 5$. Error bars represent the mean ± SEM, $^{#}p < 0.05$, $^{##}p < 0.01$, and $^{###}p < 0.0001$ vs. control; $^{*}p < 0.05$, and $^{**}p < 0.01$ vs. the LPS group.

blunted the suppressive effect of S18 on the HAVIC inflammatory responses to LPS (Figures 5(e) and 5(f)). Collectively, it is reasonable to believe that IL-37 is a potential target of S18, but not GPA, in HAVICs.

3.6. IL-37 Mediates the Protection against Mitochondrial Stress in HAVICs. To investigate whether IL-37 attenuates mitochondrial stress in HAVICs, we treated HAVICs with recombinant IL-37 (0.1 ng/mL) 1 hour prior to LPS. As shown in Figures 6(a) and 6(b), recombinant IL-37 not only significantly decreased ROS levels by 30% but also increased MMP levels in HAVICs stimulated with LPS. Conversely, IL-37 knockdown through specific siRNAs further upregulated LPS-induced ROS production and decreased MMP (Figures 6(c) and 6(d)). Thus, these results suggest that downregulating IL-37 with siRNA prevents the protective effect of S18 against LPS-induced mitochondrial stress.

3.7. Docking Analysis of S18 and GPA with IL-37. The monomeric and dimeric forms of IL-37 have a remarkable impact on its anti-inflammatory activity. Eisenmesser et al. found that, compared with native IL-37, monomeric IL-37 shows more effective suppression of inflammatory mediators in multiple cell types [34]. To order to explore the interaction between S18 and the potential target, we selected a homology model of IL-37 (PDB code: 6NCU), which was subjected to in silico molecular docking analysis. S18 comfortably combines with the monomeric and dimeric forms of IL-37 into the binding pocket (Figure 7) with negative binding free energy values (S value) -6.618 and -7.042, respectively. Heparin was selected to be the positive control drug [34]. Intriguingly, heparin appeared to fit perfectly into the monomeric form of IL-37 with an S value of -7.290 but interacted with the dimeric form of IL-37 with an S value of -2.159 (Figure S8). In addition, the docking analysis of several piericidin analogues was assessed. Similar to S18, S40, a

piericidin diglycoside, could be considered as a potential ligand of the IL-37 protein (Figure S8a). On the contrary, piericidin glycoside S14 and piericidin aglycone PA failed to dock with the IL-37 protein (Figure S8b-c).

As shown in Figure 7(b), S18 exhibited a vital role in the binding model, and its hydroxy groups formed hydrogen bonds with the active site residues LYS58, ARG158, and GLN160 in the monomeric form of IL-37. However, the glucoside with monosaccharides GPA (Figure 7(c)) and S14 (Figure S8b) displayed weak activity in the binding model of the monomeric form of IL-37 with S values ranging from -4 to -5, which was consistent with the corresponding MST assay results (Figure S8d). MST analysis also revealed that PA exhibited no binding activity with IL-37 (Figure S8d). Therefore, further exploration could be conducted to reveal the underlying mechanism of IL-37 that is induced by piericidin glucoside accompanied by disaccharide or monosaccharide.

3.8. S18 Alleviates Aortic Valve Lesions In Vivo. To further confirm the effect of S18 on CAVD, a renal dysfunction plus vitamin D-induced aortic valve calcification model was established as previously reported [29] (Figure 8(a)). IL-37 transgenic (Tg) mice were intraperitoneally injected with normal saline or S18 and fed an adenine (1.48×10^{-2} mol/kg) diet for 21 days to induce renal dysfunction. Other IL-37-Tg mice were intraperitoneally injected with normal saline and were fed a regular diet as a control. The levels of creatinine and blood urea (BUN) were detected (Figure S9a). Vitamin D (2.27×10^{-5} mol/kg) was applied to generate high calcium-induced aortic valve calcification. After vitamin D injection for 10 days, no obvious effect of vitamin D on renal function was observed (Figure S9b). After an additional 4 days of observation, the heart tissue of mice was harvested to perform H&E staining, Von Kossa staining, and immunofluorescence staining. As shown in Figure 8(b), the cardiomyocyte cross-
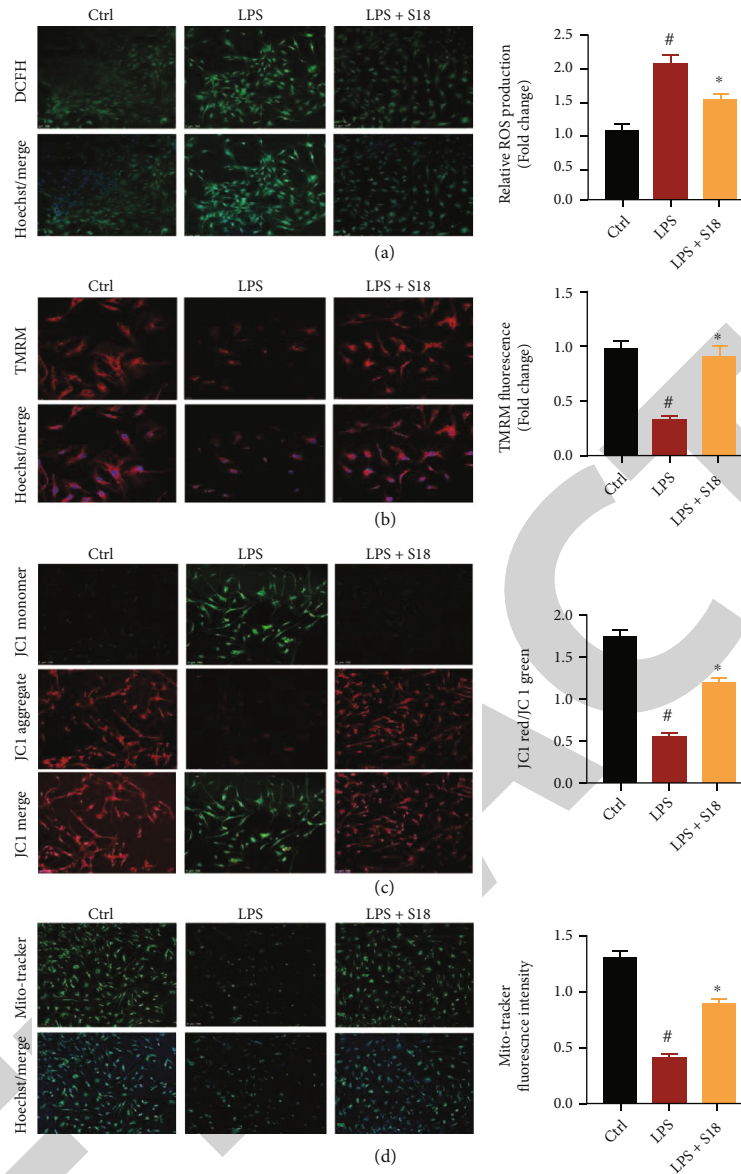
Figure 3: S18 prevents LPS-induced mitochondrial dysfunction in HAVICs. Cells were treated with LPS (200 ng/mL) in the presence or absence of S18 for 24 hours. (a) Fluorescence images show the production of ROS in HAVICs using the 2,7-dichlorodihydrofluorescein diacetate (DCFH-DA) fluorescent dye, $n = 5$. Scale bar $= 100 \, \mu$m. (b) Fluorescence images of HAVICs stained with TMRM, $n = 5$. Scale bar $= 25 \, \mu$m. (c) The MMP was detected with JC-1 staining in HAVICs, $n = 5$. Scale bar $= 100 \, \mu$m. (d) Fluorescence intensity of Mito-Tracker Green staining is shown in HAVICs, $n = 5$. Scale bar $= 100 \, \mu$m. The data are shown as the mean $\pm$ SEM. $^{\#}p < 0.05$ vs. control; $^{*}p < 0.05$ vs. the LPS group.

sectional area and the aortic valve leaflet thickness were increased in the model group compared with the control group but were markedly decreased by S18 treatment. Correspondingly, the results of the Von Kossa staining illustrated that S18 impeded the aortic valve thickening and calcium deposition induced by prolonged renal dysfunction plus vitamin D administration (Figure 8(c)). In addition, immunofluorescence analysis revealed that the levels of ALP and BMP2 were increased in the thickened aortic valve tissues from the model group, but that supplemental S18 reduced the expression of ALP, and BMP2 in valve tissues (Figures 8(d) and 8(e)).

4. Discussion

In recent decades, valvular inflammation has been considered to occur in the initial lesions and throughout the course of CAVD [35]. Upon exposure to proinflammatory stimuli, HAVICs differentiate into osteoblast-like cells, which produce and deposit collagen matrix and bone-relaxed proteins to remodel valvular structure, resulting in valvar thickening and stiffening [11]. In this regard, investigating the molecular mechanism underlying aortic valve inflammatory responses and discovering anti-inflammatory agents may promote the development of pharmacological interventions for CAVD.

(a)

(b)

(c)

(d)
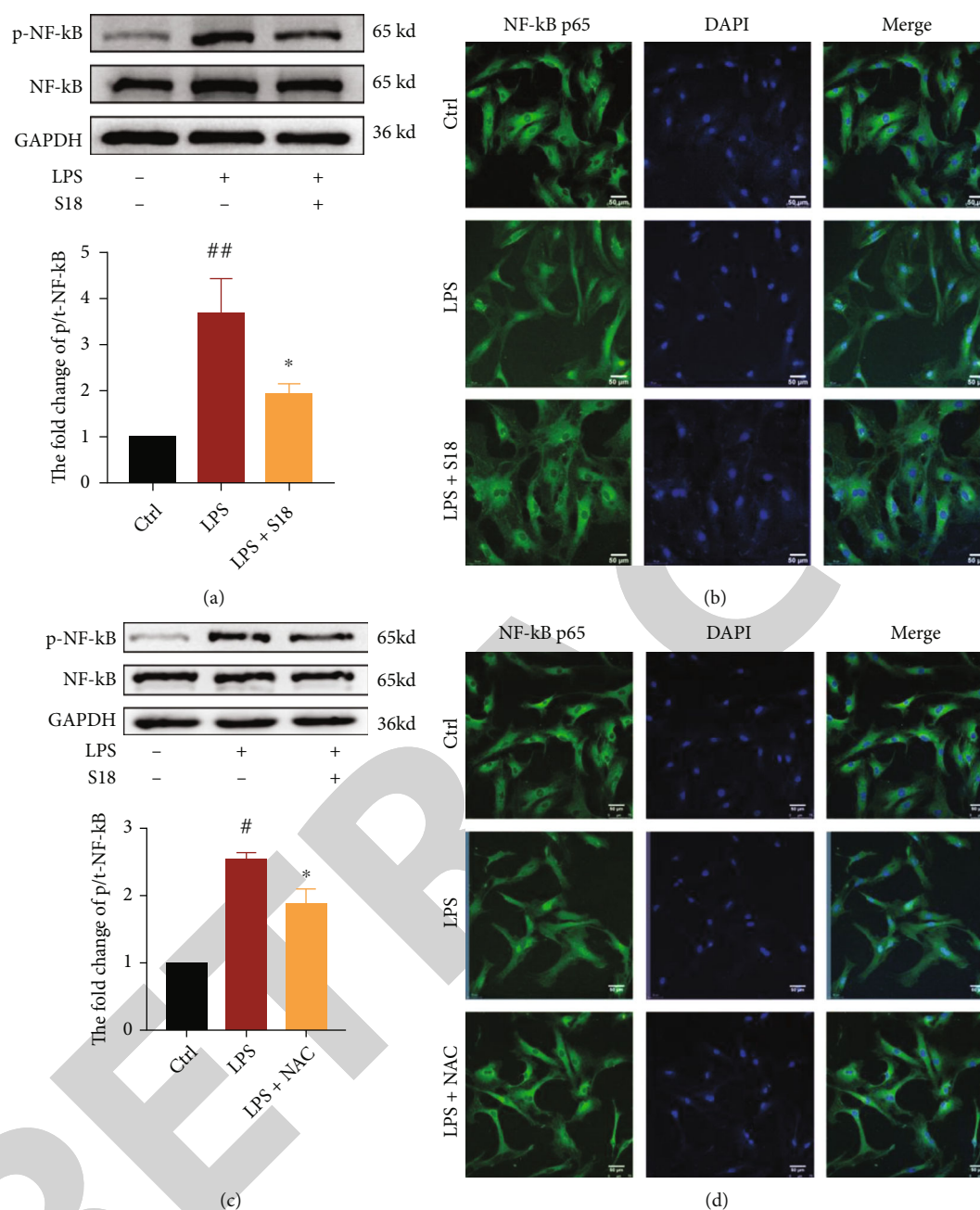
Figure 4: S18 prevents the activation of NF-κB p65 against inflammation. HAVICs were treated with LPS (200 ng/mL) for 4 hours in the presence or absence of S18. (a) Western blot analysis shows that S18 reduced the phosphorylation of NF-κB p65 in HAVICs, $n = 5$. (b) Representative images show intranuclear localization of NF-κB p65 in HAVICs stimulated with LPS and extranuclear localization of NF-κB p65 after HAVICs were treated with S18. Scale bar = 50 μm. (c, d) Data show that NAC treatment reduces NF-κB phosphorylation in HAVICs, $n = 4$. Images show that NAC treatment attenuates LPS-induced intranuclear localization of NF-κB p65 in HAVICs. Scale bar = 50 μm. Data are shown as the mean ± SEM. $^{\#}p < 0.05$, and $^{\#\#}p < 0.01$ vs. control; $^{*}p < 0.05$ vs. LPS alone.

However, few studies have yet discovered novel drugs, especially marine-derived compounds, which ameliorate the inflammatory responses of HAVICs. In this study, we discovered a marine-derived piericidin diglycoside S18 with pharmacological potential and found that (1) S18 suppressed the HAVIC inflammatory responses to LPS, (2) S18 mitigated the LPS-induced mitochondrial stress implicated in HAVICs inflammation, (3) S18 interacted with IL-37 to inhibit the NF-κB activation involved in the HAVIC pro-

inflammatory pathway, and (4) administration of S18 alleviated aortic valve calcification in IL-37-Tg mice. These findings represent the therapeutic potential of S18 for CAVD and provide new insights to aid in the discovery of anti-CAVD agents from marine-derived compounds.

4.1. S18 Suppresses LPS-Induced Inflammation and Mitochondrial Stress in HAVICs. Haemodynamic mechanical stress and shear stress on the aortic valve damage to

(a)

(b)

(c)

(d)

(e)

(f)
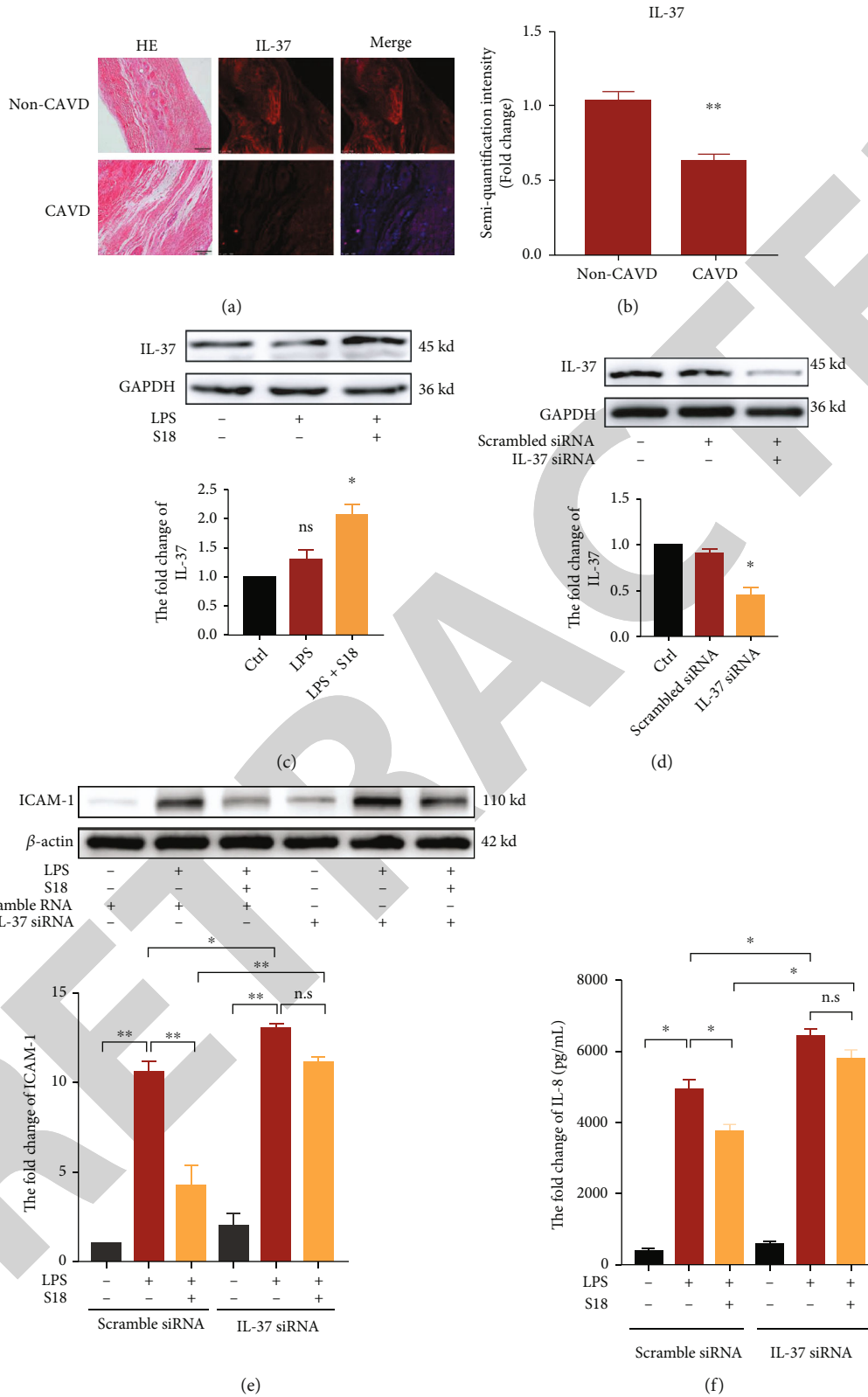
Figure 5: IL-37 activation is required for the downregulation of inflammatory cytokines caused by S18. (a, b) HE staining of aortic valve from patients with CAVD or non-CAVD patients, and the expression of IL-37 in valve tissue was detected by immunofluorescent staining. $^{**}p < 0.01$ compared with the non-CAVD group, scale bar $= 50\,\mu$m, $n = 4$. (c, d) Representative immunoblots and the corresponding quantification of IL-37 in HAVICs, $n = 5$. $^{*}p < 0.05$ compared with the LPS group. (e, f) Representative immunoblots and ELISA showing the protein expression of ICAM-1 and IL-8 in LPS and S18-treated HAVICs in combination with IL-37 knockdown. Cells with scrambled siRNA were used as controls, $n = 4$. Data are shown as the mean ± SEM. $^{**}p < 0.01$, and $^{*}p < 0.05$.
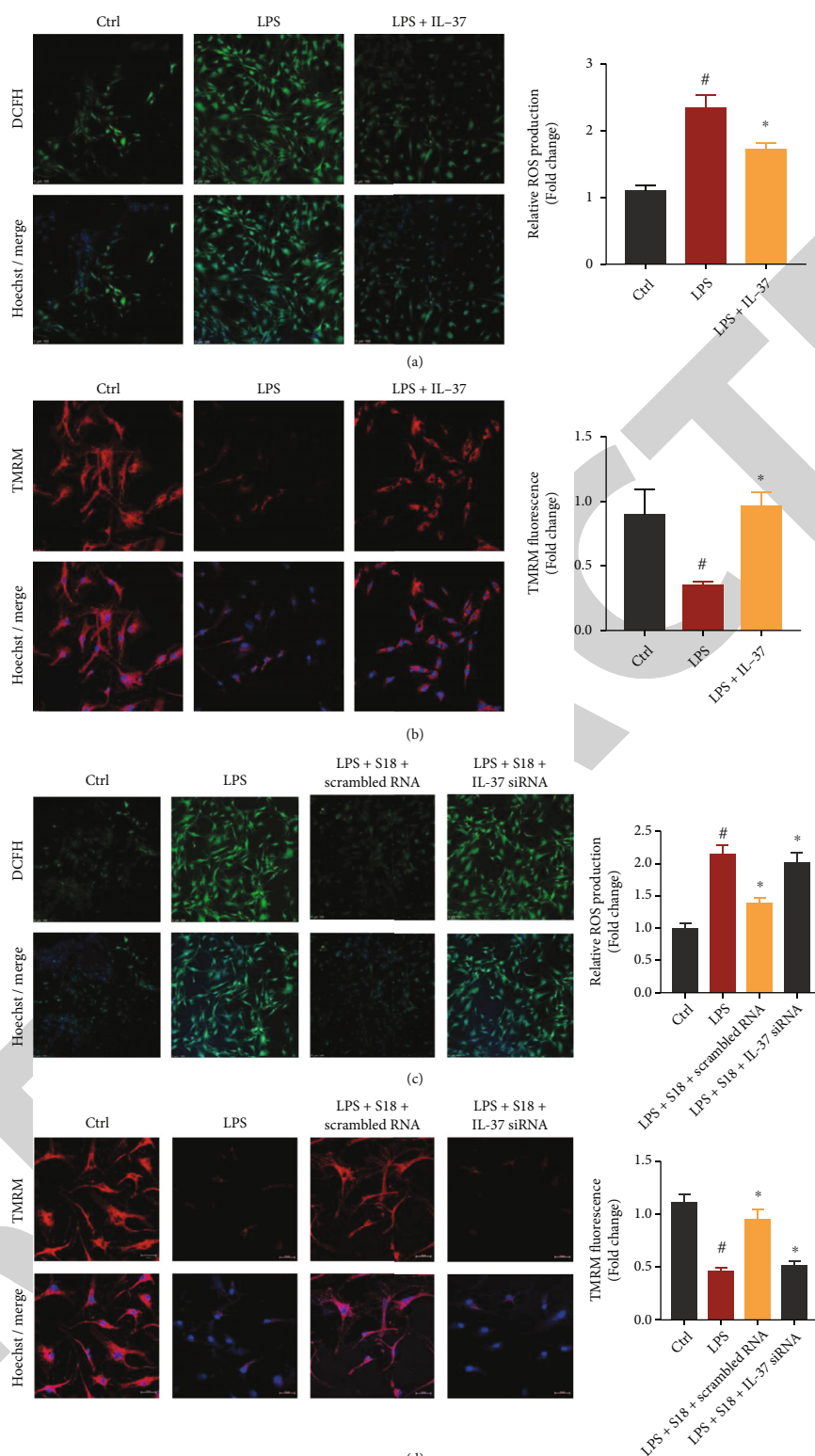
FIGURE 6: S18 prevents against mitochondrial dysfunction in an IL-37-dependent manner. HAVICs were treated with LPS (200 ng/mL) in the presence or absence of IL-37 (0.1 ng/mL) for 24 hours. (a) Fluorescence images with DCFH-DA dye show the ROS production, $n = 4$. Scale bar = 100 μm. (b) Fluorescence images of HAVICs stained with TMRM, $n = 4$. Scale bar = 50 μm. Cells were treated with IL-37 siRNA (50 nM, OBiO) following stimulation with LPS (200 ng/mL) with or without S18 (0.5 μM). (c) Fluorescence images using DCFH-DA fluorescent dye show ROS production, $n = 4$. Scale bar = 100 μm. (d) Fluorescence intensity of TMRM staining is shown, $n = 4$. Scale bar = 50 μm. Data are shown as the mean ± SEM. #$p < 0.05$ compared with the control group, *$p < 0.05$.

Heparin/IL-37

(a)

S18/IL-37

(b)

GPA/IL-37

(c)

● Heparin/IL-37 K_d = 3.60E-05 (M)

(d)

Figure 7: Continued.

(e)
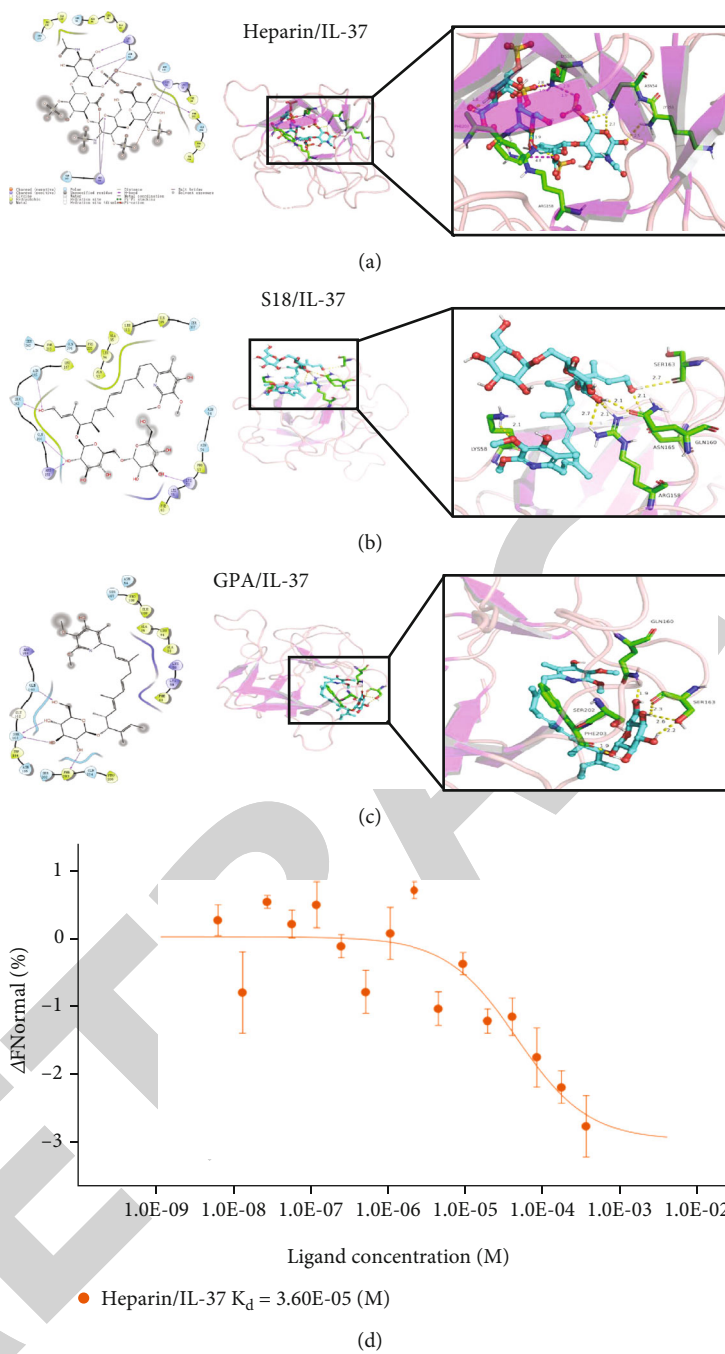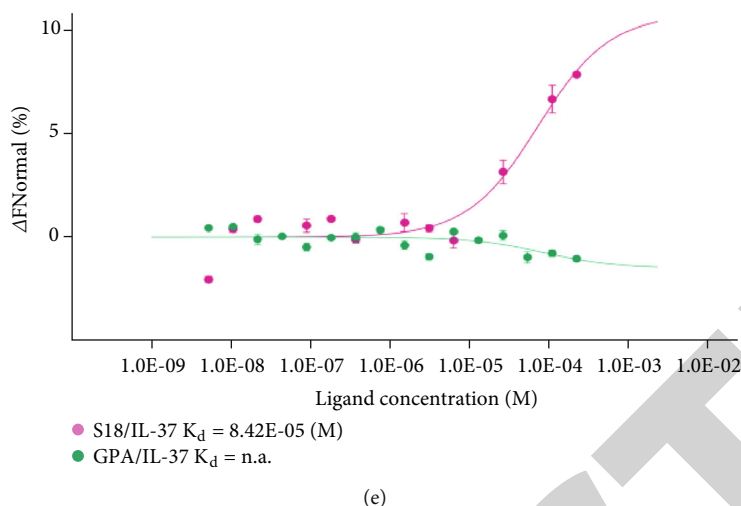
Figure 7: S18 directly binds the monomeric forms of IL-37 (6NCU). The detailed docking mode of (a) heparin/IL-37, (b) S18/IL-37, and (c) GPA/IL-37 with docking pock. The affinity of (d) heparin/IL-37 ($K_d = 36.0\,\mu M$), (e) S18/IL-37 ($K_d = 84.2\,\mu M$), and GPA/IL-37 (K_d = no binding) binding as analysed by MST assay. Data are shown as the mean ± SEM, $n = 3$.

aortic valve endothelial cells, and then, lipoprotein (a), oxidized low-density lipoprotein (oxLDL) cholesterol, and proinflammatory factors infiltrate the valvular interstitium [36]. These factors act as damage-associated molecular patterns (DAMPs) to provoke mitochondrial stress and inflammation in AVICs [4]. Subsequently, activated HAVICs produce proinflammatory factors, including ICAM-1 [37], IL-8, and MCP-1 [38, 39], resulting in the infiltration of immune cells and a resultant further inflammatory cascade in valve tissue [39, 40]. In this regard, numerous lines of evidence indicate that valvular inflammation initiates the early stage of CAVD. Moreover, our previous studies reported that proinflammatory stimuli promote the osteogenic differentiation of HAVICs [41, 42]. Therefore, it is conceivable that agents that suppress AVIC inflammatory responses might have therapeutic potential for CAVD.

Accumulating evidence suggests that mitochondria exert a pivotal effect on the inflammatory response, and mitochondrial dysfunction is involved in numerous diseases that are characterized by chronic inflammation, including atherosclerosis, cancer, and neurodegeneration [43, 44]. Mitochondria has an important effect on cell inflammation via modulating the production of ROS and the activation of NF-κB pathway. The overproduction of mitochondrial ROS and oxidative stress are the key features of mitochondrial dysfunction, which in turn leads to inflammatory responses [45]. Furthermore, inflammation induced by ROS acts as a loop, resulting in the exacerbation of tissue damage [46]. Mitochondrial dysfunction is well-known to play an essential role in the progression of atherosclerosis. Zhang et al. found that CoQ_{10} supplementation alleviates mitochondrial function, and then, the degree of atherosclerotic lesions was significantly relieved in ApoE-/- mice [47, 48]. Therefore, mitochondria are a promising therapeutic target for novel treatments of diseases with chronic inflammation.

Here, we found that S18 substantially decreased the production of ICAM-1, IL-8, MCP-1, and ROS in HAVICs treated with LPS. Additionally, S18 attenuated the LPS-induced downregulation in MMP and mitochondrial mass.

These results allude to the participation of mitochondrial stress in HAVICs and demonstrate that S18 negatively regulates HAVIC inflammatory responses to proinflammatory stimuli. These findings support that S18 may have therapeutic potential for preventing aortic valve calcification.

Although CAVD is associated with various risk factors, patients with CAVD are often accompanied with diabetes or chronic kidney disease [49]. These patients have poor calcium metabolism, which results in a high calcium load and then largely contributes to the accelerated calcification of the aortic valve [50]. Thus far, no drugs have shown therapeutic effects on the initial phases of CAVD. Hence, mounting research has focused on seeking agents against CAVD. Marine-derived compounds undoubtedly have considerable potential [51]. Similarly, our in vivo studies revealed that S18 exhibited significantly alleviated aortic valve thickening, decreased calcium nodule formation, and reduced ALP and BMP2 levels in valve leaflets after prolonged exposure to renal dysfunction plus vitamin D-induced valve calcification. To the best of our knowledge, these findings represent the first report of a beneficial role of S18 on CAVD. Furthermore, the anti-inflammatory effects of S18 have clinical significance.

4.2. IL-37 Mediates the Protective Effects of S18 against on HAVIC Inflammatory Responses via the Inhibition of NF-κB. IL-37 is a special member of the IL-1 family due to its inhibitory effects on the production of inflammatory cytokines in many kinds of cells [52]. A bulk of data corroborates the in vivo protective effect of IL-37 in disease models [53–55]. Analogously, we found that IL-37 suppresses the inflammatory and osteogenic responses to stimuli in HAVICs and ameliorates valve lesions in mice [22, 33]. In addition, as a classical inflammatory pathway mediator, NF-κB is thought to induce the activation of downstream cytokines.

Given the broad therapeutic potential of IL-37 and the extensive involvement of NF-κB in inflammation, we hypothesized that S18 promotes IL-37 expression to mitigate HAVIC inflammatory responses to LPS in an NF-κB-
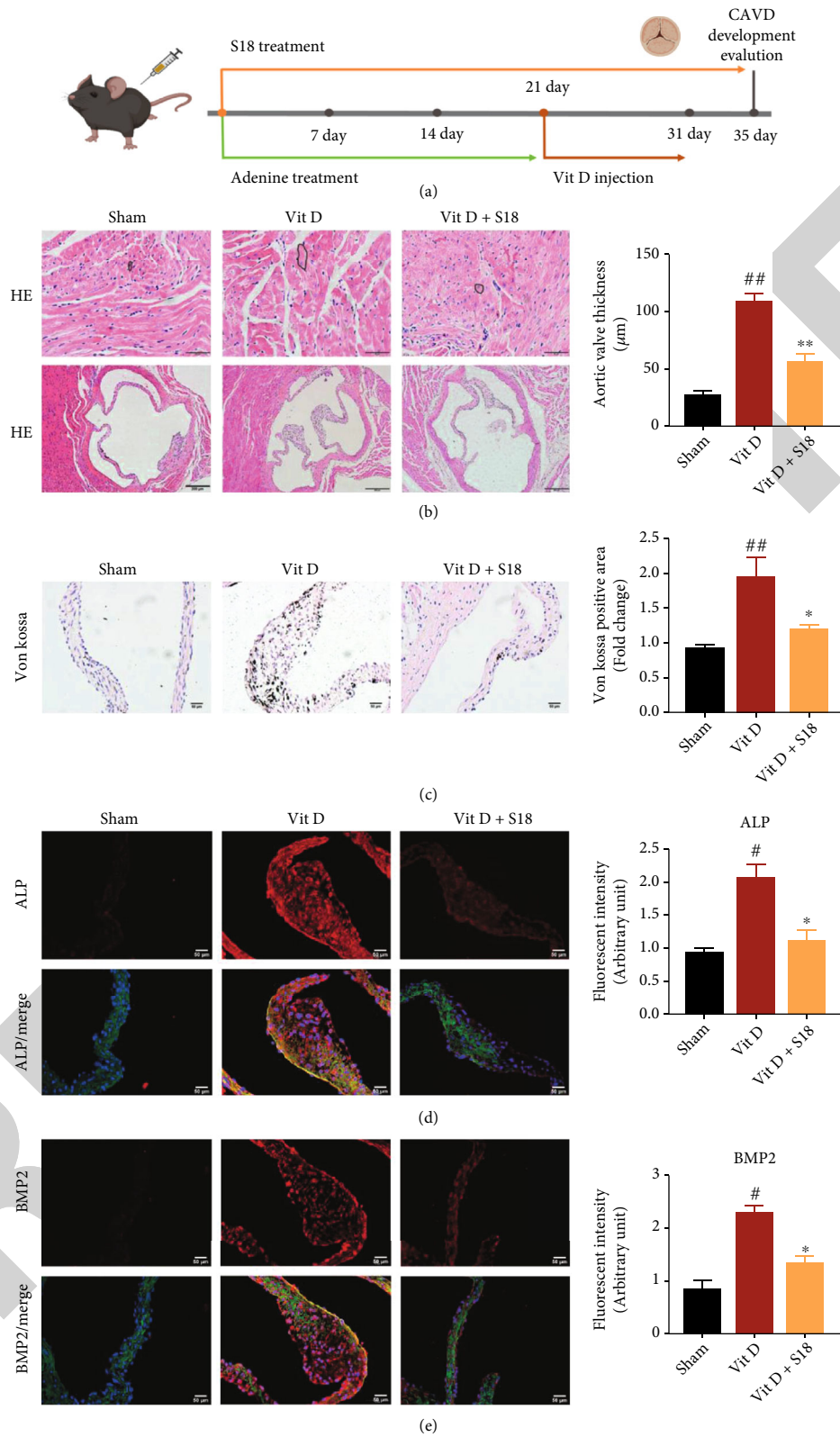
Figure 8: Evaluation of the therapeutic efficacy of S18 in IL-37-Tg mice. (a) Timeline diagram of S18 administration in the aortic valve calcification model. (b) Pathological changes in cardiomyocytes and aortic valves in the aortic valve calcification model. HE staining of cardiomyocytes and aortic valves. Scale bar = 200 μm. (c) Von Kossa staining in the aortic valve calcification model. Scale bar = 50 μm. (d, e) Representative immunofluorescence images in mouse aortic valves. Scale bar = 50 μm, $n = 5$. Data are the mean ± SEM. $^{\#\#}p < 0.01$ vs. sham; $^{**}p < 0.01$ vs. the Vit D group.

dependent fashion. While verifying this hypothesis, we found that S18 upregulated the expression of IL-37 in HAVICs. Correspondingly, LPS-induced phosphorylation and nuclear translocation of NF-κB p65 in HAVICs were suppressed by S18. Moreover, it is noteworthy that IL-37 appears to play a vital role in mediating the protective effects of S18 since IL-37 knockdown via siRNA blunted but did not abolish the anti-inflammatory and antioxidative effects of S18, as evidenced by the reduction but still high levels of ICAM-1 and IL-8.

Increasing evidence reveals that oxidative stress is involved in the progression of CAVD and mouse models of valve stenosis [12]. ROS has been characterized as activating proosteogenic signals and accelerating calcification of vascular smooth muscle cells in vitro [13]. However, uncertainty remains regarding the role of IL-37 in oxidative stress. Here, our pioneering study determined that IL-37 has a profound effect on oxidative stress in HAVICs. NAC inhibited inflammatory responses and NF-κB phosphorylation, which suggests that oxidative stress is involved in LPS-induced inflammatory responses. We also found that S18 could not alleviate oxidative-like stress in the presence of IL-37 siRNA, which suggests that S18 may exert its effect on HAVICs in an IL-37-dependent manner. Accordingly, IL-37 is a key factor for the therapeutic effect of S18 on CAVD.

4.3. IL-37 Is a Potential Target of the Piericidin Diglycoside S18 in HAVICs. To date, compounds that inhibit or activate the IL-37 protein to achieve therapeutic effects remain to be discovered. A total of 5 piericidin compounds were applied to the docking analysis, consisting of the aglycone PA, the piericidin diglycosides S18 and S40, and the piericidin monoglycosides GPA and S14. MST and docking analysis provided direct evidence that the piericidin diglycosides S18 and S40 may be potential candidates that bind to and activate the IL-37 protein. In contrast, the piericidin monoglycosides, GPA and S14, exerted no IL-37-binding activity. Moreover, the toxicity of S18 is less than that of GPA in HAVICs. In these contexts, compared to piericidin monoglycoside, piericidin diglycosides have a greater therapeutic potential for CAVD.

Agents with excellent pharmacological activity for CAVD are expected to be discovered. Numerous studies have been performed to discover novel drugs from a variety of natural products [56, 57]. Notably, marine natural products represent the most abundant source of novel compounds that maybe overcome the limitations of other anti-CAVD drug discovery approaches and become pioneering agents in the treatment of CAVD. Additionally, further exploration of the effect of these drugs on CAVD will not only have crucial complications for the understanding of cardiovascular diseases but also provide a rationale for discovering new therapeutic strategies.

There are several limitations in this study. First, the direct detection of the expression of IL-37 in animal experiments is impossible, because mice do not have a homologue gene for human IL-37. Therefore, IL-37-Tg mice were used to examine the effect of S18 in vivo. Second, hyperlipidaemia and osteoblast-like differentiation contribute to the progression of CAVD. The effects of S18 on osteogenic responses and hyperlipidaemia should be further examined. Future studies should explore the anti-CAVD mechanism of S18.

5. Conclusion

In conclusion, this study demonstrates that S18 attenuates HAVIC inflammatory responses in vitro and alleviates mouse aortic valve lesions in vivo. S18 promotes and interacts with IL-37 to inhibit mitochondrial stress and NF-κB activation which is responsible for the anti-CAVD effect of S18. Moreover, the piericidin diglycoside S18 directly combined with IL-37 protein, while monoglycosides exerted no IL-37-binding activity. Overall, our findings provide a novel potential treatment for preventing the progression of valvular calcification.

Abbreviations

AVICs:	Interstitial cells of aortic valve cells
CAVD:	Calcific aortic valve disease
CKD:	Chronic kidney disease
DAMPs:	Damage-associated molecular patterns
DCFH:	2,7-Dichlorodihydrofluorescein diacetate
ELISA:	Enzyme-linked immunosorbent assay
H&E:	Hematoxylin and eosin
HPLC:	High-performance liquid chromatography
HRMS:	High-resolution mass spectrometry
HAVICs:	Human interstitial cells of aortic valve cells
ICAM-1:	Intercellular cell adhesion molecule-1
IL-37:	Interleukin-37
BUN:	Blood urea
IL-37-Tg mice:	IL-37 transgenic mice
IL-8:	Interleukin-8
LC-MS/MS:	Liquid chromatography-tandem mass spectrometry
LPS:	Lipopolysaccharide
MCP-1:	Monocyte chemoattractant protein-1
MMP:	Mitochondrial membrane potential
MST:	Microscale thermophoresis
NAC:	N-acetyl-L-cysteine
NMR:	Nuclear magnetic resonance
oxLDL:	Oxidized low-density lipoprotein
qRT-PCR:	Quantitative real-time polymerase chain reaction
ROS:	Reactive oxygen species
siRNA:	Small interfering RNA
TLR4:	Toll-like receptor 4
TMRM:	Tetramethylrhodamine, ethyl ester.

Data Availability

The data used to support the findings of this study are included within the article.

Conflicts of Interest

The authors declare no competing financial interest.

Authors' Contributions

Shunyi Li and Jianglian She contributed equally to this work. Shunyi Li is responsible for the conceptualization, methodology, and writing—original draft; Jianglian She for methodology, data curation, and writing—original draft; Jingxin Zeng and Zichao Luo for visualization and writing—original draft; Kaiji Xie, Shuwen Su, Gaopeng Xian, and Zhengdong Chen for conceptualization and methodology; Shaoping Li and Jing Zhao for conceptualization; Xingbo Xu for validation and formal analysis; Dingli Xu, Lan Tang, and Xuefeng Zhou for resources and writing—review and editing; and Qingchun Zeng for writing—review and editing, project administration, and supervision. All authors reviewed and approved the manuscript.

Acknowledgments

Supplementary Materials

Supplementary materials and methods: additional figures illustrating structure elucidation and spectral data of S18, GPA, S40, S14, and PA, as well as their spectra (IR, MS, and NMR) (Figure S1-S6); the effect of GPA on expression of IL-37 protein (Figure S7); the structures of piericidin analogues subjected to the docking analysis, the docking results of some piericidin aglycones binding with IL-37 (6NCU) (Figures S8); renal function in mice (Figure S9); demographic characteristic of enrolled patients (Table S1); the primer information (Table S2). *(Supplementary Materials)*

References

[1] S. Yadgir, C. O. Johnson, V. Aboyans et al., "Global, regional, and national burden of calcific aortic valve and degenerative mitral valve diseases, 1990-2017," *Circulation*, vol. 141, no. 21, pp. 1670–1680, 2020.

[2] R. A. Spampinato, M. Tasca, M. A. Borger et al., "Advanced symptoms are associated with myocardial damage in patients with severe aortic stenosis," *Journal of Cardiology*, vol. 70, no. 1, pp. 41–47, 2017.

[3] K. Khan, B. Yu, C. Kiwan et al., "The role of Wnt/β-catenin pathway mediators in aortic valve stenosis," *Frontiers in cell and developmental biology*, vol. 8, p. 862, 2020.

[4] K. I. Cho, I. Sakuma, I. S. Sohn, S. H. Jo, and K. K. Koh, "Inflammatory and metabolic mechanisms underlying the calcific aortic valve disease," *Atherosclerosis*, vol. 277, pp. 60–65, 2018.

[5] N. Coté, A. Mahmut, Y. Bosse et al., "Inflammation is associated with the remodeling of calcific aortic valve disease," *Inflammation*, vol. 36, no. 3, pp. 573–581, 2013.

[6] K. D. O'Brien, "Pathogenesis of calcific aortic valve disease," *Arteriosclerosis, Thrombosis, and Vascular Biology*, vol. 26, no. 8, pp. 1721–1728, 2006.

[7] L. Osman, M. H. Yacoub, N. Latif, M. Amrani, and A. H. Chester, "Role of human valve interstitial cells in valve calcification and their response to atorvastatin," *Circulation*, vol. 114, 1 Suppl, pp. I547–I552, 2006.

[8] J. D. Miller, R. M. Weiss, D. D. Heistad, and D. A. Towler, "Calcific aortic valve stenosis: methods, models, and mechanisms," vol. 108, pp. 1392–1412, 2011.

[9] P. Mathieu, R. Bouchareb, and M.-C. Boulanger, "Innate and adaptive immunity in calcific aortic valve disease," *Journal of Immunology Research*, vol. 2015, Article ID 851945, 2015.

[10] X. Meng, L. Ao, Y. Song et al., "Expression of functional Toll-like receptors 2 and 4 in human aortic valve interstitial cells: potential roles in aortic valve inflammation and stenosis," *American Journal of Physiology. Cell Physiology*, vol. 294, no. 1, pp. C29–C35, 2008.

[11] C. García-Rodríguez, I. Parra-Izquierdo, I. Castaños-Mollor, J. López, J. A. San Román, and M. Sánchez Crespo, "Toll-like receptors, inflammation, and calcific aortic valve disease," *Frontiers in physiology*, vol. 9, pp. 201–209, 2018.

[12] H. Liu, L. Wang, Y. Pan et al., "Celastrol alleviates aortic valve calcification via inhibition of NADPH oxidase 2 in valvular interstitial cells," *JACC. Basic to translational science*, vol. 5, no. 1, pp. 35–49, 2020.

[13] E. Branchetti, R. Sainger, P. Poggio et al., "Antioxidant enzymes reduce DNA damage and early activation of valvular interstitial cells in aortic valve sclerosis," *Arteriosclerosis, Thrombosis, and Vascular Biology*, vol. 33, no. 2, pp. e66–e74, 2013.

[14] P. Bhargava and R. G. Schnellmann, "Mitochondrial energetics in the kidney," *Nature Reviews. Nephrology*, vol. 13, no. 10, pp. 629–646, 2017.

[15] J. Miao, J. Liu, J. Niu et al., "Wnt/β-catenin/RAS signaling mediates age-related renal fibrosis and is associated with mitochondrial dysfunction," *Aging Cell*, vol. 18, no. 5, pp. e13004–e13025, 2019.

[16] V. Valerio, V. A. Myasoedova, D. Moschetta et al., "Impact of oxidative stress and protein S-glutathionylation in aortic valve sclerosis patients with overt atherosclerosis," *Journal of Clinical Medicine*, vol. 8, no. 4, p. 552, 2019.

[17] J. Li, Q. Zeng, Z. Xiong et al., "Trimethylamine -N-oxide induces osteogenic responses in human aortic valve interstitial cells in vitro and aggravates aortic valve lesions in mice," *Cardiovascular Research*, vol. 118, no. 8, pp. 2018–2030, 2022.

[18] C. A. Dinarello, C. Nold-Petry, M. Nold et al., "Suppression of innate inflammation and immunity by interleukin-37," *European Journal of Immunology*, vol. 46, no. 5, pp. 1067–1081, 2016.

[19] M. F. Nold, C. A. Nold-Petry, J. A. Zepp, B. E. Palmer, P. Bufler, and C. A. Dinarello, "IL-37 is a fundamental inhibitor of innate immunity," *Nature Immunology*, vol. 11, no. 11, pp. 1014–1022, 2010.

[20] T. Zhao, F. Jin, D. Xiao et al., "IL-37/ STAT3/ HIF-1α negative feedback signaling drives gemcitabine resistance in pancreatic cancer," *Theranostics*, vol. 10, no. 9, pp. 4088–4100, 2020.

[21] H. Jia, J. Liu, and B. Han, "Reviews of interleukin-37: functions, receptors, and roles in diseases," *BioMed Research International*, vol. 2018, Article ID 3058640, 14 pages, 2018.

[22] Q. Zeng, R. Song, D. A. Fullerton et al., "Interleukin-37 suppresses the osteogenic responses of human aortic valve interstitial cells in vitro and alleviates valve lesions in mice," *Proceedings of the National Academy of Sciences of the United States of America*, vol. 114, no. 7, pp. 1631–1636, 2017.

[23] X. Zhou and W. Fenical, "The unique chemistry and biology of the piericidins," *The Journal of Antibiotics*, vol. 69, no. 8, pp. 582–593, 2016.

[24] S. M. Azad, Y. Jin, H. L. Ser et al., "Biological insights into the piericidin family of microbial metabolites," *Journal of Applied Microbiology*, vol. 132, no. 2, pp. 772–784, 2022.

[25] X. Zhou, Z. Liang, K. Li et al., "Exploring the natural piericidins as anti-renal cell carcinoma agents targeting peroxiredoxin 1," *Journal of Medicinal Chemistry*, vol. 62, no. 15, pp. 7058–7069, 2019.

[26] K. Li, Z. Liang, W. Chen et al., "Iakyricidins A-D, antiproliferative piericidin analogues bearing a carbonyl group or cyclic skeleton from Streptomyces iakyrus SCSIO NS104," *The Journal of Organic Chemistry*, vol. 84, no. 19, pp. 12626–12631, 2019.

[27] K. Li, Z. Su, Y. Gao et al., "Cytotoxic minor piericidin derivatives from the actinomycete strain Streptomyces psammoticus SCSIO NS126," *Marine Drugs*, vol. 19, no. 8, p. 428, 2021.

[28] R. A. Nishimura, C. M. Otto, R. O. Bonow et al., "2014 AHA/ACC guideline for the management of patients with valvular heart disease: a report of the American College of Cardiology/American Heart Association task force on practice guidelines," *Circulation*, vol. 129, no. 23, pp. e521–e643, 2014.

[29] Y. Wang, J. Gu, A. Du et al., "SPARC-related modular calcium binding 1 regulates aortic valve calcification by disrupting BMPR-II/p38 signalling," *Cardiovascular Research*, vol. 118, no. 3, pp. 913–928, 2022.

[30] A. Rutkovskiy, A. Malashicheva, G. Sullivan et al., "Valve interstitial cells: the key to understanding the pathophysiology of heart valve calcification," *Journal of the American Heart Association*, vol. 6, no. 9, 2017.

[31] Q. Zhou, L. L. Pan, R. Xue et al., "The anti-microbial peptide LL-37/CRAMP levels are associated with acute heart failure and can attenuate cardiac dysfunction in multiple preclinical models of heart failure," *Theranostics*, vol. 10, no. 14, pp. 6167–6181, 2020.

[32] E. E. Battin and J. L. Brumaghim, "Antioxidant activity of sulfur and selenium: a review of reactive oxygen species scavenging, glutathione peroxidase, and metal-binding antioxidant mechanisms," *Cell Biochemistry and Biophysics*, vol. 55, no. 1, pp. 1–23, 2009.

[33] Q. Zhan, Q. Zeng, R. Song et al., "IL-37 suppresses MyD88-mediated inflammatory responses in human aortic valve interstitial cells," *Molecular Medicine*, vol. 23, no. 1, pp. 83–91, 2017.

[34] E. Z. Eisenmesser, A. Gottschlich, J. S. Redzic et al., "Interleukin-37 monomer is the active form for reducing innate immunity," *Proceedings of the National Academy of Sciences of the United States of America*, vol. 116, no. 12, pp. 5514–5522, 2019.

[35] V. A. Myasoedova, A. L. Ravani, B. Frigerio et al., "Novel pharmacological targets for calcific aortic valve disease: prevention and treatments," *Pharmacological Research*, vol. 136, pp. 74–82, 2018.

[36] P. Mathieu and M. C. Boulanger, "Basic mechanisms of calcific aortic valve disease," *The Canadian Journal of Cardiology*, vol. 30, no. 9, pp. 982–993, 2014.

[37] A. S. Jaipersad, G. Y. Lip, S. Silverman, and E. Shantsila, "The role of monocytes in angiogenesis and atherosclerosis," *Journal of the American College of Cardiology*, vol. 63, no. 1, pp. 1–11, 2014.

[38] A. Schober, "Chemokines in vascular dysfunction and remodeling," *Arteriosclerosis, Thrombosis, and Vascular Biology*, vol. 28, no. 11, pp. 1950–1959, 2008.

[39] N. E. Hastings, R. E. Feaver, M. Y. Lee, B. R. Wamhoff, and B. R. Blackman, "Human IL-8 regulates smooth muscle cell VCAM-1 expression in response to endothelial cells exposed to atheroprone flow," *Arteriosclerosis, Thrombosis, and Vascular Biology*, vol. 29, no. 5, pp. 725–731, 2009.

[40] S. H. Lee and J. H. Choi, "Involvement of immune cell network in aortic valve stenosis: communication between valvular interstitial cells and immune cells," *Immune network*, vol. 16, no. 1, pp. 26–32, 2016.

[41] R. Song, Q. Zeng, L. Ao et al., "Biglycan induces the expression of osteogenic factors in human aortic valve interstitial cells via Toll-like receptor-2," *Arteriosclerosis, Thrombosis, and Vascular Biology*, vol. 32, no. 11, pp. 2711–2720, 2012.

[42] X. Yang, D. A. Fullerton, X. Su, L. Ao, J. C. Cleveland Jr., and X. Meng, "Pro-osteogenic phenotype of human aortic valve interstitial cells is associated with higher levels of Toll-like receptors 2 and 4 and enhanced expression of bone morphogenetic protein 2," *Journal of the American College of Cardiology*, vol. 53, no. 6, pp. 491–500, 2009.

[43] J. M. Suárez-Rivero, C. J. Pastor-Maldonado, S. Povea-Cabello et al., "From mitochondria to atherosclerosis: the inflammation path," *Biomedicine*, vol. 9, no. 3, 2021.

[44] E. L. Mills, B. Kelly, and L. A. J. O'Neill, "Mitochondria are the powerhouses of immunity," *Nature Immunology*, vol. 18, no. 5, pp. 488–498, 2017.

[45] D. Salnikova, V. Orekhova, A. Grechko et al., "Mitochondrial dysfunction in vascular wall cells and its role in atherosclerosis," *International Journal of Molecular Sciences*, vol. 22, no. 16, pp. 8990–9008, 2021.

[46] Z. Li, Q. Li, L. Wang et al., "Targeting mitochondria-inflammation circle by renal denervation reduces atheroprone endothelial phenotypes and atherosclerosis," *Redox Biology*, vol. 47, article 102156, 2021.

[47] T. Xie, C. Wang, Y. Jin et al., "CoenzymeQ10-induced activation of AMPK-YAP-OPA1 pathway alleviates atherosclerosis by improving mitochondrial function, inhibiting oxidative stress and promoting energy metabolism," *Frontiers in pharmacology*, vol. 11, pp. 1034–1049, 2020.

[48] X. Zhang, H. Liu, Y. Hao et al., "Coenzyme Q10 protects against hyperlipidemia-induced cardiac damage in apolipoprotein E-deficient mice," *Lipids in Health and Disease*, vol. 17, no. 1, pp. 279–288, 2018.

[49] M. Rodriguez, J. M. Martinez-Moreno, M. E. Rodríguez-Ortiz, J. R. Muñoz-Castañeda, and Y. Almaden, "Vitamin D and vascular calcification in chronic kidney disease," *Kidney & Blood Pressure Research*, vol. 34, no. 4, pp. 261–268, 2011.

[50] F. Tarrass, M. Benjelloun, M. Zamd et al., "Heart valve calcifications in patients with end-stage renal disease: analysis for risk factors," *Nephrology*, vol. 11, no. 6, pp. 494–496, 2006.

[51] W. C. Wei, P. J. Sung, C. Y. Duh, B. W. Chen, J. H. Sheu, and N. S. Yang, "Anti-inflammatory activities of natural products

Retraction

Retracted: The RPL4P4 Pseudogene Is a Prognostic Biomarker and Is Associated with Immune Infiltration in Glioma

Oxidative Medicine and Cellular Longevity

This article has been retracted by Hindawi following an investigation undertaken by the publisher [1]. This investigation has uncovered evidence of one or more of the following indicators of systematic manipulation of the publication process:

(1) Discrepancies in scope

(2) Discrepancies in the description of the research reported

(3) Discrepancies between the availability of data and the research described

(4) Inappropriate citations

(5) Incoherent, meaningless and/or irrelevant content included in the article

(6) Peer-review manipulation

The presence of these indicators undermines our confidence in the integrity of the article's content and we cannot, therefore, vouch for its reliability. Please note that this notice is intended solely to alert readers that the content of this article is unreliable. We have not investigated whether authors were aware of or involved in the systematic manipulation of the publication process.

Wiley and Hindawi regrets that the usual quality checks did not identify these issues before publication and have since put additional measures in place to safeguard research integrity.

We wish to credit our own Research Integrity and Research Publishing teams and anonymous and named external researchers and research integrity experts for contributing to this investigation.

The corresponding author, as the representative of all authors, has been given the opportunity to register their agreement or disagreement to this retraction. We have kept a record of any response received.

References

[1] Z. Wang, Y. Aili, Y. Wang et al., "The RPL4P4 Pseudogene Is a Prognostic Biomarker and Is Associated with Immune Infiltration in Glioma," *Oxidative Medicine and Cellular Longevity*, vol. 2022, Article ID 7967722, 28 pages, 2022.

Research Article

The RPL4P4 Pseudogene Is a Prognostic Biomarker and Is Associated with Immune Infiltration in Glioma

Zengliang Wang [iD],[1,2] **Yirizhati Aili** [iD],[2] **Yongxin Wang** [iD],[2]
Nuersimanguli Maimaitiming [iD],[3] **Hu Qin** [iD],[2] **Wenyu Ji** [iD],[2] **Guofeng Fan** [iD],[2] and **Bo Li** [iD][4]

[1]*Department of Neurosurgery, Xinjiang Bazhou People's Hospital, Xinjiang, China*
[2]*Department of Neurosurgery, First Affiliated Hospital of Xinjiang Medical University, Urumqi, Xinjiang, China*
[3]*Department of Oncology, First Affiliated Hospital of Xinjiang Medical University, Urumqi, Xinjiang, China*
[4]*Department of Neurosurgery, Affiliated Hospital of Jining Medical University, Jining, Shandong, China*

Correspondence should be addressed to Bo Li; libo5479937@126.com

Objective. Research over the past decade has suggested important roles for pseudogenes in gliomas. Our previous study found that the RPL4P4 pseudogene is highly expressed in gliomas. However, its biological function in gliomas remains unclear. *Methods*. In this study, we analyzed clinical data on patients with glioma obtained from The Cancer Genome Atlas (TCGA), the Chinese Glioma Genome Atlas (CGGA), the Genotype-Tissue Expression (GTEx), and the GEPIA2 databases. We used the R language for the main analysis. Correlations among RPL4P4 expression, pathological characteristics, clinical outcome, and biological function were evaluated. In addition, the correlations of RPL4P4 expression with immune cell infiltration and glioma progression were analyzed. Finally, wound healing, Transwell, and CCK-8 assays were performed to analyze the function of RPL4P4 in glioma cells. *Result*. We found that RPL4P4 is highly expressed in glioma tissues and is associated with poor prognosis, IDH1 wild type, codeletion of 1p19q, and age. Multivariate analysis and the nomogram model showed that high RPL4P4 expression was an independent risk factor for glioma prognosis and had better prognostic prediction power. Moreover, high RPL4P4 expression correlated with immune cell infiltration, which showed a significant positive association with M2-type macrophages. Finally, RPL4P4 knockdown in glioma cell lines caused decreased glioma cell proliferation, invasion, and migration capacity. *Conclusion*. Our data suggest that RPL4P4 can function as an independent prognostic predictor of glioma. It also shows that RPL4P4 expression correlates with immune cell infiltration and that targeting RPL4P4 may be a new strategy for the treatment of glioma patients.

1. Introduction

Gliomas are common primary brain tumors characterized by treatment resistance, high recurrence, and high mortality rates. Gliomas have been classified into four grades, with grades III and IV usually leading to poor clinical outcomes [1]. Lower-grade gliomas (LGGs) can progress to higher-grade gliomas (GBM, for glioblastoma multiforme), which are resistant to chemotherapy. Despite various treatment modalities, including surgical intervention, postoperative adjuvant chemoradiotherapy, and immunotherapy, patients with gliomas exhibit poor prognoses [2]. In recent years,

with the development of molecular pathology, some molecular markers in glioma have played an important role in the diagnosis and prognosis of the disease. These molecular markers include isocitrate dehydrogenase (IDH), epidermal growth factor receptor (EGFR), O-6-methylguanine-DNA methyltransferase (MGMT), and tumor protein p53 (TP53) [3]. In 2021, the WHO CNS5 placed even more emphasis on the importance of molecular markers in glioma [4]. Therefore, the new molecular classification of glioma may play a key role in its prognosis.

Pseudogenes are a class of homologous genes similar to functional genes and are unable to express truly functional

proteins due to mutations in their coding sequence (such as insertion, deletion, and code shift mutations) and to the premature appearance of stop codons [5]. For a long time since its discovery, pseudogenes have been thought to be nonfunctional, "junk genes" and "fossil genes", but some recent studies have found that some pseudogenes have certain functions, can be transcribed, and can also be regulated in other ways to encode DNA function [6]. Pseudogenes may be associated with a variety of cancers and may function as oncogenes or tumor suppressor genes involved in the development of certain cancers [7]. Pseudogenes have a variety of functions, serving as bait for mRNA and proteins and acting as competitive endogenous RNAs for microRNA sponges. There are endogenous interfering RNAs with pseudogene production, and interference mechanisms for RNA can be formed in subsequent development [8]. The pseudogene itself and the endogenous small interfering RNAs it produces can have a regulatory effect on their parent genes after transcription [9]. The significance of pseudogenes in gliomas has rarely been studied, and there are no systematic studies on prognosis-related pseudogenes and on the role of pseudogenes in the malignant evolution of gliomas.

Mutations in ribosome proteins, ribosomal RNA (rRNA) processing, and ribosome assembly factors can lead to ribosome disease, which is associated with an increased risk of developing malignancy [10]. Recent studies link ribosome protein mutations and abnormal ribosomes to poor prognosis, highlighting that ribosome protein targeted therapy is a promising treatment for cancer patients [11]. Ribosomal protein genes have the largest number of processed pseudogenes, approximately 1700; these genes include cyclophilin A, actin, keratin (keratin), GAPDH, cytochrome C (cytochrome C), and nucleophosmin [12]. There are many copies of the processed pseudogenes. Hirotsune et al. [13] found that pathological changes occur when the function of the ribosomal protein pseudogene in mice is blocked. Therefore, it has been theoretically asserted that the functional abnormalities of pseudogenes may be related to the occurrence of multiple diseases. Ribosomal protein L4 pseudogene 4 (RPL4P4) belongs to the ribosomal protein pseudogene that plays a regulatory role in protein folding and protein posttranslational modification [14]. Studies have shown that RPL4P4 is closely related to the maintenance of normal human function, and its loss of expression is associated with tumors, endocrine dysfunction, and immune diseases [15]. In our previous studies, we found that the differential expression of RPL4P4 is associated with the occurrence and development of multiple tumors (DLBC, GBM, LGG, TGCT, and THYM). Among them, there is a clear correlation with glioma, and the pattern of RPL4P4 expression, its prognostic value, and its correlation with the tumor microenvironment in glioma remain unclear.

To further understand the potential role of RPL4P4 in glioma, this study investigated the diagnostic and prognostic significance of RPL4P4 in glioma by data mining datasets from TCGA, GTEx, and CGGA. Subsequently, GO, KEGG, and GSEA analyses were used to determine the possible biological functions and mechanisms of RPL4P4 in glioma. In addition, the relationship between RPL4P4 expression and the infiltration of immune cells in glioma was assessed in the Tumor Immune Estimation Resource (TIMER) database. Finally, we investigated the effects of RPL4P4 on the biological behavior of glioma cell lines in a variety of ways. These findings indicate that RPL4P4 can regulate the infiltration of immune cells into gliomas and that the level of RPL4P4 expression may be a prognostic biomarker in patients with these tumors.

2. Materials and Methods

2.1. Microarray Data Information. The data used in our study were obtained from the public databases The Cancer Genome Atlas (TCGA, https://tcga-data.nci.nih.gov/tcga/), Genotype-Tissue Expression (GTEx, https://www.gtexportal.org), and Chinese Glioma Genome Atlas (CGGA, http://www.cgga.org.cn.). TCGA and GTEx data were used as the experimental groups, and CGGA data were used as the validation set. The expression data of TCGA glioma, including TCGA lower-grade tissues (LGG) and TCGA high-grade glioma tissues (GBM), were downloaded from the TCGA database. The dataset consisted of the clinical data of 698 glioma patients and 5 normal individuals, and patients with incomplete clinical data were excluded from subsequent analyses. In addition, the validation set (CGGA data), gene expression data, and corresponding clinical data of the glioma patients were downloaded from CGGA (LGG+GBM). Two datasets containing the clinical data of 693 and 325 patients (mRNA-seq-693 and mRNAseq-325), respectively, were downloaded. The two sets of gene expression data were corrected in batches and integrated by loading them into the Limma and SVA packages in R software (v 4.1.2). The prognostic value of RPL4P4 expression in various cancers was analyzed using the GEPIA2 [16] database.

2.2. Difference and Survival Analyses. Transcription data from TCGA and GTEx datasets were integrated, and RPL4P4 transcription data were selected. Then, the expression levels were compared between the tumor and normal groups. After integrating RPL4P4 expression with clinical data, we divided the data into high and low expression groups based on the medium level. Next, we performed survival analyses among the TCGA, GTEx, and CGGA datasets.

2.3. Clinical Analyses. Since clinical data in the TGGA database were the most comprehensive and the data volume was sufficient, conclusions drawn from it have the highest reliability. The main clinical characteristics were as follows: age, sex, chemoradiotherapy status, WHO grade, histological type, critical molecular pathology information, and survival data. Univariate and multivariate analyses were performed to explore clinical factors associated with prognosis. Subsequently, associations between RPL4P4 expression levels and various clinical subgroups were observed. On this basis, the nomogram prediction model was established, visually analyzed, and evaluated by the C-index and calibration curve. The R packages "rms," "beeswarm," and "survivalROC" were used during this process.

2.4. GO Annotation and KEGG Pathway Enrichment Analysis. Gene set enrichment analysis (GSEA) is a useful tool to interpret gene expression profiles and obtain insights into biological mechanisms; it evaluates microarray data at the level of gene sets. In our study, each sample was divided into high, medium, and low expression groups based on RPL4P4 expression levels. Through Bayesian correction, we explored major enrichment pathways for various differentially expressed genes among the high- and low-expression groups and included Kyoto Encyclopedia of Genes and Genomes (KEGG) and Gene Ontology (GO) term enrichment analyses. This reminded us to give more attention to potential pathways.

2.5. Immune Cell Infiltration Analysis. The associations between RPL4P4 expression and glioma infiltration by B cells, CD4+ T cells, CD8+ T cells, macrophages, neutrophils, and dendritic cells were examined using the TIMER database (http://timer.cistrome.org) [17], with analyses performed using the R package GSVA.

2.6. Cell Line and Cell Culture. All cell lines, including U-251 and A-172, were purchased from the Cell Bank of the Chinese Academy of Sciences (China). All cell lines were cultured in DMEM with 10% newborn bovine serum supplemented with 100 U/mL penicillin and 100 μg/mL streptomycin in a 5% CO_2 incubator with saturated humidity and 37°C constant temperature.

2.7. Construction and Transfection of Lentivirus. The cells were cultured. When the cell growth density reached more than 85%, the original medium was aspirated and 5 mL of fresh serum-free 1640 medium was added. The culture was continued for 6 h to make the cells hungry and then prepared for cell transfection. For transfection, 40 μL of lentiviral infection preparation A solution and 40 μL of P solution (HitransG A infection enhancer 25× and HitransG P infection enhancement solution 25×) (gene sequence 1 5′-GCCCAATGATATCGGTGTACT-3′, gene sequence 1 2′ GCAGAGCTATGGCTCGAATTC-3′, and gene sequence 1 3′GGGCCTGTGCATCATCTATAA-3′) were each added to 1.5 mL enzymatic EP tubes, followed by 5 μL of viral stock solution to mix it. The solution was then inoculated in a T25-well plate at a viral MOI value of 5 (the recommended concentration in the instruction manual) and gently inverted and mixed several times. The two tubes of reagents described above were mixed and gently inverted several times. The prepared transfection reagent was slowly and evenly dripped into the Petri dish, and then, the mixture was gently shaken, placed in a constant temperature cell culture incubator at 37°C and 5% CO_2, and cultured for 24 h after the fluorescence microscope began to detect the cell fluorescence strength and cell growth state. When the abundance of fluorescent cells was approximately 80%, the medium was replaced with complete medium added to puromycin to continue to culture and screen successfully transfected cells. Puromycin (biosharp purine mycin solution 10 mg/mL) was dissolved in complete medium to screen for 2-3 days at a concentration of 2 μg/mL, after which cells were cultured

with normal culture medium and passaged according to the number of cells grown. According to the Declaration of Helsinki, the samples and case data used in this study were approved by the Ethics Committee of the First Affiliated Hospital of Xinjiang Medical University.

2.8. Puromycin Kill Curve. Cells were spread in 6-well plates with approximately 80% confluence, added to the appropriate viral solution and polybrene (final concentration of 5-10 g/mL), and incubated in an incubator overnight. The medium containing the screening drug blasticidin/puromycin was replaced to screen for stable transformants. The medium was changed every 3 to 4 days until resistant clones appeared. At least five resistant clones were picked, the culture was expanded, and the target gene and protein expression were identified. Control was set as an empty vector.

2.9. Transwell Assay. Transwell cells were placed in a 24-well plate, substrate glue was added to the Transwell cells, and complete culture medium was added to the substrate. After digestion and resuspension, the cells of each group were inoculated in the upper chamber of the Transwell, and the number of cells was 3×10^4. After 48 h of culture, the cells that did not invade the subchamber were washed away. Then, the cells were fixed with 4% polymethanol and stained with 0.1% crystal violet for 20 min. The number of cells invading the subcompartment in each field was counted under an inverted microscope.

2.10. Wound Healing Assay. The cells in each group were digested by trypsin and inoculated into 6-well plates with 1 $\times 10^6$ cells in each well. Then, the cells were cultured at 37°C, 5% CO_2, and 100% relative humidity until the cells reached approximately 90% confluence. Then, cells were scratched from top to bottom with a 200 μL pipette tip, and the scratched cells were washed away with PBS buffer. Then, the culture was continued for 24 h under the same conditions. The single-layer images were observed using an inverted microscope, and the migration ability of cells was analyzed by measuring the distance moved by the cell front and the width of the scratch.

2.11. CCK-8 Kit for Cell Value-Added Experiments. After the cell density reached approximately 90%, the cell culture was washed with PBS twice, underwent pancreatic enzyme digestion, and was then resuspended into a 15 mL centrifuge tube. According to the kit instructions, the experimental protocol was performed as follows: the cell suspension was inoculated in a 96-well plate (cell count is 5000-10,000/100 μL) and then incubated at 37°C and 5% CO_2 for 2-4 hours. Cell adherence was examined at the following times: 0 h, 6 h, 12 h, 24 h, and 36 h. Subsequently, 10 μL of CCK-8 (Bioss enhanced cell counting kit-8 size: 500 T) was added to the wells for 48 h to avoid bubble production, which were then placed in the incubator for 2 h. The absorbance at 450 nm was determined with a microplate reader.

2.12. Statistical Analyses. Statistical analyses of the datasets from the TCGA database were performed using R (v 4.1.1) software. The associations between RPL4P4 and pathologic

characteristics were evaluated by the Wilcoxon rank sum tests for continuous variables and chi-square tests for categorical variables. Overall survival (OS), disease-free survival (DFS), and progression-free interval (PFS) were calculated using the Kaplan-Meier method and compared by log-rank tests. The univariate and multivariate Cox regression analyses were performed to assess the correlation between clinical features and survival (OS and DFS). For data regarding the function of RPL4P4, statistical analyses were performed using GraphPad Prism 7.0 software. Differences between two groups were assessed using Student's t tests, and differences among multiple groups were evaluated by one-way ANOVA. P values < 0.05 were considered statistically significant.

3. Results

3.1. Expression and Prognostic Potential of RPL4P4 in Pancancer Analysis.
First, we used VASH1 expression levels in cancer and normal tissue samples from the TCGGA database. Given the limited number of normal samples in the TCGGA database, we integrated the RPL4P4 expression of cancer tissue and normal tissue samples from the GTEx and TCGGA databases and found that there was a significant difference in the expression of RPL4P4 in multiple cancers compared to the normal GTEx control group (Figure 1(a)). Furthermore, through GEPIA analysis, RPL4P4 and DLBC, GBM, LGG, TGCT, and THYM were associated (Figure 1(b)), all of which suggest that they play an important role in the development of glioma. We performed a univariate analysis using the TCGA dataset. The forest plot showed that in 33 cancers, RPL4P4 had a significant effect on the survival time according to specific tumor types, and RPL4P4 had a clear correlation with prognosis in patients with gliomas (P < 0.001) (Supplemental Figure 1). For further exploration, we analyzed the differential expression of RPL4P4 in glioma and normal tissues using TCGA and then used the GEPIA online analysis website for the verification of the results. The results showed that RPL4P4 was highly expressed in glioma tissues (Figure 1(c)). Based on median RPL4P4 expression in samples from the databases used, patients were grouped according to their high or low levels of RPL4P4 expression. We found that high RPL4P4 expression was correlated with poorer OS (P < 0.001) (Figure 1(d)). We evaluated the model by the tROC curve and found that it had good specificity and sensitivity (AUC = 0.692) (Figure 1(e)).

3.2. RPL4P4 Expression Is Significantly Correlated with the Degree of Malignancy and Glioma Subtype.
We further analyzed and visualized heatmaps of RPL4P4 and glioma clinical features in the TCGA database and found that RPL4P4 was correlated with the clinical features of glioma. Through a correlation analysis with clinical data (Table 1), we found that high RPL4P4 expression was significantly correlated with that of other WHO subtypes, IDH1 mutation status, histological types, and age (Figure 1(f)) and that RPL4P4 was significantly higher in WHO IV expression. To further confirm that we used the CGGA database, high RPL4P4 expression correlated with WHO subtypes, IDH1 mutation status, codeletion of chromosomes 1p and 19, and age

(Figure 1(g)). We found that there were significant differences between the WHO grade subgroups, which were positively correlated with the malignancy of glioma (Supplemental Table 1).

3.3. Univariate and Multivariate Analysis Showed the Prognostic Significance of RPL4P4 and Its Association with Related Clinicopathological Factors in Glioma.
Based on the median RPL4P4 expression in the samples in the database, patients were divided into groups with high and low levels of RPL4P4 expression. High RPL4P4 expression was found to correlate with poor OS (Figure 2(a)), DFS (Figure 2(b)), and PFS (Figure 2(c)), and a visual forest plot was plotted (Figures 2(d)–2(f)) (Supplemental Tables 2, 3). Univariate results showed that high RPL4P4 expression in gliomas was significantly associated with a poor prognosis (Table 2). Combined with the results of multivariate analyses, high WHO grade, PD, IDH1 wild type, high RPL4P4 expression, age, and histological type are risk factors for glioma prognosis. The above results further confirm that increased RPL4P4 expression is associated with the development of malignant glioma. The ability of a nomogram that included RPL4P4 expression, age, IDH mutation status, primary therapy outcome, 1p19q codeletion, and WHO grade to accurately predict prognosis in glioma patients was tested. This nomogram was found to predict 1-, 3-, and 5-year OS in patients with glioma (Figure 2(g)), demonstrated the accuracy of the model with a calibration curve, and found that the 1-, 3-, and 5-year models had good predictive performance (Figure 2(h)). In summary, RPL4P4 is an independent risk factor for glioma prognosis, helps to predict patient prognosis and is a potential biomarker for glioma.

3.4. The Prognostic Value of RPL4P4 in Different Glioma Subgroups.
Assessment of the prognostic value of RPL4P4 expression in glioma patients subgrouped by WHO grade, 1p/19q codeletion, IDH mutation status, recurrence, and age showed that high expression of RPL4P4 was associated with poor prognosis in all of these groups (Figures 3(a)–3(h)). These results suggested that gliomas with high RPL4P4 expression were associated with poor outcomes in response to treatment.

3.5. Genes Coexpressed with RPL4P4 and Enrichment Analysis in Patients with Glioma.
To further elucidate the importance of RPL4P4 in glioma, we explored the coexpression patterns of RPL4P4 using the LinkFinder module in LinkedOmics. We obtained 316 associated genes and extracted the 10 most relevant genes using the chord diagram (Figure 4(a)). A heatmap was constructed showing the 50 most significant genes positively associated with RPL4P4 expression in glioma (Figure 4(b)). Subsequently, we performed a gene function enrichment analysis, showing the enrichment results using GO and KEGG tools with bubble plots. Annotations to the GO term suggest that many genes expressed with RPL4P4 are involved in biological processes such as negative regulation of gene expression, negative regulation at the chromatin level, nucleosome formation, participation in transcriptional regulation, and

(a)

(b)

Figure 1: Continued.

(c)

(d)

(e)

(f)

Figure 1: Continued.

(g)
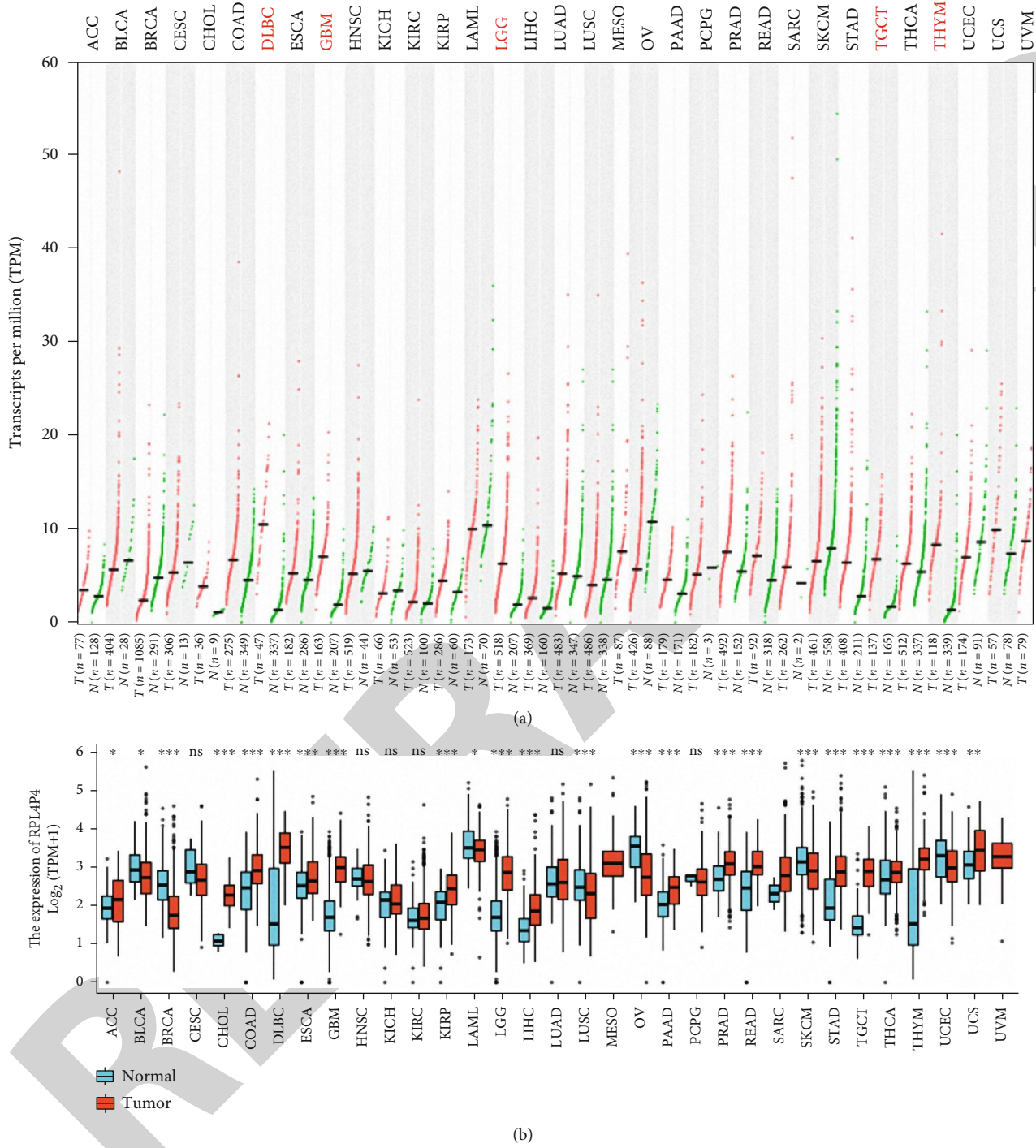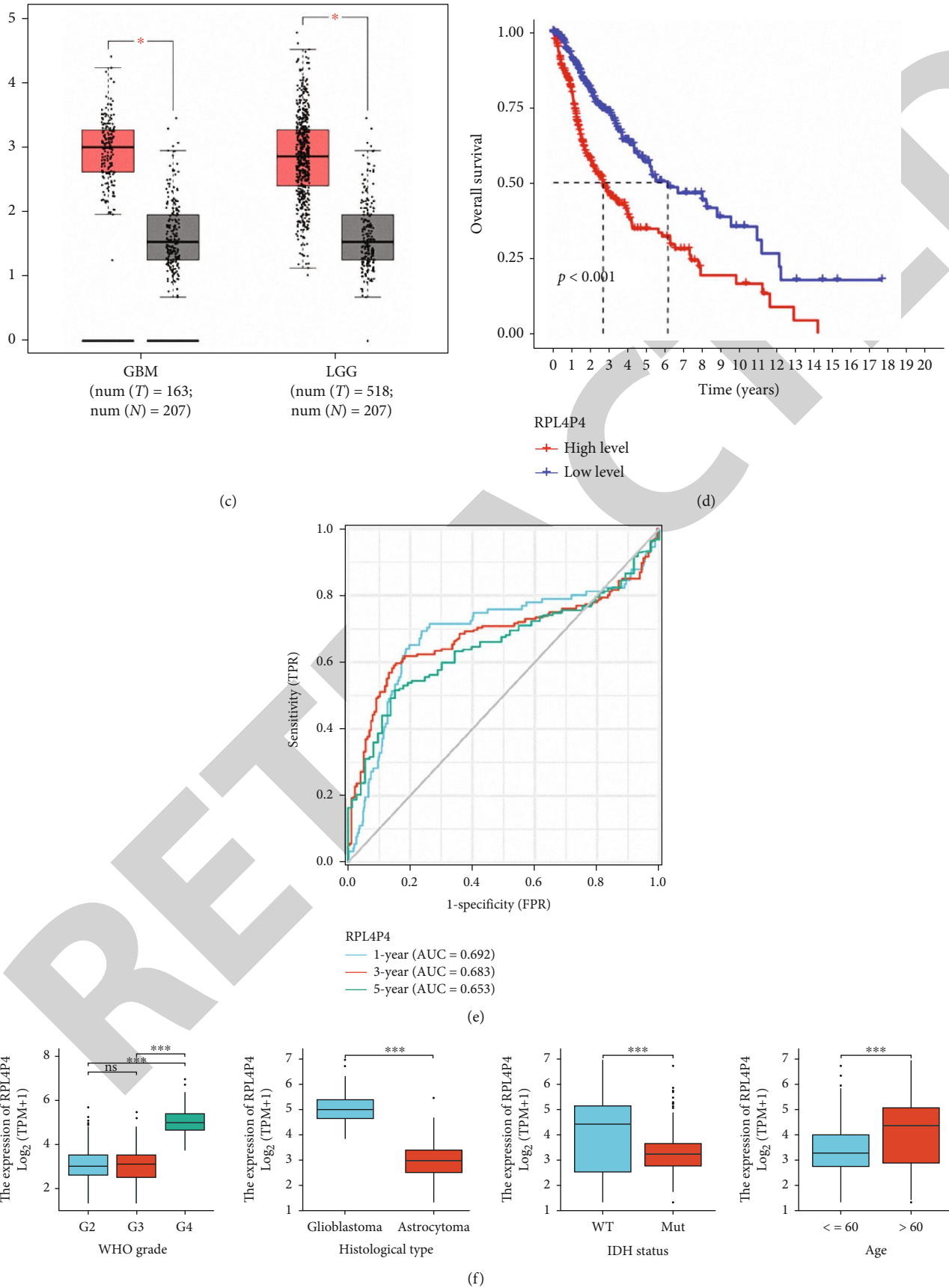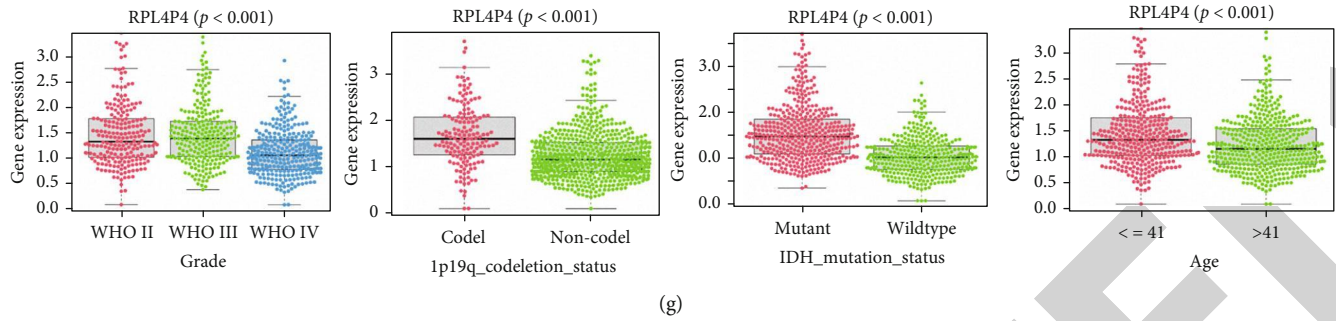
Figure 1: RPL4P4 expression and prognostic value in glioma. (a) The transcription level of RPL4P4 was determined in different tumor tissues and normal tissues by GEPIA2. (b) The mRNA expression levels of RPL4P4 in different tumor tissues and normal tissues analyzed by TCGA and GTEx. (c) RPL4P4 expression is significantly upregulated in glioma. (d) Kaplan-Meier survival analysis of all gliomas. (e) tROC analysis showing the predictive value of RPL4P4based TCGA glioma. (f) The correlation between RPL4P4 expression and different clinical features based on TCGA glioma. (g) The correlation between RPL4P4 expression and different clinical features based on CGGA. $*P < .05$, $**P < .01$, and $***P < .001$.

Table 1: The correlation between RPL4P4 and clinicopathological characteristic in TCGA-glioma dataset.

Characteristic	Low expression of RPL4P4	High expression of RPL4P4	P
n	348	348	
WHO grade, n (%)			<0.001
G2	144 (22.7%)	80 (12.6%)	
G3	166 (26.1%)	77 (12.1%)	
G4	0 (0%)	168 (26.5%)	
IDH status, n (%)			<0.001
WT	92 (13.4%)	154 (22.4%)	
Mut	255 (37.2%)	185 (27%)	
1p/19q codeletion, n (%)			0.842
Codel	88 (12.8%)	83 (12%)	
Noncodel	260 (37.7%)	258 (37.4%)	
Primary therapy outcome, n (%)			0.142
PD	77 (16.7%)	35 (7.6%)	
SD	95 (20.6%)	52 (11.3%)	
PR	44 (9.5%)	20 (4.3%)	
CR	78 (16.9%)	61 (13.2%)	
Histological type, n (%)			<0.001
Astrocytoma	139 (20%)	56 (8%)	
Glioblastoma	0 (0%)	168 (24.1%)	
Oligoastrocytoma	83 (11.9%)	51 (7.3%)	
Oligodendroglioma	126 (18.1%)	73 (10.5%)	
Age, n (%)			<0.001
≤60	300 (43.1%)	253 (36.4%)	
>60	48 (6.9%)	95 (13.6%)	

humoral immune response. Molecular functional annotations of these GO terms indicate that genes coexpressed with RPL4P4 are primarily involved in negative regulatory processes, i.e., manifested as inhibition of translational and transcriptional levels, ribosomal protein activity, and immune response correlation (Figures 4(c)–4(e)). KEGG pathway enrichment suggests that genes coexpressed with RPL4P4 participate in neuroactive ligand-receptor interactions,

alcoholism, neutrophil extracellular trap formation, nicotine addiction, morphine addiction, GABAergic synapses, EMC-receptor interactions, retrograde endocannabinoid signaling, and calcium signaling pathways (Figures 4(f) and 4(g)).

3.6. Function and Somatic Mutation of RPL4P4. GSEA tools were utilized to identify the signaling pathways involving RPL4P4 in glioma. High RPL4P4 expression was found to
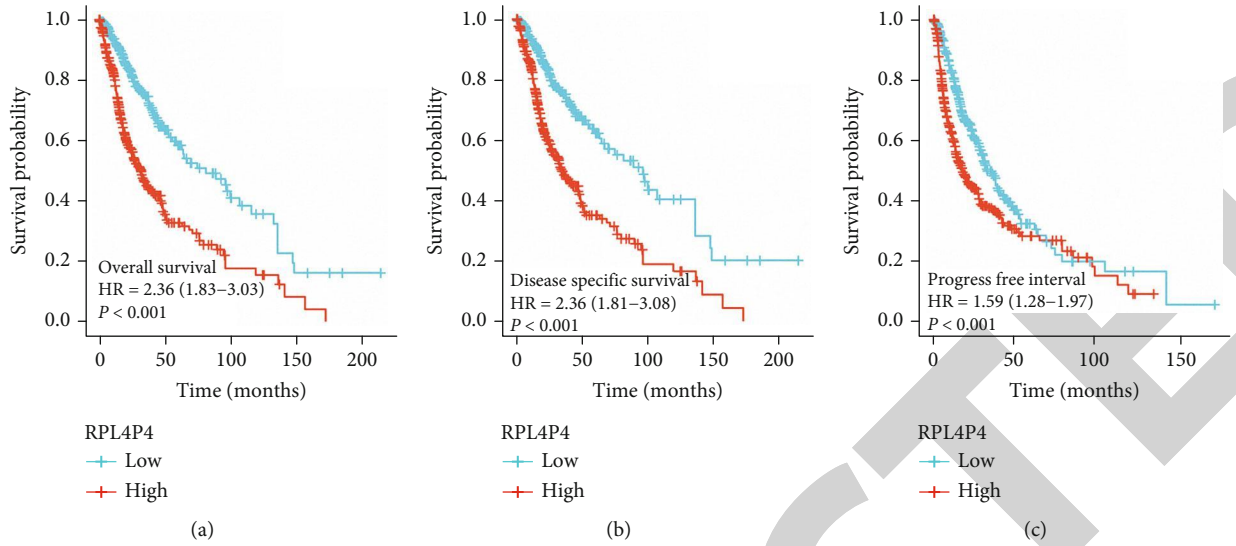
(a)

(b)

(c)

Characteristics	Total (N)	HR (95% CI) Univariate analysis		P value univariate analysis
WHO grade	634			
G2	223			
G3	243			
G4	168	18.615 (12.460–27.812)		<0.001
1p/19q codeletion	688			
Codel	170			
Non-codel	518	4.428 (2.885–6.799)		<0.001
Primary therapy outcome	259			
SD	147			
PD	112	2.288 (1.529–3.426)		<0.001
IDH status	685			
Mut	439			
WT	246	8.551 (6.558–11.150)		<0.001
MGMT	695			
Low	347			
High	348	1.783 (1.398–2.275)		<0.001
Age	695			
>60	143			
< = 60	552	0.214 (0.165–0.278)		<0.001
Histological type	695			
Astrocytoma	195			
Oligoastrocytoma	134			
Oligodendroglioma	198			
Glioblastoma	168	6.791 (4.932–9.352)		<0.001
Gender	695			
Female	297			
Male	398	1.262 (0.988–1.610)		0.062
RPL4P4	695			
Low	348			
High	347	2.357 (1.833–3.030)		<0.001

0 5 10 15 20

(d)

Figure 2: Continued.

Characteristics	Total (N)	HR (95% CI) Univariate analysis		P value univariate analysis
WHO grade	614			
G2	220			
G3	239			
G4	155	19.243 (12.572–29.455)		<0.001
1p/19q codeletion	668			
Codel	169			
Non-codel	499	4.987 (3.117–7.978)		<0.001
Primary therapy outcome	255			
SD	144			
PD	111	2.705 (1.757–4.165)		<0.001
IDH status	664			
Mut	432			
WT	232	9.055 (6.833–12.000)		<0.001
MGMT	674			
Low	337			
High	337	1.848 (1.427–2.394)		<0.001
Age	674			
>60	133			
< = 60	541	0.222 (0.168–0.293)		<0.001
Histological type	674			
Astrocytoma	192			
Oligoastrocytoma	132			
Oligodendroglioma	195			
Glioblastoma	155	6.602 (4.739–9.197)		<0.001
Gender	674			
Female	289			
Male	385	1.248 (0.965–1.614)		0.092
RPL4P4	674			
Low	340			
High	334	2.360 (1.809–3.080)		<0.001

0   5   10   15   20

(e)

Characteristics	Total (N)	HR (95% CI) Univariate analysis		P value univariate analysis
WHO grade	634			
G2	223			
G3	243			
G4	168	7.865 (5.808–10.649)		<0.001
1p/19q codeletion	688			
Codel	170			
Non-codel	518	3.373 (2.438–4.666)		<0.001
Primary therapy outcome	259			
SD	147			
PD	112	3.826 (2.700–5.421)		<0.001
IDH status	685			
Mut	439			
WT	246	6.627 (5.231–8.396)		<0.001
MGMT	695			
Low	347			
High	348	1.665 (1.344–2.062)		<0.001
Age	695			
>60	143			
< = 60	552	0.348 (0.275–0.441)		<0.001
Histological type	695			
Astrocytoma	195			
Oligoastrocytoma	134			
Oligodendroglioma	198			
Glioblastoma	168	4.416 (3.353–5.816)		<0.001
Gender	695			
Female	297			
Male	398	1.083 (0.875–1.342)		0.463
RPL4P4	695			
Low	348			
High	347	1.588 (1.282–1.967)		<0.001

0.0   2.5   5.0   7.5

(f)

Figure 2: Continued.

(g)

(h)

Figure 2: The prognostic value of RPL4P4 in glioma. (a–c) The prognosis of RPL4P4 in glioma examined by TCGA databases. (d–f) The forest plot indicates the prognosis in the presence of (d) OS, (e) DFS, and (f) PFS. (g) Construction of a nomogram to predict OS. (h) The calibration curve used to display the TCGA glioma cohort for OS.

be involved in neurotransmitter secretion, neurotransmitter transport, potassium ion transport, regulation of neurotransmitter levels, regulation of synaptic plasticity, calcium signaling pathways, long-term potentiation, neuroactive ligand receptor interactions, phosphatidylinositol signaling pathways, and ribosomes (Figures 5(a) and 5(b)).

In addition, we obtained the driver gene for gliomas and evaluated somatic mutations in patients with RPL4P4 at different levels of expression. Figure 5(c) shows the mutation distribution of the 15 driver genes with the highest frequency of change in the high and low RPL4P4 groups, of

which the high expression of RPL4P4 and the low expression of VASH1 have a strong correlation with IDH1, and further correlation analysis shows that RPL4P4 is positively correlated with the status of IDH1 ($r = 0.407$, $P < 0.001$) (Figure 5(d)). These results suggest that RPL4P4 combined with IDH1 may have some significance for glioma risk stratification and for guiding treatment.

3.7. Correlation of RPL4P4 Expression with Immune Cell Infiltration and Immune Checkpoints in Glioma Patients. To display the distribution of immune infiltration in glioma,

Table 2: Univariate regression and multivariate survival model of OS in patients with glioma.

Characteristics	Total (N)	Univariate analysis Hazard ratio (95% CI)	P value	Multivariate analysis Hazard ratio (95% CI)	P value
WHO grade	634				
G2	223				
G3	243	2.999 (2.007-4.480)	<0.001	1.815 (1.077-3.061)	0.025
G4	168	18.615 (12.460-27.812)	<0.001	3.759 (0.961-14.706)	0.057
1p/19q codeletion	688				
Codel	170				
Noncodel	518	4.428 (2.885-6.799)	<0.001	1.244 (0.589-2.624)	0.567
Primary therapy outcome	259				
SD	147				
PD	112	2.288 (1.529-3.426)	<0.001	3.508 (2.049-6.006)	<0.001
SALL4	695				
Low	348				
High	347	1.900 (1.490-2.423)	<0.001	2.275 (1.425-3.633)	<0.001
IDH status	685				
Mut	439				
WT	246	8.551 (6.558-11.150)	<0.001	1.600 (0.814-3.145)	0.173
Age	695				
>60	143				
≤60	552	0.214 (0.165-0.278)	<0.001	0.247 (0.141-0.430)	<0.001
Histological type	695				
Astrocytoma	195				
Oligoastrocytoma	134	0.657 (0.419-1.031)	0.068	1.186 (0.660-2.129)	0.568
Oligodendroglioma	198	0.580 (0.395-0.853)	0.006	0.565 (0.304-1.051)	0.071
Glioblastoma	168	6.791 (4.932-9.352)	<0.001		
Gender	695				
Female	297				
Male	398	1.262 (0.988-1.610)	0.062	1.583 (0.982-2.554)	0.060

we first explored the immune infiltration of 22 subpopulations of immune cells in glioma tissue using the CIBERSORT algorithm. The divergence in tumor-infiltrating immune cells (TIICs) may be a distinctive feature of individual differences and may have prognostic value (Figures 6(a) and 6(b)). Figure 6(a) shows that RPL4P4 expression is positively correlated with the infiltration of neutrophils, M0 and M2 macrophages, eosinophils, DCs, and Treg T cells in gliomas. It was inversely correlated with mast cell and B cell infiltrates. Next, we investigated the relationship between RPL4P4 and tumor purity based on the ESTIMATE algorithm. In gliomas, RPL4P4 expression was positively correlated with stromal score, immune score, and ESTIMATE score (Figure 6(c)). RPL4P4 was also positively correlated with tumor mutation burden (TMB) (Figure 6(d)). The above evidence suggests that RPL4P4 is a potential marker of tumor microenvironmental status.

We further confirmed the value of six types of immune-infiltrating cells in predicting LGG prognosis by TIMER (Figure 6(e)). Differential correlation analysis showed that tumor immune infiltrators were correlated with RPL4P4 in 11, of which M0 macrophages (0.4), M2 macrophages (0.23), neutrophils (0.22), CD8+ T cells (0.15), and gamma

T cells were positively correlated and DC cells, eosinophils, mast cells, eosinophils, NK cells, and CD4+ T cells were negatively correlated. The above results suggest that RPL4P4 is clearly associated with M2 macrophages, which may promote the formation of an inhibitory immune microenvironment, thereby promoting tumor progression and leading to a poor prognosis (Figure 6(f)).

Given that immunotherapy is a key treatment for tumor reduction and eradication, the relationship between RPL4P4 expression and gene expression at 47 immune checkpoints was further analyzed. Interestingly, the analysis showed that RPL4P4 expression was positively correlated with the immune checkpoint gene commonly found in multiple cancers. In gliomas, RPL4P4 is closely related to the expression of CD276, NRP1, CD40 and CD48 (Figures 7(a) and 7(b)). This suggests a potential synergy between RPL4P4 and consistent immune checkpoints. The complex pattern of RPL4P4 modulating tumor immune responses by modulating immune checkpoint genes is important. In addition, we identified the relationship between RPL4P4 and TMB, microsatellite instability (MSI), and mismatch repairs (MMRs), which showed that gliomas were inversely correlated with MSI and MMRs, which further supported the above conclusions (Figures 7(c) and 7(d)).

(a)

(b)

(c)

(d)

Figure 3: Continued.

Primary therapy outcome: SD

Overall survival
HR = 0.45 (0.22–0.91)
P = 0.027

RPL4P4
Low
High

(e)

1p/19q codeletion: non-codel

Overall survival
HR = 2.74 (2.09–3.58)
P < 0.001

RPL4P4
Low
High

(f)

Age: < = 60

Overall survival
HR = 1.78 (1.31–2.42)
P < 0.001

RPL4P4
Low
High

(g)

Age: >60

Overall survival
HR = 1.86 (1.24–2.78)
P = 0.003

RPL4P4
Low
High

(h)
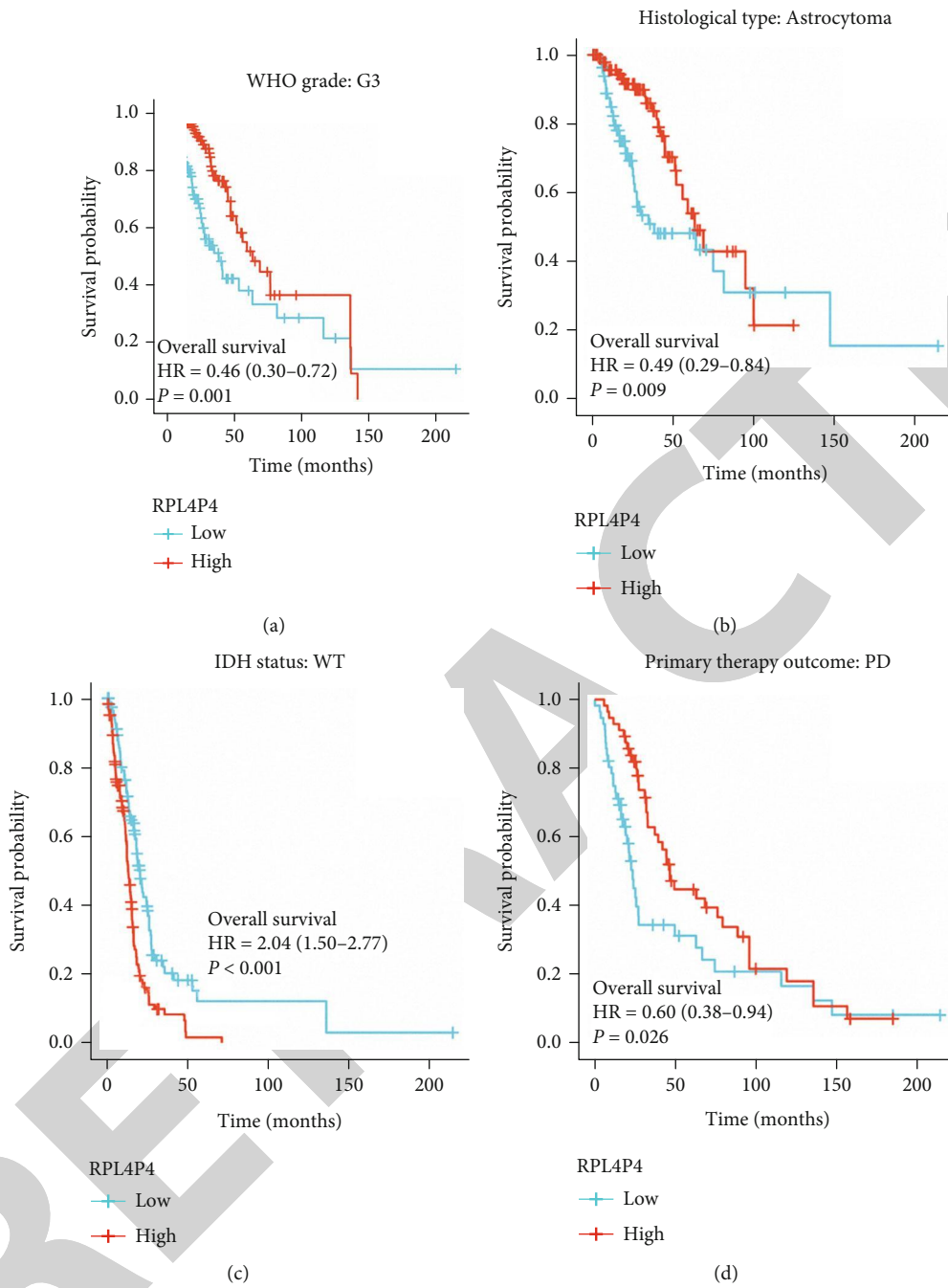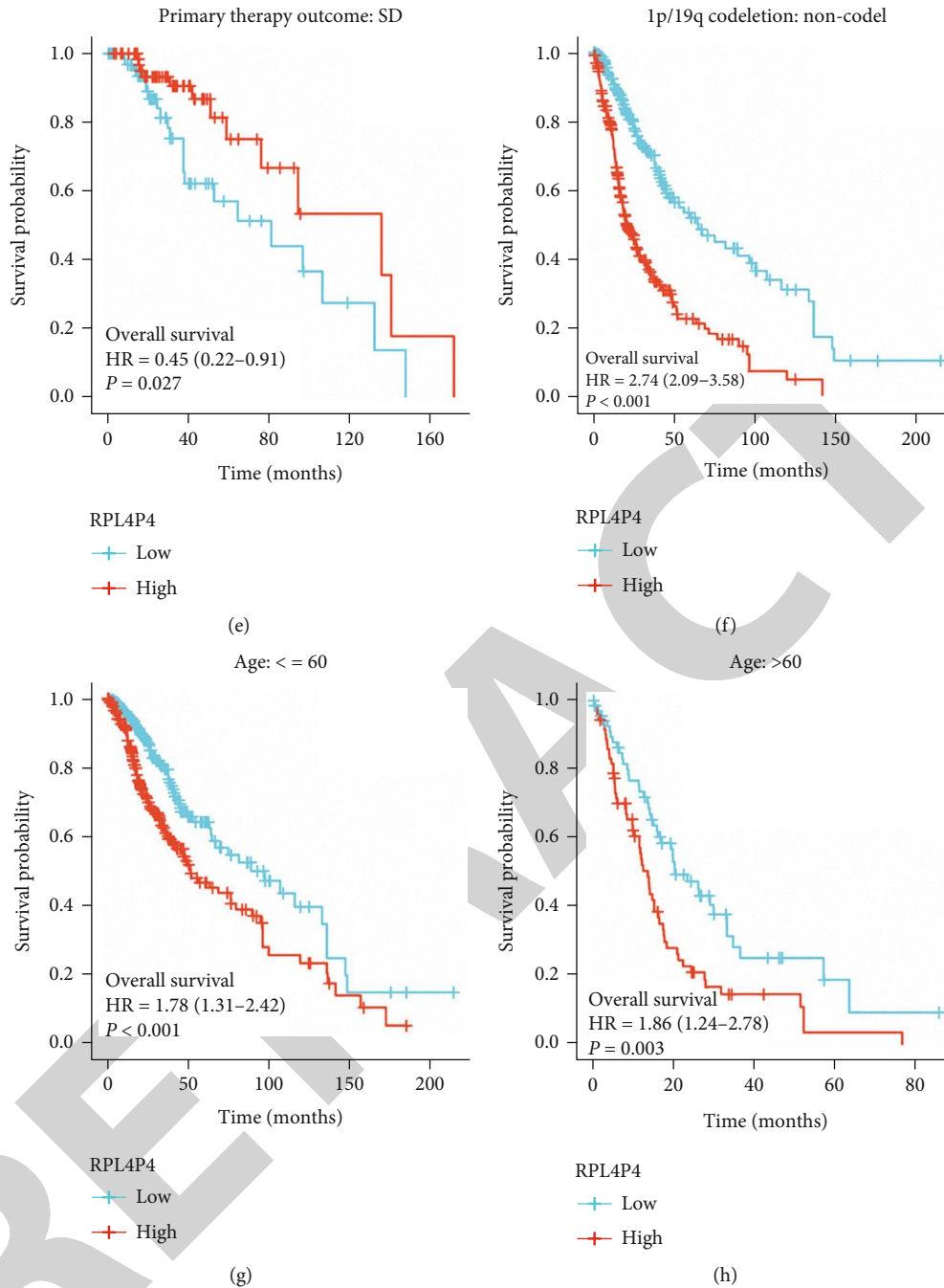
Figure 3: Analysis of the prognostic value of RPL4P4 in different glioma subgroups. (a–h) Analysis of the prognostic value of RPL4P4 in different subgroups.

3.8. RPL4P4 Knockdown Inhibits the Proliferation, Migration, and Invasion of Gliomas.

To demonstrate that RPL4P4 affects glioma cells, the RPL4P4 gene was silenced by three lentiviral transfections of glioma cell lines (A-172 and U-251). By screening stable transfection lines using the puromycin kill curve, the highest transfection efficiency was found in gene sequence 1 5′-GCCCAATGATATCGGTGTACT-3′ (53.7%), so this gene sequence was selected as the lentivirus for the next experiment (Figure 8(a)). The transfected cell lines were divided into control, si-NC, and si-RPL4P4. We confirmed

the proliferative effect of the RPL4P4 gene on glioma cells through the CCK-8 trial. After silencing RPL4P4 expression, the proliferation capacity of glioma cells (A-172 and U-251) in the si-RPL4P4 group decreased significantly compared with the that of other groups (Figures 8(b) and 8(c)). In addition, the cell scratch test found that the healing ability of si-RPL4P4 glioma cells was significantly lower than that of the control and si-NC groups (P < 0.05) (Figures 8(d) and 8(g)). Finally, we conducted a Transwell invasion test to confirm the effect of RPL4P4 on the aggressive ability of glioma cells

(a)

(b)
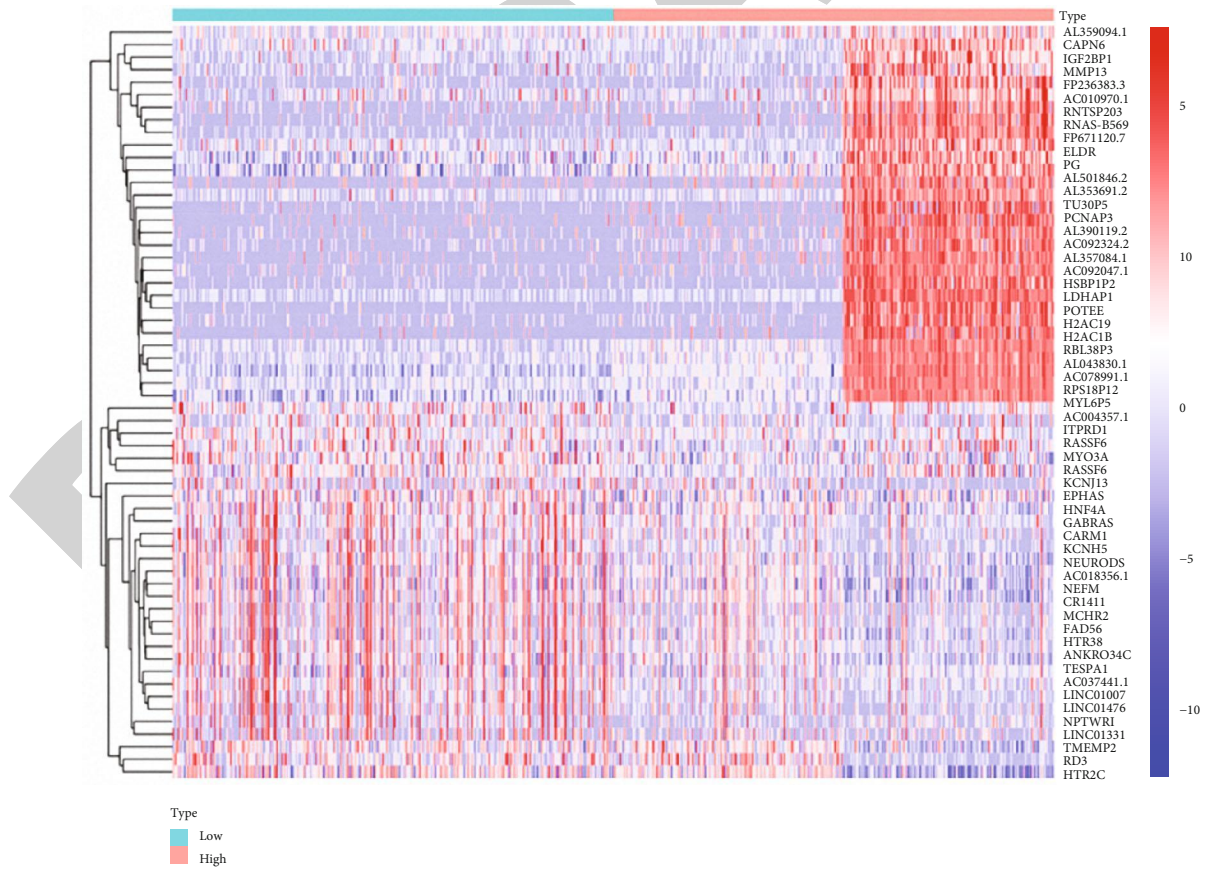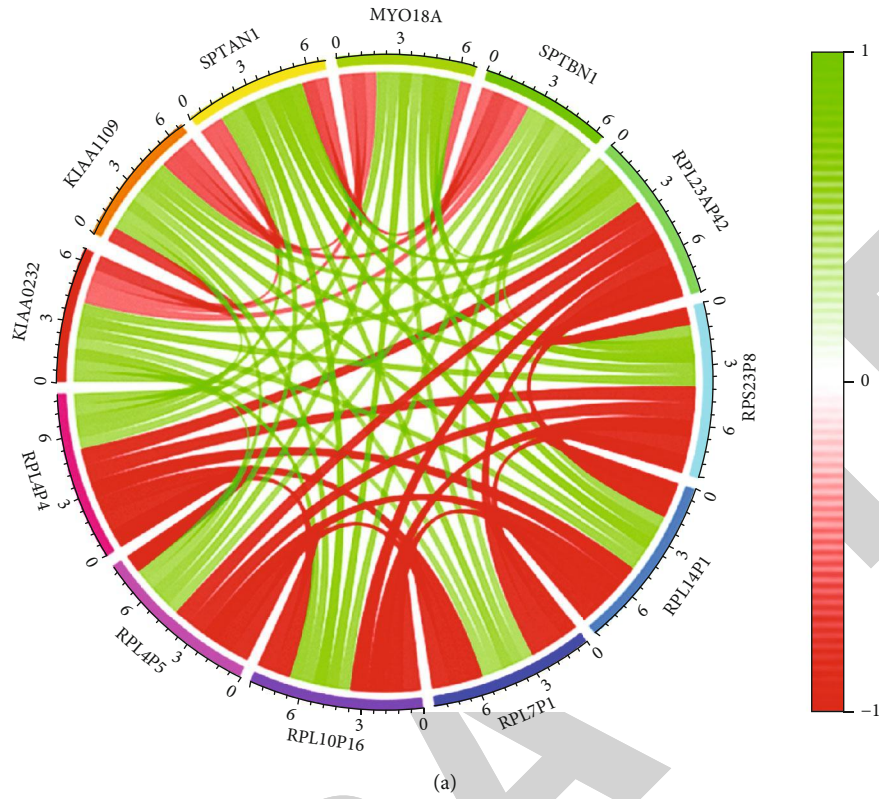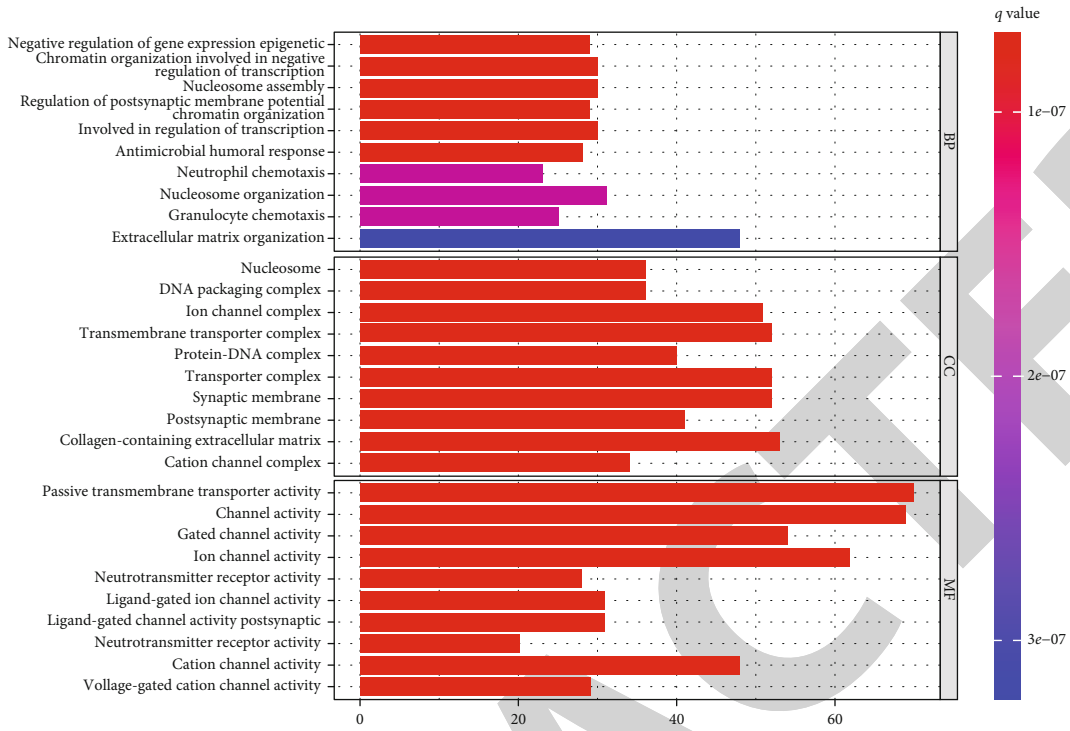
Figure 4: Continued.

(c)
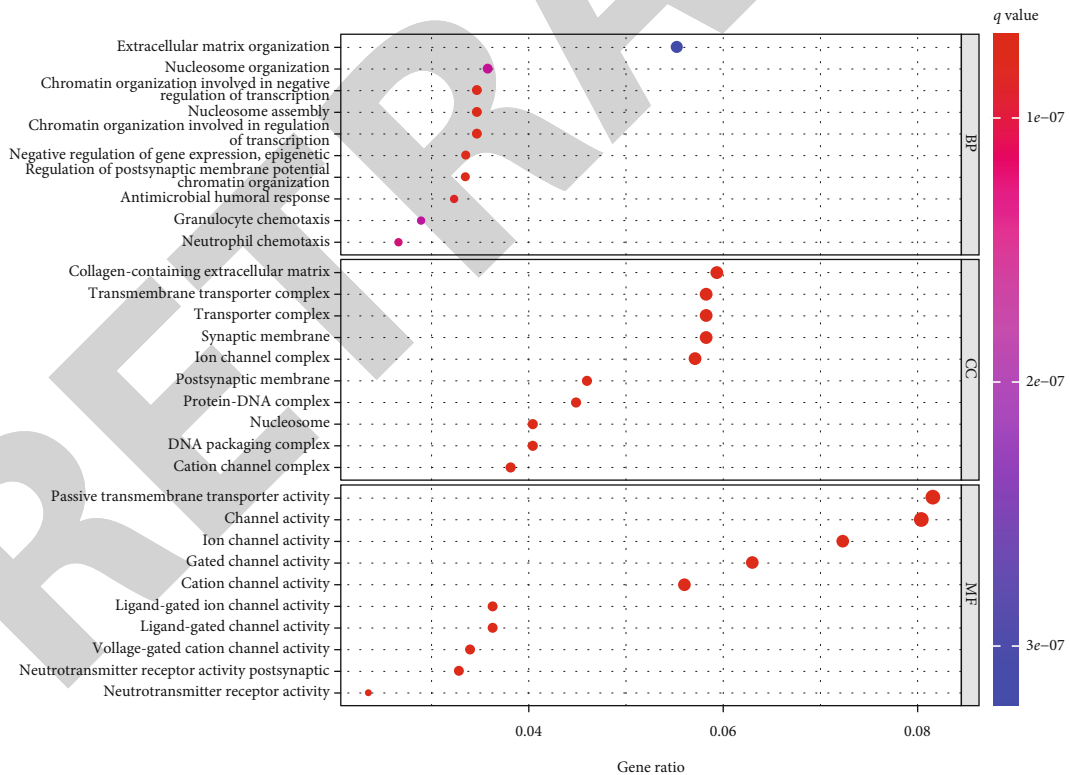
(d)

Figure 4: Continued.

(e)

(f)

Figure 4: Continued.

(g)
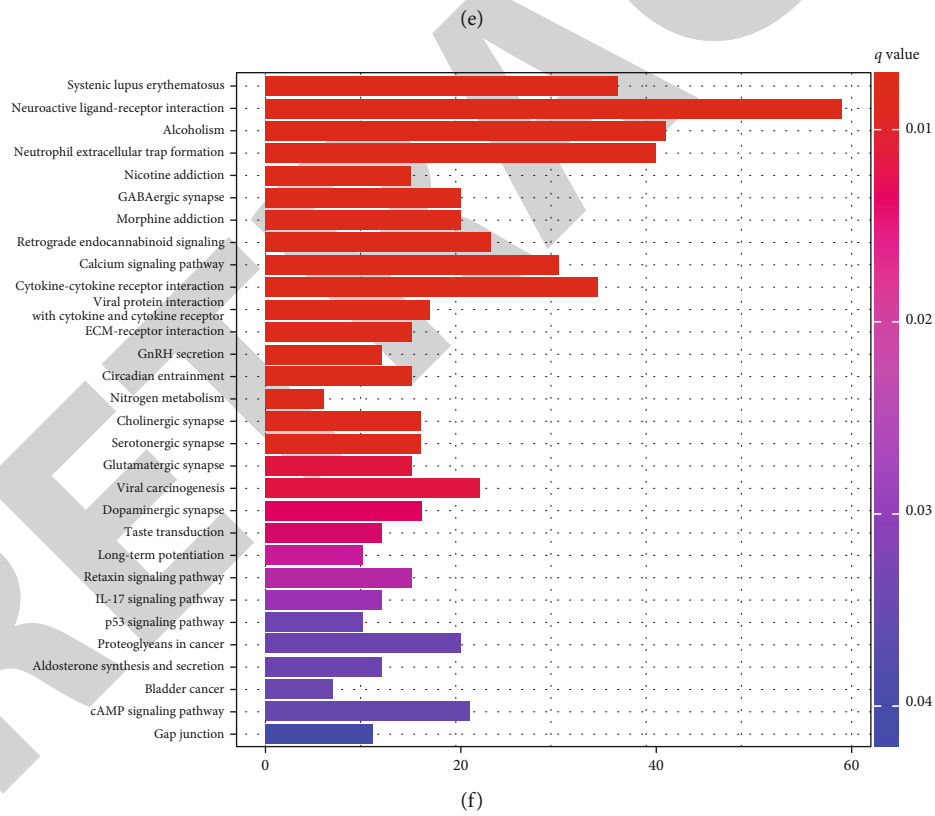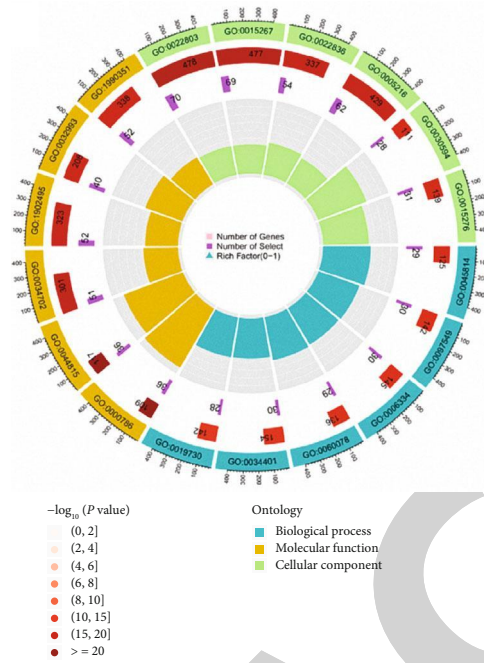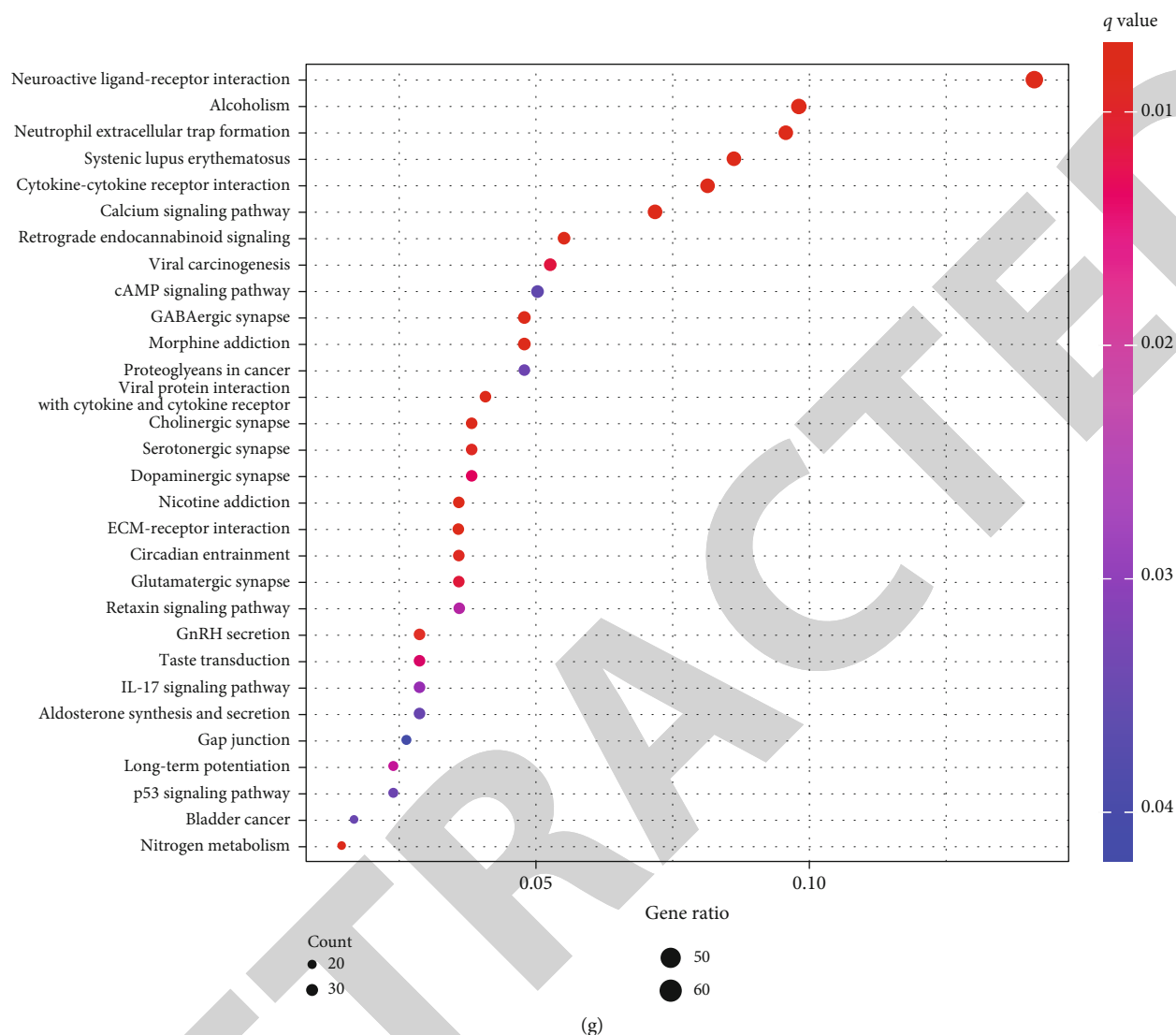
Figure 4: Analysis of the biological function of RPL4P4 in glioma. (a and b) The coexpression of the RPL4P4 gene in glioma was explored by LinkedOmics. (c–g) GO and KEGG analyses of genes coexpressed with RPL4P4 in glioma.

and found that the glioma cell invasion ability of si-RPL4P4 was significantly lower than that of the control and si-NC groups ($P < 0.05$) (Figures 8(h) and 8(i)). Overall, these results suggest that RPL4P4 expression is significantly associated with the ability of glioma cells to invade, migrate, and proliferate.

4. Discussion

Gliomas are the most common type of primary malignant brain tumor in adults [18, 19]. They are associated with short survival and direct repercussions on quality of life and cognitive functions [20]. Even with standard therapy, including surgical resection, radiotherapy, and chemotherapy, the prognosis for glioma patients remains poor [2, 21]. Further advancements in technologies that identify new biomarkers to improve the understanding of the regulation of cell processes and treatment of glioma are needed.

In recent years, the roles of pseudogenes have been reported to be associated with various human diseases,

including cancer, and have attracted much attention [22]. Several pseudogenes are differentially expressed in glioma tissues and are implicated in biological processes related to tumorigenesis and drug resistance to chemotherapy [23, 24]. To date, no report has investigated the function and mechanism of the pseudogene RPL4P4 in glioma. These findings shed new light on the importance of the orchestrated interactions among pseudogenes, microRNAs, and proteins in tumorigenesis and may be used for precision therapy in glioma patients.

To our knowledge, the present study is the first to comprehensively evaluate RPL4P4 expression and its association with clinical and prognostic outcomes in glioma using various public databases, including the CGGA, TCGA, GEPA2, and UALCAN datasets. We found that RPL4P4 was significantly overexpressed in gliomas and that increased RPL4P4 expression correlated significantly with poor outcomes, tumor grade, age, IDH mutation status, and chromosome 1p/19q codeletion status. Univariate and Cox analyses

(a)

(b)

Figure 5: Continued.

Missense_mutation
Frame_shift_del
Nonsense_mutation
Splice_site
In_frame_ins
In_frame_del
Frame_shift_ins
Translation_start_site

Sample group:
HighExp
LowExp
Code:
LGG
GBM

(c)
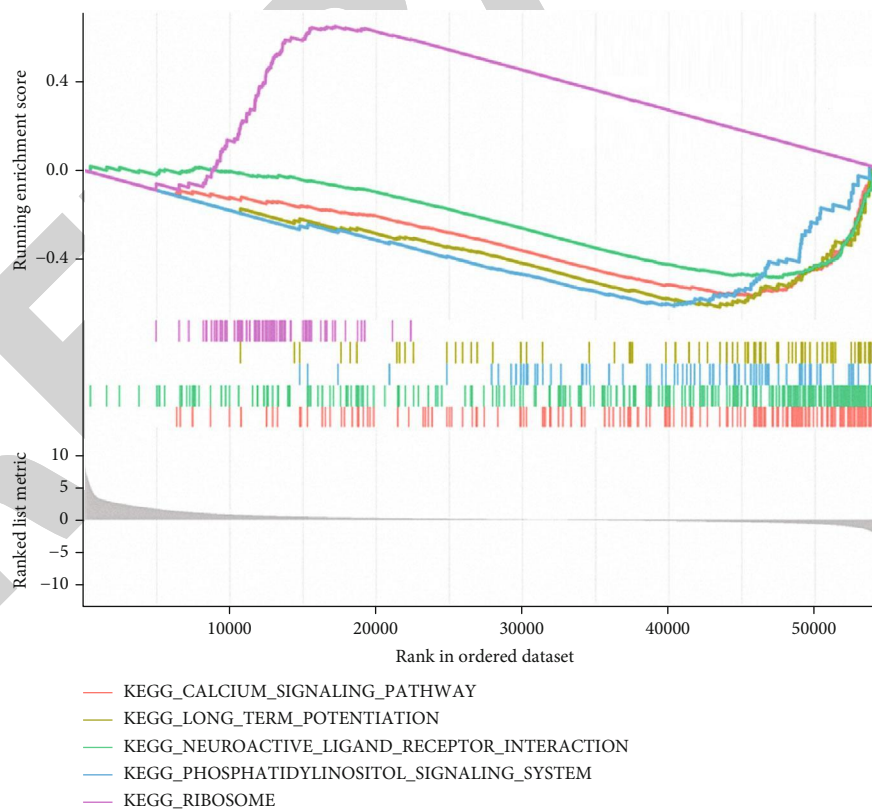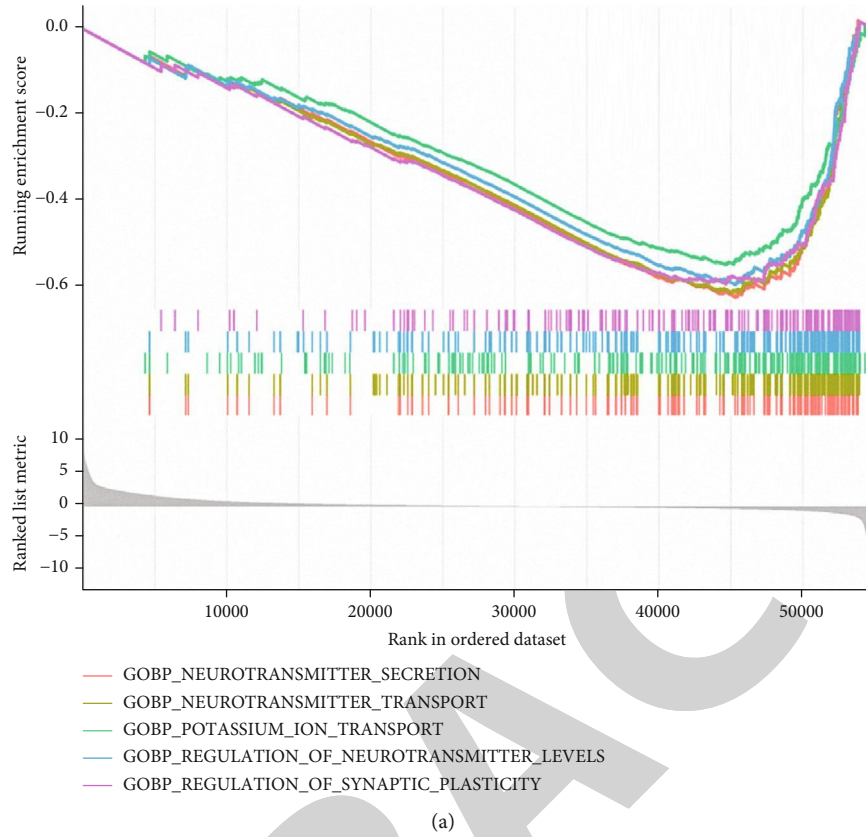
(d)
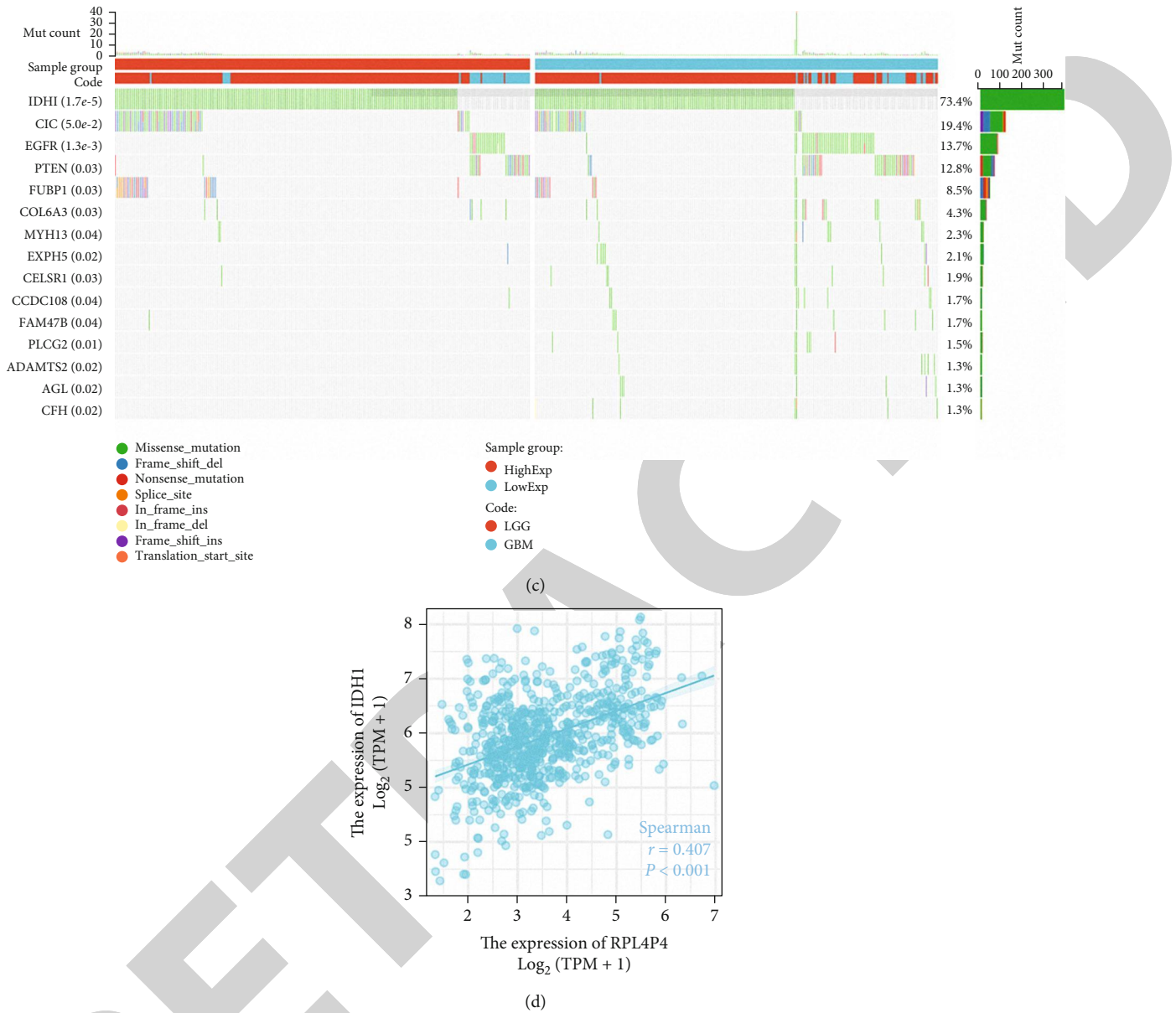
FIGURE 5: Function and somatic mutation of RPL4P4. (a and b) The involvement of genes coexpressed with RPL4P4 in glioma signaling pathways as examined by GSEA software. (c) Molecules associated with a somatic mutation describe RPL4P4 mutations in glioma. (d) Correlation between RPL4P4 and IDH1.

showed that RPL4P4 expression correlated positively with WHO grade, primary therapy outcome, IDH mutation status, age, and poor OS in patients with glioma. Based on the multivariate Cox analysis, a nomogram was constructed to predict the prognosis of patients with glioma based on the expression of RPL4P4 and to stratify glioma patients with better performance. Furthermore, GSEA showed that high RPL4P4 expression was positively correlated with neurotransmitter secretion, neurotransmitter transport, potassium ion transport, regulation of neurotransmitter levels, regulation of synaptic plasticity, calcium signaling pathways, long-term potentiation, neuroactive ligand receptor interaction, phosphatidylinositol signaling pathways, and ribosomes. Further inferred from the pathways involved,

RPL4P4 may act as an oncogene, regulating the expression of ribosomal genes at the stage, thus promoting gliogenesis.

Immunotherapy plays an increasingly important role in standard cancer treatment, as it can recruit tumor-infiltrating T cells to eradicate tumor cells. In glioma, tumor-infiltrating CD4+ T cells play an important role in immune regulation [25, 26]. GSEA showed that RPL4P4 expression was significantly involved in immune signaling pathways. Analysis of immune cell infiltration in the present study showed that high RPL4P4 expression was significantly and positively associated with levels of M0 macrophages (0.4), M2 macrophages (0.23), neutrophils (0.22), CD8+ T cells (0.15), and gamma T cells in gliomas. Among them, M2 macrophage infiltration is clearly related, and M2-like tumor-associated macrophages play an
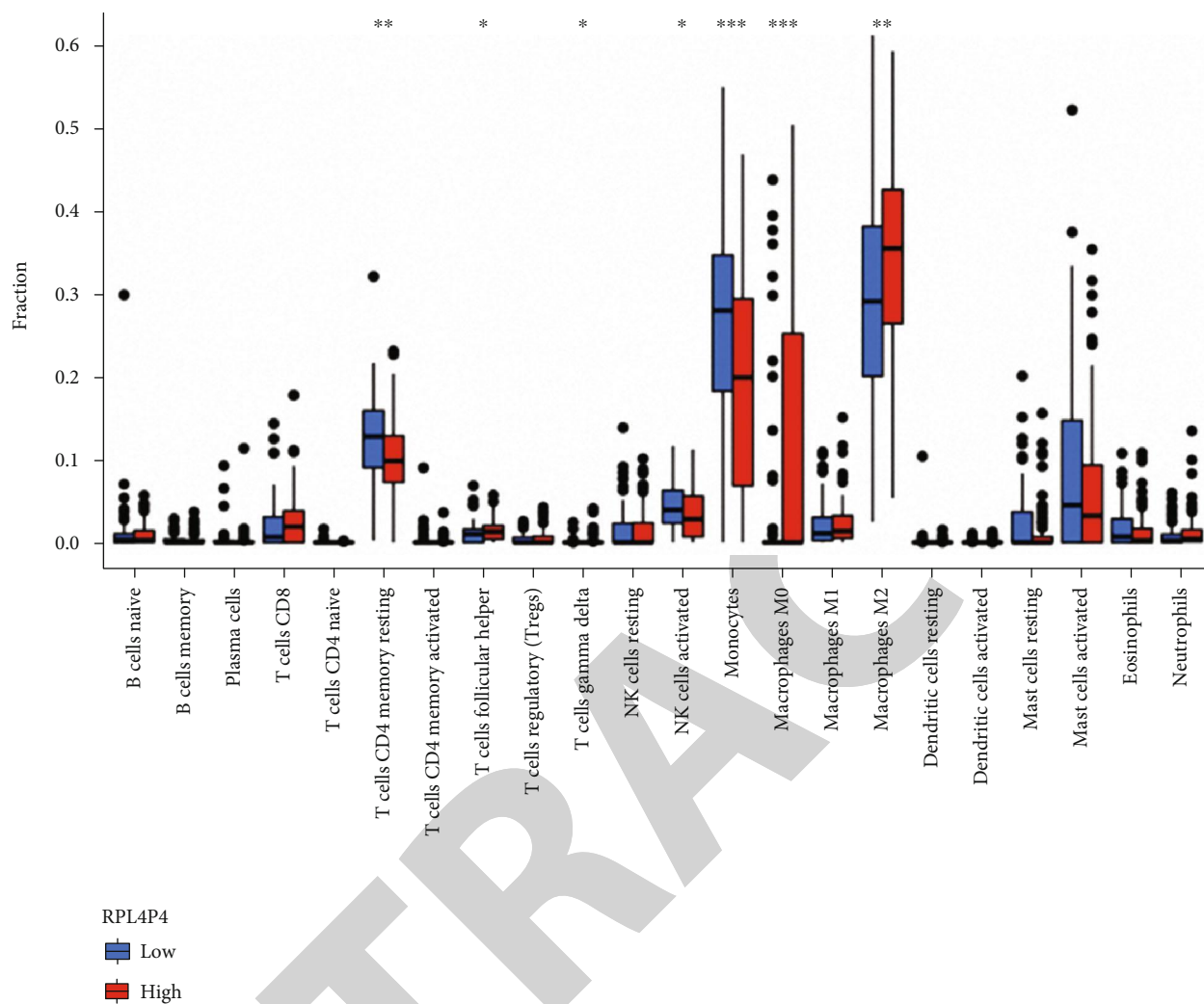
(a)

FIGURE 6: Continued.

(b)
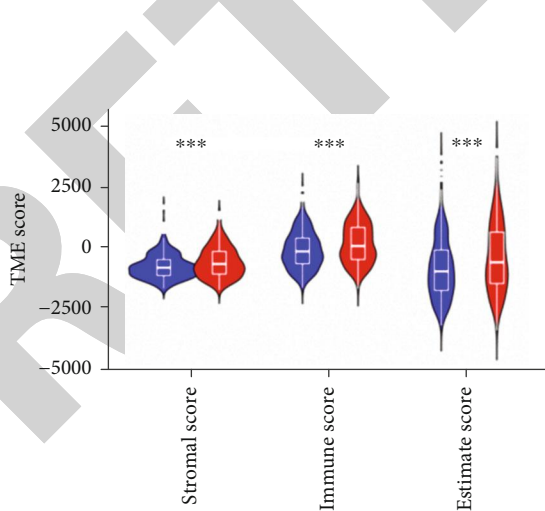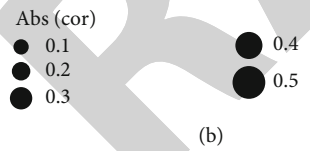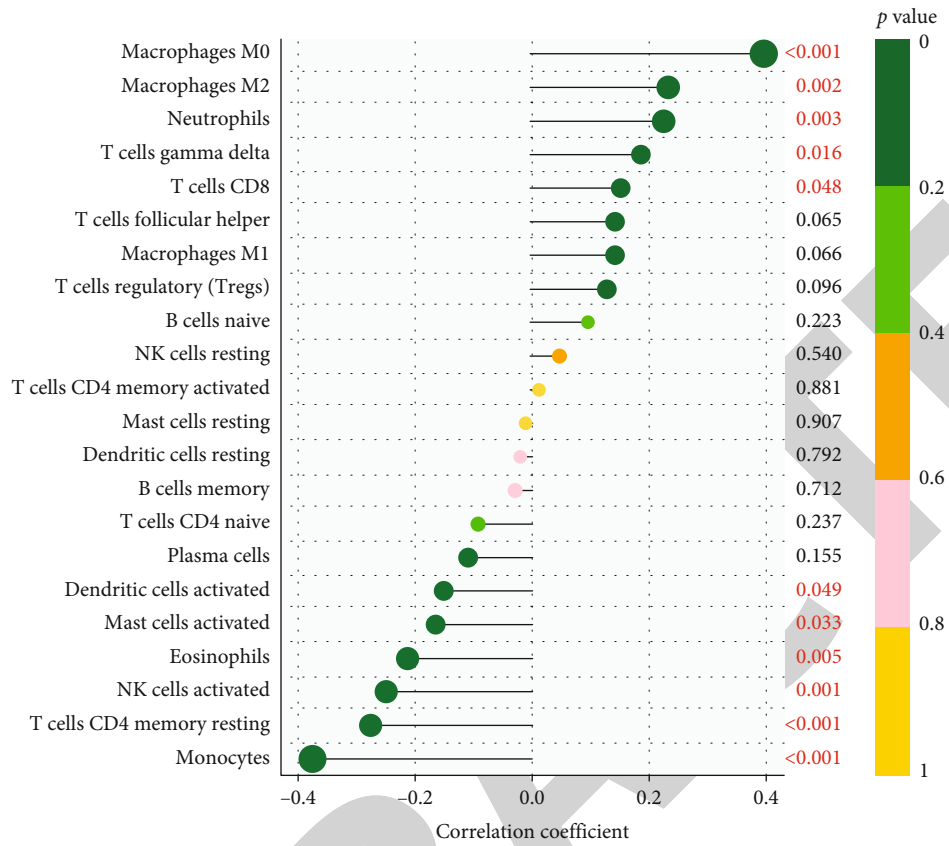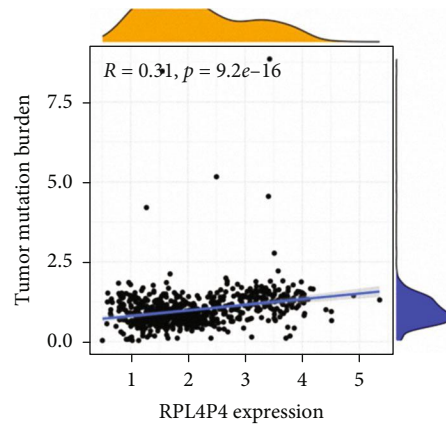
(c)

(d)

Figure 6: Continued.
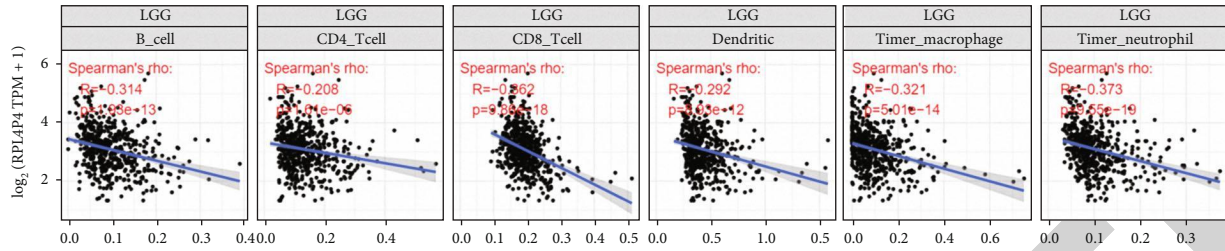
(e)
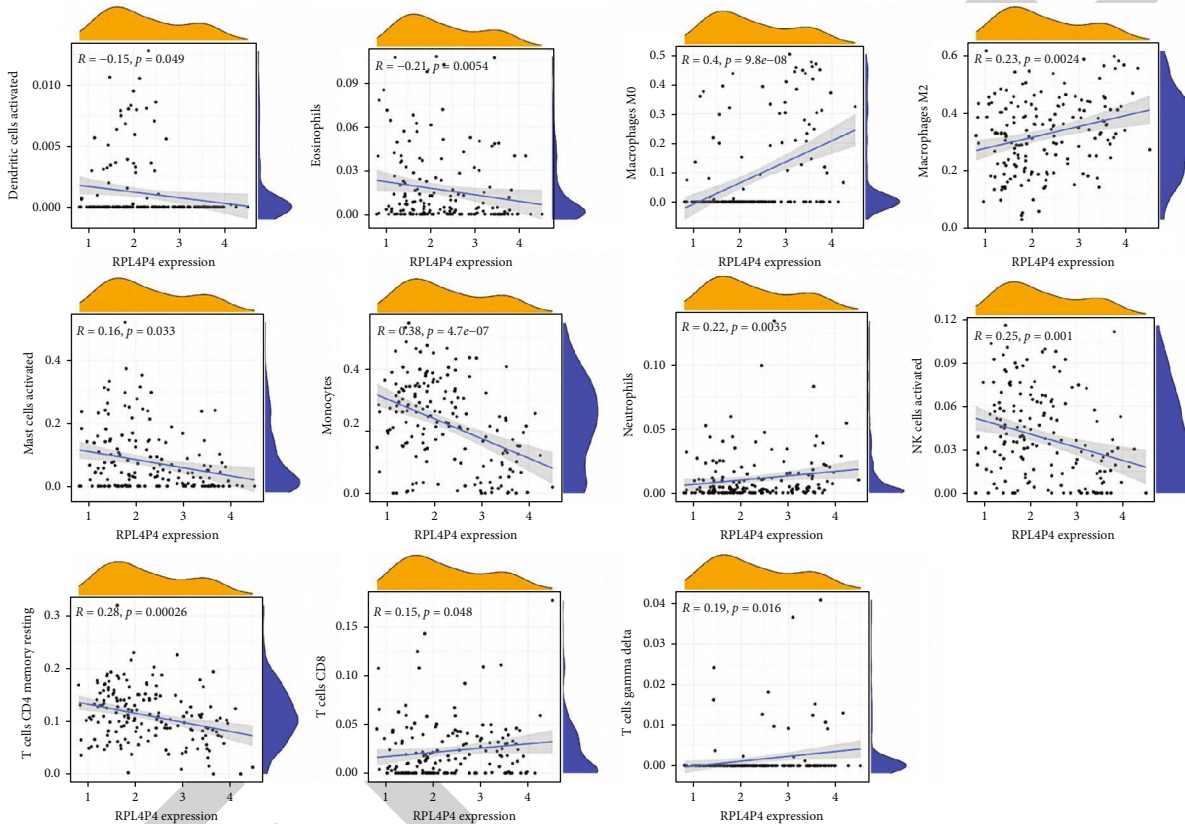
(f)
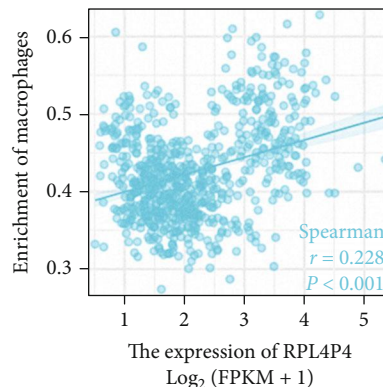
(g)

Figure 6: Relationship between the expression of RPL4P4 and the level of immune infiltration in glioma. (a and b) Correlation matrix for all 22 immune cell proportions. (c) Correlation between RPL4P4 and ImmuneScore, ESTIMATEScore, and StromalScore in glioma. (d) RPL4P4 expression was positively correlated with TMB. (e) The correlation between RPL4P4 expression and the infiltration of different immune cells based on time. (f) Correlation between RPL4P4 expression and immune-infiltrating cells in TCGA. $^*P < .05$, $^{**}P < .01$, and $^{***}P < .001$.
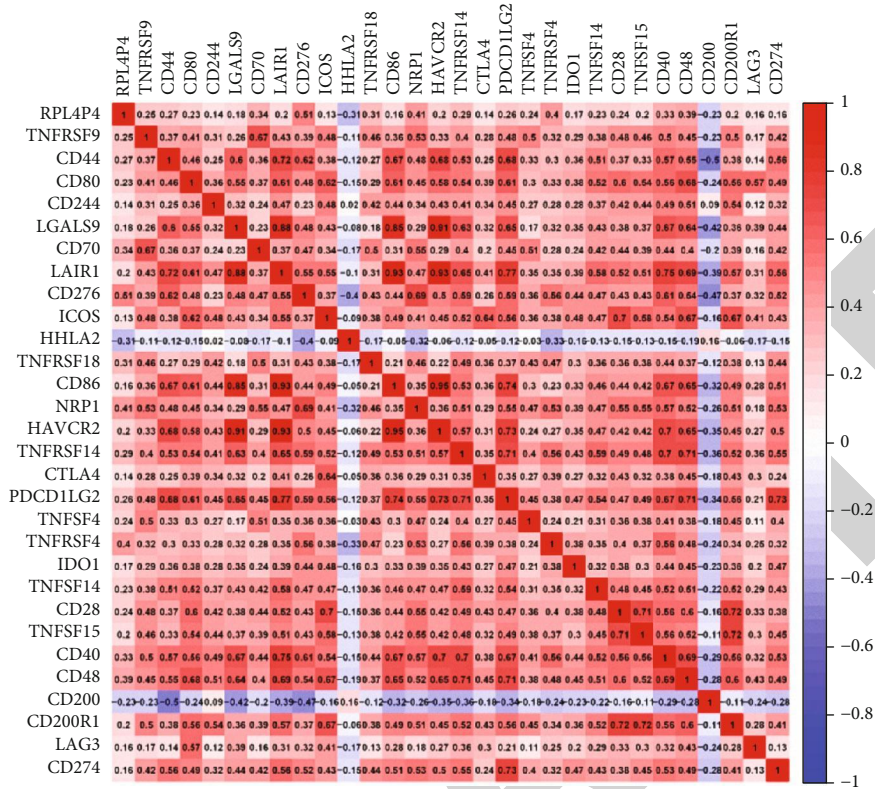
(a)
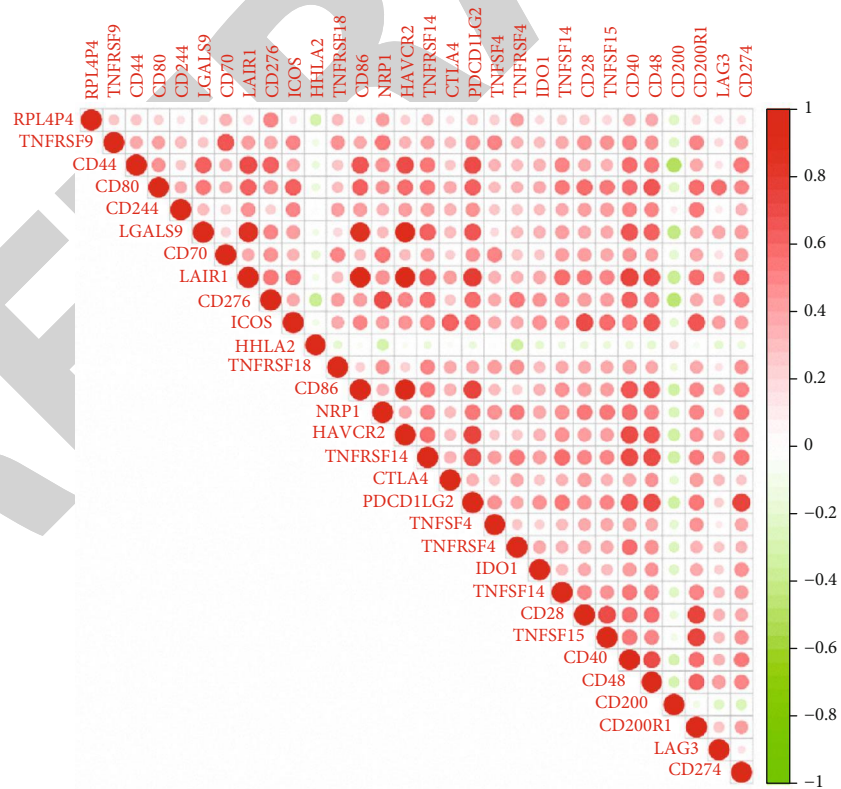
(b)

Figure 7: Continued.

(c)

(d)
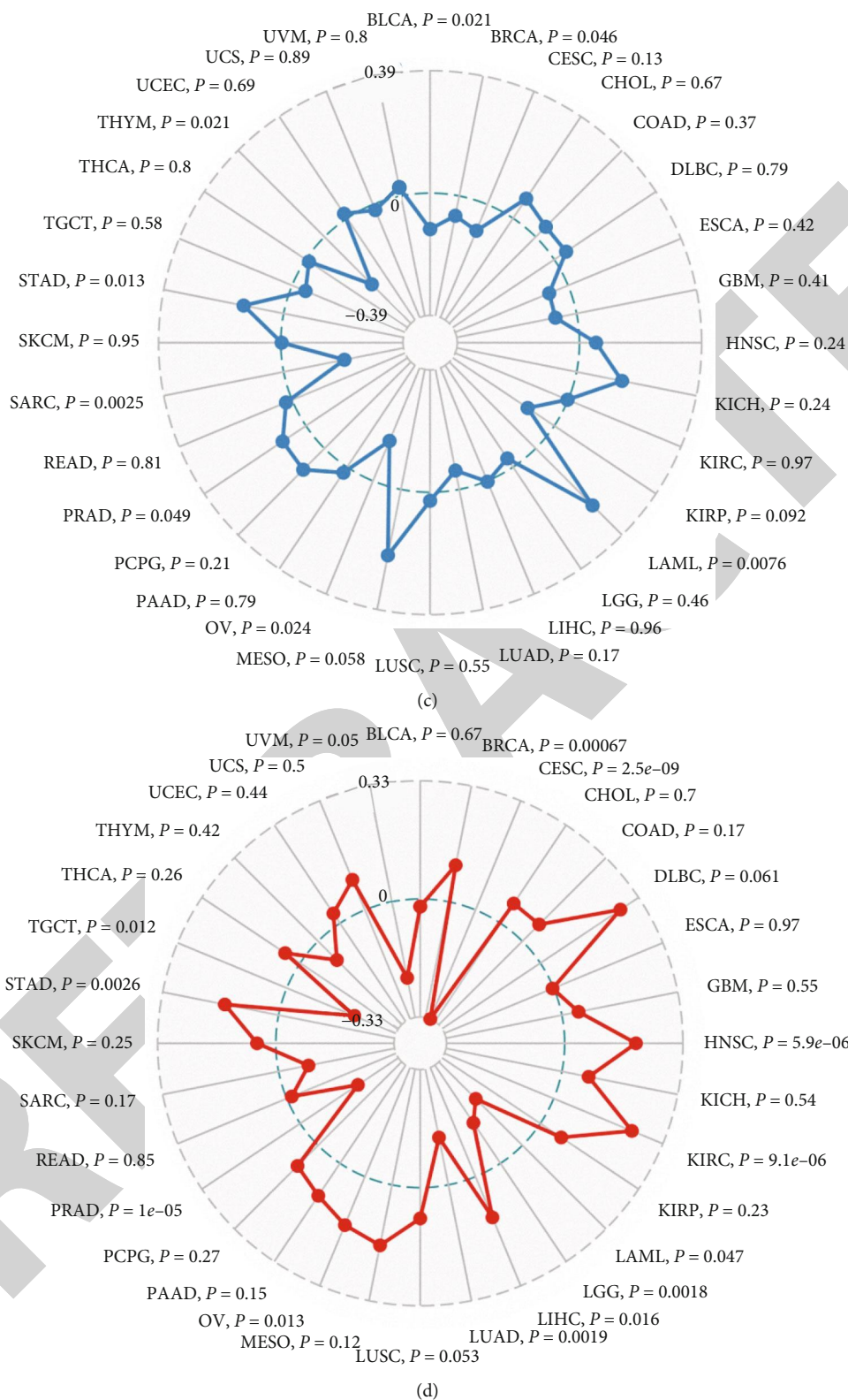
Figure 7: The relationship between RPL4P4 expression and immune checkpoints, TMB, and MSI. (a and b) Correlation analysis between RPL4P4 expression and 47 immune checkpoint genes in cancer. (c) Correlation analysis between RPL4P4 expression and TMB. (d) Correlation analysis between RPL4P4 expression and MSI.
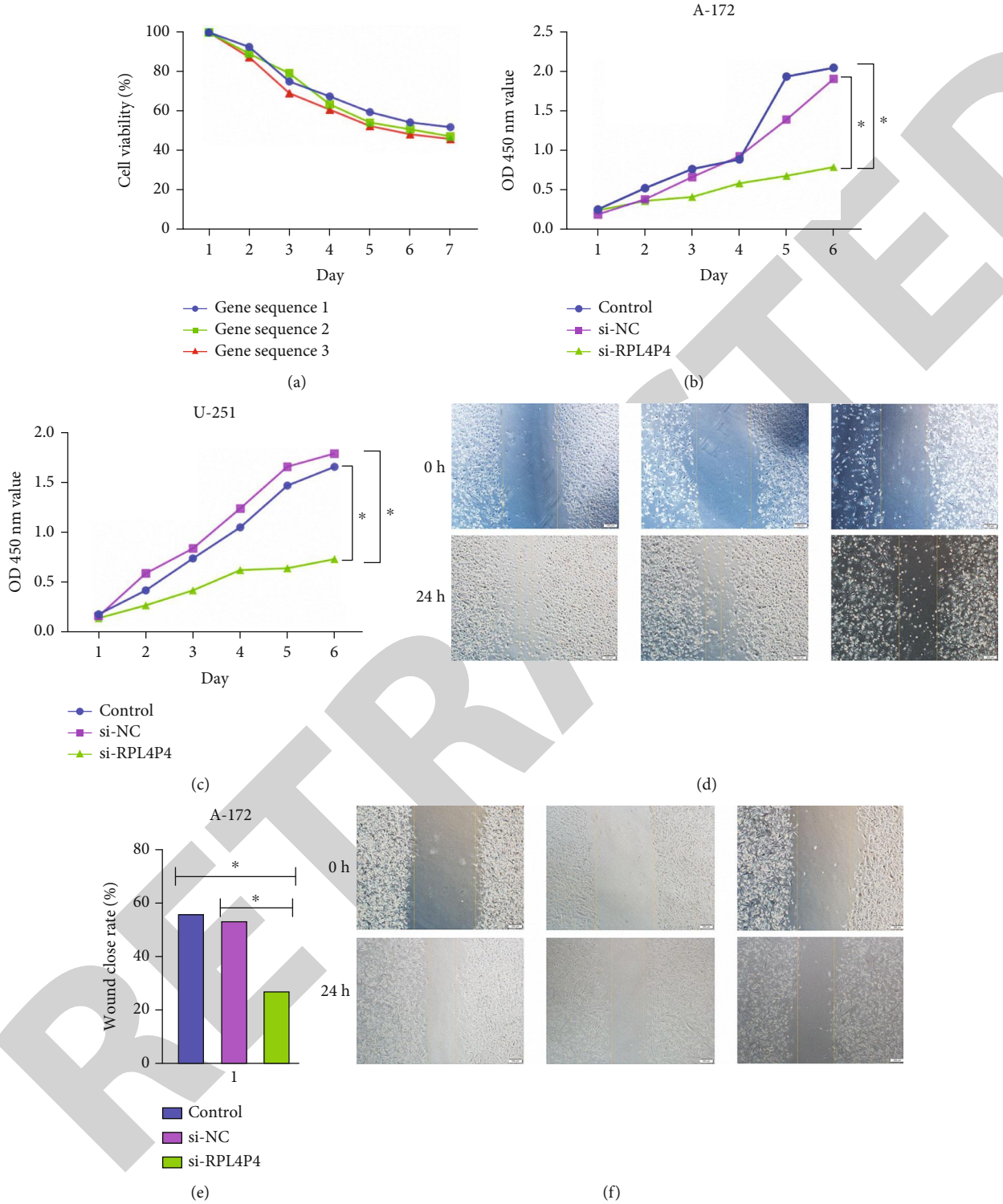
Figure 8: Continued.

A-172

U-251

(g)

(h)

U-251

(i)
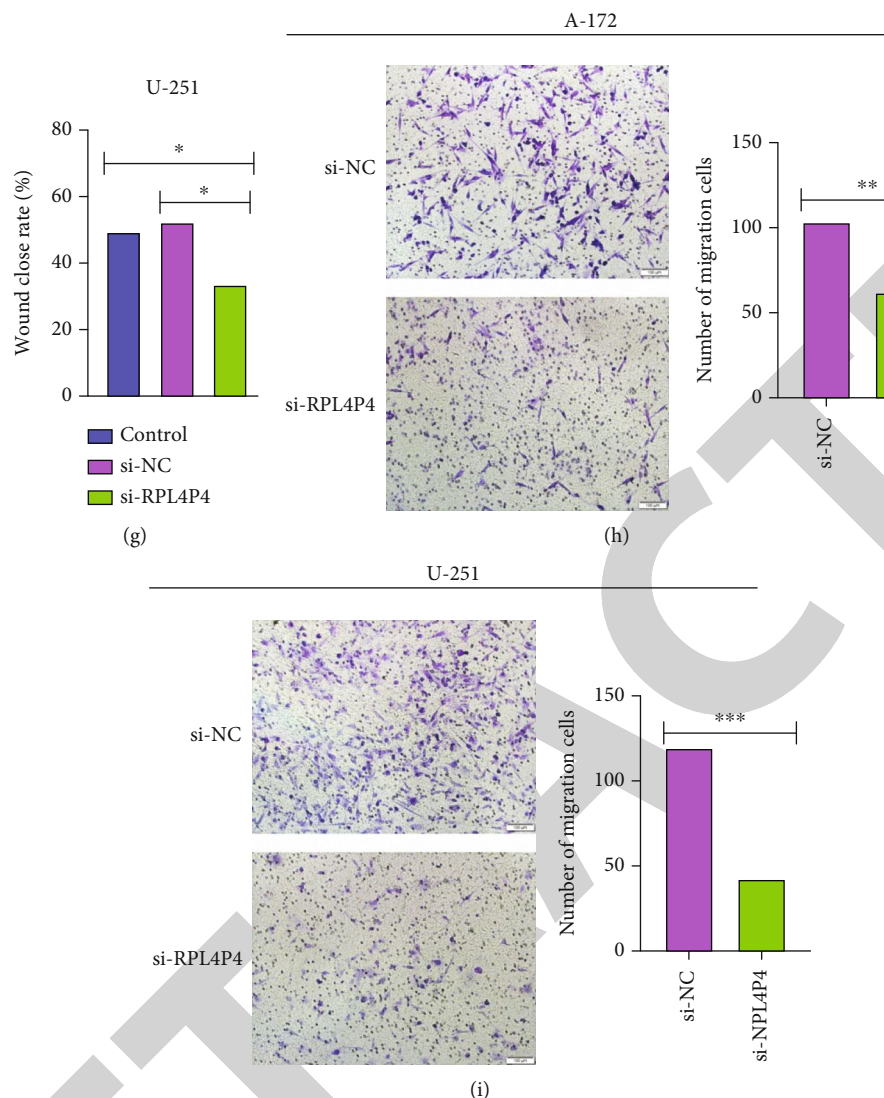
Figure 8: RPL4P4 depletion inhibits GBM cell proliferation and migration. (a) Optimal lentivirus was screened using a puromycin kill curve for the stability of the three sets of RPL4P4 lentivirus constructs. (b and c) RPL4P4 knockdown significantly inhibited A-172 and U-251 cell proliferation, as examined by CCK8 assay. (d and i) RPL4P4 knockdown significantly inhibited A-172 and U-251 cell migration as examined by wound healing and Transwell assays. $*P < .05$, $**P < .01$, and $***P < .001$.

important role in the immune microenvironment of gliomas [27], and the high expression of RPL4P4 promotes the inhibitory phenotype of macrophages, thereby promoting tumor progression, which indicates that RPL4P4 may serve as a potential biomarker. Inhibition of its expression may improve the sensitivity of gliomas to immunotherapy, and this result needs to be further confirmed.

The biological functions of RPL4P4 in these cells were evaluated by RPL4P4 knockdown, which significantly inhibited glioma cell proliferation, invasion, and migration. These results suggest that NRPL4P4 may act as an oncogene in glioma, but additional studies are needed to confirm these findings.

This study had several limitations. Although we explored the correlation between RPL4P4 and immune cell infiltration in glioma patients, we did not determine the function of RPL4P4 in regulating the tumor microenvironment in glioma. In addition, we showed that a depletion of RPL4P4

could inhibit the migration of glioma cells, but the potential molecular mechanisms of RPL4P4 in cancer metastasis remain unclear. Furthermore, the present study assessed the expression and biological roles of RPL4P4 in databases of patients with glioma and cultured cells, not in vivo. Additional studies are required to assess the function of RPL4P4 in glioma metastasis and in regulating the tumor microenvironment of glioma.

5. Conclusion

In summary, these findings shed new light on the importance of the pseudogene RPL4P4 in glioma. The results showed that RPL4P4 expression was increased in glioma tissues and that its high expression correlated with the malignant progression of gliomas. RPL4P4 knockdown in glioma cells reduced their proliferation and migration

activities. In tumor immunity, RPL4P4 was significantly associated with M2-like tumor-associated macrophages in the microenvironment of gliomas. Therefore, RPL4P4 is a prognostic biomarker linked to immunosuppression, and targeting RPL4P4 may improve the outcome of immunotherapy.

Data Availability

The data used to support the findings of this study are included within the article and supplementary information file(s).

Ethical Approval

The manuscript does not contain any studies with human participants or animals performed by any of the authors.

Conflicts of Interest

The authors have declared that no competing interests exist.

Authors' Contributions

Bo Li and Yongxin Wang conceptualized the study. Nuersimanguli Maimaitiming and Hu Qin contributed to the methodology. Wenyu Ji, Guofeng Fan carried out formal analysis and investigation. Yirizhati Aili wrote the original draft preparation. Zengliang Wang and Bo Li wrote, reviewed, and edited the manuscript. Zengliang Wang and Yirizhati Aili are co-first authors. Zengliang Wang and Yirizhati Aili contributed equally to this work.

Acknowledgments

Supplementary Materials

Supplementary 1. Supplemental Figure 1: the forest plot showed that in 33 cancers, RPL4P4 had a significant effect on the survival time according to specific tumor types, and RPL4P4 had a clear correlation with prognosis in patients with gliomas ($P < 0.001$).

Supplementary 2. Supplemental Table 1: the correlation between RPL4P4 and clinicopathological characteristic in CCGA-glioma dataset.

Supplementary 3. Supplemental Table 2: univariate regression and multivariate survival model of DFS in patients with glioma.

Supplementary 4. Supplemental Table 3: univariate regression and multivariate survival model of PFS in patients with glioma.

References

[1] F. Komboz, S. Zechel, V. Malinova, D. Mielke, V. Rohde, and T. Abboud, "Infratentorial ganglioglioma mimicking a cerebellar metastasis," *The International Journal of Neuroscience*, vol. 1-6, pp. 1–5, 2022.

[2] S. Xu, L. Tang, X. Li, F. Fan, and Z. Liu, "Immunotherapy for glioma: current management and future application," *Cancer Letters*, vol. 476, pp. 1–12, 2020.

[3] G. Reifenberger, H. G. Wirsching, C. B. Knobbe-Thomsen, and M. Weller, "Advances in the molecular genetics of gliomas - implications for classification and therapy," *Nature Reviews. Clinical Oncology*, vol. 14, no. 7, pp. 434–452, 2017.

[4] P. Y. Wen and R. J. Packer, "The 2021 WHO classification of tumors of the central nervous system: clinical implications," *Neuro-Oncology*, vol. 23, no. 8, pp. 1215–1217, 2021.

[5] Y. Ma, Z. Chen, and J. Yu, "Pseudogenes and their potential functions in hematopoiesis," *Experimental Hematology*, vol. 103, pp. 24–29, 2021.

[6] C. Sisu, "Pseudogenes as and in human cancers," *Methods in Molecular Biology*, vol. 2324, pp. 319–337, 2021.

[7] L. Tutar, A. Özgür, and Y. Tutar, "Involvement of miRNAs and pseudogenes in cancer," *Methods in Molecular Biology*, vol. 1699, pp. 45–66, 2018.

[8] L. Wang, Z. Y. Guo, R. Zhang et al., "Pseudogene OCT4-pg4 functions as a natural micro RNA sponge to regulate OCT4 expression by competing for miR-145 in hepatocellular carcinoma," *Carcinogenesis*, vol. 34, no. 8, pp. 1773–1781, 2013.

[9] O. H. Tam, A. A. Aravin, P. Stein et al., "Pseudogene-derived small interfering RNAs regulate gene expression in mouse oocytes," *Nature*, vol. 453, no. 7194, pp. 534–538, 2008.

[10] J. Pelletier, G. Thomas, and S. Volarević, "Ribosome biogenesis in cancer: new players and therapeutic avenues," *Nature Reviews. Cancer*, vol. 18, no. 1, pp. 51–63, 2018.

[11] A. Pecoraro, M. Pagano, G. Russo, and A. Russo, "Ribosome biogenesis and cancer: overview on ribosomal proteins," *International Journal of Molecular Sciences*, vol. 22, no. 11, p. 5496, 2021.

[12] A. Lari, H. G. Pourbadie, A. Sharifi-Zarchi et al., "Dysregulation of ribosome-related genes in ankylosing spondylitis: a systems biology approach and experimental method," *BMC Musculoskeletal Disorders*, vol. 22, no. 1, p. 789, 2021.

[13] S. Hirotsune, N. Yoshida, A. Chen et al., "An expressed pseudogene regulates the messenger-RNA stability of its homologous coding gene," *Nature*, vol. 423, no. 6935, pp. 91–96, 2003.

[14] H. Zhao, M. Chen, S. B. Lind, and U. Pettersson, "Distinct temporal changes in host cell lncRNA expression during the course of an adenovirus infection," *Virology*, vol. 492, pp. 242–250, 2016.

[15] S. Balasubramanian, D. Zheng, Y. J. Liu et al., "Comparative analysis of processed ribosomal protein pseudogenes in four mammalian genomes," *Genome Biology*, vol. 10, no. 1, p. R2, 2009.

[16] Z. Tang, B. Kang, C. Li, T. Chen, and Z. Zhang, "GEPIA2: an enhanced web server for large-scale expression profiling and interactive analysis," *Nucleic Acids Research*, vol. 47, no. W1, pp. W556–W560, 2019.

[17] T. Li, J. Fan, B. Wang et al., "TIMER: a web server for comprehensive analysis of tumor-infiltrating immune cells," *Cancer Research*, vol. 77, no. 21, pp. e108–e110, 2017.

[18] Q. T. Ostrom, L. Bauchet, F. G. Davis et al., "The epidemiology of glioma in adults: a "state of the science" review," *Neuro-Oncology*, vol. 16, no. 7, pp. 896–913, 2014.

[19] O. Gusyatiner and M. E. Hegi, "Glioma epigenetics: from subclassification to novel treatment options," *Seminars in Cancer Biology*, vol. 51, pp. 50–58, 2018.

Retraction

Retracted: Intermittent Hypoxia and Atherosclerosis: From Molecular Mechanisms to the Therapeutic Treatment

Oxidative Medicine and Cellular Longevity

This article has been retracted by Hindawi, as publisher, following an investigation undertaken by the publisher [1]. This investigation has uncovered evidence of systematic manipulation of the publication and peer-review process. We cannot, therefore, vouch for the reliability or integrity of this article.

Please note that this notice is intended solely to alert readers that the peer-review process of this article has been compromised.

Wiley and Hindawi regret that the usual quality checks did not identify these issues before publication and have since put additional measures in place to safeguard research integrity.

We wish to credit our Research Integrity and Research Publishing teams and anonymous and named external researchers and research integrity experts for contributing to this investigation.

The corresponding author, as the representative of all authors, has been given the opportunity to register their agreement or disagreement to this retraction. We have kept a record of any response received.

References

[1] B. Luo, Y. Li, M. Zhu, J. Cui, Y. Liu, and Y. Liu, "Intermittent Hypoxia and Atherosclerosis: From Molecular Mechanisms to the Therapeutic Treatment," *Oxidative Medicine and Cellular Longevity*, vol. 2022, Article ID 1438470, 16 pages, 2022.

Review Article

Intermittent Hypoxia and Atherosclerosis: From Molecular Mechanisms to the Therapeutic Treatment

Binyu Luo ⓘ,[1] Yiwen Li ⓘ,[1] Mengmeng Zhu ⓘ,[1] Jing Cui ⓘ,[1] Yanfei Liu ⓘ,[2] and Yue Liu ⓘ[1]

[1]*National Clinical Research Center for Chinese Medicine Cardiology, Xiyuan Hospital, Chinese Academy of Chinese Medical Sciences, Beijing 100091, China*
[2]*The Second Department of Gerontology, Xiyuan Hospital, China Academy of Chinese Medical Sciences, Beijing 100091, China*

Correspondence should be addressed to Yue Liu; liuyueheart@hotmail.com

Intermittent hypoxia (IH) has a dual nature. On the one hand, chronic IH (CIH) is an important pathologic feature of obstructive sleep apnea (OSA) syndrome (OSAS), and many studies have confirmed that OSA-related CIH (OSA-CIH) has atherogenic effects involving complex and interacting mechanisms. Limited preventive and treatment methods are currently available for this condition. On the other hand, non-OSA-related IH has beneficial or detrimental effects on the body, depending on the degree, duration, and cyclic cycle of hypoxia. It includes two main states: intermittent hypoxia in a simulated plateau environment and intermittent hypoxia in a normobaric environment. In this paper, we compare the two types of IH and summarizes the pathologic mechanisms and research advances in the treatment of OSA-CIH-induced atherosclerosis (AS), to provide evidence for the systematic prevention and treatment of OSAS-related AS.

1. Introduction

Intermittent hypoxia (IH) refers to a state of repeated hypoxia–reoxygenation alternating with periods of normoxia. In particular, chronic IH (CIH) mostly occurs in patients with obstructive sleep apnea (OSA) syndrome (OSAS) and is an important pathologic feature of OSAS [1–3], causing damage to multiple systems such as the cardiovascular, nervous, respiratory, circulatory, and endocrine systems.

The disease background of CIH is homogeneous and is mostly seen in patients with OSA. Compared with OSA-CIH, the research background of other types of IH is more complex, and there is no relatively unified and accepted research model, so they are uniformly classified as non-OSA-IH in this paper. Some non-OSA-IH models can have positive effects such as improving the hypoxia tolerance of the body and alleviating cardiac ischemia–reperfusion injury [4], suggesting that different IH patterns can mediate different biological effects.

Patients with OSAS who are exposed to CIH are at an increased risk of developing several major risk factors for atherosclerosis (AS), including obesity, hyperglycemia, hypertension, and dyslipidemia [5–7]. The association between intermittent hypoxia and atherosclerosis has been studied more frequently, but relatively few studies have been conducted on persistent hypoxia and atherosclerosis. The study [8] found that hypoxia induced proliferation of smooth muscle cells and plaque formation in the aorta of ApoE$^{-/-}$ mice after 3 weeks of feeding in a gas chamber with hypoxia ($10.0 \pm 0.5\%$ O$_2$), but not in normoxia. Smooth muscle cell proliferation and plaque formation were found to be induced by hypoxia, but not by normoxia, along with an increase in plasma LDL cholesterol, NADPH-dependent vascular superoxide (O^{2-}), and activation of matrix metalloproteinase 9. Thus, this study not only confirms that chronic sustained hypoxia accelerates the development of atherosclerosis, but also suggests possible mechanisms, such as abnormal lipid metabolism and reactive oxygen species production. We focus on the interrelationship between OSA-IH and AS. The study of sustained hypoxia and AS will be discussed specifically in future studies.

This article will focus on the bidirectional clinical impact of IH, the pathologic mechanisms by which OSA-CIH causes AS, and the current research advances in treatment methods, with the aim of providing a reference for the prevention and treatment of AS secondary to OSAS.

2. Dual Nature of IH

There are several different models of IH, capable of producing positive or negative effects on the organism, i.e., the two-sided nature of IH. Most cases of OSA-related IH are chronic (i.e., OSA-CIH), which can induce the onset of AS and hence produce various pathologic outcomes. Non-OSA-IH can exert different effects on the body depending on its intensity; that is, low-intensity IH can have several protective effects, whereas high-intensity IH mostly leads to adverse consequences, which suggests that the physiologic effects of IH are correlated with its intensity [9]. In the non-OSA-IH paradigm, central sleep apnea (CSA) as a sleep disorder is mostly a chronic process with a complex classification and different effects on the organism. Our discussion of non-OSA-IH is dominated by patterns that bring positive effects to the organism (see Table 1 and Figure 1).

2.1. OSA-CIH. OSA is mainly characterized by upper airway obstruction during sleep and discontinuous nighttime sleep, leading to repeated hypoxia-reoxygenation cycles that last from weeks to years, resulting in CIH. Upper airway narrowing is an important structural basis for this. The cross-sectional area of the pharyngeal airway is significantly reduced in OSA patients compared to non-OSA patients [24]. OSA-CIH can promote oxidative stress by increasing ROS expression, inflammation by increasing NF-κB activity, and blood pressure elevation and inflammatory response by increasing carotid body-mediated sympathetic activity [25], which leads to a variety of cardiovascular and cerebrovascular diseases occurrence and development. Patients with OSAS tend to have a chronic course of disease. Their hypoxic state usually manifests as CIH (characterized by a long duration of severe hypoxia with a high frequency of episodes and short cycles), which can result in a wide range of adverse consequences. For example, OSA-CIH can significantly increase the morbidity and mortality of various diseases and is an independent risk factor for cardiovascular diseases [26]. OSA was reported to be significantly correlated with the incidence and severity of hypertension [27]. A cross-sectional study covering 2677 adults showed that the number of patients with hypertension increased linearly with the severity of OSA and that each increase in sleep apnea was associated with a 1% increase in the odds of developing hypertension [28]. A first retrospective study describing comorbidities in Hungarian and Romanian OSA patients showed that various diseases such as cardiovascular diseases (e.g., hypertension and arrhythmias), diabetes, and asthma were strongly associated with OSA severity in the whole study population and that OSA-CIH played an important role in it [29]. Khamsai et al. found that patients with OSA combined with hypertension were much more likely to develop hypertensive crisis than the general population

[30], greatly increasing the risk of various cardiovascular and cerebrovascular diseases. It was also noted that carotid artery intima-media thickness and AS-related inflammatory markers were significantly increased in hypertensive patients with combined OSA, confirming the damage to the vascular endothelium caused by this pathological phenomenon [31]. In addition, the risk of atrial fibrillation is significantly increased by OSA-CIH and exponentially increased by the presence of both OSAS and heart failure [32–38]. OSA-CIH can also facilitate the development of coronary heart disease [39], heart failure [40], and aortic dissection [41]. Among them, OSA was significantly associated with the incidence of aortic coarctation. A meta-analysis noted an increased risk of up to 433% between moderate-to-severe OSA and aortic coarctation, but the incidence of aortic coarctation in patients with OSA has not been derived due to the relatively short follow-up period of the study [42]. In terms of metabolic diseases, a meta-analysis [43] revealed that moderate-to-severe OSA was associated with an increased incidence of type 2 diabetes mellitus. This may be because OSA-CIH can cause glucose metabolic disorders by increasing oxidative stress (OS) and inflammation and can directly affect the pancreatic β-cells, liver, and other organs and tissues, thereby influencing glucose homeostasis [44]. Furthermore, this hypoxic pattern can lead to liver fibrosis, inflammation, and liver damage by inducing inflammatory mediators such as nuclear factors, resulting in hepatic dyslipidemia that can further develop into nonalcoholic fatty liver disease [45]. Therefore, OSA-CIH plays an important role in promoting the development of many AS-related diseases.

2.2. Non-OSA-IH. The effects of non-OSA-IH on the organism are closely related to the duration, frequency, and degree of hypoxia: short, low-frequency, and mild hypoxia usually has a protective effect on the organism, while the opposite causes damage to the organism [9].

The current research on non-OSA-IH mainly includes three types of intermittent low-pressure hypoxia, intermittent normobaric hypoxia, and CSA related IH, which can have different effects on the organism depending on the duration, frequency, and cyclic cycle of hypoxia. Each of them will be discussed in the following section.

Many studies have found that residents of high altitude areas have a relatively low incidence of heart attacks and coronary heart disease mortality [46]. Therefore, many scholars have found that such intermittent hypoxia has various protective effects on the organism after intermittent low-pressure hypoxia training in a low-pressure chamber (4-8 hours per day, with the rest of the day at atmospheric pressure) simulating a high-altitude environment. For example, when expedition members underwent IH training in a hypobaric chamber at a simulated altitude of 4000–5500 m, their time spent exercising significantly increased, and their erythrocyte, reticulocyte, and platelet counts were found to be elevated [19]. These findings suggest that this type of IH can enhance the oxygen-carrying capacity and tolerance to ischemia and hypoxia of tissues, thus improving exercise endurance. Left ventricular function was assessed in isolated

TABLE 1: Comparison of animal models of OSA-CIH and non-OSA-IH.

Mode of action	OSA-CIH	Non-OSA-IH	
Pneumatic pressure	Atmospheric pressure intermittent hypoxia	Low pressure (exposure to low-pressure, low-oxygen environment for 4-8 hours per day)	Atmospheric pressure intermittent hypoxia
Cycle duration	Short cycle duration (s)	Long cycle duration (h)	Short cycle duration (min)
Inhaled oxygen	Approximately 5–21% FiO_2	$FiO_2 < 21\%$	Approximately 5–21% FiO_2
Hypoxia duration per cycle	Several seconds	Several hours	Several minutes
Duration of exposure	Several months to several years	Approximately 2–6 weeks	Approximately 2–6 weeks
Effect on the organism	Abnormal liver lipid metabolism [10], liver injury [11], endothelial cell dysfunction [12], hypercholesterolemia, and lipid peroxidation [13]	Positive (low-intensity IH): protects against myocardial ischemia-reperfusion injury [14], prevents arrhythmia [15]	Positive (low-intensity IH): prevents arrhythmia and myocardial infarction [16], improves myocardial contractile function [17], etc.
Clinical features/ applications	Seen in patients with OSAS, mostly causes adverse effects	Enhance the physical fitness and training outcomes of athletes [18, 19], relieve coronary heart disease [20]	Improvement/treatment of cognitive dysfunction [21], spinal cord injury [22], chronic obstructive pulmonary disease [23]

Note: Low-intensity IH: 9–16% inhaled oxygen + low number of cycles (3–15 cycles/d) [9].
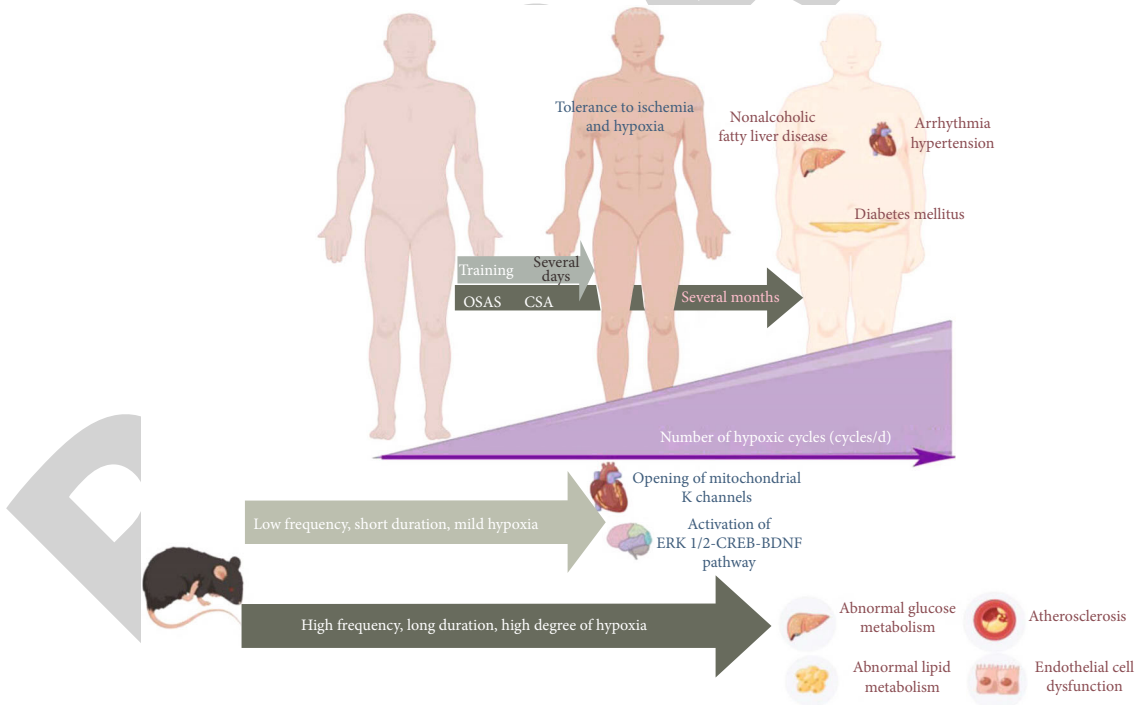
FIGURE 1: Bidirectional nature of intermittent hypoxia (blue represents the positive effect, red represents the negative effect). The bidirectional nature of intermittent hypoxia means that different patterns of IH can have positive or negative effects on the body. For example, several days of IH training in athletes may improve their tolerance to ischemic hypoxia, whereas patients with OSA or CSA may show multiple pathological outcomes after several months. Animal studies have found that low-frequency, short-duration, mild hypoxia can have a protective effect on the cardiovascular and cerebrovascular system through various mechanisms, while high-frequency, long-duration, severe hypoxia can lead to various pathological outcomes such as abnormal glycolipid metabolism.

hearts of rats treated with similar chronic intermittent low-pressure hypoxia (CIHH, at an altitude of 3000 m, CIH environment). It was found that after treatment of isolated hearts with ischemia/reperfusion injury, the recovery of cardiac function was significantly enhanced in CIHH rats compared with controls, and they had higher superoxide dismutase levels and total antioxidant capacity. These protective effects were counteracted by the addition of an ATP-sensitive potassium (KATP) channel inhibitor, a mitochondrial KATP inhibitor, and a mitochondrial permeability transition pore opener. This study not only demonstrated the protective effect of CIH, but also verified for the first time that this effect was associated with KATP channels [14] In addition to the cardiac benefits, intermittent low-pressure hypoxic training has been shown to contribute to weight loss and glycemic control in prediabetic obese patients and is expected to help restore normal fasting glucose in prediabetic patients [47].

Central sleep apnea occurs when the drive to breathe by the medullary respiratory center is temporarily stopped resulting in the disappearance of both oral and nasal airflow and thoracic and abdominal movements. Its classification is complex and includes primary central sleep apnea, central sleep apnea due to Cheyne-Stokes breathing pattern, and central sleep apnea due to high altitude periodic breathing. Unlike the intermittent hypoxia that simulates a high altitude environment above, travelers to high altitudes are in a continuous hypoxic state for a specific period of time and usually experience central sleep apnea, which manifests as restless sleep and nonresolving sleep upon awakening. Hyperventilation occurs after exposure to hypoxia and increases with time, usually after about 10 minutes of hypoxia in the form of gradual strengthening-decreasing respiration, with a gradual increase in respiratory amplitude, resulting in a gradual decrease in $PaCO_2$ and an apnea, followed by an increase in inspiration, and so on and so forth, showing periodic breathing. The main mechanism is hypoxemia. Chronic respiratory stimulants and CO_2 inhalation can reduce or even eliminate this periodic respiration [48].

Multiple factors can contribute to the development of CSA and often coexist with OSA, making the classification complex. CSA is associated with a variety of diseases, such as heart failure, renal failure, and stroke. Similar to OSA, CSA is also associated with intermittent hypoxia, but due to the complexity of the respiratory pattern and the diversity of classification of CSA, there are few animal studies on CSA-IH, and a relatively perfect animal model cannot be summarized for reference. In contrast, the animal model of OSA is relatively simple to construct, so most of the current animal studies on IH use OSA as the research background, and Table 1 is also compiled through these literatures.

In addition to the low-pressure environment similar to the plateau environment, IH at atmospheric pressure has also been shown to have positive effects [49, 50]. For example, IH can improve mitochondrial efficiency and enhance tissue perfusion by activating hypoxia-inducible factor 1α (HIF-1α), which enhances muscle oxygen homeostasis [51–53]. In addition, under IH conditions, blood pressure

in hypertensive patients is significantly reduced or even normalized [54, 55]. A study conducted in patients with stage I hypertension demonstrated for the first time that IH conditioning can lower blood pressure by affecting nitric oxide (NO) synthesis. Hence, IH conditioning can be a nonpharmacologic treatment option for patients with stage I hypertension [55]. Furthermore, IH preconditioning in rats [50] and dogs [56] led to a reduction in infarct size in both animal models, as well as to a lower incidence of ventricular arrhythmias in dogs. This protective effect may be achieved through increased NO production or adrenergic receptor activation [56].

In addition, non-OSA-IH can improve neurocognitive function [57], enhance innate immunity [58], and induce endogenous cardioprotection through oxidative stress [59]. Hence, it is expected to provide new ideas and methods for the treatment of many diseases.

3. Pathophysiologic Mechanisms Underlying OSA-CIH-Induced AS

3.1. Inflammation.
Because inflammation plays a crucial role in AS development, AS is considered a chronic inflammatory disease [60, 61]. Studies have shown that CIH can induce AS through the activation of inflammatory [62] pathways, including HIF, nuclear factor kappa-B (NF-κB), and Toll-like receptor 4 (TLR4).

HIF belongs to the family of transcriptional activators. HIF-1, the first member of its family to be identified, consists of oxygen-sensitive HIF-1α and constitutively expressed HIF-1β, which are present in all mammalian cells and are able to respond sensitively to hypoxic environments [63, 64]. Animal studies have found that CIH significantly upregulates HIF-1α levels in vivo [65]. HIF-1α has been clearly demonstrated to be associated with atherosclerosis: it promotes macrophage activation and conversion into proinflammatory cells, releasing IL, TNF, and other cytokines, which have an impact on plaque formation and stability [66]. In vivo studies in LDL$^{-/-}$ mice have found that HIF-1α deficiency in bone marrow cells substantially reduces atherosclerosis by a mechanism associated with HIF-1α affecting its inflammatory properties [67]. In addition, HIF-1α can also promote the formation and development of atherosclerosis by affecting glucose metabolism and apoptosis of macrophages, migration and proliferation of vascular smooth muscle cells, and permeability of endothelial cells [68].

The NF-κB pathway is one of the major inflammatory pathways. One study [69] found that CIH exposure not only increased NF-κB binding activity in a time-dependent manner across multiple organs and tissues in mice but also increased the expression of inducible NO synthase, an NF-κB-dependent gene product. Furthermore, patients with OSAS showed significantly increased monocyte NF-κB activity compared with controls, which significantly decreased when their CIH was corrected. These findings suggest that CIH is an important pathologic mechanism leading to NF-κB activation in patients with OSAS. In an experimental study [70], CIH + a high-cholesterol diet

(HCD) induced AS development, whereas knockdown of the NF-κB P50 subunit eliminated the AS lesions induced by CIH + HCD by significantly inhibiting three major atherogenic mechanisms: vascular inflammation, hypercholesterolemia, and macrophage foam cell formation. Therefore, NF-κB may serve as a common pathway through which CIH activates multiple atherogenic mechanisms that can synergistically act to cause the onset and development of AS. In addition, elevated plasma levels of several NF-κB target gene products, such as tumor necrosis factor alpha (TNF-α), interleukin-6 (IL-6), and vascular cell adhesion molecule-1 (VCAM-1), have been observed in patients with OSAS [71–73]. NF-κB activation not only accelerates the development of metabolic syndrome [74] but also mediates the expression of factor VIII [75] and tissue factor [76], thereby promoting coagulopathies. Thus, NF-κB plays an important role in various AS-promoting mechanisms, such as proinflammatory and procoagulatory processes.

TLR4 is the upstream molecule of NF-κB. As a pattern recognition receptor, it may be involved in the activation of plaque inflammation [77]. Akinnusi et al. [78] demonstrated that TLR4 influenced the activation of the inflammatory response in patients with OSAS. Zeng et al. [79] found that IH could promote TLR4 expression in endothelial cells and TLR4/NF-κB activation, which was followed by the production of inflammatory factors. Furthermore, TLR4 interference not only led to a significant reduction in inflammation but also decreased the AS plaque load and plaque vulnerability by more than half. These findings have helped elucidate the effects of TLR4 on inflammation and atherosclerotic plaque formation, suggesting that IH may promote inflammation by activating the TLR4/NF-κB pathway, thereby inducing AS. Therefore, TLR4 may play an important role in interventions for AS induced by OSAS (or IH) in the near future.

In addition, inflammatory markers such as adhesion molecules and tumor necrosis factor have been strongly associated with atherosclerosis [80, 81]. In clinical studies, Dyugovskaya et al. found that the expression of two adhesion molecules, CD15 and CD11c, was significantly increased in OSA patients compared to controls, and their monocytes adhered more readily to endothelial cells than controls. Treatment with nasal continuous positive airway pressure ventilation significantly suppressed both of these changes [82]. Minoguchi et al. found that TNF-α levels were significantly increased in patients with moderate to severe OSAS compared to the other three groups, possibly accelerating the development of atherosclerosis, in a study of healthy people, obese people, patients with mild OSAS, and patients with moderate to severe OSAS. This alteration was independently associated with the duration of hypoxia during sleep. Treatment with nasal continuous positive airway pressure ventilation significantly improved this change [83]. Thus, hypoxia can activate the inflammatory response and promote the development and progression of atherosclerosis through multiple pathways.

3.2. Abnormal Platelet Function. Platelet aggregation and activation are abnormally enhanced in patients with OSAS [84, 85]; hence, they play an important role in promoting the pathogenesis of AS and plaque rupture [62]. An increase in OSA severity is associated with an increase in both platelet aggregation and activation [86]. More specifically, IH and reoxygenation can enhance platelet aggregation through substances such as adenosine diphosphate and TNF-α in vivo [87, 88]. Furthermore, treatment with continuous positive airway pressure (CPAP) can improve platelet aggregation [84, 89], which may delay the development of AS.

Mean platelet volume (MPV) reflects the average size of circulating platelets and is used to assess platelet activity [90]. It is not only associated with various risk factors for cardiovascular diseases, such as hypertension and diabetes [91], but is also closely related to thromboembolic complications and adverse outcomes of cardiovascular events [92]. MPV has been found to increase with the severity of OSA [93] and was reported to be positively correlated with the apnea–hypopnea index [94, 95]. Meanwhile, patients who underwent uvulopalatal flap surgery showed significantly decreased MPV [96]. Notably, both the frequency and level of nocturnal hypoxemia can promote platelet activation [97], which can have a further impact on AS.

Platelet-derived particles (PMP) are nanoscale fragments released by platelets and are the most abundant particles in human blood, reflecting the degree of platelet activation. Because of its highly procoagulant effect, it has been considered as a prognostic marker for atherosclerosis [98]. Researchers who studied patients with mild OSA versus control subjects without OSA found that patients with mild OSA had significantly higher PMP levels compared to controls [99]. Another study of patients with different degrees of OSAS showed that plasma PMP levels were significantly higher in patients with severe OSAS compared to both patients with mild to moderate OSAS and the normal group, and that PMP levels correlated with AHI. The study also demonstrated that CPAP was able to reduce the level of this particle [100]. All of the above studies can demonstrate the effect of OSA on PMP levels, in which IH plays an important role.

In addition to platelets, coagulation factor levels were also altered in OSA patients. The thrombin-antithrombin (TAT) complex marks the formation of intravascular thrombin, indicating enhanced coagulation. A clinical study showed increased levels of several activated coagulation factors, including TAT, in patients with OSA [101]. As a major coagulation protein, fibrinogen can form insoluble clots or gels when converted to fibrin by thrombin, thus affecting platelet aggregation, and its levels are associated with atherosclerosis [102], which is an important risk factor for cardiovascular disease [103]. Clinical studies have found not only an increase in fibrinogen in patients with OSA, but also a linear relationship between its levels and AHI [104].

3.3. Glycolipid Metabolism Disorder. OSAS can alter the patient's metabolic status and significantly increase the incidence of metabolic syndrome [105]; CIH induces abnormal glucose metabolism not only by causing the replication and apoptosis of pancreatic β-cells [106, 107] but also by promoting β-cell damage and dysfunction [108]. An

experimental study [109] found that mice in the CIH group had significantly higher fasting blood glucose and serum insulin levels, compared with mice in the normoxic group, while also exhibiting abnormal glucose metabolism and insulin resistance (IR). The specific mechanisms involved in CIH-mediated IR mainly include reduced phosphorylation, action, and sensitivity of tyrosine kinase (an insulin receptor); inhibition of insulin secretion; and increased production of glucocorticoids and epinephrine [110]. CIH also affects lipid metabolism by increasing the total cholesterol and low-density lipoprotein (LDL) cholesterol (LDL-C) levels in mice, leading to dyslipidemia. Among ApoE$^{-/-}$ mice fed a high-fat diet, those that were also exposed to CIH showed significant differences in AS damage to the aortic sinus and descending aorta compared with normoxic mice [111]. LDL can undergo oxidative modification to produce oxidized LDL (Ox-LDL), which can affect inflammation and AS formation. Studies have demonstrated that the upregulation of Ox-LDL is influenced by CIH [112]. Thus, CIH can mediate the development of AS through an abnormal glycolipid metabolism (see Figure 2).

The current clinical evidence on OSA and dyslipidemia is dominated by cross-sectional studies. Trzepizur et al. found by oxygen saturation index (ODI) in 2081 patients that high triglyceride levels and low HDL cholesterol levels were associated with nocturnal IH and OSA severity and may increase the incidence of cardiovascular disease in patients with OSA [113]. Another clinical study showed that OSA can dynamically increase plasma free fatty acid levels during sleep and that CPAP can attenuate this change, again suggesting an important role for IH in this [114]. This change may be due to the fact that IH regulates hormone-sensitive lipase (HSL) by activating the sympathetic nervous system, thus triggering lipolysis [115].

Recent studies have shown that sex hormones have a regulatory effect on glucose metabolism under CIH conditions. Marcouiller et al. [116] treated mice using either excipients or estradiol and placed them in normoxic or CIH environments, respectively. The results showed that IH impaired glucose tolerance in female mice, particularly in ovariectomized mice, but this effect was reversed by estradiol supplementation, and pancreatic b-cell function was improved. This provides new evidence for improving glycolipid metabolism in the CIH environment.

3.4. Oxidative Stress. The continuous and repetitive hypoxia–reoxygenation cycle in CIH causes extensive OS, resulting in endothelial damage and accelerated AS formation [117]. The CIH environment induces the upregulation of peroxidation markers such as malondialdehyde and ROS [118–120]. Of these, excessive ROS can promote VCAM production, leukocyte activation, and systemic inflammation, leading to vascular endothelial damage and dysfunction [110], thereby resulting in the development of AS. In addition, CIH can inhibit endothelial nitric oxide synthase (eNOS) activity and reduce NO levels, causing platelet aggregation and vasoconstriction [121]. Furthermore, metallothionein is a strong antioxidant and is one of the most effective proteins in eliminating free radicals. Under CIH,

metallothionein-deficient mice showed more severe arterial inflammation, fibrosis, and oxidative damage, whereas the arterial metallothionein levels of normal mice showed a sharp increase, followed by a decrease. This suggests that CIH mediates OS via the metallothionein pathway [122], thereby promoting the onset and development of AS. In addition, it has been found that the activation of oxidative stress by CIH can be inhibited by progesterone. According to Joseph et al. [123], ovaries of female rats were excised, implanted with osmotic pumps delivering excipients or progesterone, and exposed to room air or CIH, respectively, and divided into three groups: Veh-AIR, Veh-CIH, and Prog-CIH. The results showed that progesterone not only reduced the frequency of CIH-induced apnea and increased hypoxic and hypercapnic ventilatory responses, but also prevented the occurrence of increased NOX activity and decreased cytosolic and mitochondrial SOD activity by CIH. Thus, sex hormones are expected to intervene in the development of related AS by inhibiting CIH-induced oxidative stress.

Cofta et al. responded to oxidative stress levels in OSA patients by plasma total antioxidant status (TAS) and thiobarbituric acid reactive substances (TBARs), which have been shown to be associated with atherosclerosis. This study found that TAS decreased and TBARs increased with increasing severity of OSA [124]. This result is consistent with the findings of Barceló et al. on lipid peroxidation in patients with OSA [125], suggesting the presence of significant oxidative stress alterations in OSA patients.

As one of the intermediate mechanisms of CIH-induced AS, OS also synergistically acts with inflammation, causing damage to the vascular endothelium and hence inducing AS. Tuleta et al. [12] divided ApoE$^{-/-}$ mice into the intermittent air exposure group and the CIH group and found that endothelial function was more severely impaired in the CIH group after 6 weeks; however, they also found that vascular damage can be inhibited by a combination of anti-inflammatory and antioxidant therapy (infliximab + glutathione). Their findings imply that CIH can cause vascular endothelial damage through the synergistic effects of inflammation and OS, which can lead to AS development in severe cases, but it can be effectively treated using combined anti-inflammatory and antioxidant therapy.

3.5. Apoptosis. Apoptosis is involved in several pathophysiologic processes and has received increasing research attention as one of the intermediate mechanisms of CIH-induced AS. Apoptosis can suppress injury by attenuating the phagocytosis, migration, and ROS production of neutrophils, whereas delayed apoptosis can exacerbate injury [126–128]. One study [129] reported that IH in patients with OSAS triggered increased neutrophil apoptosis, which induced cardiovascular injury. By conducting *in vitro* experiments on human neutrophils [130], researchers found that IH-treated neutrophils showed an imbalance between Bax of the Bcl-2 protein family (pro-apoptotic) and Mcl-1 (antiapoptotic), as well as prolonged neutrophil survival, which led to persistent inflammation. This process may be affected by the proteolytic enzymes and free radicals released through the interaction of neutrophils and endothelial cells [118]. In addition,
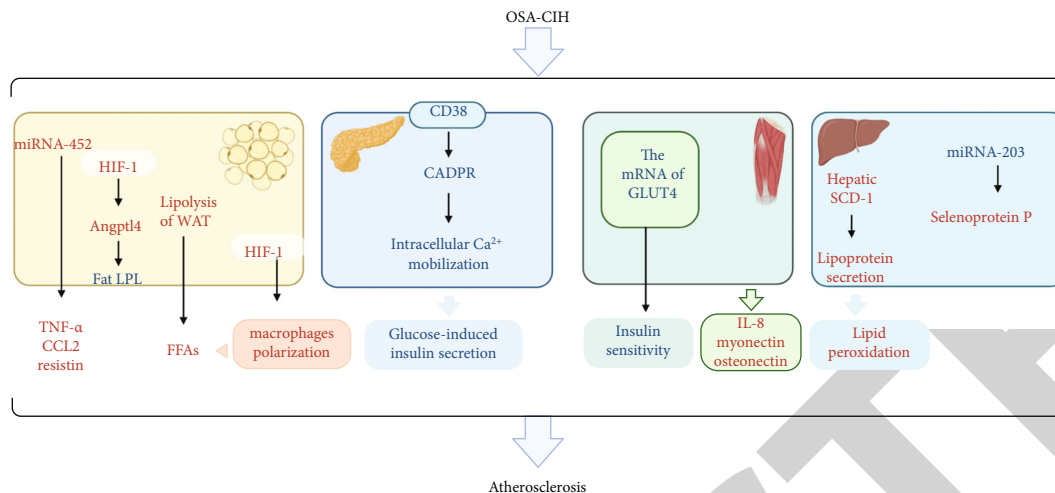
FIGURE 2: Possible mechanisms by which OSA-CIH induces atherosclerosis through abnormal glycolipid metabolism (red represents promoted expression and blue represents inhibited expression). OSA-CIH promoted the expression of microRNA-452 in adipose tissue, increased the levels of TNF-α, CCL-2, and Resistin; at the same time, it can accelerate lipolysis of white adipose tissue, activation of hypoxia-inducible factor-1, and polarization of macrophages to proinflammatory subtype M1, resulting in the release of more free fatty acids, resulting in fat aggregation; under CIH stimulation, hypoxia-inducible factor-1 (HIF-1) is activated, and lipoangiogenin 4 (Angptl4) is upregulated, leading to the inactivation of lipoprotein lipase (LPL); intracellular mobilization of Ca^{2+} stored in the er and extracellular Ca^{2+} influx play an important role in glucose-induced insulin secretion (GIS). Cyclic ADP-ribose (CADPR) is a second messenger that mobilizes Ca^{2+} from intracellular Ca^{2+} pools. CD38 has the activities of ADP-ribose cyclase and CADPR hydrolase for the synthesis and hydrolysis of CADPR, respectively. In the occurrence of OSA-CIH, CD38mRNA transcription level is significantly inhibited, cADPR level is reduced, and intracellular Ca^{2+} mobilization is impaired, which leads to decreased GIS and may induce T2DM. Studies have shown that OSA-CIH inhibits the expression of glucose transporter 4 (GLUT4) in skeletal muscle, leading to decreased insulin sensitivity and glucose uptake, accelerating the occurrence of T2DM. In addition, OSA-CIH can induce T2DM by promoting the expression of various muscle factors (IL-8, osteonectin, and myonectin). When severe OSA-CIH occurs, liver stearoyl-CoA desaturase 1 (SCD-1) is significantly increased, which increases the secretion of lipoprotein in the body, induces the occurrence of liver lipid peroxidation, and promotes the occurrence of hyperlipidemia. In addition, OSA-CIH also inhibits the expression of microRNA-203 and promotes the expression of selenophenol P to accelerate T2DM.

lysophosphatidylcholine, one of the components of Ox-LDL, can induce apoptosis in vascular endothelial cells via the p38 mitogen-activated protein kinase (MAPK) pathway, which may lead to AS formation [131].

Survivin is a member of a family of apoptosis inhibitors with complex immunomodulatory effects. A study by Kunos et al. found that plasma survivin was significantly lower in OSA patients compared to non-OSA subjects, correlating not only with OSA severity but also with high BMI, low HDL-C, and high TG levels [132]. This suggests that immune regulation is impaired in OSA patients, and the exact mechanism needs further study and explanation. Klotho is a protein secreted mainly by the kidneys and known for its antiaging properties [133]. Pákó et al. studied plasma klotho levels in OSA patients and non-OSA volunteers and found that CIH decreased the levels of this protein in OSA patients, which may not only promote the development of hypertension but may also have an impact on the inflammatory process [134].

Under IH conditions, the apoptosis of different cells can have different effects on AS. More specifically, insufficient or delayed apoptosis of inflammatory cells can lead to persistent inflammation and contribute to the onset and progression of AS, whereas excessively high levels of apoptosis of vascular endothelial cells can induce IH-mediated cardiovascular diseases. Furthermore, CPAP has been shown to have

an ameliorative effect on the apoptosis of vascular endothelial cells [135]. Therefore, apoptosis plays an important role in the process of IH-mediated AS.

3.6. Neuroendocrine Disorders. Patients with OSAS experience frequent nocturnal awakenings, IH, and daytime sleepiness, which can lead to sustained excitation of the sympathetic nervous system. This, in turn, increases catecholamine release and activates the renin–angiotensin–aldosterone system (RAAS), resulting in neurohumoral dysregulation. Neuroendocrine abnormalities can accelerate the formation and development of AS in several ways. Trombetta et al. [136] found that patients with multiple sclerosis and OSAS showed stronger muscle sympathetic reflex activation than those without OSAS, which could be attributed to the enhanced peripheral and central chemoreflex responses in OSAS. Other studies [137, 138] have also demonstrated that the occurrence of CIH in patients with OSAS may lead to the inability of the carotid body to maintain a normal dynamic balance of oxygen in the body, which may induce AS through mechanisms involving RAAS upregulation, OS, and inflammatory response in the carotid body.

3.7. Small-Molecule RNAs. The occurrence of CIH-mediated AS is accompanied by the abnormal expression of small-molecule RNAs. Most of the existing studies have mainly

Table 2: Basic research on drugs for the treatment of OSA-related AS.

Drug name	Research subjects	Hypoxic conditions in the experimental group	Intervention period (weeks)	Experimental dose	Mechanism of action
DHA [148]	Male ApoE$^{-/-}$ mice	5–21% FiO$_2$, 60 s/cycle, 8 h/d	8	Dietary intake of 0.5% fish oil (containing 80% DHA/4% eicosapentaenoic acid)	AA↓, MMP-2 expression↓ → AS↓
Mirabegron [156]	Male ApoE$^{-/-}$ mice	5–21% FiO$_2$, 60 s/cycle, 8 h/d	6	10 mg/kg/d	Nitrotyrosine↓, dihydroglutaraldehyde↓, SOD↑, GSH↑ → OS↓ → AS↓
	Male C57BL/6 mice	6–21% FiO$_2$, 60 s/cycle, 8 h/d	12	5 mg/kg/d	OS↓ → AS↓
Atorvastatin [158, 163]	Male Wistar rats	5–21% FiO$_2$, 60 s/cycle, 8 h/d	Simultaneous protocol for 2 weeks Delayed protocol for 4 weeks	10 mg/kg/d	
Chinese medicine [162]	Male ApoE$^{-/-}$ mice	(10 ± 0.5 %)–(21 ± 0.5%) FiO$_2$, 180 s/cycle, 8 h/d	8	Medium dose: 1500 mg Zhenyuan capsule +500 mg ligustrazine phosphate tablet. The high-dose and low-dose groups were administered 2 times and 1/2 of the medium dose, respectively.	LDL-C↓, TNF-α↓, HIF-1α↓, SREBP-1c↓, FAS↓; SOD↑, HDL-C↑ → blood lipid↓, inflammation↓, OS↓ → AS↓
Montelukast [164]	Male ApoE$^{-/-}$ mice	21–5% FiO$_2$, 60 s/cycle, 8 h/d	8	1 mg/kg/d	CysLT 1 receptor blocking → vascular remodeling↓ → AS↓
DMB [165]	Male Ldlr$^{-/-}$ mice; male ApoE$^{-/-}$ mice	21–8% FiO$_2$, 0.5–8% CO$_2$, 8 min/cycle, 10 h/d	8	1.0%, vol/vol	TMA↓ → TMAO↓ → inflammation, dyslipidemia↓ → AS↓
Propofol [161]	Human endothelial cell line EA.hy926 cells	1% O$_2$ 10 min +21% O$_2$ 5 min, 15 min/cycle	64 cycles	0, 25, 50, and 100 μM (four concentrations)	p38 MAPK↓ → NF-κB↓, IL-6↓, TNF↓, IL-1β↓ → inflammation↓ → AS↓
Salidroside [166]	Male ApoE$^{-/-}$ mice; HUVECs	Hypoxic conditions for mice: 21%–5%–21% FiO$_2$, 120 s/cycle, 12 h/d Hypoxic conditions for HUVECs: 21%–5%–21%, 40 min/cycle	7 weeks for mice; 72 cycles for HUVECs	Mice: 100 mg/kg/d; HUVECs: 10 or 100 μM	cAMP/PKA↑ → RhoA/ROCK↓ → ROS↓ → endothelial barrier function↑ → AS↓

GSH: glutathione; SOD: superoxide dismutase; FiO$_2$: fraction of inspiration oxygen; AA: arachidonic acid; MMP-2: matrix metalloproteinase 2; DHA: docosahexaenoic acid; SREBP: sterol-regulatory element-binding protein; FAS: a downstream molecule of SREBP-1c; SOD: superoxide dismutase; HDL-C: high-density lipoprotein cholesterol; IHR: intermittent hypoxia/reoxygenation; HUVECs: human umbilical vein endothelial cells; ROS: reactive oxygen species; RhoA: ras homolog gene family member A; ROCK: rho-associated protein kinase; PKA: protein kinase A; CysLT: cysteinyl leukotriene; DMB: 3,3-dimethyl-1-butanol; ApoE$^{-/-}$, apolipoprotein E deficient; Ldlr$^{-/-}$: low-density lipoprotein receptor deficient; IHC: intermittent hypoxia and hypercapnia; RA: room air; HFD: high-fat diet; TMA: trimethylamine; TMAO: trimethylamine N-oxide.

focused on mRNAs, microRNAs, and long noncoding RNAs. In a study that analyzed the differential expression of mRNAs and long noncoding RNAs in atherosclerotic vascular tissues of ApoE$^{-/-}$ mice, markedly fewer genes were significantly upregulated in mice exposed to CIH for 12 weeks than in mice exposed to CIH for 8 weeks, which leads to weakening of atherosclerotic vascular tissue. The specific mechanism involved was related to the abnormal expression

of heat shock proteins caused by CIH via the endoplasmic reticulum protein processing pathway [139]. This study also showed that the long-term CIH exposure resulted in reduced mRNA expression of Rev-erb (a member of the nuclear receptor superfamily that is important for the regulation of immunity, metabolic function, and circadian rhythm) and exacerbated the development of atherosclerosis, suggesting that Rev-erb may be involved in the development of CIH-related AS and play an important role in it. An experiment on male volunteers revealed that after exposure to IH, plasma exosomal microRNAs disrupted the impedance levels while also significantly enhancing the expression of intercellular adhesion molecule-1 and significantly reducing the expression of eNOS in endothelial cells [140]. Thus, IH can alter the exosomes circulating in the body, increase the permeability and affect the function of endothelial cells, and promote the onset and development of AS.

3.8. *Intestinal Microorganism.* There is now growing evidence that gut microbes play an important role in the development of CIH-induced AS. Hu et al. [141] divided ApoE$^{-/-}$ mice into control, AS, and AS+CIH groups and fed them with normal and high-fat diets, respectively. It was found that (i) there was a disturbed gut microbiota in the AS mice; (ii) CIH promoted the development of AS while interfering with the gut microbiota and worsened the disturbed gut microbiota in the mice. Xue et al. [142] used similar experimental methods to confirm the AS-causing effect of CIH and its effect on intestinal microbiota, which may act on the development of AS in various ways, including inflammation and lipid metabolism. Clinical studies have also demonstrated a link between OSA and intestinal flora. Studies in patients with OSA have found altered intestinal epithelial barrier markers and increased intestinal permeability, and this intestinal damage may lead to abnormal lipid metabolism in the liver, which is associated with atherosclerosis [143]. Kheirandish-Gozal, L et al. showed that obese children with OSA had the highest levels of bacterial lipopolysaccharide-binding protein (LBP), a surrogate for intestinal bacterial lipopolysaccharide-induced hypoendotoxemia marker. Therefore, it can be speculated that OSA may disrupt the intestinal microbiota and cause other damage to the body [144].

Therefore, although the mechanisms involved are not yet clear, the link between gut microbes and OSA-associated AS is gradually being recognized and is expected to be used for the prevention and treatment of OSA-associated AS in the near future.

4. Advances in Drug Research for OSA-Related AS

New treatment methods are continuously being developed with the gradual increase in the incidence of OSAS. Individuals at a high risk of developing AS require not only correction of IH but also prevention and treatment of AS. Currently, CIH is corrected using nonpharmacologic methods (e.g. CPAP, oral appliances, and sublingual nerve stimulation) supplemented with pharmacologic treatment, whereas the treatment of CIH-related AS is primarily based on drugs, which include drugs for controlling traditional AS risk factors and improving the tolerance of the body to IH. In this section, we will review and summarize the current research advances in the pharmacological treatment of OSA-related atherosclerosis. But most pharmacologic studies related to OSAS are currently in the preclinical stage.

4.1. *Ethyl Polyenoate.* Docosahexaenoic acid (DHA) is an n-3 polyunsaturated fatty acid derived from alternating elongation and desaturation reactions of linolenic acid (a type of essential fatty acid) or eicosapentaenoic acid. This fatty acid is a precursor of several anti-inflammatory lipid mediators (e.g., resolvins and protectins [145]). It has a wide range of actions that can have a role in the regulation of inflammation, thus exerting positive effects [146]. Studies have shown that supplementation with DHA and eicosapentaenoic acid is effective in reducing the production of several pro-inflammatory cytokines, such as IL-6 and TNF-α, in healthy individuals [147]. In the study by Van Noolen et al. [148] in ApoE$^{-/-}$ mice, DHA prevented CIH-induced AS. This effect was associated with a decrease in arachidonic acid content in tissues and organs and in aortic matrix metalloproteinase-2 expression caused by the increase in DHA and eicosapentaenoic acid.

4.2. *β3-Adrenoreceptor Agonists.* β-Adrenoreceptors (βARs) may serve as a new target for the treatment of IH-related AS. Bae et al. [149] found elevated levels of β1AR in fetal rat hearts under hypoxic conditions. Arioglu-Inan et al. [150] showed that β3AR levels were elevated in patients with cancer, diabetes, and other diseases under hypoxic conditions and also elevated in rat macrophages under IH conditions [151]. As a selective β3AR agonist, mirabegron exerts several physiologic effects. It not only relaxes the smooth muscles of the bladder in the treatment of overactive bladder syndrome [152] but also improves left ventricular ejection fraction in patients with heart failure [153–155]. Wang et al. [156] treated ApoE$^{-/-}$ mice with mirabegron and found that mirabegron was able to prevent CIH-induced AS progression. The underlying mechanism was related to the ability of mirabegron to inhibit OS after β3AR stimulation.

4.3. *Statins.* Statins are widely used in clinical practice for their lipid-lowering, mainly LDL-lowering, effects. However, in addition to lipid lowering, statins have also been demonstrated to improve endothelial function and to have anti-inflammatory effects [157]. They can inhibit the activation of Rho protein, which increases NOS activity and accelerates its expression, accompanied by an increase in endogenous NO, which ultimately reduces the contraction and proliferation of vascular smooth muscle cells. One study [158] showed that CIH exposure for 14 days in rats led to a wide range of deleterious effects, including blood pressure elevation, OS, and vascular sclerosis, with remodeling of the carotid vessel wall occurring after 28 days, all of which were significantly alleviated by the administration of atorvastatin. Therefore, statins are expected to improve CIH-induced AS.

4.4. Propofol. Propofol (2,6-diisopropylphenol) is widely used as an intravenous anesthetic and has been shown to have various anti-inflammatory properties, including inhibition of neutrophil function, alteration of NO production, and reduction of pro-inflammatory cytokine production [159]. Studies have found that the anti-inflammatory effect of propofol is associated with the inhibition of p38 MAPK activation [160]. Li et al. [161] cultured human umbilical vein endothelial cells *in vitro* under an IH/reoxygenation environment, to observe the effects of different propofol doses on NF-κB and HIF-1 activity, as well as on the level of proinflammatory cytokines. Their results showed that 25 and 50 μM propofol had a dose-dependent inhibitory effect on NF-κB activity, which may be based on the inhibition of the p38 MAPK signaling pathway, whereas 100 μM propofol had no significant effect on NF-κB activity. Meanwhile, propofol had no effect on HIF-1 activity regardless of the dose. In addition, 50 or 100 μM propofol had a significant inhibitory effect on various downstream proinflammatory cytokines of NF-κB, such as TNF-α, IL-1β, and IL-6, under IH/reoxygenation. Thus, propofol may prevent OSAS (CIH)-mediated AS by inhibiting NF-κB-mediated inflammation in vascular endothelial cells.

4.5. Chinese Medicine. During the course of research on therapeutic drugs for OSAS or CIH-related AS, marked progress has been made in the field of Chinese medicine. Ma et al. [162] administered a combination of Chinese herbal medicines (ginsenosides and ligustrazine) for supplementing Qi and activating blood circulation to a composite IH- and IR-mediated AS mouse model. Their results showed that ApoE$^{-/-}$ mice in the high-dose group had significantly lower blood glucose, LDL-C, and mRNA and protein expression (TNF-α, HIF-1α, sterol regulatory element-binding protein 1c [(SREBP-1c], and FAS) levels; significantly higher high-density lipoprotein cholesterol and superoxide dismutase levels; and significantly reduced AS plaque area than mice in the CIH group. This experiment demonstrated that the Chinese herbal medicine combination could significantly improve composite IH- and IR-mediated AS through a number of ways, including regulation of blood lipids and mitigation of inflammation, IR, and OS. The specific mechanism may be related to the inhibition of signaling molecules such as SREBP-1c. This study provides a new basis for the treatment of OSAS (CIH)-related AS with Chinese medicine.

In addition to the drugs mentioned above, salidroside and montelukast have also been shown to have therapeutic effects on CIH-AS (see Table 2).

5. Perspective

OSA-CIH generally has adverse consequences in the body, whereas non-OSA-IH exerts different effects under different IH intensities. At present, non-OSA-IH has been applied in sports training to improve exercise tolerance in a hypobaric environment; however, its positive effects remain predominantly reported in animal studies. Future clinical studies conducted in a relatively safe IH environment are warranted

to further confirm its positive effects and lay the clinical foundation for its early and widespread application.

With improvements in living conditions, the number of individuals with obesity has steadily increased, and the incidence of OSAS has gradually increased. OSA-CIH can lead to the formation of AS, and IR plays an important role in this process. However, drug research on this pathologic mechanism is scarce, and only a few studies on Chinese medicine are available. Therefore, more studies are needed to fill the gap and provide new evidence for the drug treatment of this disease.

In conclusion, CIH can contribute to the occurrence and development of AS through multiple mechanisms. Since there are no uniform criteria for classifying IH, this paper classifies them into OSA-IH and non-OSA-IH according to whether they are associated with OSA. it is undeniable that there is some irrationality in this classification, but there is no more uniform and reasonable way to classify them. Patients with OSA usually have many coexisting pathologies, such as obesity, diabetes, and hyperlipidemia, and there is no clear evidence that OSA-CIH directly causes AS and further research is needed. The focus of current research is on the indirect aggravation of risk factors by CIH leading to AS, with fewer studies conducted on the direct relationship between CIH and AS. In addition, owing to the complexity of the underlying mechanisms and the interactions among the different mechanisms, it is difficult to clarify the role of a specific mechanism. Furthermore, molecular research on these mechanisms is still in the early stages, involving only a few molecular pathways and insufficient clinical evidence. Therefore, more thorough investigations are needed to gain a better understanding of the pathogenesis of this disease in order to reduce the incidence of complications and mortality.

Abbreviations

AS: Atherosclerosis
CIH: Chronic intermittent hypoxia
CPAP: Continuous positive airway pressure
DHA: Docosahexaenoic acid
eNOS: Endothelial nitric oxide synthase
HIF: Hypoxia-inducible factor
IH: Intermittent hypoxia
IL: Interleukin
LDL-C: Low-density lipoprotein cholesterol
MAPK: Mitogen-activated protein kinase
NF-κB: Nuclear factor kappa-B
NO: Nitric oxide
OS: Oxidative stress
OSAS: Obstructive sleep apnea syndrome
Ox-LDL: Oxidized low-density lipoprotein
RAAS: Renin–angiotensin–aldosterone system
ROS: Reactive oxygen species
SREBP-1c: Sterol regulatory element binding protein 1c
TLR4:   Toll-like receptor 4
TNF-α: Tumor necrosis factor alpha
VCAM: Vascular cell adhesion molecule.

Data Availability

The data used to support the findings of this study are available from the corresponding author upon request.

Conflicts of Interest

The authors declare that the research was conducted in the absence of any commercial or financial relationships that could be construed as a potential conflict of interest.

Authors' Contributions

Binyu Luo and Yiwen Li performed the reference collection, conducted the reference analysis, and wrote the manuscript and are considered as co-first authors. Yue Liu contributed to the topic conception, manuscript revision, and decision to submit for publication and is the corresponding author. Jing Cui, Mengmeng Zhu, and Yanfei Liu contributed to reference analysis and helped in the revision of the manuscript. All authors contributed to the article and approved the submitted version.

Acknowledgments

References

[1] J. A. Dempsey, S. C. Veasey, B. J. Morgan, and C. P. O'Donnell, "Pathophysiology of sleep apnea," *Physiological Reviews*, vol. 90, no. 1, pp. 47–112, 2010.

[2] J. A. Neubauer, "Invited review: physiological and pathophysiological responses to intermittent hypoxia," *Journal of Applied Physiology*, vol. 90, no. 4, pp. 1593–1599, 2001.

[3] E. C. Fletcher, "Invited review: physiological consequences of intermittent hypoxia: systemic blood pressure," *Journal of Applied Physiology*, vol. 90, no. 4, pp. 1600–1605, 2001.

[4] I. Almendros, Y. Wang, and D. Gozal, "The polymorphic and contradictory aspects of intermittent hypoxia," *American Journal of Physiology. Lung Cellular and Molecular Physiology*, vol. 307, no. 2, pp. L129–L140, 2014.

[5] F. Li, H. Huang, L. Song, H. Hao, and M. Ying, "Effects of obstructive sleep apnea hypopnea syndrome on blood pressure and C-reactive protein in male hypertension patients," *Journal of Clinical Medical Research*, vol. 8, no. 3, pp. 220–224, 2016.

[6] I. W. Seetho, R. Asher, R. J. Parker et al., "Effect of CPAP on arterial stiffness in severely obese patients with obstructive sleep apnoea," *Sleep & Breathing*, vol. 19, no. 4, pp. 1155–1165, 2015.

[7] L. N. Diogo, S. A. Pereira, A. R. Nunes, R. A. Afonso, A. I. Santos, and E. C. Monteiro, "Efficacy of carvedilol in reversing hypertension induced by chronic intermittent hypoxia in rats," *European Journal of Pharmacology*, vol. 765, pp. 58–67, 2015.

[8] D. Nakano, T. Hayashi, N. Tazawa et al., "Chronic hypoxia accelerates the progression of atherosclerosis in apolipoprotein E-knockout mice," *Hypertension Research*, vol. 28, no. 10, pp. 837–845, 2005.

[9] A. Navarrete-Opazo and G. S. Mitchell, "Therapeutic potential of intermittent hypoxia: a matter of dose," *American Journal of Physiology. Regulatory, Integrative and Comparative Physiology*, vol. 307, no. 10, pp. R1181–R1197, 2014.

[10] H. Wang, Y. Wang, T. Xia et al., "Pathogenesis of abnormal hepatic lipid metabolism induced by chronic intermittent hypoxia in rats and the therapeutic effect of N-acetylcystein," *Medical Science Monitor*, vol. 24, pp. 4583–4591, 2018.

[11] V. Savransky, A. Nanayakkara, A. Vivero et al., "Chronic intermittent hypoxia predisposes to liver injury," *Hepatology*, vol. 45, no. 4, pp. 1007–1013, 2007.

[12] I. Tuleta, C. N. França, D. Wenzel et al., "Hypoxia-induced endothelial dysfunction in apolipoprotein E-deficient mice; effects of infliximab and L-glutathione," *Atherosclerosis*, vol. 236, no. 2, pp. 400–410, 2014.

[13] J. Li, V. Savransky, A. Nanayakkara, P. L. Smith, C. P. O'Donnell, and V. Y. Polotsky, "Hyperlipidemia and lipid peroxidation are dependent on the severity of chronic intermittent hypoxia," *Journal of Applied Physiology*, vol. 102, no. 2, pp. 557–563, 2007.

[14] H. M. Bu, C. Y. Yang, M. L. Wang, H. J. Ma, H. Sun, and Y. Zhang, "K (ATP) channels and MPTP are involved in the cardioprotection bestowed by chronic intermittent hypobaric hypoxia in the developing rat," *The Journal of Physiological Sciences*, vol. 65, no. 4, pp. 367–376, 2015.

[15] G. Asemu, J. Neckár, O. Szárszoi, F. Papousek, B. Ostádal, and F. Kolar, "Effects of adaptation to intermittent high altitude hypoxia on ischemic ventricular arrhythmias in rats," *Physiological Research*, vol. 49, no. 5, pp. 597–606, 2000.

[16] P. Zong, S. Setty, W. Sun et al., "Intermittent hypoxic training protects canine myocardium from infarction," *Experimental Biology and Medicine (Maywood, N.J.)*, vol. 229, no. 8, pp. 806–812, 2004.

[17] E. B. Manukhina, L. M. Belkina, O. L. Terekhina et al., "Normobaric, intermittent hypoxia conditioning is cardio- and vasoprotective in rats," *Experimental Biology and Medicine (Maywood, N.J.)*, vol. 238, no. 12, pp. 1413–1420, 2013.

[18] M. Casas, H. Casas, and T. Pagés, "Effect of intermittent exposure to hypobaric hypoxia and exercise on human physical performance," *Journal of Physiology and Biochemistry*, vol. 53, p. 160, 1997.

[19] F. A. Rodríguez, H. Casas, M. Casas et al., "Intermittent hypobaric hypoxia stimulates erythropoiesis and improves aerobic capacity," *Medicine and Science in Sports and Exercise*, vol. 31, no. 2, pp. 264–268, 1999.

[20] V. M. Del Pilar, F. García-Godos, O. O. Woolcott et al., "Improvement of myocardial perfusion in coronary patients after intermittent hypobaric hypoxia," *Journal of Nuclear Cardiology*, vol. 13, no. 1, pp. 69–74, 2006.

[21] Z. O. Serebrovska, T. V. Serebrovska, V. A. Kholin et al., "Intermittent hypoxia-hyperoxia training improves cognitive function and decreases circulating biomarkers of Alzheimer's disease in patients with mild cognitive impairment: a pilot study," *International Journal of Molecular Sciences*, vol. 20, no. 21, p. 5405, 2019.

[22] H. B. Hayes, A. Jayaraman, M. Herrmann, G. S. Mitchell, W. Z. Rymer, and R. D. Trumbower, "Daily intermittent hypoxia enhances walking after chronic spinal cord injury: a randomized trial," *Neurology*, vol. 82, no. 2, pp. 104–113, 2014.

[23] M. Burtscher, T. Haider, W. Domej et al., "Intermittent hypoxia increases exercise tolerance in patients at risk for or with

mild COPD," *Respiratory Physiology & Neurobiology*, vol. 165, no. 1, pp. 97–103, 2009.

[24] B. C. Neelapu, O. P. Kharbanda, H. K. Sardana et al., "Craniofacial and upper airway morphology in adult obstructive sleep apnea patients: a systematic review and meta-analysis of cephalometric studies," *Sleep Medicine Reviews*, vol. 31, pp. 79–90, 2017.

[25] N. A. Dewan, F. J. Nieto, and V. K. Somers, "Intermittent hypoxemia and OSA: implications for comorbidities," *Chest*, vol. 147, no. 1, pp. 266–274, 2015.

[26] A. Lebkuchen, L. S. Freitas, K. H. M. Cardozo, and L. F. Drager, "Advances and challenges in pursuing biomarkers for obstructive sleep apnea: implications for the cardiovascular risk," *Trends in Cardiovascular Medicine*, vol. 31, no. 4, pp. 242–249, 2021.

[27] E. Perger, M. F. Pengo, and C. Lombardi, "Hypertension and atrial fibrillation in obstructive sleep apnea: is it a menopause issue?," *Maturitas*, vol. 124, pp. 32–34, 2019.

[28] P. Lavie, P. Herer, and V. Hoffstein, "Obstructive sleep apnoea syndrome as a risk factor for hypertension: population study," *BMJ*, vol. 320, no. 7233, pp. 479–482, 2000.

[29] A. Bikov, S. Frent, R. Pleava et al., "The burden of associated comorbidities in patients with obstructive sleep apnea-regional differences in two central-eastern European sleep centers," *Journal of Clinical Medicine*, vol. 9, no. 11, p. 3583, 2020.

[30] S. Khamsai, A. Chootrakool, P. Limpawattana et al., "Hypertensive crisis in patients with obstructive sleep apnea-induced hypertension," *BMC Cardiovascular Disorders*, vol. 21, no. 1, p. 310, 2021.

[31] M. F. Damiani, A. Zito, P. Carratù et al., "Obstructive sleep apnea, hypertension, and their additive effects on atherosclerosis," *Biochemistry Research International*, vol. 2015, Article ID 984193, 16 pages, 2015.

[32] E. J. Benjamin, P. A. Wolf, R. B. D'agostino, H. Silbershatz, W. B. Kannel, and D. Levy, "Impact of atrial fibrillation on the risk of death: the Framingham Heart Study," *Circulation*, vol. 98, no. 10, pp. 946–952, 1998.

[33] R. Mehra, K. L. Stone, P. D. Varosy et al., "Nocturnal arrhythmias across a spectrum of obstructive and central sleep-disordered breathing in older men: outcomes of sleep disorders in older men (MrOS sleep) study," *Archives of Internal Medicine*, vol. 169, no. 12, pp. 1147–1155, 2009.

[34] R. Mehra, E. J. Benjamin, E. Shahar et al., "Association of nocturnal arrhythmias with sleep-disordered breathing: the Sleep Heart Health Study," *American Journal of Respiratory and Critical Care Medicine*, vol. 173, no. 8, pp. 910–916, 2006.

[35] C. Y. Ng, T. Liu, M. Shehata, S. Stevens, S. S. Chugh, and X. Wang, "Meta-analysis of obstructive sleep apnea as predictor of atrial fibrillation recurrence after catheter ablation," *The American Journal of Cardiology*, vol. 108, no. 1, pp. 47–51, 2011.

[36] S. K. Goyal and A. Sharma, "Atrial fibrillation in obstructive sleep apnea," *World Journal of Cardiology*, vol. 5, no. 6, pp. 157–163, 2013.

[37] F. Holmqvist, N. I. Guan, Z. Zhu et al., "Impact of obstructive sleep apnea and continuous positive airway pressure therapy on outcomes in patients with atrial fibrillation-results from the Outcomes Registry for Better Informed Treatment of Atrial Fibrillation (ORBIT-AF)," *American Heart Journal*, vol. 169, no. 5, pp. 647–654.e2, 2015.

[38] G. Cadby, N. McArdle, T. Briffa et al., "Severity of OSA is an independent predictor of incident atrial fibrillation hospitalization in a large sleep-clinic cohort," *Chest*, vol. 148, no. 4, pp. 945–952, 2015.

[39] C. H. Lee, S. M. Khoo, B. C. Tai et al., "Obstructive Sleep Apnea in Patients Admitted for Acute Myocardial Infarction: Prevalence, Predictors, and Effect on Microvascular Perfusion," *Chest*, vol. 135, no. 6, pp. 1488–1495, 2009.

[40] E. Shahar, C. W. Whitney, S. Redline et al., "Sleep-disordered breathing and cardiovascular disease: cross-sectional results of the Sleep Heart Health Study," *American Journal of Respiratory and Critical Care Medicine*, vol. 163, no. 1, pp. 19–25, 2001.

[41] R. Naito, K. Sakakura, T. Kasai et al., "Aortic dissection is associated with intermittent hypoxia and re-oxygenation," *Heart and Vessels*, vol. 27, no. 3, pp. 265–270, 2012.

[42] X. Zhou, F. Liu, W. Zhang et al., "Obstructive sleep apnea and risk of aortic dissection: a meta-analysis of observational studies," *Vascular*, vol. 26, no. 5, pp. 515–523, 2018.

[43] X. Wang, Y. Bi, Q. Zhang, and F. Pan, "Obstructive sleep apnoea and the risk of type 2 diabetes: a meta-analysis of prospective cohort studies," *Respirology*, vol. 18, no. 1, pp. 140–146, 2013.

[44] Y. Mok, C. W. Tan, H. S. Wong, C. H. How, K. L. A. Tan, and P. P. Hsu, "Obstructive sleep apnoea and type 2 diabetes mellitus: are they connected," *Singapore Medical Journal*, vol. 58, no. 4, pp. 179–183, 2017.

[45] G. Musso, C. Olivetti, M. Cassader, and R. Gambino, "Obstructive sleep apnea-hypopnea syndrome and nonalcoholic fatty liver disease: emerging evidence and mechanisms," *Seminars in Liver Disease*, vol. 32, no. 1, pp. 49–64, 2012.

[46] J. J. Savla, B. D. Levine, and H. A. Sadek, "The effect of hypoxia on cardiovascular disease: friend or foe," *High Altitude Medicine & Biology*, vol. 19, no. 2, pp. 124–130, 2018.

[47] N. R. Fuller and R. Courtney, "A case of remission from pre-diabetes following intermittent hypoxic training," *Obesity Research & Clinical Practice*, vol. 10, no. 4, pp. 487–491, 2016.

[48] S. Javaheri and J. A. Dempsey, "Central sleep apnea," *Comprehensive Physiology*, vol. 3, no. 1, pp. 141–163, 2013.

[49] J. A. Estrada, A. G. Williams, J. Sun et al., "δ-Opioid receptor (DOR) signaling and reactive oxygen species (ROS) mediate intermittent hypoxia induced protection of canine myocardium," *Basic Research in Cardiology*, vol. 111, no. 2, pp. 1–12, 2016.

[50] P. C. Béguin, M. Joyeux-Faure, D. Godin-Ribuot, P. Lévy, and C. Ribuot, "Acute intermittent hypoxia improves rat myocardium tolerance to ischemia," *Journal of Applied Physiology*, vol. 99, no. 3, pp. 1064–1069, 2005.

[51] E. Ponsot, S. P. Dufour, J. Zoll et al., "Exercise training in normobaric hypoxia in endurance runners. II. Improvement of mitochondrial properties in skeletal muscle," *Journal of Applied Physiology*, vol. 100, no. 4, pp. 1249–1257, 2006.

[52] S. Toffoli, A. Roegiers, O. Feron et al., "Intermittent hypoxia is an angiogenic inducer for endothelial cells: role of HIF-1," *Angiogenesis*, vol. 12, no. 1, pp. 47–67, 2009.

[53] G. L. Semenza, "Regulation of oxygen homeostasis by hypoxia-inducible factor 1," *Physiology (Bethesda)*, vol. 24, pp. 97–106, 2009.

[54] T. V. Serebrovskaya, E. B. Manukhina, M. L. Smith, H. F. Downey, and R. T. Mallet, "Intermittent hypoxia: cause of or therapy for systemic hypertension," *Experimental Biology*

and Medicine (Maywood, N.J.), vol. 233, no. 6, pp. 627–650, 2008.

[55] N. P. Lyamina, S. V. Lyamina, V. N. Senchiknin, R. T. Mallet, H. F. Downey, and E. B. Manukhina, "Normobaric hypoxia conditioning reduces blood pressure and normalizes nitric oxide synthesis in patients with arterial hypertension," *Journal of Hypertension*, vol. 29, no. 11, pp. 2265–2272, 2011.

[56] R. T. Mallet, M. G. Ryou, A. G. Williams, L. Howard, and H. F. Downey, "Beta 1-adrenergic receptor antagonism abrogates cardioprotective effects of intermittent hypoxia," *Basic Research in Cardiology*, vol. 101, no. 5, pp. 436–446, 2006.

[57] E. Rybnikova, T. Glushchenko, E. Tyulkova, K. Baranova, and M. Samoilov, "Mild hypobaric hypoxia preconditioning up-regulates expression of transcription factors c-Fos and NGFI-A in rat neocortex and hippocampus," *Neuroscience Research*, vol. 65, no. 4, pp. 360–366, 2009.

[58] T. V. Serebrovskaya, I. S. Nikolsky, V. V. Nikolska, R. T. Mallet, and V. A. Ishchuk, "Intermittent hypoxia mobilizes hematopoietic progenitors and augments cellular and humoral elements of innate immunity in adult men," *High Altitude Medicine & Biology*, vol. 12, no. 3, pp. 243–252, 2011.

[59] F. Kolar, J. Jezkova, P. Balkova et al., "Role of oxidative stress in PKC-delta upregulation and cardioprotection induced by chronic intermittent hypoxia," *American Journal of Physiology. Heart and Circulatory Physiology*, vol. 292, no. 1, pp. H224–H230, 2007.

[60] P. Libby, P. M. Ridker, and G. K. Hansson, "Progress and challenges in translating the biology of atherosclerosis," *Nature*, vol. 473, no. 7347, pp. 317–325, 2011.

[61] R. Ross, "Atherosclerosis–an inflammatory disease," *The New England Journal of Medicine*, vol. 340, no. 2, pp. 115–126, 1999.

[62] L. Ma, J. Zhang, and Y. Liu, "Roles and mechanisms of obstructive sleep apnea-hypopnea syndrome and chronic intermittent hypoxia in atherosclerosis: evidence and prospective," *Oxidative Medicine and Cellular Longevity*, vol. 2016, Article ID 8215082, 10 pages, 2016.

[63] G. L. Semenza, "Oxygen sensing, hypoxia-inducible factors, and disease pathophysiology," *Annual Review of Pathology*, vol. 9, pp. 47–71, 2014.

[64] G. L. Wang and G. L. Semenza, "Purification and characterization of hypoxia-inducible factor 1," *The Journal of Biological Chemistry*, vol. 270, no. 3, pp. 1230–1237, 1995.

[65] Y. J. Peng, G. Yuan, D. Ramakrishnan et al., "Heterozygous HIF-1alpha deficiency impairs carotid body-mediated systemic responses and reactive oxygen species generation in mice exposed to intermittent hypoxia," *The Journal of Physiology*, vol. 577, no. 2, pp. 705–716, 2006.

[66] E. L. Mills, B. Kelly, A. Logan et al., "Succinate dehydrogenase supports metabolic repurposing of mitochondria to drive inflammatory macrophages," *Cell*, vol. 167, no. 2, pp. 457–470, 2016.

[67] A. Aarup, T. X. Pedersen, N. Junker et al., "Hypoxia-inducible factor-1α expression in macrophages promotes development of atherosclerosis," *Arteriosclerosis, Thrombosis, and Vascular Biology*, vol. 36, no. 9, pp. 1782–1790, 2016.

[68] A. K. Knutson, A. L. Williams, W. A. Boisvert, and R. V. Shohet, "HIF in the heart: development, metabolism, ischemia, and atherosclerosis," *The Journal of Clinical Investigation*, vol. 131, no. 17, 2021.

[69] H. Greenberg, X. Ye, D. Wilson, A. K. Htoo, T. Hendersen, and S. F. Liu, "Chronic intermittent hypoxia activates nuclear factor-kappa B in cardiovascular tissues in vivo," *Biochemical and Biophysical Research Communications*, vol. 343, no. 2, pp. 591–596, 2006.

[70] D. Song, G. Fang, S. Z. Mao et al., "Chronic intermittent hypoxia induces atherosclerosis by NF-kappa B-dependent mechanisms," *Biochimica et Biophysica Acta*, vol. 1822, no. 11, pp. 1650–1659, 2012.

[71] K. Minoguchi, T. Yokoe, T. Tazaki et al., "Increased carotid intima-media thickness and serum inflammatory markers in obstructive sleep apnea," *American Journal of Respiratory and Critical Care Medicine*, vol. 172, no. 5, pp. 625–630, 2005.

[72] T. Yokoe, K. Minoguchi, H. Matsuo et al., "Elevated levels of C-reactive protein and interleukin-6 in patients with obstructive sleep apnea syndrome are decreased by nasal continuous positive airway pressure," *Circulation*, vol. 107, no. 8, pp. 1129–1134, 2003.

[73] E. Ohga, T. Tomita, H. Wada, H. Yamamoto, T. Nagase, and Y. Ouchi, "Effects of obstructive sleep apnea on circulating ICAM-1, IL-8, and MCP-1," *Journal of Applied Physiology*, vol. 94, no. 1, pp. 179–184, 2003.

[74] M. C. Arkan, A. L. Hevener, F. R. Greten et al., "IKK-beta links inflammation to obesity-induced insulin resistance," *Nature Medicine*, vol. 11, no. 2, pp. 191–198, 2005.

[75] M. S. Figueiredo and G. G. Brownlee, "Cis-acting elements and transcription factors involved in the promoter activity of the human factor VIII gene," *The Journal of Biological Chemistry*, vol. 270, no. 20, pp. 11828–11838, 1995.

[76] P. A. Oeth, G. C. Parry, C. Kunsch, P. Nantermet, C. A. Rosen, and N. Mackman, "Lipopolysaccharide induction of tissue factor gene expression in monocytic cells is mediated by binding of c-Rel/p 65 heterodimers to a kappa B-like site," *Molecular and Cellular Biology*, vol. 14, no. 6, pp. 3772–3781, 1994.

[77] L. Yvan-Charvet, C. Welch, T. A. Pagler et al., "Increased inflammatory gene expression in ABC transporter-deficient macrophages: free cholesterol accumulation, increased signaling via toll-like receptors, and neutrophil infiltration of atherosclerotic lesions," *Circulation*, vol. 118, no. 18, pp. 1837–1847, 2008.

[78] M. Akinnusi, P. Jaoude, T. Kufel, and A. A. el-Solh, "Toll-like receptor activity in patients with obstructive sleep apnea," *Sleep & Breathing*, vol. 17, no. 3, pp. 1009–1016, 2013.

[79] X. Zeng, R. Guo, M. Dong, J. Zheng, H. Lin, and H. Lu, "Contribution of TLR4 signaling in intermittent hypoxia-mediated atherosclerosis progression," *Journal of Translational Medicine*, vol. 16, no. 1, p. 106, 2018.

[80] A. Munjal and R. Khandia, "Atherosclerosis: orchestrating cells and biomolecules involved in its activation and inhibition," *Advances in Protein Chemistry and Structural Biology*, vol. 120, pp. 85–122, 2020.

[81] Y. Zhu, X. Xian, Z. Wang et al., "Research progress on the relationship between atherosclerosis and inflammation," *Biomolecules*, vol. 8, no. 3, 2018.

[82] L. Dyugovskaya, P. Lavie, and L. Lavie, "Increased adhesion molecules expression and production of reactive oxygen species in leukocytes of sleep apnea patients," *American Journal of Respiratory and Critical Care Medicine*, vol. 165, no. 7, pp. 934–939, 2002.

[83] K. Minoguchi, T. Tazaki, T. Yokoe et al., "Elevated production of tumor necrosis factor-alpha by monocytes in patients with obstructive sleep apnea syndrome," *Chest*, vol. 126, no. 5, pp. 1473–1479, 2004.

[84] G. Bokinsky, M. Miller, K. Ault, P. Husband, and J. Mitchell, "Spontaneous platelet activation and aggregation during obstructive sleep apnea and its response to therapy with nasal continuous positive airway pressure. A preliminary investigation," *Chest*, vol. 108, no. 3, pp. 625–630, 1995.

[85] T. Geiser, F. Buck, B. J. Meyer, C. Bassetti, A. Haeberli, and M. Gugger, "In vivo platelet activation is increased during sleep in patients with obstructive sleep apnea syndrome," *Respiration*, vol. 69, no. 3, pp. 229–234, 2002.

[86] T. Oga, K. Chin, A. Tabuchi et al., "Effects of obstructive sleep apnea with intermittent hypoxia on platelet aggregability," *Journal of Atherosclerosis and Thrombosis*, vol. 16, no. 6, pp. 862–869, 2009.

[87] P. Pignatelli, L. De Biase, L. Lenti et al., "Tumor necrosis factor-alpha as trigger of platelet activation in patients with heart failure," *Blood*, vol. 106, no. 6, pp. 1992–1994, 2005.

[88] J. Bar, A. Zosmer, M. Hod, M. G. Elder, and M. H. Sullivan, "The regulation of platelet aggregation in vitro by interleukin-1beta and tumor necrosis factor-alpha: changes in pregnancy and in pre-eclampsia," *Thrombosis and Haemostasis*, vol. 78, no. 4, pp. 1255–1261, 1997.

[89] D. S. Hui, F. W. Ko, J. P. Fok et al., "The effects of nasal continuous positive airway pressure on platelet activation in obstructive sleep apnea syndrome," *Chest*, vol. 125, no. 5, pp. 1768–1775, 2004.

[90] S. Tsiara, M. Elisaf, I. A. Jagroop, and D. P. Mikhailidis, "Platelets as predictors of vascular risk: is there a practical index of platelet activity," *Clinical and Applied Thrombosis/Hemostasis*, vol. 9, no. 3, pp. 177–190, 2003.

[91] F. Karim, Q. S. Akter, A. Khanom, S. Haque, and S. Nahar, "Mean platelet volume in type 2 diabetes male," *Mymensingh Medical Journal*, vol. 29, no. 3, pp. 659–663, 2020.

[92] G. Slavka, T. Perkmann, H. Haslacher et al., "Mean platelet volume may represent a predictive parameter for overall vascular mortality and ischemic heart disease," *Arteriosclerosis, Thrombosis, and Vascular Biology*, vol. 31, no. 5, pp. 1215–1218, 2011.

[93] A. Kanbay, N. Tutar, E. Kaya et al., "Mean platelet volume in patients with obstructive sleep apnea syndrome and its relationship with cardiovascular diseases," *Blood Coagulation & Fibrinolysis*, vol. 24, no. 5, pp. 532–536, 2013.

[94] S. N. Sokucu, C. Ozdemir, L. Dalar, L. Karasulu, S. Aydın, and S. Altın, "Is mean platelet volume really a severity marker for obstructive sleep apnea syndrome without omorbidities?," *Pulmonary Medicine*, vol. 2014, Article ID 754839, 7 pages, 2014.

[95] M. S. Karakas, R. E. Altekin, A. O. Baktir, M. Kucuk, A. Cilli, and S. Yalcinkaya, "Association between mean platelet volume and severity of disease in patients with obstructive sleep apnea syndrome without risk factors for cardiovascular disease," *Türk Kardiyoloji Derneği Arşivi*, vol. 41, no. 1, pp. 14–20, 2013.

[96] G. Simsek, S. Haytoglu, N. B. Muluk, O. K. Arikan, M. Cortuk, and K. Kiraz, "Mean platelet volume decreases in adult patients with obstructive sleep apnea after uvulopalatal flap surgery," *The Journal of Craniofacial Surgery*, vol. 26, no. 7, pp. 2152–2154, 2015.

[97] E. Varol, O. Ozturk, T. Gonca et al., "Mean platelet volume is increased in patients with severe obstructive sleep apnea," *Scandinavian Journal of Clinical and Laboratory Investigation*, vol. 70, no. 7, pp. 497–502, 2010.

[98] C. M. Boulanger, N. Amabile, and A. Tedgui, "Circulating microparticles: a potential prognostic marker for atherosclerotic vascular disease," *Hypertension*, vol. 48, no. 2, pp. 180–186, 2006.

[99] L. Ayers, B. Ferry, S. Craig, D. Nicoll, J. R. Stradling, and M. Kohler, "Circulating cell-derived microparticles in patients with minimally symptomatic obstructive sleep apnoea," *The European Respiratory Journal*, vol. 33, no. 3, pp. 574–580, 2009.

[100] K. Maruyama, E. Morishita, A. Sekiya et al., "Plasma levels of platelet-derived microparticles in patients with obstructive sleep apnea syndrome," *Journal of Atherosclerosis and Thrombosis*, vol. 19, no. 1, pp. 98–104, 2012.

[101] G. V. Robinson, J. C. Pepperell, H. C. Segal, R. J. Davies, and J. R. Stradling, "Circulating cardiovascular risk factors in obstructive sleep apnoea: data from randomised controlled trials," *Thorax*, vol. 59, no. 9, pp. 777–782, 2004.

[102] D. Tousoulis, N. Papageorgiou, E. Androulakis, A. Briasoulis, C. Antoniades, and C. Stefanadis, "Fibrinogen and cardiovascular disease: genetics and biomarkers," *Blood Reviews*, vol. 25, no. 6, pp. 239–245, 2011.

[103] J. J. Stec, H. Silbershatz, G. H. Tofler et al., "Association of fibrinogen with cardiovascular risk factors and cardiovascular disease in the Framingham offspring population," *Circulation*, vol. 102, no. 14, pp. 1634–1638, 2000.

[104] A. Shamsuzzaman, R. S. Amin, A. D. Calvin, D. Davison, and V. K. Somers, "Severity of obstructive sleep apnea is associated with elevated plasma fibrinogen in otherwise healthy patients," *Sleep & Breathing*, vol. 18, no. 4, pp. 761–766, 2014.

[105] S. K. Sharma, E. V. Reddy, A. Sharma et al., "Prevalence and risk factors of syndrome Z in urban Indians," *Sleep Medicine*, vol. 11, no. 6, pp. 562–568, 2010.

[106] J. Xu, Y. S. Long, D. Gozal, and P. N. Epstein, "Beta-cell death and proliferation after intermittent hypoxia: role of oxidative stress," *Free Radical Biology & Medicine*, vol. 46, no. 6, pp. 783–790, 2009.

[107] T. Yokoe, L. C. Alonso, L. C. Romano et al., "Intermittent hypoxia reverses the diurnal glucose rhythm and causes pancreatic β-cell replication in mice," *The Journal of Physiology*, vol. 586, no. 3, pp. 899–911, 2008.

[108] N. Wang, S. A. Khan, N. R. Prabhakar, and J. Nanduri, "Impairment of pancreatic β-cell function by chronic intermittent hypoxia," *Experimental Physiology*, vol. 98, no. 9, pp. 1376–1385, 2013.

[109] V. Savransky, A. Nanayakkara, J. Li et al., "Chronic intermittent hypoxia induces atherosclerosis," *American Journal of Respiratory and Critical Care Medicine*, vol. 175, no. 12, pp. 1290–1297, 2007.

[110] P. Levy, J. L. Pepin, C. Arnaud et al., "Intermittent hypoxia and sleep-disordered breathing: current concepts and perspectives," *The European Respiratory Journal*, vol. 32, no. 4, pp. 1082–1095, 2008.

[111] J. Jun, C. Reinke, D. Bedja et al., "Effect of intermittent hypoxia on atherosclerosis in apolipoprotein E-deficient mice," *Atherosclerosis*, vol. 209, no. 2, pp. 381–386, 2010.

[112] X. Su, S. Peng, R. He, C. Hu, J. He, and P. Pan, "Endarterium injury and the related pathway in chronic intermittent

hypoxia rats," *Zhong Nan Da Xue Xue Bao. Yi Xue Ban*, vol. 38, no. 7, pp. 676–680, 2013.

[113] W. Trzepizur, M. Le Vaillant, N. Meslier et al., "Independent association between nocturnal intermittent hypoxemia and metabolic dyslipidemia," *Chest*, vol. 143, no. 6, pp. 1584–1589, 2013.

[114] S. Chopra, A. Rathore, H. Younas et al., "Obstructive sleep apnea dynamically increases nocturnal plasma free fatty acids, glucose, and cortisol during sleep," *The Journal of Clinical Endocrinology and Metabolism*, vol. 102, no. 9, pp. 3172–3181, 2017.

[115] M. Lafontan and D. Langin, "Lipolysis and lipid mobilization in human adipose tissue," *Progress in Lipid Research*, vol. 48, no. 5, pp. 275–297, 2009.

[116] F. Marcouiller, A. Jochmans-Lemoine, G. Ganouna-Cohen et al., "Metabolic responses to intermittent hypoxia are regulated by sex and estradiol in mice," *American Journal of Physiology. Endocrinology and Metabolism*, vol. 320, no. 2, pp. e316–e325, 2021.

[117] Q. B. Liu, L. L. Liu, Y. M. Lu et al., "The induction of reactive oxygen species and loss of mitochondrial Omi/Htr A2 is associated with S-nitrosoglutathione-induced apoptosis in human endothelial cells," *Toxicology and Applied Pharmacology*, vol. 244, no. 3, pp. 374–384, 2010.

[118] A. Anogeianaki, D. Angelucci, E. Cianchetti et al., "Atherosclerosis: a classic inflammatory disease," *International Journal of Immunopathology and Pharmacology*, vol. 24, no. 4, pp. 817–825, 2011.

[119] G. L. Semenza and N. R. Prabhakar, "Neural regulation of hypoxia-inducible factors and redox state drives the pathogenesis of hypertension in a rodent model of sleep apnea," *Journal of Applied Physiology*, vol. 119, no. 10, pp. 1152–1156, 2015.

[120] E. Vatansever, E. Surmen-Gur, A. Ursavas, and M. Karadag, "Obstructive sleep apnea causes oxidative damage to plasma lipids and proteins and decreases adiponectin levels," *Sleep & Breathing*, vol. 15, no. 3, pp. 275–282, 2011.

[121] H. J. Eisele, P. Markart, and R. Schulz, "Obstructive sleep apnea, oxidative stress, and cardiovascular disease: evidence from human studies," *Oxidative Medicine and Cellular Longevity*, vol. 2015, Article ID 608438, 9 pages, 2015.

[122] S. Zhou, Y. Wang, Y. Tan et al., "Deletion of metallothionein exacerbates intermittent hypoxia-induced oxidative and inflammatory injury in aorta," *Oxidative Medicine and Cellular Longevity*, vol. 2014, Article ID 141053, 11 pages, 2014.

[123] V. Joseph, S. Laouafa, F. Marcouiller, D. Roussel, V. Pialoux, and A. Bairam, "Progesterone decreases apnoea and reduces oxidative stress induced by chronic intermittent hypoxia in ovariectomized female rats," *Experimental Physiology*, vol. 105, no. 6, pp. 1025–1034, 2020.

[124] S. Cofta, H. M. Winiarska, A. Płóciniczak et al., "Oxidative stress markers and severity of obstructive sleep apnea," *Advances in Experimental Medicine and Biology*, vol. 1222, pp. 27–35, 2019.

[125] A. Barceló, C. Miralles, F. Barbé, M. Vila, S. Pons, and A. G. Agustí, "Abnormal lipid peroxidation in patients with sleep apnoea," *The European Respiratory Journal*, vol. 16, no. 4, pp. 644–647, 2000.

[126] N. A. Maianski, A. N. Maianski, T. W. Kuijpers, and D. Roos, "Apoptosis of neutrophils," *Acta Haematologica*, vol. 111, no. 1-2, pp. 56–66, 2003.

[127] C. Akgul, D. A. Moulding, and S. W. Edwards, "Molecular control of neutrophil apoptosis," *FEBS Letters*, vol. 487, no. 3, pp. 318–322, 2001.

[128] S. P. Hart, J. A. Ross, K. Ross, C. Haslett, and I. Dransfield, "Molecular characterization of the surface of apoptotic neutrophils: implications for functional downregulation and recognition by phagocytes," *Cell Death and Differentiation*, vol. 7, no. 5, pp. 493–503, 2000.

[129] L. Dyugovskaya, A. Polyakov, P. Lavie, and L. Lavie, "Delayed neutrophil apoptosis in patients with sleep apnea," *American Journal of Respiratory and Critical Care Medicine*, vol. 177, no. 5, pp. 544–554, 2008.

[130] L. Dyugovskaya, A. Polyakov, V. Cohen-Kaplan, P. Lavie, and L. Lavie, "Bax/Mcl-1 balance affects neutrophil survival in intermittent hypoxia and obstructive sleep apnea: effects of p38MAPK and ERK1/2 signaling," *Journal of Translational Medicine*, vol. 10, p. 211, 2012.

[131] M. Takahashi, H. Okazaki, Y. Ogata, K. Takeuchi, U. Ikeda, and K. Shimada, "Lysophosphatidylcholine induces apoptosis in human endothelial cells through a p 38-mitogen-activated protein kinase-dependent mechanism," *Atherosclerosis*, vol. 161, no. 2, pp. 387–394, 2002.

[132] L. Kunos, P. Horvath, A. Kis et al., "Circulating survivin levels in obstructive sleep apnoea," *Lung*, vol. 196, no. 4, pp. 417–424, 2018.

[133] M. Yamamoto, J. D. Clark, J. V. Pastor et al., "Regulation of oxidative stress by the anti-aging hormone klotho," *The Journal of Biological Chemistry*, vol. 280, no. 45, pp. 38029–38034, 2005.

[134] J. Pákó, L. Kunos, M. Mészáros et al., "Decreased levels of anti-aging klotho in obstructive sleep apnea," *Rejuvenation Research*, vol. 23, no. 3, pp. 256–261, 2020.

[135] S. Jelic, D. J. Lederer, T. Adams et al., "Endothelial repair capacity and apoptosis are inversely related in obstructive sleep apnea," *Vascular Health and Risk Management*, vol. 5, pp. 909–920, 2009.

[136] I. C. Trombetta, C. Maki-Nunes, E. Toschi-Dias et al., "Obstructive sleep apnea is associated with increased chemoreflex sensitivity in patients with metabolic syndrome," *Sleep*, vol. 36, no. 1, pp. 41–49, 2013.

[137] M. L. Fung, G. L. Tipoe, and P. S. Leung, "Mechanisms of maladaptive responses of peripheral chemoreceptors to intermittent hypoxia in sleep-disordered breathing," *Sheng Li Xue Bao*, vol. 66, no. 1, pp. 23–29, 2014.

[138] S. Y. Lam, Y. Liu, K. M. Ng et al., "Chronic intermittent hypoxia induces local inflammation of the rat carotid body via functional upregulation of proinflammatory cytokine pathways," *Histochemistry and Cell Biology*, vol. 137, no. 3, pp. 303–317, 2012.

[139] J. Zhang, C. Hu, X. Jiao et al., "Potential role of mRNAs and Lnc RNAs in chronic intermittent hypoxia exposure-aggravated atherosclerosis," *Frontiers in Genetics*, vol. 11, p. 290, 2020.

[140] A. Khalyfa, C. Zhang, A. A. Khalyfa et al., "Effect on intermittent hypoxia on plasma exosomal micro RNA signature and endothelial function in healthy adults," *Sleep*, vol. 39, no. 12, pp. 2077–2090, 2016.

[141] C. Hu, P. Wang, Y. Yang et al., "Chronic intermittent hypoxia participates in the pathogenesis of atherosclerosis and perturbs the formation of intestinal microbiota," *Frontiers in Cellular and Infection Microbiology*, vol. 11, p. 392, 2021.

Retraction

Retracted: Mitochondrial Dysfunction and Cardiovascular Disease: Pathophysiology and Emerging Therapies

Oxidative Medicine and Cellular Longevity

This article has been retracted by Hindawi, as publisher, following an investigation undertaken by the publisher [1]. This investigation has uncovered evidence of systematic manipulation of the publication and peer-review process. We cannot, therefore, vouch for the reliability or integrity of this article.

Please note that this notice is intended solely to alert readers that the peer-review process of this article has been compromised.

Wiley and Hindawi regret that the usual quality checks did not identify these issues before publication and have since put additional measures in place to safeguard research integrity.

We wish to credit our Research Integrity and Research Publishing teams and anonymous and named external researchers and research integrity experts for contributing to this investigation.

The corresponding author, as the representative of all authors, has been given the opportunity to register their agreement or disagreement to this retraction. We have kept a record of any response received.

References

[1] C. A. Stamerra, P. Di Giosia, P. Giorgini, C. Ferri, V. N. Sukhorukov, and A. Sahebkar, "Mitochondrial Dysfunction and Cardiovascular Disease: Pathophysiology and Emerging Therapies," *Oxidative Medicine and Cellular Longevity*, vol. 2022, Article ID 9530007, 16 pages, 2022.

Review Article

Mitochondrial Dysfunction and Cardiovascular Disease: Pathophysiology and Emerging Therapies

Cosimo Andrea Stamerra,[1,2] Paolo Di Giosia,[1,2] Paolo Giorgini,[1] Claudio Ferri,[1] Vasily N. Sukhorukov,[3] and Amirhossein Sahebkar [ID] [4,5,6]

[1]*University of L'Aquila, Department of Life, Health and Environmental Sciences, Building Delta 6, San Salvatore Hospital, Via Vetoio, Coppito 67100 L'Aquila, Italy*

[2]*Department of Internal Medicine, Mazzoni Hospital, Ascoli Piceno, Italy*

[3]*Institute for Atherosclerosis Research, Osennyaya Street 4-1-207, Moscow 121609, Russia*

[4]*Biotechnology Research Center, Pharmaceutical Technology Institute, Mashhad University of Medical Sciences, Mashhad, Iran*

[5]*Applied Biomedical Research Center, Mashhad University of Medical Sciences, Mashhad, Iran*

[6]*Department of Biotechnology, School of Pharmacy, Mashhad University of Medical Sciences, Mashhad, Iran*

Correspondence should be addressed to Amirhossein Sahebkar; amir_saheb2000@yahoo.com

Mitochondria ensure the supply of cellular energy through the production of ATP via oxidative phosphorylation. The alteration of this process, called mitochondrial dysfunction, leads to a reduction in ATP and an increase in the production of reactive oxygen species (ROS). Mitochondrial dysfunction can be caused by mitochondrial/nuclear DNA mutations, or it can be secondary to pathological conditions such as cardiovascular disease, aging, and environmental stress. The use of therapies aimed at the prevention/correction of mitochondrial dysfunction, in the context of the specific treatment of cardiovascular diseases, is a topic of growing interest. In this context, the data are conflicting since preclinical studies are numerous, but there are no large randomized studies.

1. Introduction and Methods

Mitochondria are responsible for regulating processes for maintaining cellular health; the onset of mitochondrial dysfunction involves energy deficits, increased production of harmful catabolites of oxidative phosphorylation (OXPHOS), increased autophagy and apoptosis, and metabolic abnormalities, causing the development of cardiovascular diseases (CVD).

The purpose of this narrative review is to investigate the mechanisms by which mitochondrial dysfunction leads to the development of CVD; in fact, these alterations represent the target towards which new therapeutic strategies for the treatment of cardiovascular pathologies are aimed.

We performed a review of the available literature in the "PubMed" database. To find relevant articles, we combined each of the following key words: "cardiovascular disease", "mitochondrial dysfunction", "oxidative stress", and "therapy".

2. Mitochondrial Physiology

Mitochondria are involved in many physiological processes: production of adenosine triphosphate (ATP), synthesis and degradation of organic macromolecules (carbohydrates, proteins, lipids), thermogenesis, regulation of cytoplasmic calcium levels, triggering of apoptosis, production of reactive oxygen species (ROS), and synthesis of the heme group and steroid hormones [1, 2].

Mitochondria perform the synthesis and degradation of fatty acids and proteins. These organelles are also the site of the Krebs cycle, known as the common final pathway of

metabolism because it allows the products of the catabolism of carbohydrates, lipids, and proteins to be converted into molecules of carbon dioxide and water, with the simultaneous reduction of protons and transporters electrons: nicotinamide adenine dinucleotide (NAD) and flavin adenine dinucleotide (FAD). The reduced forms of these cofactors (NADH and FADH2) release protons and electrons to the respiratory chain, located in the inner mitochondrial membrane.

Respiratory chain complexes I, III, and IV oxidize NADH and FADH2 and use the energy thus obtained to transport protons across the inner mitochondrial membrane, creating an electrochemical gradient [3]. The proton gradient is then used to activate the enzyme ATP synthase (V complex of the respiratory chain), which catalyzes the synthesis of ATP, the main energy source for the cell [2, 3].

At the mitochondrial level, heat is produced due to the chemical reactions that occur in these organelles and due to the presence of uncoupling proteins (UCP). UCPs are ion channels that allow to dissipate the proton gradient existing across the inner mitochondrial membrane [1, 4]. The expression of the known isoforms (UCP1-5) is tissue-specific [5].

Mitochondria also regulate cytoplasmic levels of calcium [6]. The molecular mechanisms by which mitochondria internalize or release calcium ions have not yet been fully elucidated; it is supposed that there are various systems of regulation of calcium dynamics and that different tissues use different systems [6]. The main mechanisms characterized include a mitochondrial calcium transporter (mitochondrial calcium uniporter), a calcium-proton exchanger, and a transmembrane protein leucine zipper Ef-hand containing transmembrane protein 1 (LETM1); the latter would also mediate the escape of calcium from the mitochondria [6].

An excessive accumulation of calcium in the mitochondria seems to lead to the opening of a protein channel at the level of the inner mitochondrial membrane (mitochondrial permeability transition pore (mPTP)), thus triggering apoptosis [7]. This mechanism is believed to be crucial in myocardial damage from ischemia and reperfusion, a condition in which cellular calcium overload occurs [7].

Excessive ROS production has also been implicated in ischemic and reperfusion injury (IRI) [7, 8]. ROS are normally produced at very low levels by the respiratory chain. In the past, it was believed that these molecules were uniquely harmful to cells, since at high concentrations they cause oxidative damage and cell death [8]. However, it has been shown that the production of low-moderate ROS levels is essential for the regulation of various cellular processes (gene expression, signal transduction, and cellular adaptation to stress conditions) [9].

A fine regulation of the cellular levels of ROS is therefore essential and is operated by the mitochondria through a balance between the production and degradation of these molecules [9]. Among the main enzymes responsible for the degradation of ROS are superoxide dismutase and glutathione reductase, located at the mitochondrial level, and catalase, which is expressed in other cellular organelles, the peroxisomes [8, 9]. Mitochondria also synthesize the heme group, localized in various proteins, the main ones being hemoglobin, myoglobin, and some subunits of the respiratory chain [10].

Finally, various enzymes involved in the synthesis of steroid hormones are localized at the mitochondrial level [11].

2.1. Mitochondrial Dysfunction and Pathogenesis of Cardiovascular Diseases

2.1.1. Primary Mitochondrial Dysfunction. Many mutations have been associated with pathological pictures attributable to mitochondrial dysfunction. The common denominator of these mutations appears to be the ability to cause global mitochondrial dysfunction by altering processes such as protein synthesis or mitochondrial genome replication [12]. The prevalence of heart disease linked to mtDNA mutations is estimated to be 1 case: 10-15,000 in the general population; there are no prevalence data for nDNA mutations, which appear to be more frequent than mtDNA mutations [13].

An inverse correlation has been documented between the residual activity of complex I and the extent of ROS production [14]; on the other hand, there does not seem to be any correlation between the extent of ROS production and the severity of the clinical phenotype [12, 14]. A direct correlation between the severity of the ATP synthesis defect and the severity of the clinical manifestations is likely but has not yet been definitively demonstrated [12]. DiMauro and Hirano hypothesized that the mutations responsible for severe clinical manifestations determine a severe deficiency of ATP synthesis and modest oxidative stress, while the mutations that cause milder clinical phenotypes mainly determine severe oxidative stress [12].

Alterations of calcium homeostasis have been shown using the cybrid cell line model [12]. Cells expressing mutations associated with mitochondrial encephalomyopathy, lactic acidosis, and stroke-like episodes (MELAS) and myoclonic epilepsy with ragged red fibers (MERRF) syndrome showed abnormal increases in cytoplasmic calcium concentrations following the induction of calcium release from the smooth endoplasmic reticulum; this phenomenon demonstrated a reduced ability of the mitochondria to internalize calcium [15, 16].

The presence of alterations in calcium dynamics should be evaluated in further studies, since these alterations are potentially responsible for apoptosis and alterations in the excitability of neurons and cardiomyocytes. Among other things, the increased susceptibility to apoptosis of cells with altered mitochondrial function is likely but not established.

Mitochondrial heart disease can be defined as an impairment of the structure and/or function of the heart due to mitochondrial pathology; the diagnosis therefore requires the exclusion of other etiologies, for example, coronary hypertensive and valvular or congenital pathology [17]. Cardiac involvement can present in the form of cardiomyopathy and/or alterations in electrical activity [18]. Hypertrophic cardiomyopathy (HCM) is the most frequent form of cardiomyopathy, developing in an estimated 40% of patients with mitochondrial disease [19, 20].

The exact mechanisms of heart damage in mitochondrial heart disease have not been elucidated. Ventricular hypertrophy has been hypothesized to constitute an adaptive change to mitochondrial dysfunction. However, ultrastructural analyses never found evidence of expansion of the sarcomeric structures, while they frequently showed a marked increase in the number and size of mitochondria, which cause an enlargement of the cardiomyocytes. Abnormal mitochondria cause the disarray of sarcomeres and mechanically hinders contractile activity. It is also plausible that these dysfunctional mitochondria produce large amounts of ROS, causing significant oxidative stress. Other possible consequences of mitochondrial dysfunction are oxidative stress, cytoplasmic calcium overload (with consequent alterations in the excitability of cardiomyocytes), anomalies in the use of energy substrates, and a greater tendency to apoptosis [17, 18]. The ultimate outcomes of these alterations would be hypokinesia and ventricular dilatation, the appearance of areas of fibrosis, and abnormalities of cardiac electrical activity.

2.1.2. Acquired Mitochondrial Dysfunction. Mitochondrial dysfunction has been considered as a crucial player in the development of cardiovascular diseases. Mitochondrial dysfunction implies mitochondrial complex disruption, mitochondrial uncoupling, and cristae remodelling and swelling, which results in ROS increase, energy stress, and cell death [21]. For instance, the generation of mitochondrial ROS is the main process involved in cardiac remodelling in diabetes, and it is caused by mechanisms that are redox-sensitive, including inflammation, organelle dysfunction, alterations in ion homeostasis, cardiomyocyte hypertrophy, apoptosis, fibrosis, and contractile dysfunction [22].

Mitochondrial health is enabled by specific control mechanisms, namely, mitophagy, a cargo-specific form of autophagy selective for the elimination of damaged mitochondria.

The importance of autophagy and mitophagy abnormalities in aging-induced CVD has been widely described. In particular, aging results in a decline of autophagy that leads to age-related CVD, due to perturbations in cellular energy metabolism and adaption to stress [23]. On the same hand, several studies have established that genetic and pharmacological interventions promoting enhanced mitophagy also lead to an extended life span, while disrupting mitophagy leads to accelerated aging phenotypes [24]. However, it is still unclear how aging impacts on mitophagy. Recently, it has been proposed that PINK1/Parkin-mediated mitophagy plays a minimal role in basal mitophagy and that this pathway plays a more significant role in stress adaptation and repair [25]. Thus, increased oxidative stress and inflammation due to the aging process could play a pivotal role in disrupting Parkin-mediated mitophagy with consequent accumulation of damaged mitochondria. This activates NLRP3 inflammasome that is a cytosolic protein complex that promotes inflammatory responses by provoking cell death and triggering the release of proinflammatory cytokines. Perturbation in NLRP3 inflammasome has been linked to inhibition of autophagy and aging [26].

In addition, proteostasis is also considered as an emerging mechanism regulating mitochondrial quality control in the heart. Mitochondrial proteostasis controls biogenesis, folding, and degradation of mitochondrial proteins. Proteostasis seems impaired during cardiac stress [26].

In the presence of misfolded protein increase in mitochondria, the mitochondrial unfolded protein response (mtUPR) is enhanced by activating transcription factor 5 (ATF5), which translocates to the nucleus and stimulates the upregulation of genes that promote the restoration of mitochondrial protein folding and proteostasis [27].

Previous work showed that stimulation of mtUPR improves mitochondrial function and reduces cardiac damage in response to IRI and pressure overload [28]. Mitochondrial biogenesis is also critical for the regulation of mitochondrial turnover and function in cardiovascular pathophysiology. The transcriptional coactivator peroxisome proliferator-activated receptor γ coactivator 1 alpha (PGC-1α) plays a critical role as a metabolic sensor and is a regulator of mitochondrial biogenesis and metabolism. A dysregulation of PGC-1α signaling during heart failure takes place at the transcriptional and posttranscriptional level, leading to the progression of cardiac dysfunction by multiple mechanisms, particularly those involved in mitochondrial metabolism [29]. Finally, perturbations of epigenetic mechanisms implicated in mitochondrial function could promote CVD. Recent studies showed a complex interplay between epigenetic signals, environment, and mitochondrial metabolism, resulting in dysfunction of vascular phenotype and greater cardiovascular risk [30].

Epigenetic modifications might interrupt the expression of genes implicated in mitochondrial homeostasis.

Epigenetic changes impair mitochondrial function, with a decrease in mitochondrial metabolites (i.e., NAD and FAD) used as cofactors by components involved in chromatin modifications. Conversely, metabolic changes taking place in mitochondria shrink the availability of cofactors for chromatin-modifying proteins and consequently give rise to maladaptive epigenetic changes altering gene transcription. In fact, numerous components of the epigenetic apparatus have a need of substrates of cellular metabolism (ATP, acetyl coenzyme A, NADH, and α-ketoglutarate) for enzymatic function [31].

(1) Cardiovascular Risk Factors and Mitochondrial Dysfunction. Several modifiable factors increase cardiovascular risk by triggering mitochondrial dysfunction and oxidative stress [32–43].

There are many studies about the correlations between atherosclerosis and DNA damage [44–46]; in particular, in agreement with these studies, an increase in mtDNA damage was found in the tissues of patients affected by atherosclerosis and CVD [46]. Both low density lipoprotein-oxidized (oxLDL) and free cholesterol cause mitochondrial damage. Endothelial cells incubated with oxLDL had an increase in the activity of mitochondrial complex I and oxidative stress [47]; this leads to an increase in the transcription and expression of superoxide dismutase 2 (SOD2) in macrophages [48]. Furthermore,

the mitochondrial production of oxidants contributes to the formation of oxLDL [49].

The administration of cholesterol in rabbits led to an alteration in mitochondrial energy production and a reduction in the activity of mitochondrial dehydrogenase [50].

The activity of SOD2 and the concentration of reduced glutathione (GSH) are inversely related to the age and size of the atherosclerotic plaque, showing that they are both induced by early stages of atherosclerosis [48]. Therefore, the activity of SOD2 in subjects with initial hypercholesterolemia is protective against mitochondrial dysfunction at early stages of atherogenesis.

A high-fat diet causes a reduction in the transcription of genes involved in the production of enzymes that counteract free radicals, such as SOD1, SOD2, and glutathione peroxidase (GPX); furthermore, an increase in UCP2 but not in UCP3 was detected. The administration of antioxidants caused a reduction of these alterations [51]. Conversely, calorie restriction is associated with an increase in SOD2 and GPX and in mitochondrial genes involved in energy metabolism (complexes I, III, IV, and V); furthermore, there was a reduction in UCP3 but not in UCP2 [52].

It is now known that diabetes causes mitochondrial dysfunction and an increase in the production of free radicals, lipid peroxides, isoprostanes, and DNA damage [53, 54]. Hyperglycemia, through the overproduction of electron donors like NADH and flavin adenine dinucleotide FADH2 through the Krebs cycle, increases the production of free radicals and, therefore, leads to an increase in the proton gradient of the inner mitochondrial membrane [53–55]. The hyperactivity of antioxidant mitochondrial enzymes, such as SOD2, prevents the proliferation of hyperglycemic-related free radicals [53–55] and induction of inducible nitric oxide synthase (iNOS) in insulin-producing cells [56]. On the other hand, suppression of SOD2 causes a 2-fold increase in iNOS promoter cells [56].

The majority of individuals chronically exposed to cigarette smoke die from CVD. Smoking induces dysfunction of OXPHOS with a reduction in the activity of cytochrome oxidase in heart cells and causes an increase in the production of free radicals [38, 43, 57, 58]. After thirty minutes exposure to second-hand smoke, there is a 25% reduction in the activity of mitochondrial cytochrome oxidase [57]. Cigarette smoke, causing mitochondrial dysfunction, leads to an increased susceptibility to the development of ischemic heart disease and myocardial injury revascularization [42]. A reduction in coenzyme Q levels has also been demonstrated [43, 58]. Rats exposed to cigarette smoke showed damage to aortic mtDNA, reduction in the activity of adenine nucleotide translocase (ANT), increased nitration, and inactivation of SOD2, as well as mitochondrial dysfunction [33].

Smoking, associated with other cardiovascular risk factors, accelerates the processes of mitochondrial dysfunction and atherogenesis [33].

The overexpression of SOD2 is instead associated with a reduction in cigarette smoke cytotoxicity [59].

Another significant cardiovascular risk factor is age. Aging contributes significantly to the development of mitochondrial damage and dysfunction [60, 61] with a reduction in the efficiency of OXPHOS and an increase in mtDNA damage.

There is a gender difference in the development of mitochondrial dysfunction: it is known, in fact, that premenopausal women have a reduced cardiovascular risk compared to men of the same age; this risk, on the other hand, is equal between the two sexes after menopause [62–64]. After menopause, estrogen levels drop significantly, leading to an increase in the susceptibility to developing cardiovascular risk factors, including atherogenesis [64, 65]. The cardioprotective effects of estrogen are attributed, in addition to the anti-inflammatory and antiproliferative properties, to its antioxidant properties, and to the ability to increase the production of nitrogen monoxide, to activate mitochondrial K^{ATP} channels, which is important in the regulation of intramitochondrial calcium levels during ischemia [66–70]. Furthermore, premenopausal rats have less peroxide/oxidative-related mtDNA damage and higher concentrations of GSH, SOD2, and GPX than male rats [71, 72].

Estrogens, acting on specific mitochondrial receptors (ERα and ERβ) [73], modulate mtDNA transcription, electron transport activity, ATP production, membrane potential, calcium concentration, apoptosis, and increase in intramitochondrial GSH [73–76].

Mitochondrial dysfunction can also be iatrogenic. Associations between some drugs such as protease inhibitors, antiretroviral agents, doxorubicin, and arsenic with the onset of mtDNA deletion [77–81], mitochondrial dysfunction with reduction of antioxidant enzyme activity, and increase in the production of free radicals have been reported [82, 83].

(2) Heart Failure and Mitochondrial Dysfunction. In heart failure (HF), mitochondria are commonly injured because of membrane rupture and matrix depletion [84]: these mitochondria show inadequate capacity for ATP synthesis because of the impairment of the respiratory chain related to a decreased activity of complexes I and IV [85]. The ATP necessary for cardiac metabolism is initially obtained by the mitochondrial oxidative metabolism of fatty acids [86]. Pathological cardiac remodelling causes an alteration of cardiac metabolism with an increase in glycolysis and a reduction in the oxidation of fatty acids [86]. Since the ATP generated by glycolysis alone provides less than 5% of the necessary energy [87], an energy deficit is thus created [88], which leads to ventricular dysfunction.

In end-stage HF, the activities of other redox enzymes, NADPH-transhydrogenase, and the Krebs cycle enzymes such as isocitrate dehydrogenase, malate dehydrogenase, and aconitase are severely impaired. Decreased activities of mitochondrial enzymes are induced by some chemical modifications [89]. Mitochondrial proteins can be modified by acetylation of the lysine residue by thioester-CoAs, such as acetyl-CoA, succinyl-CoA, and malonyl-CoA. [90]. Levels of acetylated proteins increase in HF [91–93]. HF is therefore associated with the acetylation of antioxidant proteins, enzymes involved in the oxidation of fatty acids, enzymes of the Krebs cycle, and proteins of the electron transport chain [95, 96]. There is therefore a reduction in the activity of succinate dehydrogenase, pyruvate dehydrogenase, ATP

synthase, and malate-aspartate shuttle enzymes; in addition, the acetylation of the oligomycin sensitivity–conferring protein (OSCP) leads to an increase in the sensitivity of the mPTP opening [91–95]. Furthermore, acetylation of the malate-aspartate shuttle impairs the transport of NADH from the cytosol into the mitochondrion and alters the cytosolic redox state and glycolytic ATP production during the transition between ventricular hypertrophy and HF [94, 96].

The underlying causes of hyperacetylation of mitochondrial proteins during HF are uncertain. A possible mechanism is the increase in short-chain acyl-CoAs in the myocardium, due to the reduced oxidation of fatty acids [96]. Another possible mechanism is the reduction of protein deacetylation mediated by the sirtuin family of NAD$^+$-dependent deacetylases: among the three mitochondrial sirtuins (SIRT3, SIRT4, and SIRT5), SIRT3 is responsible for deacetylation [94] and is downregulated in HF [91]. The activity of sirtuins requires NAD$^+$; however, since in HF, there is a reduction in NAD$^+$, and in the NAD$^+$/NADH ratio [91, 97–99], there is a reduced activity of sirtuins and, therefore, a reduction in the deacetylation of mitochondrial proteins, leading to mitochondrial dysfunction [92, 99].

HF is associated with an alteration of calcium homeostasis: damaged cardiomyocytes have a reduction in calcium entry into the sarcoplasmic reticulum and an increase in calcium loss through the ryanodine receptor. It leads to an increase in cytosolic calcium at baseline and a reduction during excitation. Since the sarcoplasmic reticulum and mitochondria are adjacent, an increase in intramitochondrial calcium concentrations is caused, leading to mitochondrial dysfunction [100].

At normal levels, calcium activates important enzymes involved in OXPHOS such as pyruvate dehydrogenase, isocitrate dehydrogenase, and α-ketoglutarate dehydrogenase [104, 105] and in the regulation of mitochondrial function, ROS scavenging, or mPTP opening [102, 103]. However, calcium overload involves the alteration of these functions and, through mitochondrial dysfunction, induces HF [100, 104].

An important regulator of mitochondrial calcium concentrations is the mitochondrial Ca^{2+} uniporter (MCU) complex [105]: a loss of function of the MCU prevents the internalization of calcium [106]. In dysfunctional hearts, hyperactivity of the MCU and a reduction in efflux via Na/Ca^{2+} exchanger (NCLX) have been found, leading to an overload of intramitochondrial calcium [106]: this process, while representing an initial attempt by the cell to compensate for the energy deficit [107], it appears to be harmful in the long term [108].

Since ventricular remodeling causes a greater demand for energy, there is an increase in the activity of the mitochondrial ATP synthase, however impaired by hyperacetylation [93]; this therefore implies the compromise of the production of ATP, of the electron transport chain and, therefore, an increase in the production of free radicals [109]. The altered function of antioxidant enzymes [110] and the intramitochondrial calcium overload caused by inefficiency of control proteins lead to a further worsening of mitochondrial free radical production [111], generating a

mechanism called ROS-induced ROS release in mitochondria [107]. Furthermore, high levels of free radicals trigger mPTP opening and, therefore, cell death [104].

Postischemic HF is also characterized by a reduction in the activity of the protein responsible for the fusion of the inner mitochondrial membrane optic atrophy (OPA) 1 and the proteins responsible for the fusion of the external mitochondrial membrane mitofusins (Mfn) 1 and 2. The activities of Mfn 1/2 are also increased in nonischemic dilated heart disease, a condition in which there is also an increase in the activity of the protein responsible for mitochondrial fission dynamin-related protein (Drp) 1 [112]. In addition, the alteration of mitochondrial fusion and fission processes is exacerbated by the accumulation of intramitochondrial calcium [112]. All of this aggravates the mitochondrial energy deficit of HF [113].

All of these hypotheses are plausible, and it is reasonable to assume that heart damage depends on a combination of these mechanisms (Figure 1).

2.2. Mitochondria-Targeted Therapies for Cardiovascular Diseases.

Mitochondria are not only the site of OXPHOS but are also involved in the control of calcium signaling, fatty acid oxidation, apoptosis, heme complex biosynthesis, and transduction in the innate immune response [114–116]. During recent years, several molecules having different pharmacological targets and mechanisms of action have been developed to treat mitochondrial dysfunction. New therapeutic strategies for CVD restore the ability of mitochondria to produce ATP and to counteract the damaging effects of ROS, cellular apoptosis, and autophagy, typically found in CVD [116, 117]. Therapeutic agents of CVD secondary to mitochondrial dysfunction may, therefore, have biological and exogenous targets.

2.2.1. Biological Targets.

ROS are a by-product of mitochondrial OXPHOS. While their role in the genesis of oxidative damage is now known, their role as signaling molecules in CV processes and in the regulation of myocardial metabolic functions and vascular endothelial permeability is still under study.

However, mitochondrial dysfunction is generally associated with excessive ROS generation [118].

In human hearts explanted from patients with nonischemic CMD, superoxide anion concentrations were found to be double those in healthy hearts [119].

Mitochondrial dysfunction is a pathological process also present in subjects with diabetes and hypertensive heart disease [116, 120]. Furthermore, an animal study has shown that during aging, mitochondria have an increase in oxidative stress under conditions of hyperlipidemia, causing the instability of the atherosclerotic plaque [121]. Therefore, it appears that oxidative stress is implicated in several forms of CVD, including aging.

Therefore, in the context of cardiovascular risk prevention, the development of antioxidant therapies that is aimed at inhibiting mitochondrial dysfunction would reduce oxidative stress, atherosclerosis, and chronic inflammation [122].
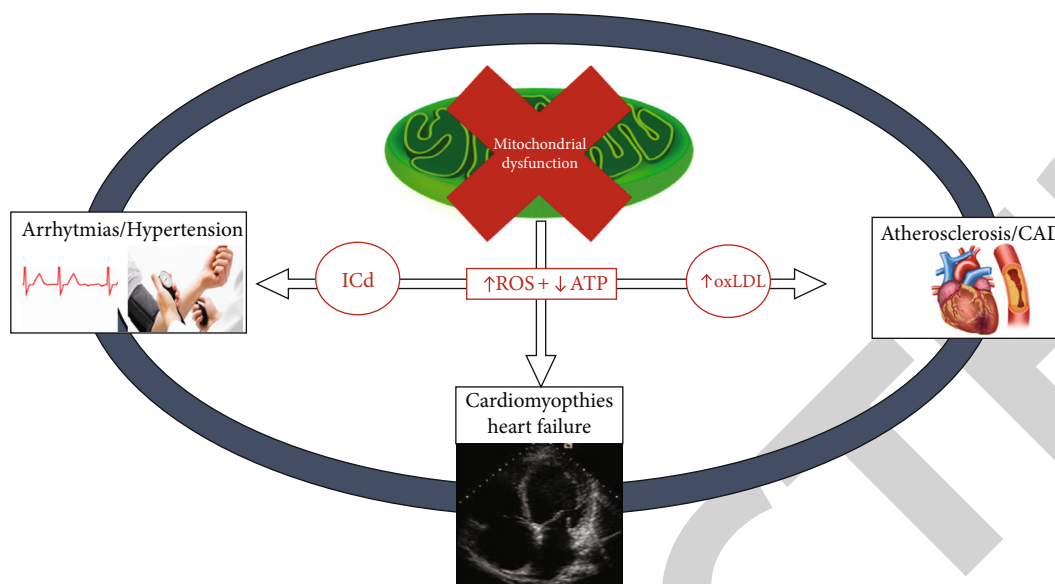
FIGURE 1: Connection between mitochondrial dysfunction and cardiovascular disease. ROS: reactive oxygen species; ATP: adenosine triphosphate; oxLDL: oxidized low density lipoproteins; ICd: ion channel dysregulated; CAD: coronary artery disease.

Coenzyme Q10 (CoQ10), vitamin E (α-tocopherol), vitamin C (ascorbic acid), and β-carotene (the precursor vitamin A) have all been clinically studied for the prevention and treatment of atherosclerosis, HF, and acute myocardial infarction [123–125]. The data in this regard are conflicting: despite the high blood concentrations of antioxidants administered, no clinically important benefits have been reported [124–126], with the sole exception of CoQ10 administered in HF [123] or in acute myocardial infarction [127] and possibly the use of elamipretide [128].

Ongoing studies are testing CoQ10, or its reduced form (ubiquinol), elamipretide, and mitoquinone (mitoQ) in patients with peripheral vascular disease, HF, and ischemic heart disease [116, 117, 129–132]; other studies are testing vitamin C and N-acetylcysteine in the prevention of atrial fibrillation after heart surgery [133–136].

CoQ10 is an antioxidant naturally present in the organism. Autosomal recessive mutations, aging-related oxidative stress, type 2 diabetes, CVD, carcinogenic processes, and statin intake are all conditions associated with CoQ10 deficiency [136–139]. There are many CoQ10 studies: in a study including 420 patients with HF, long-term treatment with CoQ10 (100 mg tid) caused an improvement in symptoms and a reduction in mortality from cardiovascular events [123]; the same conclusions were reported from a meta-analysis of 14 studies with 2149 enrolled subjects [140]. The results of another study in 144 patients with acute myocardial infarction showed that CoQ10 can produce rapid benefits when administered within 3 days of onset of symptoms [127]. Statin therapy is associated with reduced CoQ10 levels [141]; in a meta-analysis of 12 randomized studies (575 patients), it was found that CoQ10 supplementation significantly reduces muscle problems resulting from the use of beneficial statins [141].

Although the therapeutic goal is to inhibit mitochondrial dysfunction, common antioxidants are mostly ineffective because they are unable to enter the mitochondria. To solve this problem, the antioxidants were synthetically modified: MitoQ (mitoquinone), for example, is the classical ubiquinol linked to the triphenylphosphonium lipophilic cation (TPP), which allows the antioxidant to penetrate into the mitochondria, preventing oxidative damage [130].

Administration of MitoQ in mice and humans caused an inhibition in ROS production, reducing arterial stiffness and improving endothelial function (FMD) [142]. An animal study indicated that administration of MitoQ10 (500 μmol/L) prevents the development of hypertension, improves endothelial function, and limits cardiac hypertrophy in young hypertensive stroke-prone rats [143].

A preliminary cross-over study of 20 healthy adults aged 60 to 79 years with endothelial dysfunction (defined as flow-mediated dilation of the brachial artery < 6%) demonstrated that oral administration of MitoQ (20 mg/day) caused a statistically significant improvement in FMD, a reduction in arterial stiffness, and a reduction in oxLDL, thanks to a reduction in ROS [142].

Elamipretide is a new molecule capable of reaching very high concentrations within the mitochondria and, by increasing their energy, reducing apoptosis [128]. Elamipretide inhibits the oxidation of cardiolipin and therefore blocks the production of ROS and increases the production of ATP [144].

An animal study (2007) demonstrated the cardioprotective effects of elamipretide, which thanks to its antioxidant action reduces myocardial lipid peroxidation and therefore the size of the ischemic area in patients with heart attack [145]. The administration of high doses of elamipretide (0.25 mg/kg/h) in 24 patients with HF with reduced ejection fraction caused a reduction in the end-diastolic and end-systolic volumes of the left ventricle [146]. However, the EVOLVE and EMBRACE STEMI studies demonstrated the ineffectiveness of elamipretide

in reducing restenosis of the renal and coronary arteries, respectively [147, 148].

Mito-Tempo and Mito-Tempol are potent antioxidants [149] derived by a combination of the pleiotropic intracellular antioxidant piperidine nitroxide Tempo (2,2,6,6-tetramethylpiperidine-1-yloxy), respectively, with the TPP lipophilic cation, and the less hydrophobic molecule 4-hydroxy-Tempo Mito-Tempol protects mitochondria from the oxidative damage: once inside the mitochondria, it is rapidly converted by ubiquinol to the hydroxylamine Mito-Tempol-H that prevents lipid peroxidation, acting as a chain-breaking antioxidant against free radicals by donating a hydrogen atom [149].

The available data demonstrate that Mito-Tempol exerts antiatherogenic effects by inhibiting lipid peroxidation and favoring the phagocytosis of foamy cells [150], antiarrhythmic effects via control of mitochondrial-Ca^{2+} and preventing spontaneous action potentials [151], and the cardiotoxic effects deriving from administration of doxorubicin [152].

Sirtuins are a family of NAD^+-dependent deacetylases and deacylases responsible for cellular energy homeostasis, as they are involved in the regulation of mitochondrial function and redox balance, as well as glucose and lipid metabolism [153]. Three of the seven sirtuins produced in the human body are mitochondrial (SIRT3, SIRT4, and SIRT5). Activation of sirtuins leads to cardioprotective effects and to extend cellular life [117], mitigating oxidative stress, inflammation, hypertrophy, and cell death and promoting autophagy in an experimental models of cardiac dysfunction [153, 154]. Factors capable of activating sirtuins are calorie restriction [155], polyphenols such as resveratrol and curcumin, and drugs such as metformin and sodium glucose co-transporter-2 (SGLT2) inhibitors [156–159]. All this leads to a reduction in cardiovascular risk [155, 160].

Other molecules can exert indirect antioxidant effects such as melatonin and empagliflozin. Melatonin, produced by the pineal gland, is capable of neutralizing free radicals and exerting an indirect antioxidant effect [161]. In fact, melatonin stimulates glutathione peroxidase, glutathione reductase, superoxide dismutase, and glucose-6-phosphate dehydrogenase; all this leads to a stabilization of the cell membrane and to a greater resistance to oxidative insult [161]. Melatonin exerts a protective action against mitochondrial degeneration due to stimuli such as chemotherapeutic agents like doxorubicin [162], aging, ischemic cardiac injury, hypertension, diabetes mellitus, obesity, and metabolic disorders [163, 167].

Recent data indicate that SGLT2 inhibitors, in addition to being effective in maintaining euglycemia, have beneficial effects in pathological conditions such as heart and renal failure, even in nondiabetic patients [153]. Empagliflozin in fact exerts anti-inflammatory, antioxidant, antiatherosclerotic, and antiarrhythmic activities [155]. In a recent study, Canet et al. showed that empagliflozin reduces mitochondrial ROS production; this reduction was associated with a significant increase in the mRNA expression of the antioxidant enzymes SOD1 and GPX1 [168]. The administration of empagliflozin in subjects affected by HF with preserved ejection fraction led to a reduction in myocardial inflammation and oxidative stress, causing an increase in the bioavailability of nitric oxide (NO) in cardiomyocytes and thus exercising cardioprotection [158, 159, 168].

Many molecules have been tested in the modulation of mitochondrial ion channels for the treatment of myocardial infarction [169, 170]. The MPTP is a transmembrane mitochondrial channel which is closed under physiological conditions but which opens under certain conditions such as calcium accumulation, oxidative cell damage, and adenine depletion, causing apoptosis [171–175]. There are no clear data on the structure of MPTP: cyclophilin D (Cyp D) is an important regulatory component of the MPTP [180]; the c-subunit of ATP synthase appears to form the porotic component of MPTP in the deepest portion of the mitochondrial membrane [177–179]. During the period of myocardial ischemia, the MPTP remains closed and opens only in the first 2-3 minutes of reperfusion [180].

In IRI, pathological situations are created such as a reduction in ATP, an increase in intramitochondrial calcium concentration, and oxidative stress, which induce the opening of the MPTP, causing the death of the myocardiocyte; this process can be inhibited by cyclosporin A (CsA) which is able to prevent the binding between Cyp D and ANT [170–172, 181, 182]. Cyp D-deprived mice have small size myocardial revascularization damage [183, 184]. Therefore, the administration of CsA at the beginning of the myocardial reperfusion process reduces the extent of the damage [185]; on the contrary, the inhibition of CsA-related MPTP, initiated 15 minutes after reperfusion, does not exert any cardioprotective effect [186]; however, its efficacy was not confirmed in the CIRCUS trial [187, 188].

The mitochondrial calcium uniporter (MCU) is a multiprotein complex that regulates the entry of Ca^{2+} into the mitochondria and, therefore, the production of energy; the release of Ca^{2+} is regulated by the Na^+/Ca^{2+} exchanger (mNCX). Acute MCU dysfunction causes blockage of mitochondrial activity and therefore an imbalance between metabolic demands and energy produced [189]. However, MCU hyperfunction is responsible for the excessive mitochondrial uptake of Ca^{2+} with subsequent hyperactivation of mPTP and mNCX, causing cardiomyocyte necrosis during revascularization damage and the onset of arrhythmias [190, 191]. MCU and mNCX are therefore a possible therapeutic target in the treatment of cardiovascular pathologies: the pharmacological inhibition of mNCX with CGP-37157 reduces, in fact, the incidence of ventricular arrhythmias [191].

Numerous K^+ channels have been identified in the inner membrane of the mitochondria, such as the ATP-dependent (mitoK $_{ATP}$), voltage-gated Kv1.3 (mitoKv1.3), calcium-activated (mitoBKCa), and the two-pore domain TASK-3 (mitoTASK) potassium channels [192]. Potassium channels contribute to the maintenance of cell membrane integrity and regulate mitochondrial functions as they influence the integrity of the inner membrane and thus regulate mitochondrial functions such as energy transduction processes and ROS production; therefore, they are a possible therapeutic target in cytoprotection [193].

In particular, the ATP-dependent potassium channel (mitoK $_{ATP}$), activated in conditions of ischemia by ATP

reduction, is an energy saver [194]. Drugs such as diazoxide (channel activator) and sulfonylureas (channel inhibitors) protect the myocardium in IRI [195].

Activators of the BKCa channel, a large conductance Ca^{2+}-sensitive and voltage-activated K^+ mitochondrial channel, are able to reduce ischemic damage during the acute phase of IRI [194, 196].

UCP 1, UCP 2, and UCP 3 are internal membrane transport proteins of myocardiocytes that inhibit ROS production secondary to the acute phase of postischemic myocardial revascularization [169, 196]. Among the activators of UCP are antioxidant biofactor, aspalathin, ghrelin, losartan, ramipril, melatonin, resveratrol, metformin, glitazones, and sitagliptin [196].

Mitochondrial concentrations of Ca^{2+} modulate the energy balance and antioxidant activity against ROS [116]. In pathological conditions such as HF, the accumulation of Ca^{2+} in the mitochondria is impaired; therefore, the use of molecules capable of normalizing the mitochondrial Ca^{2+} content could represent a therapeutic option in HF.

Another therapeutic strategy could consist in the normalization of the mitochondrial redox balance, through the reduction of the Na^+ concentration in the cardiomyocytes. In this context, ranolazine and empagliflozin improve the balance of the ionic currents of Ca^{2+} and/or Na^+, generating beneficial effects in terms of energy and antioxidants [197–199]; ivabradine, a calcium channel blocker, is used in HF to increase calcium-dependent myocardial relaxation time [200]; omecamtiv mecarbil, on the other hand, exerts positive inotropic effects by increasing the calcium sensitivity of myofibrils [201, 202].

Calcium flux from the sarcoplasmic/endoplasmic reticulum (SR/ER) to mitochondria is one of the major regulatory mechanisms of many mitochondrial processes [203]. The cardiac isoform of the SR/ER calcium ATPase (SERCA2a) is a calcium ion pump activated by the hydrolysis of ATP that transfers Ca^{2+} from the cytosol of the cardiomyocyte to the lumen of the SR diastole [204]. In HF, SERCA2a is downregulated [205]; therefore, an overexpressing of SERCA2a in patients with HF may be a therapeutic approach to increase the ejection fraction and reduce the rate of arrhythmias [205].

2.2.2. Exogenous Targets. The balance between mitochondrial division (fission) and fusion processes determines the number, morphology, and function of mitochondria within each cell and is important for maintaining cardiovascular health in physiological or pathological conditions [206, 207].

The fission and fusion processes are regulated by specific enzymes and proteins; mitochondrial division is regulated by mitochondrial fission protein 1 (FIS1), mitochondrial fission factor, and dynamin-1-like protein (DNM1L); proteins that promote fusion include MFN1, MFN2, and optic atrophy protein 1 [208]. In conditions of CVD, such as HCM, ischemic heart disease, and HF, alterations of many of these proteins have been found [209, 210].

Autophagy is a process that preserves intracellular homeostasis, including myocardial and endothelial smooth muscle cells, through the seizure and lysosomal destruc-

tion of old or damaged cytoplasmic material [113, 211]. Mitophagy, aimed at the destruction of damaged and therefore potentially cytotoxic mitochondria, is important for the maintenance of cardiovascular homeostasis in physiological or pathological conditions [210]. In this context, genetic defects in autophagy or mitophagy favor the development of degenerative CVD; similarly, in pathological conditions such as atherosclerosis or acute myocardial ischemia, autophagy is impaired, causing cardiac remodeling [113, 211–216].

Calorie restriction and selected phytochemicals such as resveratrol, as activators of sirtuins, promote autophagy [212, 217–220]. Other promoters of autophagy/mitophagy include pharmacological agents, such as spermidine, anacardic acid, acetylsalicylic acid, curcumin, and garcinol [221–224], which inhibit the p300 protein associated with acetyltransferase E1A (EP300), as well as sirolimus, statins, and suberanylohydroxamic acid (SAHA), which block mammalian target of rapamycin (mTOR) [225–231].

The promoters of autophagy/mitophagy processes contribute to the reduction of cardiovascular risk [113, 232]. It has been shown that the intake of spermidine, by increasing the phosphorylation of titin, causes a reduction in blood pressure, limits cardiac hypertrophy, and slows the progression towards HF [225]. In the acute postinfarct phase, it is also able to reduce the inflammatory response and ventricular remodeling [224–226].

Sirolimus and other "limus agents" (mTOR inhibitors) are used in medicated coronary stents to reduce restenosis after myocardial revascularization [133]. In fact, they exert anti-inflammatory and antiproliferative effects, which stimulate autophagy/mitophagy leading to the degradation of oxLDL and macrophages of the atherosclerotic plaque [233].

In addition to suppressing ROS and activating SIRT1, SGLT2 inhibitors stimulate autophagy in cardiomyocytes, leading to improved cardiac performance in HF patients [157].

3. Conclusions and Limitations

Mitochondrial dysfunction, whatever its genesis, causes an energy deficit in the cell, aggravated by ROS overproduction. Cardiovascular pathologies such as ischemic heart disease, HF, arterial hypertension, and cardiac arrhythmias are characterized by mitochondrial dysfunction. Therefore, studies are ongoing to define the role of molecules capable of hampering mitochondrial dysfunction at different levels [234, 235]. Although the premises are promising, the data available are still few. New randomized clinical trials should be carried out to further investigate this field.

Data Availability

There is no raw data associated with this review article.

Conflicts of Interest

The authors declare that they have no conflicts of interest.

Acknowledgments

References

[1] R. A. Busiello, S. Savarese, and A. Lombardi, "Mitochondrial uncoupling proteins and energy metabolism," *Frontiers in Physiology*, vol. 6, p. 36, 2015.

[2] S. S. Sheu, R. T. Dirksen, and E. N. Pugh Jr., "Perspectives on: SGP symposium on mitochondrial physiology and medicine: mitochondria take center stage," *The Journal of General Physiology*, vol. 139, no. 6, pp. 391–393, 2012.

[3] P. Mitchell, "The protonmotive Q cycle: a general formulation," *FEBS Letters*, vol. 59, no. 2, pp. 137–139, 1975.

[4] J. Santo-Domingo and N. Demaurex, "Perspectives on: SGP symposium on mitochondrial physiology and medicine: the renaissance of mitochondrial pH," *The Journal of General Physiology*, vol. 139, no. 6, pp. 415–423, 2012.

[5] F. S. Celi, T. N. le, and B. Ni, "Physiology and relevance of human adaptive thermogenesis response," *Trends in Endocrinology and Metabolism*, vol. 26, no. 5, pp. 238–247, 2015.

[6] J. O-Uchi, S. Pan, and S. S. Sheu, "Perspectives on: SGP symposium on mitochondrial physiology and medicine: molecular identities of mitochondrial Ca2+ influx mechanism: updated passwords for accessing mitochondrial Ca2+-linked health and disease," *The Journal of General Physiology*, vol. 139, no. 6, pp. 435–443, 2012.

[7] L. K. Seidlmayer, V. V. Juettner, S. Kettlewell, E. V. Pavlov, L. A. Blatter, and E. N. Dedkova, "Distinct mPTP activation mechanisms in ischaemia-reperfusion: contributions of Ca2 +, ROS, pH, and inorganic polyphosphate," *Cardiovascular Research*, vol. 106, no. 2, pp. 237–248, 2015.

[8] L. Wei and R. T. Dirksen, "Perspectives on: SGP symposium on mitochondrial physiology and medicine: mitochondrial superoxide flashes: from discovery to new controversies," *The Journal of General Physiology*, vol. 139, no. 6, pp. 425–434, 2012.

[9] A. Weidinger and A. Kozlov, "Biological activities of reactive oxygen and nitrogen species: oxidative stress versus signal transduction," *Biomolecules*, vol. 5, no. 2, pp. 472–484, 2015.

[10] H. J. Kim, O. Khalimonchuk, P. M. Smith, and D. R. Winge, "Structure, function, and assembly of heme centers in mitochondrial respiratory complexes," *Biochimica et Biophysica Acta*, vol. 1823, no. 9, pp. 1604–1616, 2012.

[11] V. Papadopoulos and W. L. Miller, "Role of mitochondria in steroidogenesis," *Best Practice & Research. Clinical Endocrinology & Metabolism*, vol. 26, no. 6, pp. 771–790, 2012.

[12] S. DiMauro and M. Hirano, "Pathogenesis and treatment of mitochondrial disorders," *Advances in Experimental Medicine and Biology*, vol. 652, pp. 139–170, 2009.

[13] T. C. G. Vydt, R. F. M. de Coo, O. I. I. Soliman et al., "Cardiac Involvement in Adults With m.3243A>G MELAS Gene Mutation," *The American Journal of Cardiology*, vol. 99, no. 2, pp. 264–269, 2007.

[14] S. Verkaart, W. J. H. Koopman, S. E. van Emst-de Vries et al., "Superoxide production is inversely related to complex I activity in inherited complex I deficiency," *Biochimica et Biophysica Acta*, vol. 1772, no. 3, pp. 373–381, 2007.

[15] M. Brini, P. Pinton, M. P. King, M. Davidson, E. A. Schon, and R. Rizzuto, "A calcium signaling defect in the pathogenesis of a mitochondrial DNA inherited oxidative phosphorylation deficiency," *Nature Medicine*, vol. 5, no. 8, pp. 951–954, 1999.

[16] A. M. Moudy, S. D. Handran, M. P. Goldberg et al., "Abnormal calcium homeostasis and mitochondrial polarization in a human encephalomyopathy," *Proceedings of the National Academy of Sciences of the United States of America*, vol. 92, no. 3, pp. 729–733, 1995.

[17] D. E. Meyers, H. I. Basha, and M. K. Koenig, "Mitochondrial cardiomyopathy: pathophysiology, diagnosis, and management," *Texas Heart Institute Journal*, vol. 40, no. 4, pp. 385–394, 2013.

[18] M. G. Bates, J. P. Bourke, C. Giordano, G. d'Amati, D. M. Turnbull, and R. W. Taylor, "Cardiac involvement in mitochondrial DNA disease: clinical spectrum, diagnosis, and management," *European Heart Journal*, vol. 33, no. 24, pp. 3023–3033, 2012.

[19] G. Limongelli, M. Tome-Esteban, C. Dejthevaporn, S. Rahman, M. G. Hanna, and P. M. Elliott, "Prevalence and natural history of heart disease in adults with primary mitochondrial respiratory chain disease," *European Journal of Heart Failure*, vol. 12, no. 2, pp. 114–121, 2010.

[20] F. Scaglia, J. A. Towbin, W. J. Craigen et al., "Clinical spectrum, morbidity, and mortality in 113 pediatric patients with mitochondrial disease," *Pediatrics*, vol. 114, no. 4, pp. 925–931, 2004.

[21] J. Sadoshima, R. N. Kitsis, and S. Sciarretta, "Editorial: Mitochondrial Dysfunction and Cardiovascular Diseases," *Frontiers in Cardiovascular Medicine*, vol. 8, article 645986, 2021.

[22] N. Kaludercic and F. di Lisa, "Mitochondrial ROS Formation in the Pathogenesis of Diabetic Cardiomyopathy," *Frontiers in Cardiovascular Medicine*, vol. 7, p. 12, 2020.

[23] W. J. Liang and Å. B. Gustafsson, "The Aging Heart: Mitophagy at the Center of Rejuvenation," *Frontiers in Cardiovascular Medicine*, vol. 7, p. 18, 2020.

[24] D. A. Kubli, M. N. Quinsay, and Å. B. Gustafsson, "Parkin deficiency results in accumulation of abnormal mitochondria in aging myocytes," *Communicative & Integrative Biology*, vol. 6, no. 4, article e24511, 2013.

[25] M. Song, G. Gong, Y. Burelle et al., "Interdependence of parkin-mediated mitophagy and mitochondrial fission in adult mouse hearts," *Circulation Research*, vol. 117, no. 4, pp. 346–351, 2015.

[26] E. Latz and P. Duewell, "NLRP3 inflammasome activation in inflammaging," *Seminars in Immunology*, vol. 40, pp. 61–73, 2018.

[27] W. Neupert and M. Brunner, "The protein import motor of mitochondria," *Nature Reviews Molecular Cell Biology*, vol. 3, no. 8, pp. 555–565, 2002.

[28] I. Smyrnias, S. P. Gray, D. O. Okonko et al., "Cardioprotective effect of the mitochondrial unfolded protein response during chronic pressure overload," *Journal of the American College of Cardiology*, vol. 73, no. 14, pp. 1795–1806, 2019.

[29] S. I. Oka, A. D. Sabry, K. M. Cawley, and J. S. Warren, "Multiple Levels of PGC-1α Dysregulation in Heart Failure," *Front Cardiovasc Med.*, vol. 7, p. 2, 2020.

[30] S. A. Mohammed, S. Ambrosini, T. Lüscher, F. Paneni, and S. Costantino, "Epigenetic Control of Mitochondrial

Function in the Vasculature," *Frontiers in Cardiovascular Medicine*, vol. 7, p. 28, 2020.

[31] S. T. Keating and A. el-Osta, "Epigenetics and metabolism," *Circulation Research*, vol. 116, no. 4, pp. 715–736, 2015.

[32] J. A. Holland, L. M. Ziegler, and J. W. Meyer, "Atherogenic levels of lowdensity lipoprotein increase hydrogen peroxide generation in cultured human endothelial cells: possible mechanism of heightened endocytosis," *Journal of Cellular Physiology*, vol. 166, no. 1, pp. 144–151, 1996.

[33] C. A. Knight-Lozano, C. G. Young, D. L. Burow et al., "Cigarette smoke exposure and hypercholesterolemia increase mitochondrial damage in cardiovascular tissues," *Circulation*, vol. 105, no. 7, pp. 849–854, 2002.

[34] S. W. Ballinger, C. Patterson, C. A. Knight-Lozano et al., "Mitochondrial integrity and function in atherogenesis," *Circulation*, vol. 106, no. 5, pp. 544–549, 2002.

[35] M. Reilly, N. Delanty, J. A. Lawson, and G. A. FitzGerald, "Modulation of oxidant stress in vivo in chronic cigarette smokers," *Circulation*, vol. 94, no. 1, pp. 19–25, 1996.

[36] D. Praticò, O. P. Barry, J. A. Lawson et al., "IPF2α-I: An index of lipid peroxidation in humans," *Proceedings of the National Academy of Sciences of the United States of America*, vol. 95, no. 7, pp. 3449–3454, 1998.

[37] H. Ito, M. Torii, and T. Suzuki, "Decreased superoxide dismutase activity and increased superoxide anion production in cardiac hypertrophy of spontaneously hypertensive rats," *Clinical and Experimental Hypertension*, vol. 17, no. 5, pp. 803–816, 1995.

[38] G. F. Watts and D. A. Playford, "Dyslipoproteinaemia and hyperoxidative stress in the pathogenesis of endothelial dysfunction in non-insulin dependent diabetes mellitus: an hypothesis," *Atherosclerosis*, vol. 141, no. 1, pp. 17–30, 1998.

[39] D. B. Rousselot, J. P. Bastard, and M. C. Jaudon, "Consequences of the diabetic status on the oxidant/antioxidant balance," *Diabetes & Metabolism*, vol. 26, pp. 163–176, 2000.

[40] P. M. Yao and I. Tabas, "Free Cholesterol Loading of Macrophages Is Associated with Widespread Mitochondrial Dysfunction and Activation of the Mitochondrial Apoptosis Pathway*," *Journal of Biological Chemistry*, vol. 276, no. 45, pp. 42468–42476, 2001.

[41] R. Asmis and J. G. Begley, "Oxidized LDL promotes peroxide mediated mitochondrial dysfunction and cell death in human macrophages," *Circulation Research*, vol. 92, no. 1, pp. e20–e29, 2003.

[42] H. van Jaarsveld, J. M. Kuyl, and D. W. Alberts, "Exposure of rats to low concentration of cigarette smoke increases myocardial sensitivity to ischaemia/reperfusion," *Basic Research in Cardiology*, vol. 87, no. 4, pp. 393–399, 1992.

[43] A. Gvozdjakova, V. Bada, L. Sany et al., "Smoke cardiomyopathy: disturbance of oxidative processes in myocardial mitochondria," *Cardiovascular Research*, vol. 18, no. 4, pp. 229–232, 1984.

[44] M. G. Andreassi and N. Botto, "DNA Damage as a New Emerging Risk Factor in Atherosclerosis," *Trends in Cardiovascular Medicine*, vol. 13, no. 7, pp. 270–275, 2003.

[45] B. Binkova, Z. Smerhovsky, P. Strejc et al., "DNA-adducts and atherosclerosis: a study of accidental and sudden death males in the Czech Republic," *Mutation Research*, vol. 501, no. 1-2, pp. 115–128, 2002.

[46] W. Martinet, M. W. M. Knaapen, G. R. Y. DeMeyer, A. G. Herman, and M. M. Kockx, "Elevated levels of oxidative DNA damage and DNA repair enzymes in human atherosclerotic plaques," *Circulation*, vol. 106, no. 8, pp. 927–932, 2002.

[47] E. Ceaser, A. Ramachandran, A. L. Levonen, and V. M. Darley-Usmar, "Oxidized low-density lipoprotein and 15-deoxy-$\Delta^{12,14}$-PGJ$_2$ increase mitochondrial complex I activity in endothelial cells," *American Journal of Physiology-Heart and Circulatory Physiology*, vol. 285, no. 6, pp. H2298–H2308, 2003.

[48] R. Kinscherf, H.-P. Deigner, C. Usinger et al., "Induction of mitochondrial manganese superoxide dismutase in macrophages by oxidized LDL: its relevance in atherosclerosis of humans and heritable hyperlipidemic rabbits," *The FASEB Journal*, vol. 11, no. 14, pp. 1317–1328, 1997.

[49] L. Mabile, O. Meilhac, I. Escargueil-Blanc et al., "Mitochondrial function is involved in LDL oxidation mediated by human cultured endothelial cells," *Arteriosclerosis, Thrombosis, and Vascular Biology*, vol. 17, no. 8, pp. 1575–1582, 1997.

[50] N. P. Mikaelian, E. M. Khalilov, A. S. Ivanov, E. S. Fortinskaia, and I. M. Lopukhin, "Study of some Mitochondrial enzymes in circulating lymphocytes during hemoperfusion for experimental hypercholesterolemia," *Bulletin of Experimental Biology and Medicine*, vol. 96, no. 3, pp. 1230–1232, 1983.

[51] R. Sreekumar, J. Unnikrishnan, A. Fu et al., "Impact of high-fat diet and antioxidant supplement on mitochondrial functions and gene transcripts in rat muscle," *American Journal of Physiology. Endocrinology and Metabolism*, vol. 282, no. 5, pp. E1055–E1061, 2002.

[52] R. Sreekumar, J. Unnikrishnan, A. Fu et al., "Effects of caloric restriction on mitochondrial function and gene transcripts in rat muscle," *American Journal of Physiology. Endocrinology and Metabolism*, vol. 283, no. 1, pp. E38–E43, 2002.

[53] T. Nishikawa, D. Edelstein, X. L. Du et al., "Normalizing mitochondrial superoxide production blocks three pathways of hyperglycaemic damage," *Nature*, vol. 404, no. 6779, pp. 787–790, 2000.

[54] T. Nishikawa, D. Edelstein, and M. Brownlee, "The missing link: a single unifying mechanism for diabetic complications," *Kidney International*, vol. 58, pp. S26–S30, 2000.

[55] S. Vega-Lopez, S. Devaraj, and I. Jialal, "Oxidative stress and antioxidant supplementation in the management of diabetic cardiovascular disease," *Journal of Investigative Medicine*, vol. 52, no. 1, pp. 24–32, 2004.

[56] A. K. Azevedo-Martins, S. Lortz, S. Lenzen, R. Curi, D. L. Eizirik, and M. Tiedge, "Improvement of the mitochondrial antioxidant defense status prevents cytokine-induced nuclear Factor-κB activation in insulin-producing cells," *Diabetes*, vol. 52, no. 1, pp. 93–101, 2003.

[57] J. Gvozdjak, A. Gvozdjakova, J. Kucharska, and V. Bada, "The effect of smoking on myocardial metabolism," *Czechoslovak Medicine*, vol. 10, no. 1, pp. 47–53, 1987.

[58] A. Gvozdjakova, F. Simko, J. Kucharska, Z. Braunova, P. Psenek, and J. Kyselovic, "Captopril increased mitochondrial coenzyme Q10level, improved respiratory chain function and energy production in the left ventricle in rabbits with smoke mitochondrial cardiomyopathy," *BioFactors*, vol. 10, no. 1, pp. 61–65, 1999.

[59] D. K. St Clair, J. A. Jordan, X. S. Wan, and C. G. Gairola, "Protective role of manganese superoxide dismutase against cigarette smokeinduced cytotoxicity," *Journal of Toxicology and Environmental Health*, vol. 43, no. 2, pp. 239–249, 1994.

[60] G. A. Cortopassi and N. Arnheim, "Detection of a specific mitochondrial DNA deletion in tissues of older humans," *Nucleic Acids Research*, vol. 18, no. 23, pp. 6927–6933, 1990.

[61] I. Trounce, E. Byrne, and S. Marzuki, "Decline in skeletal muscle mitochondrial respiration chain function with ageing," *Lancet*, vol. 334, no. 8653, pp. 44-45, 1989.

[62] American Heart Association, *Heart disease and stroke statistics— 2005 update*, American Heart Association, Dallas, TX pp, 2005.

[63] P. Di Giosia, P. Giorgini, C. A. Stamerra, M. Petrarca, C. Ferri, and A. Sahebkar, "Gender differences in epidemiology, pathophysiology, and treatment of hypertension," *Current Atherosclerosis Reports*, vol. 20, no. 3, p. 13, 2018.

[64] P. Di Giosia, G. Passacquale, M. Petrarca, P. Giorgini, A. M. Marra, and A. Ferro, "Gender differences in cardiovascular prophylaxis: focus on antiplatelet treatment," *Pharmacological Research*, vol. 119, pp. 36–47, 2017.

[65] J. D. Wagner, J. R. Kaplan, and R. T. Burkman, "Reproductive hormones and cardiovascular disease: Mechanism of action and clinical implications," *Obstetrics and Gynecology Clinics of North America*, vol. 29, no. 3, pp. 475–493, 2002.

[66] K. Node, M. Kitakaze, H. Kosaka, T. Minamino, H. Funaya, and M. Hori, "Amelioration of ischemia- and reperfusion-induced myocardial injury by 17β-Estradiol," *Circulation*, vol. 96, no. 6, pp. 1953–1963, 1997.

[67] A. Nadal, A. B. Ropero, O. Laribi, M. Maillet, E. Fuentes, and B. Soria, "Nongenomic actions of estrogens and xenoestrogens by binding at a plasma membrane receptor unrelated to estrogen receptor alpha and estrogen receptor beta," *Proceedings of the National Academy of Sciences of the United States of America*, vol. 97, no. 21, pp. 11603–11608, 2000.

[68] E. A. Booth, M. Marchesi, E. J. Kilbourne, and B. R. Lucchesi, "17Beta-estradiol as a receptor-mediated cardioprotective agent," *Journal of Pharmacology and Experimental Therapeutics*, vol. 307, no. 1, pp. 395–401, 2003.

[69] T. M. Lee, S. F. Su, C. C. Tsai, Y. T. Lee, and C. H. Tsai, "Cardioprotective Effects of 17β-Estradiol Produced by Activation of Mitochondrial ATP-Sensitive K$^+$Channels in Canine Hearts," *Journal of Molecular and Cellular Cardiology*, vol. 32, no. 7, pp. 1147–1158, 2000.

[70] P. Geraldes, M. G. Sirois, P. N. Bernatchez, and J. F. Tanguay, "Estrogen regulation of endothelial and smooth muscle cell migration and proliferation: role of p38 and p42/44 mitogen-activated protein kinase," *Arteriosclerosis, Thrombosis, and Vascular Biology*, vol. 22, no. 10, pp. 1585–1590, 2002.

[71] C. Borras, J. Sastre, D. Garcia-Sala, A. Lloret, F. V. Pallardo, and J. Vina, "Mitochondria from females exhibit higher antioxidant gene expression and lower oxidative damage than males," *Free Radical Biology and Medicine*, vol. 34, no. 5, pp. 546–552, 2003.

[72] J. Vina, J. Sastre, F. Pallardo, and C. Borras, "Mitochondrial theory of aging: importance to explain why females live longer than males," *Antioxidants & Redox Signaling*, vol. 5, no. 5, pp. 549–556, 2003.

[73] J. Q. Chen, M. Delannoy, C. Cooke, and J. D. Yager, "Mitochondrial localization of ERalpha and ERbeta in human MCF7 cells," *American Journal of Physiology. Endocrinology and Metabolism*, vol. 286, no. 6, pp. E1011–E1022, 2004.

[74] J. Nilsen and B. R. Diaz, "Mechanism of estrogen-mediated neuroprotection: regulation of mitochondrial calcium and Bcl-2 expression," *Proceedings of the National Academy of Sciences of the United States of America*, vol. 100, no. 5, pp. 2842–2847, 2003.

[75] J. Q. Chen, M. Eshete, W. L. Alworth, and J. D. Yager, "Binding of MCF-7 cell mitochondrial proteins and recombinant human estrogen receptors alpha and beta to human mitochondrial DNA estrogen response elements," *Journal of Cellular Biochemistry*, vol. 93, no. 2, pp. 358–373, 2004.

[76] X. Wang, J. W. Simpkins, J. A. Dykens, and P. R. Cammarata, "Oxidative damage to human lens epithelial cells in culture: estrogen protection of mitochondrial potential, ATP, and cell viability," *Investigative Ophthalmology & Visual Science*, vol. 44, no. 5, pp. 2067–2075, 2003.

[77] K. Adachi, Y. Fujiura, F. Mayumi et al., "A deletion of mitochondrial DNA in murine doxorubicin-induced cardiotoxicity," *Biochemical and Biophysical Research Communications*, vol. 195, no. 2, pp. 945–951, 1993.

[78] W. Lewis and M. C. Dalakas, "Mitochondrial toxicity of antiviral drugs," *Nature Medicine*, vol. 1, no. 5, pp. 417–422, 1995.

[79] W. Lewis, "Atherosclerosis in AIDS: Potential Pathogenetic Roles of Antiretroviral Therapy and HIV," *Journal of Molecular and Cellular Cardiology*, vol. 32, no. 12, pp. 2115–2129, 2000.

[80] M. N. Swartz, "Mitochondrial toxicity—new adverse drug effects," *The New England Journal of Medicine*, vol. 333, no. 17, pp. 1146–1148, 1995.

[81] K. Brinkman, H. J. ter Hofstede, D. M. Burger, J. A. Smeitink, and P. P. Koopmans, "Adverse effects of reverse transcriptase inhibitors," *AIDS*, vol. 12, no. 14, pp. 1735–1744, 1998.

[82] C. A. Stamerra, P. Di Giosia, C. Ferri et al., "Statin therapy and sex hormones," *European Journal of Pharmacology*, vol. 890, no. 890, article 173745, 2021.

[83] P. P. Simeonova, T. Hulderman, D. Harki, and M. I. Luster, "Arsenic exposure accelerates atherogenesis in apolipoprotein E / mice," *Environmental Health Perspectives*, vol. 111, no. 14, pp. 1744–1748, 2003.

[84] V. G. Sharov, A. Goussev, M. Lesch, S. Goldstein, and H. N. Sabbah, "Abnormal mitochondrial function in myocardium of dogs with chronic heart failure," *Journal of Molecular and Cellular Cardiology*, vol. 30, no. 9, pp. 1757–1762, 1998.

[85] E. Arbustini, M. Diegoli, R. Fasani et al., "Mitochondrial DNA mutations and mitochondrial abnormalities in dilated cardiomyopathy," *The American Journal of Pathology*, vol. 153, no. 5, pp. 1501–1510, 1998.

[86] G. D. Lopaschuk, J. R. Ussher, C. D. Folmes, J. S. Jaswal, and W. C. Stanley, "Myocardial fatty acid metabolism in health and disease," *Physiological Reviews*, vol. 90, no. 1, pp. 207–258, 2010.

[87] M. F. Allard, B. O. Schönekess, S. L. Henning, D. R. English, and G. D. Lopaschuk, "Contribution of oxidative metabolism and glycolysis to ATP production in hypertrophied hearts," *American Journal of Physiology*, vol. 267, 2 Part 2, pp. H742–H750, 1994.

[88] T. G. von Lueder, D. Kotecha, D. Atar, and I. Hopper, "Neurohormonal blockade in heart failure," *Cardiac Failure Review*, vol. 3, no. 1, pp. 19–24, 2017.

[89] J. M. Grillon, K. R. Johnson, K. Kotlo, and R. S. Danziger, "Non-histone lysine acetylated proteins in heart failure," *Biochimica et Biophysica Acta*, vol. 1822, no. 4, pp. 607–614, 2012.

[90] C. Carrico, J. G. Meyer, W. He, B. W. Gibson, and E. Verdin, "The mitochondrial acylome emerges: proteomics, regulation by sirtuins, and metabolic and disease implications," *Cell Metabolism*, vol. 27, no. 3, pp. 497–512, 2018.

[91] J. L. Horton, O. J. Martin, L. Lai et al., "Mitochondrial protein hyperacetylation in the failing heart," *JCI Insight*, vol. 1, no. 2, article e84897, 2016.

[92] C. F. Lee, J. D. Chavez, L. Garcia-Menendez et al., "Normalization of NAD+ redox balance as a therapy for heart failure," *Circulation*, vol. 134, no. 12, pp. 883–894, 2016.

[93] X. Zhang, R. Ji, X. Liao et al., "MicroRNA-195 regulates metabolism in failing myocardium via alterations in sirtuin 3 expression and mitochondrial protein acetylation," *Circulation*, vol. 137, no. 19, pp. 2052–2067, 2018.

[94] L. W. Finley, W. Haas, V. Desquiret-Dumas et al., "Succinate dehydrogenase is a direct target of sirtuin 3 deacetylase activity," *PLoS One*, vol. 6, no. 8, article e23295, 2011.

[95] A. V. Hafner, J. Dai, A. P. Gomes et al., "Regulation of the mPTP by SIRT3-mediated deacetylation of CypD at lysine 166 suppresses age-related cardiac hypertrophy," *Aging*, vol. 2, no. 12, pp. 914–923, 2010.

[96] E. D. Lewandowski, J. M. O'Donnell, T. D. Scholz, N. Sorokina, and P. M. Buttrick, "Recruitment of NADH shuttling in pressure-overloaded and hypertrophic rat hearts," *American Journal of Physiology-Cell Physiology*, vol. 292, no. 5, pp. C1880–C1886, 2007.

[97] L. Lai, T. C. Leone, M. P. Keller et al., "Energy metabolic reprogramming in the hypertrophied and early stage failing heart: a multisystems approach," *Circulation: Heart Failure*, vol. 7, no. 6, pp. 1022–1031, 2014.

[98] N. Diguet, S. A. J. Trammell, C. Tannous et al., "Nicotinamide riboside preserves cardiac function in a mouse model of dilated cardiomyopathy," *Circulation*, vol. 137, no. 21, pp. 2256–2273, 2018.

[99] G. Karamanlidis, C. F. Lee, L. Garcia-Menendez et al., "Mitochondrial complex I deficiency increases protein acetylation and accelerates heart failure," *Cell Metabolism*, vol. 18, no. 2, pp. 239–250, 2013.

[100] G. Santulli, W. Xie, S. R. Reiken, and A. R. Marks, "Mitochondrial calcium overload is a key determinant in heart failure," *Proceedings of the National Academy of Sciences of the United States of America*, vol. 112, no. 36, pp. 11389–11394, 2015.

[101] R. M. Denton, D. A. Richards, and J. G. Chin, "Calcium ions and the regulation of NAD+-linked isocitrate dehydrogenase from the mitochondria of rat heart and other tissues," *Biochemical Journal*, vol. 176, no. 3, pp. 899–906, 1978.

[102] R. K. Hopper, S. Carroll, A. M. Aponte et al., "Mitochondrial matrix phosphoproteome: effect of extra mitochondrial calcium," *Biochemistry*, vol. 45, no. 8, pp. 2524–2536, 2006.

[103] B. Glancy, W. T. Willis, D. J. Chess, and R. S. Balaban, "Effect of calcium on the oxidative phosphorylation cascade in skeletal muscle mitochondria," *Biochemistry*, vol. 52, no. 16, pp. 2793–2809, 2013.

[104] D. B. Zorov, M. Juhaszova, and S. J. Sollott, "Mitochondrial reactive oxygen species (ROS) and ROS-induced ROS release," *Physiological Reviews*, vol. 94, no. 3, pp. 909–950, 2014.

[105] J. M. Baughman, F. Perocchi, H. S. Girgis et al., "Integrative genomics identifies MCU as an essential component of the mitochondrial calcium uniporter," *Nature*, vol. 476, no. 7360, pp. 341–345, 2011.

[106] G. S. Williams, L. Boyman, and W. J. Lederer, "Mitochondrial calcium and the regulation of metabolism in the heart," *Journal of Molecular and Cellular Cardiology*, vol. 78, pp. 35–45, 2015.

[107] S. Sommakia, P. R. Houlihan, S. S. Deane et al., "Mitochondrial cardiomyopathies feature increased uptake and diminished efflux of mitochondrial calcium," *Journal of Molecular and Cellular Cardiology*, vol. 113, pp. 22–32, 2017.

[108] T. S. Luongo, J. P. Lambert, P. Gross et al., "The mitochondrial Na$^+$/Ca^{2+} exchanger is essential for Ca^{2+} homeostasis and viability," *Nature*, vol. 545, no. 7652, pp. 93–97, 2017.

[109] E. T. Chouchani, V. R. Pell, E. Gaude et al., "Ischaemic accumulation of succinate controls reperfusion injury through mitochondrial ROS," *Nature*, vol. 515, no. 7527, pp. 431–435, 2014.

[110] N. Ardanaz, X. P. Yang, M. E. Cifuentes et al., "Lack of glutathione peroxidase 1 accelerates cardiac-specific hypertrophy and dysfunction in angiotensin II hypertension," *Hypertension*, vol. 55, no. 1, pp. 116–123, 2010.

[111] F. Billia, L. Hauck, F. Konecny, V. Rao, J. Shen, and T. W. Mak, "PTEN-inducible kinase 1 (PINK1)/Park6 is indispensable for normal heart function," *Proceedings of the National Academy of Sciences of the United States of America*, vol. 108, no. 23, pp. 9572–9577, 2011.

[112] L. Chen, Q. Gong, J. P. Stice, and A. A. Knowlton, "Mitochondrial OPA1, apoptosis, and heart failure," *Cardiovascular Research*, vol. 84, no. 1, pp. 91–99, 2009.

[113] L. Kane and R. Youle, "Mitochondrial fission and fusion and their roles in the heart," *Journal of Molecular Medicine*, vol. 88, no. 10, pp. 971–979, 2010.

[114] D. A. Brown, J. B. Perry, M. E. Allen et al., "Mitochondrial function as a therapeutic target in heart failure," *Nature Reviews Cardiology*, vol. 14, no. 4, pp. 238–250, 2017.

[115] D. A. Chistiakov, T. P. Shkurat, A. A. Melnichenko, A. V. Grechko, and A. N. Orekhov, "The role of mitochondrial dysfunction in cardiovascular disease: a brief review," *Annals of Medicine*, vol. 50, no. 2, pp. 121–127, 2018.

[116] M. Bonora, M. R. Wieckowski, D. A. Sinclair, G. Kroemer, P. Pinton, and L. Galluzzi, "Targeting mitochondria for cardiovascular disorders: therapeutic potential and obstacles," *Nature Reviews Cardiology*, vol. 16, no. 1, pp. 33–55, 2019.

[117] D. F. Dai, T. Chen, H. Szeto et al., "Mitochondrial targeted antioxidant peptide ameliorates hypertensive cardiomyopathy," *Journal of the American College of Cardiology*, vol. 58, no. 1, pp. 73–82, 2011.

[118] J. N. Peoples, A. Saraf, N. Ghazal, T. T. Pham, and J. Q. Kwong, "Mitochondrial dysfunction and oxidative stress in heart disease," *Experimental & Molecular Medicine*, vol. 51, no. 12, pp. 1–13, 2019.

[119] F. Sam, D. L. Kerstetter, D. R. Pimental et al., "Increased reactive oxygen species production and functional alterations in antioxidant enzymes in human failing myocardium," *Journal of Cardiac Failure*, vol. 11, no. 6, pp. 473–480, 2005.

[120] D. Montaigne, X. Marechal, A. Coisne et al., "Myocardial contractile dysfunction is associated with impaired mitochondrial function and dynamics in type 2 diabetic but not in obese patients," *Circulation*, vol. 130, no. 7, pp. 554–564, 2014.

[121] A. E. Vendrov, M. D. Stevenson, S. Alahari et al., "Attenuated superoxide dismutase 2 activity induces atherosclerotic

plaque instability during aging in hyperlipidemic mice," *Journal of the American Heart Association*, vol. 6, no. 11, 2017.

[122] A. N. Orekhov, A. V. Poznyak, I. A. Sobenin, N. N. Nikifirov, and E. A. Ivanova, "Mitochondrion as a selective target for treatment of atherosclerosis: role of mitochondrial DNA mutations and defective mitophagy in the pathogenesis of atherosclerosis and chronic inflammation," *Current Neuropharmacology*, vol. 17, p. 1, 2019.

[123] S. A. Mortensen, F. Rosenfeldt, A. Kumar et al., "The effect of coenzyme Q_{10} on morbidity and mortality in chronic heart failure: results from Q-SYMBIO: a randomized double-blind trial," *JACC: Heart Failure*, vol. 2, no. 6, pp. 641–649, 2014.

[124] Heart Protection Study Collaborative Group, "MRC/BHF Heart Protection Study of antioxidant vitamin supplementation in 20 536 high-risk individuals: a randomised placebo-controlled trial," *The Lancet*, vol. 360, pp. 23–33, 2002.

[125] H. D. Sesso, J. E. Buring, W. G. Christen et al., "Vitamins E and C in the prevention of cardiovascular disease in men: the Physicians' Health Study II randomized controlled trial," *JAMA*, vol. 300, no. 18, pp. 2123–2133, 2008.

[126] N. Katsiki and C. Manes, "Is there a role for supplemented antioxidants in the prevention of atherosclerosis?," *Clinical Nutrition*, vol. 28, no. 1, pp. 3–9, 2009.

[127] R. B. Singh, "Effect of coenzyme Q10 on risk of atherosclerosis in patients with recent myocardial infarction," *Molecular and Cellular Biochemistry*, vol. 246, no. 1/2, pp. 75–82, 2003.

[128] A. Aimo, V. Castiglione, C. Borrelli et al., "Oxidative stress and inflammation in the evolution of heart failure: from pathophysiology to therapeutic strategies," *European Journal of Preventive Cardiology*, vol. 27, no. 5, pp. 494–510, 2020.

[129] R. F. Ribeiro Jr., E. R. Dabkowski, K. C. Shekar, K. A. O'Connell, P. A. Hecker, and M. P. Murphy, "MitoQ improves mitochondrial dysfunction in heart failure induced by pressure overload," *Free Radical Biology and Medicine*, vol. 117, pp. 18–29, 2018.

[130] V. J. Adlam, J. C. Harrison, C. M. Porteous et al., "Targeting an antioxidant to mitochondria decreases cardiac ischemia-reperfusion injury," *The FASEB Journal*, vol. 19, no. 9, pp. 1088–1095, 2005.

[131] D. A. Brown, S. L. Hale, C. P. Baines et al., "Reduction of early reperfusion injury with the mitochondria-targeting peptide bendavia," *Journal of Cardiovascular Pharmacology and Therapeutics*, vol. 19, no. 1, pp. 121–132, 2014.

[132] J. Shi, W. Dai, S. L. Hale et al., "Bendavia restores mitochondrial energy metabolism gene expression and suppresses cardiac fibrosis in the border zone of the infarcted heart," *Life Sciences*, vol. 141, pp. 170–178, 2015.

[133] J. Gambardella, D. Sorriento, M. Ciccarelli et al., "Functional role of mitochondria in arrhythmogenesis," *Advances in Experimental Medicine and Biology*, vol. 982, pp. 191–202, 2017.

[134] L. Konya, V. Kekesi, S. Juhasz-Nagy, and J. Feher, "The effect the superoxide dismutase in the myocardium during reperfusion in the dog," *Free Radical Biology and Medicine*, vol. 13, no. 5, pp. 527–532, 1992.

[135] M. Ozaydin, O. Peker, D. Erdogan et al., "N-acetylcysteine for the prevention of postoperative atrial fibrillation: a prospective, randomized, placebo-controlled pilot study," *European Heart Journal*, vol. 29, no. 5, pp. 625–631, 2008.

[136] A. Sahebkar, A. F. G. Cicero, P. Di Giosia et al., "Pathophysiological mechanisms of statin-associated myopathies: possible role of the ubiquitin-proteasome system," *Journal of Cachexia, Sarcopenia and Muscle*, vol. 11, no. 5, pp. 1177–1186, 2020.

[137] J. M. Villalba, C. Parrado, M. Santos-Gonzalez, and F. J. Alcain, "Therapeutic use of coenzyme Q10 and coenzyme Q10-related compounds and formulations," *Expert Opinion on Investigational Drugs*, vol. 19, no. 4, pp. 535–554, 2010.

[138] M. Banach, C. Serban, S. Ursoniu et al., "Statin therapy and plasma coenzyme Q10 concentrations–A systematic review and meta-analysis of placebo-controlled trials," *Pharmacological Research*, vol. 99, pp. 329–336, 2015.

[139] A. F. G. Cicero, A. Colletti, G. Bajraktari et al., "Lipid lowering nutraceuticals in clinical practice: position paper from an International Lipid Expert Panel," *Archives of Medical Science*, vol. 13, no. 5, pp. 965–1005, 2017.

[140] L. Lei and Y. Liu, "Efficacy of coenzyme Q10 in patients with cardiac failure: a meta-analysis of clinical trials," *BMC Cardiovascular Disorders*, vol. 17, no. 1, p. 196, 2017.

[141] H. Qu, M. Guo, H. Chai, W. T. Wang, Z. Y. Gao, and D. Z. Shi, "Effects of coenzyme Q10 on statin-induced myopathy: an updated meta-analysis of randomized controlled trials," *Journal of the American Heart Association*, vol. 7, no. 19, article e009835, 2018.

[142] M. J. Rossman, J. R. Santos-Parker, C. A. C. Steward et al., "Chronic supplementation with a mitochondrial antioxidant (MitoQ) improves vascular function in healthy older adults," *Hypertension*, vol. 71, no. 6, pp. 1056–1063, 2018.

[143] D. Graham, N. N. Huynh, C. A. Hamilton et al., "Mitochondria-targeted antioxidant MitoQ10Improves endothelial function and attenuates cardiac hypertrophy," *Hypertension*, vol. 54, no. 2, pp. 322–328, 2009.

[144] H. H. Szeto, "First-in-class cardiolipin-protective compound as a therapeutic agent to restore mitochondrial bioenergetics," *British Journal of Pharmacology*, vol. 171, no. 8, pp. 2029–2050, 2014.

[145] J. Cho, K. Won, D. Wu et al., "Potent mitochondria-targeted peptides reduce myocardial infarction in rats," *Coronary Artery Disease*, vol. 18, no. 3, pp. 215–220, 2007.

[146] M. A. Daubert, E. Yow, G. Dunn et al., "Novel mitochondria-targeting peptide in heart failure Treatment," *Circulation: Heart Failure*, vol. 10, no. 12, article e004389, 2017.

[147] A. Saad, S. M. S. Herrmann, A. Eirin et al., "Phase 2a clinical trial of mitochondrial protection (elamipretide) during stent revascularization in patients with atherosclerotic renal artery stenosis," *Circulation. Cardiovascular Interventions*, vol. 10, no. 9, article e005487, 2017.

[148] C. M. Gibson, R. P. Giugliano, R. A. Kloner et al., "EMBRACE STEMI study: a Phase 2a trial to evaluate the safety, tolerability, and efficacy of intravenous MTP-131 on reperfusion injury in patients undergoing primary percutaneous coronary intervention," *European Heart Journal*, vol. 37, no. 16, pp. 1296–1303, 2016.

[149] J. Trnka, F. H. Blaikie, A. Logan, R. A. Smith, and M. P. Murphy, "Antioxidant properties of MitoTEMPOL and its hydroxylamine," *Free Radical Research*, vol. 43, no. 1, pp. 4–12, 2009.

[150] Y. Ma, Z. Huang, Z. Zhou et al., "A novel antioxidant Mito-Tempol inhibits ox-LDL-induced foam cell formation

through restoration of autophagy flux," *Free Radical Research*, vol. 129, pp. 463–472, 2018.

[151] Y. Olgar, D. Billur, E. Tuncay, and B. Turan, "MitoTEMPO provides an antiarrhythmic effect in aged-rats through attenuation ∗∗of∗∗ mitochondrial reactive oxygen species," *Experimental Gerontology*, vol. 136, article 110961, 2020.

[152] J. S. Dickey, Y. Gonzalez, B. Aryal et al., "Mito-tempol and dexrazoxane exhibit cardioprotective and chemotherapeutic effects through specific protein oxidation and autophagy in a syngeneic breast tumor preclinical model," *PLoS One*, vol. 8, no. 8, article e70575, 2013.

[153] A. Planavila, R. Iglesias, M. Giralt, and F. Villarroya, "Sirt1 acts in association with PPARα to protect the heart from hypertrophy, metabolic dysregulation, and inflammation," *Cardiovascular Research*, vol. 90, no. 2, pp. 276–284, 2011.

[154] R. H. Houtkooper, E. Pirinen, and J. Auwerx, "Sirtuins as regulators of metabolism and healthspan," *Nature Reviews. Molecular Cell Biology*, vol. 13, no. 4, pp. 225–238, 2012.

[155] P. Di Giosia, C. A. Stamerra, P. Giorgini, T. Jamialahamdi, A. E. Butler, and A. Sahebkar, "The role of nutrition in inflammaging," *Ageing Research Reviews*, vol. 77, article 101596, 2022.

[156] E. Zendedel, A. E. Butler, S. L. Atkin, and A. Sahebkar, "Impact of curcumin on sirtuins: a review," *Journal of Cellular Biochemistry*, vol. 119, no. 12, pp. 10291–10300, 2018.

[157] A. S. Manolis and A. A. Manolis, "Use of sodium–glucose cotransporter 2 (SGLT2) inhibitors beyond diabetes: on the verge of a paradigm shift?," *Rhythmos*, vol. 15, pp. 1–5, 2020.

[158] D. Kolijn, S. Pabel, Y. Tian et al., "Empagliflozin improves endothelial and cardiomyocyte function in human heart failure with preserved ejection fraction via reduced pro-inflammatory-oxidative pathways and protein kinase Gα oxidation," *Cardiovascular Research*, vol. 117, no. 2, pp. 495–507, 2021.

[159] M. Mizuno, A. Kuno, T. Yano et al., "Empagliflozin normalizes the size and number of mitochondria and prevents reduction in mitochondrial size after myocardial infarction in diabetic hearts," *Physiological Reports*, vol. 6, no. 12, article e13741, 2018.

[160] M. Banach, A. M. Patti, R. V. Giglio et al., "The role of nutraceuticals in statin intolerant patients," *Journal of the American College of Cardiology*, vol. 72, no. 1, pp. 96–118, 2018.

[161] R. J. Reiter, J. M. Guerrero, J. J. Garcia, and D. Acuna-Castroviejo, "Reactive oxygen intermediates, molecular damage, and aging. Relation to melatonin," *Annals of the New York Academy of Sciences*, vol. 854, no. 1, pp. 410–424, 1998.

[162] E. Balli, U. O. Mete, A. Tuli, O. Tap, and M. Kaya, "Effect of melatonin on the cardiotoxicity of doxorubicin," *Histology and Histopathology*, vol. 19, pp. 1101–1108, 2004.

[163] O. C. Baltatu, F. G. Amaral, L. A. Campos, and J. Cipolla-Neto, "Melatonin, mitochondria and hypertension," *Cellular and Molecular Life Sciences*, vol. 74, no. 21, pp. 3955–3964, 2017.

[164] M. I. Rodríguez, M. Carretero, G. Escames et al., "Chronic melatonin treatment prevents age-dependent cardiac mitochondrial dysfunction in senescence-accelerated mice," *Free Radical Research*, vol. 41, no. 1, pp. 15–24, 2007.

[165] G. Petrosillo, G. Colantuono, N. Moro et al., "Melatonin protects against heart ischemia-reperfusion injury by inhibiting mitochondrial permeability transition pore opening," *American Journal of Physiology. Heart and Circulatory Physiology*, vol. 297, no. 4, pp. H1487–H1493, 2009.

[166] G. Petrosillo, N. Di Venosa, N. Moro et al., "In vivo hyperoxic preconditioning protects against rat-heart ischemia/reperfusion injury by inhibiting mitochondrial permeability transition pore opening and cytochrome c release," *Free Radical Biology and Medicine*, vol. 50, no. 3, pp. 477–483, 2011.

[167] I. B. Zavodnik, E. A. Lapshina, V. T. Cheshchevik et al., "Melatonin and succinate reduce rat liver mitochondrial dysfunction in diabetes," *Journal of Physiology and Pharmacology*, vol. 62, no. 4, pp. 421–427, 2011.

[168] F. Canet, F. Iannantuoni, A. M. . Marañon et al., "Does empagliflozin modulate leukocyte–endothelium interactions, oxidative stress, and inflammation in type 2 diabetes?," *Antioxidants*, vol. 10, no. 8, p. 1228, 2021.

[169] P. Bernardi and F. di Lisa, "The mitochondrial permeability transition pore: molecular nature and role as a target in cardioprotection," *Journal of Molecular and Cellular Cardiology*, vol. 78, pp. 100–106, 2015.

[170] F. Di Lisa and P. Bernardi, "A CaPful of mechanisms regulating the mitochondrial permeability transition," *Journal of Molecular and Cellular Cardiology*, vol. 46, no. 6, pp. 775–780, 2009.

[171] M. Crompton, H. Ellinger, and A. Costi, "Inhibition by cyclosporin A of a Ca2+-dependent pore in heart mitochondria activated by inorganic phosphate and oxidative stress," *Biochemical Journal*, vol. 255, no. 1, pp. 357–360, 1988.

[172] R. A. Haworth and D. R. Hunter, "The Ca^{2+}-induced membrane transition in mitochondria," *Archives of Biochemistry and Biophysics*, vol. 195, no. 2, pp. 460–467, 1979.

[173] D. R. Hunter and R. A. Haworth, "The Ca^{2+}-induced membrane transition in mitochondria: I. The protective mechanisms," *Archives of Biochemistry and Biophysics*, vol. 195, no. 2, pp. 453–459, 1979.

[174] D. R. Hunter and R. A. Haworth, "The Ca^{2+}-induced membrane transition in mitochondria:," *Archives of Biochemistry and Biophysics*, vol. 195, no. 2, pp. 468–477, 1979.

[175] C. P. Baines, R. A. Kaiser, T. Sheiko, W. J. Craigen, and J. D. Molkentin, "Voltage-dependent anion channels are dispensable for mitochondrial-dependent cell death," *Nature Cell Biology*, vol. 9, no. 5, pp. 550–555, 2007.

[176] E. Basso, L. Fante, J. Fowlkes, V. Petronilli, M. A. Forte, and P. Bernardi, "Properties of the Permeability Transition Pore in Mitochondria Devoid of Cyclophilin D∗," *Journal of Biological Chemistry*, vol. 280, no. 19, pp. 18558–18561, 2005.

[177] M. Bonora, A. Bononi, M. E. De et al., "Role of the c subunit of the FO ATP synthase in mitochondrial permeability transition," *Cell Cycle*, vol. 12, no. 4, pp. 674–683, 2013.

[178] V. Giorgio, S. von Stockum, M. Antoniel et al., "Dimers of mitochondrial ATP synthase form the permeability transition pore," *Proceedings of the National Academy of Sciences of the United States of America*, vol. 110, no. 15, pp. 5887–5892, 2013.

[179] K. N. Alavian, G. Beutner, E. Lazrove et al., 2014.

[180] E. J. Griffiths and A. P. Halestrap, "Mitochondrial non-specific pores remain closed during cardiac ischaemia, but open upon reperfusion," *Biochemical Journal*, vol. 307, no. 1, pp. 93–98, 1995.

[181] K. Woodfield, A. Ruck, D. Brdiczka, and A. P. Halestrap, "Direct demonstration of a specific interaction between cyclophilin-D and the adenine nucleotide translocase

confirms their role in the mitochondrial permeability transition," *Biochemical Journal*, vol. 336, no. 2, pp. 287–290, 1998.

[182] T. Nakagawa, S. Shimizu, T. Watanabe et al., "Cyclophilin D-dependent mitochondrial permeability transition regulates some necrotic but not apoptotic cell death," *Nature*, vol. 434, no. 7033, pp. 652–658, 2005.

[183] C. P. Baines, R. A. Kaiser, N. H. Purcell et al., "Loss of cyclophilin D reveals a critical role for mitochondrial permeability transition in cell death," *Nature*, vol. 434, no. 7033, pp. 658–662, 2005.

[184] D. J. Hausenloy, H. L. Maddock, G. F. Baxter, and D. M. Yellon, "Inhibiting mitochondrial permeability transition pore opening: a new paradigm for myocardial preconditioning?," *Cardiovascular Research*, vol. 55, no. 3, pp. 534–543, 2002.

[185] D. J. Hausenloy and D. M. Yellon, "The mitochondrial permeability transition pore: its fundamental role in mediating cell death during ischaemia and reperfusion," *Journal of Molecular and Cellular Cardiology*, vol. 35, no. 4, pp. 339–341, 2003.

[186] S. Verheye, W. Martinet, M. M. Kockx et al., "Selective clearance of macrophages in atherosclerotic plaques by autophagy," *Journal of the American College of Cardiology*, vol. 49, no. 6, pp. 706–715, 2007.

[187] D. J. Hausenloy, R. Schulz, H. Girao et al., "Mitochondrial ion channels as targets for cardioprotection," *Journal of Cellular and Molecular Medicine*, vol. 24, no. 13, pp. 7102–7114, 2020.

[188] M. Carraro, A. Carrer, A. Urbani, and P. Bernardi, "Molecular nature and regulation of the mitochondrial permeability transition pore(s), drug target(s) in cardioprotection," *Journal of Molecular and Cellular Cardiology*, vol. 144, pp. 76–86, 2020.

[189] C. Piot, P. Croisille, P. Staat et al., "Effect of cyclosporine on reperfusion injury in acute myocardial infarction," *The New England Journal of Medicine*, vol. 359, no. 5, pp. 473–481, 2008.

[190] T. T. Cung, O. Morel, G. Cayla et al., "Cyclosporine before PCI in patients with acute myocardial infarction," *The New England Journal of Medicine*, vol. 373, no. 11, pp. 1021–1031, 2015.

[191] J. C. Liu, "Is MCU dispensable for normal heart function?," *Journal of Molecular and Cellular Cardiology*, vol. 143, pp. 175–183, 2020.

[192] J. F. Garbincius, T. S. Luongo, and J. W. Elrod, "The debate continues - What is the role of MCU and mitochondrial calcium uptake in the heart?," *Journal of Molecular and Cellular Cardiology*, vol. 143, pp. 163–174, 2020.

[193] S. Sventzouri, I. Nanas, S. Vakrou et al., "Pharmacologic inhibition of the mitochondrial Na^+/Ca^{2+} exchanger protects against ventricular arrhythmias in a porcine model of ischemia-reperfusion," *Hellenic Journal of Cardiology*, vol. 59, no. 4, pp. 217–222, 2018.

[194] I. Szabo and M. Zoratti, "Mitochondrial channels: ion fluxes and more," *Physiological Reviews*, vol. 94, no. 2, pp. 519–608, 2014.

[195] M. Laskowski, B. Augustynek, B. Kulawiak et al., "What do we not know about mitochondrial potassium channels?," *Biochimica et Biophysica Acta*, vol. 1857, no. 8, pp. 1247–1257, 2016.

[196] A. Paggio, V. Checchetto, A. Campo et al., "Identification of an ATP-sensitive potassium channel in mitochondria," *Nature*, vol. 572, no. 7771, pp. 609–613, 2019.

[197] Y. Shintani, K. Node, H. Asanuma et al., "Opening of Ca^{2+}-activated K^+ channels is involved in ischemic preconditioning in canine hearts," *Journal of Molecular and Cellular Cardiology*, vol. 37, no. 6, pp. 1213–1218, 2004.

[198] P. V. Dludla, B. B. Nkambule, L. Tiano, J. Louw, M. Jastroch, and S. E. Mazibuko-Mbeje, "Uncoupling proteins as a therapeutic target to protect the diabetic heart," *Pharmacological Research*, vol. 137, pp. 11–24, 2018.

[199] A. Dietl and C. Maack, "Targeting mitochondrial calcium handling and reactive oxygen species in heart failure," *Current Heart Failure Reports*, vol. 14, no. 4, pp. 338–349, 2017.

[200] M. Maczewski and U. Mackiewicz, "Effect of metoprolol and ivabradine on left ventricular remodelling and Ca^{2+} handling in the post-infarction rat heart," *Cardiovascular Research*, vol. 79, no. 1, pp. 42–51, 2008.

[201] A. M. Swenson, W. Tang, C. A. Blair et al., "Omecamtiv Mecarbil Enhances the Duty Ratio of Human β-Cardiac Myosin Resulting in Increased Calcium Sensitivity and Slowed Force Development in Cardiac Muscle," *Journal of Biological Chemistry*, vol. 292, no. 9, pp. 3768–3778, 2017.

[202] J. R. Teerlink, G. M. Felker, J. J. V. Mcmurray et al., "Acute treatment with omecamtiv mecarbil to increase contractility in acute heart failure: the ATOMIC-AHF study," *Journal of the American College of Cardiology*, vol. 67, no. 12, pp. 1444–1455, 2016.

[203] J. R. Teerlink, G. M. Felker, J. J. Mcmurray et al., "Chronic oral study of myosin activation to increase contractility in heart failure (COSMIC-HF): a phase 2, pharmacokinetic, randomised, placebo-controlled trial," *The Lancet*, vol. 388, pp. 2895–2903, 2016.

[204] V. Eisner, G. Csordas, and G. Hajnoczky, "Interactions between sarco-endoplasmic reticulum and mitochondria in cardiac and skeletal muscle - pivotal roles in Ca^{2+} and reactive oxygen species signaling," *Journal of Cell Science*, vol. 126, Part 14, pp. 2965–2978, 2013.

[205] Y. Kawase and R. J. Hajjar, "The cardiac sarcoplasmic/endoplasmic reticulum calcium ATPase: a potent target for cardiovascular diseases," *Nature Reviews Cardiology*, vol. 5, pp. 554–565, 2008.

[206] I. Scott and R. J. Youle, "Mitochondrial fission and fusion," *Essays in Biochemistry*, vol. 47, pp. 85–98, 2010.

[207] P. Mishra and D. C. Chan, "Mitochondrial dynamics and inheritance during cell division, development and disease," *Nature Reviews Molecular Cell Biology*, vol. 15, no. 10, pp. 634–646, 2014.

[208] L. Fang, X. L. Moore, X. M. Gao, A. M. Dart, Y. L. Lim, and X. J. Du, "Down-regulation of mitofusin-2 expression in cardiac hypertrophy in vitro and in vivo," *Life Sciences*, vol. 80, pp. 2154–2160, 2007.

[209] S. Javadov, V. Rajapurohitam, A. Kilić et al., "Expression of mitochondrial fusion-fission proteins during post-infarction remodeling: the effect of NHE-1 inhibition," *Basic Research in Cardiology*, vol. 106, no. 1, pp. 99–109, 2011.

[210] L. Galluzzi, E. H. Baehrecke, A. Ballabio et al., "Molecular definitions of autophagy and related processes," *The EMBO Journal*, vol. 36, no. 13, pp. 1811–1836, 2017.

[211] M. Bagherniya, A. E. Butler, G. E. Barreto, and A. Sahebkar, "The effect of fasting or calorie restriction on autophagy induction: a review of the literature," *Ageing Research Reviews*, vol. 47, pp. 183–197, 2018.

Retraction

Retracted: The Effects of Statin Therapy on Oxidized LDL and Its Antibodies: A Systematic Review and Meta-Analysis

Oxidative Medicine and Cellular Longevity

This article has been retracted by Hindawi, as publisher, following an investigation undertaken by the publisher [1]. This investigation has uncovered evidence of systematic manipulation of the publication and peer-review process. We cannot, therefore, vouch for the reliability or integrity of this article.

Please note that this notice is intended solely to alert readers that the peer-review process of this article has been compromised.

Wiley and Hindawi regret that the usual quality checks did not identify these issues before publication and have since put additional measures in place to safeguard research integrity.

We wish to credit our Research Integrity and Research Publishing teams and anonymous and named external researchers and research integrity experts for contributing to this investigation.

The corresponding author, as the representative of all authors, has been given the opportunity to register their agreement or disagreement to this retraction. We have kept a record of any response received.

References

[1] T. Jamialahmadi, F. Baratzadeh, Ž. Reiner et al., "The Effects of Statin Therapy on Oxidized LDL and Its Antibodies: A Systematic Review and Meta-Analysis," *Oxidative Medicine and Cellular Longevity*, vol. 2022, Article ID 7850659, 15 pages, 2022.

Hindawi

Review Article

The Effects of Statin Therapy on Oxidized LDL and Its Antibodies: A Systematic Review and Meta-Analysis

Tannaz Jamialahmadi,[1] **Fatemeh Baratzadeh,**[2] **Željko Reiner,**[3] **Massimo R. Mannarino,**[4] **Vladimiro Cardenia,**[5] **Luis E. Simental-Mendía,**[6] **Matteo Pirro,**[4] **Gerald F. Watts,**[7] **and Amirhossein Sahebkar** [8,9,10]

[1]*Surgical Oncology Research Center, Mashhad University of Medical Sciences, Mashhad, Iran*
[2]*Department of Clinical Pharmacy, School of Pharmacy, Isfahan University of Medical Sciences, Isfahan, Iran*
[3]*Department of Internal Medicine, University Hospital Centre Zagreb, School of Medicine, University of Zagreb, Zagreb, Croatia*
[4]*Unit of Internal Medicine, Angiology and Arteriosclerosis Diseases, Department of Medicine, University of Perugia, Perugia, Italy*
[5]*Department of Agricultural, Forest and Food Sciences (DISAFA), University of Turin, Grugliasco 10095, Italy*
[6]*Biomedical Research Unit, Mexican Social Security Institute, Durango, Mexico*
[7]*Cardiometabolic Service, Department of Cardiology, Royal Perth Hospital, School of Medicine, The University of Western Australia, Perth, Western Australia, Australia*
[8]*Applied Biomedical Research Center, Mashhad University of Medical Sciences, Mashhad, Iran*
[9]*Biotechnology Research Center, Pharmaceutical Technology Institute, Mashhad University of Medical Sciences, Mashhad, Iran*
[10]*Department of Biotechnology, School of Pharmacy, Mashhad University of Medical Sciences, Mashhad, Iran*

Correspondence should be addressed to Amirhossein Sahebkar; amir_saheb2000@yahoo.com

Background. Elevated serum low-density lipoproteins (LDL), the substrate for the formation of atherogenic oxidized LDLs (oxLDL), are a causal factor for atherosclerotic cardiovascular disease (ASCVD). Statins are well known to decrease LDL particle concentration and reduce ASCVD morbidity and mortality. *Objective*. To perform a meta-analysis of the effects of statins (i.e., type, dose, and duration of treatment) on serum levels of oxLDL and on immunoglobulin M (IgM) and immunoglobulin G (IgG) antibody levels against oxLDL. *Methods*. PubMed, Scopus, Embase, and Web of Science were searched up to February 5th, 2021, for randomized controlled trials (RCT) evaluating the effect of statins on oxLDL and anti-oxLDL antibody levels. Meta-analysis was performed using Comprehensive Meta-Analysis (CMA) V2 software. To evaluate the influence of each study on the overall effect size, a sensitivity analysis was performed using the leave-one-out method. Evaluation of the funnel plot, Begg's rank correlation, and Egger's weighted regression tests was used to assess the presence of publication bias in the meta-analysis. *Results*. A total of 28 RCTs including 4019 subjects were finally included in the meta-analysis. The results indicated a significant decrease in circulating concentrations of oxLDL after treatment with statins (SMD: -2.150, 95% CI: -2.640, -1.697, $p < 0.001$). Subgroup analysis found no significant effect of the intensity of statin treatment or statin lipophilicity on the reduction of circulating concentrations of oxLDL. An additional meta-analysis of 3 trials showed that statins did not change the serum levels of IgM and IgG antibodies to oxLDL. *Conclusion*. Statin therapy decreases serum oxLDL concentrations but does not affect circulating levels of anti-oxLDL antibodies.

1. Introduction

Elevated serum low-density lipoprotein cholesterol (LDL-C) is a causal factor for atherosclerotic cardiovascular disease (ASCVD) morbidity and mortality [1]. Statins are drugs of choice to decrease LDL-C levels and ASCVD risk in both primary and secondary prevention [2, 3]. The oxidation of LDL particles, which typically occurs in patients with

elevated LDL-C levels as well as in the presence of other pro-oxidative conditions, is considered to be the major atherogenic modification of LDL [4]. Among LDL subclasses, small and very small dense particles are most susceptible to oxidation [5]. Oxidized LDL (oxLDL) can trigger the expression of adhesion molecules (e.g., intracellular adhesion molecule-1 (ICAM-1), vascular adhesion molecule-1 (VCAM-1), and E-selectin) on the endothelial cell surface resulting in activation of endothelial cells [6, 7]. These adhesion molecules along with integrins, selectins, and chemokines stimulate the recruitment and adhesion of leukocytes, mostly monocytes, to the endothelium and their infiltration into intima. Monocytes differentiate to macrophages, recognize and internalize oxLDL particles by scavenger receptors, and transform into foam cells, thus initiating the formation of the atherosclerotic plaque [8]. Moreover, the overexpression of the lectin-like oxidized low-density lipoprotein receptor-1 (LOX-1), the main oxLDL receptor in endothelial cells, promotes endothelial cell activation and dysfunction, triggering the activation of proinflammatory signaling pathways and the development of atherosclerotic process [9]. oxLDL particles participate in the destabilization of atherosclerotic plaques leading to clinical manifestations, such as myocardial infarction (MI) and unstable angina. In addition to promoting plaque appearance, growth, inflammation, and destabilization, oxLDLs act as immune antigens inducing the innate immune response to produce immunoglobulin M (IgM) and immunoglobulin G (IgG) antibodies against oxLDL [8]. The role of these antibodies as markers of oxLDL exposure and pathogenic determinants of ASCVD has been proposed [10]. Namely, as a consequence of the macrophage activation, matrix metalloproteinases are produced causing matrix degradation, fissuring of the plaque, and thrombus formation on this site [11].

In the armamentarium of different lipid-lowering drugs [12–14], statins still remain the most widely prescribed class. This is due to their efficient LDL-lowering activity and pleiotropic effects of these drugs ([15–21]). Although the effects of statins on LDL-C are well known, inconsistency about the effects of statin therapy on circulating levels of oxLDL and anti-oxLDL antibodies is still present. Moreover, the impact of statin therapy intensity and lipophilicity on these highly atherogenic modified LDL particles remains unexplored, and it is not known whether different statins have different effects on serum concentrations of oxLDL. Therefore, the aim of this systematic review and meta-analysis was to analyze the magnitude of the effect of statins on oxLDL and anti-oxLDL antibody levels.

2. Methods

2.1. Search Strategy.
We followed the methods of Jamialahmadi et al. as follows [22]. The present systematic review and meta-analysis was designed according to the 2009 Preferred Reporting Items for Systematic Reviews and Meta-Analysis (PRISMA) guidelines [23]. PubMed, Scopus, Embase, and Web of Science were searched from inception to February 5th, 2021, using the following keywords in titles and abstracts (also in combination with MESH terms):

("Hydroxymethylglutaryl-CoA Reductase Inhibitors" OR simvastatin OR rosuvastatin OR atorvastatin OR pravastatin OR pitavastatin OR mevastatin OR fluvastatin OR lovastatin OR cerivastatin) AND ("oxidized low density lipoprotein" OR "oxidized LDL" OR OxLDL OR ox-LDL OR "oxidized Low-Density Lipoprotein" OR "minimally modified oxidized-LDL" OR MM-LDL OR MMLDL OR "malondialdehyde-low density lipoprotein" OR "malondialdehyde low density lipoprotein" OR "MDA-LDL" OR "MDALDL" OR "MDA-LDL IgM" OR "MDA-LDL IgG" OR "autoantibodies against oxidized low-density lipoprotein" OR "autoantibodies against oxidized low density lipoprotein" OR "AuAb-oxLDL" OR "antibodies against oxidized LDL" OR "Anti-oxLDL"). The search was performed consecutively using the search engines and search terms which are presented in Supplementary Material Table S1.

2.2. Study Selection.
Human studies were included if they met the following inclusion criteria: (i) randomized controlled trial with either parallel or cross-over design, (ii) the study which investigated the effect of statins on oxLDL and/or antibodies against oxLDL, and (iii) presentation of sufficient information at baseline and at the end of follow-up in each group or studies which provided the net change values. Exclusion criteria were as follows: (i) nonrandomized trials, (ii) uncontrolled trials, (iii) observational studies with case-control, cross-sectional, or cohort design, and (iv) lack of sufficient information at baseline or follow-up and of an active comparator in the control group.

2.3. Data Extraction.
We followed the methods of Jamialahmadi et al. as follows [22]. After removal of duplicate studies, two independent and blinded authors (JB, MR) evaluated eligibility by screening the titles and abstracts of the studies. Full reports of eligible studies were obtained. Any disagreements were resolved by discussion and consensus. Eligible studies were reviewed, and the following data were abstracted: (1) the name of the first author, (2) the year of publication, (3) study design, (4) type of statins used in the study, (5) dose of statin, (6) treatment duration, (7) patient characteristics, and (8) clinical outcomes.

2.4. Quality Assessment.
We followed the methods of Jamialahmadi et al. as follows [22]. Risk of bias in the studies included in this meta-analysis was evaluated according to the Cochrane instructions [24]. Selection bias, performance bias, attrition bias, detection bias, reporting bias, and other sources of bias were estimated to be high, low, or unclear for each of the included studies.

2.5. Quantitative Data Synthesis.
We followed the methods of Jamialahmadi et al. as follows [22]. Meta-analysis was performed using Comprehensive Meta-Analysis (CMA) V2 software (Biostat, NJ) [25]. Values were reported in different units. Sample sizes, means, and standard deviations from each group were obtained for each relevant outcome to calculate standardized mean differences (SMDs). We applied SMDs because of the different metrics used to assess

Table 1: Characteristics of studies that measured circulating concentrations of oxidized LDL and MDA LDL.

Study, year	Study design	Follow-up	Treatment	Control	Clinical outcome oxLDL	Clinical outcome MDA-LDL	Patients	No. of patients
Diepeveen et al., 2005 [31]	Double-blind randomized placebo-controlled study	12 weeks	A (40 mg/day)	Placebo	Significant decrease in serum level of oxLDL	—	Dialysis patients	23
Dogra et al., 2005 [32]	Double-blind, randomized cross-over study	6 weeks	A (40 mg/day)	Placebo	Significant decrease in serum level of oxLDL	—	T1DM with microalbuminuria	32
Dogra et al., 2007 [33]	Double-blind, randomized, placebo-controlled, parallel-group study	6 weeks	A (40 mg/day)	Placebo	Significant decrease in serum level of oxLDL	—	CKD stages 3 to 5	63
Vlachopoulos et al., 2007 [34]	Randomized, placebo-controlled, double-blind study	4 days	A (40 mg/day)	Placebo	Significant decrease in serum level of oxLDL	—	Acute systemic inflammation-induced endothelial dysfunction in hypercholesterolaemic patients	50
Singh et al., 2008 [35]	Randomized double-blind placebo-controlled study	12 weeks	A (10, 80 mg/day)	Placebo	Significant decrease in serum level of oxLDL	—	Metabolic syndrome	70
Nou et al., 2016 [36]	Randomized, placebo-controlled study	12 months	A (40 mg/day)	Placebo	Significant decrease in serum level of oxLDL	—	HIV-infected patients with subclinical coronary atherosclerosis	37
Nixon et al., 2017 [37]	Multicenter, prospective, randomized, double-blind, placebo controlled, cross-over pilot study	20 weeks	A (20 mg/day)	Placebo	Significant decrease in serum level of oxLDL	—	HIV-infected patients	146
deFilippi et al., 2018 [38]	Single-center randomized double-blind placebo-controlled study	12 months	A (40 mg/day)	Placebo	Significant decrease in serum level of oxLDL	—	HIV-infected patients	39
Yamada et al., 2007 [39]	Prospective randomized controlled study	6 months	A (10 mg/day)	Placebo	—	Significant decrease in serum level of MDA-LDL	CHF	38
Oka et al., 2008 [40]	Randomized controlled study	12 weeks	A (10 mg/day)	Only diet therapy	—	Decrease in serum level of MDA-LDL	CAD and hyperlipidemia	48
El-Sisi et al., 2015 [41]	Single-center, blind randomized investigational study	3 months	A (20 mg/day)	Conventional therapy of HF	Significant decrease in serum level of oxLDL	—	CHF	48
Andreou et al., 2010 [42]	Randomized placebo-controlled study	1 month	R (10 mg/day)	Placebo	Significant decrease in serum level of oxLDL	—	CHF	39
Erbs et al., 2011 [43]	Randomized, double-blind, and placebo-controlled study	12 weeks	R (40 mg/day)	Placebo	Significant decrease in serum level of oxLDL	—	CHF	40
				Placebo		—	Familial combined hyperlipidemia	36

TABLE 1: Continued.

Study, year	Study design	Follow-up	Treatment	Control	Clinical outcome		Patients	No. of patients
					oxLDL	MDA-LDL		
ter Avest et al., 2005 [44]	Double-blind, randomized cross-over study	12 weeks	R (40 mg/day)		Significant decrease in serum level of oxLDL		HIV-infected patients	147
Hileman et al., 2016 [45]	Randomized, placebo-controlled trial	48 weeks	R (10 mg/day)	Placebo	Increase in serum level of oxLDL	—		
Abe et al., 2011 [46]	Randomized, prospective, open-label, parallel-group, controlled study	6 months	R (10 mg/day)	Patients without statin prescription	—	Significant decrease in serum level of MDA-LDL	Diabetic nephropathy	101
Rydén et al., 2012 [47]	Randomized, double-blind, placebo-controlled study	6 weeks	S (40 mg/day)	Placebo	Significant decrease in serum level of oxLDL	—	Mild to moderate hypercholesterolemia	76
Krysiak et al., 2011 [48]	Prospective, randomized, placebo-controlled study	90 days	S (40 mg/day)	Placebo	Significant decrease in serum level of oxLDL	—	Isolated primary hypercholesterolemia	49
Kirmizis et al., 2010 [49]	Prospective, controlled, single-center study	6 months	S (10 mg/day)	Patients without prescriptions	Significant decrease in serum level of oxLDL	—	Patients with chronic hemodialysis	50
Kishimoto et al., 2010 [50]	Randomized controlled study	16 weeks	S (5, 10 mg/day)	Patients without prescriptions	Significant decrease in serum level of oxLDL	—	Patients with chronic hemodialysis	37
Ichihara et al., 2002 [51]	Randomized, double-blind, placebo-controlled study	6 months	F (20 mg/day)	Placebo	—	Significant decrease in serum level of MDA-LDL	T2DM hemodialysis patients with normal serum lipid levels	22
Yoshida et al., 2010 [52]	Randomized controlled study	4 weeks	Pi (2 mg/day)	Patients without prescriptions	—	Significant decrease in serum level of MDA-LDL	Chronic smokers	30
Janatuinen et al., 2004 [53]	Randomized, double-blind, placebo-controlled study	4 months	P (40 mg/day)	Placebo	Significant decrease in serum level of oxLDL	—	T1DM	42
Tani et al., 2005 [54]	Prospective, single-center, randomized, open study	6 months	P (5-20 mg/day)	Patients without prescriptions	—	Significant decrease in serum level of MDA-LDL	Stable coronary artery disease	75
Ky et al., 2008 [55]	Randomized, parallel-arm, double-blind, placebo-controlled study	16 weeks	P (40 mg/day); A (10, 80 mg/day)	Placebo	Significant decrease in serum level of oxLDL	—	Hypercholesterolemic patients	106

Abbreviation: A: atorvastatin; OxLDL: oxidized low-density lipoprotein; MDA-LDL: malondialdehyde-modified low-density lipoprotein; T1DM: type 1 diabetes mellitus; CKD: chronic kidney disease; HIV: human immunodeficiency virus; CHF: chronic heart failure; CAD: coronary artery disease; HF: heart failure; R: rosuvastatin; CHF: chronic heart failure; S: simvastatin; T2DM: type 2 diabetes mellitus; F: fluvastatin; Pi: pitavastatin; P: pravastatin.

TABLE 2: Characteristics of studies that measured antibodies to oxidized LDL and MDA LDL.

Study, year	Study design	Follow-up	Treatment	Control	Clinical outcome AuAb-oxLDL	Clinical outcome AuAb-MDA-LDL	Patients	No. of patients
Tsimikas et al., 2004 [56]	Randomized, double-blinded, placebo-controlled study	16 weeks	A (80 mg/day)	Placebo	—	Significant increase in serum level of AuAb-MDA-LDL	ACS	2341
Kuklinska et al., 2010 [57]	Randomized prospective open-label study	3 months	A (80 mg/day)	Statin free patients	Serum level of AuAb-oxLDL decreased, but the alterations were not significant	—	Normolipidemic patients	56
Rodenburg et al., 2006 [58]	Double-blind, randomized placebo-controlled study	2 years	P (20-40 mg/day)	Placebo	—	Significant changes in serum level of AuAb-MDA-LDL	Children with familial hypercholesterolemia	178

Abbreviation: A: atorvastatin; AuAb-oxLDL: autoantibodies against oxidized LDL; AuAb-MDA-LDL: autoantibodies against malondialdehyde-modified LDL; NICM: nonischemic cardiomyopathy; ACS: acute coronary syndrome; P: pravastatin.
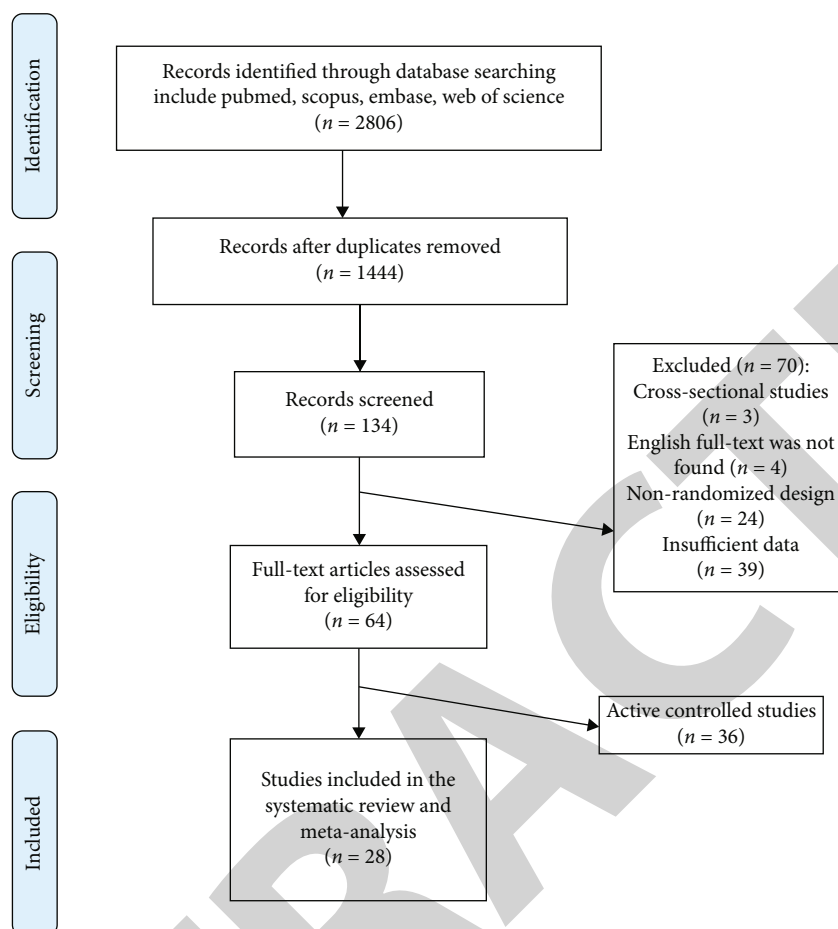
Figure 1: Flow chart of studies identified and included in meta-analysis.

outcomes. Effect size was calculated as (measured at the end of follow − up in the treatment group − measured at baseline in the treatment group) − (measured at the end of follow-up in the control group − measured at baseline in the control group). A random-effects model and the generic inverse variance weighting method were used to compensate for the heterogeneity of the studies in terms of study design, treatment duration, and the characteristics of the studied populations [23]. If the outcome measures were reported in the median and range (or 95% confidence interval (CI)), mean and SD values were estimated using the method described by Hozo et al. [26]. Where only the standard error of the mean (SEM) was reported, SD was estimated using the following formula: $SD = SEM \times sqrt(n)$, where n is the number of subjects. Given the variations in the assay methods and reporting different oxLDL concentrations, effect sizes were expressed as SMD and 95% CI. To evaluate the influence of each study on the overall effect size, a sensitivity analysis was performed using the leave-one-out method (i.e., removing one study each time and repeating the analysis) [27, 28].

2.6. Metaregression. We followed the methods of Jamialahmadi et al. as follows [22]. As potential confounders of treatment response, the baseline levels of oxLDL and duration of statin treatment were included into a random-effects metar-

egression model to explore their association with the estimated effect size.

2.7. Publication Bias. We followed the methods of Jamialahmadi et al. as follows [22]. Evaluation of the funnel plot, Begg's rank correlation, and Egger's weighted regression tests was used to assess the presence of publication bias in the meta-analysis. When there was evidence of funnel plot asymmetry, potentially missing studies were included using the "trim and fill" method. In case of a significant result, the number of potentially missing studies required to make the p value nonsignificant was estimated using the "failsafe N" method as another marker of publication bias [29].

2.8. GRADE Scoring. We assessed the strength of evidence for each outcome using the Grading of Recommendations, Assessment, Development and Evaluation (GRADE) system [30]. GRADEpro GDT software was used to summarise the finding for each outcome, which is presented in Supplementary Material Table S2. According to the GRADE system, RCTs start as high-quality evidence. Four points were given for each outcome, and then, we assessed factors reducing the quality of the evidence. For each outcome, points were reduced based on the presence of the following: the overall risk of bias for each RCT, inconsistency, indirectness, and imprecision. Accordingly,

FIGURE 2: Quality of bias assessment of the included studies in this meta-analysis.

we graded the evidence in four categories based on the overall GRADE scores for each intervention: high-grade evidence (at least 4 points), moderate-grade evidence (3 points), low-grade evidence (2 points), and very low-grade evidence (1 point).

3. Results

Among the 1444 published studies identified by a systematic database search, 134 were directly related to the topic of this study. However, 106 studies were excluded after

careful evaluation (3 studies were cross-sectional, 21 studies were not found, 24 studies were not randomized clinical trials, 39 studies did not report sufficient data, 36 studies were actively controlled, 22 studies were poster presentations, and 1 study investigated cerivastatin, a drug currently withdrawn from almost all markets). Therefore, 28 RCTs were finally included in the systematic review and meta-analysis. A total of 25 studies evaluated the circulating concentrations of oxLDL and malondialdehyde (MDA) LDL (Table 1), while 3 studies measured antibodies against oxLDL and MDA LDL (Table 2). The study selection process is shown in Figure 1.

3.1. Risk of Bias Assessment of Clinical Trials. Most of the selected trials showed insufficient information regarding both random sequence generation and allocation concealment. Furthermore, seven studies showed a high risk of bias for blinding of participants, personnel, and outcome assessment [40, 46, 49, 52, 54]. Finally, all included trials had a low risk of bias for incomplete outcome data and selective reporting. The evaluation of the risk of bias in the selected studies is presented in Figure 2.

3.2. Assays for oxLDL. In most of the included studies, serum oxLDL was measured using the enzyme-linked immunosorbent assay (ELISA) method. Thirteen studies used the Mercodia oxLDL kit (Mercodia, Uppsala, Sweden) [31–37, 44, 45, 47–49, 55], three studies used the SRL kit (Tokyo, Japan) [39, 40, 51], one study used the USCNK Life Science Inc. kit (Wuhan, China) [41], one study used the R&D Systems Inc. kit (Minneapolis, Minnesota, USA) [42], one study used the Immundiagnostik kit (Bensheim, Germany) [43], one study used the Kyowa Medex MX kit (Kyowa Medex, Inc., Tokyo) [50], one study used the Daiichi kit (Tokyo, Japan) [52], one study used the Biomedica kit (Wien, Austria) [57], one study used ML25 (monoclonal antibody against MDA-LDL) [54], and five studies did not mention the methods used or assay kits [38, 46, 53, 56, 58].

3.3. Effect of Statins on Circulating Concentrations of Oxidized LDL. Meta-analysis from 25 trials including 1444 subjects demonstrated a significant decrease in circulating concentrations of oxLDL (SMD: -2.150, 95% CI: -2.604, -1.697, $p < 0.001$) (Figure 3(a)). The reduction in circulating concentrations of oxLDL because of statin treatment was robust in the leave-one-out sensitivity analysis (Figure 3(b)).

3.4. Effect of Statins on Antibodies to Oxidized LDL (IgG and IgM). Meta-analysis from 3 clinical trials including 2575 subjects did not show a significant change in serum IgM antibodies to oxLDL (SMD: -10.842, 95% CI: -32.091, 10.406, $p = 0.317$) and IgG (SMD: 0.048, 95% CI: -0.030, 0.125, $p = 0.229$) following treatment with statins (Figures 4(a) and 4(b)).

3.5. Metaregression. Random-effects metaregression was performed to assess the effect of potential confounders on the circulating concentrations of oxLDL-lowering activity of statins. The results did not suggest any significant association

Stydy name	Std diff in means	Standard error	Variance	Lower limit	Upper limit	Z–Value	p–Value
Diepeveen 2005 (U/I) Mercodia kit	−1.195	0.456	0.208	−2.089	−0.302	−2.621	0.009
Dogra et al, 2005	−0.949	0.373	0.139	−1.679	−0.218	−2.544	0.011
Dogra et al, 2007	−1.411	0.282	0.079	−1.963	−0.859	−5.011	0.000
Vlachopoulos 2007	−1.754	0.333	0.111	−2.406	−1.101	−5.289	0.000
Singh et al, 2008 a	−1.014	0.376	0.142	−1.751	−0.277	−2.696	0.007
Singh et aI,2008 b	−1.267	0.387	0.150	−2.025	−0.508	−3.273	0.001
Nou at al, 2016	−1.407	0.368	0.136	−2.129	−0.686	−3.822	0.000
Nixon et al, 2017 a	−1.439	0.261	0.068	−1.950	−0.928	−5.516	0.000
Nixon el al. 2017 b	−2.503	0.315	0.099	−3.120	−1.886	−7.952	0.000
deFipps at al, 2018	−1.218	0.350	0.122	−1.904	−0.533	−3.485	0.000
EI–Sisi at al, 2015	−0.928	0.304	0.092	−1.524	−0.333	−3.055	0.002
Andreou at al, 2020	−0.435	0.325	0.106	−1.072	0.202	−1.339	0.181
Erbs et al. 2011	−2.505	0.422	0.178	−3.333	−1.677	−5.930	0.000
Ter Avast et al, 2005	−2.923	0.479	0.230	−3.863	−1.984	−6.098	0.000
Hileman et al, 2016	0.006	0.165	0.027	−0.318	0.329	0.035	0.972
Ryden et al, 2012	−1.411	0.258	0.066	−1.914	−0.908	−5.502	0.000
Krysiak et al, 2011	−5.786	0.651	0.423	−7.061	−4.511	−8.893	0.000
Kirmizis at al, 2010	−0.559	0.288	0.083	−1.125	0.006	−1.940	0.052
Kishimoto et al, 2010 a	−7.322	1.346	1.811	−9.959	−4.685	−5.441	0.000
Kishimoto et al, 2010 b	−10.525	1.785	3.186	14.023	−7.026	−5.896	0.000
Ichhihara at al, 2002	−3.197	0.645	0.418	−4.461	−1.933	−4.959	0.000
Janatuinen et al, 2004	−0.558	0.315	0.099	−1.175	0.059	−1.773	0.076
Ky et al, 2008 a	−8.839	1.083	1.174	10.963	−6.716	−8.159	0.000
Ky et al, 2008 b	−7.975	1.029	1.058	−9.991	−5.959	−7.753	0.000
ky et al, 2008 c	−5.657	0.799	0.638	−7.222	−4.092	−7.084	0.000
Yamada et al, 2007	−1.188	0.352	0.124	−1.878	−0.498	−3.376	0.001
Oka et al. 2008	−1.276	0.317	0.100	−1.897	−0.655	−4.027	0.000
Abe at al, 2011	−1.279	0.218	0.048	−1.707	−0.851	−5.856	0.000
Yoshida et al, 2010	−2.904	0.523	0.274	−3.930	−1.878	−5.549	0.000
Tani at al, 2005	−0.743	0.258	0.066	−1.248	−0.238	−2.884	0.004
	−2.150	0.232	0.054	−2.604	−1.697	−9.285	0.000

Meta analysis

(a)

Stydy name	Point	Standard error	Variance	Lower limit	Upper limit	Z–Value	p–Value
Diepeveen 2005 (U/I) Mercodia kit	−2.191	0.238	0.057	−2.658	−1.724	−9.201	0.000
Dogra et al, 2005	−2.204	0.239	0.057	−2.673	−1.735	−9.216	0.000
Dogra et al, 2007	−2.194	0.242	0.058	−2.668	−1.720	−9.073	0.000
Vlachopoulos 2007	−2.175	0.240	0.057	−2.645	−1.706	−9.079	0.000
Singh et al, 2008 a	−2.202	0.239	0.057	−2.670	−1.733	−9.204	0.000
Singh et aI,2008 b	−2.192	0.239	0.057	−2.661	−1.723	−9.186	0.000
Nou at al, 2016	−2.188	0.239	0.057	−2.657	−1.718	−9.137	0.000
Nixon et al, 2017 a	−2.196	0.243	0.059	−2.672	−1.720	−9.045	0.000
Nixon el al. 2017 b	−2.136	0.236	0.055	−2.598	−1.674	−9.086	0.000
deFipps at al, 2018	−2.196	0.240	0.058	−2.666	−1.726	−9.155	0.000
EI–Sisi at al, 2015	−2.210	0.241	0.058	−2.682	−1.738	−9.180	0.000
Andreou at al, 2020	−2.222	0.238	0.057	−2.689	−1 755	−9.324	0.000
Erbs et al. 2011	−2.138	0.238	0.056	−2.600	−1.675	−9.067	0.000
Ter Avast et al, 2005	−2.119	0.234	0.055	−2.578	−1 880	−9.055	0.000
Hileman et al, 2016	−2.215	0.228	0.052	−2.681	−1.789	−9.727	0.000
Ryden et al, 2012	−2.198	0.243	0.059	−2.674	−1.721	−9.043	0.000
Krysiak et al, 2011	−1.999	0.221	0.049	−2.431	−1.566	−9.058	0.000
Kirmizis at al, 2010	−2.222	0.240	0.057	−2.692	−1.752	−9.269	0.000
Kishimoto et al, 2010 a	−2.048	0.228	0.052	−2.494	−1.602	−8.993	0.000
Kishimoto et al, 2010 b	−2.033	0.225	0.051	−2.474	−1.592	−9.041	0.000
Ichhihara at al, 2002	−2.114	0.234	0.055	−2.572	−1.656	−9 045	0.000
Janatuinen et al, 2004	−2.220	0.239	0.057	−2.688	−1.751	−9 283	0.000
Ky et al, 2008 a	−1.971	0.219	0.048	−2.400	−1 542	−9 006	0.000
Ky et al, 2008 b	−1.988	0.221	0.049	−2.421	−1.554	−8.988	0.000
ky et al, 2008 c	−2.031	0.226	0.051	−2.474	−1.588	−8.986	0.000
Yamada et al, 2007	−2.197	0.240	0.058	−2.667	−1.727	−9.161	0.000
Oka et al. 2008	−2.196	0.241	0.058	−2.668	−1 725	−9.124	0.000
Abe at al, 2011	−2.210	0.246	0.060	−2.691	−1.728	−8.995	0.000
Yoshida et al, 2010	−2.121	0.234	0.055	−2.581	−1.882	−9.055	0.000
Tani at al, 2005	−2.220	0.242	0.058	−2.694	−1.747	−9.187	0.000
	−2.150	0.232	0.054	−2 604	−1.697	−9.285	0.000

Meta analysis

(b)

Figure 3: (a) Forest plot displaying standardized mean difference and 95% confidence intervals for the effect of statins on circulating concentrations of oxidized LDL. (b) Leave-one-out sensitivity analyses for the effect of statins on circulating concentrations of oxidized LDL.

Study name	Statistics for each study							Std diff in means and 95% CI
	Std diff in means	Standard error	Variance	Lower limit	Upper limit	Z-value	p-value	
Tsimikas et al, 2004	−0.032	0.041	0.002	−0.113	0.049	−0.776	0.438	
Rodenburg et al, 2006	−21.715	1.161	1.347	−23.990	−19.440	−18.710	0.000	
	−10.842	10.841	117.534	−32.091	10.406	−1.000	0.317	

Meta analysis

(a)

Study name	Statistics for each study							Std diff in means and 95% CI
	Std diff in means	Standard error	Variance	Lower limit	Upper limit	Z-value	p-value	
Tsimikas et al, 2004	0.042	0.041	0.002	−0.039	0.123	1.016	0.309	
Rodenburg et al, 2006	−0.040	0.150	0.022	−0.334	0.254	−0.269	0.788	
Kuklinska et al, 2010	0.679	0.298	0.089	0.096	1.262	2.281	0.023	
	0.048	0.040	0.002	−0.030	0.125	1.203	0.229	

Meta analysis

(b)

Figure 4: Forest plot displaying standardized mean difference and 95% confidence intervals for the effect of statins on (a) IgM antibodies to oxidized LDL and (b) IgG antibodies to oxidized LDL.

between the changes in circulating concentrations of oxLDL and either baseline level (slope: -0.00069; 95% CI: -0.00685, 0.00547; $p = 0.826$), treatment duration (slope: 0.0255; 95% CI: -0.00961, 0.06068; $p = 0.154$), or delta LDL (slope: -0.0121; 95% CI: -0.0591, 0.0349; $p = 0.613$) (Figures 5(a)–5(c)).

3.6. Subgroup Analysis. A subgroup analysis was also performed based on statin type and lipophilicity, statin dose, and treatment duration (≤12 weeks and >12 weeks). Subgroup analyses showed significant associations between the statin type and oxLDL level changes ($p = 0.024$). There was no significant effect of statin lipophilicity ($p = 0.102$) and doses ($p = 0.491$) on the reduction of circulating concentrations of oxLDL. A negative association between the treatment duration and change in oxLDL levels ($p = 0.039$) was found (Table 3).

3.7. Publication Bias. Given the asymmetric funnel plot, Egger's linear regression test (intercept = −7.33, standard error = 0.83; 95%CI = −9.04, −5.62, $t = 8.79$, df = 28, two-tailed $p < 0.001$) and Begg's rank correlation test (Kendall's tau with continuity correction = −0.48, $z = 3.74$, two-tailed p value < 0.001) suggest the presence of publication bias in the meta-analysis of the effects of statins on serum oxLDL and antibodies. Using the "trim and fill" method, three potentially missing studies were included showing an adjusted effect size (SMD) of -2.53 (95% CI: -3.12, -1.93). The "fail-safe N" test showed that 4904 missing studies would be needed to bring the effect size down to a nonsignificant ($p > 0.05$) value (Figure 6).

4. Discussion

The results of our meta-analysis suggest that treatment with statins significantly decreases circulating oxLDL concentrations and that such an effect is independent of the intensity (dose) and lipophilicity of statin. Meta-analysis of 3 clinical trials showed that statin treatment did not change serum levels of IgM and IgG antibodies to oxLDL.

The results of earlier studies suggested that elevated levels of circulating oxLDL might be associated with preclinical arterial injury, coronary and peripheral arterial atherosclerosis, and ASCVD outcomes [59]. Circulating levels of oxLDL are associated with all stages of atherosclerosis, from the earliest asymptomatic phases such as endothelial dysfunction to the clinical manifestations of ASCVD and events. It has been reported that oxLDL levels were associated with ASCVD risk factors including hyperlipidemia, hypertension, diabetes, obesity, and metabolic syndrome [60, 61].

After the first small study published in 2004 showing that the level of circulating oxLDL was significantly decreased by treatment with statins (fluvastatin and pravastatin) and that this effect was independent of their lipid-lowering effect [62], a number of mostly small studies was published supporting the same finding. In recent years, several smaller studies were performed showing the beneficial effects of statins on oxLDL [63] suggesting that high-dose atorvastatin and rosuvastatin induce similar decreases in oxLDL [64]. The pleiotropic effects of statins (e.g., antioxidative and anti-inflammatory) might have contributed to the reduction of oxLDL formation [65, 66]. For instance, since

(a)

(b)

(c)
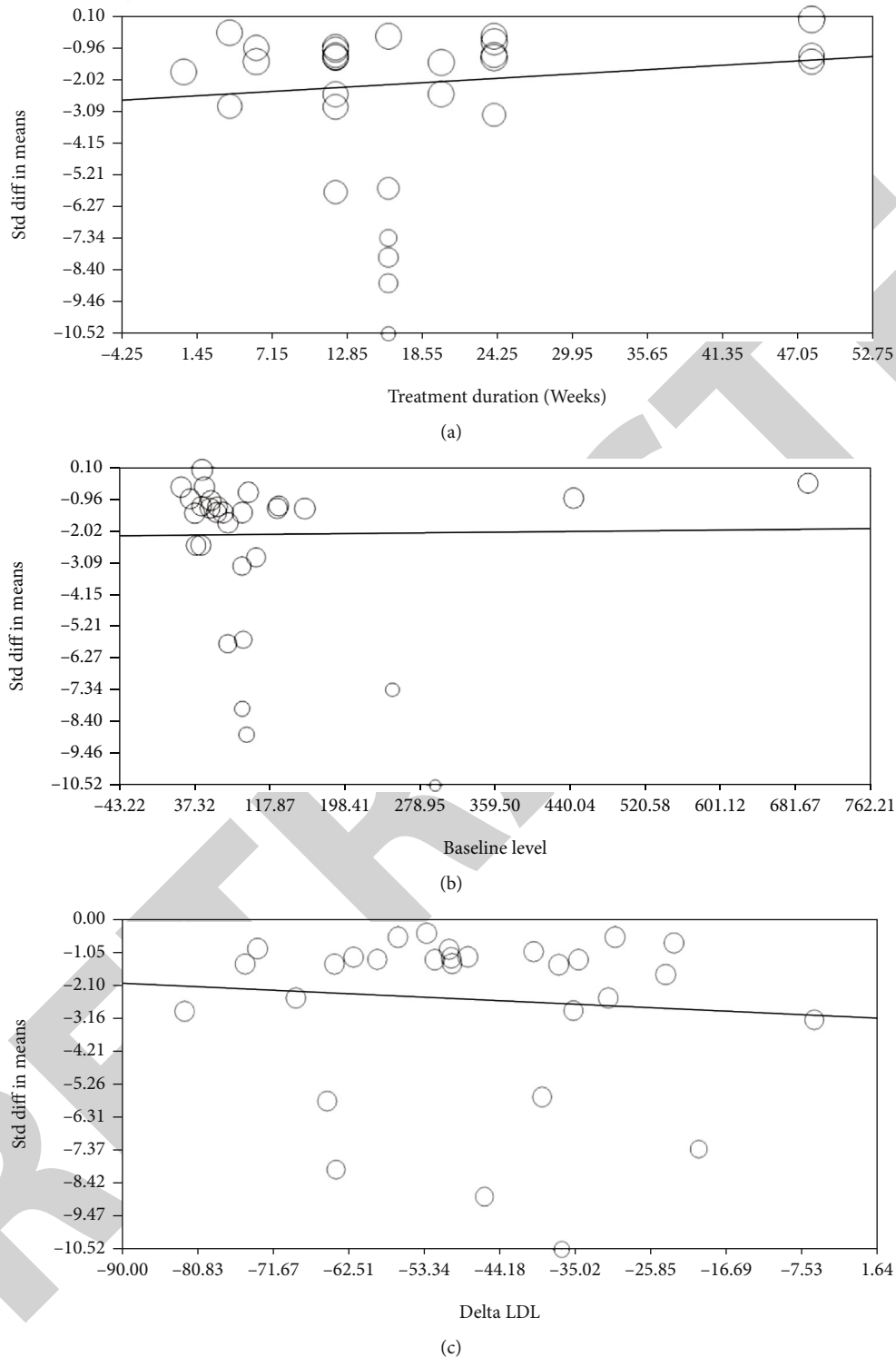
Figure 5: Random-effects metaregression for assessing the effect of (a) treatment duration, (b) baseline level, and (c) delta LDL-C.

C-reactive protein (CRP) and oxLDL are interlinked in pathophysiological pathways [67], the reduction in plasma CRP levels with statins [68] could be related to the lowering of oxLDL. Furthermore, statin-induced lowering of LDLs decreases the circulating level of the substrate (i.e., LDL particles) for oxidation, and this could partially account for reduction in the generation of oxLDL.

Irrespective of cholesterol-dependent or cholesterol-independent (pleiotropic) effects of statins [69–72], plaque oxLDL levels might be associated with plaque inflammation. However, a recent study showed that plaque oxLDL levels were not associated with future ASCVD events [73]. It is important to stress that plaque levels of oxLDL were lower in patients who were treated with statins.

TABLE 3: Subgroup analysis based on treatment duration, statin type, lipophilicity, and intensity.

Subgroup		SMD	95% CI	p value	I^2 value (%)
Statin type	Atorvastatin	-1.85	-2.36, -1.33	<0.001	86.86
	Simvastatin	-4.52	-6.69, -2.35	<0.001	95.92
	Rosuvastatin	-1.36	-2.36, -0.372	0.007	93.90
	Fluvastatin	-3.19	-4.46, -1.93	<0.001	0
	Pitavastatin	-2.90	-3.93, -1.87	<0.001	0
	Pravastatin	-2.10	-3.96, -0.253	0.026	94.58
Statin lipophilicity	Hydrophilic	-1.57	-2.37, -0.77	<0.001	93.23
	Lipophilic	-2.37	-2.91, -2.83	<0.001	90.38
Statin dose	High	-1.95	-2.58, -1.33	<0.001	84.27
	Low to moderate	-2.25	-2.85, -1.66	<0.001	93.42
Treatment duration	>12 months	-1.73	-2.23, -1.24	<0.001	84.75
	<12 months	-2.67	-3.41, -1.93	<0.001	94.32
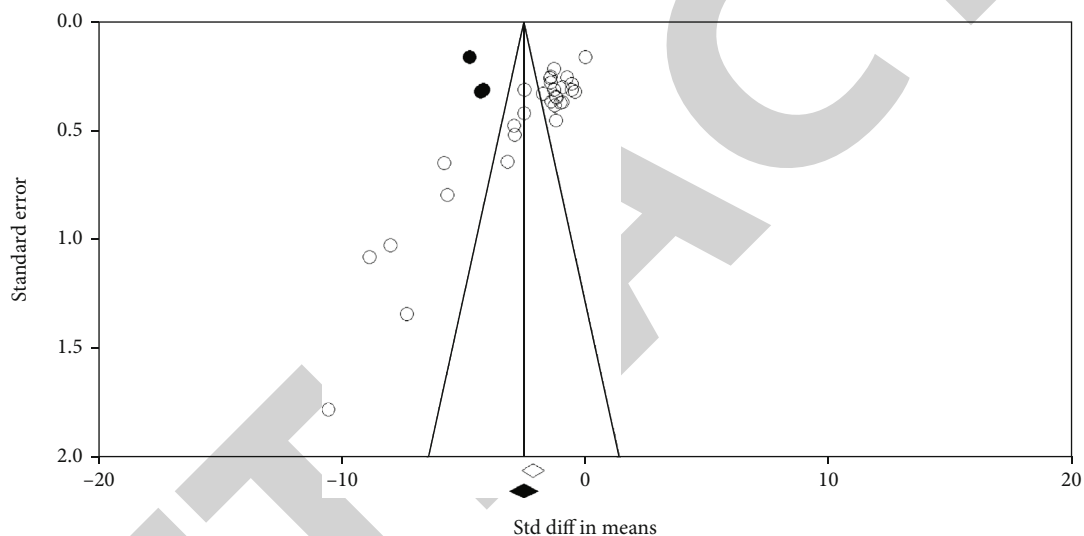
FIGURE 6: Funnel plot detailing publication bias in studies reporting the effect of statin treatment on circulating concentrations of oxidized LDL.

Based upon the results of studies showing that elevated oxLDL levels can independently predict recurrent stroke in patients with minor stroke or TIA [74], several recent studies have shown that prestroke treatment with statins can reduce serum oxLDL levels and that statins improve clinical outcomes in patients with atrial fibrillation-related acute ischemic stroke [75, 76]. Overall, the results of this meta-analysis and of previous studies may support the hypothesis that the beneficial effects of statins on ASCVD may be related, at least in part, to their ability to reduce oxLDL levels.

Antibodies to oxLDL have been associated with atherosclerosis presence, progression, and related clinical events, with the latter association being independent of and additive to LDL-C levels [10]. It is important to note that when normolipemic patients were treated with a high dose of atorvastatin, this resulted in a decrease in the levels of autoantibodies against oxLDL [57]. However, our meta-analysis could not find a significant effect of statins on antibodies against oxLDL. Although anti-oxLDL antibodies may

have a pathogenic role in ASCVD, our results suggest that the beneficial effect of statins on ASCVD may be independent of the detrimental impact of anti-oxLDL antibodies.

This meta-analysis has some strengths and some limitations. Several studies and a relatively recently published meta-analysis have shown that increased levels of circulating oxLDL are associated with clinical ASCVD events [77], but no meta-analysis has so far investigated the effects of statin therapy on circulating oxLDL levels. This is the novelty of our analysis. A limitation is that not all studies uniformly measured and reported oxLDL values, thereby justifying the use of SMD as a summary statistic for the pooled effect size in this meta-analysis. Another limitation is that the meta-analysis of data on antibodies against oxLDL included only 3 studies (although with 2575 subjects), which might have introduced a bias towards a negative finding. Also, the PROSPERO protocol has not been preregistered for this review. Besides, the methods for measuring oxLDL concentrations in some studies included in this meta-analysis were different and might explain heterogeneity in our findings,

although the use of standardization analysis reduces this error. Additionally, LDL oxidation can be affected by a number of concomitant factors, such as obesity, triglyceride levels, systemic inflammation, or LDL particle size, which were not fully evaluated in this study. Furthermore, dietary patterns, level of physical activity, smoking, and some drugs may modify LDL oxidation, which have not been considered in the included studies.

5. Conclusions

This meta-analysis suggests that patients treated with statins have significantly lower circulating concentrations of oxLDL and that this effect is not related to the intensity or lipophilicity of the statins used. Beyond well-known reduction in LDL-C, the beneficial effect of statins may partly be associated with the reduction of oxidative modifications of LDL and its effect on different stages of the atherosclerotic process. Further studies should address the association between statin-induced reduction of oxLDL and its effect on cardiovascular outcomes, particularly in patients with diabetes, metabolic syndrome, and chronic kidney disease. Furthermore, the effect of other lipid-lowering drugs, such as ezetimibe, PCSK9 inhibitors, and fibrates, on oxLDL levels also merits further investigation.

Data Availability

There is no primary dataset associated with this study.

Conflicts of Interest

The authors declare that they have no conflicts of interest.

Authors' Contributions

Fatemeh Baratzadeh and Željko Reiner equally contributed as the first author.

Supplementary Materials

Table S1: summary of the search strategy. Table S2: summary of the strength of evidence using the Grade of Recommendations, Assessment, Development and Evaluation (GRADE) system. (Supplementary Materials)

References

[1] I. Graham, M.-T. Cooney, D. Bradley, A. Dudina, and Z. Reiner, "Dyslipidemias in the prevention of cardiovascular disease: risks and causality," *Current cardiology reports*, vol. 14, no. 6, pp. 709–720, 2012.

[2] Ž. Reiner, "Statins in the primary prevention of cardiovascular disease," *Nature Reviews Cardiology*, vol. 10, no. 8, pp. 453–464, 2013.

[3] Ž. Reiner, G. De Backer, Z. Fras et al., "Lipid lowering drug therapy in patients with coronary heart disease from 24 European countries-Findings from the EUROASPIRE IV survey," *Atherosclerosis*, vol. 246, pp. 243–250, 2016.

[4] H. Jiang, Y. Zhou, S. M. Nabavi et al., "Mechanisms of Oxidized LDL-Mediated Endothelial Dysfunction and Its Consequences for the Development of Atherosclerosis," *Frontiers in Cardiovascular Medicine*, vol. 9, Article ID 925923, 2022.

[5] E. A. Ivanova, V. A. Myasoedova, A. A. Melnichenko, A. V. Grechko, and A. N. Orekhov, "Small dense low-density lipoprotein as biomarker for atherosclerotic diseases," *Oxidative Medicine and Cellular Longevity*, vol. 2017, Article ID 1273042, 10 pages, 2017.

[6] G. Obermayer, T. Afonyushkin, and C. Binder, "Oxidized low-density lipoprotein in inflammation-driven thrombosis," *Journal of Thrombosis and Haemostasis*, vol. 16, no. 3, pp. 418–428, 2018.

[7] O. Guardamagna, F. Abello, P. Saracco, V. Baracco, E. Rolfo, and M. Pirro, "Endothelial activation, inflammation and premature atherosclerosis in children with familial dyslipidemia," *Atherosclerosis*, vol. 207, no. 2, pp. 471–475, 2009.

[8] C. J. Binder, N. Papac-Milicevic, and J. L. Witztum, "Innate sensing of oxidation-specific epitopes in health and disease," *Nature Reviews Immunology*, vol. 16, no. 8, pp. 485–497, 2016.

[9] A. Pirillo, G. D. Norata, and A. L. Catapano, "LOX-1, OxLDL, and atherosclerosis," *Mediators of Inflammation*, vol. 2013, Article ID 152786, 12 pages, 2013.

[10] M. Puurunen, M. Mänttäri, V. Manninen et al., "Antibody against oxidized low-density lipoprotein predicting myocardial infarction," *Archives of Internal Medicine*, vol. 154, no. 22, pp. 2605–2609, 1994.

[11] C. Chen and D. B. Khismatullin, "Oxidized low-density lipoprotein contributes to atherogenesis via co-activation of macrophages and mast cells," *PlosOne*, vol. 10, no. 3, article e0123088, 2015.

[12] M. Ruscica, N. Ferri, R. D. Santos, C. R. Sirtori, and A. Corsini, "Lipid lowering drugs: present status and future developments," *Current Atherosclerosis Reports*, vol. 23, no. 5, p. 17, 2021.

[13] A. Sahebkar and G. F. Watts, "New therapies targeting apoB metabolism for high-risk patients with inherited dyslipidaemias: what can the clinician expect?," *Cardiovascular Drugs and Therapy*, vol. 27, no. 6, pp. 559–567, 2013.

[14] A. Sahebkar and G. F. Watts, "New LDL-cholesterol lowering therapies: pharmacology, clinical trials, and relevance to acute coronary syndromes," *Clinical Therapeutics*, vol. 35, no. 8, pp. 1082–1098, 2013.

[15] F. Amin, F. Fathi, Ž. Reiner, M. Banach, and A. Sahebkar, "The role of statins in lung cancer," *Archives of Medical Science*, vol. 18, no. 1, pp. 141–152, 2022.

[16] A. Bahrami, N. Parsamanesh, S. L. Atkin, M. Banach, and A. Sahebkar, "Effect of statins on toll-like receptors: a new insight to pleiotropic effects," *Pharmacological Research*, vol. 135, pp. 230–238, 2018.

[17] M. Khalifeh, P. E. Penson, M. Banach, and A. Sahebkar, "Statins as anti-pyroptotic agents," *Archives of Medical Science*, vol. 17, no. 5, pp. 1414–1417, 2021.

[18] Ž. Reiner, M. Hatamipour, M. Banach et al., "Statins and the Covid-19 main protease: in silico evidence on direct interaction," *Archives of Medical Science*, vol. 16, no. 3, pp. 490–496, 2020.

[19] N. Shakour, M. Ruscica, F. Hadizadeh et al., "Statins and C-reactive protein: in silico evidence on direct interaction," *Archives of Medical Science*, vol. 16, no. 6, pp. 1432–1439, 2020.

[20] S. M. Sohrevardi, F. S. Nasab, M. R. Mirjalili et al., "Effect of atorvastatin on delirium status of patients in the intensive care unit: a randomized controlled trial," *Archives of Medical Science*, vol. 17, no. 5, pp. 1423–1428, 2021.

[21] A. Vahedian-Azimi, S. M. Mohammadi, F. H. Beni et al., "Improved COVID-19 ICU admission and mortality outcomes following treatment with statins: a systematic review and meta-analysis," *Archives of Medical Science*, vol. 17, no. 3, pp. 579–595, 2021.

[22] T. Jamialahmadi, F. Baratzadeh, Z. Reiner et al., "The effects of statin dose, lipophilicity, and combination of statins plus ezetimibe on circulating oxidized low-density lipoprotein levels: a systematic review and meta-analysis of randomized controlled trials," *Mediators of Inflammation*, vol. 2021, Article ID 9661752, 12 pages, 2021.

[23] A. J. Sutton, K. R. Abrams, D. R. Jones, D. R. Jones, T. A. Sheldon, and F. Song, "Methods for meta-analysis in medical research," *Wiley Chichester*, vol. 348, 2000.

[24] J. P. T. G. S. Higgins, *Handbook for Systematic Reviews of Interventions. Version 5.0.2 ed*, The Cochrane Collaboration, London, 2009.

[25] M. Borenstein, L. Hedges, J. Higgins, and H. Rothstein, *Comprehensive Meta-Analysis, Version 2 Biostat*, Englewood, 2005.

[26] S. P. Hozo, B. Djulbegovic, and I. Hozo, "Estimating the mean and variance from the median, range, and the size of a sample," *BMC Medical Research Methodology*, vol. 5, no. 1, pp. 1–10, 2005.

[27] M. Banach, C. Serban, A. Sahebkar et al., "Impact of statin therapy on coronary plaque composition: a systematic review and meta-analysis of virtual histology intravascular ultrasound studies," *BMC Medicine*, vol. 13, no. 1, p. 229, 2015.

[28] M. Banach, C. Serban, S. Ursoniu et al., "Statin therapy and plasma coenzyme Q10 concentrations-a systematic review and meta-analysis of placebo-controlled trials," *Pharmacological Research*, vol. 99, pp. 329–336, 2015.

[29] S. Duval and R. Tweedie, "Trim and fill: a simple funnel-plot–based method of testing and adjusting for publication bias in meta-analysis," *Biometrics*, vol. 56, no. 2, pp. 455–463, 2000.

[30] G. H. Guyatt, A. D. Oxman, G. E. Vist et al., "GRADE: an emerging consensus on rating quality of evidence and strength of recommendations," *BMJ*, vol. 336, no. 7650, pp. 924–926, 2008.

[31] S. H. Diepeveen, G. W. Verhoeven, J. Van Der Palen et al., "Effects of atorvastatin and vitamin E on lipoproteins and oxidative stress in dialysis patients: a randomised-controlled trial," *Journal of Internal Medicine*, vol. 257, no. 5, pp. 438–445, 2005.

[32] G. K. Dogra, G. F. Watts, D. C. Chan, and K. Stanton, "Statin therapy improves brachial artery vasodilator function in patients with type 1 diabetes and microalbuminuria," *Diabetic Medicine*, vol. 22, no. 3, pp. 239–242, 2005.

[33] G. Dogra, A. Irish, D. Chan, and G. Watts, "A randomized trial of the effect of statin and fibrate therapy on arterial function in CKD," *American Journal of Kidney Diseases*, vol. 49, no. 6, pp. 776–785, 2007.

[34] C. Vlachopoulos, K. Aznaouridis, A. Dagre et al., "Protective effect of atorvastatin on acute systemic inflammation-induced endothelial dysfunction in hypercholesterolaemic subjects," *European Heart Journal*, vol. 28, no. 17, pp. 2102–2109, 2007.

[35] U. Singh, S. Devaraj, I. Jialal, and D. Siegel, "Comparison effect of atorvastatin (10 versus 80 mg) on biomarkers of inflammation and oxidative stress in subjects with metabolic syndrome," *The American Journal of Cardiology*, vol. 102, no. 3, pp. 321–325, 2008.

[36] E. Nou, M. T. Lu, S. E. Looby et al., "Serum oxidized low-density lipoprotein decreases in response to statin therapy and relates independently to reductions in coronary plaque in patients with HIV," *AIDS*, vol. 30, no. 4, pp. 583–590, 2016.

[37] D. E. Nixon, R. J. Bosch, E. S. Chan et al., "Effects of atorvastatin on biomarkers of immune activation, inflammation, and lipids in virologically suppressed, human immunodeficiency virus-1–infected individuals with low-density lipoprotein cholesterol <130 mg/dL (AIDS Clinical Trials Group study A5275)," *Journal of Clinical Lipidology*, vol. 11, no. 1, pp. 61–69, 2017.

[38] C. DeFilippi, R. Christenson, J. Joyce et al., "Brief report: statin effects on myocardial fibrosis markers in people living with HIV," *Journal of Acquired Immune Deficiency Syndromes*, vol. 78, no. 1, pp. 105–110, 2018.

[39] T. Yamada, K. Node, T. Mine et al., "Long-term effect of atorvastatin on neurohumoral activation and cardiac function in patients with chronic heart failure: a prospective randomized controlled study," *American Heart Journal*, vol. 153, no. 6, p. 1055e1-e8, 2007.

[40] H. Oka, S. Ikeda, S. Koga, Y. Miyahara, and S. Kohno, "Atorvastatin induces associated reductions in platelet P-selectin, oxidized low-density lipoprotein, and interleukin-6 in patients with coronary artery diseases," *Heart and Vessels*, vol. 23, no. 4, pp. 249–256, 2008.

[41] A. El-Sisi, S. K. Hegazy, M. K. Ahmed, and M. A. Hamouda, "Evaluation of short term effect of atorvastatin on myocardial performance and its pleiotropic effects on ischemic heart failure," *British Journal of Pharmaceutical Research*, vol. 6, no. 5, pp. 343–357, 2015.

[42] I. Andreou, D. Tousoulis, A. Miliou et al., "Effects of rosuvastatin on myeloperoxidase levels in patients with chronic heart failure: a randomized placebo-controlled study," *Atherosclerosis*, vol. 210, no. 1, pp. 194–198, 2010.

[43] S. Erbs, E. B. Beck, A. Linke et al., "High-dose rosuvastatin in chronic heart failure promotes vasculogenesis, corrects endothelial function, and improves cardiac remodeling-results from a randomized, double-blind, and placebo-controlled study," *International Journal of Cardiology*, vol. 146, no. 1, pp. 56–63, 2011.

[44] E. ter Avest, E. J. Abbink, J. de Graaf, C. J. Tack, and A. F. Stalenhoef, "Effect of rosuvastatin on insulin sensitivity in patients with familial combined hyperlipidaemia," *European Journal of Clinical Investigation*, vol. 35, no. 9, pp. 558–564, 2005.

[45] C. O. Hileman, R. Turner, N. T. Funderburg, R. D. Semba, and G. A. McComsey, "Changes in oxidized lipids drive the improvement in monocyte activation and vascular disease after statin therapy in HIV," *AIDS*, vol. 30, no. 1, pp. 65–73, 2016.

[46] M. Abe, N. Maruyama, K. Okada, S. Matsumoto, K. Matsumoto, and M. Soma, "Effects of lipid-lowering therapy with rosuvastatin on kidney function and oxidative stress in patients with diabetic nephropathy," *Journal of Atherosclerosis and Thrombosis*, vol. 18, no. 11, pp. 1018–1028, 2011.

[47] M. Rydén, P. Leanderson, K. O. Kastbom, and L. Jonasson, "Effects of simvastatin on carotenoid status in plasma,"

Nutrition, Metabolism and Cardiovascular Diseases, vol. 22, no. 1, pp. 66–71, 2012.

[48] R. Krysiak, W. Zmuda, and B. Okopień, "The effect of ezetimibe and simvastatin on hemostasis in patients with isolated hypercholesterolemia," *Fundamental and Clinical Pharmacology*, vol. 26, no. 3, pp. 424–431, 2012.

[49] D. Kirmizis, A. Papagianni, F. Dogrammatzi et al., "Effects of simvastatin on markers of inflammation, oxidative stress and endothelial cell apoptosis in patients on chronic hemodialysis," *Journal of Atherosclerosis and Thrombosis*, vol. 17, no. 12, pp. 1256–1265, 2010.

[50] N. Kishimoto, T. Hayashi, I. Sakuma et al., "A hydroxymethylglutaryl coenzyme A reductase inhibitor improves endothelial function within 7 days in patients with chronic hemodialysis," *International Journal of Cardiology*, vol. 145, no. 1, pp. 21–26, 2010.

[51] A. Ichihara, M. Hayashi, M. Ryuzaki, M. Handa, T. Furukawa, and T. Saruta, "Fluvastatin prevents development of arterial stiffness in haemodialysis patients with type 2 diabetes mellitus," *Nephrology Dialysis Transplantation*, vol. 17, no. 8, pp. 1513–1517, 2002.

[52] O. Yoshida, T. Kondo, Y. Kureishi-Bando et al., "Pitavastatin, an HMG-CoA reductase inhibitor, ameliorates endothelial function in chronic smokers," *Circulation Journal*, vol. 74, no. 1, pp. 195–202, 2010.

[53] T. Janatuinen, J. Knuuti, J. O. Toikka et al., "Effect of pravastatin on low-density lipoprotein oxidation and myocardial perfusion in young adults with type 1 diabetes," *Arteriosclerosis, Thrombosis, and Vascular Biology*, vol. 24, no. 7, pp. 1303–1308, 2004.

[54] S. Tani, I. Watanabe, T. Anazawa et al., "Effect of pravastatin on malondialdehyde-modified low-density lipoprotein levels and coronary plaque regression as determined by three-dimensional intravascular ultrasound," *The American Journal of Cardiology*, vol. 96, no. 8, pp. 1089–1094, 2005.

[55] B. Ky, A. Burke, S. Tsimikas et al., "The influence of pravastatin and atorvastatin on markers of oxidative stress in hypercholesterolemic humans," *Journal of the American College of Cardiology*, vol. 51, no. 17, pp. 1653–1662, 2008.

[56] S. Tsimikas, J. L. Witztum, E. R. Miller et al., "High-dose atorvastatin reduces total plasma levels of oxidized phospholipids and immune complexes present on apolipoprotein B-100 in patients with acute coronary syndromes in the MIRACL trial," *Circulation*, vol. 110, no. 11, pp. 1406–1412, 2004.

[57] A. M. Kuklinska, B. Mroczko, W. J. Musial et al., "Influence of atorvastatin on blood pressure control in treated hypertensive, normolipemic patients – an open, pilot study," *Blood Pressure*, vol. 19, no. 4, pp. 260–266, 2010.

[58] J. Rodenburg, M. N. Vissers, A. Wiegman et al., "Oxidized low-density lipoprotein in children with familial hypercholesterolemia and unaffected siblings: effect of pravastatin," *Journal of the American College of Cardiology*, vol. 47, no. 9, pp. 1803–1810, 2006.

[59] A. E. Fraley and S. Tsimikas, "Clinical applications of circulating oxidized low-density lipoprotein biomarkers in cardiovascular disease," *Current Opinion in Lipidology*, vol. 17, no. 5, pp. 502–509, 2006.

[60] P. Luo, M. Yan, E. D. Frohlich, J. L. Mehta, and C. Hu, "Novel concepts in the genesis of hypertension: role of LOX-1," *Cardiovascular Drugs and Therapy*, vol. 25, no. 5, pp. 441–449, 2011.

[61] M. Yan, J. L. Mehta, and C. Hu, "LOX-1 and obesity," *Cardiovascular Drugs and Therapy*, vol. 25, no. 5, pp. 469–476, 2011.

[62] S. Inami, K. Okamatsu, M. Takano et al., "Effects of statins on circulating oxidized low-density lipoprotein in patients with hypercholesterolemia," *Japanese Heart Journal*, vol. 45, no. 6, pp. 969–975, 2004.

[63] R. X. Xu, Y. Zhang, Y. Zhang et al., "Effects of pitavastatin on lipoprotein subfractions and oxidized low-density lipoprotein in patients with atherosclerosis," *Medical Science*, vol. 40, no. 5, pp. 879–884, 2020.

[64] B. B. Altunkeser, A. Tuncez, B. Ozturk et al., "Comparative effects of high-dose atorvastatin versus rosuvastatin on lipid parameters, oxidized low-density lipoprotein, and proprotein convertase subtilisin kexin 9 in acute coronary syndrome," *Coronary Artery Disease*, vol. 30, no. 4, pp. 285–290, 2019.

[65] M. Pirro, L. E. Simental-Mendía, V. Bianconi, G. F. Watts, M. Banach, and A. Sahebkar, "Effect of statin therapy on arterial wall inflammation based on 18F-FDG PET/CT: a systematic review and meta-analysis of interventional studies," *Journal of Clinical Medicine*, vol. 8, no. 1, p. 118, 2019.

[66] A. Sahebkar, N. Kiaie, A. M. Gorabi et al., "A comprehensive review on the lipid and pleiotropic effects of pitavastatin," *Progress in Lipid Research*, vol. 84, article 101127, 2021.

[67] M. M. Obradovic, A. Trpkovic, V. Bajic et al., "Interrelatedness between C-reactive protein and oxidized low-density lipoprotein," *Clinical Chemistry and Laboratory Medicine*, vol. 53, no. 1, pp. 29–34, 2015.

[68] P. M. Ridker, E. Danielson, F. A. Fonseca et al., "Reduction in C-reactive protein and LDL cholesterol and cardiovascular event rates after initiation of rosuvastatin: a prospective study of the JUPITER trial," *The Lancet*, vol. 373, no. 9670, pp. 1175–1182, 2009.

[69] O. Hofnagel, B. Luechtenborg, G. Weissen-Plenz, and H. Robenek, "Statins and foam cell formation: impact on LDL oxidation and uptake of oxidized lipoproteins via scavenger receptors," *Lipids*, vol. 1771, no. 9, pp. 1117–1124, 2007.

[70] J. Geng, H. Xu, X. Yu et al., "Rosuvastatin protects against oxidized low-density lipoprotein-induced endothelial cell injury of atherosclerosis in vitro," *Molecular Medicine Reports*, vol. 19, no. 1, pp. 432–440, 2019.

[71] M. Pirro, G. Schillaci, M. R. Mannarino et al., "Effects of rosuvastatin on 3-nitrotyrosine and aortic stiffness in hypercholesterolemia," *Nutrition, Metabolism and Cardiovascular Diseases*, vol. 17, no. 6, pp. 436–441, 2007.

[72] M. Pirro, G. Schillaci, P. F. Romagno et al., "Influence of short-term rosuvastatin therapy on endothelial progenitor cells and endothelial function," *Journal of cardiovascular pharmacology and therapeutics*, vol. 14, no. 1, pp. 14–21, 2009.

[73] P. Singh, I. Goncalves, C. Tengryd et al., "Reduced oxidized LDL in T2D plaques is associated with a greater statin usage but not with future cardiovascular events," *Cardiovascular Diabetology*, vol. 19, no. 1, pp. 1–12, 2020.

[74] A. Wang, J. Xu, G. Chen et al., "Oxidized low-density lipoprotein predicts recurrent stroke in patients with minor stroke or TIA," *Neurology*, vol. 91, no. 10, pp. e947–e955, 2018.

[75] L. He, R. Xu, J. Wang et al., "Prestroke statins use reduces oxidized low density lipoprotein levels and improves clinical

Retraction

Retracted: Hemodynamic and Geometric Risk Factors for In-Stent Restenosis in Patients with Intracranial Atherosclerotic Stenosis

Oxidative Medicine and Cellular Longevity

This article has been retracted by Hindawi following an investigation undertaken by the publisher [1]. This investigation has uncovered evidence of one or more of the following indicators of systematic manipulation of the publication process:

(1) Discrepancies in scope

(2) Discrepancies in the description of the research reported

(3) Discrepancies between the availability of data and the research described

(4) Inappropriate citations

(5) Incoherent, meaningless and/or irrelevant content included in the article

(6) Manipulated or compromised peer review

The presence of these indicators undermines our confidence in the integrity of the article's content and we cannot, therefore, vouch for its reliability. Please note that this notice is intended solely to alert readers that the content of this article is unreliable. We have not investigated whether authors were aware of or involved in the systematic manipulation of the publication process.

Wiley and Hindawi regrets that the usual quality checks did not identify these issues before publication and have since put additional measures in place to safeguard research integrity.

We wish to credit our own Research Integrity and Research Publishing teams and anonymous and named external researchers and research integrity experts for contributing to this investigation.

The corresponding author, as the representative of all authors, has been given the opportunity to register their agreement or disagreement to this retraction. We have kept a record of any response received.

References

[1] X. Song, H. Qiu, S. Wang, Y. Cao, and J. Zhao, "Hemodynamic and Geometric Risk Factors for In-Stent Restenosis in Patients with Intracranial Atherosclerotic Stenosis," *Oxidative Medicine and Cellular Longevity*, vol. 2022, Article ID 6951302, 14 pages, 2022.

Research Article

Hemodynamic and Geometric Risk Factors for In-Stent Restenosis in Patients with Intracranial Atherosclerotic Stenosis

Xiaowen Song,[1,2,3,4] **Hancheng Qiu,**[1,2,3,4] **Shuo Wang** ⬚[1,2,3,4] **Yong Cao,**[1,2,3,4] **and Jizong Zhao** ⬚[1,2,3,4]

¹*Department of Neurosurgery, Beijing Tiantan Hospital, Capital Medical University, Beijing, China*
²*China National Clinical Research Center for Neurological Diseases, Beijing, China*
³*Center of Stroke, Beijing Institute for Brain Disorders, Beijing, China*
⁴*Beijing Key Laboratory of Translational Medicine for Cerebrovascular Disease, Beijing, China*

Correspondence should be addressed to Jizong Zhao; zhaojizong@bjtth.org

Problem. Investigating the importance of vessel geometry and hemodynamics in intracranial atherosclerotic stenosis (ICAS) might provide a more profound understanding about the underlying mechanisms of in-stent restenosis (ISR). *Methods*. Severe ICAS patients managed with percutaneous transluminal angioplasty and stenting (PTAS) were included in the retrospective cohort study and were divided into two groups according to whether ISR occurred at follow-up (ISR group and no-ISR group). Computational fluid dynamics models were built based on digital subtraction angiography before and after PTAS to simulate blood flow and quantify hemodynamic parameters. The associations between vessel geometry, hemodynamics, and ISR in ICAS patients were investigated. *Results*. Among 39 patients, ISR occurred in seven patients (17.95%) after a mean follow-up period of 6.69 ± 3.24 months. Stenting decreased vessel angulation (51.11° [40.07°–67.27°] vs. 15.97° [0.00°–36.16°], $P = 0.000$) and vessel tortuosity (0.09 [0.06–0.13] vs. 0.01 [0.00–0.03], $P = 0.000$). Meanwhile, the translational pressure ratio (PR) dramatically increased (0.07 [0.00–0.31] vs. 0.62 [0.41–0.82], $P = 0.000$) with the wall shear stress ratio decreased (13.93 [8.37–40.30] vs. 2.90 [1.69–4.48], $P = 0.000$). In the multivariate analysis, smaller Δ tortuosity ($P = 0.038$) was independently associated with the occurrence of ISR, and smaller post-PTAS translesional PR was also a predictive factor of marginal significance ($P = 0.059$). *Conclusion*. PTAS decreased vessel angulation, vessel tortuosity, and translesional wall shear stress ratio while it increased translesional pressure ratio (PR) dramatically in ICAS patients. Smaller Δ tortuosity was found to be a risk factor for ISR, and smaller post-PTAS translesional PR was also a predictive factor of marginal significance, indicating that both geometric and hemodynamic parameters played important roles in the occurrence of ISR after PTAS.

1. Introduction

Hemodynamic factors had a profound influence on vascular physiology and homeostasis, thus playing important roles in the development and progression of various vascular diseases such as atherosclerosis or stenosis [1]. Vessel geometry had been proven to affect the blood flow pattern through the artery, regulating the function of arterial endothelium and attributing to atherosclerotic stenosis [2].

Intracranial atherosclerotic stenosis (ICAS) was a major ischemic stroke subtype of high recurrence, causing approximately 5% to 10% of strokes in White people, 15% to 29% of transient ischemic attacks (TIAs) or strokes in Black people, and up to 30% to 50% of strokes in Asian people [3]. For patients with high-grade ICAS, despite optimal medical treatment, the risk of recurrent stroke that might result from embolic events and hemodynamic insufficiency was as high as 12.6% in the SAMMPRIS (Stenting and Aggressive Medical Management for Preventing Recurrent Stroke in Intracranial

Stenosis) trial [4] and 23% in the WASID (Warfarin-Aspirin Symptomatic Intracranial Disease) trial during the first year [5]. For Chinese population, the rate of recurrent stroke within 3 months could be 11.3% for ICAS patients with aggressive medical treatment [6].

Percutaneous transluminal angioplasty and stenting (PTAS) had emerged as a possible treatment option. With a 2.6% periprocedural stroke and death rate, the WEAVE (Wingspan StEnt System Post MArket SurVEillance) trial revealed the excellent safety and efficiency of this treatment [7]. Stenting could not only normalize the lumen diameter but also change the geometry of target vessels, resulting in underlying hemodynamic alterations. However, the hemodynamic influences of PTAS in small-caliber intracranial vessels had not been well demonstrated [8–10].

In the long term, clinicians should pay attention to challenges such as restenosis or delayed stent thrombosis after PTAS. With a 6.81% to 31.18% occurrence rate [11–19], the in-stent restenosis (ISR) in ICAS might be affected by features of the lesion and characteristics of the stent, which was controversial and not definite [11, 15, 16, 20]. In carotid and coronary arteries, local hemodynamic changes caused by geometric variations had been suggested to govern the risk and mechanism of ISR [21–24]. However, the hemodynamic and geometric features prone to adverse events, especially ISR in ICAS, had never been studied before.

This current study sought to evaluate the geometrical and hemodynamic changes caused by PTAS using computational fluid dynamic (CFD) analysis of patient-specific digital subtraction angiography (DSA) data, delineate associations between hemodynamics and vessel geometry, and identify hemodynamic and geometric factors implicated in the initiation and progression of ISR.

2. Materials and Methods

2.1. Patient Selection. This was a retrospective cohort study. We retrospectively screened eligible patients admitted to Beijing Tiantan Hospital from January 2020 to June 2021. Thirty-nine adult patients with severe ICAS (70%–99%) treated with PTAS were identified according to the following criteria: (1) history of ischemic stroke or TIA attributed to 70% to 99% atherosclerotic stenosis of a major intracranial artery (intracranial portion of the internal carotid artery (ICA), M1 middle cerebral artery (MCA-M1), V4 vertebral artery (VA-V4), or basilar artery (BA)), as revealed by DSA; (2) computed tomography perfusion imaging showing apparent hypoperfusion in the corresponding territory of the target intracranial artery; and (3) receiving PTAS for the severe ICAS. We excluded patients with the following conditions: (1) the index ischemic stroke or TIA was attributed to nonatherosclerotic intracranial arterial stenosis such as moyamoya disease, vasculitis or dissection, restenosis within a stented artery, or tandem stenosis of extracranial and intracranial arteries; (2) there was any potential cardioembolic source; and (3) there was known intracranial tumor, arteriovenous malformation, or aneurysm.

Patients' demographics, history of common cardiovascular risk factors, onset symptoms, lesion locations, and stroke severity by the National Institutes of Health Stroke Scale were obtained from electronic medical database. In each case, geometric metrics were assessed on three-dimensional-(3D-) DSA images, and a CFD model was built based on DSA images before and after PTAS to quantify the hemodynamic features.

This retrospective study was in accordance with the 1964 Helsinki Declaration and its later amendments or comparable ethical standards, and the research flow chart is shown in Figure 1. Informed consent was waived by the ethics committee of Beijing Tiantan Hospital because of the retrospective nature of the study (KY2016-034-02).

2.2. Treatment and Follow-Up. All patients had been pretreated with dual antiplatelet therapy (aspirin 300 mg and clopidogrel 75 mg daily) started at least 5 days before stenting. The PTAS procedures were successfully fulfilled using self-expanding stents by highly experienced neurosurgeons. After stent deployment, patients were maintained on dual antiplatelet therapy for at least 3 months, which was replaced by antiplatelet monotherapy (aspirin or clopidogrel) afterward.

According to the standard follow-up regimen after PTAS at our center, initial follow-up angiography would be performed at 3 to 12 months following the stent deployment procedure in all included patients. Further follow-up or treatment would be performed as dictated by clinical symptoms and findings on the initial angiogram. The follow-up DSA images were collected from the radiological database for ISR evaluation. If the luminal narrowing in the affected vessel was greater than 50%, it would be considered restenosis.

2.3. Assessment of Geometric Features. Patient-specific models were reconstructed from pre- and post-PTAS DSA source images for further quantitative analysis. Multiplanar reconstructions were oriented at the working angles for stenting to enable the measurement. Centerlines of the interested vessels were generated in 3-Matic from the catheter 3D rotational angiography. The vessel angulation was referred to as the angle between the local vessel centerlines of the proximal and distal vessels to the local stenosis (Figure 2). Angles were measured in the direction of the flow. As shown in Figure 3, vessel tortuosity was defined as $T/D - 1$, where T was the length of the centerline between two points proximal and distal to the local stenosis and D was the straight-line distance between these 2 points [25, 26]. Geometric parameters were measured before and after stenting and at subsequent angiographic follow-up. The differences of vessel tortuosity and angulation between pre- and post-PTAS defined as Δ tortuosity and Δ angulation were calculated, respectively.

2.4. CFD Modeling and Quantification of Hemodynamic Features of ICAS. CFD analysis was performed using the patients' 3D-DSA data before and after stenting for comparison of hemodynamic alteration caused by PTAS. 3D geometry of the arteries of interest was reconstructed from DSA source images with Mimics and Magics, covering the ICA;
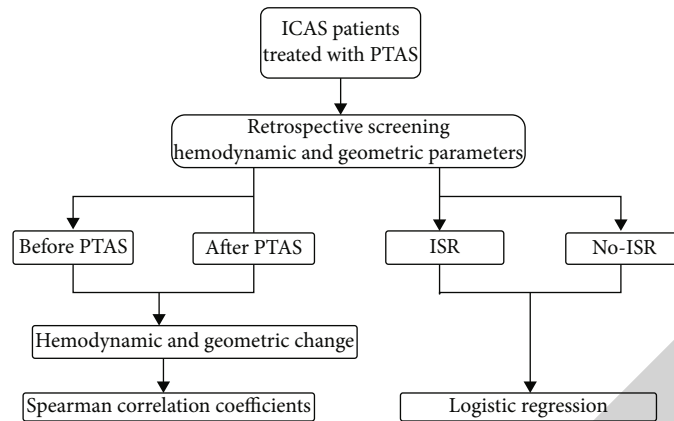
FIGURE 1: Research flow chart. ICAS: intracranial atherosclerotic stenosis; PTAS: percutaneous transluminal angioplasty and stenting; ISR: in-stent restenosis.
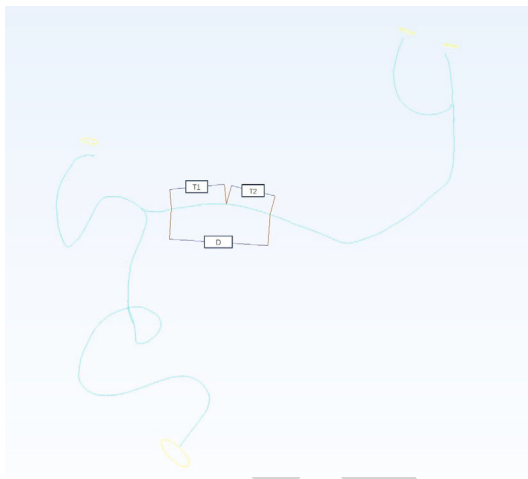
FIGURE 2: A patient-specific model reconstructed from DSA images and the generated centerlines of the proximal and distal vessel to the local stenosis before and after PTAS. The vessel angulation is referred to as the angle between the centerlines (displayed by dotted arrows). DSA: digital subtraction angiography; PTAS: percutaneous transluminal angioplasty and stenting.
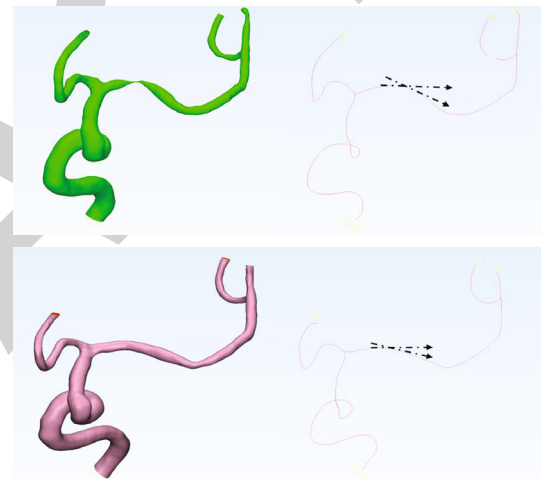
FIGURE 3: Centerline extracted from the interested vessel. Vessel tortuosity is defined as $T/D - 1$, where T, equal to T1 + T2, is the length of the centerline between two points proximal and distal to the local stenosis, respectively, and D is the straight-line distance between these 2 points.

MCA-M1, M2; and ACA-A1, A2 segments for cases with ICA or MCA-M1 lesion and VA-V4, BA, PCA-P1 segments and SCA for cases with a VA-V4 or BA lesion. A mesh was then created on the vessel surface in ANSYS ICEM CFD, with the maximal element sizes of 0.1 for the inlet(s) and outlets and 0.2 for other parts of the mesh, containing at least 1 million elements in total for each case. The procedure of CFD modeling was shown in Figure 4. Blood flow simulation was performed on this mesh using ANSYS CFX software. The following settings and assumptions were applied in simulation of the blood flow: (1) rigid, noncompliant walls with no-slip boundary conditions were assumed; (2) the outlet pressure was set to be 0 Pa, as we primarily focused on the relative translesional pressure change across the ICAS lesion; (3) the individualized mean flow velocity at the inlet was obtained from each patient's transcranial Doppler; (4) blood flow simulation was conducted in ANSYS CFX by solving the Navier-Stokes equations; convergence was achieved when the root mean square residual value reached below 10^{-4}; and (5) blood was an incompressible Newtonian fluid with a constant viscosity of 0.0035 kg/ (m ∗ s) and a density of 1060 kg/m^3.

We quantified the relative changes of pressure and wall shear strain (WSS) across each ICAS lesion, by obtaining translesional pressure ratio (PR) and WSS ratio (WSSR) on the CFD models in ANSYS CFD-post. In the pre-PTAS model, translesional PR was calculated as pressure$_{poststenotic}$/pressure$_{prestenotic}$, and pressure$_{poststenotic}$ and pressure$_{prestenotic}$ were measured at the first normal diameter distal to the ICAS lesion and at the proximal normal vessel segment, respectively. Translesional WSSR was calculated as WSS$_{stenotic-apex}$/WSS$_{prestenotic}$; and WSS$_{stenotic-apex}$ was measured
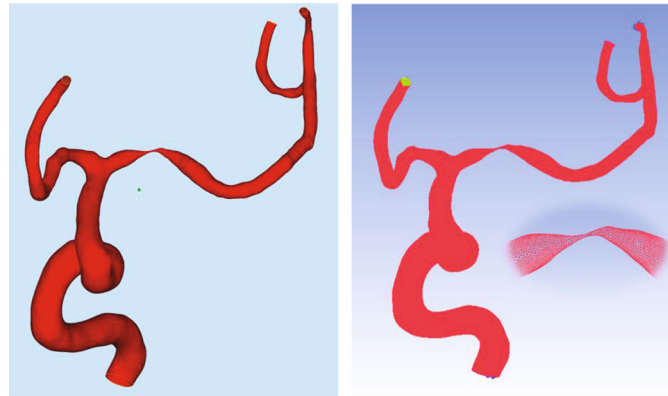
FIGURE 4: A patient-specific three-dimensional geometry of the arteries of interest reconstructed from DSA source images and the mesh created on the vessel surface and within the vessel lumen. DSA: digital subtraction angiography.

at the most severely narrowed cross-section of the diseased intracranial artery referred to as the stenotic throat, and $WSS_{prestenotic}$ was measured at the proximal normal vessel segment. In the post-PTAS model, these hemodynamic indices were measured at the correspondingly the same locations as in the pre-PTAS model. The difference between pre- and post-PTAS hemodynamic features was calculated.

2.5. Statistical Analysis. Continuous variables and ordinal variables (National Institutes of Health Stroke Scale) were expressed as median and interquartile range, and frequency and categorical variables were expressed as the frequency and percentage. We compared the geometric and hemodynamic metrics between pre- and post-PTAS by Wilcoxon rank sum test. The Mann–Whitney U test was used for univariable comparisons of continuous variables and χ^2 tests or Fisher exact test for categorical variables between patients with ISR and no-ISR during follow-up period. Nonparametric tests were adopted while needed. Multivariate logistic regression model was established to predict ISR, adjusting for other factors with $P < 0.1$ in univariate logistic regression. In addition, we analyzed the associations between geometric and hemodynamic features by using Spearman correlation coefficients. We considered $P < 0.05$ as statistically significant. We conducted all statistical analyses in IBM SPSS Statistics version 22.0 (IBM Corp, Armonk, New York).

3. Results

Among 52 potentially eligible patients with severe ICAS confirmed in DSA who were scheduled a second follow-up DSA at 6 months, we excluded 12 cases with poor DSA image quality or complex vessel geometry that did not allow CFD model construction and one case for failure in solving the Navier-Stokes equations in simulation of blood flow. Therefore, 39 patients were included in the current study (mean age, 57.51 years; 22 males; Table 1). Twenty-two patients (56%) had the ICAS lesion in the anterior circulation (20 in MCA-M1, 2 in intracranial ICA). No difference was found between the baseline characteristics of the ISR and no-ISR group.

As shown in Tables 2–3, at the affected arteries, prominent hemodynamic changes were brought about by PTAS (Figure 5). Translesional PR (0.07 [0.00–0.31] vs. 0.62 [0.41–0.82], $P = 0.000$) increased, whereas WSSR (13.93 [8.37–40.30] vs. 2.90 [1.69–4.48], $P = 0.000$) decreased significantly after PTAS. Besides minimizing the luminal narrowness, stenting straightened the target vessel, significantly decreasing vessel tortuosity (0.01 [0.00–0.03] vs. 0.09 [0.06–0.13], $P = 0.000$) and vessel angulation (15.97° [0.00°–36.16°] vs. 51.11° [40.07°–67.27°], $P = 0.000$).

All patients underwent angiographic follow-up from 3 to 24 months (mean, 6.41 months). After PTAS, the deployed stent exerted a continuous outwardly directed radial force resulting in persistent vascular remodeling. At the angiographic follow-up, a significant difference existed in vessel tortuosity (0.01 [0.00–0.03] vs. 0.09 [0.06–0.13], $P = 0.000$) and angulation (21.46° [0.00°–31.34°] vs. 51.11° [40.07°–67.27°], $P = 0.000$) compared with those measured before PTAS (Figure 6). Nevertheless, when compared with the vessel geometry after PTAS, no significant differences were found (0.01 [0.00–0.03] vs. 0.01 [0.00–0.03], $P = 0.575$; 21.46° [0.00°–31.34°] vs. 15.97° [0.00°–36.16°], $P = 0.112$) (Table 3).

Seven patients (17.95%) were diagnosed with ISR during follow-up. Compared with those without ISR, ICAS lesions with ISR had significantly larger vessel tortuosity (0.06 [0.02–0.10] vs. 0.05 [0.00–0.01], $P = 0.001$) and lower PR (0.36 [0.05–0.62] vs. 0.67 [0.50–0.89], $P = 0.024$) after PTAS. In addition, ISR lesions had smaller Δ tortuosity (0.05 [0.02–0.06] vs. 0.08 [0.06–0.12], $P = 0.006$) and smaller Δ angulation (14.08° [6.00°–29.24°] vs. 33.53° [22.85°–44.05°], $P = 0.016$) (Table 4).

As shown in Table 5, there was a strong linear correlation between translesional PR and WSSR ($r_s = -0.672$, $P = 0.000$; $r_s = -0.566$, $P = 0.000$) both before and after PTAS (Figure 7). Besides, after PTAS, vessel tortuosity was negatively linearly correlated with PR ($r_s = -0.673$, $P = 0.000$) and positively with WSSR ($r_s = 0.547$, $P = 0.000$) (Figure 8), indicating the underlying interactions between vascular geometry and hemodynamics.

In the univariate logistic model, larger post-PTAS vessel tortuosity ($P = 0.012$), larger post-PTAS vessel angulation

TABLE 1: Comparison of baseline characteristics between ICAS patients with ISR and no ISR.

Variables	Overall $n = 39$	No ISR $n = 32$	ISR $n = 7$	P
Age (y)	58.00 (50.00–65.00)	57.50 (50.50–64.50)	59.00 (49.00–65.00)	0.985
Male	22 (56.41)	16 (50.00)	6 (85.71)	0.113
Smoker	15 (38.41)	12 (37.50)	3 (42.86)	1.000
Hypertension	26 (66.67)	22 (68.75)	4 (57.14)	0.666
Diabetes mellitus	13 (33.33)	12 (37.50)	1 (14.29)	0.388
Coronary artery disease	4 (10.26)	4 (12.50)	0 (0.00)	1.000
Dyslipidemia	27 (69.23)	21 (65.63)	6 (85.71)	0.403
Glucose (mmol/L)	5.62 (5.02–6.67)	5.78 (5.09–6.84)	5.02 (5.00–5.63)	0.143
NIHSS at admission	0 (0–1)	0 (0–1)	0 (0–1)	0.578
Symptom				
Headache/dizziness	19 (48.72)	17 (53.13)	2 (28.57)	
Limb weakness	17 (43.59)	12 (37.50)	5 (71.43)	
Limb numbness	10 (25.64)	9 (28.13)	1 (14.29)	
Aphasia	10 (25.64)	8 (25.00)	2 (28.57)	
Ataxia	1 (2.56)	1 (3.13)	0 (0.00)	
Blurred vision	4 (10.26)	4 (12.50)	0 (0.00)	
ICAS lesion				0.413
ICA	2 (5.13)	1 (3.13)	1 (14.29)	
MCA	20 (51.28)	16 (50.00)	4 (57.14)	
BA	11 (28.21)	9 (28.13)	2 (28.57)	
VA	6 (15.38)	6 (18.75)	0 (0)	

BA: basilar artery; ICA: internal carotid artery; ICAS: intracranial atherosclerotic stenosis; ISR: in-stent restenosis; MCA: middle cerebral artery; NIHSS: National Institutes of Health Stroke Scale; VA: vertebral artery.

TABLE 2: Hemodynamic changes after PTAS.

Variables	Pre-PTAS	Post-PTAS	P
PR	0.07 (0.00 to 0.31)	0.62 (0.41 to 0.82)	0.000
Pressures$_{stenotic-apex}$(Pa)	$-1.84 * 10^4$ ($-2.75 * 10^5$ to $-7.21 * 10^3$)	$1.47 * 10^3$ (-3.14 to $4.19 * 10^3$)	0.000
SSR$_{stenotic-apex}$ (s^{-1})	$9.84 * 10^3$ ($3.32 * 10^3$ to $2.30 * 10^4$)	$2.49 * 10^3$ ($1.47 * 10^3$ to $4.55 * 10^3$)	0.000
WSS$_{stenotic-apex}$ (Pa)	$2.93 * 10^2$ ($1.61 * 10^2$ to $8.74 * 10^2$)	$6.91 * 10^1$ ($3.51 * 10^1$ to $1.11 * 10^2$)	0.000
WSSR	13.93 (8.37 to 40.30)	2.90 (1.69 to 4.48)	0.000

PR: pressure ratio (PR = pressure$_{poststenotic}$/pressure$_{prestenotic}$); PTAS: percutaneous transluminal angioplasty and stenting; SSR: shear strain rate; WSS: wall shear stress; WSSR: wall shear strain ratio. (WSSR = WSS$_{stenotic–apex}$/WSS$_{prestenotic}$). Italic characters indicate $P < 0.05$.

TABLE 3: Vessel remodeling caused by PTAS.

	Tortuosity	Angulation (°)
Pre-PTAS	0.09 (0.06–0.13)	51.11 (40.07–67.27)
Post-PTAS	0.01 (0.00–0.03)	15.97 (0.00–36.16)
Follow-up	0.01 (0.00–0.03)	21.46 (0.00–31.34)
P_1 value	0.000	0.000
P_2 value	0.000	0.000
P_3 value	0.112	0.575

PTAS: percutaneous transluminal angioplasty and stenting; P_1: P value of comparison between pre-PTAS and post-PTAS; P_2: P value of comparison between pre-PTAS and angiographic follow-up; P_3: P value of comparison between post-PTAS and angiographic follow-up. Italic characters indicate $P < 0.05$.

($P = 0.053$), lower post-PTAS PR ($P = 0.025$), and smaller Δ tortuosity ($P = 0.018$), as well as smaller Δ angulation ($P = 0.027$), were closely related with ISR and should be consequently taken into account in the multivariate logistic regression. However, because post-PTAS tortuosity and Δ tortuosity were intrinsically related, which also applied to post-PTAS angulation and Δ angulation, and there was a negative linear correlation between vessel tortuosity and PR after PTAS, we included only Δ tortuosity, Δ angulation, and post-PTAS PR in the multivariate logistic regression. It turned out that smaller Δ tortuosity (odds ratio, 0.00; 95% confidence interval, 0.00–0.02; $P = 0.038$) was an independent risk factor of ISR in our multivariate model, and post-PTAS translesional PR was also a predictive factor of marginal significance (odds ratio, 0.00; 95% confidence interval, 0.00–1.34; $P = 0.059$) (Table 6).

(a)

(b)
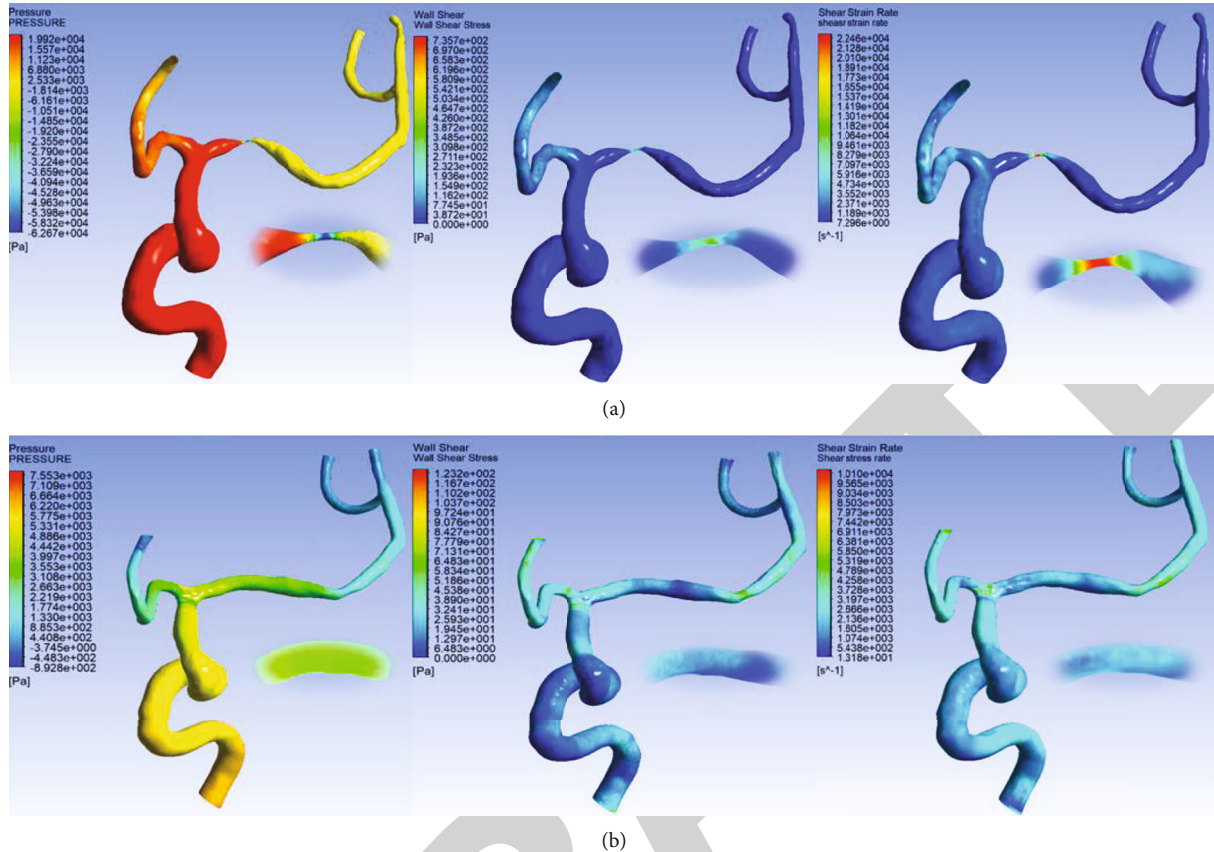
FIGURE 5: CFD models showing distribution of pressure, WSS, and SSR across a 90% stenotic lesion over the left MCA-M1 before and after PTAS. (a) Shows a significant decrease of pressure distal to the lesion and a significant elevated WSS and SSR adjacent to the stenotic throat before PTAS. (b) Displays increased pressure and decreased WSS and SSR adjacent to the stenotic throat after PTAS. CFD: computational fluid dynamics; WSS: wall shear stress; SSR: shear strain rate; MCA: middle cerebral artery; PTAS: percutaneous transluminal angioplasty and stenting.

4. Discussion

The current study was among the first studies using CFD to investigate the roles of hemodynamics and vessel geometry in governing ISR risk in severe ICAS patients after PTAS. Establishing simplified CFD models with generic blood properties and individualized boundary conditions extracted from transcranial Doppler, this article found that local hemodynamic and geometric features of ICAS lesions were significantly influenced by PTAS and played an important role in the occurrence of ISR.

It had been previously shown that vessel morphology and local hemodynamics were closely related and played an important role in the initiation and development of various cerebrovascular diseases. In addition to systemic risk factors, atherosclerosis was a chronic and systemic inflammatory disease with the interactions of hemodynamic, geometrical, and biological factors [27, 28]. Stent implantation induced vessel straightening, significantly decreased vessel curvature, remodeled the vessel, and changed hemodynamic patterns [10, 29]. In coronary and carotid atherosclerosis, stenting showed its ability to change the vessel geometry and the local hemodynamics [23, 24, 30]. In intracranial arteries, previous studies have described the effect of stent-

induced straightening of vessels [31] and vascular angel remodeling [32–34] during stent-assisted coiling of intracranial aneurysms. With five PTAS cases, Schirmer and Malek described the WSS dynamic fluctuations in ICAS using CFD, showing the complex dynamic directional and amplitude oscillations across the lesion, which could be normalized by stenting [9]. The geometric and hemodynamic changing ability of stents was also proved by the current study in ICAS patients. PTAS resulted in significant decrease of vessel tortuosity (0.09 vs. 0.01, $P = 0.000$) and vessel angulation (51.11° vs. 15.97°, $P = 0.000$), elevation of PR (0.07 vs. 0.62, $P = 0.000$) and reduction of WSSR (13.93 vs. 2.90, $P = 0.000$) through stenotic lesions. In stent coiling patients, with the passage of time, these stents showed persistent self-straightening tendency and continually exerted on the cerebral vasculature, leading to longer-term delayed angular and vascular remodeling [32]. In the current study of ICAS patients, during the follow-up period, the remodeling of vessel geometry persisted because of the continuous outwardly directed radial force of stents, but the geometrical parameters did not show much difference compared with immediate poststenting vessel angulation ($P = 0.112$) and tortuosity ($P = 0.575$). In PTAS, the balloon inflation also attributed a lot to the vascular remodeling, which was absent
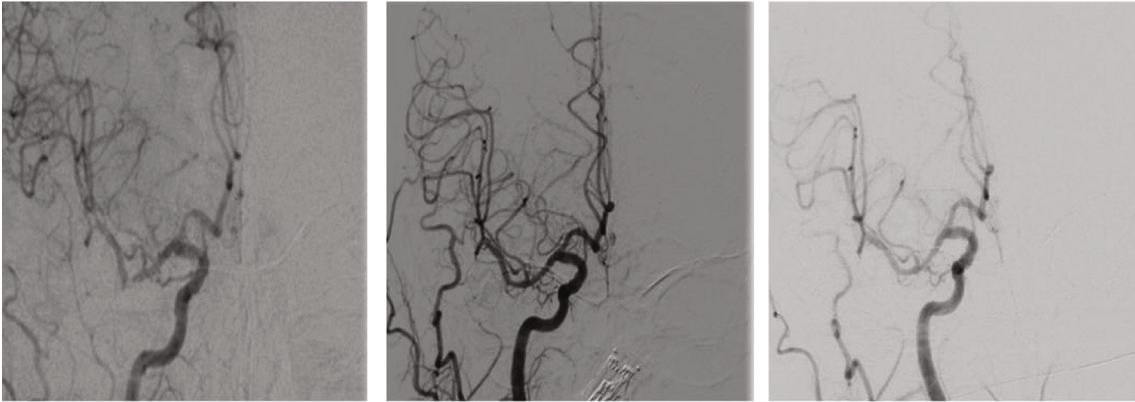
(a)
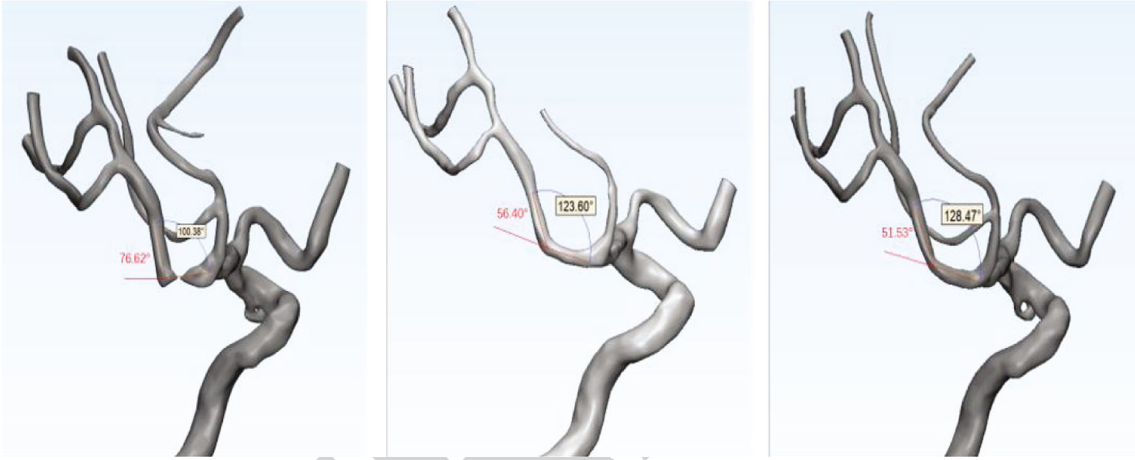
(b)
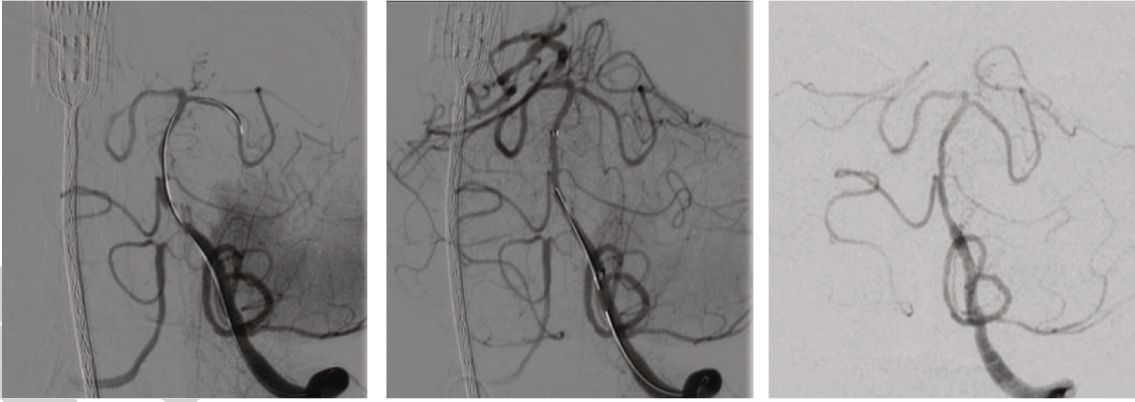
(c)

Figure 6: Continued.

(d)
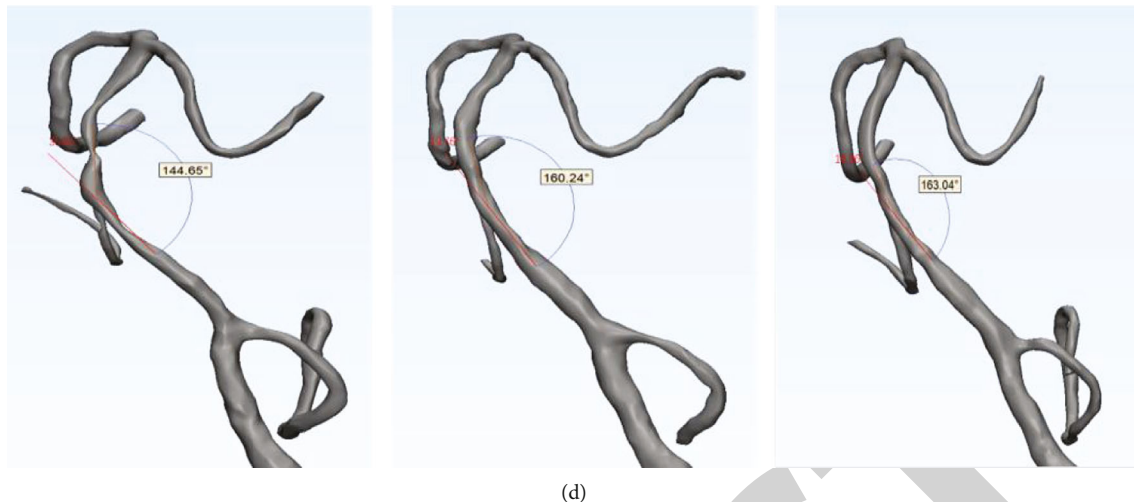
Figure 6: (a, b) Show a 68-year-old man diagnosed with a severe right MCA-M1 stenosis, with pretreatment vessel angulation of 76.62°. After PTAS, the vessel angulation was 56.40°. 4 months later, vessel angulation was 51.53°. (c, d) Show a 62-year-old man having a severe basilar stenosis, with pretreatment vessel angulation of 35.65°. Following PTAS, vessel angulation changed to 19.76°. At 6.5-month follow-up, vessel angulation was 16.96°.

in stent coiling, indicating that the most striking geometry change might occur during the intervention process for ICAS patients instead of during the early follow-up for intracranial aneurysm patients [32].

In-stent restenosis could be caused by four key processes following stenting: thrombus formation, arterial inflammation, neointimal hyperplasia (NIH), and remodeling. NIH was the predominant attributor [21]. The balloon inflation and stent deployment inevitably resulted in endothelial disruption and the subsequent proliferation and activation of regional smooth muscle cells, thus causing NIH and ISR [35, 36]. The degree of NIH was linked directly to the severity of endothelial injury induced by the angioplasty balloon and intravascular stent. In coronary atherosclerotic lesions, quantitative angiographic analysis revealed a triphasic luminal response characterized by early restenosis (until 6 months), intermediate regression (6 months to 3 years), and late renarrowing (beyond 4 years), which could probably be explained by the fibrotic scar formation and reduction in matrix proteoglycans [37]. Similarly, in stenting for intracranial aneurysm treatment, dynamic and spontaneously resolvable ISR has also been reported [36, 38, 39]. However, regression of ISR has not been seen in ICAS yet, which was consistent with the current study. This divergence might be attributed to the difference in the incidence and natural history of ISR between stent-assisted coiling and PTAS [40].

Tortuosity of cerebral artery [26] and arteries in other body districts (e.g., coronary artery [41], carotid artery [42], and peripheral artery [43]) has been found to correlate with the development of atherosclerotic disease or thickening of wall intima. From the hemodynamic point of view, the increased tortuosity might induce disturbances of local hemodynamic environment characterized by low wall shear stress that have been demonstrated to associate with the initiation and progression of atherosclerosis [44–46]. For coronary [23, 47, 48] and carotid stents [11, 21, 24, 42, 49], geometry of the blood vessels, especially tortuosity, had been

suggested to attribute to not only atherogenesis but also in-stent NIH [1]. The current study showed an ISR rate of 17.95% in severe ICAS patients and also revealed the important role of vessel tortuosity. The stented arteries with ISR were much more tortuous (0.06 vs. 0.05, $P = 0.001$), and the reduction of tortuosity caused by stenting (Δ tortuosity) was also much smaller (0.05 vs. 0.08, $P = 0.006$), which turned out to be the independent risk factor for ISR ($P = 0.038$).

Studies focusing on the hemodynamics of ICAS were still scarce because the cerebral artery had a smaller vascular caliber, a more complex and tortuous architecture of the arterial tree, and different histological features from coronary arteries. Translesional PR, calculated as the ratio of the pressures distal and proximal to an ICAS lesion obtained in a CFD model, had been proven to be highly correlated with invasive fractional flow ratio [50], a variable adapted from the coronary circulation and could be used to reflect the hemodynamic significance of ICAS, thus being a promising diagnostic parameter in cerebrovascular disorders [51]. It was an index that took into account of the degree of stenosis, lesion length, eccentricity, and other geometric features of a lesion, reflecting the fractional or residual flow across a stenotic artery, with lower values indicating hemodynamically more significant lesions [52, 53]. Translesional PR played an important role in sustaining cerebral perfusion in patients with symptomatic ICAS [54]. Lower PR at the ICAS lesion significantly increased the risk of recurrent stroke despite optimal medical treatment [55]. The current study also proved the important role of PR in ICAS lesions by revealing the borderline independent predictive value of lower PR for ISR after PTAS.

WSS was the tangential stress of the flowing blood on arterial wall, a major force on the endothelial surface. Physiological WSS modulated the endothelial functions, thus influencing the initiation and progression of atherosclerosis [56, 57]. And it was also related with ISR after coronary

Table 4: Comparison of geometric and hemodynamic parameters between ISR and no ISR lesions.

Variables	Overall $n = 39$	No ISR $n = 32$	ISR $n = 7$	P
Tortuosity				
Pre-PTAS	0.09 (0.06–0.13)	0.10 (0.06–0.13)	0.08 (0.07–0.15)	0.661
Post-PTAS	0.01 (0.00–0.03)	0.05 (0.00–0.01)	0.06 (0.02–0.10)	0.001
Δ tortuosity	0.08 (0.05–0.11)	0.08 (0.06–0.12)	0.05 (0.02–0.06)	0.006
Angulation (°)				
Pre-PTAS	51.11 (40.07–67.27)	53.00 (40.48–66.55)	47.11 (37.81–68.57)	0.826
Post-PTAS	15.97 (0.00–36.16)	13.01 (0.00–32.90)	36.16 (8.57–62.57)	0.096
Δ angulation (°)	31.76 (18.29–41.27)	33.53 (22.85–44.05)	14.08 (6.00–29.24)	0.016
PR				
Pre-PTAS	0.07 (0.00–0.31)	0.08 (0.01–0.27)	0.01 (0.00–0.58)	0.884
Post-PTAS	0.62 (0.41–0.82)	0.67 (0.50–0.89)	0.36 (0.05–0.62)	0.024
Pressure$_{stenotic-apex}$ (Pa)				
Pre-PTAS	$-1.84 * 10^4$ ($-2.75 * 10^5$ to $-7.21 * 10^3$)	$-3.71 * 10^4$ ($-3.95 * 10^5$ to $-7.75 * 10^3$)	$-1.27 * 10^4$ ($-4.27 * 10^4$ to $-5.19 * 10^3$)	0.487
Post-PTAS	$1.47 * 10^3$ (-3.14 to $4.19 * 10^3$)	$2.22 * 10^3$ ($1.72 * 10^1$ to $4.66 * 10^3$)	$6.49 * 10^2$ ($-1.81 * 10^2$ to $2.42 * 10^3$)	0.442
WSS$_{stenotic-apex}$ (Pa)				
Pre-PTAS	$2.93 * 10^2$ ($1.61 * 10^2$ to $8.74 * 10^2$)	$3.28 * 10^2$ ($1.57 * 10^2$ to $9.16 * 10^2$)	$2.28 * 10^2$ ($2.08 * 10^2$ to $3.06 * 10^2$)	0.534
Post-PTAS	$6.91 * 10^1$ ($3.51 * 10^1$ to $1.11 * 10^2$)	$7.02 * 10^1$ ($3.32 * 10^1$ to $1.11 * 10^2$)	$5.53 * 10^1$ ($4.31 * 10^1$ to $1.97 * 10^2$)	0.798
WSSR				
Pre-PTAS	13.93 (8.37 to 40.30)	13.70 (7.90 to 39.77)	19.97 (10.41 to 48.39)	0.634
Post-PTAS	2.90 (1.69 to 4.48)	2.64 (1.58 to 4.41)	3.60 (2.34 to 5.68)	0.188
SSR$_{stenotic-apex}$ (s^{-1})				
Pre-PTAS	$9.84 * 10^3$ ($3.32 * 10^3$ to $2.30 * 10^4$)	$1.06 * 10^4$ ($2.97 * 10^3$ to $2.32 * 10^4$)	$7.91 * 10^3$ ($4.77 * 10^3$ to $1.17 * 10^4$)	0.742
Post-PTAS	$2.49 * 10^3$ ($1.47 * 10^3$ to $4.55 * 10^3$)	$2.52 * 10^3$ ($1.55 * 10^3$ to $4.05 * 10^3$)	$2.28 * 10^3$ ($1.30 * 10^3$ to $8.11 * 10^3$)	0.971

Δ angulation: pre $-$ PTAS angulation $-$ post $-$ PTAS angulation; ISR: in-stent restenosis; PR: pressure ratio (PR = pressure$_{poststenotic}$/pressure$_{prestenotic}$); PTAS: percutaneous transluminal angioplasty and stenting; WSS: wall shear stress; WSSR: wall shear stress ratio (WSSR = WSS$_{stenotic-apex}$/WSS$_{prestenotic}$); Δ tortuosity: pre $-$ PTAS tortuosity $-$ post $-$ PTAS tortuosity. Italic characters indicate $P < 0.05$.

TABLE 5: Linear correlation between indices of vessel geometry and hemodynamics of ICAS.

Variable 1	Variable 2	P	r
Pre-PTAS PR	Pre-PTAS WSSR	*0.000*	−0.672
Post-PTAS PR	Post-PTAS WSSR	*0.000*	−0.566
Post-PTAS tortuosity	Post-PTAS PR	*0.000*	−0.673
Post-PTAS tortuosity	Post-PTAS WSSR	*0.000*	0.547

ISR: in-stent restenosis; PR: pressure ratio (PR = pressure$_{poststenotic}$/pressure$_{prestenotic}$); PTAS: percutaneous transluminal angioplasty and stenting; WSS: wall shear stress; WSSR: wall shear stress ratio (WSSR = WSS$_{stenotic-apex}$/WSS$_{prestenotic}$). Italic characters indicate $P < 0.05$.
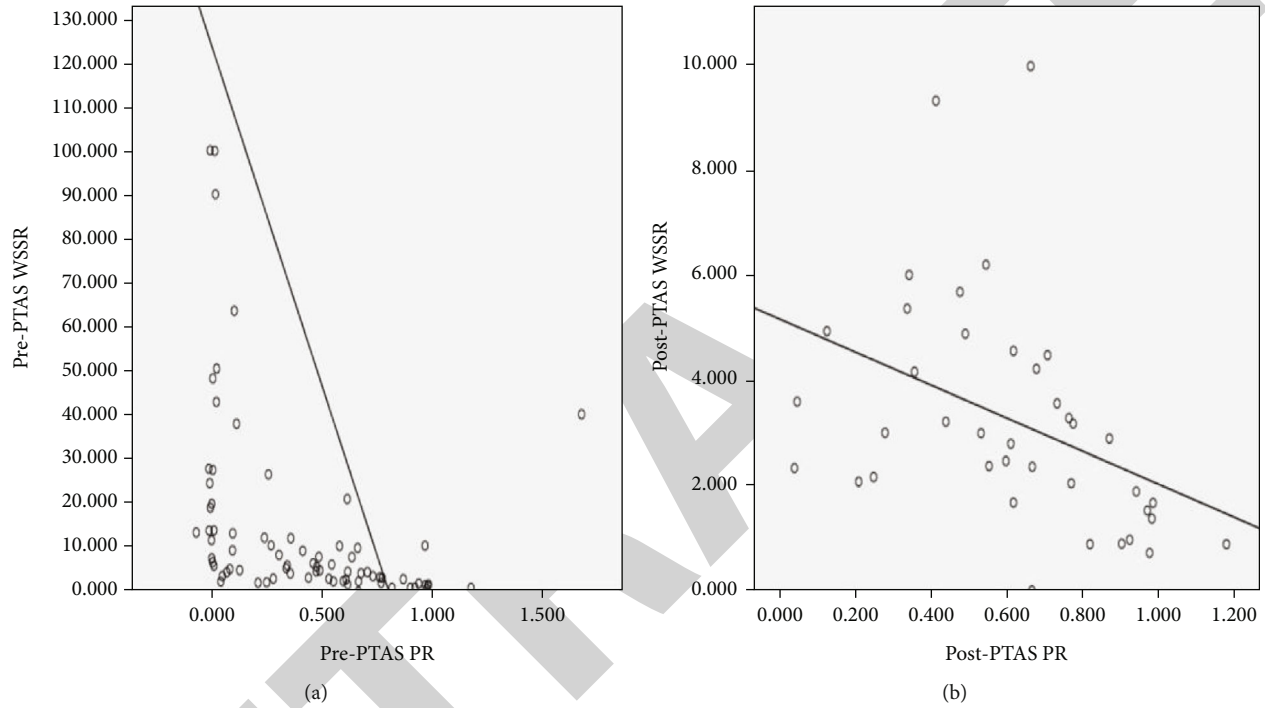
FIGURE 7: The scatterplots of correlations between hemodynamic indices. (a) Shows the correlation between WSS$_{stenotic-apex}$ and PG before and after PTAS. (b) Shows the correlation between translesional PR and WSSR before and post PTAS. WSS: wall shear stress; PR: pressure ratio; WSSR: wall shear stress ratio; PTAS: percutaneous transluminal angioplasty and stenting.

stenting [23, 47] and carotid stenting [24, 49]. For intracranial arteries, elevated focal WSS at ICAS lesions significantly increased the risk of recurrent stroke despite optimal medical treatment [55]. In the current study, both WSS and WSSR significantly decreased after PTAS but showed no relationship with ISR. However, there was a strong linear correlation between PG and WSS as well as PR and WSSR both before (r_s =0.750, r_s = −0.672) and after stenting (r_s =0.548, r_s = −0.566), which was also demonstrated by previous studies in ICAS [58] and coronary artery [30]. And because of the positive linear correlation between WSSR and vessel tortuosity after stenting, which was proven to be the independent predictor for ISR in ICAS, it was reasonable to deduce that WSS or WSSR could have some influence on ISR in ICAS, which might be proven by future studies with larger sample and more advanced CFD models.

The current study had several limitations. First, because of the retrospective nature, there was some bias that could be avoided, such as the patients' selection and the quantification of geometric and hemodynamic parameters. Second, the sample size was relatively small, which might lower the accuracy of the statistical analyses. Because of the controversial conclusions on the outcome of PTAS, the population of ICAS patients receiving PTAS was still not large, which could explain the small sample size of our study to some degree. Furthermore, only simplified CFD models with the diseased artery and adjacent arteries were reconstructed, and although individualized inlet velocity was adopted, uniform outlet conditions and blood properties were still used. Adopting patient-specific boundary conditions such as the proximal and distal pressure measured by the pressure wire and blood properties in CFD simulation might increase the accuracy of quantification of hemodynamic metrics. In order to offset the confounders, relative rather than absolute values in the current study were adopted for analysis. In future studies, more advanced CFD models might provide more information about the general and local hemodynamics of intracranial arteries. Moreover, morphological features or

(a)

(b)
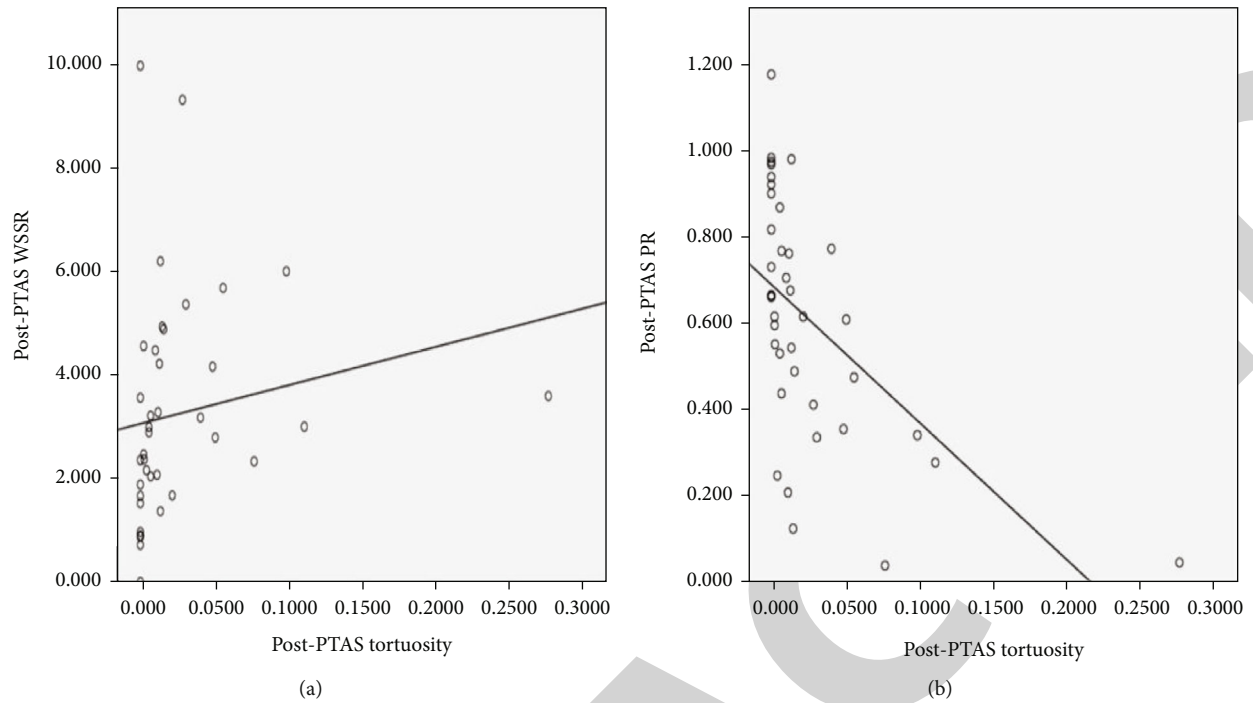
Figure 8: The scatterplots of correlations between geometric and hemodynamic metrics. (a) Shows the correlation between vessel tortuosity and WSSR after PTAS. (b) Shows the correlation between vessel tortuosity and translational PR after PTAS. WSSR: wall shear stress ratio; PR: pressure ratio; PTAS: percutaneous transluminal angioplasty and stenting.

Table 6: Univariate and multivariate logistic regression analyses for associations between geometric and hemodynamic metrics of ICAS and ISR after PTAS.

Variables	No-ISR ($n = 32$)	ISR ($n = 7$)	Unadjusted P	Adjusted Odds ratio (95% confidence interval)	P
Male	16 (50.00)	6 (85.71)	0.115		
Age (y)	57.50 (50.50–64.50)	59.00 (49.00–65.00)	0.984		
Hypertension	22 (68.75)	4 (57.14)	0.557		
Diabetes mellitus	12 (37.50)	1 (14.29)	0.261		
Coronary artery disease	4 (12.50)	0 (0.00)	0.999		
Dyslipidemia	21 (65.63)	6 (85.71)	0.316		
Glucose (mmol/L)	5.78 (5.09–6.84)	5.02 (5.00–5.63)	0.186		
Smoker	12 (37.50)	3 (42.86)	0.792		
Post-PTAS tortuosity	0.05 (0.00–0.01)	0.06 (0.02–0.10)	*0.012*		
Δ tortuosity	0.08 (0.06–0.12)	0.05 (0.02–0.06)	*0.018*	0.00 (0.00–0.02)	**0.038**
Post-PTAS angulation (°)	13.01 (0.00–32.90)	36.16 (8.57–62.57)	*0.053*		
Δ angulation (°)	33.53 (22.85–44.05)	14.08 (6.00–29.24)	*0.027*	1.02 (0.89–1.16)	0.772
Post-PTAS PR	0.67 (0.50–0.89)	0.36 (0.05–0.62)	*0.025*	0.00 (0.00–1.34)	0.059
Post-PTAS pressure (Pa)	$2.22 * 10^3$ ($1.72 * 10^1$ to $4.66 * 10^3$)	$6.49 * 10^2$ ($-1.81 * 10^2$ to $2.42 * 10^3$)	0.756		
Post-PTAS SSR (s⁻¹)	$2.52 * 10^3$ ($1.55 * 10^3$ to $4.05 * 10^3$)	$2.28 * 10^3$ ($1.30 * 10^3$ to $8.11 * 10^3$)	0.843		
Post-PTAS WSS (Pa)	$7.02 * 10^1$ ($3.32 * 10^1$ to $1.11 * 10^2$)	$5.53 * 10^1$ ($4.31 * 10^1$ to $1.97 * 10^2$)	0.720		
Post-PTAS WSSR	2.64 (1.58 to 4.41)	3.60 (2.34 to 5.68)	0.441		

Δ angulation: pre − PTAS angulation − post − PTAS angulation; ISR: in-stent restenosis; PR: pressure ratio (PR = pressure$_{poststenotic}$/pressure$_{prestenotic}$); PTAS: percutaneous transluminal angioplasty and stenting; WSS: wall shear stress; WSSR: wall shear stress ratio (WSSR = WSS$_{stenotic-apex}$/WSS$_{prestenotic}$); Δ tortuosity = pre − PTAS tortuosity − post − PTAS tortuosity. Italic characters indicate unadjusted $P < 0.1$. Bold characters indicate adjusted $P < 0.05$.

components of the plaques were not included in this study. Combination of CFD techniques and high-resolution magnetic resonance imaging was needed for further analysis.

5. Conclusion

The current study was among the first attempts to use CFD-based cerebral blood flow simulation methods to describe the geometric and hemodynamic changes caused by stent implantation, explore the possible relationships between vessel geometry and local hemodynamics in ICAS, and investigate the role of vessel geometry and hemodynamics played on ISR after PTAS. It turned out that stenting resulted in predominant change of vessel geometry and consequently influenced the local hemodynamics significantly. After PTAS, both translesional PR and WSSR were linearly correlated with vessel tortuosity, indicating interactions between vessel geometry and hemodynamics in ICAS. Δ Tortuosity turned out to be an independent risk factor for ISR, and ICAS lesions with lower translesional PR after PTAS demonstrated a somewhat higher rate of ISR, suggesting the predominant roles of vessel geometry and hemodynamics played in ISR. Further studies with larger sample size, more accurate CFD modeling and blood flow simulation, and multimodel neuroimaging evaluations would be needed.

Data Availability

The datasets generated during the current study are available from the corresponding author on reasonable request.

Conflicts of Interest

The authors declare that there is no conflict of interest regarding the publication of this article.

Supplementary Materials

Supplemental material: STROBE Statement—checklist of items that should be included in reports of observational studies. (Supplementary Materials)

References

[1] C. Zhang, S. Xie, S. Li et al., "Flow patterns and wall shear stress distribution in human internal carotid arteries: the geometric effect on the risk for stenoses," *Journal of Biomechanics*, vol. 45, no. 1, pp. 83–89, 2012.

[2] K. T. Nguyen, C. D. Clark, T. J. Chancellor, and D. V. Papavassiliou, "Carotid geometry effects on blood flow and on risk for vascular disease," *Journal of Biomechanics*, vol. 41, no. 1, pp. 11–19, 2008.

[3] C. A. Holmstedt, T. N. Turan, and M. I. Chimowitz, "Atherosclerotic intracranial arterial stenosis: risk factors, diagnosis, and treatment," *The Lancet Neurology*, vol. 12, no. 11, pp. 1106–1114, 2013.

[4] C. P. Derdeyn, M. I. Chimowitz, M. J. Lynn et al., "Aggressive medical treatment with or without stenting in high-risk patients with intracranial artery stenosis (SAMMPRIS): the final results of a randomised trial," *The Lancet*, vol. 383, no. 9914, pp. 333–341, 2014.

[5] S. E. Kasner, M. I. Chimowitz, M. J. Lynn et al., "Predictors of ischemic stroke in the territory of a symptomatic intracranial arterial stenosis," *Circulation*, vol. 113, no. 4, pp. 555–563, 2006.

[6] L. Liu, K. S. Wong, X. Leng et al., "Dual antiplatelet therapy in stroke and ICAS: subgroup analysis of CHANCE," *Neurology*, vol. 85, no. 13, pp. 1154–1162, 2015.

[7] M. J. Alexander, A. Zauner, J. C. Chaloupka et al., "WEAVE trial," *Stroke*, vol. 50, no. 4, pp. 889–894, 2019.

[8] C. M. Schirmer and A. M. Malek, "Prediction of complex flow patterns in intracranial atherosclerotic disease using computational fluid dynamics," *Neurosurgery*, vol. 61, no. 4, pp. 842–852, 2007.

[9] C. M. Schirmer and A. M. Malek, "Estimation of wall shear stress dynamic fluctuations in intracranial atherosclerotic lesions using computational fluid dynamics," *Neurosurgery*, vol. 63, no. 2, pp. 326–335, 2008.

[10] D. C. Suh, Y. B. Ko, S. T. Park et al., "Computational flow dynamics of the severe m1 stenosis before and after stenting," *Neurointervention*, vol. 6, no. 1, pp. 13–16, 2011.

[11] K. Zhang, T. X. Li, Z. L. Wang et al., "Factors affecting in-stent restenosis after angioplasty with the Enterprise stent for intracranial atherosclerotic diseases," *Scientific Reports*, vol. 11, no. 1, p. 10479, 2021.

[12] Z. Feng, G. Duan, P. Zhang et al., "Enterprise stent for the treatment of symptomatic intracranial atherosclerotic stenosis: an initial experience of 44 patients," *BMC Neurology*, vol. 15, no. 1, p. 187, 2015.

[13] Z. Vajda, E. Schmid, T. Güthe et al., "The modified Bose method for the endovascular treatment of intracranial atherosclerotic arterial stenoses using the Enterprise stent," *Neurosurgery*, vol. 70, no. 1, pp. 91–101, 2012.

[14] K. Groschel, S. Schnaudigel, S. M. Pilgram, K. Wasser, and A. Kastrup, "A systematic review on outcome after stenting for intracranial atherosclerosis," *Stroke*, vol. 40, no. 5, pp. e340–e347, 2009.

[15] W. J. Jiang, E. Cheng-Ching, A. Abou-Chebl et al., "Multicenter analysis of stenting in symptomatic intracranial atherosclerosis," *Neurosurgery*, vol. 70, no. 1, pp. 25–31, 2012, discussion 31.

[16] X. Guo, N. Ma, F. Gao, D. P. Mo, G. Luo, and Z. R. Miao, "Long-term risk factors for intracranial in-stent restenosis from a multicenter trial of stenting for symptomatic intracranial artery stenosis registry in China," *Frontiers in Neurology*, vol. 11, article 601199, 2021.

[17] N. Ma, Y. Zhang, J. Shuai et al., "Stenting for symptomatic intracranial arterial stenosis in China: 1-year outcome of a multicentre registry study," *Stroke and Vascular Neurology*, vol. 3, no. 3, pp. 176–184, 2018.

[18] B. Sun, C. Xu, P. Wu et al., "Intracranial angioplasty with Enterprise stent for intracranial atherosclerotic stenosis: a single-center experience and a systematic review," *BioMed Research International*, vol. 2021, Article ID 6645500, 12 pages, 2021.

[19] A. S. Turk, E. I. Levy, F. C. Albuquerque et al., "Influence of patient age and stenosis location on wingspan in-stent restenosis," *AJNR. American Journal of Neuroradiology*, vol. 29, no. 1, pp. 23–27, 2008.

[20] M. Haidegger, M. Kneihsl, K. Niederkorn et al., "Blood biomarkers of progressive atherosclerosis and restenosis after stenting of symptomatic intracranial artery stenosis," *Scientific Reports*, vol. 11, no. 1, p. 15599, 2021.

[21] J. Murphy and F. Boyle, "Predicting neointimal hyperplasia in stented arteries using time-dependant computational fluid dynamics: a review," *Computers in Biology and Medicine*, vol. 40, no. 4, pp. 408–418, 2010.

[22] D. Birchall, A. Zaman, J. Hacker, G. Davies, and D. Mendelow, "Analysis of haemodynamic disturbance in the atherosclerotic carotid artery using computational fluid dynamics," *European Radiology*, vol. 16, no. 5, pp. 1074–1083, 2006.

[23] J. F. LaDisa Jr., L. E. Olson, H. A. Douglas, D. C. Warltier, J. R. Kersten, and P. S. Pagel, "Alterations in regional vascular geometry produced by theoretical stent implantation influence distributions of wall shear stress: analysis of a curved coronary artery using 3D computational fluid dynamics modeling," *Biomedical Engineering Online*, vol. 5, no. 1, p. 40, 2006.

[24] X. Yao, Z. Dai, X. Zhang et al., "Carotid geometry as a predictor of in-stent neointimal hyperplasia- a computational fluid dynamics study," *Circulation Journal*, vol. 83, no. 7, pp. 1472–1479, 2019.

[25] J. B. Thomas, L. Antiga, S. L. Che et al., "Variation in the carotid bifurcation geometry of young versus older adults: implications for geometric risk of atherosclerosis," *Stroke*, vol. 36, no. 11, pp. 2450–2456, 2005.

[26] B. J. Kim, S. M. Kim, D. W. Kang, S. U. Kwon, D. C. Suh, and J. S. Kim, "Vascular tortuosity may be related to intracranial artery atherosclerosis," *International Journal of Stroke*, vol. 10, no. 7, pp. 1081–1086, 2015.

[27] C. Oviedo, A. Maehara, G. S. Mintz et al., "Intravascular ultrasound classification of plaque distribution in left main coronary artery bifurcations: where is the plaque really located?," *Circulation: Cardiovascular Interventions*, vol. 3, no. 2, pp. 105–112, 2010.

[28] P. Eshtehardi, M. C. McDaniel, J. Suo et al., "Association of coronary wall shear stress with atherosclerotic plaque burden, composition, and distribution in patients with coronary artery disease," *Journal of the American Heart Association*, vol. 1, no. 4, article e002543, 2012.

[29] R. M. King, J. Y. Chueh, I. M. van der Bom et al., "The effect of intracranial stent implantation on the curvature of the cerebrovasculature," *AJNR. American Journal of Neuroradiology*, vol. 33, no. 9, pp. 1657–1662, 2012.

[30] K. E. Lee, G. T. Kim, J. S. Lee, J. H. Chung, E. S. Shin, and E. B. Shim, "A patient-specific virtual stenotic model of the coronary artery to analyze the relationship between fractional flow reserve and wall shear stress," *International Journal of Cardiology*, vol. 222, pp. 799–805, 2016.

[31] M. A. Zenteno, J. A. Santos-Franco, J. M. Freitas-Modenesi et al., "Use of the sole stenting technique for the management of aneurysms in the posterior circulation in a prospective series of 20 patients," *Journal of Neurosurgery*, vol. 108, no. 6, pp. 1104–1118, 2008.

[32] B. Gao, M. I. Baharoglu, A. D. Cohen, and A. M. Malek, "Stent-assisted coiling of intracranial bifurcation aneurysms leads to immediate and delayed intracranial vascular angle remodeling," *AJNR. American Journal of Neuroradiology*, vol. 33, no. 4, pp. 649–654, 2012.

[33] A. M. Malek, A. D. Cohen, M. I. Baharoglu, and B. Gao, "Y-stent coiling of basilar bifurcation aneurysms induces a dynamic angular vascular remodeling with alteration of the apical wall shear stress pattern," *Neurosurgery*, vol. 72, no. 4, pp. 617–629, 2013.

[34] B. Gao and A. M. Malek, "Possible mechanisms for delayed migration of the closed cell–designed enterprise stent when used in the adjunctive treatment of a basilar artery aneurysm," *AJNR. American Journal of Neuroradiology*, vol. 31, no. 10, pp. E85–E86, 2010.

[35] N. Kipshidze, G. Dangas, M. Tsapenko et al., "Role of the endothelium in modulating neointimal formation: vasculoprotective approaches to attenuate restenosis after percutaneous coronary interventions," *Journal of the American College of Cardiology*, vol. 44, no. 4, pp. 733–739, 2004.

[36] D. Fiorella, F. C. Albuquerque, H. Woo, P. A. Rasmussen, T. J. Masaryk, and C. G. McDougall, "Neuroform in-stent stenosis: incidence, natural history, and treatment strategies," *Neurosurgery*, vol. 59, no. 1, pp. 34–42, 2006.

[37] T. Kimura, K. Abe, S. Shizuta et al., "Long-term clinical and angiographic follow-up after coronary stent placement in native coronary arteries," *Circulation*, vol. 105, no. 25, pp. 2986–2991, 2002.

[38] B. Gao, M. G. Safain, and A. M. Malek, "Enterprise stenting for intracranial aneurysm treatment induces dynamic and reversible age-dependent stenosis in cerebral arteries," *Journal of NeuroInterventional Surgery*, vol. 7, no. 4, pp. 297–302, 2015.

[39] N. Chalouhi, R. Drueding, R. M. Starke et al., "In-stent stenosis after stent-assisted coiling: incidence, predictors and clinical outcomes of 435 cases," *Neurosurgery*, vol. 72, no. 3, pp. 390–396, 2013.

[40] S. S. Investigators, "Stenting of symptomatic atherosclerotic lesions in the vertebral or intracranial arteries (SSYLVIA): study results," *Stroke*, vol. 35, no. 6, pp. 1388–1392, 2004.

[41] C. A. Bulant, P. J. Blanco, A. Pereira et al., "On the search of arterial geometry heritability," *International Journal of Cardiology*, vol. 221, pp. 1013–1021, 2016.

[42] S. W. Lee, L. Antiga, J. D. Spence, and D. A. Steinman, "Geometry of the carotid bifurcation predicts its exposure to disturbed flow," *Stroke*, vol. 39, no. 8, pp. 2341–2347, 2008.

[43] X. Li, X. Liu, X. Li, L. Xu, X. Chen, and F. Liang, "Tortuosity of the superficial femoral artery and its influence on blood flow patterns and risk of atherosclerosis," *Biomechanics and Modeling in Mechanobiology*, vol. 18, no. 4, pp. 883–896, 2019.

[44] A. Lauric, J. Hippelheuser, M. G. Safain, and A. M. Malek, "Curvature effect on hemodynamic conditions at the inner bend of the carotid siphon and its relation to aneurysm formation," *Journal of Biomechanics*, vol. 47, no. 12, pp. 3018–3027, 2014.

[45] F. Rikhtegar, J. A. Knight, U. Olgac et al., "Choosing the optimal wall shear parameter for the prediction of plaque location–a patient-specific computational study in human left coronary arteries," *Atherosclerosis*, vol. 221, no. 2, pp. 432–437, 2012.

[46] C. Cheng, D. Tempel, R. van Haperen et al., "Atherosclerotic lesion size and vulnerability are determined by patterns of fluid shear stress," *Circulation*, vol. 113, no. 23, pp. 2744–2753, 2006.

[47] J. J. Wentzel, R. Krams, J. C. Schuurbiers et al., "Relationship between neointimal thickness and shear stress after Wallstent implantation in human coronary arteries," *Circulation*, vol. 103, no. 13, pp. 1740–1745, 2001.

[48] T. Konishi, T. Yamamoto, N. Funayama, H. Nishihara, and D. Hotta, "Relationship between left coronary artery bifurcation angle and restenosis after stenting of the proximal left anterior descending artery," *Coronary Artery Disease*, vol. 27, no. 6, pp. 449–459, 2016.

Retraction

Retracted: Provisional Decision-Making for Perioperative Blood Pressure Management: A Narrative Review

Oxidative Medicine and Cellular Longevity

This article has been retracted by Hindawi following an investigation undertaken by the publisher [1]. This investigation has uncovered evidence of one or more of the following indicators of systematic manipulation of the publication process:

(1) Discrepancies in scope

(2) Discrepancies in the description of the research reported

(3) Discrepancies between the availability of data and the research described

(4) Inappropriate citations

(5) Incoherent, meaningless and/or irrelevant content included in the article

(6) Manipulated or compromised peer review

The presence of these indicators undermines our confidence in the integrity of the article's content and we cannot, therefore, vouch for its reliability. Please note that this notice is intended solely to alert readers that the content of this article is unreliable. We have not investigated whether authors were aware of or involved in the systematic manipulation of the publication process.

Wiley and Hindawi regrets that the usual quality checks did not identify these issues before publication and have since put additional measures in place to safeguard research integrity.

We wish to credit our own Research Integrity and Research Publishing teams and anonymous and named external researchers and research integrity experts for contributing to this investigation.

The corresponding author, as the representative of all authors, has been given the opportunity to register their agreement or disagreement to this retraction. We have kept a record of any response received.

References

[1] Q. Song, J. Li, and Z. Jiang, "Provisional Decision-Making for Perioperative Blood Pressure Management: A Narrative Review," *Oxidative Medicine and Cellular Longevity*, vol. 2022, Article ID 5916040, 17 pages, 2022.

Review Article

Provisional Decision-Making for Perioperative Blood Pressure Management: A Narrative Review

Qiliang Song, Jipeng Li, and Zongming Jiang [ID]

Department of Anesthesiology, Shaoxing People's Hospital (Shaoxing Hospital, Zhejiang University School of Medicine), Shaoxing, 312000 Zhejiang Province, China

Correspondence should be addressed to Zongming Jiang; jiangzhejiang120@163.com

Blood pressure (BP) is a basic determinant for organ blood flow supply. Insufficient blood supply will cause tissue hypoxia, provoke cellular oxidative stress, and to some extent lead to organ injury. Perioperative BP is labile and dynamic, and intraoperative hypotension is common. It is unclear whether there is a causal relationship between intraoperative hypotension and organ injury. However, hypotension surely compromises perfusion and causes harm to some extent. Because the harm threshold remains unknown, various guidelines for intraoperative BP management have been proposed. With the pending definitions from robust randomized trials, it is reasonable to consider observational analyses suggesting that mean arterial pressures below 65 mmHg sustained for more than 15 minutes are associated with myocardial and renal injury. Advances in machine learning and artificial intelligence may facilitate the management of hemodynamics globally, including fluid administration, rather than BP alone. The previous mounting studies concentrated on associations between BP targets and adverse complications, whereas few studies were concerned about how to treat and multiple factors for decision-making. Hence, in this narrative review, we discussed the way of BP measurement and current knowledge about baseline BP extracting for surgical patients, highlighted the decision-making process for BP management with a view to providing pragmatic guidance for BP treatment in the clinical settings, and evaluated the merits of an automated blood control system in predicting hypotension.

1. Introduction

Approximately 300 million surgical operations are conducted globally every year [1, 2], with most of the concerned patients being at risk of perioperative hemodynamic instability. The American College of Cardiology/American Heart Association (ACC/AHA) updated its guidelines for blood pressure (BP) management in patients with chronic hypertension in 2017, and the European Society of Cardiology/European Society of Hypertension updated its guidelines in 2018 [3, 4]. However, these guidelines are not fully applicable to perioperative patients because of the dynamic nature of the patients' physiological status, characterized by increased stress and immune response, inflammation, hypercoagulable state, and pain [5–8]. For long, anesthesiologists have been taught and believed that perioperative BP should be maintained within ±20% of the baseline values in practice; however, this recommendation is not evidence-based. Consequently, BP management varies considerably among clinicians. To provide pragmatic guidance and highlight the importance of optimizing BP perioperatively, this manuscript is a review of recent research on perioperative BP management, especially those on the targets and decision-making process.

2. The Physiology of BP and Organ Perfusion

BP is one of the routinely measured variables in the perioperative period; it is the force that propels blood to the tissues and organs. BP is the interplay between cardiac output or stroke volume and systemic vascular resistance at a given filling pressure, which is affected by various hemodynamic elements [5] such as intravascular volume, myocardial contractility, cardiac compliance, heart rate, and vascular radius (Figure 1). A change in one or more of these elements will not necessarily cause a change in BP. Besides, biological
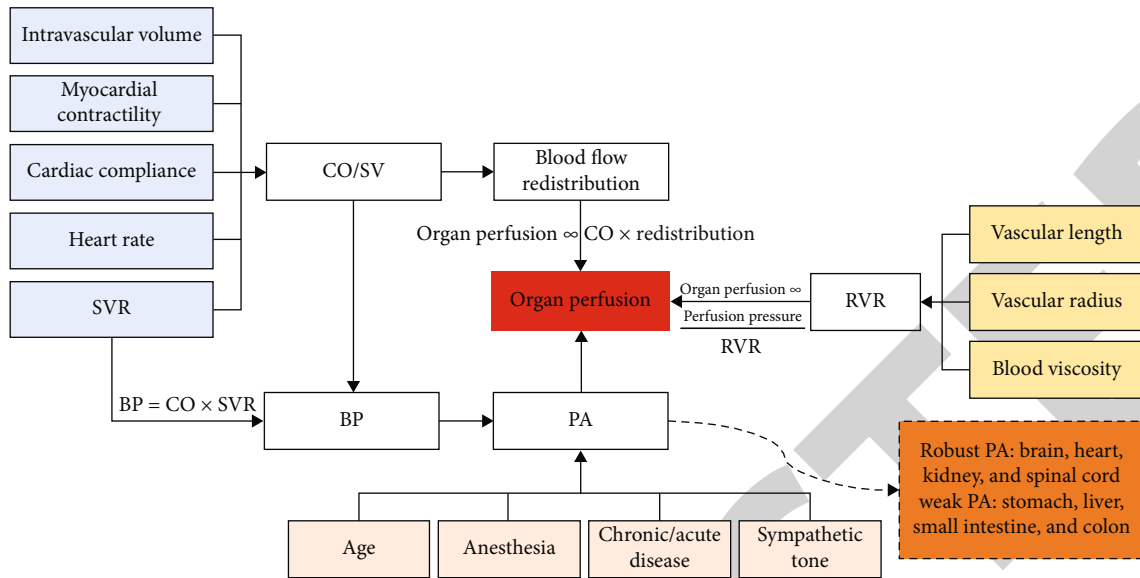
Figure 1: The physiology of BP and miscellaneous factors affecting organ perfusion. BP is determined by production of CO and SVR. PA: blood flow redistribution and organ-specific RVR influence the organ perfusion. BP: blood pressure; CO: cardiac output; SV: stroke volume; SVR: systemic vascular resistance; PA: pressure autoregulation; RVR: regional vascular resistance.

rhythms, hormones, and emotional states can also affect BP [9, 10]. BP is an important determinant for organ blood flow supply. Insufficient blood supply causes tissue hypoxia, provokes cellular oxidative stress, and leads to organ injury and even dysfunction to some extent. The BP levels that trigger cellular oxidative stress or tissue injury vary with organs. Therefore, the underlying pathophysiological mechanisms of hypotension or hypertension may be individualized and have different influences on organ perfusion.

Pressure autoregulation is a self-regulation mechanism of an organ to maintain stable perfusion amidst fluctuations in BP or perfusion pressure [11]. When BP fluctuates violently and exceeds the pressure autoregulation threshold, the organs get into a hypo/hyperperfusable state. Of course, the autoregulation ability varies with organs, a feature known as heterogeneity. Vital organs (the brain, heart, kidneys, and spinal cord) have robust pressure autoregulation mechanisms. In contrast, the visceral organs, such as the stomach, small intestines, and colon, have weaker pressure autoregulation mechanisms, which bear the brunt when BP fluctuates violently [12]. Besides, pressure autoregulation is also influenced by intraindividual heterogeneity factors including age, chronic or acute disease, anesthesia, and sympathetic tone [12]. For example, the lower threshold of cerebral perfusion pressure in healthy participants varies from a mean arterial pressure (MAP) of 53 to 113 mmHg, with a gap of up to 60 mmHg [13].

Organ perfusion is regulated by perfusion pressure and organ-specific resistance. Perfusion pressure is determined by the gradient between the upstream pressure and downstream pressure (Figure 1). MAP decreases progressively from central to peripheral arteries given the relatively low resistance of the arterial system. Hence, MAP is a reference for organ input pressure [5]. Organ perfusion depends on BP via pressure autoregulation and the cardiac output

among organs, since the total perfusion shared by all organs is equal to the cardiac output [14]. Decreased cardiac output results in blood flow redistribution to different organs, with vital organs being prioritized [15]. In a previous study, this kind of blood flow redistribution was examined in cardiac surgery; it was observed that compared to a low MAP (40–50 mmHg), a higher MAP (70–80 mmHg) did not significantly decrease the severity of brain infarcts diagnosed postoperatively [16]. This is explained by the fact that the same laminal pump flow of 2.4 L min^{-1}2009m^{-2}, which provides the same cardiac output, was used for both groups. Even though the BP was much lower in the low MAP group, the perfusion of the brain was well guaranteed. In contrast, the BP was maintained within the normal range in the perioperative period by surgical stress or vasopressor infusion, which may mask insufficient organ perfusion due to decreased cardiac output. Therefore, the goal of perioperative BP management is to optimize adequate blood flow supply, not just to concentrate on the BP values.

3. Perioperative BP Monitoring and Baseline BP

Appropriate BP monitoring is a prerequisite for obtaining accurate BP values and providing reliable guidance for perioperative BP management. The two most used methods for BP monitoring are intermittent oscillometric manometry with a noninvasive cuff and continuous intra-arterial invasive catheterization; however, cuffless BP measurement is an emergent popular field due to the clinical need and technology advances [17, 18]. Intraoperative BP is measured using intermittent oscillometric manometry [19], which allows automatic, intermittent BP measurement, usually at 3–5 min intervals. The measurement accuracy depends on the selection of a suitable cuff

that matches the circumference of the patients' biceps, patients' posture and ambient temperature, etc.

Continuous intra-arterial invasive manometry is performed using intraperipheral arterial cannula placement, which allows for continuous, real-time, and accurate BP measurement. Conventionally, it is believed that the accuracy of BP measured invasively is more than that measured with cuffs, and invasive BP measurements are often regarded as the reference method due to cuff pressure shows large limits of agreement compared to invasive BP [20]. However, there may be differences between noninvasive cuff pressure and invasive arterial pressure in different situations. In a study by Wax et al. [21] involving 24225 patients, the BP of 63% of the patients were measured both noninvasively (cuff BP) and invasively (radial artery BP), while that of 37% was measured only invasively (radial artery BP). They observed that in patients with hypotension, particularly those with an arterial systolic BP below 111 mmHg, the noninvasive cuff BP was higher than the invasive arterial pressure in most cases. However, in the patients with hypertension, the invasive measurements were higher than the noninvasive cuff pressure in most cases, especially the systolic BP values [22]. This is mainly because of the amplification of the pulse pressure difference as the pulse wave propagates from the aorta to the peripheral arteries [23], especially in patients with chronic hypertension. In patients receiving vasopressors, such as patients with sepsis [24], liver transplantation [25], and cardiac surgery under extracorporeal circulation [26], BP measured by invasive manometry is often lower than the central BP. In clinical settings, the noninvasive cuff pressure should be measured simultaneously when there is a significant difference between the two values, especially when the invasive BP is significantly low. Because the noninvasive cuff pressure is closer to the actual BP, it should be the basis for relevant management measures [27]. When encountering this condition, the merits of invasive BP should not be ignored and should be considered supplement for BP treatment.

In addition to accurate BP monitoring, obtaining a reliable and true baseline BP might be critical for BP titration and decision-making. As for the definition of baseline BP, it lacks standard definition and also varies with studies. Several studies [28–31] on the relationship between intraoperative hypotension (IOH) and BP-related complications reported that the BP value obtained before anesthesia induction should be considered the baseline BP; however, this definition is debatable and vague. Saugel et al. [9] selected patients under general anesthesia aged 40–65 years undergoing elective noncardiac surgery as the study population; they compared preoperative 24 h ambulatory BP with preanesthesia induction, postanesthesia induction BP, and intraoperative MAP. They observed that the correlation between the first BP value obtained before anesthesia induction and preoperative ambulatory MAP was poor ($r = 0.429$), which suggested that BP before anesthesia induction cannot be regarded as the baseline BP. To obtain an accurate baseline BP, Ard et al. [32] conducted a prospective and observational trial involving 2087

patients and measured the BP in three locations (surgical visiting clinic, unit for preoperative punctuality, and the first BP at the operating theatre). They observed that the BP obtained in the theatre was markedly higher ($P < 0.01$ for all comparisons), specifically systolic BP (138 ± 23 mmHg), diastolic BP (77 ± 14 mmHg), and MAP (97 ± 14 mmHg), whereas no difference was observed between the first two measurements with 128 ± 17 mmHg and 74 ± 11 mmHg and 124 ± 18 mmHg, 73 ± 11 mmHg, and 92 ± 12 mmHg, respectively. Consequently, they concluded that the BP before anesthesia induction could not be used as the baseline BP, while the BP measured in the preoperative holding area could be used as the baseline BP. Hu et al. had consistent findings with theirs [33]: the BP measured at the holding area before surgery was considered the baseline BP, and there was an association between baseline MAP and acute kidney injury (AKI) in patients after cardiac surgery, implying that this baseline BP could be used as an important predicting factor for AKI. To ascertain whether baseline BP obtained at different time points can optimize intraoperative brain function, Drummond et al. [34] defined the baseline BP as the average of three or more ambulatory clinic BP values 7 months earlier and compared them to the first BP measured in the operating cabinet in a retrospective study. They observed that if the first BP measured in the operating theatre was suggestive of hypertension, the BP was greater than ambulatory clinic recordings 7 months earlier. Furthermore, if the first BP was consistent with normotension, the BP reflected the baseline BP. Based on the previous literatures, a widely accepted protocol to determine awake baseline BP is to take BP measurement 3 to 5 times in the ward or visiting clinic after resting 5 to 10 minutes in a quiet and comfortable site, and the average of all readings can be regarded as baseline BP [35, 36].

Currently, it is hypothesized that the preoperative 24 h ambulatory BP is the best reflection of the daily BP, which can be used as the baseline BP [5]. However, performing 24 h ambulatory BP monitoring preoperatively for each surgical patient to obtain the baseline BP is not practical. Therefore, further research is needed to determine a clinically practical and easy method for determining baseline BP.

4. The Importance of Preoperative BP Optimization

Preoperative hypertension increases the risk of perioperative adverse events. The ACC/AHA guidelines recommend postponing any elective surgery for a patient with a preoperative BP above 180/110 mmHg [3, 4]. However, a previous study [37] revealed that there is no relationship between BP > 180/110 mmHg and perioperative adverse events. Moreover, there is no clear evidence that the delay in performing the surgery will improve perioperative outcomes. This is because for a timely surgery the BP should be titrated to the ideal level within a short preoperative time if it was delayed. Moreover, the rapid control of BP with medications increases the risk of postoperative complications, especially in patients with significantly elevated

preoperative BP [38]. Consequently, Howell et al. [37] reported that surgery should not be delayed because of isolated elevated preoperative BP values only in a healthy patient. Certainly, a goal of ±20% baseline BP during surgery should be kept, and measures should be taken to ensure a stable cardiovascular system intraoperatively. On the other hand, the importance of preoperative BP optimization in patients with hypertension should not be ignored.

Commonly used antihypertensive agents include angiotensin-converting enzyme inhibitors, angiotensin receptor inhibitors, β-blockers, and calcium channel blockers. Studies have observed that angiotensin-converting enzyme inhibitors and angiotensin receptor inhibitors often complicate protracted IOH [39] and may increase the incidence of perioperative AKI, stroke, myocardial injury, and mortality [40]. Therefore, the Canadian Cardiovascular Society, the European Cardiovascular Society, and the European Society of Anesthesiologists recommend the discontinuation of both drugs on the day of surgery [4, 41, 42]. Patients with chronic β-blocker intake, especially those with congestive heart failure or recent myocardial infarction, can continue during the perioperative period [43, 44]. However, β-blockers may be deleterious in the perioperative period, as their intake is characterized by frequent hypotension and end-organ hypoperfusion. The 2008 PeriOperative ISchemic Evaluation (POISE) trial found that although preoperative initiation of β-blockers reduced the risk of nonfatal myocardial infarction, it increased the risk of cardiovascular adverse events (including bradycardia, stroke, and hypotension) and mortality in the perioperative period [45]. This finding was consistent with the results of a large retrospective cohort study, which showed that continuing β-blockers increased the 30-day mortality after surgery in elderly patients with hypertension having elevated systolic BP [46]. While Kertai et al. [47] found that although withdrawal of β-blockers reduced the need of vasopressor and shortened stay in the postanesthesia care unit, it increased risk for mortality within 48 hours after noncardiac surgery. Over the past 30 years, multiple studies have concerned about the best strategy for the perioperative approach to patients receiving β-blockers. Due to the use of β-blockers are not limited perioperatively, whether withholding or continuing and timing is still a debate and needs further study [48].

Preoperative hypotension also increases the risk of postoperative adverse events. Venkatesan et al. [7] found that preoperative systolic BP < 119 mmHg and diastolic BP < 63 mmHg were associated with increased 30-day mortality in elderly patients undergoing elective noncardiac surgery, lower preoperative BP, and higher postoperative mortality. Preoperative hypotension increases the incidence of IOH, decreases coronary perfusion pressure, and shifts the autoregulation curve to the left, which leads to ischemia of vital organs. Preoperative hypertension or hypotension in patients awaiting surgery should be normalized preoperatively, and aggressive BP management is needed to reduce or avoid adverse events.

5. Intraoperative BP Control Target and Its Implications

Hypotension is common during the operative period. However, the definition of IOH remains controversial. Bijker et al. [49] identified 140 definitions of IOH after a review of 130 articles. The most used definition of IOH was as follows: a decrease in the systolic BP of more than 20% from the baseline BP or a MAP < 65 mmHg [50, 51]. The latter, also known as absolute thresholds, is used more frequently for the following reasons: (1) baseline BP measurements are often unknown, and approximately one-third of patients do not have a baseline BP value preoperatively, as described by Monk et al. [28]; (2) relative thresholds are not superior to absolute thresholds in predicting unfavorable outcomes as reported by Salmasi et al. [52] in a large-sample retrospective cohort analysis; (3) absolute thresholds are concrete and easier to use in decision-making; and (4) preoperative BP measurements are often elevated due to tension and anxiety. Therefore, in daily practice, absolute thresholds are adopted frequently as the baseline for BP regulation.

IOH may lead to inadequate blood supply and various degrees of organ dysfunction. Several studies [16, 28, 52–76] found that IOH was associated with postoperative detrimental outcomes (such as AKI, myocardial injury, and neurocognitive disorders), which is related to the duration and magnitude of hypotension [77], suggesting that IOH should be avoided perioperatively (Table 1). Based on existing evidence [51, 56, 58, 74, 75], intraoperative MAP should be maintained above 65 mmHg in normal adult patients, and in patients with other comorbidities (for example, coronary artery disease and carotid stenosis), the intraoperative MAP must be individualized based on the patient's pathophysiology and clinical situation. For example, the MAP of patients with chronic hypertension should be maintained above 70 mmHg. Of note, the advocation of absolute thresholds in BP management does not mean that one-size-fits-all methods should be used. Conversely, it will lead to hypoperfusion. For instance, in chronic hypertension cases, the autoregulatory mechanisms of the kidneys are likely compromised [78], with a right shift of the threshold [79, 80]. Therefore, higher MAP values should be maintained to ensure sufficient blood flow. A combination of absolute thresholds in BP management and individualized BP tailoring should be implemented for patients with comorbidities.

6. Postoperative BP Management

Postoperative BP is a basic component of the perioperative period, and its appropriate management is essential for a smooth postoperative recovery. Postoperative hypotension (POH) management is an important component of postoperative BP management [81].

Considering the controversy in POH, the incidence of POH varies considerably (from 8%–48%) when based on different MAP thresholds of 60–75 mmHg [82]. The secondary analysis from the POISE-2 trial [54] showed that the incidence of POH was 7.6% in the first four postoperative

TABLE 1: Recent studies on the association between IOH and perioperative outcomes.

Author (year)	Study design	Study population	IOH definition	Baseline BP	Target BP	Main findings
Vedel et al. (2018) [16]	Randomized controlled trial	197 patients undergoing cardiac surgery under CPB	/	/	High pressure group: MAP 70–80 mmHg Low pressure group: MAP 40–50 mmHg during CPB	Targeting a higher versus lower MAP during CPB did not seem to affect the volume or number of new cerebral infarcts.
Monk et al. (2015) [28]	Retrospective cohort study	18,576 patients undergoing noncardiac surgery	Systolic BP < 90 mmHg, MAP < 60 mmHg, diastolic BP < 50 mmHg, or ↓>30, 40, 50% from the baseline, respectively	The average of all noninvasive BP measurements before the appearance of end-tidal carbon dioxide	/	IOH, defined as systolic BP <70 mmHg, MAP < 50 mmHg, diastolic BP < 30 mmHg, MAP↓>50% from the baseline for ≥5 min, is associated with high operative morbidity and 30-day mortality.
Salmasi et al. (2017) [52]	Retrospective cohort study	53,315 patients undergoing noncardiac surgery	MAP < 75, 70, 65, 60, 55 mmHg MAP↓>10, 15, 20, 25% from the baseline	The average of all MAP readings in the 6 months before surgery	/	MAP < 65 mmHg for more than 13 min or a cumulative time exceeding 90 min with a MAP less than 20% below the baseline was related to MINS and AKI. Both absolute and relative MAP thresholds had comparable ability to discriminate patients with MINS or AKI.
Hallqvist et al. (2018) [53]	Observational study	23,140 patients undergoing major noncardiac surgery	Systolic BP↓>40 or 50% from the baseline, and lasting more than 5 min	The average of all MAP readings within 2 preoperative months	/	Reduction of systolic BP more than 40% from the baseline was associated with an elevated risk of AKI. Reduction of more than 50% was associated with a more than doubled risk of AKI.
Sessler et al. (2018) [54]	Retrospective cohort study	9765 patients undergoing noncardiac surgery	Systolic BP < 90 mmHg requiring treatment	/	/	IOH and POH were significantly and independently associated with the composite outcomes of myocardial infarction and death within 30 days.
Walsh et al. (2013) [55]	Observational study	33,330 patients undergoing noncardiac surgery	MAP < 55 – 75 mmHg	/	/	MAP < 55 mmHg even for short durations was associated with AKI and MINS. The risk increased with an increasing hypotension duration.
Loffel et al. (2020) [56]		416 patients undergoing	MAP < 65 mmHg	/	/	

Table 1: Continued.

Author (year)	Study design	Study population	IOH definition	Baseline BP	Target BP	Main findings
	Retrospective cohort analysis	noncardiac surgery				MAP < 65 mmHg, especially 60 mmHg, is associated with an increased risk of AKI.
Sun et al. (2015) [57]	Retrospective cohort study	5127 patients undergoing noncardiac surgery	MAP < 65, 60, 55 mmHg	/	/	AKI was associated with MAP < 60 mmHg for 11–20 min and MAP < 55 mmHg for >10 min.
Joosten et al. (2021) [58]	Historical cohort study	242 patients undergoing liver transplantation	MAP < 65 mmHg	/	/	IOH was independently associated with AKI after liver transplant surgery. The longer the MAP stays below 65 mmHg, the higher the risk of AKI, and the greater the severity.
Ahuja et al. (2020) [59]	Retrospective cohort study	23,140 patients undergoing noncardiac surgery	/	/	/	Systolic BP < 90 mmHg, MAP < 65 mmHg, and PP > 35 mmHg were all related to postoperative AKI, and MAP < 65 mmHg was the most sensitive predictor of postoperative MINS and AKI.
Jang et al. (2019) [60]	Retrospective study	248 patients undergoing femoral neck fracture surgery	Systolic BP < 80 mmHg or MAP < 55 – 60 mmHg, persisting for more than 5 min	/	/	IOH was an independent risk factor for AKI (OR = 5.14).
Hallqvist et al. (2016) [61]	Observational cohort study	300 patients undergoing major noncardiac surgery	A 50% decrease in systolic BP relative to the baseline and lasting more than 5 min	The average of all MAP readings for the 2 months before surgery	/	An intraoperative reduction in systolic BP of more than 50% from baseline lasting more than 5 min was independently associated with both myocardial damages on postoperative day 1 and MI within 30 days after surgery.
Hallqvist et al. (2021) [62]	Nested case-control study	652 patients undergoing noncardiac surgery	Systolic BP↓≤20, 21 – 40, 41 – 50, or > 50 mmHg from baseline Systolic BP < 100 mmHg	5 on average, documented within 2 months before surgery, obtained from the surgical ward, preoperative anesthetic consultation, or documen4tations from the primary health care	/	IOH as an independent risk factor of perioperative MI. A reduction of 41–50 mmHg from baseline systolic BP was associated with more than a tripled MI risk.

TABLE 1: Continued.

Author (year)	Study design	Study population	IOH definition	Baseline BP	Target BP	Main findings
Abbott et al. (2018) [63]	Prospective cohort study	15,109 patients undergoing noncardiac surgery				Prolonged HR > 100 bpm in combination with SBP < 100 mmHg was associated with an increased risk of MINS. A combination of the lowest HR >55 bpm and highest systolic BP >160 mmHg was also associated with MINS.
van Waes et al. (2016) [64]	Retrospective cohort study	890 patients undergoing vascular surgery	MAP < 50, <60 mmHg, MAP↓>30%, 40% from the baseline	Preinduction MAP	/	A 40% decrease from the baseline with a cumulative duration of >30 min was associated with postoperative MINS. Postoperative MI and death within 30 days occurred more often when the MAP was <60 mmHg.
Sang et al. (2020) [65]	Retrospective study	2517 patients with prior coronary stents undergoing noncardiac surgery	MAP↓≥50%, 40%, or 30% rom the baseline or MAP < 70, <60, or < 50 mmHg	Preinduction MAP	/	The predefined levels of IOH were not significantly associated with postoperative MINS, but intraoperative continuous inotrope/vasopressor use was significantly higher in patients with MINS.
Hu et al. (2021) [66]	A prospective randomized controlled trial	322 patients undergoing noncardiac surgery	/	/	/	High MAP (90–100 mmHg) was associated with a shorter delirium span and a higher intraoperative urine volume than low MAP (60–70 mmHg).
Mathis et al. (2020) [67]	Retrospective cohort study	138,021 patients undergoing major noncardiac surgery	MAP < 50 mmHg, 50 – 54 mmHg, 55 – 59 mmHg, and 60 – 64 mmHg or MAP↓>40%, 30 – 40%, and 20 – 30% from the baseline	Preinduction MAP, measured in the preoperative holding room on the date of surgery	/	There were no associations between IOH and AKI in patients with a low risk. Patients with a medium risk demonstrated associations between severe IOH (MAP < 50 mmHg) and AKI. Patients with the highest risk and mild IOH (MAP <55–59 mmHg) were associated with AKI.
Stapelfeldt et al. (2017) [68]	Retrospective study	152,445 patients undergoing	/	/	/	The greater the hypotension duration, the greater the 30-day mortality risk.

Table 1: Continued.

Author (year)	Study design	Study population	IOH definition	Baseline BP	Target BP	Main findings
		noncardiac surgery				These exposure time limit sets were shorter in patients with chronic hypertension.
Wu et al. (2017) [69]	Randomized clinical trial	678 patients with chronic hypertension undergoing major gastrointestinal surgery	/	The average of all cuff pressure 2 to 3 days (at least 3 times) before surgery in the ward	Target MAP: Low (65–79 mmHg) Intermediate (80–95 mmHg) High (96–110 mmHg)	Maintaining intraoperative MAP levels to 80–95 mmHg could reduce postoperative AKI after major abdominal surgery.
Gold et al. (1995) [70]	Randomized clinical trial	248 patients undergoing coronary bypass	/	/	High pressure: MAP 80–100 mmHg Low pressure: MAP 50–60 mmHg during CPB	Maintaining a high MAP during CPB could reduce the total mortality rate and the overall incidence of combined cardiac and neurologic complications at 6 months after operation.
Siepe et al. (2011) [71]	Randomized controlled trial	92 patients undergoing coronary bypass	/	/	High pressure: MAP 80–90 mmHg Low pressure: MAP 60–70 mmHg during CPB	Maintaining perfusion pressure at physiologic levels during CPB was associated with less early postoperative cognitive dysfunction and delirium.
Azau et al. (2014) [72]	Randomized controlled trial	300 patients undergoing cardiac surgery under CPB	/	/	High pressure: MAP 75–85 mmHg Control: MAP 50–60 mmHg during CPB	Maintaining a high level of MAP during CPB did not reduce the risk of postoperative AKI or the mortality rate.
Futier et al. (2017) [73]	Randomized clinical trial	298 patients undergoing major noncardiac surgery	/	BP measured at rest in supine position one day before surgery or obtained from the patients' medical records	Individualized treatment: systolic BP within 10% of the baseline BP Standard treatment: systolic BP > 80 mmHg or > 40% baseline	Individualized BP management reduced the incidence of systemic inflammatory response syndrome and renal, cardiovascular, coagulation, and neurological impairment of at least one vital organ system better than routine management.
de la Hoz et al. (2022) [74]	Retrospective cohort study	4984 patients undergoing cardiac surgery	MAP < 65 mmHg MAP < 65 mmHg	/ /	Fraction of overall hypotension >80%, 80–60%, <60%	The total duration of IOH (MAP < 65 mmHg) per 10 min exposure was associated with stroke, AKI, or death in patients undergoing cardiac surgery with CPB.

TABLE 1: Continued.

Author (year)	Study design	Study population	IOH definition	Baseline BP	Target BP	Main findings
Murabito et al. (2017) [75]	Randomized controlled trial	40 patients undergoing major general surgery			MAP < 65 mmHg and hypotension prediction index 50–85	The combined use of the early warning system and hemodynamic algorithm for intraoperative BP management can reduce the incidence of IOH and organ injury.

IOH: intraoperative hypotension; OR: odds ratio; MINS: myocardial injury after noncardiac surgery; AKI: acute kidney injury; MI: myocardial infarction; HR: heart rate; BP: blood pressure; CPB: coronary pulmonary bypass.

days. There are very few studies on the association between postoperative BP and organ insufficiency. Recent studies have shown that POH contributes to the occurrence of myocardial injury [40, 82, 83] and infarction [54]. To the best of our knowledge, the optimal postoperative BP target and BP threshold that leads to organ injury remains unclear [84]. Besides, duration of POH > 10 min is associated with increased risk of postoperative myocardial infarction and 30-day mortality in elderly patients. Furthermore, longer duration and greater magnitude of hypotension (systolic BP < 90 mmHg) significantly increase the risk of myocardial injury [54]. Similarly, Mohammed et al. [85] and Kause et al. [86] also observed that systolic BP < 90 mmHg was associated with postoperative emergency events in the general ward. Based on existing literature [82, 87, 88], POH is an independent surrogate predictor for postoperative myocardial injury, and avoiding POH helps to attenuate myocardial injury.

Whether there are causal interactions between POH and IOH is unclear. To ascertain the severity of IOH on the occurrence of POH and outcomes, a study involving 2833 patients who were transferred to the surgical intensive care unit postoperatively was conducted to investigate whether there is an association between hypotension and cardiovascular incidents or death within seven postoperative days; there was a strong association between POH and IOH severity, especially the lowest intraoperative MAP [89]. Contrarily, a retrospective study conducted in 2008–2017 and involving 67968 patients (with POH and not IOH) undergoing noncardiac surgery was conducted to assess the relationship between major adverse cardiovascular or cerebrovascular events within 30 postoperative days [90]; it was revealed that in the patients without IOH, POH was not associated with major adverse cardiovascular or cerebrovascular events at any MAP threshold (≤75, ≤65, and ≤55 mmHg). Therefore, they suggested that there was no interaction between POH and IOH. Notably, due to the inherent study limitations and the few patients with a MAP below 55 mmHg, the applicability of the conclusion in clinical practice is limited. Further studies are necessary to assess the interactions between POH and IOH.

Timely detection and prompt intervention is essential in POH correction. In the general ward, unlike the conditions in the operating theatre, monitoring of vital signs is usually intermittent with 30 min to 4–6 h intervals. Therefore, POH is often ignored or undetected during the monitoring; approximately 50% of the patients with POH are not identified, and if they are identified, it implies that the POH has been ongoing for a long time [91]. Given this situation, there is a growing interest in continuous monitoring of patients postoperatively in the general ward, which allows earlier detection of POH and thus prompt treatment, improved patient outcomes, and fewer resuscitation events, especially for high-risk patients [92–94]. Besides, stopping antihypertensive medication preoperatively favors postoperative BP management. When and how to initiate antihypertension agents should be weighted based on risks and benefits [41, 42, 84].

7. Individualized Hemodynamic Management in Perioperative Care Is Promising

In the past decades, BP thresholds from popular studies were used as therapeutic targets for perioperative BP management. A BP management strategy using one-size-fits-all principles does not represent an accurate personalized BP threshold for organ perfusion and oxygen supply. The current ACC/AHA guidelines [44] recommend individualized care for noncardiac surgical patients with associated comorbidities.

With the rapid advances in medical science and improved disease knowledge, perioperative individualized BP management is attracting clinical attention [73, 95–97]. Perioperative individualized BP management could be defined as intraoperative BP target values based on each patient's physiological and surgical characteristics, while considering acute and chronic pathophysiological cardiovascular alterations [98].

In 2017, a randomized clinical trial involving 678 elderly patients with hypertension who underwent major gastrointestinal operations were enrolled into three MAP groups (65–79, 80–95, and 96–110 mmHg) receiving intraoperative goal-directed fluid therapy (stroke volume variation: 8%–13%). Also, four vasopressor agents were used to titrate BPs within the target range. This suggested that a MAP level of 80–95 mmHg markedly lowers the possibility of postoperative AKI [69]. Intriguingly, an intermediate MAP is conducive for postoperative renal function recovery, although the authors assigned the patients to three preset MAP groups arbitrarily, suggesting that strict BP control is beneficial for organ functioning in patients with a normal BP range. Similarly, in a multicenter randomized study, 322 elderly patients were assigned to two groups based on intraoperative MAP levels (60–70 or 90–100 mmHg), and the results concluded that a high MAP significantly reduces the occurrence of postoperative delirium [66]. In nonsurgical patients, the BP management strategy affects cognitive function, and a good control for hypertension reduces the risk of cognitive impairment. In this regard, patients with Alzheimer's disease were randomly allocated into standard BP control (systolic BP goal < 120 mmHg) or intensive BP control (systolic BP goal < 140 mmHg) groups; the latter was associated with a mild and significant decrease in cerebral volume [99]. This might be the robust evidence supporting the fact that BP control and intensive BP may influence cerebral volume better than standard care in patients with hypertension.

Individualized BP control considering baseline BP might meet the demands for individuals, and perioperative BP should be tailored in an individual pattern. Futier et al. [73] pioneered individualized BP tailoring in 2017, and in their study, the eligible patients were randomly allocated into individualized BP management groups (systolic BP was controlled within 10% of the baseline value during surgery under the administration of norepinephrine) and conventional BP management group (ephedrine was injected when the systolic BP was less than 80 mmHg or was 40%
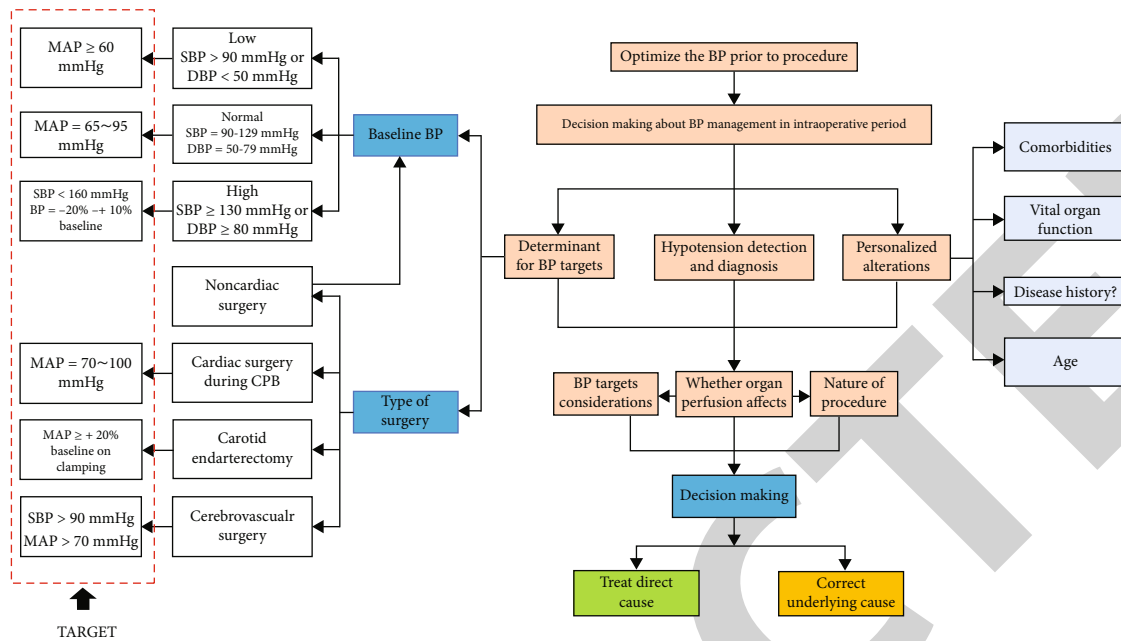
FIGURE 2: The flow chart for decision-making for BP targets and hypotension interventions during surgery. The main determinants for BP targets are baseline BP, type of surgery, and specific pathophysiological alterations and weight between organ ischemia and impending surgical bleeding. The BP targets are initial values and a fixed threshold, and maintaining sufficient oxygen supply is priority to a fixed BP value. Individualized BP management highlights the importance of balancing conflicting risks. BP: blood pressure; SBP: systolic blood pressure; DBP: diastolic blood pressure; MAP: mean arterial pressure; and CPB: cardiopulmonary bypass.

lower than the preoperative values). They observed that individualized BP management reduced the incidence of systemic inflammatory response syndrome; renal, cardiovascular, coagulation, or neurological impairment; or impairment of at least one vital organ system, compared to routine management [73]. However, this study did not evaluate the volume status objectively. Titration of vasoconstrictors to maintain individualized arterial pressure might cover the hypovolemic status, which would reduce end-organ blood flow and result in tissue hypoperfusion.

Lately, individualized hemodynamic management requiring optimizing the volume simultaneously during individualized BP management was introduced into clinical practice [100]. Typically, this entails using a closed-loop autonomous system and incorporating machine learning (a subset of artificial intelligence) to control and predict BP variations during the operative period. In a randomized clinical trial on individualized hemodynamic management published in 2020, 188 high-risk patients undergoing major abdominal surgery were divided into a conventional management group and an individualized management group, which required anesthesiologists to use a proprietary algorithm, based on a noninvasive pulse wave analysis to guided intraoperative fluid infusion and/or dobutamine administration, thus maintaining the intraoperative cardiac index at the baseline values. The results showed that the individualized management group had a lower composite outcome of major postoperative complications or death within 30 days [97]. In 2021, Joosten et al. [101] developed a hybrid system including a computer-assisted closed-loop system for vasopressors and a decision-support system for bolus fluid challenge for intermediate to high-risk surgical patients. They

observed that the prevalence of IOH in the computer-assisted group was 1.2% and 21.5% in the individualized management group. This suggests that individualized hemodynamic optimization decreases the incidence of IOH and may be a potential BP management strategy.

Fundamentally, there are frequent serial fluctuations in cardiocirculatory parameters prior to hypotension. Hence, the development of a hypotension prediction index will help prevent hypotension. By analyzing BP waveform characteristics using machine deep learning algorithms, Hatib et al. [102] pioneered the prediction of hypotension occurrence with MAP values below 65 mmHg 1 min, 5 min, or even earlier, thus allowing clinicians to intervene during hypotension or even prevent hypotension. The algorithm was verified in 204 surgical patients. It showed that the sensitivity and specificity of predicting hypotension 15 min before the onset of hypotension were 88% and 87%, respectively. However, the algorithm was unable to predict hypotension due to clinical interventions, including intraoperative compression of large vessels or changes in position, such as the Trendelenburg position. Schneck et al. [103] found that the application of the algorithm conferred a significantly lower IOH incidence and a significantly shorter IOH duration than conventional BP management. However, in a single-center trial by Maheshwari et al. [104] involving 214 patients undergoing medium- and high-risk noncardiac surgery, the algorithm predicted hypotension but did not reduce the amount of IOH. The investigators concluded that the algorithm for treatment recommendations in the treatment algorithm system was too complex and needed further optimization to ensure timely clinical intervention. Based on this, considering the large proportion of low-risk patients who undergo

conventional common surgery, we should weigh the risk-benefit ratio when using expensive noninvasive hemodynamic devices, as it is a valuable tool or a superfluous toy for the right patients [105]. Fully automated individualized hemodynamic management has broad prospects with advances in computer technology, especially in high-risk patients, as supported by recent studies [75, 106, 107].

8. Provisional Decision-Making and Targets in Practice

Given the dynamic nature of BP, perioperative individualized BP management is not to set a fixed threshold, but rather an individualized BP target value that considers the baseline BP, pathophysiology, comorbidities, perioperative agent use, and surgery.

In clinical practice, individualized BP targets can be achieved, which will ultimately improve patient outcomes through an easy and rapid process. The "5 Ts" (target patients, timing and type of intervention, target variables, and values) may provide a reference for rapid individualized BP management [108, 109].

Targeting an appropriate BP is a challenge. Clinically, several factors should be considered when setting an appropriate BP target [110, 111]: (1) hypotension does not always appear to be harmful and lead to organ hypoperfusion [112]; (2) the goal is to ensure sufficient perfusion pressure and oxygen delivery, not to correct a number [113]; (3) the pressure regulation ability and ischemia tolerability varies with organs [110, 111]; (4) an absolute threshold is easy to use and often adopted in decision-making; (5) intravascular volume status is fundamental and essential for organ perfusion and should be evaluated simultaneously when correcting hypotension [114, 115]; (6) specific pathophysiology alterations of the surgical patient (e.g., shock, hemorrhage, and sepsis); (7) the BP requirements for high-risk elderly patients undergoing major surgery is quite different from those of normal patients undergoing a brief surgery; (8) strict BP management is more conducive for the protection of organ functions than laissez-faire or lenient BP management [116]; (9) a "one-size-fits-all" approach should be abandoned and personalized BP targets that vary with time should be adopted; and (10) a holistic attitude when treating refractory hypotension should be adopted.

BP targets vary with the population characteristics and surgical type. The patient's baseline BP measurements are a major determinant for perioperative BP targets. Based on the BP values, the baseline BP can be classified into three categories: the low (systolic BP < 90 mmHg and diastolic BP < 50 mmHg), normal (systolic BP 90–139 mmHg and diastolic BP 50–89 mmHg), and high baseline BP (systolic BP ≥ 140 mmHg and diastolic BP ≥ 90 mmHg) categories. The BP target for patients with a low baseline BP undergoing noncardiac surgery should be maintained at a MAP ≥ 60 mmHg based on results of multiple studies [52, 55–57, 64] and a MAP > 65 mmHg for patients with a normal BP [30, 50, 73, 117]. BP should be maintained within 80%–110% of the baseline BP in patients with a high baseline BP [30, 52, 73, 118, 119] and at a systolic BP of ≤160 mmHg [63, 120], which is favorable for the outcomes. For cardiac surgery, the requirements for BP during and before or after extracorporeal circulation are different. Before and after extracorporeal circulation, the target BP may be the optimal value for patients undergoing noncardiac surgery: the intraoperative systolic BP should not be higher than 140 mmHg [50, 121], and the MAP should be kept at 70–100 mmHg during cardiopulmonary bypass [70, 71, 122, 123]. BP targets for patients with specific pathophysiological alterations should be tailored in an individualized manner. In a perioperative setting, two conditions are often encountered: the BP targets and management of hypotension. The pragmatic decision-making flow chart is depicted in Figure 2.

For postoperative BP, maintaining a systolic BP of 90–160 mmHg is a reasonable target for patients with a normal baseline BP. However, for patients with an abnormal baseline BP, these targets should be adjusted according to the preoperative baseline values [84].

9. Conclusion and Perspectives

BP can be corrected, and hypotension should be avoided. Given the nature of BP, perioperative BP management is a dynamic process and not a fixed point. From existing evidence, maintaining the MAP of normal patients at ≥65 mmHg perioperatively is widely accepted, MAP value at 65 mmHg can be considered a minimum level for BP management and adjustment and at the same time not solely concentrates on the value but tailors individually suffice for organ blood supply.

Both IOH and POH have detrimental effects on patient prognosis, and there is paucity of evidence on the direct relationship between hypotension and adverse outcomes, and an absolute BP target is usually selected as the initial target for perioperative BP management. The baseline BP is helpful for setting an appropriate BP target, and personalized BP targets may change over time owing to abrupt pathophysiological alterations perioperatively. Strict BP management relying on baseline BP and maintaining fluctuations within ±20% or ±10% of the baseline BP is an optimal BP control method. Further research is needed to define individual BP harm thresholds and to develop therapeutic strategies to treat and avoid IOH.

The newly emerged hypotension prediction index algorithm and automated BP control system are helpful for individualized hemodynamic management, especially for high-risk patients. It is necessary to validate whether the machine learning algorithm or artificial intelligence-based intervention for BP management is valuable for all patients, especially for high-risk patients.

Conflicts of Interest

The authors declare that there is no conflict of interest regarding the publication of this paper.

Acknowledgments

References

[1] T. G. Weiser, A. B. Haynes, G. Molina et al., "Size and distribution of the global volume of surgery in 2012," *Bulletin of the World Health Organization*, vol. 94, no. 3, pp. 201–209F, 2016.

[2] T. G. Weiser, A. B. Haynes, G. Molina et al., "Estimate of the global volume of surgery in 2012: an assessment supporting improved health outcomes," *Lancet*, vol. 385, Suppl 2, p. S11, 2015.

[3] B. Williams, G. Mancia, W. Spiering et al., "2018 ESC/ESH Guidelines for the management of arterial hypertension," *European Heart Journal*, vol. 39, no. 33, pp. 3021–3104, 2018.

[4] R. D. Brook and S. Rajagopalan, "2017 ACC/AHA/AAPA/ABC/ACPM/AGS/APhA/ASH/ASPC/NMA/PCNA Guideline for the prevention, detection, evaluation, and management of high blood pressure in adults. A report of the American College of Cardiology/American Heart Association Task Force on clinical practice guidelines," *Journal of the American Society of Hypertension*, vol. 12, no. 3, p. 238, 2018.

[5] G. L. Ackland, C. S. Brudney, M. Cecconi et al., "Perioperative Quality Initiative consensus statement on the physiology of arterial blood pressure control in perioperative medicine," *British Journal of Anaesthesia*, vol. 122, no. 5, pp. 542–551, 2019.

[6] D. I. Sessler, J. A. Bloomstone, S. Aronson et al., "Perioperative Quality Initiative consensus statement on intraoperative blood pressure, risk and outcomes for elective surgery," *British Journal of Anaesthesia*, vol. 122, no. 5, pp. 563–574, 2019.

[7] S. Venkatesan, P. R. Myles, H. J. Manning et al., "Cohort study of preoperative blood pressure and risk of 30-day mortality after elective non-cardiac surgery," *British Journal of Anaesthesia*, vol. 119, no. 1, pp. 65–77, 2017.

[8] W. J. Gu, B. L. Hou, J. S. W. Kwong et al., "Association between intraoperative hypotension and 30-day mortality, major adverse cardiac events, and acute kidney injury after non-cardiac surgery: a meta-analysis of cohort studies," *International Journal of Cardiology*, vol. 258, pp. 68–73, 2018.

[9] B. Saugel, P. C. Reese, D. I. Sessler et al., "Automated ambulatory blood pressure measurements and intraoperative hypotension in patients having noncardiac surgery with general anesthesia: a prospective observational study," *Anesthesiology*, vol. 131, no. 1, pp. 74–83, 2019.

[10] F. N. Buijs, L. León-Mercado, M. Guzmán-Ruiz, N. N. Guerrero-Vargas, F. Romo-Nava, and R. M. Buijs, "The circadian system: a regulatory feedback network of periphery and brain," *Physiology (Bethesda, Md.)*, vol. 31, no. 3, pp. 170–181, 2016.

[11] P. C. Johnson, "Autoregulation of blood flow," *Circulation Research*, vol. 59, no. 5, pp. 483–495, 1986.

[12] L. Meng, Y. Wang, L. Zhang, and D. L. McDonagh, "Heterogeneity and variability in pressure autoregulation of organ blood flow: lessons learned over 100+ years," *Critical Care Medicine*, vol. 47, no. 3, pp. 436–448, 2019.

[13] F. S. Larsen, K. S. Olsen, B. A. Hansen, O. B. Paulson, and G. M. Knudsen, "Transcranial Doppler is valid for determination of the lower limit of cerebral blood flow autoregulation," *Stroke*, vol. 25, no. 10, pp. 1985–1988, 1994.

[14] L. Meng, W. Hou, J. Chui, R. Han, and A. W. Gelb, "Cardiac output and cerebral blood Flow," *Anesthesiology*, vol. 123, no. 5, pp. 1198–1208, 2015.

[15] S. Ogoh, R. M. Brothers, Q. Barnes et al., "The effect of changes in cardiac output on middle cerebral artery mean blood velocity at rest and during exercise," *Journal of Physiology*, vol. 569, no. 2, pp. 697–704, 2005.

[16] A. G. Vedel, F. Holmgaard, L. S. Rasmussen et al., "High-target versus low-target blood pressure management during cardiopulmonary bypass to prevent cerebral injury in cardiac surgery patients: a randomized controlled trial," *Circulation*, vol. 137, no. 17, pp. 1770–1780, 2018.

[17] N. D. Agham and U. M. Chaskar, "Learning and non-learning algorithms for cuffless blood pressure measurement: a review," *Medical and Biological Engineering and Computing*, vol. 59, no. 6, pp. 1201–1222, 2021.

[18] R. Mukkamala, G. S. Stergiou, and A. P. Avolio, "Cuffless blood pressure measurement," *Annual Review of Biomedical Engineering*, vol. 24, no. 1, pp. 203–230, 2022.

[19] K. Bartels, S. A. Esper, and R. H. Thiele, "Blood pressure monitoring for the Anesthesiologist," *Anesthesia and Analgesia*, vol. 122, no. 6, pp. 1866–1879, 2016.

[20] T. Kaufmann, E. G. M. Cox, R. Wiersema et al., "Non-invasive oscillometric versus invasive arterial blood pressure measurements in critically ill patients: a post hoc analysis of a prospective observational study," *Journal of Critical Care*, vol. 57, pp. 118–123, 2020.

[21] D. B. Wax, H. M. Lin, and A. B. Leibowitz, "Invasive and concomitant noninvasive intraoperative blood pressure monitoring: observed differences in measurements and associated therapeutic interventions," *Anesthesiology*, vol. 115, no. 5, pp. 973–978, 2011.

[22] A. P. Avolio, L. M. Van Bortel, P. Boutouyrie et al., "Role of pulse pressure amplification in arterial Hypertension," *Hypertension*, vol. 54, no. 2, pp. 375–383, 2009.

[23] A. L. Pauca, S. L. Wallenhaupt, N. D. Kon, and W. Y. Tucker, "Does radial artery pressure accurately reflect aortic pressure?," *Chest*, vol. 102, no. 4, pp. 1193–1198, 1992.

[24] W. Y. Kim, J. H. Jun, J. W. Huh, S. B. Hong, C. M. Lim, and Y. Koh, "Radial to femoral arterial blood pressure differences in septic shock patients receiving high-dose norepinephrine therapy," *Shock*, vol. 40, no. 6, pp. 527–531, 2013.

[25] M. Lee, L. Weinberg, B. Pearce et al., "Agreement between radial and femoral arterial blood pressure measurements during orthotopic liver transplantation," *Critical Care and Resuscitation*, vol. 17, no. 2, pp. 101–107, 2015.

[26] G. Fuda, A. Denault, A. Deschamps et al., "Risk factors involved in central-to-radial arterial pressure gradient during cardiac surgery," *Anesthesia and Analgesia*, vol. 122, no. 3, pp. 624–632, 2016.

[27] J. van Egmond, M. Hasenbos, and J. F. Crul, "Invasive v. non-invasive measurement of arterial pressure. Comparison of two automatic methods and simultaneously measured direct intra-arterial pressure," *British Journal of Anaesthesia*, vol. 57, no. 4, pp. 434–444, 1985.

[28] T. G. Monk, M. R. Bronsert, W. G. Henderson, M. P. Mangione, and K. E. Hammermeister, "Association between intraoperative hypotension and hypertension and 30-day postoperative mortality in noncardiac surgery," *Anesthesiology*, vol. 123, no. 2, pp. 307–319, 2015.

[29] C. C. Cheung, A. Martyn, N. Campbell, S. Frost, and N. A. Khan, "Predictors of intraoperative hypotension and bradycardia," *American Journal of Medicine*, vol. 128, no. 5, pp. 532–538, 2015.

[30] J. B. Bijker, S. Persoon, L. M. Peelen et al., "Intraoperative hypotension and perioperative ischemic stroke after general surgery: a nested case-control study," *Anesthesiology*, vol. 116, no. 3, pp. 658–664, 2012.

[31] S. Toyama, M. Kakumoto, M. Morioka et al., "Perfusion index derived from a pulse oximeter can predict the incidence of hypotension during spinal anaesthesia for caesarean delivery," *British Journal of Anaesthesia*, vol. 111, no. 2, pp. 235–241, 2013.

[32] J. L. Ard and S. Kendale, "Searching for baseline blood pressure: a comparison of blood pressure at three different care points," *Journal of Clinical Neuroscience*, vol. 34, pp. 59–62, 2016.

[33] R. Hu, Y. Kalam, J. Broad, T. Ho, and R. Bellomo, "Decreased mean perfusion pressure as an independent predictor of acute kidney injury after cardiac surgery," *Heart and Vessels*, vol. 35, no. 8, pp. 1154–1163, 2020.

[34] J. C. Drummond, J. L. Blake, P. M. Patel, P. Clopton, and G. Schulteis, "An observational study of the influence of "white-coat hypertension" on day-of-surgery blood pressure determinations," *Journal of Neurosurgical Anesthesiology*, vol. 25, no. 2, pp. 154–161, 2013.

[35] S. Czernichow, A. Zanchetti, F. Turnbull et al., "The effects of blood pressure reduction and of different blood pressure-lowering regimens on major cardiovascular events according to baseline blood pressure: meta-analysis of randomized trials," *Journal of Hypertension*, vol. 29, no. 1, pp. 4–16, 2011.

[36] D. S. Nuyujukian, M. S. Newell, J. J. Zhou, J. Koska, and P. D. Reaven, "Baseline blood pressure modifies the role of blood pressure variability in mortality: results from the ACCORD trial," *Diabetes, Obesity & Metabolism*, vol. 24, no. 5, pp. 951–955, 2022.

[37] S. J. Howell, J. W. Sear, and P. Foëx, "Hypertension, hypertensive heart disease and perioperative cardiac risk," *British Journal of Anaesthesia*, vol. 92, no. 4, pp. 570–583, 2004.

[38] J. Varon and P. E. Marik, "The diagnosis and management of hypertensive crises," *Chest*, vol. 118, no. 1, pp. 214–227, 2000.

[39] D. J. Rosenman, F. S. McDonald, J. O. Ebbert, P. J. Erwin, M. LaBella, and V. M. Montori, "Clinical consequences of withholding versus administering renin-angiotensin-aldosterone system antagonists in the preoperative period," *Journal of Hospital Medicine*, vol. 3, no. 4, pp. 319–325, 2008.

[40] P. S. Roshanov, B. Rochwerg, A. Patel et al., "Withholding versusContinuing angiotensin-converting enzyme inhibitors or angiotensin ii receptor blockers before noncardiac surgery," *Anesthesiology*, vol. 126, no. 1, pp. 16–27, 2017.

[41] K. G. Vazquez-Narvaez and M. Ulibarri-Vidales, "The patient with hypertension and new guidelines for therapy," *Current Opinion in Anaesthesiology*, vol. 32, no. 3, pp. 421–426, 2019.

[42] R. D. Sanders, F. Hughes, A. Shaw et al., "Perioperative Quality Initiative consensus statement on preoperative blood pressure, risk and outcomes for elective surgery," *British Journal of Anaesthesia*, vol. 122, no. 5, pp. 552–562, 2019.

[43] C. Andersson, D. Shilane, A. S. Go et al., "Beta-Blocker Therapy and Cardiac Events Among Patients With Newly Diagnosed Coronary Heart Disease," *Journal of the American College of Cardiology*, vol. 64, no. 3, pp. 247–252, 2014.

[44] L. A. Fleisher, K. E. Fleischmann, A. D. Auerbach et al., "2014 ACC/AHA guideline on perioperative cardiovascular evaluation and management of patients undergoing noncardiac surgery: a report of the American College of Cardiology/ American Heart Association Task Force on practice guidelines," *Journal of the American College of Cardiology*, vol. 64, no. 22, pp. e77–137, 2014.

[45] P. J. Devereaux, H. Yang, S. Yusuf et al., "Effects of extended-release metoprolol succinate in patients undergoing non- cardiac surgery (POISE trial): a randomised controlled trial," *Lancet*, vol. 371, no. 9627, pp. 1839–1847, 2008.

[46] S. Venkatesan, M. E. Jorgensen, H. J. Manning et al., "Preoperative chronic beta-blocker prescription in elderly patients as a risk factor for postoperative mortality stratified by preoperative blood pressure: a cohort study," *British Journal of Anaesthesia*, vol. 123, no. 2, pp. 118–125, 2019.

[47] M. D. Kertai, M. Cooter, R. J. Pollard et al., "Is Compliance With Surgical Care Improvement Project Cardiac (SCIP-Card-2) measures for perioperative β-blockers associated with reduced incidence of mortality and cardiovascular-related critical quality indicators after noncardiac surgery?," *Anesthesia and Analgesia*, vol. 126, no. 6, pp. 1829–1838, 2018.

[48] P. Foëx and J. W. Sear, "Perioperative beta-blockade: a conundrum still in need of study!," *Anesthesia and Analgesia*, vol. 126, no. 6, pp. 1819–1821, 2018.

[49] J. B. Bijker, W. A. van Klei, T. H. Kappen, L. van Wolfswinkel, K. G. Moons, and C. J. Kalkman, "Incidence of intraoperative hypotension as a function of the chosen definition: literature definitions applied to a retrospective cohort using automated data collection," *Anesthesiology*, vol. 107, no. 2, pp. 213–220, 2007.

[50] M. L. van Zuylen, A. Gribnau, M. Admiraal et al., "The role of intraoperative hypotension on the development of postoperative cognitive dysfunction: a systematic review," *Journal of Clinical Anesthesia*, vol. 72, article 110310, 2021.

[51] L. Weinberg, S. Y. Li, M. Louis et al., "Reported definitions of intraoperative hypotension in adults undergoing non-cardiac surgery under general anaesthesia: a review," *BMC Anesthesiology*, vol. 22, no. 1, p. 69, 2022.

[52] V. Salmasi, K. Maheshwari, D. Yang et al., "Relationship between intraoperative hypotension, defined by either reduction from baseline or absolute thresholds, and acute kidney and myocardial injury after noncardiac surgery: a retrospective cohort analysis," *Anesthesiology*, vol. 126, no. 1, pp. 47–65, 2017.

[53] L. Hallqvist, F. Granath, E. Huldt, and M. Bell, "Intraoperative hypotension is associated with acute kidney injury in noncardiac surgery," *European Journal of Anaesthesiology*, vol. 35, no. 4, pp. 273–279, 2018.

[54] D. I. Sessler, C. S. Meyhoff, N. M. Zimmerman et al., "Period-dependent associations between hypotension during and for four days after noncardiac surgery and a composite of myocardial infarction and death: a substudy of the POISE-2 trial," *Anesthesiology*, vol. 128, no. 2, pp. 317–327, 2018.

[55] M. Walsh, P. J. Devereaux, A. X. Garg, A. Kurz, and D. I. Sessler, "Relationship between intraoperative mean arterial pressure and clinical outcomes after noncardiac surgery: toward an empirical definition of hypotension," *Anesthesiology*, vol. 119, no. 3, pp. 507–515, 2013.

[56] L. M. Loffel, K. F. Bachmann, M. A. Furrer, and P. Y. Wuethrich, "Impact of intraoperative hypotension on early postoperative acute kidney injury in cystectomy patients - a retrospective cohort analysis," *Journal of Clinical Anesthesia*, vol. 66, p. 109906, 2020.

[57] L. Y. Sun, D. N. Wijeysundera, G. A. Tait, and W. S. Beattie, "Association of intraoperative hypotension with acute kidney injury after elective noncardiac surgery," *Anesthesiology*, vol. 123, no. 3, pp. 515–523, 2015.

[58] A. Joosten, V. Lucidi, B. Ickx et al., "Intraoperative hypotension during liver transplant surgery is associated with postoperative acute kidney injury: a historical cohort study," *BMC Anesthesiology*, vol. 21, no. 1, p. 12, 2021.

[59] S. Ahuja, E. J. Mascha, D. Yang et al., "Associations of intraoperative radial arterial systolic, diastolic, mean, and pulse pressures with myocardial and acute kidney injury after noncardiac surgery: a retrospective cohort analysis," *Anesthesiology*, vol. 132, no. 2, pp. 291–306, 2020.

[60] W. Y. Jang, J. K. Jung, D. K. Lee, and S. B. Han, "Intraoperative hypotension is a risk factor for postoperative acute kidney injury after femoral neck fracture surgery: a retrospective study," *BMC Musculoskeletal Disorders*, vol. 20, no. 1, p. 131, 2019.

[61] L. Hallqvist, J. Mårtensson, F. Granath, A. Sahlén, and M. Bell, "Intraoperative hypotension is associated with myocardial damage in noncardiac surgery: an observational study," *European Journal of Anaesthesiology*, vol. 33, no. 6, p. 450, 2016.

[62] L. Hallqvist, F. Granath, M. Fored, and M. Bell, "Intraoperative hypotension and myocardial infarction development among high-risk patients undergoing noncardiac surgery: a nested case-control study," *Anesthesia and Analgesia*, vol. 133, no. 1, pp. 6–15, 2021.

[63] T. E. F. Abbott, R. M. Pearse, R. A. Archbold et al., "A prospective international multicentre cohort study of intraoperative heart rate and systolic blood pressure and myocardial injury after noncardiac surgery: results of the VISION study," *Anesthesia and Analgesia*, vol. 126, no. 6, pp. 1936–1945, 2018.

[64] J. A. van Waes, W. A. van Klei, D. N. Wijeysundera, L. van Wolfswinkel, T. F. Lindsay, and W. S. Beattie, "Association between intraoperative hypotension and myocardial injury after vascular surgery," *Anesthesiology*, vol. 124, no. 1, pp. 35–44, 2016.

[65] H. L. Sang, A. K. Jie, B. Y. Heo, Y. R. Kim, and S. Ahn, "Association between intraoperative hypotension and postoperative myocardial injury in patients with prior coronary stents undergoing high-risk surgery: a retrospective study," *Journal of Anesthesia*, vol. 34, no. 2, pp. 257–267, 2020.

[66] A. M. Hu, Y. Qiu, P. Zhang et al., "Higher versus lower mean arterial pressure target management in older patients having non-cardiothoracic surgery: a prospective randomized controlled trial," *Journal of Clinical Anesthesia*, vol. 69, p. 110150, 2021.

[67] M. R. Mathis, B. I. Naik, R. E. Freundlich et al., "Preoperative risk and the association between hypotension and postoperative acute kidney injury," *Anesthesiology*, vol. 132, no. 3, pp. 461–475, 2020.

[68] W. H. Stapelfeldt, H. Yuan, J. K. Dryden et al., "The SLU-Score: a novel method for detecting hazardous hypotension in adult patients undergoing noncardiac surgical procedures," *Anesthesia and Analgesia*, vol. 124, no. 4, pp. 1135–1152, 2017.

[69] X. Wu, Z. Jiang, J. Ying, Y. Han, and Z. Chen, "Optimal blood pressure decreases acute kidney injury after gastrointestinal surgery in elderly hypertensive patients: a randomized study: optimal blood pressure reduces acute kidney injury," *Journal of Clinical Anesthesia*, vol. 43, pp. 77–83, 2017.

[70] J. P. Gold, M. E. Charlson, P. Williams-Russo et al., "Improvement of outcomes after coronary artery bypass: A randomized trial comparing intraoperative high versus low mean arterial pressure," *Journal of Thoracic and Cardiovascular Surgery*, vol. 110, no. 5, pp. 1302–1314, 1995.

[71] M. Siepe, T. Pfeiffer, A. Gieringer et al., "Increased systemic perfusion pressure during cardiopulmonary bypass is associated with less early postoperative cognitive dysfunction and delirium," *European Journal of Cardio-Thoracic Surgery*, vol. 40, no. 1, pp. 200–207, 2011.

[72] A. Azau, P. Markowicz, J. J. Corbeau et al., "Increasing mean arterial pressure during cardiac surgery does not reduce the rate of postoperative acute kidney injury," *Perfusion*, vol. 29, no. 6, pp. 496–504, 2014.

[73] E. Futier, J. Y. Lefrant, P. G. Guinot et al., "Effect of individualized vs standard blood pressure management strategies on postoperative organ dysfunction among high-risk patients undergoing major surgery: a randomized clinical trial," *JAMA*, vol. 318, no. 14, pp. 1346–1357, 2017.

[74] M. A. de la Hoz, V. Rangasamy, A. B. Bastos et al., "Intraoperative hypotension and acute kidney injury, stroke, and mortality during and outside cardiopulmonary bypass: a retrospective observational cohort study," *Anesthesiology*, vol. 136, no. 6, pp. 927–939, 2022.

[75] P. Murabito, M. Astuto, F. Sanfilippo et al., "Proactive management of intraoperative hypotension reduces biomarkers of organ injury and oxidative stress during elective noncardiac surgery: a pilot randomized controlled trial," *Journal of Clinical Medicine*, vol. 11, no. 2, p. 392, 2022.

[76] A. Gregory, W. H. Stapelfeldt, A. K. Khanna et al., "Intraoperative hypotension is associated with adverse clinical outcomes after noncardiac surgery," *Anesthesia and Analgesia*, vol. 132, no. 6, pp. 1654–1665, 2021.

[77] E. M. Wesselink, T. H. Kappen, H. M. Torn, A. J. C. Slooter, and W. A. van Klei, "Intraoperative hypotension and the risk of postoperative adverse outcomes: a systematic review," *British Journal of Anaesthesia*, vol. 121, no. 4, pp. 706–721, 2018.

[78] B. F. Palmer, "Renal dysfunction complicating the treatment of hypertension," *New England Journal of Medicine*, vol. 347, no. 16, pp. 1256–1261, 2002.

[79] A. Polese, N. De Cesare, P. Montorsi et al., "Upward shift of the lower range of coronary flow autoregulation in hypertensive patients with hypertrophy of the left ventricle," *Circulation*, vol. 83, no. 3, pp. 845–853, 1991.

[80] J. B. Almeida, M. A. Saragoça, A. Tavares, M. L. Cezareti, S. A. Draibe, and O. L. Ramos, "Severe hypertension induces disturbances of renal autoregulation," *Hypertension*, vol. 19, 2_supplement, 1992.

[81] L. Briesenick, M. Flick, and B. Saugel, "Postoperative blood pressure management in patients treated in the ICU after noncardiac surgery," *Current Opinion in Critical Care*, vol. 27, no. 6, pp. 694–700, 2021.

[82] V. G. B. Liem, S. E. Hoeks, K. Mol et al., "Postoperative hypotension after noncardiac surgery and the association with myocardial injury," *Anesthesiology*, vol. 133, no. 3, pp. 510–522, 2020.

[83] F. van Lier, F. H. I. M. Wesdorp, V. G. B. Liem et al., "Association between postoperative mean arterial blood pressure and myocardial injury after noncardiac surgery," *British Journal of Anaesthesia*, vol. 120, no. 1, pp. 77–83, 2018.

[84] M. D. McEvoy, R. Gupta, E. J. Koepke et al., "Perioperative Quality Initiative consensus statement on postoperative blood pressure, risk and outcomes for elective surgery," *British Journal of Anaesthesia*, vol. 122, no. 5, pp. 575–586, 2019.

[85] S. Mohammed Iddrisu, J. Considine, and A. Hutchinson, "Frequency, nature and timing of clinical deterioration in the early postoperative period," *Journal of Clinical Nursing*, vol. 27, no. 19-20, pp. 3544–3553, 2018.

[86] J. Kause, G. Smith, D. Prytherch, M. Parr, A. Flabouris, and K. Hillman, "A comparison of antecedents to cardiac arrests, deaths and emergency intensive care admissions in Australia and New Zealand, and the United Kingdom–the ACADEMIA study," *Resuscitation*, vol. 62, no. 3, pp. 275–282, 2004.

[87] Y. L. Liu, P. John, L. Elisa, U. Shigehiko, and B. Rinaldo, "Changes in blood pressure before the development of nosocomial acute kidney injury," *Nephrology, Dialysis, Transplantation*, vol. 24, no. 2, pp. 504–511, 2008.

[88] N. J. Smischney, A. D. Shaw, W. H. Stapelfeldt et al., "Postoperative hypotension in patients discharged to the intensive care unit after non-cardiac surgery is associated with adverse clinical outcomes," *Critical Care*, vol. 24, no. 1, p. 682, 2020.

[89] A. K. Khanna, K. Maheshwari, G. Mao et al., "Association between mean arterial pressure and acute kidney injury and a composite of myocardial injury and mortality in postoperative critically ill patients: a retrospective cohort analysis," *Critical Care Medicine*, vol. 47, no. 7, pp. 910–917, 2019.

[90] A. K. Khanna, A. D. Shaw, W. H. Stapelfeldt et al., "Postoperative hypotension and adverse clinical outcomes in patients without intraoperative hypotension, after noncardiac surgery," *Anesthesia and Analgesia*, vol. 132, no. 5, pp. 1410–1420, 2021.

[91] A. Turan, C. Chang, B. Cohen et al., "Incidence, severity, and detection of blood pressure perturbations after abdominal surgery: a prospective blinded observational study," *Anesthesiology*, vol. 130, no. 4, pp. 550–559, 2019.

[92] M. H. Mcgillion, E. Duceppe, K. Allan, M. Marcucci, and P. J. Devereaux, "Postoperative remote automated monitoring: need for and state of the science," *Canadian Journal of Cardiology*, vol. 34, no. 7, pp. 850–862, 2018.

[93] F. Michard, R. Bellomo, and A. Taenzer, "The rise of ward monitoring: opportunities and challenges for critical care specialists," *Intensive Care Medicine*, vol. 45, no. 5, pp. 671–673, 2019.

[94] A. K. Khanna, P. Hoppe, and B. Saugel, "Automated continuous noninvasive ward monitoring: future directions and challenges," *Critical Care*, vol. 23, no. 1, p. 194, 2019.

[95] J. D. Williamson, M. A. Supiano, W. B. Applegate et al., "Intensive vs standard blood pressure control and cardiovascular disease outcomes in adults aged ≥75 years: a randomized clinical trial," *JAMA*, vol. 315, no. 24, pp. 2673–2682, 2016.

[96] I. D. Croall, D. J. Tozer, B. Moynihan et al., "Effect of standard vs intensive blood pressure control on cerebral blood flow in small vessel disease: the PRESERVE randomized clinical trial," *JAMA Neurology*, vol. 75, no. 6, pp. 720–727, 2018.

[97] J. Y. Nicklas, O. Diener, M. Leistenschneider et al., "Personalised haemodynamic management targeting baseline cardiac index in high- risk patients undergoing major abdominal surgery: a randomised single-centre clinical trial," *British Journal of Anaesthesia*, vol. 125, no. 2, pp. 122–132, 2020.

[98] T. Godet, R. Grobost, and E. Futier, "Personalization of arterial pressure in the perioperative period," *Current Opinion in Critical Care*, vol. 24, no. 6, pp. 554–559, 2018.

[99] I. M. Nasrallah, S. A. Gaussoin, R. Pomponio et al., "Association of intensive vs standard blood pressure control with magnetic resonance imaging biomarkers of alzheimer disease: secondary analysis of the SPRINT MIND randomized trial," *JAMA Neurology*, vol. 78, no. 5, pp. 568–577, 2021.

[100] O. Gottesman, S. A. Scott, S. B. Ellis et al., "The CLIPMERGE PGx program: clinical implementation of personalized medicine through electronic health records and genomics-pharmacogenomics," *Clinical Pharmacology and Therapeutics*, vol. 94, no. 2, pp. 214–217, 2013.

[101] A. Joosten, J. Rinehart, P. Van der Linden et al., "Computer-assisted individualized hemodynamic management reduces intraoperative hypotension in intermediate- and high-risk surgery: a randomized controlled trial," *Anesthesiology*, vol. 135, no. 2, pp. 258–272, 2021.

[102] F. Hatib, Z. Jian, S. Buddi et al., "Machine-learning algorithm to predict hypotension based on high-fidelity arterial pressure waveform analysis," *Anesthesiology*, vol. 129, no. 4, pp. 663–674, 2018.

[103] E. Schneck, D. Schulte, L. Habig et al., "Hypotension Prediction Index based protocolized haemodynamic management reduces the incidence and duration of intraoperative hypotension in primary total hip arthroplasty: a single centre feasibility randomised blinded prospective interventional trial," *Journal of Clinical Monitoring and Computing*, vol. 34, no. 6, pp. 1149–1158, 2020.

[104] K. Maheshwari, T. Shimada, D. Yang et al., "Hypotension prediction index for prevention of hypotension during moderate- to high-risk noncardiac surgery," *Anesthesiology*, vol. 133, no. 6, pp. 1214–1222, 2020.

[105] A. Joosten, J. L. Vincent, and B. Saugel, "Continuous noninvasive haemodynamic monitoring in patients having surgery: valuable tool or superfluous toy?," *Anaesthesia, Critical Care & Pain Medicine*, vol. 39, no. 3, pp. 417-418, 2020.

[106] B. Alexander, J. Rinehart, M. Cannesson, J. Duranteau, and A. Joosten, "Closed-loop hemodynamic management," *Best Practice & Research. Clinical Anaesthesiology*, vol. 33, no. 2, pp. 199–209, 2019.

[107] J. Rinehart, S. Lee, B. Saugel, and A. Joosten, "Automated blood pressure control," *Seminars in Respiratory and Critical Care Medicine*, vol. 42, no. 1, pp. 47–58, 2021.

Retraction

Retracted: Association between Oxidative Burden and Restenosis: A Case-Control Study

Oxidative Medicine and Cellular Longevity

This article has been retracted by Hindawi, as publisher, following an investigation undertaken by the publisher [1]. This investigation has uncovered evidence of systematic manipulation of the publication and peer-review process. We cannot, therefore, vouch for the reliability or integrity of this article.

Please note that this notice is intended solely to alert readers that the peer-review process of this article has been compromised.

Wiley and Hindawi regret that the usual quality checks did not identify these issues before publication and have since put additional measures in place to safeguard research integrity.

We wish to credit our Research Integrity and Research Publishing teams and anonymous and named external researchers and research integrity experts for contributing to this investigation.

The corresponding author, as the representative of all authors, has been given the opportunity to register their agreement or disagreement to this retraction. We have kept a record of any response received.

References

[1] S. Ganjali, A. Mansouri, M. Abbasifard, S. A. Moallem, Z. Tayarani-Najaran, and A. Sahebkar, "Association between Oxidative Burden and Restenosis: A Case-Control Study," *Oxidative Medicine and Cellular Longevity*, vol. 2022, Article ID 3577761, 10 pages, 2022.

Research Article

Association between Oxidative Burden and Restenosis: A Case-Control Study

Shiva Ganjali,[1] Atena Mansouri,[2,3] Mitra Abbasifard ⓘ,[4,5] Seyed Adel Moallem,[6,7] Zahra Tayarani-Najaran,[8,9] and Amirhossein Sahebkar ⓘ[2,10,11]

[1]*Department of Medical Biotechnology and Nanotechnology, Mashhad University of Medical Sciences, Mashhad, Iran*
[2]*Biotechnology Research Center, Pharmaceutical Technology Institute, Mashhad University of Medical Sciences, Mashhad, Iran*
[3]*Cellular & Molecular Research Center, Birjand University of Medical Sciences, Birjand, Iran*
[4]*Immunology of Infectious Diseases Research Center, Research Institute of Basic Medical Sciences, Rafsanjan University of Medical Sciences, Rafsanjan, Iran*
[5]*Department of Internal Medicine, Ali-Ibn Abi-Talib Hospital, School of Medicine, Rafsanjan University of Medical Sciences, Rafsanjan, Iran*
[6]*Department of Pharmacology and Toxicology, College of Pharmacy, Al-Zahraa University for Women, Karbala, Iraq*
[7]*Department of Pharmacodynamics and Toxicology, School of Pharmacy, Mashhad University of Medical Sciences, Mashhad, Iran*
[8]*Targeted Drug Delivery Research Center, Pharmaceutical Technology Institute, Mashhad University of Medical Sciences, Mashhad, Iran*
[9]*Medical Toxicology Research Center, Mashhad University of Medical Sciences, Mashhad, Iran*
[10]*Applied Biomedical Research Center, Mashhad University of Medical Sciences, Mashhad, Iran*
[11]*Department of Biotechnology, School of Pharmacy, Mashhad University of Medical Sciences, Mashhad, Iran*

Correspondence should be addressed to Mitra Abbasifard; dr.mabbasifard@gmail.com
and Amirhossein Sahebkar; amir_saheb2000@yahoo.com

Background. In-stent restenosis (ISR) is an important clinical complication that occurs following stent implantation. The application of drug-eluting stents (DES) and even consumption of drugs such as antiplatelet agents and statins are not completely effective in reducing ISR risk. Since the number of these patients continues to rise, it is pivotal to detect patients who are at a higher risk of ISR. In addition, identification of biochemical markers of ISR could give the right perspective on choosing the proper strategy to treat these patients. Several pathophysiological pathways including oxidative stress (OS) are implicated in the progression of ISR. Hence, this study aimed to evaluate the association between oxidative/anti-oxidative markers and ISR. *Methods*. This was a case-control study which comprised 21 ISR, 26 NISR (non-ISR), and 20 healthy subjects. The serum levels of OS markers including malondialdehyde (MDA), thiol groups (GSH), total antioxidant capacity (TAC), and the activity of serum antioxidant enzymes such as glutathione peroxidase (GPx) and superoxide dismutase (SOD) were assessed by colorimetric methods. The overall oxidative burden was assessed using a pro-oxidant-antioxidant balance (PAB) assay. *Results*. MDA levels were considerably higher in the ISR group when compared to healthy subjects ($P = 0.004$). PAB also indicated significantly higher values in both ISR ($P < 0.001$) and NISR ($P < 0.001$) groups related to healthy subjects. No significant differences were observed between the studied groups regarding thiol levels, antioxidant enzyme activities, and TAC. Multinomial logistic regression analysis showed that elevated serum levels of MDA (OR: 1.028, 95% CI: 1.008-1.048; $P = 0.006$) and PAB (OR: 1.076, 95% CI: 1.017-1.139; $P = 0.011$) were significantly associated with higher ISR risk; however, increased values of TAC (OR: 0.990, 95% CI: 0.982-0.999; $P = 0.030$) were significantly associated with decreased ISR risk, while after adjustment for confounders, only SOD activity (OR: 0.0, 95% CI: 0.0-0.0; $P < 0.001$) and PAB value (OR: 1.866, 95% CI: 1.856-1.900; $P < 0.001$) showed association with ISR risk. *Conclusion*. According to the present findings, some oxidative and antioxidative markers like PAB and SOD activity showed the potential in the prediction of ISR risk.

1. Introduction

Atherosclerotic cardiovascular disease (ASCVD) is one of the main causes of mortality worldwide [1]. Percutaneous coronary intervention (PCI) with stent implantation is one of the most effective approaches to restore coronary blood flow in atherosclerosis, especially in high-risk patients for whom coronary artery bypass surgery may be considered threatening. However, in-stent restenosis (ISR) is a principal clinical drawback occurring in these patients [2, 3].

Despite many advances in this field like the use of drug-eluting stents (DES) and antiplatelet agents that reduce neointimal hyperplasia to some extent, ISR still remains a major clinical problem occurring in patients who undergo stent implantation [4, 5]. Since the number of these patients continues to rise, it is pivotal to identify patients who are at a higher risk of ISR. In fact, identification of biochemical markers of ISR could give the right perspective on choosing the proper strategy to treat these patients in order to lessen the need for reintervention, improve patient outcomes, and reduce healthcare costs.

Several pathophysiological pathways including alterations of plasma lipids and lipoproteins, endothelial dysfunction, chronic vascular inflammation, elevated oxidative stress (OS), and diminished redox processes are involved in the progression of ISR [4, 6, 7]. Tissue injury followed by stent implantation may lead to increased production of reactive oxygen species (ROS) that contribute to the initial proliferation, migration, and apoptosis of vascular smooth muscle cells as part of the restenosis progression [8–10]. On the other hand, the capacity of intrinsic antioxidant defense system as vascular repair responses in tissue damage [9] has been suggested to be diminished in restenosis. In this regard, the association between reduced glutathione peroxidase (GPx) activity, as well as increased lipid peroxidation with ISR risk, has been illustrated previously [4, 11].

Therefore, this study aimed to evaluate the association of oxidative/antioxidative markers with ISR, in order to find a sensitive and reliable potential marker for accurate and timely diagnosis of patients who are at increased risk of ISR.

2. Material and Methods

2.1. Study Population.

This was a case-control study performed between December 2014 and April 2017, and based on nonprobability (purposive) sampling, we enrolled 47 unrelated Iranian patients (18-75 years old) with a history of coronary angioplasty with stent implantation at least 1 month earlier who were eventually returned due to the chest pain or equivalent symptoms. According to the angiographic results, patients who had >50% and <50% stenosis within the stent were placed into the in-stent restenosis (ISR; $N = 21$) and non-ISR (NISR; $N = 26$) groups, respectively. Patients with primary PCI, positive troponin, and restenosis in the first month after angioplasty due to thrombosis, autoimmune disorder, active cancer, thrombophilia, or chronic kidney disease were excluded. Furthermore, 20 healthy controls were considered as a validation group. Demographic data including sex, age, smoking history, drug history, past history of diabetes mellitus (DM), hypertension (HTN), dyslipidemia, and duration between coronary stenting and subsequent angiography were collected from medical records. The study protocol was given approval by the Ethics Committee of the Mashhad University of Medical Sciences, and written informed consent was obtained from all participants. Inclusion and exclusion criteria were defined previously [12]. Peripheral femoral or brachial blood was drawn right after entering the catheter; serum samples were separated immediately by centrifugation (20 min, 1000 RCF) and then stored at –80°C until further investigation. Biochemical analysis including fasting blood glucose (FBG), triglycerides (TG), total cholesterol (TC) and high-density lipoprotein cholesterol (HDL-C) was performed by commercial kits (Pars Azmoon, Iran) according to the previously described method [12]. Low-density lipoprotein cholesterol (LDL-C) was calculated using the Friedewald formula.

2.2. Assessment of Oxidative Stress and Antioxidant Markers.

The serum levels of OS markers including malondialdehyde (MDA) (nmol/mL), thiol groups (GSH) (uM), and total antioxidant capacity (TAC) and the activity of serum antioxidant enzymes such as glutathione peroxidase (GPx) (mU/mL) and superoxide dismutase (SOD) (U) were assessed by colorimetric methods using commercial kits (Kiazist, Iran) according to the manufacturer's protocol as describe in our previous article [13]. Pro-oxidant-antioxidant balance (HK unit) was also measured using a pro-oxidant-antioxidant balance (PAB) assay according to the previously described method [14].

2.3. Total Antioxidant Capacity (TAC) Assay.

In addition, total antioxidant capacity (TAC) was measured by CUPric Reducing Anti-oxidant Capacity kit (CUPRAC assay kit) (Kiazist, Iran) in accordance with the manufacturer's protocol. In this assay, in the presence of antioxidants, cupric (Cu^{2+}) is reduced to cuprous (Cu^{+}), and the color which is produced in the presence of chromogen is recorded at 450 nm. TAC was calculated based on a standard curve constructed by Trolox standard available in the kit and was reported as nmol of Trolox equivalent/mL.

2.4. Statistical Analysis.

SPSS software, version 11.5 (Chicago, IL, USA) was used for statistical analysis. Normal distributed variables which are tested using the Kolmogorov–Smirnov test are presented as mean ± standard error (SE), and one-way analysis of variance (ANOVA) and the Tukey multiple comparison post-test or independent sample t-test were used to distinguish changes in variables between the groups. In addition, Chi squared analysis and Fisher's exact test were applied for comparison of qualitative variables between the groups. Binary logistic regression was used to estimate the association between OS markers with ISR (ref: NISR) after adjustment for age, sex, low-density lipoprotein cholesterol (LDL-C), high-density lipoprotein cholesterol (HDL-C) and fasting blood glucose (FBG) levels, Stent type, and use of statins. Moreover, multinomial logistic

TABLE 1: Baseline characteristics of subjects.

	Healthy ($n = 20$)	NISR ($n = 26$)	ISR ($n = 21$)	P value
Sex (%)				
Male	8 (40%)	13 (50%)	11 (52.4%)	0.700
Female	12 (60%)	13 (50%)	10 (47.6%)	
Age (y)	34.50 ± 1.70[a,b]	60.38 ± 2.14	59.48 ± 2.60	0.000*
FBG (mg/dL)	90.60 ± 1.24[a,b]	138.90 ± 15.72	155.62 ± 17.00	0.006*
TC (mg/dL)	155.50 ± 5.10[b]	124.40 ± 8.74	145.62 ± 7.90	0.016*
LDL-C (mg/dL)	93.40 ± 5.72[b]	70.84 ± 6.40	81.70 ± 6.70	0.045*
TG (mg/dL)	91.80 ± 4.54[a]	97.31 ± 11.80[a]	144.80 ± 21.20	0.022*
HDL-C (mg/dL)	46.90 ± 2.40[a,b]	34.11 ± 2.20	36.60 ± 1.64	0.000*

Data are shown as mean ± SE or number (percentage). [a]Significant in comparison with ISR group. [b]Significant in comparison with NISR group. IRS: in-stent restenosis; NISR: non-in-stent restenosis; FBG: fasting blood glucose; TC: total cholesterol; LDL-C: low-density lipoprotein cholesterol; TG: triglycerides; HDL-C: high-density lipoprotein cholesterol.

TABLE 2: Clinical characteristics of ISR and NISR groups.

Variables	ISR ($n = 21$)	NISR ($n = 26$)	P value
Dyslipidemia %	71.4	46.2	0.081
Diabetics %	61.9	46.2	0.282
Hypertension %	71.4	65.4	0.659
Stent type %			
Bare	50.0	11.1	0.015*
Drug	50.0	88.9	
Stent number %			
1	66.7	65.4	0.927
>1	33.3	34.6	
De novo stenosis in other vessels %	57.1	60.9	0.802
Duration of stent implantation (month)	32.8 ± 5.9	22.4 ± 5.4	0.200
Ejection fraction (%)	46.2 ± 2.9	45.2 ± 2.5	0.806
hs-CRP (mg/L)	3.90 ± 0.8	4.62 ± 0.8	0.509
Drugs consumption %			
Statin	100.0	88.0	0.239
Aspirin	90.5	84.0	0.257
Clopidogrel	68.4	92.0	0.095
NSAID	15.0	4.0	0.197
β blocker	5.9	12.5	
ARB	58.8	50.0	0.555
ACE inhibitor	29.4	12.5	
CCB	5.9	18.8	
Insulin	19.0	19.2	0.324
Oral diabetic drugs	38.1	19.2	

Data are expressed as mean ± SE or percentage; *statistically significant ($P < 0.05$). ISR: in-stent restenosis; NIRS: non-in-stent restenosis; hs-CRP: high-sensitivity C-reactive protein; ARB: angiotensin receptor blockers; ACE: angiotensin converting enzyme; CCB: channel calcium blocker; NSAID: nonsteroidal anti-inflammatory drugs.

regression was used to estimate the association between OS markers with ISR (ref: healthy) and NISR (ref: healthy) after adjustment for age, LDL-C, HDL-C, and FBG levels. $P < 0.05$ were considered statistically significant.

3. Results

3.1. Baseline Characteristics of Subjects. 67 participants were enrolled. 20, 26, and 21 were classified into healthy, NISR,
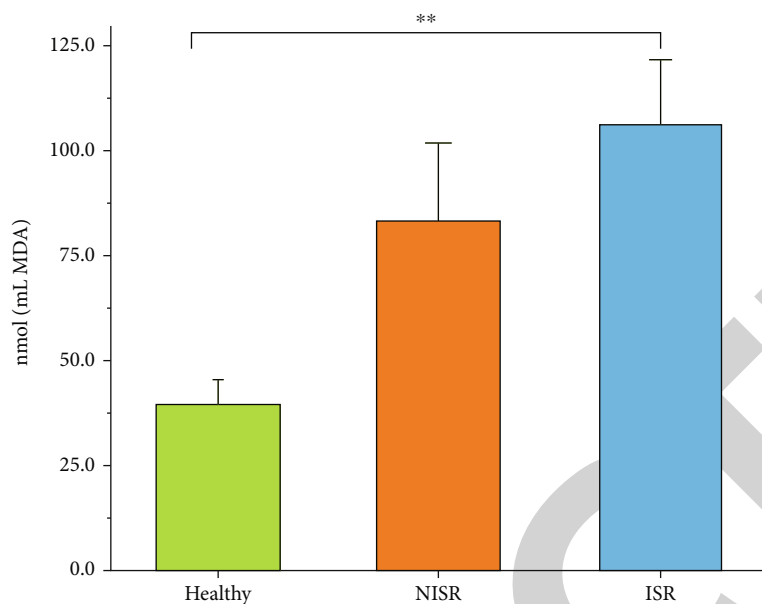
FIGURE 1: Comparison of the MDA levels between the studied groups. Data are expressed as mean ± SE. ∗∗$P < 0.01$. MDA: malondialdehyde; ISR: in-stent restenosis; NISR: non-in-stent-restenosis.
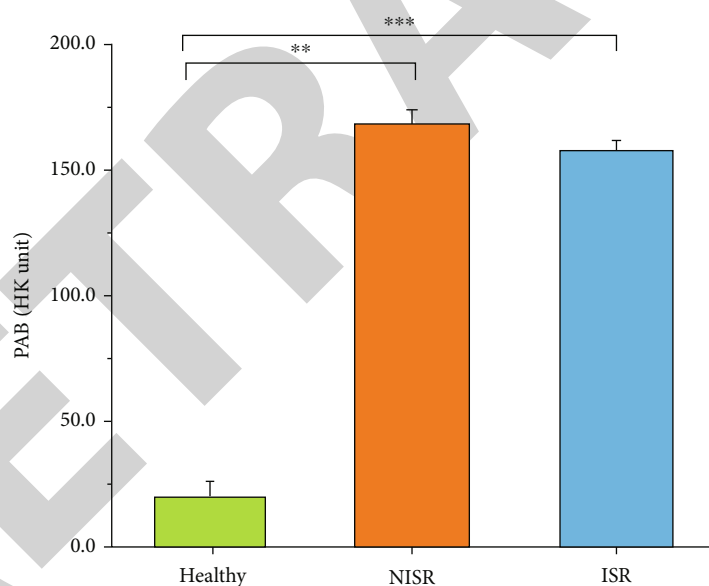
FIGURE 2: Comparison of the PAB between the studied groups. Data are expressed as mean ± SE. ∗∗∗$P < 0.001$. PAB: pro-oxidant-antioxidant balance.

and ISR groups, respectively. Groups were not different in terms of gender, although the healthy group included younger individuals in comparison with ISR ($P < 0.001$) and NISR ($P < 0.001$) groups. Significantly great levels of FBG were observed in both ISR ($P = 0.006$) and NISR ($P = 0.043$) groups relative to healthy subjects. Triglyceride (TG) concentrations also showed higher levels in ISR group when compared to NISR ($P = 0.048$) and healthy ($P = 0.036$) groups. The levels of TC ($P = 0.015$), LDL-C ($P = 0.035$), and HDL-C ($P < 0.001$) were significantly higher in healthy individuals in comparison with NISR group. In addition, a higher level of HDL-C was also found in the healthy group when compared to ISR group ($P = 0.005$) (Table 1).

Moreover, the percentage of patients with DES was significantly higher in the NISR group related to the ISR group (Table 2). Totally, most (71.9%) of the patients (the sum of both ISR and NISR) underwent DES implantation, although about half of them (44.7%) had experienced ISR complications.

3.2. Oxidative Stress Marker Comparison between the Groups. Serum MDA levels were significantly higher in ISR

(a)

(b)

(c)

(d)
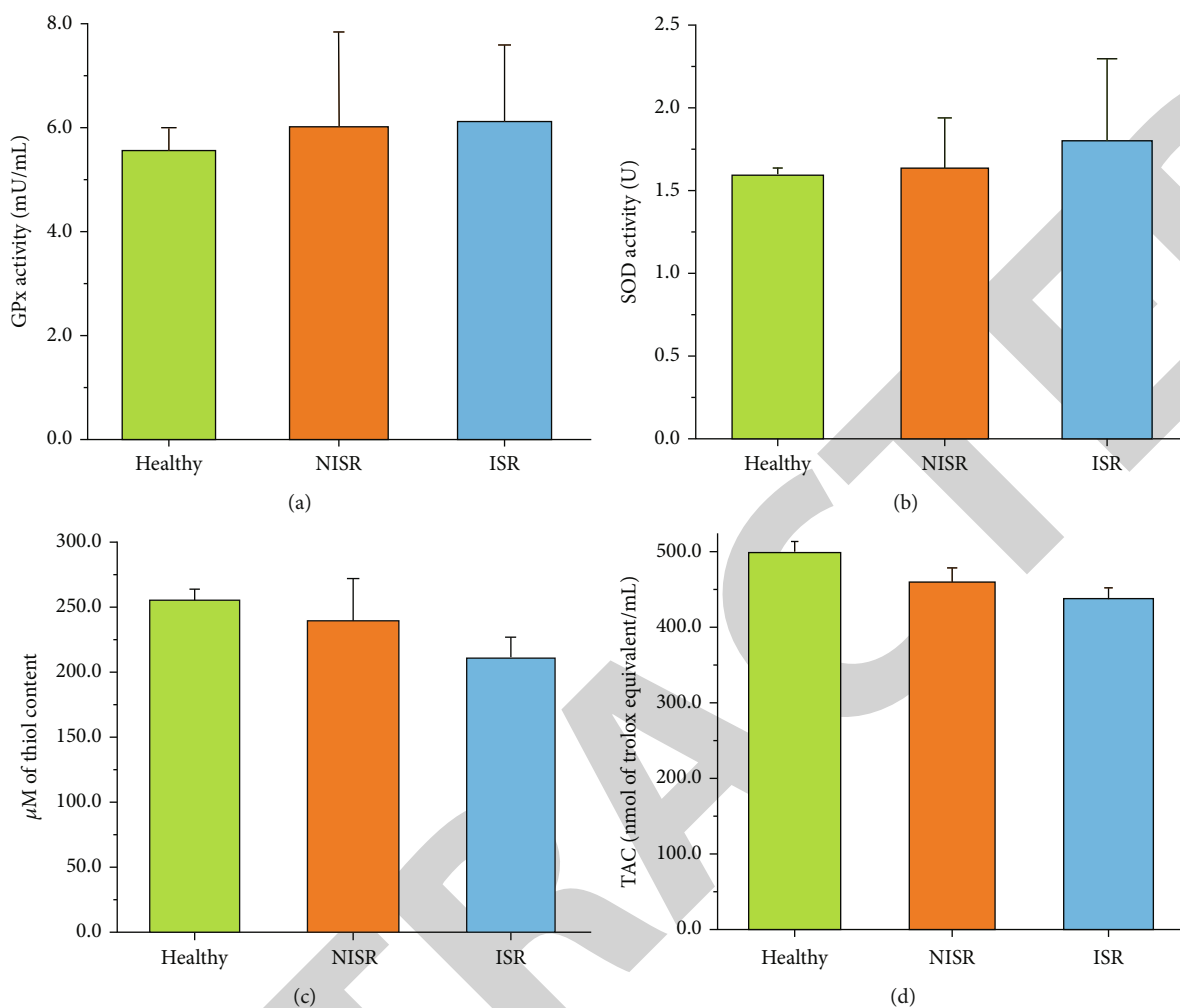
FIGURE 3: Comparison of the (a) GPx activity; (b) SOD activity; (c) total thiol content of serum; (d) TAC of serum between the studied groups. Data are expressed as mean ± SE. GPX: glutathione peroxidase; SOD: superoxide dismutase; TAC: total antioxidant capacity.

TABLE 3: Binary logistic regression for oxidative stress markers in relation to ISR (Ref: NISR).

	ISR			
Variables	Unadjusted		Adjusted[#]	
	OR (95% CI)	P value	OR (95% CI)	P value
GPX activity (mU/mL)	1.003 (0.915-1.100)	0.947	1.249 (0.870-1.794)	0.228
MDA concentration (nmol/mL)	1.004 (0.995-1.013)	0.347	0.986 (0.958-1.015)	0.341
SOD activity (U)*	1.077 (0.709-1.636)	0.727	0.995 (0.367-2.694)	0.992
Thiol concentration (uM)	0.998 (0.993-1.003)	0.436	0.994 (0.984-1.005)	0.268
TAC (nmol of Trolox equivalent/mL)	0.997 (0.990-1.004)	0.432	0.991 (0.976-1.006)	0.242
PAB (HK unit**)	0.984 (0.963-1.006)	0.161	0.996 (0.963-1.030)	0.823

[#]Adjusted for age, sex, LDL-C, HDL-C, and FBG levels, stent type, and use of statins. LDL-C: low-density lipoprotein cholesterol; HDL-C: high-density lipoprotein cholesterol; FBG: fasting blood glucose; ISR: in-stent restenosis; NISR: non-in-stent-restenosis; GPX: glutathione peroxidase; MDA: malondialdehyde; SOD: superoxide dismutase; TAC: total antioxidant capacity; PAB: pro-oxidant-antioxidant balance; OR: odds ratio; CI: confidence interval.

group in comparison with healthy subjects ($P = 0.004$) (Figure 1). PAB also showed greater levels in both ISR ($P < 0.001$) and NISR ($P < 0.001$) groups when compared to healthy subjects (Figure 2). However, no significant differences in the activities of the antioxidant enzymes GPx and

SOD (Figures 3(a) and 3(b), respectively), in thiol levels (Figure 3(c)), and in TAC (Figure 3(d)) were found between the studied groups.

The results of binary logistic regression also failed to show any association between OS markers as well as

TABLE 4: Multinomial logistic regression for oxidative stress markers in relation to ISR and NISR (ref: healthy).

Variables	NISR				ISR			
	Unadjusted OR (95% CI)	P value	Adjusted# OR (95% CI)	P value	Unadjusted OR (95% CI)	P value	Adjusted# OR (95% CI)	P value
GPX activity (mU/mL)	1.017 (0.909-1.138)	0.771	0.820 (0.455-1.476)	0.507	1.021 (0.910-1.146)	0.722	0.841 (0.467-1.514)	0.564
MDA concentration (nmol/mL)	1.023 (1.004-1.043)	0.019*	1.026 (0.966-1.089)	0.409	1.028 (1.008-1.048)	0.006*	1.031 (0.970-1.095)	0.325
SOD activity (U)*	1.030 (0.602-1.762)	0.915	0.0 (0.0)	0.000*	1.144 (0.692-1.893)	0.599	0.0 (0.0)	0.000*
Thiol concentration (uM)	0.999 (0.994-1.004)	0.748	0.988 (0.970-1.006)	0.201	0.995 (0.988-1.003)	0.197	0.985 (0.966-1.003)	0.108
TAC (nmol of Trolox equivalent/mL)	0.994 (0.987-1.002)	0.153	0.987 (0.967-1.008)	0.140	0.990 (0.982-0.999)	0.030*	0.984 (0.964-1.005)	0.227
PAB (HK unit**)	1.094 (1.030-1.162)	0.004*	1.891 (1.847-1.935)	0.000*	1.076 (1.017-1.139)	0.011*	1.866 (1.856-1.900)	0.000*

#Adjusted for age, LDL-C, HDL-C, and FBG levels. LDL-C: low-density lipoprotein cholesterol; HDL-C: high-density lipoprotein cholesterol; FBG: fasting blood glucose; ISR: in-stent restenosis; NISR: non-in-stent-restenosis; GPX: glutathione peroxidase; MDA: malondialdehyde; SOD: superoxide dismutase; TAC: total antioxidant capacity; PAB: pro-oxidant-antioxidant balance; OR: odds ratio; CI: confidence interval.

antioxidant enzyme activities with ISR (reference group: NISR), even after adjustment for age, sex, LDL-C, HDL-C and FBG levels, stent type, and use of statins as confounder factors (Table 3). While multinomial logistic regression showed that elevated levels of MDA (OR: 1.028, 95% CI: 1.008-1.048; $P = 0.006$) and PAB (OR: 1.076, 95% CI: 1.017-1.139; $P = 0.011$) were significantly associated with higher ISR risk (reference group: healthy), increased values of TAC (OR: 0.990, 95% CI: 0.982-0.999; $P = 0.030$) were significantly associated with decreased ISR risk. After adjustment for age, LDL-C, HDL-C, and FBG levels, only elevated PAB and lower SOD activity showed an association with increased ISR risk (Table 4).

High levels of MDA (OR: 1.023, 95% CI: 1.004-1.043; $P = 0.019$) and PAB (OR: 1.094, 95% CI: 1.030-1.162; $P = 0.004$) were also significantly related to the NISR risk. After adjustment for age, LDL-C, HDL-C, and FBG levels, only elevated PAB and lower SOD activity showed an association with increased NISR risk (Table 4).

4. Discussion

It is widely accepted that OS, as an imbalance between pro-oxidants and antioxidants [15], is a major factor involved in the vascular injury that leads to the initiation and progression of ASCVD [15]. In this study, for the first time, several oxidative and antioxidative markers were evaluated simultaneously in Iranian patients who underwent stent implantation. The results indicated some changes in OS markers in patients with ISR. Considerably higher levels of MDA were found in the ISR group compared to the healthy subjects. PAB also illustrated significantly higher values in both ISR and NISR groups compared with the healthy individuals. However, no significant differences were observed between the studied groups regarding other OS markers including thiol levels, antioxidant enzyme activities, and TAC. Previously, an increase in markers of OS has been observed after coronary stent implantation, suggesting OS as a trigger of a complex chain of events leading to restenosis [16, 17]. Limitations of the evaluation of MDA, which showed a higher levels in ISR patients compared to the healthy group, have been discussed; however, the test is very simple, rapid, inexpensive, and relatively reliable [18]. Several studies have shown that the plasma levels of TBARS are significantly elevated in patients with ischemic heart disease [19, 20], and it has been suggested that measurement of this parameter may be clinically useful. In fact, significantly higher levels of MDA were observed in patients with angiographically diagnosed coronary artery disease (CAD) relative to the healthy subjects [21]. Moreover, TBARS levels are significantly higher in patients with restenosis after coronary balloon angioplasty [22]. MDA is one of the most commonly used biomarkers for lipid peroxidation, which is associated with atherosclerosis progression [23]. Increase in serum levels of MDA suggests lipid peroxidation of biological membranes and/or lipoproteins in ISR patients. This hypothesis is supported by previous studies, which have shown the presence of elevated levels of antioxidized LDL antibodies in patients at a high risk for restenosis [24].

The activity of the enzyme Gpx, which protects against lipid peroxidation through reduction of free hydrogen peroxide and lipid hydroperoxides [25], showed no significant difference between the studied groups. In contrast, other authors have demonstrated decreased activity of Gpx in ISR groups in comparison with normal controls [4], as well as in human atherosclerotic tissue [26]. Even the activity of SOD, another endogenous enzymatic free radical scavenger which can efficiently detoxify generated ROS [27], showed no statistically significant differences between our studied groups. Our results on SOD are compliant with previous studies in which no differences between ISR, NISR, and normal controls have been demonstrated [4]. The levels of total thiol content and TAC indicated decreased values in ISR and NISR groups compared with the healthy subjects, but the differences were not statistically significant. Other authors have shown lower thiols [21] and lower TAC levels in CAD patients relative to healthy individuals [28]. The discrepancies might be due to the larger sample size of the referred study relative to the current one. On the other hand, the results of PAB assay, which determines the pro-oxidant burden and antioxidant capacity in a single assay [15], revealed an increase in both ISR and NISR groups, when compared to healthy individuals. Increased values of PAB were observed in patients with CAD compared with healthy subjects and a correlation with the severity of angiographic findings was found [15]. Although antioxidant enzyme activities and TAC had not shown any significant alteration between the groups of this study, elevated value of PAB in ISR and NISR patients might be due to the increased pro-oxidant burden in these patients. Moreover, the results of multinomial logistic regression showed that elevated levels of MDA and PAB and decreased levels of TAC were significantly associated with increased risk of ISR. After adjustment for age, LDL-C, HDL-C, and FBG levels, only elevated PAB and lower SOD activity showed a significant association with increased ISR risk. As reported previously, OS levels represented a strong and independent prognostic predictor of cardiovascular events in patients with CAD [29, 30].

The pleiotropic actions of statins have been previously reported [31–40]. Among these pleiotropic activities are antioxidant effects [41]. Through reduction of superoxide anion formation, increasing eNOS activity, and direct antioxidant activity, statins could decrease OS burden [42–46]. Hence, pre-PCI statin therapy could reduce the major adverse cardiac events including death, MI, and target vessel revascularization [47]. In this study, most of the patients in both ISR and NISR group were on statin medication, which might be the reason for increased antioxidant status in patients as high as healthy subjects. Nevertheless, when the use of statins was considered a confounding variable, the results of multinomial logistic regression just showed a significant association between higher MDA levels and higher ISR risk (OR: 1.049, 95% CI: 1.00-1.099; $P = 0.048$) as well as between higher PAB values and higher NISR risk (OR: 1.587, 95% CI: 1.551-1.623; $P < 0.001$) (data are not shown). In addition, the use of DES in patients who undergo angioplasty therapy could reduce the ISR risk by

30-40% [48, 49]. In the United States, the estimated ISR rate is about 10% [50]. In this study, the number of patients who underwent DES implantation was about 71.9%, though about half of them had experienced ISR complications. Nevertheless, when stent type was considered a confounding parameter, the results of binary logistic regression failed to show any association between OS markers as well as antioxidant enzyme activities with ISR. This might be due to the other characteristics of stents like the size and brand of DESs. This information was not available for our studied patients, and this was a limitation of this study. Furthermore, the small sample size of this study along with the lack of sufficient data regarding other confounders like restenosis in more than one stent, *de novo* stenosis in other vessels, and vessel caliber were other limitations of the current study. In addition, the current findings are confined to the Iranian population and further supportive evidence from other ethnic groups is warranted.

In conclusion, according to our findings, oxidative and antioxidative markers could not distinct ISR from NISR; however, variables like PAB and SOD activity showed a potential for the prediction of both ISR and NISR risk. Therapeutic strategies addressing ROS production and antioxidant systems may prevent OS and complications like ISR in patients who undergo stent implantation. To verify this hypothesis, interventional and prospective studies with larger sample sizes are needed.

Abbreviations

ACE: Angiotensin converting enzyme
ANOVA: One-way analysis of variance
ARB: Angiotensin receptor blockers
CCB: Channel calcium blocker
CI: Confidence interval
CU+:   Cuprous
Cu2+:   Cupric
CVD: Cardiovascular disease
DES: Drug eluting stents
DM: Diabetes mellitus
FBG: Fasting blood glucose
HDL-C: High-density lipoprotein cholesterol
HK unit: Hamidi-Koliakos unit
HTN: Hypertension
hs-CRP: High-sensitivity C-reactive protein
GSH: Glutathione
GPx: Glutathione peroxidase
ISR: In-stent restenosis
LDL-C: Low-density lipoprotein cholesterol
MDA: Malondialdehyde
mg/dL: Milligrams per deciliter
nmol/mL: Nanomole per milliliter
NIRS: Non-in-stent restenosis
NSAID: Nonsteroidal anti-inflammatory drugs
OR: Odds ratio
OS: Oxidative stress
PAB: Pro-oxidant-antioxidant balance
PCI: Percutaneous coronary intervention
ROS: Reactive oxygen species
SE: Standard error
SOD: Superoxide dismutase
TAC: Total antioxidant capacity
TC: Total cholesterol
TG: Triglycerides
Y: Year.

Data Availability

The data are available upon request.

Conflicts of Interest

The authors declare that they have no conflicts of interest.

Authors' Contributions

Shiva Ganjali and Atena Mansouri contributed equally to this work.

References

[1] H. Wang, A. A. Abajobir, K. H. Abate et al., "Global, regional, and national under-5 mortality, adult mortality, age-specific mortality, and life expectancy, 1970–2016: a systematic analysis for the Global Burden of Disease Study 2016," *The Lancet*, vol. 390, no. 10100, pp. 1084–1150, 2017.

[2] E. D. Grech, "Percutaneous coronary intervention. I: history and development," *British Medical Journal*, vol. 326, no. 7398, pp. 1080–1082, 2003.

[3] D. P. Taggart, "Coronary-artery stents," *The New England Journal of Medicine*, vol. 354, no. 19, pp. 2076–2078, 2006.

[4] P. Misra, P. C. Reddy, D. Shukla, G. C. Caldito, L. Yerra, and T. Y. Aw, "In-stent stenosis: potential role of increased oxidative stress and glutathione-linked detoxification mechanisms," *Angiology*, vol. 59, no. 4, pp. 469–474, 2008.

[5] L. Räber, L. Wohlwend, M. Wigger et al., "Five-year clinical and angiographic outcomes of a randomized comparison of sirolimus-eluting and paclitaxel-eluting stents: results of the sirolimus-eluting versus paclitaxel-eluting stents for coronary revascularization LATE trial," *Circulation*, vol. 123, no. 24, pp. 2819–2828, 2011.

[6] K. Yin and D. K. Agrawal, "High-density lipoprotein: a novel target for antirestenosis therapy," *Clinical and Translational Science*, vol. 7, no. 6, pp. 500–511, 2014.

[7] F. G. Welt and C. Rogers, "Inflammation and restenosis in the stent era," *Arteriosclerosis, Thrombosis, and Vascular Biology*, vol. 22, no. 11, pp. 1769–1776, 2002.

[8] V. W. Liu and P. L. Huang, "Cardiovascular roles of nitric oxide: a review of insights from nitric oxide synthase gene disrupted mice," *Cardiovascular Research*, vol. 77, no. 1, pp. 19–29, 2008.

[9] R. P. Juni, H. J. Duckers, P. M. Vanhoutte, R. Virmani, and A. L. Moens, "Oxidative stress and pathological changes after coronary artery interventions," *Journal of the American College of Cardiology*, vol. 61, no. 14, pp. 1471–1481, 2013.

[10] L. C. Azevedo, M. A. Pedro, L. C. Souza et al., "Oxidative stress as a signaling mechanism of the vascular response to injury: the redox hypothesis of restenosis," *Cardiovascular Research*, vol. 47, no. 3, pp. 436–445, 2000.

[11] Y. A. Shuvalova, A. Kaminnyi, A. Meshkov, R. Shirokov, and A. Samko, "Association between polymorphisms of eNOS and GPx-1 genes, activity of free-radical processes and in-stent restenosis," *Molecular and Cellular Biochemistry*, vol. 370, no. 1-2, pp. 241–249, 2012.

[12] M. Baktashian, S. S. Soflaei, N. Kosari et al., "Association of high level of hs-CRP with in-stent restenosis: a case-control study," *Cardiovascular Revascularization Medicine*, vol. 20, no. 7, pp. 583–587, 2019.

[13] S. Ganjali, R. Keshavarz, S. Hosseini et al., "Evaluation of oxidative stress status in familial hypercholesterolemia," *Journal of Clinical Medicine*, vol. 10, no. 24, p. 5867, 2021.

[14] M. Ghayour-Mobarhan, D. H. Alamdari, M. Moohebati et al., "Determination of prooxidant–antioxidant balance after acute coronary syndrome using a rapid assay: a pilot study," *Angiology*, vol. 60, no. 6, pp. 657–662, 2009.

[15] D. H. Alamdari, M. Ghayour-Mobarhan, S. Tavallaie et al., "Prooxidant–antioxidant balance as a new risk factor in patients with angiographically defined coronary artery disease," *Clinical Biochemistry*, vol. 41, no. 6, pp. 375–380, 2008.

[16] X. Li, D. Guo, Y. Chen, Y. Hu, and F. Zhang, "Complex coronary instent chronic total occlusion lesions: oxidative stress, inflammation, and coronary stent lengths," *Oxidative Medicine and Cellular Longevity*, vol. 2021, Article ID 8815048, 11 pages, 2021.

[17] J.-C. Tardif, J. Grégoire, and P. L. L'Allier, "Prevention of restenosis with antioxidants," *American Journal of Cardiovascular Drugs*, vol. 2, no. 5, pp. 323–334, 2002.

[18] R. Lee, M. Margaritis, K. M. Channon, and C. Antoniades, "Evaluating oxidative stress in human cardiovascular disease: methodological aspects and considerations," *Current Medicinal Chemistry*, vol. 19, no. 16, pp. 2504–2520, 2012.

[19] B. R. Maharjan, J. C. Jha, D. Adhikari, R. S. Akila, V. M. Alurkar, and P. P. Singh, "Oxidative stress, antioxidant status and lipid profile in ischemic heart disease patients from western region of Nepal," *Nepal Medical College Journal: NMCJ*, vol. 10, no. 1, pp. 20–24, 2008.

[20] S. V. Drinitsina, T. I. Torkhovskaia, O. A. Azizova et al., "Relation between resistance to oxidation and cholesterol acceptance of high density lipoproteins in patients with ischemic heart disease," *Kardiologiia*, vol. 44, no. 5, pp. 36–39, 2004.

[21] A. Bridges, N. Scott, J. Belch, T. Pringle, and G. Mcneill, "Relationship between the extent of coronary artery disease and indicators of free radical activity," *Clinical Cardiology*, vol. 15, no. 3, pp. 169–174, 1992.

[22] K. Imai, T. Matsubara, M. Kanashiro, S. Ichimiya, and N. Hotta, "Lipid peroxidation may predict restenosis after coronary balloon angioplasty," *Japanese Circulation Journal*, vol. 65, no. 6, pp. 495–499, 2001.

[23] F. Ito, Y. Sono, and T. Ito, "Measurement and clinical significance of lipid peroxidation as a biomarker of oxidative stress: oxidative stress in diabetes, atherosclerosis, and chronic inflammation," *Antioxidants*, vol. 8, no. 3, p. 72, 2019.

[24] J. George, D. Harats, E. Bakshi et al., "Anti-oxidized low density lipoprotein antibody determination as a predictor of restenosis following percutaneous transluminal coronary angioplasty," *Immunology Letters*, vol. 68, no. 2-3, pp. 263–266, 1999.

[25] E. Lubos, J. Loscalzo, and D. E. Handy, "Glutathione peroxidase-1 in health and disease: from molecular mechanisms to therapeutic opportunities," *Antioxidants & Redox Signaling*, vol. 15, no. 7, pp. 1957–1997, 2011.

[26] D. Lapenna, S. de Gioia, G. Ciofani et al., "Glutathione-related antioxidant defenses in human atherosclerotic plaques," *Circulation*, vol. 97, no. 19, pp. 1930–1934, 1998.

[27] E. B. Kurutas, "The importance of antioxidants which play the role in cellular response against oxidative/nitrosative stress: current state," *Nutrition Journal*, vol. 15, no. 1, pp. 1–22, 2015.

[28] S. Nojiri, H. Daida, H. Mokuno et al., "Association of serum antioxidant capacity with coronary artery disease in middle-aged men," *Japanese Heart Journal*, vol. 42, no. 6, pp. 677–690, 2001.

[29] J. Kotur-Stevuljevic, L. Memon, A. Stefanovic et al., "Correlation of oxidative stress parameters and inflammatory markers in coronary artery disease patients," *Clinical Biochemistry*, vol. 40, no. 3-4, pp. 181–187, 2007.

[30] M. F. Walter, R. F. Jacob, B. Jeffers et al., "Serum levels of thiobarbituric acid reactive substances predict cardiovascular events in patients with stable coronary artery disease: a longitudinal analysis of the PREVENT study," *Journal of the American College of Cardiology*, vol. 44, no. 10, pp. 1996–2002, 2004.

[31] A. R. Afshari, H. Mollazadeh, N. C. Henney, T. Jamialahmad, and A. Sahebkar, "Effects of statins on brain tumors: a review," *Seminars in Cancer Biology*, vol. 73, pp. 116–133, 2021.

[32] A. M. Gorabi, N. Kiaie, M. Pirro, V. Bianconi, T. Jamialahmadi, and A. Sahebkar, "Effects of statins on the biological features of mesenchymal stem cells and therapeutic implications," *Heart Failure Reviews*, vol. 26, no. 5, pp. 1259–1272, 2021.

[33] A. Bahrami, N. Parsamanesh, S. L. Atkin, M. Banach, and A. Sahebkar, "Effect of statins on toll-like receptors: a new insight to pleiotropic effects," *Pharmacological Research*, vol. 135, pp. 230–238, 2018.

[34] P. Chruściel, A. Sahebkar, M. Rembek-Wieliczko et al., "Impact of statin therapy on plasma adiponectin concentrations: a systematic review and meta-analysis of 43 randomized controlled trial arms," *Atherosclerosis*, vol. 253, pp. 194–208, 2016.

[35] M. Khalifeh, P. E. Penson, M. Banach, and A. Sahebkar, "Statins as anti-pyroptotic agents," *Archives of Medical Science*, vol. 17, no. 5, pp. 1414–1417, 2021.

[36] N. Shakour, M. Ruscica, F. Hadizadeh et al., "Statins and C-reactive protein: in silico evidence on direct interaction," *Archives of Medical Science*, vol. 16, no. 6, pp. 1432–1439, 2020.

[37] A. Vahedian-Azimi, S. M. Mohammadi, F. H. Beni et al., "Improved COVID-19 ICU admission and mortality outcomes following treatment with statins: a systematic review and meta-analysis," *Archives of Medical Science*, vol. 17, no. 3, pp. 579–595, 2021.

[38] D. Yu and J. K. Liao, "Emerging views of statin pleiotropy and cholesterol lowering," *Cardiovascular Research*, vol. 118, no. 2, pp. 413–423, 2022.

[39] S. Dehnavi, A. Kiani, M. Sadeghi et al., "Targeting AMPK by statins: A potential therapeutic approach," *Drugs*, vol. 81, no. 8, pp. 923–933, 2021.

[40] A. Sahebkar, K. Kotani, C. Serban et al., "Statin therapy reduces plasma endothelin-1 concentrations: a meta-analysis of 15 randomized controlled trials," *Atherosclerosis*, vol. 241, no. 2, pp. 433–442, 2015.

Hindawi

Retraction

Retracted: Conservative Therapy vs. Endovascular Approach for Intracranial Vertebrobasilar Artery Trunk Large Aneurysms: A Prospective Multicenter Cohort Study

Oxidative Medicine and Cellular Longevity

This article has been retracted by Hindawi following an investigation undertaken by the publisher [1]. This investigation has uncovered evidence of one or more of the following indicators of systematic manipulation of the publication process:

(1) Discrepancies in scope
(2) Discrepancies in the description of the research reported
(3) Discrepancies between the availability of data and the research described
(4) Inappropriate citations
(5) Incoherent, meaningless and/or irrelevant content included in the article
(6) Peer-review manipulation

The presence of these indicators undermines our confidence in the integrity of the article's content and we cannot, therefore, vouch for its reliability. Please note that this notice is intended solely to alert readers that the content of this article is unreliable. We have not investigated whether authors were aware of or involved in the systematic manipulation of the publication process.

In addition, our investigation has also shown that one or more of the following human-subject reporting requirements has not been met in this article: ethical approval by an Institutional Review Board (IRB) committee or equivalent, patient/participant consent to participate, and/or agreement to publish patient/participant details (where relevant).

Wiley and Hindawi regrets that the usual quality checks did not identify these issues before publication and have since put additional measures in place to safeguard research integrity.

We wish to credit our own Research Integrity and Research Publishing teams and anonymous and named external researchers and research integrity experts for contributing to this investigation.

The corresponding author, as the representative of all authors, has been given the opportunity to register their agreement or disagreement to this retraction. We have kept a record of any response received.

References

[1] Q. Wu, T. Li, W. Jiang, J. A. Hernesniemi, L. Li, and Y. He, "Conservative Therapy vs. Endovascular Approach for Intracranial Vertebrobasilar Artery Trunk Large Aneurysms: A Prospective Multicenter Cohort Study," *Oxidative Medicine and Cellular Longevity*, vol. 2022, Article ID 9682507, 10 pages, 2022.

Research Article

Conservative Therapy vs. Endovascular Approach for Intracranial Vertebrobasilar Artery Trunk Large Aneurysms: A Prospective Multicenter Cohort Study

Qiaowei Wu [1,2] **Tianxiao Li,**[1] **Weijian Jiang,**[3] **Juha Antero Hernesniemi,**[1] **Li Li,**[1] **and Yingkun He** [1]

[1]*Cerebrovascular Department of Interventional Center, Zhengzhou University People's Hospital, Henan University People's Hospital and Henan Provincial People's Hospital, Zhengzhou, Henan, China*
[2]*Department of Neurosurgery, The First Affiliated Hospital of Harbin Medical University, Harbin, Heilongjiang, China*
[3]*Department of Vascular Neurosurgery, Chinese People's Liberation Army Rocket Force Characteristic Medical Center, Beijing, China*

Correspondence should be addressed to Yingkun He; heyingkun@henu.edu.cn

Background. Intracranial vertebrobasilar trunk large (≥10 mm) aneurysms (IVBTLAs) are rare and challenging to manage. In this study, we describe the natural prognosis and evaluate the safety and efficacy of endovascular treatment of IVBTLAs compared with conservative therapy. *Methods*. This prospective multicenter cohort study included patients with IVBTLAs, who chose either endovascular treatment (endovascular group) or conservative therapy (conservative group) after discussion with their doctors. The primary endpoint was the incidence of serious adverse events (SAEs) related to the target vessel, while secondary endpoints included target vessel-related mortality, major stroke, other serious adverse events, and aneurysm occlusion rate. *Results*. In total, 258 patients were referred to our two centers for the management of vertebrobasilar aneurysms, and 69 patients had IVBTLAs. Among them, 51 patients underwent endovascular treatment, and 18 patients received conservative therapy. The incidence of target vessel-related SAEs was 15.7% (8/51) in the endovascular group and 44.4% (8/18) in the conservative group ($P = 0.031$). The target vessel-related mortality was 2.0% (1/51) in the endovascular group and 38.9% (7/18) in the conservative group ($P < 0.001$). The cumulative survival rates in the endovascular group and conservative group within 1-year, 3-year, and 5-year were 98.0% vs. 83.3%, $P = 0.020$; 98.0% vs. 66.7%, $P = 0.001$; and 98.0% vs. 35.6%, $P < 0.001$, respectively. Multivariate analysis revealed conservative therapy, giant aneurysm, and ischemic onset as risks factor for SAEs. *Conclusions*. Compared with conservative treatment, endovascular treatment of the IVBTLAs may be associated with a lower incidence of SAEs, with higher 1-year, 3-year, and 5-year survival rates. Conservative therapy, giant aneurysm, and ischemic onset were associated with a high risk of SAEs.

1. Introduction

The intracranial vertebrobasilar trunk artery is defined as the arterial segment extending from the origin of the intracranial vertebral artery up to the origin of the superior cerebellar artery. Aneurysms originating from the branch of the vertebrobasilar artery and basilar tip aneurysms are excluded from intracranial vertebrobasilar trunk aneurysms [1]. Endovascular treatment is the most commonly used method

for treatment of these aneurysms, which have always posed a great challenge to physicians due to their location, pathological features, relation to perforating branches of the vertebrobasilar artery, higher risks of procedural complications, and poorer outcomes compared with anterior circulation aneurysms [2–5]. According to published studies, aneurysms could be defined as small aneurysms (<10 mm in maximum diameter), large aneurysms (10 to <25 mm), and giant aneurysms (≥25 mm) [6, 7]. As intracranial vertebrobasilar trunk

large (≥10 mm) aneurysms (IVBTLAs) rarely occur, there are limited data on the epidemiology, natural history, and management, besides case reports [1, 8–10]. The natural prognosis of IVBTLAs and the safety and efficacy of endovascular treatment still need to be further confirmed. Therefore, this study was conducted to explore the natural prognosis of conservative therapy and the safety and efficacy of endovascular treatment of IVBTLAs.

2. Materials and Methods

2.1. Study Design and Participants. This prospective multicenter cohort study of conservative therapy versus endovascular approach for IVBTLAs was conducted in Henan Provincial People's Hospital and Chinese People's Liberation Army Rocket Force Characteristic Medical Center between October 2012 and October 2018. The date of follow-up was ended in March 2019. The institutional review board of the lead center (Henan Provincial People's Hospital) approved the study (No. 12072), and the ethics approval documents were recorded and registered in Chinese People's Liberation Army Rocket Force Characteristic Medical Center. The study was carried out in accordance with the 1964 Declaration of Helsinki. Informed consent was obtained from the patients before the enrollment of the study, and the treatment decision was made. The doctors informed the patients of all treatment options, after which the patients individually discussed with their doctors and chose endovascular treatment (endovascular group) or refused to receive further surgical treatment (conservative group).

The major criterion for inclusion in the study was aneurysm arising from the intracranial vertebrobasilar trunk artery, measuring ≥10 mm in diameter and modified Rankin Scale (mRS) ≤ 2 before the symptom onset. The major cause for exclusion was an aneurysm involving the extracranial segment of vertebral artery, basilar tip, and superior cerebellar artery aneurysms, complicated by other intracranial aneurysms. Patients with vertebrobasilar dolichoectasia were also excluded. Patients' inclusion and exclusion criteria are detailed in Supplemental Table 1.

2.2. Endovascular Treatment. The endovascular strategies for all patients in the endovascular group can be divided into 3 following techniques: reconstructive technique, deconstructive technique, and combination therapy.

2.2.1. Reconstructive Technique. The reconstructive technique included coiling, stent-assisted coiling, and flow diversion (FD). The parent artery maintained patency after the procedure. The technique was mostly used in patients with saccular aneurysms, patients with insufficient collateral circulation, or other aneurysms at the discretion of the neurointerventionists. The procedures were performed under general anesthesia and systemic heparinization (50–70 U/kg). After sheath placement, a suitable guiding catheter was placed in the distal vertebral artery. Three-dimensional (3D) rotational angiography was performed, and 3D reconstruction was used to determine the work projection, measure the parent artery and aneurysms, and determine the treatment

protocol. Depending on operator preferences, aneurysms were coiled with stent-assisted by LVIS (MicroVention-Terumo, California, USA), Enterprise (Codman Neurovascular, Massachusetts, USA), Solitaire (ev3, Irvine, California, USA), and LEO (Balt, Montmorency, France). A Pipeline embolization device (Covidien, Irvine, California, USA) was used for patients with FD treatment.

2.2.2. Deconstructive Technique. The deconstructive technique included parent artery sacrifice and aneurysm embolization combined with parent artery sacrifice. Preliminary digital subtraction angiography (DSA) with a collateral circulation test and a balloon occlusion test (BOT) under local infiltration anesthesia and systemic heparinization was performed before the procedure. The balloon was placed in the proximal parent artery. In addition, prior to balloon inflation, the mean arterial pressure was pharmacologically decreased by a third, in order to maximize the sensitivity of the BOT. After the balloon inflation, a 30 min observation was maintained [11]. If the neurological status remained unchanged during the BOT, the aneurysm occlusion and parent artery sacrifice were performed using coils.

2.2.3. Reconstruction and Deconstruction Combined Technique. The combined technique of reconstruction and deconstruction incorporated the characteristics of the two methods, where reconstruction therapy ensured the unobstructed parent artery, and unilateral vertebral artery sacrificing reduced the blood flow to the aneurysm.

2.3. Antiplatelet Therapy. For patients with unruptured aneurysms who underwent reconstructive therapy or combined therapy, daily dual antiplatelet therapy (75 mg clopidogrel and 100 mg aspirin) was prescribed for at least 3-5 days before the procedural. For patients with ruptured aneurysms, a loading dose of 300 mg clopidogrel and 300 mg aspirin or tirofiban (intravenous bolus (8 μg/kg) over 3 min followed by a maintenance dose of 0.1 mg/kg/min for 24-48 h) was administrated [12, 13]. At least 3 days after the dual antiplatelet administration, thromboelastography (TEG) was used to evaluate the platelet function. For clopidogrel hyporesponders, the clopidogrel would be changed to ticagrelor 90 mg, twice daily. Daily antiplatelet therapy (75 mg clopidogrel and 100 mg aspirin) was maintained for at least 3 months, while 100 mg aspirin was continued indefinitely.

2.4. Conservative Therapy. Conservative therapy was divided into 2 strategies: antiplatelet therapy and risk factors control. For patients with ischemic onset, the daily antiplatelet agent was used (75 mg clopidogrel or 100 mg aspirin) infinitely. TEG was also used to test the platelet function, and for clopidogrel hyporesponders, the clopidogrel would be changed to ticagrelor. In addition, risk factors such as hypertension, diabetes, and smoking were controlled. Patients with hemorrhage or other onset were treated by controlling risk factors. Daily blood pressure and blood glucose measurements were instructed to all the patients with hypertension and diabetes to ensure the modification.
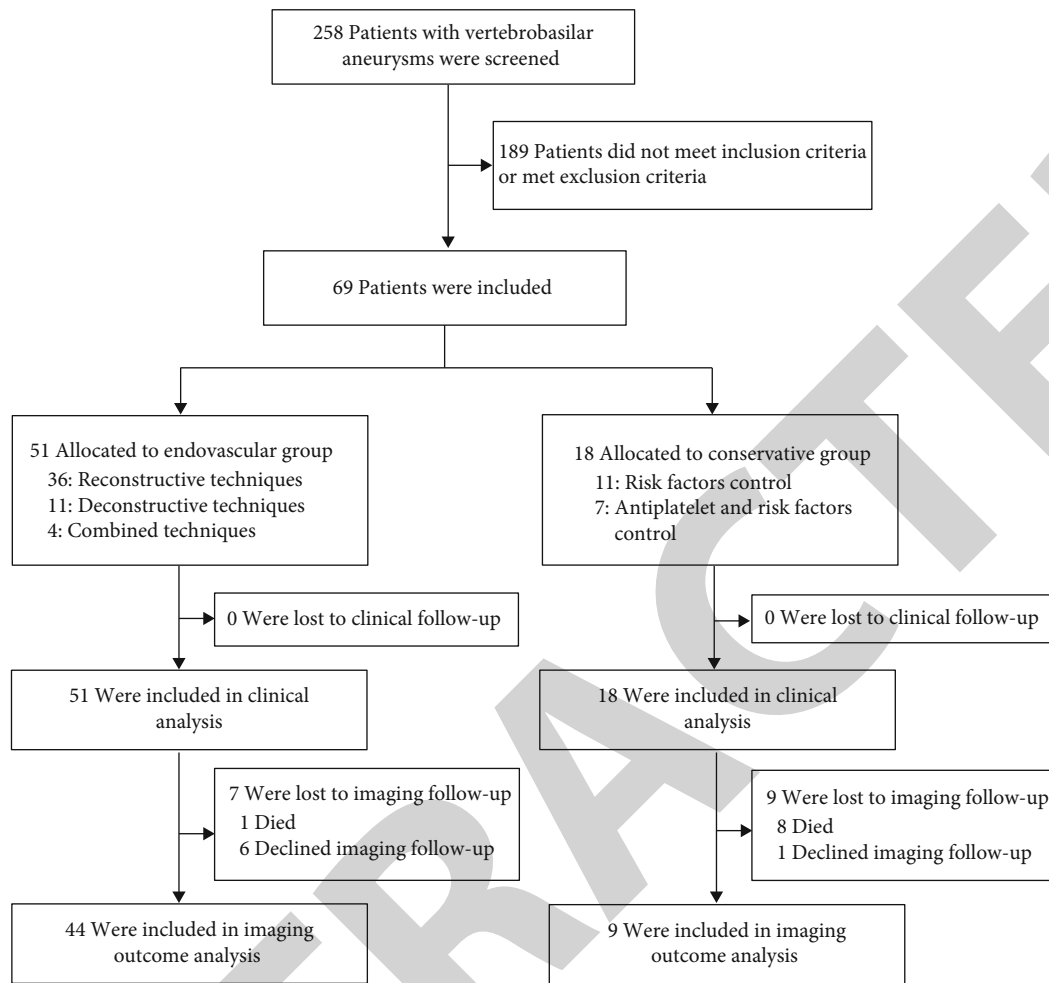
```
┌──────────────────────────────┐
│ 258 Patients with vertebrobasilar │
│ aneurysms were screened       │
└──────────────────────────────┘
              │
              │    ┌────────────────────────────────────┐
              ├───▶│ 189 Patients did not meet inclusion criteria │
              │    │ or met exclusion criteria           │
              │    └────────────────────────────────────┘
              ▼
┌──────────────────────────────┐
│ 69 Patients were included     │
└──────────────────────────────┘
```

FIGURE 1: Flow chart of the patient selection process.

2.5. Follow-Up. Patients underwent clinical assessments at day 1, day 7, day 30, 6 months, 1 year, and annual follow-up postprocedure. Imaging follow-up (DSA or MR) was performed at 6 months postprocedure. All clinical and imaging data were submitted for assessment by an independent laboratory. Investigators were requested to report all adverse events and to judge the relationship to the target vessel. Ischemic stroke was evaluated by the National Institute of Health Stroke Scale (NIHSS); NIHSS increase < 6 was defined as minor stroke, while NIHSS increase ≥ 6 was defined as major stroke. Clinical outcomes were evaluated by mRS, and mRS ≤ 2 was defined as a good outcome. The degree of aneurysm occlusion status was evaluated according to the Roy–Raymond grading scale [14].

2.6. Study Endpoints. The primary endpoint was the incidence of serious adverse events (SAEs) related to the target vessel, which included death, thromboembolic events (partial or complete occlusion of parent artery on DSA or thromboembolism symptoms with or without cerebral infarction on postprocedural MRI/CT), hemorrhagic events (new intracranial hemorrhage on postprocedural head CT/MRI with or without certain clinical symptoms), or other threatening events, leading to hospitalizations or prolonged hospitalizations.

Secondary endpoints included target vessel-related mortality, major stroke (ischemic or hemorrhagic), other SAEs, and aneurysm occlusion rate.

2.7. Statistical Analysis. Statistical analysis was performed using SPSS 22.0 software (IBM SPSS Inc., Chicago, IL, USA) by independent statisticians. Continuous variables were presented as mean ± SD, median, and interquartile range (IQR). Qualitative variables were presented as numbers followed by percentages. Independent-sample t-test, chi-square test, and Fisher's exact test were used to verify the differences between variables. Kaplan-Meier survival analysis was used to compare the cumulative incidence of SAEs and death in the endovascular and conservative groups. Univariate and multivariate Cox regression analysis was performed to identify the independent risk factors for SAEs. $P < 0.05$ was considered as statistically significant.

3. Results

3.1. Patients' Characteristics. Between October 2012 and October 2018, a total of 258 patients were referred to our two centers for the management of vertebrobasilar aneurysms, and 69 patients were enrolled in our study (Figure 1). The

TABLE 1: Baseline characteristics of patients and aneurysms.

Characteristics	Endovascular group ($n = 51$)	Conservative group ($n = 18$)	P value
Male, n (%)	38 (74.5)	10 (55.6)	0.133
Age (years) (IQR)	56.0 (43.0, 62.0)	58.5 (51.0, 66.3)	0.107
Risk factors, n (%)			
Hypertension	33 (64.7)	17 (94.4)	0.034
Diabetes mellitus	1 (2.0)	0	1.000
Smoking	11 (21.6)	2 (11.1)	0.532
Family history	1 (2.0)	0	0.739
Onset symptoms, n (%)			0.119
Ischemic stroke	12 (23.5)	7 (38.9)	
Hemorrhage	8 (15.7)	0	
Others	31 (60.8)	11 (61.1)	
Aneurysm location, n (%)			<0.001
BA	21 (41.2)	6 (33.3)	
VBJ	5 (9.8)	11 (61.1)	
VA	25 (49.0)	1 (5.6)	
Aneurysm shape, n (%)			1.000
Saccular	14 (27.5)	5 (27.8)	
Fusiform and/or dissecting	37 (72.5)	13 (72.2)	
Aneurysm's size, n (%)			0.030
Large	41 (80.4)	9 (50.0)	
Giant	10 (19.6)	9 (50.0)	
Wide-necked aneurysms, n (%)	47 (92.2)	17 (94.4)	1.000
Aneurysms involving side branches, n (%)	17 (33.3)	9 (50.0)	0.210

IQR: interquartile range; BA: basilar artery; VBJ: vertebrobasilar junction; VA: vertebral artery.

cohort comprised 48 (69.6%) males and 21 (30.4%) females, with a median age of 56.0 years (IQR, 47.5-62.5). The maximal median diameter of the aneurysms was 14.8 mm (IQR, 12.0-20.0). Most aneurysms were located in the basilar artery ($n = 27$, 39.1%), followed by vertebral artery ($n = 26$, 37.7%), and vertebrobasilar junction ($n = 16$, 23.2%). Among the 69 patients, 51 underwent the endovascular treatment (endovascular group), and 18 received the antiplatelet and (or) risk factors control treatment (conservative group). The conservative group had higher rates of hypertension and giant aneurysms compared to the endovascular group (94.4% vs. 64.7%, $P = 0.034$; 50.0% vs. 19.6%, $P = 0.030$). Detailed baseline patient and aneurysm characteristics are shown in Table 1.

Of the 51 patients in the endovascular group, 36 (70.6%) underwent the reconstructive treatment, 11 (21.6%) underwent the deconstructive treatment, and 4 (7.8%) underwent the combined treatment. Detailed procedure-related data are shown in Table 2. In the conservative group, 11 (61.1%) patients received the risk factor control, and 7 (38.9%) received the antiplatelet and risk factor control treatment.

3.2. Primary Endpoint. The clinical follow-up was available for all the 69 patients, with a median of 34.0 (IQR, 6.5-47.5) months. The incidence of all SAEs associated with the target vessel was 15.7% (8/51) in the endovascular group and 44.4% (8/18) in the conservative group (RR = 0.35, 95% CI, 0.16-0.80; $P = 0.031$). The proportion

of cases with good outcomes (mRS ≤ 2) in the endovascular group was higher than that in the conservative group (88.2% vs. 55.6%, $P = 0.009$) (Table 3).

Among 8 patients with SAEs in the endovascular group, 4 had ischemic symptoms with the final mRS of 3, 3, 4, and 4, respectively. Transient ischemic symptoms were found in 3 patients with the final mRS of 1, 0, and 0, respectively. One patient suffered subarachnoid hemorrhage (SAH) 3 months after the procedure and subsequently died (Supplemental Figure 1). Among 8 patients with SAEs in the conservative group, 4 died due to the aneurysm rupture. One patient died due to brainstem compression, and 2 due to an ischemic stroke. The remaining patient had persistent ischemic symptoms and a final mRS of 1.

3.3. Other Outcomes. During the follow-up, significantly lower mortality was found in the endovascular group compared to the conservative group (2.0% vs. 38.9%, $P < 0.001$). The proportion of patients with hemorrhagic stroke was also higher in the conservative group (2.0% vs. 22.2%, $P = 0.020$). The proportion of patients with ischemic stroke was similar between the endovascular group and conservative group (13.7% vs. 16.7%, $P = 1.000$). Fifty-three imaging follow-ups were analyzed at a median of 6.0 (IQR, 6.0-12.5) months, revealing 56.8% (25/44) of the aneurysms in the endovascular group with complete occlusion (Supplemental Figure 2), while no aneurysms occluded (0/9) in the

Table 2: Endovascular procedure-related data.

Procedure details	$n = 51$ patients
Catheter access, n (%)	51 (100)
Femoral access	47 (92.2)
Radial access	3 (5.9)
Brachial access	1 (2.0)
Reconstructive treatment, n (%)	36 (70.6)
Sole stenting	6/36 (16.7)
Single stent	2/6 (33.3)
Series stents	4/6 (66.7)
Stent-assisted coiling	26/36 (72.2)
Single stent-assisted	11/26 (42.3)
Series stent-assisted	15/26 (57.7)
Flow diverter treatment	4/36 (11.1)
Flow diverter alone	2/4 (50)
Adjunct coiling	2/4 (50)
Deconstructive treatment, n (%)	11 (21.6)
Reconstruction and deconstruction combined treatment, n (%)	4 (7.8)
Stent-assisted coiling and unilateral vertebral artery sacrifice	3/4 (75)
FD implantation and unilateral vertebral artery sacrifice	1/4 (25)
Antiplatelet treatment application after the procedure, n (%)	40 (78.4)
Type of stent placed, n (%)	$n = 67$ stents
LVIS	22 (32.8)
Enterprise	34 (50.7)
LEO	4 (6.0)
Solitaire	2 (3.0)
Pipeline embolization device	5 (7.5)

conservation group. The detailed outcomes are described in Table 3.

3.4. Survival Analysis. The 1- and 3-year SAE-free cumulative survival rates of patients in the endovascular group were similar to those in the conservative group (88.2%, 95% CI: 29.5% to 99.3% vs. 76.9%, 95% CI: 18.8% to 97.9%, $P = 0.322$; 85.5%, 95% CI: 28.7% to 98.9% vs. 61.5%, 95% CI: 13.1% to 94.4%, $P = 0.085$). The 5-year SAE-free cumulative survival rate of patients in the endovascular group was higher compared to that in the conservative group (85.5%, 95% CI: 28.7% to 98.9% vs. 32.8%, 95% CI: 3.1% to 88.1%, $P = 0.007$) (Figure 2). Also, the 1-year, 3-year, and 5-year overall cumulative survival rates of patients in the endovascular group were higher than those in the conservative group (98.0%, 95% CI: 19.5% to 99.9% vs. 83.3%, 95% CI: 20.4% to 99.0%, $P = 0.020$; 98.0%, 95% CI: 19.5% to 99.9% vs. 66.7%, 95% CI: 14.5% to 95.9%, $P = 0.001$; and 98.0%, 95% CI: 19.5% to 99.9% vs 35.6%, 95% CI: 3.6% to 89.2%, $P < 0.001$) (Figure 2, Supplemental Table 2).

3.5. Subgroup Analysis. There was no significant difference ($P = 1.000$) in the overall SAEs between constructive treat-

ment (5/36, 13.9%) and deconstructive treatment (1/11, 9.1%). For patients with unruptured aneurysms, the incidence of overall SAEs in the endovascular group was lower than that in the conservative group (7/43, 16.3% vs 8/18, 44.4%, $P = 0.045$). For patients treated with reconstructive techniques, stent-assisted coiling showed a higher complete aneurysm occlusion rate compared with sole stenting or sole FD implantation (13/24, 54.2% vs 0/7, 0%, $P = 0.025$). Deconstructive treatment was associated with high rates of complete occlusion of aneurysms in comparison to reconstructive treatment (10/10, 100% vs. 13/31, 41.9%, $P = 0.004$).

3.6. Risk Factors of SAEs. Univariate analysis showed that ischemic onset ($P = 0.006$), aneurysms involving basilar artery ($P = 0.054$), giant aneurysms ($P = 0.011$), and conservative treatment ($P = 0.002$) were related to SAEs. Multivariate analysis revealed fewer SAEs in the endovascular group than in the conservative group (HR = 4.42, 95% CI: 1.48 to 13.19; $P = 0.008$). Also, ischemic onset (HR = 3.33, 95% CI: 1.19 to 9.32; $P = 0.022$) and giant aneurysms (HR = 2.85, 95% CI: 1.01 to 8.04; $P = 0.049$) resulted as statistically significant risk factors associated with SAEs after controlling for fusiform and/or dissecting aneurysms and aneurysms involved basilar artery (Table 4).

4. Discussion

Currently, there are limited reports on the epidemiology of IVBTLAs. Previous studies have shown that the percentage of vertebrobasilar or posterior cerebral artery aneurysms (basilar tip aneurysms were not included) among the overall aneurysm locations is 6.6% [6], with an overall dismal prognosis after the aneurysm rupture [5]. In addition, Mizutani et al. [15] reported that the recurrent rupture rate of untreated ruptured vertebrobasilar was 71.4%, and it most commonly occurred within 24 hours after the first rupture, resulting in a mortality of 46.7%. Due to the high risk of rupture and poor natural history of IVBTLAs, once detected, it is important to individualize surgical intervention on the basis of the patient's overall medical condition, and aneurysm obliteration should be performed as soon as the patient is medically stabilized because of rebleeding [15]. In our study, the mortality of the conservative group was 38.9% (7/18), where 4 (4/7, 57.1%) cases were due to ruptured aneurysms.

The anatomy location and pathological feature of large vertebrobasilar aneurysms, such as the limited surgical accessibility and the relation to perforating branches, limit open surgical options, including clipping, wrapping, vessel occlusion, and bypass, which are often associated with high morbidity and mortality [16, 17]. Endovascular treatment has been increasingly used for treating such aneurysms, which can avoid the extensive surgical invasion and cranial nerve deficits associated with open surgery [2, 16, 18]. In this study, the overall target vessel-related SAE rate in the endovascular group was 15.7%, which was significantly lower compared to that in the conservative group. Especially low mortality (2.0%) and hemorrhagic stroke rate (2.0%) were also observed. Endovascular therapy can be divided into two methods according to different therapeutic concepts:

Table 3: Treatment and imaging outcomes of patients.

Characteristics	Endovascular group	Conservative group	RR (95% CI)	P value
Number of patients with clinical FU	51	18	—	—
Median clinical FU (m) (IQR)	39.0 (9.0, 48.0)	19.5 (4.8, 38.3)	—	0.030
Overall SAEs, n (%)	8 (15.7)	8 (44.4)	0.35 (0.16-0.80)	0.031
Death	1 (2.0)	7 (38.9)	0.05 (0.01-0.38)	<0.001
Ischemic stroke	7 (13.7)	3 (16.7)	0.82 (0.24-2.8)	1.000
Major stroke	4 (7.8)	2 (11.1)		
Minor stroke	3 (5.9)	1 (5.6)		
Hemorrhage	1 (2.0)	4 (22.2)	0.09 (0.01-0.74)	0.020
Others	2 (3.9)	1 (5.6)	0.71 (0.07-7.33)	1.000
SAEs within 30 d of enrollment*, n (%)	6 (11.8)	2 (11.1)	1.06 (0.24-4.78)	1.000
Death	0	2 (11.6)	0.07 (0.01-1.45)	0.065
Ischemic stroke	5 (9.8)	1 (5.6)	1.77 (0.22-14.11)	0.949
Major stroke	2 (3.9)	1 (5.6)		
Minor stroke	3 (5.9)	0		
Hemorrhage	1 (2.0)	1 (5.6)	0.35 (0.02-5.53)	0.457
SAEs 30 d after enrollment*, n (%)	4 (7.8)	6 (33.3)	0.24 (0.08-0.74)	0.024
Death	1 (2.0)	5 (27.8)	0.07 (0.01-0.56)	0.004
Ischemic stroke	2 (3.9)	2 (11.6)	0.35 (0.05-2.32)	0.592
Major stroke	2 (3.9)	1 (5.6)		
Minor stroke	0	1(5.6)		
Intracranial hemorrhage	1 (2.0)	3 (16.7)	0.12 (0.01-1.06)	0.086
Others	1 (2.0)	1 (5.6)	0.35 (0.02-5.35)	0.457
mRS at last follow-up, n (%)			—	0.009
0-2	45 (88.2)	10 (55.6)		
3-6	6 (11.8)	8 (44.4)		
Number of patients with imaging FU	44	9		
Median imaging FU (m) (IQR)	6.0 (6.0, 12.0)	12.0 (12.0, 22.0)		
Aneurysm imaging finding, n (%)			—	<0.001
Occluded	25 (56.8)	0		
Improved	3 (6.8)	0		
Stable	9 (20.5)	5 (55.6)		
Recanalized	5 (11.4)	0		
Enlarged	2 (4.5)	4 (44.4)		

FU: follow-up; IQR: interquartile range; SAEs: serious adverse events; mRS: modified Rankin Scale. *One patient experienced two intracranial hemorrhage events, one within 30 days of enrollment and one 30 days after enrollment. One patient experienced a minor stroke within 30 days and an SAE (gross hematuria) after 30 days. One patient had a major stroke within 30 days and a minor stroke after 30 days.

(1) aneurysm treated by coiling, stent-assisted coiling, or FD (reconstructive treatment) and (2) parent artery sacrifice (deconstructive treatment). In specific cases, it is also possible to combine these two methods. BOT is necessary before the deconstructive treatment so as to avoid severe ischemic stroke after occlusion, especially fatal brainstem ischemia. Parent artery sacrifice should only be considered if the collateral circulation is good. Nevertheless, patients with a negative BOT are still at risk for ischemia, and sometimes, bypass procedures are needed [2, 19, 20]. Then again, a large meta-analysis reported that aneurysms were more likely to be completely occluded after the deconstructive treatment, with the complete occlusion rate which was 93% and 71% after deconstructive and reconstructive treatments, respec-

tively [2]. Another meta-analysis also demonstrated that the deconstructive treatment was associated with higher rates of complete aneurysmal occlusion compared with reconstructive treatment (88.0% vs. 81.0%) [21]. In the present study, the complete occlusion rate was 100% without an increase in ischemic complications.

With the development of new intracranial stents, reconstructive treatments of large intracranial aneurysms have become more widely used, especially in patients with insufficient collateral circulation [2, 22, 23]. However, single stenting or series stenting of IVBTLAs cannot completely obliterate the aneurysm sac. In our study, 2 cases underwent the single stenting, and 4 underwent the series stenting; however, all the aneurysms remained unchanged during
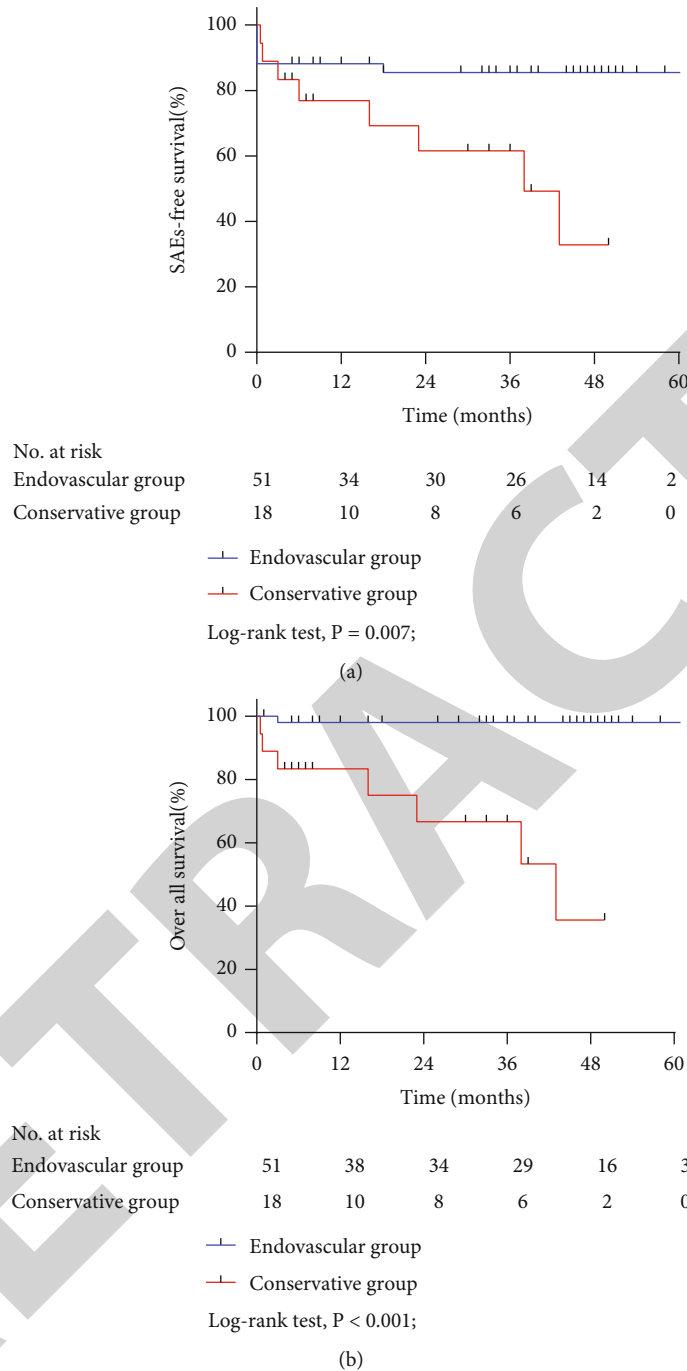
FIGURE 2: Kaplan–Meier survival curves for SAE-free cumulative survival rates (a) and overall cumulative survival rates (b) according to treatment.

the follow-up. The concomitant coiling was needed to facilitate the aneurysmal occlusion and prevent the rupture of aneurysms. For large or giant vertebrobasilar aneurysms treated with stent-assisted coiling, Li et al. [24] reported a recurrence rate of 33.3%, while Mu and colleagues [25] reported a recanalization rate of 66.6%, with a complication rate of 36.4%. In our study, the complete occlusion rate was 54.2% during the follow-up after stent-assisted coiling, and the SAE rate was 15.4%, including mortality of 3.9%. Over recent years, FD has been used as a reconstructive option.

In the present study, only a few patients were treated with FD, and the long-term results remain to be observed. Nonetheless, previous studies have shown promising results after FD treatment of intracranial vertebrobasilar aneurysms [22, 26–28]. Kumar et al. [27] compared the long-term imaging outcomes of intradural vertebral artery aneurysms following parent artery sacrifice or FD treatment, revealing a complete occlusion rate of 81.5% in the FD group and comparable intraprocedural complications and long-term clinical and imaging outcomes. Bhogal et al. [28] reported

Table 4: Univariable and multivariable analysis for serious adverse events.

Variable	Univariable			Multivariable		
	HR	95% CI	P value	HR	95% CI	P value
Conservative treatment	5.40	1.84-15.90	0.002	4.42	1.48-13.19	0.008
Aneurysms involving side branches	0.90	0.33-2.47	0.844	—	—	—
Aneurysm's size (≥25 mm)	3.72	1.35-10.22	0.011	2.85	1.01-8.04	0.049
Fusiform and/or dissecting aneurysms	0.52	0.15-1.85	0.316	1.90	0.50-7.29	0.348
Age (>60 years)	1.63	0.59-4.52	0.344	—	—	—
Sex (male)	1.00	0.34-2.94	0.998	—	—	—
Aneurysms involved basilar artery	3.51	0.98-12.62	0.054	2.42	0.49-11.96	0.280
Hypertension	2.34	0.52-10.46	0.226	—	—	—
Ischemic onset	4.21	1.51-11.71	0.006	3.33	1.19-9.32	0.022
Ruptured aneurysms	0.411	0.05-3.16	0.411	—	—	—
Diabetes mellitus	0.76	0.17-3.39	0.720	—	—	—
Smoking	0.37	0.05-2.85	0.341	—	—	—

a case series of 56 nonsaccular posterior circulation aneurysms (mean diameter = 11 mm) treated with FD, with a complete occlusion rate of 75% in fusiform aneurysms and an overall complication rate of 15.5%.

In the present study, we found a significantly lower SAE rate in the endovascular group compared to the conservative group (15.7% vs. 44.4%, $P = 0.031$). In the endovascular group, 7 (13.7%) patients presented with procedure-related ischemic stroke, and there was 1 (2.0%) death case. The specific reasons for the 7 ischemic strokes are not yet clarified. Of these, 5 out of 7 patients experienced complications within 30 days following the procedure, which may be due to the procedure-related branch vessels or perforator occlusion [29]. In addition, the detachment of parent artery mural thrombus or intraluminal thrombus during the stenting or coiling may also be the potential cause. The other 2 out of 7 patients experienced complications during the follow-up period. Meanwhile, the follow-up DSA revealed that the former dissecting aneurysms were enlarged, and the dissecting lesions that involved vital perforators may be the possible cause. Our study results suggested that giant aneurysms were associated with a high risk of SAEs after managing IVB-TLAs. Giant aneurysms often present with intraluminal thrombosis, brainstem compression, and branch vessels or perforator involvement [30, 31]. Patients with giant aneurysms have a higher rate of poor outcomes after surgical or endovascular procedures [5, 30], and giant aneurysms have often been related to a worse natural history, frequently leading to aneurysm rupture, ischemic stroke, and mass effect [5, 6]. Moreover, we found that the ischemic onset was also associated with a high risk of SAEs. Flemming et al. [32] found that the history of prior ischemia was a predictor of cerebral ischemia related to the nonsaccular vertebrobasilar aneurysms. For patients initially presenting with ischemic onset, recurrent ischemic stroke risk was 6.7% per year, with the median time to second ischemic stroke of 1.73 years. The risk of aneurysm-related ischemic stroke was reported to increase from 2.7% at 1 year to 15.9% at 10 years. IVBTLAs are often accompanied by intraluminal thrombus, and the intraluminal thrombus detachment may

cause occlusion of perforating vessels or distal vessels, leading to ischemic stroke [33]. The in situ thrombus formation within the parent artery or within perforating vessels may also cause ischemia before and after the aneurysm management.

To the best of our knowledge, this is the first study that evaluated the safety and efficacy of endovascular treatment of IVBTLAs compared with conservative therapy in order to gain a better understanding of which management methods might be the most beneficial to the patients. Deconstructive treatment seems to be associated with a higher rate of complete aneurysm occlusion; however, we did not find a significant difference in safety between constructive treatment, deconstructive treatment, and the combined treatment. Therefore, when deconstructive treatment is not feasible, the parent artery reconstruction with various manners can be used as a safe and effective choice.

The present study has some limitations. First, the conservative group had a small sample size, which was insufficient to conclude the natural prognosis of IVBTLAs. In addition, even though the study had a prospective design, due to the selection bias or the insufficient sample size, the baseline characteristics of the two groups were not completely balanced, and there were more giant aneurysms and hypertension patients in the conservative group. Moreover, 16 (23.2%) patients were lost to imaging follow-up, which might impact the evaluation of changes in aneurysms.

5. Conclusions

Endovascular treatment of IVBTLAs may be associated with lower rates of SAEs, death, and intracranial hemorrhage as compared with conservative treatment, with high 1-year, 3-year, and 5-year overall cumulative survival rates. Deconstructive treatments led to higher rates of complete occlusion of aneurysms, while stent-assisted coiling showed favorable complete occlusion rates in reconstructive treatments. In addition to conservative treatment, giant aneurysms and ischemic onset could increase the risk of SAEs.

Data Availability

Unpublished data are available upon reasonable request from the corresponding author.

Ethical Approval

The institutional review board of the lead center (Henan Provincial People's Hospital) approved the study (No. 12072), and the ethics approval documents were recorded and registered in Chinese People's Liberation Army Rocket Force Characteristic Medical Center. The study was carried out in accordance with the 1964 Declaration of Helsinki.

Conflicts of Interest

The authors declare that they have no conflict of interest.

Authors' Contributions

Qiaowei Wu, Tianxiao Li, and Weijian Jiang are joint first authors and contributed equally to this work. All authors made a significant contribution to the study and manuscript preparation. QW, TL, WJ, and YH contributed to study conception and design. QW, LL, and YH contributed to data acquisition, data interpretation, and analysis. QW and YH drafted the manuscript. TL, WJ, and JH contributed to the major revision of the manuscript. JH contributed to significant intellectual content. All authors critically revised the paper and approved the final version of the manuscript.

Supplementary Materials

Supplemental Table 1: summary of inclusion and exclusion criteria. Supplemental Table 2: survival analysis results. Figure 1: (A) pretreatment anteroposterior DSA showing a basilar giant saccular aneurysm. (B) High-resolution magnetic resonance-enhanced scanning showing the aneurysm wall was enhanced (arrow). (C) Double LVIS stent-assisted coiling was performed; the immediate postprocedural DSA showing the aneurysm sac was completely occluded. (D) The patient presented with severe headaches the second day after the procedure, and the emergency head CT showed the subarachnoid hemorrhage. (E) The followed DSA showing that the coils were compressed. (F) Additional double enterprise stent-assisted coiling was performed. The patient died of aneurysm rerupture 2 months after discharge. Figure 2: (A, B) pretreatment anteroposterior DSA (A) three-dimensional construction (B) showing a vertebrobasilar junction giant saccular aneurysm. (C) Magnetic resonance image revealed severe brain stem compression. (D) Enterprise stent-assisted coiling was performed; the immediate postprocedural DSA showing the embolization result (E). (F) The follow-up DSA at 6 months demonstrated that the aneurysm was completely occluded. *(Supplementary Materials)*

References

[1] G. Saliou, R. H. Sacho, S. Power et al., "Natural history and management of basilar trunk artery aneurysms," *Stroke*, vol. 46, no. 4, pp. 948–953, 2015.

[2] F. Cagnazzo, D. Mantilla, A. Rouchaud et al., "Endovascular treatment of very large and giant intracranial aneurysms: comparison between reconstructive and deconstructive techniques-a meta-analysis," *American Journal of Neuroradiology*, vol. 39, no. 5, pp. 852–858, 2018.

[3] Y. B. Fang, A. Lin, A. Kostynskyy et al., "Endovascular treatment of intracranial vertebrobasilar artery dissecting aneurysms: parent artery occlusion versus flow diverter," *European Journal of Radiology*, vol. 99, pp. 68–75, 2018.

[4] J. Wang, L. Jia, X. Yang et al., "Outcomes in symptomatic patients with vertebrobasilar dolichoectasia following endovascular treatment," *Frontiers in Neurology*, vol. 10, p. 610, 2019.

[5] D. O. Wiebers, J. P. Whisnant, Huston J 3rd et al., "Unruptured intracranial aneurysms: natural history, clinical outcome, and risks of surgical and endovascular treatment," *The Lancet*, vol. 362, no. 9378, pp. 103–110, 2003.

[6] Investigators ISoUIA, "Unruptured intracranial aneurysms — risk of rupture and risks of surgical intervention," *The New England Journal of Medicine*, vol. 339, no. 24, pp. 1725–1733, 1998.

[7] D. O. Wiebers, "Unruptured intracranial aneurysms: natural history and clinical management. Update on the international study of unruptured intracranial aneurysms," *Neuroimaging Clinics of North America*, vol. 16, no. 3, pp. 383–390, 2006.

[8] J. Chung, H. Park, Y. C. Lim, D. K. Hyun, and Y. S. Shin, "Endovascular treatment of basilar artery trunk aneurysms," *Acta Neurochirurgica*, vol. 153, no. 11, pp. 2137–2145, 2011.

[9] T. Higa, H. Ujiie, K. Kato, H. Kamiyama, and T. Hori, "Basilar artery trunk saccular aneurysms: morphological characteristics and management," *Neurosurgical Review*, vol. 32, no. 2, pp. 181–191, 2009.

[10] Y. Zhang, Y. Zhou, P. Yang et al., "Comparison of the flow diverter and stent-assisted coiling in large and giant aneurysms: safety and efficacy based on a propensity score-matched analysis," *European Radiology*, vol. 26, no. 7, pp. 2369–2377, 2016.

[11] W. S. Lesley and R. Rangaswamy, "Balloon test occlusion and endosurgical parent artery sacrifice for the evaluation and management of complex intracranial aneurysmal disease," *Journal of NeuroInterventional Surgery*, vol. 1, no. 2, pp. 112–120, 2009.

[12] X. D. Liang, Z. L. Wang, T. X. Li et al., "Safety and efficacy of a new prophylactic tirofiban protocol without oral intraoperative antiplatelet therapy for endovascular treatment of ruptured intracranial aneurysms," *Journal of NeuroInterventional Surgery*, vol. 8, no. 11, pp. 1148–1153, 2016.

[13] W. Zi-Liang, L. Xiao-Dong, L. Tian-Xiao et al., "Intravenous administration of tirofiban versus loading dose of oral clopidogrel for preventing thromboembolism in stent-assisted coiling of intracranial aneurysms," *International Journal of Stroke*, vol. 12, no. 5, pp. 553–559, 2017.

Retraction

Retracted: Combined Association of Low-Density Lipoprotein Cholesterol Levels and Systolic Blood Pressure to the Outcome of Intracerebral Hemorrhage: Data from the China Stroke Center Alliance

Oxidative Medicine and Cellular Longevity

This article has been retracted by Hindawi following an investigation undertaken by the publisher [1]. This investigation has uncovered evidence of one or more of the following indicators of systematic manipulation of the publication process:

(1) Discrepancies in scope

(2) Discrepancies in the description of the research reported

(3) Discrepancies between the availability of data and the research described

(4) Inappropriate citations

(5) Incoherent, meaningless and/or irrelevant content included in the article

(6) Manipulated or compromised peer review

The presence of these indicators undermines our confidence in the integrity of the article's content and we cannot, therefore, vouch for its reliability. Please note that this notice is intended solely to alert readers that the content of this article is unreliable. We have not investigated whether authors were aware of or involved in the systematic manipulation of the publication process.

In addition, our investigation has also shown that one or more of the following human-subject reporting requirements has not been met in this article: ethical approval by an Institutional Review Board (IRB) committee or equivalent, patient/participant consent to participate, and/or agreement to publish patient/participant details (where relevant).

Wiley and Hindawi regrets that the usual quality checks did not identify these issues before publication and have since put additional measures in place to safeguard research integrity.

We wish to credit our own Research Integrity and Research Publishing teams and anonymous and named external researchers and research integrity experts for contributing to this investigation.

The corresponding author, as the representative of all authors, has been given the opportunity to register their agreement or disagreement to this retraction. We have kept a record of any response received.

References

[1] Y. Ding, Y. Wang, L. Liu et al., "Combined Association of Low-Density Lipoprotein Cholesterol Levels and Systolic Blood Pressure to the Outcome of Intracerebral Hemorrhage: Data from the China Stroke Center Alliance," *Oxidative Medicine and Cellular Longevity*, vol. 2022, Article ID 6206315, 8 pages, 2022.

Research Article

Combined Association of Low-Density Lipoprotein Cholesterol Levels and Systolic Blood Pressure to the Outcome of Intracerebral Hemorrhage: Data from the China Stroke Center Alliance

Yarong Ding [ID],[1,2,3] **Yu Wang** [ID],[1,2,4] **Liping Liu** [ID],[1,2,5] **Hongqiu Gu** [ID],[1,2] **Kaixuan Yang**,[2,6,7] **Zixiao Li** [ID],[1,2,5] and **Xingquan Zhao** [ID] [1,2,5]

[1]Department of Neurology, Beijing Tiantan Hospital, Capital Medical University, Beijing, China
[2]China National Clinical Research Center for Neurological Diseases, Beijing, China
[3]Department of Neurology, Beijing Luhe Hospital, Capital Medical University, Beijing, China
[4]Department of Neurology, Beijing Hospital, National Center of Gerontology, Beijing, China
[5]Research Unit of Artificial Intelligence in Cerebrovascular Disease, Chinese Academy of Medical Sciences, Beijing, China
[6]Department of Epidemiology and Health Statistics, School of Public Health, Capital Medical University, Beijing, China
[7]Beijing Municipal Key Laboratory of Clinical Epidemiology, Beijing, China

Correspondence should be addressed to Zixiao Li; lizixiao2008@hotmail.com and Xingquan Zhao; zxq@vip.163.com

Limited data were available about the combined impact of systolic blood pressure (SBP) and low-density lipoprotein cholesterol (LDL-C) levels on intracerebral hemorrhage (ICH) prognosis. The objective of this study is to explore whether the relationship between LDL-C and ICH outcomes was modified by SBP levels in a Chinese population. From August 1, 2015, to July 31, 2019, 75,443 ICH patients enrolled from the Chinese Stroke Center Alliance program were included in our study. Patients were divided into LDL-C levels of <70 mg/dL, 70-100 mg/dL, and ≥100 mmol/L. SBP was stratified as <140 mmHg, 140-180 mmHg, and ≥180 mmHg. The primary outcome was the occurrence of hematoma expansion (HE), and the second outcome was in-hospital mortality. Correlation between LDL-C levels and SBP on ICH outcomes were assessed by logistic regression. 6,116 (8.1%) and 1,576 (2.1%) patients suffered HE and in-hospital mortality. Compared with the ≥100 mg/dL group, patients with LDL-C concentrations under 70 mg/dL had a 19% and 24% increase in the relative risk of HE (crude OR 1.19, 95% CI 1.11-1.28) and in-hospital mortality (crude OR 1.24, 95% CI 1.08-1.42). When SBP was added as a stratification variable, the above-mentioned association was attenuated in patients under a threshold SBP of 140 mmHg ($P > 0.05$). However, no statistical interaction was detected between SBP and LDL-C levels. Lower LDL-C levels (<70 mg/dL) are related to a higher risk of HE and in-hospital mortality confined to ICH patients with elevated SBP (≥140 mmHg).

1. Introduction

Intracerebral hemorrhage (ICH) has significant high morbidity and mortality [1–3]. Interventional trials, involving intensive antihypertensive treatment [4], hypoglycemic therapy [5], hemostatic agents [6, 7], and hematoma evacuation [8, 9], achieved only marginally therapeutic efficacy. As interest

in multifactorial interventions is increasing, integrated approaches to the management of ICH are urgently needed.

Elevated blood pressure (BP), especially systolic BP (SBP), is the cornerstone of ICH prevention as is closely related to the occurrence of hematoma expansion (HE) and subsequent poor prognosis [10]. Meanwhile, growing attention has been paid to the effect of low-density lipoprotein
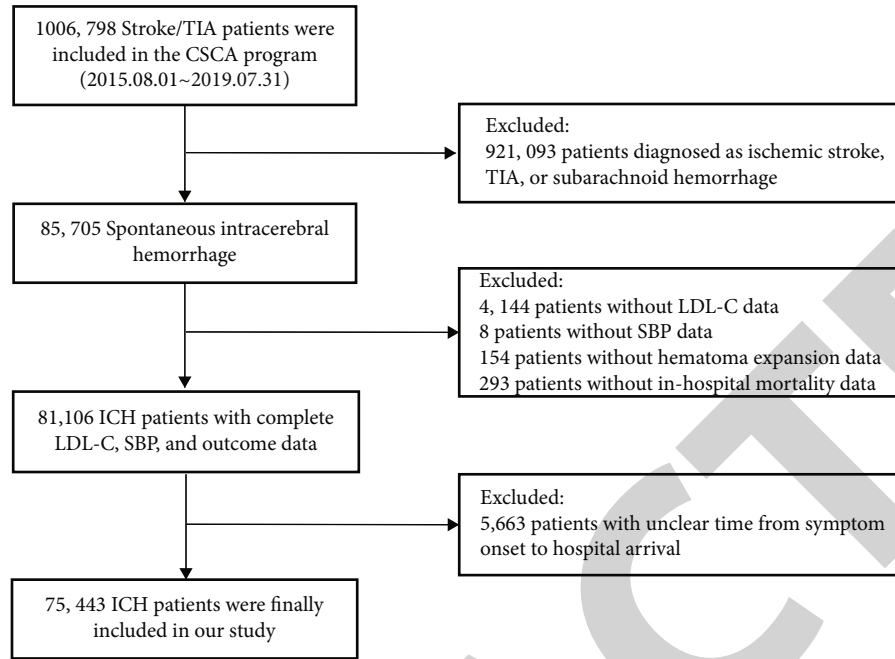
Figure 1: Flow chart for selection of study participants. TIA: transit ischemic attack; CSCA: Chinese Stroke Center Alliance; LDL-C: low-density lipoprotein cholesterol; SBP: systolic blood pressure; ICH: intracerebral hemorrhage.
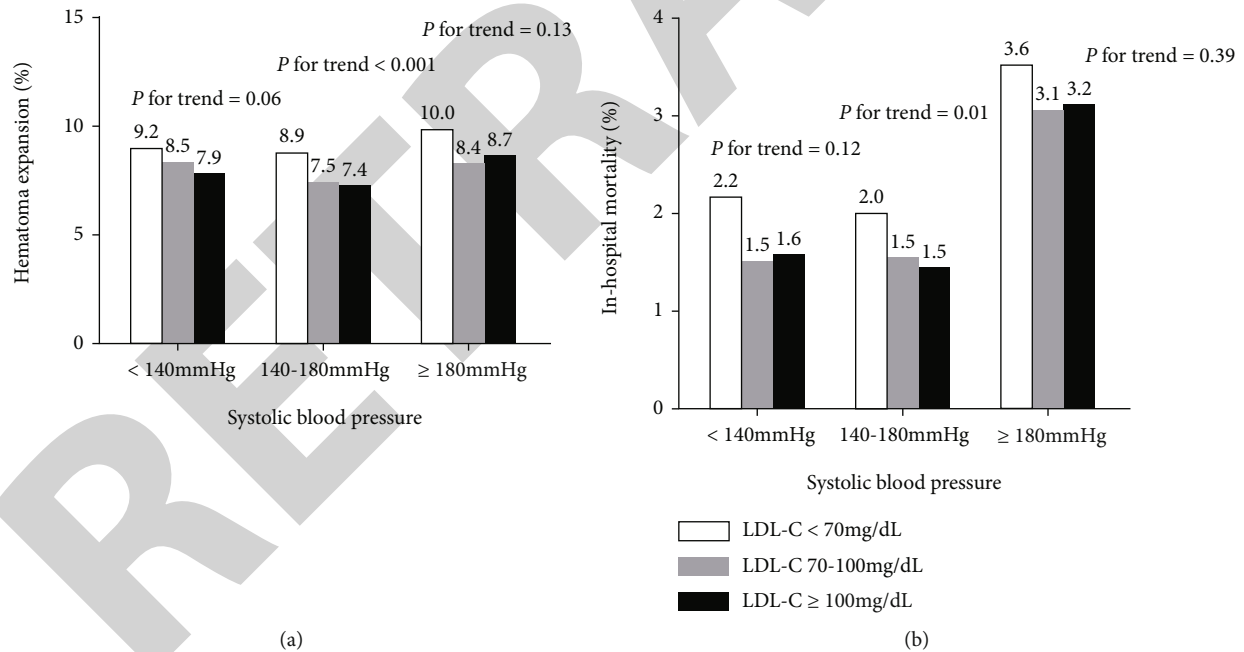
Figure 2: Prevalence of (a) hematoma expansion and (b) in-hospital mortality according to LDL-C levels across systolic blood pressure subgroups. LDL-C: low-density lipoprotein cholesterol.

cholesterol (LDL-C) on ICH prognosis [11–13]. In the series of China Stroke Center Alliance (CSCA) studies, we found that in acute ICH patients, lower LDL-C levels are related to a high risk of HE and mortality [14]. Researches regarding the joint effects of SBP and LDL-C on atherosclerotic cardiovascular risk showed an additive, even synergetic association [15–17]. While limited data were available about the com-bined impact of SBP and LDL-C levels on ICH prognosis. It is worth noting that one observational research indicated that the proportional risk of cerebral hemorrhage associated with lower LDL-C was confined to patients with elevated BP [18].

Therefore, the purpose of our study was to investigate whether the association between LDL-C and ICH prognosis was modified by SBP levels in a Chinese population.

Table 1: Characteristics of enrolled participants according to LDL-C levels.

Variables	Total	LDL-C levels			P value
		<70 mg/dL	70-100 mg/dL	≥100 mg/dL	
n (%)	75433	11899 (15.8)	24952 (33.1)	38592 (51.2)	
Age, years	63.0 ± 12.8	64.2 ± 12.8	63.6 ± 12.9	62.2 ± 12.8	<0.001
Male, n (%)	47079 (62.4)	8306 (69.8)	16134 (64.7)	22639 (58.7)	<0.001
BMI, kg/m^2	23.9 ± 4.2	23.5 ± 3.7	23.7 ± 3.7	24.1 ± 4.7	<0.001
SBP, mmHg	164.7 ± 27.9	162.4 ± 28.2	164.3 ± 27.7	165.6 ± 27.9	<0.001
DBP, mmHg	95.3 ± 16.8	93.5 ± 16.4	94.8 ± 16.5	96.2 ± 16.9	<0.001
Current smoker, n (%)	14905 (19.8)	2561 (21.5)	5088 (20.4)	7256 (18.8)	<0.001
Current alcoholic, n (%)	18373 (24.4)	3101 (26.1)	6049 (24.2)	9223 (23.9)	<0.001
Previous history, n (%)					
Hypertension	53939 (71.5)	8377 (70.4)	17562 (70.4)	28000 (72.6)	<0.001
Diabetes mellitus	7200 (9.5)	1301 (10.9)	2107 (8.4)	3792 (9.8)	<0.001
Dyslipidemia	3108 (4.1)	416 (3.5)	764 (3.1)	1928 (5.0)	<0.001
Heart failure	347 (0.5)	83 (0.7)	114 (0.5)	150 (0.4)	<0.001
Previous ICH	12877 (17.1)	2190 (18.4)	4174 (16.7)	6513 (16.9)	<0.001
Previous ischemic stroke	21333 (28.3)	3875 (32.6)	6994 (28.0)	10464 (27.1)	<0.001
Medication history, n (%)					
Antiplatelet	5296 (7.0)	1265 (10.6)	1731 (6.9)	2300 (6.0)	<0.001
Anticoagulant	1332 (1.8)	267 (2.2)	386 (1.5)	679 (1.8)	<0.001
Antihypertensive agent	35928 (47.6)	5765 (48.4)	11642 (46.7)	18521 (48.0)	<0.001
Statins	4380 (5.8)	1017 (8.5)	1356 (5.4)	2007 (5.2)	<0.001
In-hospital treatment, n (%)					
Hematoma evacuation	7511 (10.0)	1408 (11.8)	2457 (9.8)	3646 (9.4)	<0.001
Antihypertensive agent	54635 (72.4)	8254 (69.4)	17899 (71.7)	28482 (73.8)	<0.001
Statins	18310 (24.3)	2693 (22.6)	5312 (21.3)	10305 (26.7)	<0.001
Creatinine, μmol/L	67.6 (55.0, 84.3)	67.0 (54.6, 83.1)	67.0 (55.0, 82.0)	68.0 (55.0, 86.0)	<0.001
GCS score on admission*	14.0 (8.0, 15.0)	13.0 (7.0, 15.0)	14.0 (8.0, 15.0)	14.0 (9.0, 15.0)	<0.001
Time from onset to arrival, hours	3.8 (1.5, 21.0)	3.5 (1.5, 18.3)	3.8 (1.6, 20.5)	3.9 (1.5, 22.0)	0.918
Hematoma expansion, n (%)	6116 (8.1)	1102 (9.3)	1977 (7.9)	3037 (7.9)	<0.001
In-hospital mortality, n (%)	1576 (2.1)	296 (2.5)	500 (2.0)	780 (2.0)	0.004

Values are (%) for categorical variables and mean ± SD or median (IQR) for continuous variables. SD: standard deviation; LDL-C: low-density lipoprotein cholesterol; BMI: body mass index; SBP: systolic blood pressure; DBP: diastolic blood pressure; ICH: intracerebral hemorrhage; GCS: Glasgow coma scale. *GCS score on admission was evaluated in 39,216 (52.0%) patients.

2. Materials and Methods

2.1. Study Population.
The CSCA program was initiated by the Chinese Stroke Association in June 2015 to establish a national, hospital-based stroke care quality assessment and improvement platform, the protocol of which has been previously reported [19]. From August 1, 2015, to July 31, 2019, 1,006,798 stroke or transit ischemic attack patients within 7 days from the onset were recruited consecutively from 1,576 hospitals. A total of 85,705 spontaneous ICH patients were selected for the initial assessment in our study. Among all the recruited patients, 4,152 individuals were excluded due to incomplete data on baseline SBP or LDL-C levels, 154 individuals without data on HE, and 293 individuals with incomplete in-hospital mortality data were also excluded. Besides, 5,663 individuals with unclear time from symptom onset to hospital arrival were excluded. Eventually, 75,443

patients were included in this final analysis (Figure 1). Baseline characteristics between included and excluded ICH patients are shown in Table S1; the clinical features of which were similar in general.

The study was conducted in compliance with the Helsinki Declaration and approved by the central Institutional Review Board at Beijing Tiantan Hospital.

2.2. LDL-C, SBP, and Other Baseline Covariates.
Laboratory variables were collected within 24 hours after admission to each subcenter. LDL-C levels were categorized into three groups regarding the 2018 American Heart Association guidelines for the management of cholesterol: <70 mg/dL, 70-100 mg/dL, and ≥100 mg/dL [20].

Three BP readings were recorded separately in the supine position after at least two-minute resting by trained nurses at baseline, and the average of the three measurements was

TABLE 2: Odds ratios of ICH outcomes for LDL-C and SBP levels measured at baseline.

Variables		Case (%)	Univariate analysis	Multivariate analysis		
				Model 1	Model 2	Model 3
			Hematoma expansion			
LDL-C	<70 mg/dL	1102 (9.26)	1.19 (1.11, 1.28)	1.19 (1.11, 1.28)	1.17 (1.09, 1.26)	1.22 (1.10, 1.35)
	70-100 mg/dL	1977 (7.92)	1.01 (0.95, 1.07)	1.00 (0.95, 1.07)	1.02 (0.96, 1.08)	1.02 (0.94, 1.11)
	≥100 mg/dL	3037 (7.87)	Ref.	Ref.	Ref.	Ref.
			In-hospital mortality			
	<70 mg/dL	296 (2.49)	1.24 (1.08, 1.42)	1.16 (1.01, 1.33)	1.16 (1.01, 1.33)	0.91 (0.76, 1.08)
	70-100 mg/dL	500 (2.00)	0.99 (0.88, 1.11)	0.95 (0.85, 1.06)	0.96 (0.86, 1.08)	0.87 (0.75, 1.00)
	≥100 mg/dL	780 (2.02)	Ref.	Ref.	Ref.	Ref.
			Hematoma expansion			
SBP	<140 mmHg	1055 (8.33)	0.95 (0.87, 1.02)	0.95 (0.88, 1.02)	0.90 (0.83, 0.98)	0.82 (0.73, 0.93)
	140-180 mmHg	3074 (7.66)	0.86 (0.81, 0.91)	0.86 (0.81, 0.91)	0.83 (0.78, 0.88)	0.78 (0.72, 0.85)
	≥180 mmHg	1987 (8.78)	Ref.	Ref.	Ref.	Ref.
			In-hospital mortality			
	<140 mmHg	213 (1.68)	0.51 (0.44, 0.60)	0.52 (0.45, 0.61)	0.51 (0.43, 0.59)	0.74 (0.60, 0.90)
	140-180 mmHg	633 (1.58)	0.48 (0.43, 0.54)	0.47 (0.43, 0.53)	0.47 (0.42, 0.52)	0.67 (0.58, 0.76)
	≥180 mmHg	730 (3.22)	Ref.	Ref.	Ref.	Ref.

Data are OR (95% CI) unless otherwise stated. Model 1 adjusted for age and sex. Model 2 adjusted for variables in model 1 plus body mass index (<25.0 or ≥25.0 kg/m^2), systolic blood pressure, diastolic blood pressure, smoking status, drinking status, hypertension, diabetes mellitus, previous ICH, medication history (including prior use of antiplatelet, anticoagulant, antihypertensive agent, and stains), and creatinine. Model 3 adjusted for variables in model 2 plus GCS score on admission as a sensitivity analysis.

regarded as the admission BP. Admission SBP was then classified into three categories based on the 2018 European Society of Hypertension as <140 mmHg, 140-180 mmHg, and ≥180 mmHg [21].

Other baseline characteristics including demographic information, body mass index (BMI), smoking and drinking history, medical and medication history, Glasgow coma scale (GCS) score on admission, and time from symptom onset to arrival were also extracted.

2.3. Outcomes. The primary outcome was HE event, and the second outcome was in-hospital mortality. A cranial CT scan was obtained in the emergency department and repeated after admission. Hematoma volume was estimated using the ABC/2 method by two experienced neurologists [22]. According to the radiographic criteria, HE was diagnosed by follow-up image as the intraparenchymal hematoma increased >33% or an absolute increment of >6 mL from initial hematoma [23].

2.4. Statistical Analysis. Data were presented as mean ± standard deviation (SD) or median (interquartile range, IQR) for continuous variables and count (percentage) for categorical variables. The ANOVA or nonparametric Kruskal-Wallis test and the chi-squared test were used in the comparison of baseline variables.

The independent correlation between LDL-C, SBP, and ICH prognosis was assessed by odds ratios (ORs) and 95% confidence interval (CI) using logistic regression. The subgroups with the highest LDL-C (≥100 mg/dL) and SBP levels (≥180 mmHg) were used as the reference. Model 1 was cor-

rected for age and sex. Model 2 was further adjusted for BMI (<25.0 or ≥25.0 kg/m^2), systolic and diastolic BP, smoking, drinking, hypertension, diabetes mellitus, previous ICH, medication history (including prior use of the antiplatelet, anticoagulant, antihypertensive agent, and stains), and creatinine. Since the GCS score was only recorded in 39,216 (52.0%) patients, model 3 was performed as a sensitivity analysis in those with complete GCS score information on admission. Besides, to assess whether a differential correlation between lower LDL-C with HE or in-hospital mortality is observed in different SBP categories, an interaction term (LDL-C × SBP, both as a polytomous variable) was added among all the included patients as well as patients admitted within 24 h of symptom onset.

Differences were considered to be significant at $P < 0.05$. Analyses were performed using the SAS software (version 9.4; SAS Institute, Cary, NC, USA).

3. Results

75,443 patients were finally enrolled in our study; 6,116 (8.1%) and 1,576 (2.1%) of them were identified as HE and in-hospital mortality, separately. Among them, the lowest LDL-C group (<70 mg/dL) together with the highest SBP group (≥180 mmHg) tended to have more events. The prevalence of adverse outcomes according to LDL-C levels across SBP subgroups is shown in Figure 2.

3.1. Baseline Characteristics. Significant differences were found in age, sex, BMI, BP, behavior history, previous history, medication history, in-hospital treatment, creatinine,

TABLE 3: Association between LDL-C and ICH outcomes in different blood pressure levels among all the included patients.

SBP	LDL-C levels	Case (%)	Univariate analysis	Multivariate analysis		
				Model 1	Model 2	Model 3
Hematoma expansion						
	<70 mg/dL	214 (9.18)	1.18 (0.99, 1.39)	1.17 (0.99, 1.38)	1.14 (0.96, 1.35)	1.16 (0.90, 1.49)
<140 mmHg	70-100 mg/dL	364 (8.45)	1.07 (0.93, 1.24)	1.07 (0.93, 1.23)	1.07 (0.93, 1.24)	0.98 (0.79, 1.22)
	≥100 mg/dL	477 (7.92)	Ref.	Ref.	Ref.	Ref.
	<70 mg/dL	563 (8.93)	1.23 (1.11, 1.36)	1.23 (1.11, 1.36)	1.20 (1.08, 1.33)	1.33 (1.14, 1.54)
140-180 mmHg	70-100 mg/dL	996 (7.51)	1.02 (0.94, 1.11)	1.02 (0.94, 1.11)	1.04 (0.96, 1.13)	1.13 (1.00, 1.28)
	≥100 mg/dL	1515 (7.36)	Ref.	Ref.	Ref.	Ref.
	<70 mg/dL	325(9.97)	1.16 (1.02, 1.32)	1.15 (1.01, 1.31)	1.16 (1.02, 1.33)	1.14 (0.97, 1.35)
≥180 mmHg	70-100 mg/dL	617 (8.35)	0.95 (0.86, 1.06)	0.95 (0.86, 1.06)	0.97 (0.87, 1.07)	0.93 (0.81, 1.06)
	≥100 mg/dL	1045 (8.71)	Ref.	Ref.	Ref.	Ref.
P for interaction			0.649	0.646	0.608	0.255
In-hospital mortality						
	<70 mg/dL	51 (2.19)	1.38 (0.98, 1.95)	1.32 (0.93, 1.86)	1.34 (0.95, 1.90)	1.13 (0.72, 1.76)
<140 mmHg	70-100 mg/dL	66 (1.53)	0.96 (0.70, 1.32)	0.94 (0.69, 1.30)	0.96 (0.70, 1.32)	0.98 (0.66, 1.46)
	≥100 mg/dL	96 (1.59)	Ref.	Ref.	Ref.	Ref.
	<70 mg/dL	128 (2.03)	1.39 (1.13, 1.71)	1.27 (1.03, 1.57)	1.25 (1.01, 1.54)	0.99 (0.76, 1.30)
140-180 mmHg	70-100 mg/dL	203 (1.53)	1.04 (0.87, 1.25)	0.98 (0.82, 1.17)	0.99 (0.82, 1.18)	0.86 (0.69, 1.08)
	≥100 mg/dL	302 (1.47)	Ref.	Ref.	Ref.	Ref.
	<70 mg/dL	117 (3.59)	1.13 (0.92, 1.40)	1.06 (0.86, 1.32)	1.07 (0.87, 1.33)	0.80 (0.61, 1.04)
≥180 mmHg	70-100 mg/dL	231 (3.13)	0.98 (0.83, 1.16)	0.94 (0.80, 1.11)	0.97 (0.82, 1.14)	0.86 (0.70, 1.06)
	≥100 mg/dL	382 (3.19)	Ref.	Ref.	Ref.	Ref.
P for interaction			0.667	0.697	0.715	0.647

Data are OR (95% CI) unless otherwise stated. Model 1 adjusted for age and sex. Model 2 adjusted for variables in model 1 plus body mass index (<25.0 or ≥25.0 kg/m^2), systolic blood pressure, diastolic blood pressure, smoking status, drinking status, hypertension, diabetes mellitus, previous ICH, medication history (including prior use of antiplatelet, anticoagulant, antihypertensive agent, and stains), and creatinine. Model 3 adjusted for variables in model 2 plus GCS score on admission as a sensitivity analysis.

and GCS score on admission among LDL-C groups. Baseline characteristics and ICH prognosis according to LDL-C categories are shown in Table 1.

3.2. Independent Association of LDL-C and SBP Levels for ICH Outcomes. Lower LDL-C levels had a significant correlation with ICH outcomes in the univariate analysis ($P < 0.001$). Compared with the ≥100 mg/dL group, patients with LDL-C concentrations under 70 mg/dL had a 19% and 24% increase in the relative risk of HE (OR 1.19, 95% CI 1.11-1.28) and in-hospital mortality (OR 1.24, 95% CI 1.08-1.42). In the multivariate analysis, similar results were obtained after adjusting for potential covariates in model 1 and 2. The adjusted ORs of HE were 1.17 (95% CI 1.09-1.26) for $LDL-C$ levels < 70 mg/dL, 1.02 (95% CI 0.96-1.08) for LDL-C levels of 70 mg/dL to 100 mg/dL, and 1.0 (reference) for $LDL-C$ levels ≥ 100 mg/dL in model 2. Correspondingly, the adjusted ORs of in-hospital mortality were 1.16 (95% CI 1.01-1.33), 0.96 (95% CI 0.86-1.08), and 1.0 (reference) among the three LDL-C groups from low to high. However, increasing mortality risk with lower LDL-C levels (<70 mg/dL) was not pronounced when further adjusted for admission GCS score in the sensitivity analysis.

The fully adjusted ORs of the lowest SBP group (<140 mmHg) were 0.82 (95% CI 0.73-0.93) and 0.74 (95% CI 0.60-0.90) for HE and in-hospital mortality, respectively. Additional detailed information was given in Table 2.

3.3. Combined Association of LDL-C and SBP to ICH Outcomes. When examining the association of LDL-C with ICH outcomes across SBP categories, it was noteworthy that no statistical significance was obtained in those with SBP under 140 mmHg, irrespective of LDL-C concentration ($P > 0.05$). While for those with SBP between 140 mmHg and 180 mmHg and SBP above 180 mmHg, lower LDL-C levels (<70 mg/dL) conferred a 1.23-fold, 1.16-fold greater likelihood of HE presence ($P < 0.001$, Table 3). When it comes to in-hospital mortality, its significant correlation with lower LDL-C levels diminished among the highest SBP category (≥180 mmHg). In multivariate analyses, the results were essentially unaltered in both model 1 and model 2. While after further adjustment for admission GCS score in model 3, the association became nonsignificant between lower LDL-C levels and adverse outcomes among ICH patients with normal SBP. There was, however, no apparent interaction detected between LDL-C and SBP with either HE ($P = 0.649$) or in-hospital mortality ($P = 0.667$).

To differentiate the effect of time from symptom onset to admission, additional sensitivity analyses were performed among the 60,024 patients admitted within 24 h of symptom

SBP	LDL-C levels	Case (%)	Univariate analysis	Odds ratio (95% CI)
Hematoma expansion				
< 140 mmHg	< 70 mg/dL	158 (9.72)	1.21 (1.00, 1.48)	
	70-100 mg/dL	254 (8.66)	1.07 (0.90, 1.27)	
	≥ 100 mg/dL	339 (8.15)	Ref.	
140-180 mmHg	< 70 mg/dL	480 (9.52)	1.26 (1.13, 1.41)	
	70-100 mg/dL	811 (7.76)	1.01 (0.92, 1.10)	
	≥ 100 mg/dL	1237 (7.71)	Ref.	
≥ 180 mmHg	< 70 mg/dL	307 (10.51)	1.17 (1.02, 1.33)	
	70-100 mg/dL	569 (8.76)	0.95 (0.85, 1.06)	
	≥ 100 mg/dL	947 (9.15)	Ref.	
In-hospital mortality				
< 140 mmHg	< 70 mg/dL	45 (2.77)	1.40 (0.97, 2.02)	
	70-100 mg/dL	56 (1.91)	0.96 (0.68, 1.35)	
	≥ 100 mg/dL	83 (2.00)	Ref.	
140-180 mmHg	< 70 mg/dL	120 (2.38)	1.40 (1.13, 1.74)	
	70-100 mg/dL	183 (1.75)	1.03 (0.85, 1.24)	
	≥ 100 mg/dL	274 (1.71)	Ref.	
≥ 180 mmHg	< 70 mg/dL	114 (3.90)	1.11 (0.90, 1.38)	
	70-100 mg/dL	222 (3.42)	0.97 (0.82, 1.15)	
	≥ 100 mg/dL	364 (3.52)	Ref.	
				0.5 1.0 1.5 2.0

Figure 3: Association of LDL-C with HE or in-hospital mortality across SBP categories among patients admitted within 24 h of symptom onset[‡]. LDL-C: low-density lipoprotein cholesterol; HE: hematoma expansion; SBP: systolic blood pressure. $P = 0.747$ for HE; $P = 0.604$ for in-hospital mortality. [‡]60,024 (79.6%) patients were admitted within 24 h of symptom onset.

onset. In these analyses, consistent with the overall population, lower LDL-C level (<70 mg/dL) was accompanied by a higher risk of HE and in-hospital mortality, particularly in individuals with a baseline SBP above 140 mmHg (Figure 3).

4. Discussion

We provided evidence of ICH risk stratification regarding LDL-C concentrations across SBP categories in acute ICH patients. Those with $LDL - C < 70$ mg/dL conferred a higher risk of HE and in-hospital mortality compared to patients with $LDL - C \geq 100$ mg/dL. When SBP was added as a stratification variable, it was noteworthy that the above-mentioned association was attenuated in patients under a threshold SBP of 140 mmHg. Patients admitted within 24 h of symptom onset presented robust consistent results. However, no statistical interaction was detected between SBP and LDL-C levels. Our results indicated that the adverse outcome occurs commonly in the high-risk ICH patients, those with lower LDL-C levels and uncontrolled BP, for whom intensive control of SBP is recommended.

Although with the popular belief of lipid-lowering goal towards "the lower, the better" in atherosclerotic cardiovascular disease [24], appropriate LDL-C levels are still a matter of debate when weighing atherosclerosis and bleeding in acute ICH. Observational studies with small sample size demonstrated that lower LDL-C levels were independently related to HE in ICH patients [25, 26]. What is more, recent studies suggested that lower LDL-C levels carried an increased hazard of mortality [12, 25]. Of the 75,443 ICH patients enrolled in our study, the fully adjusted OR of HE

for the lowest versus the highest LDL-C group was 1.22 (95% CI 1.10-1.35). When it comes to in-hospital mortality, full adjustment with admission GCS score attenuated the significant association with LDL-C. In the series of CSCA studies, the correlation between LDL-C and adverse events weakened with the aggravation of ICH [14].

Research about the strength and shape of the joint effects of SBP and LDL-C levels on hemorrhagic risk was limited. Data from the China Kadoorie Biobank prospective study showed that lowering LDL-C by 1 mmol/L increased the risk of ICH by about one-seventh, irrespective of baseline BP level [11], while another Korean observational study suggested that the inverse association between serum cholesterol and hemorrhagic stroke was restricted to hypertensive [18]. The results of our study added to the evidence that the bleeding risk associated with lower LDL-C (<70 mg/dL) in acute ICH patients with elevated SBP (≥140 mmHg). BP in the hyperacute phase of ICH was strongly related to adverse outcomes [10]; we thus performed a sensitivity analysis among patients admitted within 24 h of symptom onset which yielded identical results to the overall population. However, no apparent modification effect of SBP subgroups was discovered in the relationship between LDL-C and ICH prognosis. Our investigation suggested that acute ICH patients with lower LDL-C and elevated BP are more susceptible to HE and ensuing mortality; simultaneous control of these two factors may have therapeutic potential.

Hypertension is a well-recognized hazard factor for adverse outcomes in ICH patients, and intensive BP reduction was associated with reduced HE and improved functional outcomes [10]. Furthermore, cholesterol is important for the

integrity of vessel walls. While in the pathological state of ICH with poor BP control, decreased cholesterol levels could lead to the fragility of cerebrovascular endothelium [27], promote the necrosis of arterial smooth muscle cells [28], inhibit platelet aggregation [29], affect erythrocyte osmotic fragility [30], and eventually cause bleeding [31]. A combined but noninteractive effect of circulating LDL-C and SBP levels on ICH outcomes was observed in our study. Intensive control of SBP to 140 mmHg is rational and necessary, especially for acute ICH patients with lower LDL-C levels.

Our study confirmed and extended the results of our previous investigation by further adding SBP categories; lower LDL-C levels are related to an increased hazard of HE and in-hospital mortality in patients with poorly-controlled BP. Nonetheless, there are still some limitations. First, hematoma volume at baseline and follow-up were unaccessible, and the determination of HE relied on subcenters. Meanwhile, the time from symptom onset to CT scans was unobtainable in the CSCA program. Secondly, our study included patients who underwent surgery, which may cause selection bias. While the statistical significance remained after excluding 7,511 patients taken operation (data was not shown). Thirdly, despite no statistical significance being reached between lower LDL-C and poor prognosis in ICH patients with SBP controlled under 140 mmHg, these results should be interpreted with caution as the exact value of ORs were all above 1.00. Besides, further analysis focused on different hypertension grades (grade 1 and 2) compared with normotension was needed given the wide SBP thresholds in our study.

5. Conclusions

A combined but noninteractive effect of LDL-C and SBP levels on ICH outcomes was observed in our study. Lower LDL-C levels (<70 mg/dL) are associated with a higher risk of HE and in-hospital mortality confined to ICH individuals with elevated SBP (≥140 mmHg).

Data Availability

Data are available to researchers on request for purpose of reproducing the results or replicating the procedure by directly contacting the corresponding author.

Conflicts of Interest

The authors declare that there is no conflict of interest regarding the publication of this paper.

Authors' Contributions

Yarong Ding and Yu Wang contributed equally to this article.

Acknowledgments

Supplementary Materials

See Table S1 in the Supplementary Material for baseline characteristics between included and excluded ICH patients. (Supplementary Materials)

References

[1] V. L. Feigin, C. M. Lawes, D. A. Bennett, S. L. Barker-Collo, and V. Parag, "Worldwide stroke incidence and early case fatality reported in 56 population- based studies: a systematic review," Lancet Neurology, vol. 8, no. 4, pp. 355–369, 2009.

[2] W. Wang, B. Jiang, H. Sun et al., "Prevalence, incidence, and mortality of stroke in China," Circulation, vol. 135, no. 8, pp. 759–771, 2017.

[3] W. J. Tu, B. H. Chao, L. Ma et al., "Case-fatality, disability and recurrence rates after first-ever stroke: a study from bigdata observatory platform for stroke of China," Brain Research Bulletin, vol. 175, pp. 130–135, 2021.

[4] T. J. Moullaali, X. Wang, R. H. Martin et al., "Blood pressure control and clinical outcomes in acute intracerebral haemorrhage: a preplanned pooled analysis of individual participant data," Lancet Neurology, vol. 18, no. 9, pp. 857–864, 2019.

[5] C. S. Gray, A. J. Hildreth, P. A. Sandercock et al., "Glucose-potassium-insulin infusions in the management of post-stroke hyperglycaemia: the UK Glucose Insulin in Stroke Trial (GIST-UK)," Lancet Neurology, vol. 6, no. 5, pp. 397–406, 2007.

[6] M. N. Diringer, B. E. Skolnick, S. A. Mayer et al., "Thrombo-embolic events with recombinant activated factor VII in spontaneous intracerebral hemorrhage: results from the Factor Seven for Acute Hemorrhagic Stroke (FAST) trial," Stroke, vol. 41, no. 1, pp. 48–53, 2010.

[7] N. Sprigg, K. Flaherty, J. P. Appleton et al., "Tranexamic acid for hyperacute primary intracerebral haemorrhage (TICH-2): an international randomised, placebo-controlled, phase 3 superiority trial," Lancet, vol. 391, no. 10135, pp. 2107–2115, 2018.

[8] A. D. Mendelow, B. A. Gregson, E. N. Rowan et al., "Early surgery versus initial conservative treatment in patients with spontaneous supratentorial lobar intracerebral haematomas (STICH II): a randomised trial," Lancet, vol. 382, no. 9890, pp. 397–408, 2013.

[9] D. F. Hanley, R. E. Thompson, M. Rosenblum et al., "Efficacy and safety of minimally invasive surgery with thrombolysis in intracerebral haemorrhage evacuation (MISTIE III): a randomised, controlled, open-label, blinded endpoint phase 3 trial," Lancet, vol. 393, no. 10175, pp. 1021–1032, 2019.

[10] Q. Li, A. D. Warren, A. I. Qureshi et al., "Ultra-early blood pressure reduction attenuates hematoma growth and improves outcome in intracerebral hemorrhage," Annals of Neurology, vol. 88, no. 2, pp. 388–395, 2020.

[11] L. Sun, R. Clarke, D. Bennett et al., "Causal associations of blood lipids with risk of ischemic stroke and intracerebral

Retraction

Retracted: Sirtuin 1 Induces Choroidal Neovascularization and Triggers Age-Related Macular Degeneration by Promoting LCN2 through SOX9 Deacetylation

Oxidative Medicine and Cellular Longevity

This article has been retracted by Hindawi, as publisher, following an investigation undertaken by the publisher [1]. This investigation has uncovered evidence of systematic manipulation of the publication and peer-review process. We cannot, therefore, vouch for the reliability or integrity of this article.

Please note that this notice is intended solely to alert readers that the peer-review process of this article has been compromised.

Wiley and Hindawi regret that the usual quality checks did not identify these issues before publication and have since put additional measures in place to safeguard research integrity.

We wish to credit our Research Integrity and Research Publishing teams and anonymous and named external researchers and research integrity experts for contributing to this investigation.

The corresponding author, as the representative of all authors, has been given the opportunity to register their agreement or disagreement to this retraction. We have kept a record of any response received.

References

[1] S. Zhao, Z. Huang, H. Jiang et al., "Sirtuin 1 Induces Choroidal Neovascularization and Triggers Age-Related Macular Degeneration by Promoting LCN2 through SOX9 Deacetylation," *Oxidative Medicine and Cellular Longevity*, vol. 2022, Article ID 1671438, 16 pages, 2022.

Research Article

Sirtuin 1 Induces Choroidal Neovascularization and Triggers Age-Related Macular Degeneration by Promoting LCN2 through SOX9 Deacetylation

Su Zhao,[1,2] Zhi Huang,[3] Hao Jiang,[1] Jiangfan Xiu,[3] Liying Zhang,[1] Qiurong Long,[1] Yuhan Yang,[1] Lu Yu,[1] Lu Lu ⓘ,[4] and Hao Gu ⓘ[1]

[1]*Department of Ophthalmology, The Affiliated Hospital of Guizhou Medical University, Guiyang 550002, China*
[2]*School of Clinical Medicine, Guizhou Medical University, Guiyang 550002, China*
[3]*School of Basic Medical Science, Guizhou Medical University, Guiyang 550002, China*
[4]*Shenzhen Key Laboratory of Ophthalmology, Shenzhen Eye Hospital, Shenzhen 5180403, China*

Correspondence should be addressed to Lu Lu; 19188508@qq.com and Hao Gu; guhao@gmc.edu.cn

Increasing studies have identified the function of sirtuin-1 (SIRT1) in ocular diseases. Hence, this study is aimed at exploring the potential role of SIRT1 in choroidal neovascularization- (CNV-) induced age-related macular degeneration (AMD) development and the associated mechanism. Expression of SIRT1/SOX9/LCN2 in the hypoxic cells was determined, and their interactions were predicted by bioinformatics websites and followed by the verification by luciferase assay and chromatin immunoprecipitation (ChIP). Their *in vitro* effects on hypoxic cells concerning cell viability, apoptosis, migration, and angiogenesis were detected through gain- and loss-of-function assays. Besides, their *in vivo* effect was explored using the established CNV mouse models. Highly expressed LCN2, SOX9, and SIRT1 were observed in hypoxic cells. LCN2 was increased by SOX9 and SIRT1 deacetylated SOX9 to promote its nuclear translocation, which further inhibited the viability of human retinal pigment epithelial cells and promoted cell apoptosis and angiogenesis as well as CNV-induced AMD formation. The relieving role of LCN2 inhibition on CNV-induced AMD without toxicity for mice was also demonstrated by *in vivo* experiments. Overall, SIRT1 promoted the formation of CNV-induced AMD through SOX9 deacetylation-caused LCN2 upregulation, representing a promising target for CNV-induced AMD management.

1. Introduction

Choroidal neovascularization (CNV), as the pathological process of the invasion of abnormal blood vessels into the subretinal space of the mammalian eye, is known as a feature of the age-related macular degeneration (AMD) [1]. AMD, the main cause of visual impairment and even blindness, is a multifactorial disorder involving the dysregulation of complement, lipid, inflammation-related, angiogenesis-related, and extracellular matrix-related pathways [2]. AMD has two types: dry AMD with the presence of drusen and atrophy and wet AMD with the features of edema and hemorrhage within or below the retina or retinal pigment epithelium besides drusen and atrophy [3]. Vascular endo-

thelial growth factor inhibitor (anti-VEGF) is a well-known medical treatment for AMD; however, this therapy is inadequate for many patients and might experience a slow loss of efficacy with repeated use [4]. Hence, new approaches are expected. Therefore, this study is aimed at providing a novel therapeutic target for CNV-induced AMD management.

Sirtuin-1 (SIRT1) can regulate a variety of cellular functions such as metabolism, inflammation, and oxidative stresses [5–7]. Meantime, SIRT1 is a key mediator in the pathogenesis of AMD [8]. More specifically, SIRT1 also serves as a therapeutic target for CNV treatment [9]. Additionally, SIRT1 can regulate the acetylation of sex determining region Y- (SRY-) box 9 (SOX9) through nuclear translocation [10]. SOX9 belongs to the SOX gene family

expressed in several organisms and involved in numerous physiological processes such as sex determination and development gonad [11]. A previous study has shown the key roles of SOX9 in the progression of CNV [1]. Moreover, SOX9 together with lipocalin 2 (LCN2) has been identified to be partially correlated with the extent of tubulointerstitial fibrosis and tubular cell injury [12]. LCN2 is a member of secreted adipokines which engaged in the pathogenesis of several diseases including cancer, diabetes, obesity, and AMD [13]. Therefore, it can be hypothesized that SIRT1/SOX9/LCN2 axis may exert great functions on the progression of CNV in AMD, but their specific interactions in CNV-induced AMD remain unclear. Hence, the present study was conducted to verify the hypothesis and explore the specific mechanism among SIRT1, SOX9, and LCN2 in the development of CNV-induced AMD, which will be greatly helpful to enlarge the understanding of CNV-induced AMD and to validate a novel therapy.

2. Materials and Methods

2.1. Ethics Statement.
Animal experiments were implemented in the light of the recommendations in the Guide for the Care and Use of Laboratory Animals issued by the US National Institutes of Health.

2.2. Bioinformatics Analysis.
AMD-related mRNA expression datasets GSE29801 and GSE103060 were downloaded from the Gene Expression Omnibus database. GSE29801 contains 151 normal samples and 142 AMD samples, while GSE103060 contains 8 normal samples and 8 AMD samples. Differential analysis was conducted using R language "limma" package to identify differentially expressed genes (DEGs) in AMD with $|\log \text{fold change (FC)}| > 1$, p value < 0.05 as the threshold. Transcription factors of the DEGs were predicted using the KnockTF and CistromeDB databases.

2.3. Cell Culture and Hypoxia Model Construction.
Human retinal pigment epithelial cells (ARPE-19, Cat.#CRL-2302) and human umbilical vein endothelial cells (HUVEC, Cat.#CRL-1730) were all purchased from the American Type Culture Collection (Manassas, VA, USA) and cultured in Dulbecco's modified Eagle's medium/F12 medium containing 10% fetal bovine serum (FBS) and 1% penicillin/streptomycin at 37°C with normoxia (consisting of 21% O_2, 5% CO_2, and 74% N_2). ARPE-19 cells for hypoxia model construction were cultured in an incubator under 1% O_2, 5% CO_2, and 94% N_2.

2.4. Cell Transfection.
Lentiviruses carrying short-hairpin RNA- (sh-) SOX9, sh-SIRT1, sh-LCN2, sh-negative control (NC), overexpression- (oe-) SIRT1, oe-LCN2, oe-SOX9, and oe-NC were purchased from GenePharma (Shanghai, China). ARPE-19 cells were seeded in a 6-well plate with 2 mL culture medium per well. Cell transfection was implemented upon 50% confluency. A total of 800 μL fresh virus solution (multiplicity of infection (MOI) = 30) was mixed with 800 μL FBS and added with Polybrene to a final concentration of 6 μg/mL. After 48 h of transfection, the cells were

cultured in a medium containing puromycin (1 μg/mL) for 2 weeks to select stable transfected cell lines. In order to evaluate the effect of sh-SOX9, sh-SIRT1, sh-LCN2, sh-NC, oe-SIRT1, oe-LCN2, and oe-SOX9, ARPE-19 cells were cultured in 1% serum for 2 weeks and used for the subsequent experiments.

2.5. Western Blot Analysis.
Total protein was extracted, electrophoresed, and then electroblotted to polyvinylidene fluoride membranes. The membrane was then incubated with diluted mouse anti-SIRT1 antibody (sc-8422, 1:500, Santa Cruz Biotechnology, Santa Cruz, CA, USA), rabbit anti-SOX9 antibody [8242, 1:1000, Cell Signaling Technologies (CST), Danvers, MA, USA], acetylated-Lysine (9441, 1:500, CST), rabbit anti-LCN2 antibody (26991-1-AP, 1:1000, Proteintech, Rosemont, IL, US), and rabbit anti-β-actin antibody (ab8227, 1:1000, Abcam, Cambridge, UK) overnight at 4°C as well as with horseradish peroxidase- (HRP-) labeled secondary antibody goat anti-rabbit (ab205718, 1:2000, Abcam) or goat anti-mouse (ab6789, 1:2000, Abcam) at room temperature for 1 h. Afterwards, the membrane visualized with enhanced chemiluminescence reagent (EMD Millipore, Billerica, MA, USA) and detected by ImageQuant LAS 4000 system (General Electric Co., Boston, MA, USA). ImageJ software was used to quantify the gray values of target bands, with β-actin used as an internal reference.

2.6. Enzyme-Linked Immunosorbent Assay (ELISA).
The hypoxic ARPE-19 cells were plated and treated for 24 h. The culture medium was collected, centrifuged at 1000 g for 5 min to remove particles, and the remaining was stored at -80°C until ELISA was performed. The retinal and choroid tissues were separated from CNV mice (post-laser, 21 days), homogenized in ice-cold RIPA lysis buffer (Boster) containing 1% protease inhibitor mixture and 1% phosphatase mixture, and centrifuged at 15000 g for 15 min with the supernatant harvested for detection of the content of VEGF (human DY293B and mouse DY493, R&D Systems, Minneapolis, MN, USA), tumor necrosis factor α (TNF-α, human DY210 and mouse DY410, R&D Systems), and interleukin-6 (IL-6, human DY206 and Mouse DY406, R&D Systems) utilizing ELISA Duoset system.

2.7. Cell Counting Kit 8 (CCK-8) Assay.
The hypoxic ARPE-19 cells were separated, resuspended, seeded into a 96-well plate at a density of 1×10^5 cells/mL (100 μL) and cultured overnight. CCK-8 kit (C0037, Beyotime, Shanghai, China) was used to detect cell viability, with 3 duplicated well set. Next, the cells were incubated with 10 μL of CCK-8 solution for 4 h in an incubator. Finally, the optical density (OD) value at 450 nm was measured with the help of a microplate reader followed by construction of a growth curve.

2.8. Flow Cytometry.
The hypoxic ARPE-19 cells were resuspended and seeded in a six-well plate for overnight culture. Afterwards, the corresponding treatment was performed, and Annexin-V-fluorescein isothiocyanate/propidium iodide (AV/PI staining, 556547, BD Bioscience, San Jose, CA, USA) and flow cytometry (FACSCalibur, BD

company) were applied to determine the apoptosis of ARPE-19 cells. Early apoptosis (AV single positive cells) and necrosis (AV and PI double positive cells) were quantified using FlowJo software.

2.9. Tube Formation Experiment. Matrigel (354234, Corning Incorporated, Corning, NY, USA) was frozen and thawed at 4°C overnight. Next, 75 μL Matrigel was added to each well of a pre-chilled 96-well plate and cultured at 37°C for 60 min. HUVEC suspension was added to a 96-well plate (2.5×10^4 cells/well) and incubated with the corresponding conditioned medium (CM) of ARPE-19 cells for 12-24 h, and then the appropriate field of view was selected for observation and photography under a microscope.

2.10. Transwell Assay. After ARPE-19 cells were treated with hypoxia and other corresponding treatments, the culture medium supernatant was collected. HUVECs were cultured in serum-free medium for 12 h, harvested, and resuspended with different CMs (1×10^5/mL) in the basolateral chamber. A Transwell chamber was added with 100 μL of HUVEC suspension for incubation at 37°C for 24 h. The cells migrated to the basolateral chamber were fixed with 100% methanol, dyed (Sigma-Aldrich, St. Louis, MO, USA) and counted under an inverted optical microscope (Zeiss, Jena, Germany) in 5 randomly selected visual fields.

2.11. Luciferase Assay. Based on the study [14], a full-length human SOX9 cDNA was synthesized according to the UCSC (http://genome.ucsc.edu) sequence and cloned into pcDNA3.1(+) vector (Promega, Madison, WI, USA) to generate pcDNA3.1-h_SOX9. The binding motif of the transcription factor SOX9 on the promoter region of human LCN2 was predicted on the website (http://cisbp.ccbr.utoronto.ca/index.php). The human LCN2 promoter region was constructed into pGL3-Basic vector (E1751, Promega) to obtain a human LCN2-wild-type (WT) recombinant vector, and the binding motif of SOX9 on LCN2 was mutated and constructed into pGL3-Basic vector (Promega) to produce a recombinant vector of human LCN2 mutant (MUT). The constructed luciferase reporter plasmids WT and MUT were cotransfected with pcDNA3.1 (empty) or pcDNA3.1-h_SOX9 into HEK-293T cells. The luciferase activity was checked using Dual Luciferase Reporter Gene Assay Kit (E1910, Promega) and SpectraMaxi3 reader multifunctional microplate reader (Molecular Devices, San Jose, CA, USA) with Renilla luciferase as the internal control.

2.12. Chromatin Immunoprecipitation (ChIP) Assay. When reaching 90% confluence, cells were fixed with 1% formaldehyde for 10 min to cross-link DNA and protein, which was then terminated by glycine. The precipitate was resuspended, treated with ribozyme for 20 min, sonicated into 200-1000 bp fragments with ultrasonic wave, and randomly centrifuged at 13000 g at 4°C. The supernatant was collected and divided into four tubes. One was used as input; the remaining three were incubated with positive control antibody Histone H3, NC antibody IgG, and rabbit anti-SOX9 (82630, 1: 20, CST), respectively, overnight at 4°C. The endogenous DNA-protein complexes were precipitated with

magnetic beads and centrifuged with the supernatant aspirated. The nonspecific complexes were washed, and the de-cross-linking was performed overnight at 65°C. The DNA fragments were extracted and purified to recover the DNA fragments, and the expression of the LCN2 promoter was checked by PCR. Primer sequence: forward: 5′-TGCAGA AATCTTGCCAAGTG-3′ and reverse: 5′-AGGAGACCT AGGGGCATGAT-3′.

2.13. Mice Model of CNV Construction. Mouse models of CNV were established by the laser irradiation. Six-week-old male C57BL/6 mice (Shanghai SLAC Laboratory Animal Co., Ltd., Shanghai, China) were housed at 22-25°C in a 12 h light/dark cycle with free access to food and water. In order to induce experimental CNV, laser-induced Bruch membrane rupture was performed on the eyes of mice after isoflurane gas anesthesia. Medical sodium hyaluronate gel was added into the experimental eye, and a 2×2 cm cover glass was placed in front of eyes; photocoagulation was conducted with the optic disc as the center using a slit lamp (SL120, Zeiss) with a laser (power, 200 mW; spot diameter, 100 μm; exposure time, 0.1 s; wavelength, 532 nm) at 1.5-2 PD from the optic disc.

A vitreous body was injected with lentivirus or synthetic peptide immediately after laser treatment. The mice were randomly assigned and intravitreally injected with sh-NC+ oe-NC, sh-SIRT1+oe-NC, sh-NC+oe-LCN2, sh-SIRT1+oe-LCN2, 2 μL of LCN2 inhibitor (RGDS peptide, $n = 8$; 5000 ng/μL, ab230365, Abcam), and 2 μL of placebo (RGES peptide, $n = 8$, 5000 ng/μL, APC038, Shanghai Apeptide Co., Ltd., Shanghai, China). Efficacy was evaluated by isolectin B4 immunofluorescence staining.

2.14. Immunofluorescence Staining. After fixation, the tissue sections were sealed by 0.3% Triton X-100 in PBS and 5% goat serum protein (Beyotime, Shanghai, China) for 1 h, reacted with isolectin (1 : 1000, Santa Cruz Biotechnology) at 4°C overnight, and incubated further with secondary antibody labeled with Alexa Fluor 488 or Alexa Fluor 594 (1 : 1000, Thermo Fisher Scientific Inc., Waltham, MA, USA) for 45 min. The images were captured with the help of a fluorescence microscope (Olympus, Japan) and a Leica TCS SP8 confocal laser scanning microscope (Leica TCS NT, Wetzlar, Germany). Quantification of the CNV area was performed with the help of an image analysis software.

Cells were washed with PBS, fixed with 4% formaldehyde for 15 min, treated with 0.2% Triton X-100 PBS at 4°C for 15 min, sealed with 1% BSA for 1 h, and incubated with anti-SOX9 antibody (sc-166505, 1 : 100, Santa Cruz Biotechnology). After PBS washing for 3 times, the cells were incubated with Alexa Fluor 568-labled secondary antibody (1 : 200) for 30 min, stained with DAPI, fixed, and observed under an inverted fluorescence microscope.

2.15. Statistical Analysis. SPSS 22.0 statistical software (IBM Corp., Armonk, NY, USA) was utilized for analysis with measurement data summarized as the mean ± standard deviation (SD). Comparison of data between two groups was performed by an unpaired t-test was selected for two

group comparisons, while one-way analysis of variance (one-way ANOVA) for multiple groups. $p < 0.05$ was concluded statistically significant.

3. Results

3.1. LCN2 Inhibited Hypoxic Cell Viability and Promoted Cell Apoptosis and Angiogenesis. An *in vitro* cell model of hypoxia was established using ARPE-19 cells. Western blot analysis results showed that the protein expression of E-cadherin was decreased while that of N-cadherin, Snail, and Vimentin was increased in ARPE-19 cells exposed to hypoxia (Fig. S1A), demonstrating that hypoxic ARPE-19 cells have an EMT phenotype. Furthermore, elevated LCN2 was seen in hypoxia-exposed ARPE-19 cells (Figure 1(a)). The *in vitro* effect of LCN2 on AMD was then explored. Silencing efficiency of LCN2 was confirmed by Western blot analysis, with sh-LCN2#2 presenting with higher silencing efficiency (Figure 1(b)) and thus selected for follow-up experiments. As shown in Figures 1(c)–1(g), cells transfected with sh-LCN2 presented decreased expression of VEGF, TNF-α, and IL-6; enhanced cell viability; and decreased cell apoptosis, migration, and angiogenesis. However, transfection with oe-LCN2 led to opposite results. Altogether, LCN2 inhibited the viability of hypoxic cells and promoted cell apoptosis and angiogenesis.

3.2. SOX9 Promoted the Expression of LCN2. To explore the mechanism of LCN2 in CNV-induced AMD, potential transcription factors were predicted through the KnockTF and CistromeDB databases, and AMD-related transcription factor SOX9 was obtained after the intersection analysis with the 2015 and 1334 DEGs obtained from the GSE29801 and GSE103060 datasets, respectively (Figures 2(a)–2(c)). SOX9 was elevated in the GSE29801 (Figure 2(d)) and GSE103060 (Figure 2(e)) datasets. In addition, ARPE-19 cells after hypoxia exposure also showed increased SOX9 expression (Figure 2(f)). Western blot analysis confirmed the silencing efficiency of SOX9, evidenced by decreased SOX9 protein expression in hypoxic ARPE-19 cells following transfection of sh-SOX9#1 and sh-SOX9#2, with sh-SOX9#2 exhibiting the higher silencing efficiency (Figure 2(g)). Thus, sh-SOX9#2 (sh-SOX9) was selected for follow-up experiments. ChIP-PCR data unraveled that SOX9 was enriched in the LCN2 promoter region (Figure 2(h)). The luciferase activity of LCN2-WT in hypoxic cells transfected with oe-SOX9 was increased while that of LCN2-MUT was unaffected compared with cells transfected with oe-NC (Figure 2(i)), indicating that SOX9 elevated LCN2. Moreover, the protein expression of LCN2 in hypoxic ARPE-19 cells transfected with sh-SOX9 was reduced while oe-SOX9 caused elevated LCN2 protein expression (Figure 2(j)). To conclude, SOX9 was capable of elevating LCN2.

3.3. SIRT1 Inhibited the Activity of Hypoxic Cells and Promoted Cell Apoptosis and Angiogenesis by Elevating the Expression of LCN2 through SOX9 Deacetylation. Previous evidence demonstrated that SIRT1 deacetylated SOX9 [15]. We further investigated whether SIRT1 could regulate LCN2 expression by promoting SOX9 nuclear translocation through SOX9 deacetylation. We found that the expression of SIRT1 was increased in hypoxia-exposed ARPE-19 cells (Figure 3(a)). The silencing efficiency of sh-SIRT1 was confirmed by Western blot analysis, as shown by decreased protein expression of SIRT1 in cells transfected with sh-SIRT1#1 or sh-SIRT1#2, among which the silencing efficiency of sh-SIRT1# 2 was higher (Figure 3(b)), so sh-SIRT1#2 (sh-SIRT1) was selected for subsequent experiments. Besides, overexpressed SIRT1 exerted no effect on the protein expression of SOX9 but decreased the protein expression of acetylated SOX9 in the nucleus, and SIRT1 silencing upregulated the expression of acetylated SOX9 in the nucleus (Figure 3(c)). Moreover, the SOX9 fluorescence in the nucleus was notably increased in response to oe-SIRT1 but decreased upon sh-SIRT1 (Figure 3(d)), indicating that SIRT1 can promote the nuclear translocation of SOX9 through deacetylation.

Next, it was investigated whether SIRT1 can promote SOX9 nuclear translocation by deacetylating SOX9, thereby affecting the expression of LCN2. Western blot data disclosed that SIRT1 silencing decreased SIRT1 and LCN2 and increased acetylated SOX9 expression; LCN2 overexpression played the opposite role to SIRT1 silencing; and downregulation of SIRT1 and LCN2 and upregulation of acetylated SOX9 mediated by SIRT1 silencing also could be reversed by LCN2 overexpression in hypoxic ARPE-19 cells (Figure 3(e)). In summary, SIRT1 could promote nuclear translocation of SOX9 through deacetylation, thereby promoting the expression of LCN2.

Furthermore, functional assays revealed that SIRT1 silencing causes a reduction in VEGF, TNF-α, and IL-6 expression, an enhancement in cell viability and an attenuation in cell apoptosis, while LCN2 overexpression could reverse the above conditions in hypoxia-exposed ARPE-19 cells (Figures 3(f)–3(h)). As shown in Figures 3(i) and 3(j), migration and tube formation of HUVECs were noted to be attenuated in the presence of SIRT1 silencing, while further overexpression of LCN2 led to opposite results.

Thus, SIRT1 promoted the SOX9 nuclear translocation through the deacetylation of SOX9, thereby promoting the expression of LCN2 to inhibit the viability of hypoxic cells and promote cell apoptosis and angiogenesis.

3.4. SIRT1 Promoted Laser-Induced CNV Formation in Mice by Promoting LCN2 through the Deacetylation of SOX9. Next, we focused on the role of SIRT1/SOX9/LCN2 in the laser-induced CNV model in mice. At 7 days after CNV induction by laser, the mice were treated. Western blot data revealed that SIRT1 and LCN2 were notably upregulated, while acetylated SOX9 was downregulated in the choroid/RPE tissues of mice after laser treatment (Figure 4(a)). Besides, we proved that SIRT1 silencing downregulated SIRT1 and LCN2 and upregulated acetylated SOX9 in the choroid/RPE tissues of mice, which also could be reversed by LCN2 overexpression (Figure 4(b)). We also discovered that SIRT1 silencing could reduce CNV area and LCN2 overexpression could increase CNV area. And the CNV area reduced by SIRT1 silencing can be reversed by LCN2
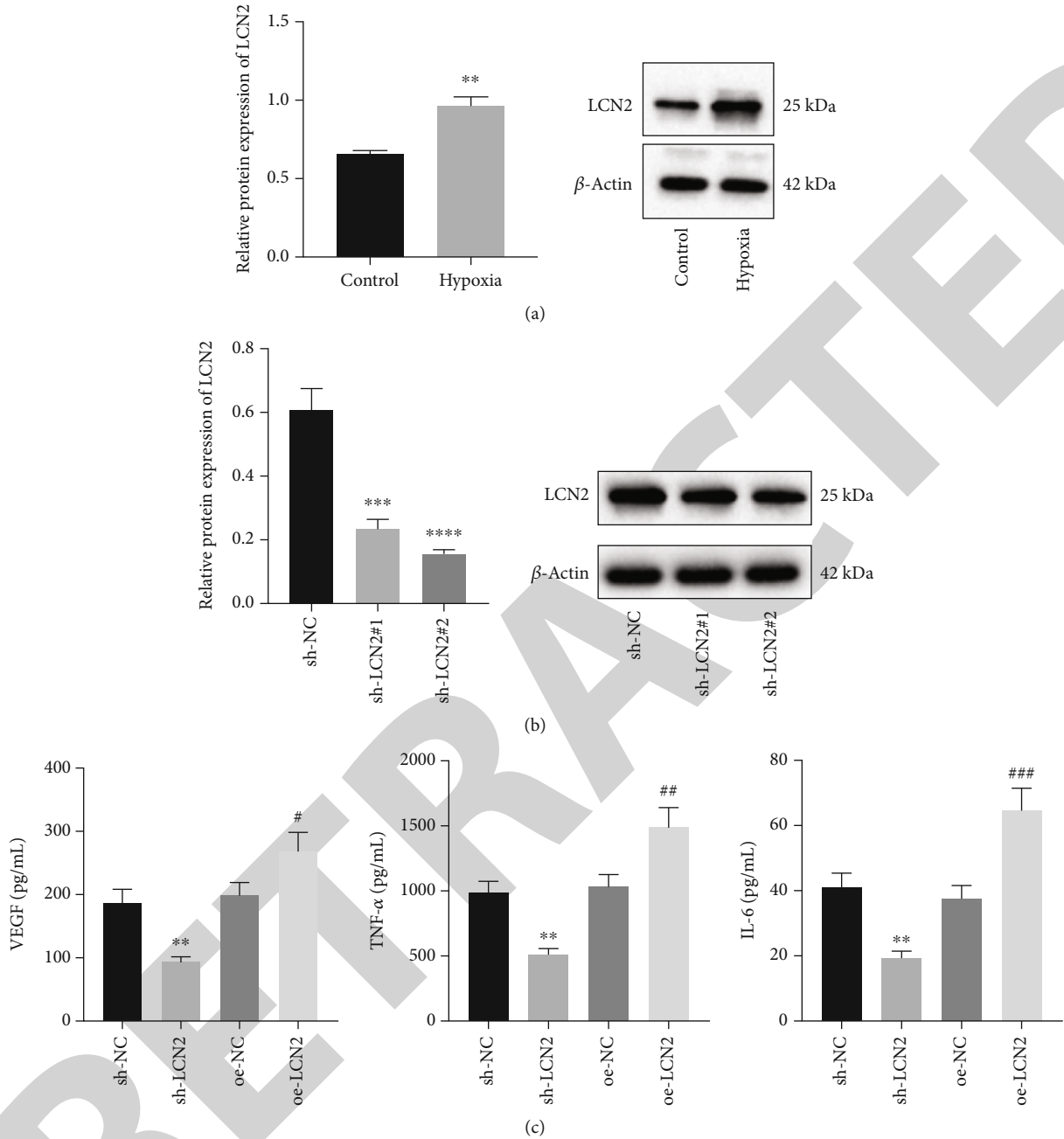
(a)

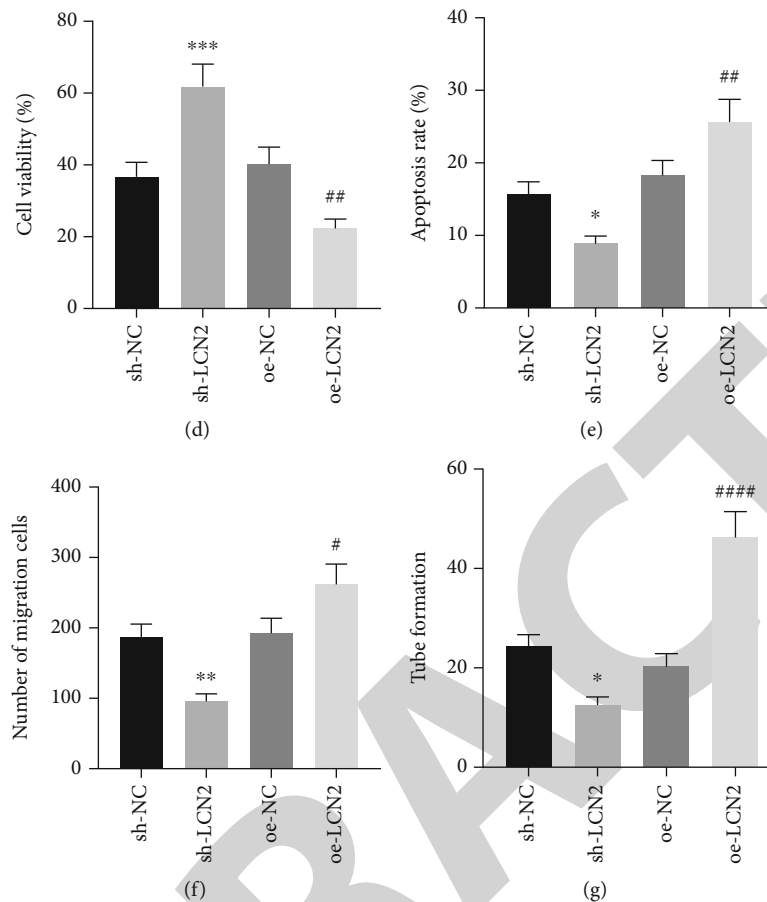(b)

(c)

Figure 1: Continued.

FIGURE 1: LCN2 inhibits the viability of hypoxic cells and promotes cell apoptosis and angiogenesis. (a) The protein expression of LCN2 in ARPE-19 cells exposed to hypoxia determined by Western blot analysis. (b) The protein expression of LCN2 in hypoxic cells after different transfections determined by Western blot analysis. (c) The content of VEGF, TNF-α and IL-6 in the cell culture fluid determined by ELISA. (d) The viability of hypoxic cells after different transfections determined by CCK-8. (e) The apoptosis of hypoxic cells after different transfections determined by flow cytometry. (f) The migration of hypoxic cells after different transfections determined by Transwell. (g) The angiogenesis of hypoxic cells after different transfection determined by tube formation experiment. $^*p < 0.05$, compared with control or cells transfected with sh-NC; $^\#p < 0.05$, compared with cells transfected with oe-NC. $^{**}p < 0.01$, $^{***}p < 0.001$, and $^{****}p < 0.0001$. $^{\#\#}p < 0.01$, $^{\#\#\#}p < 0.001$, and $^{\#\#\#\#}p < 0.0001$.

overexpression, and the CNV area increased by LCN2 overexpression can also be reversed by SIRT1 silencing (Figures 4(c) and 4(d)). In summary, SIRT1 promoted the expression of LCN2 by deacetylating SOX9 to promote the formation of laser-induced CNV in mice.

3.5. LCN2 Inhibitors Inhibited the Formation of CNV in Mice with Rare Toxicity to Tissues. In order to further explore the potential of LCN2 inhibition in the clinical treatment of CNV, LCN2 inhibitor RGDS and placebo RGES were used for follow-up studies. Western blot analysis results showed that the protein expression of LCN2 was upregulated in the choroid/RPE tissues of mice after laser treatment. Compared with the Laser+RGES group, the protein expression of LCN2 was downregulated in the choroid/RPE tissues of mice in the Laser+RGDS group (Figure 5(a)). Additionally, CNV formation in mice after laser treatment was increased. Compared with mice treated by Laser+RGES, the Laser+RGDS treatment decreased the formation of CNV in the choroid/

RPE tissues (Figures 5(b) and 5(c)). Subsequently, the maximum lesion diameter of CNV and CNV/choroid ratio were higher in mice after laser treatment than those of the control mice. To sum up, RGDS can inhibit the formation of laser-induced CNV.

4. Discussion

CNV is the feature of late-stage AMD and the greatest contributor for irreversible central visual loss among the elderly with AMD (Wang et al., 2016, [16, 17]). The hallmark of AMD pathogenesis is the retinal pigment epithelial cell damage induced by drusen accumulation, in which oxidative stress and inflammation are the well-known molecular mechanisms [18]. A recent study has identified the crucial role of SIRT1 in ocular diseases [19]. Here, we designed to investigate the potential mechanism of SIRT1 in CNV-induced AMD, and our final results demonstrated that SIRT1 elevated LCN2 through SOX9 deacetylation,
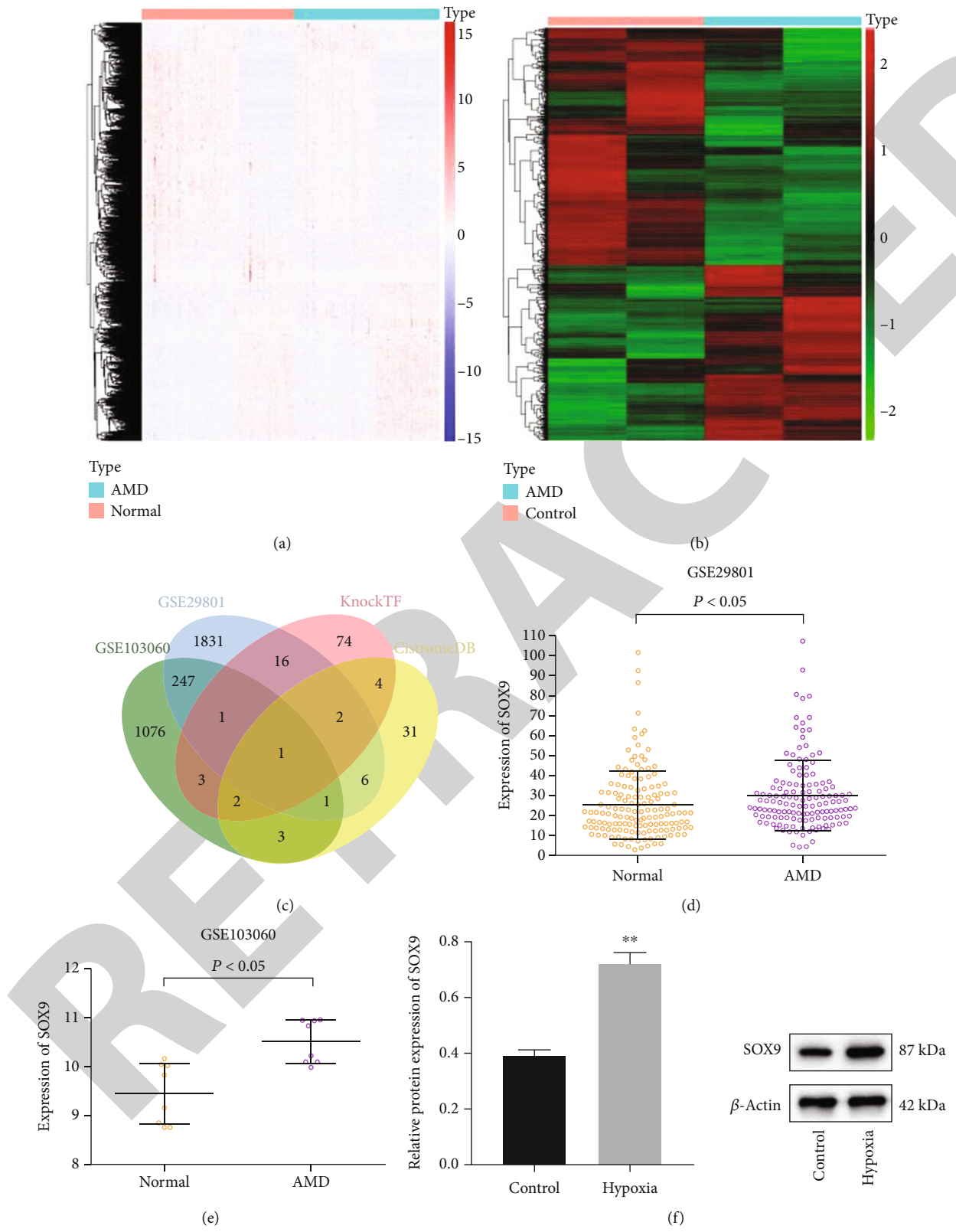
(a)

(b)
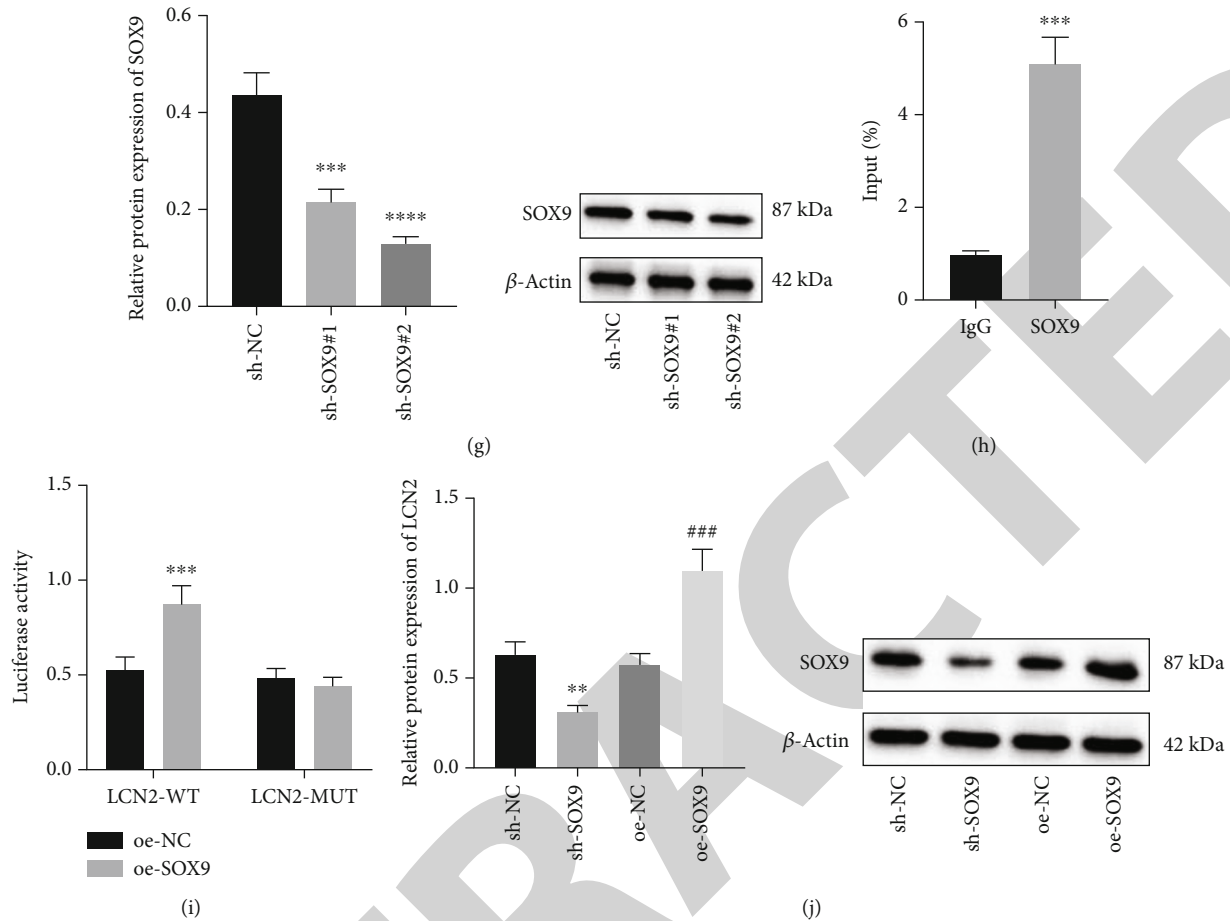
(c)

(d)

(e)

(f)

Figure 2: Continued.

Figure 2: SOX9 upregulates LCN2 expression. (a) A heat map of DEGs between 151 normal samples and 142 AMD samples in GSE29801 dataset. (b) A heat map of DEGs between 8 normal samples and 8 AMD samples in GSE103060 dataset. (c) Venn diagram of the intersection among 4 datasets. (d) The expression of SOX9 in GSE29801 dataset (151 normal samples and 142 AMD samples). (e) The expression of SOX9 in GSE103060 dataset. (f) The protein expression of SOX9 in control and hypoxia-exposed ARPE-19 cells determined by Western blot analysis; $*p < 0.05$, compared with control ARPE-19 cells. (g) The protein expression of SOX9 in hypoxia-exposed ARPE-19 cells after different transfection determined by Western blot analysis. (h) Binding sites between SOX9 and LCN2 determined by ChIP-PCR; $*p < 0.05$, compared with IgG. (i) The effect of SOX9 on LCN2 promoter activity in HEK-293T cells determined by dual luciferase reporter gene assay; $*p < 0.05$, compared with HEK-293T cells transfected with oe-NC. (j) The protein expression of LCN2 in hypoxia-exposed ARPE-19 cells after different transfection determined by Western blot analysis. The experiment was repeated three times. $*p < 0.05$ and $**p < 0.01$, compared with hypoxia-exposed ARPE-19 transfected with sh-NC; $#p < 0.05$, compared with hypoxia-exposed ARPE-19 cells transfected with oe-NC. $***p < 0.001$ and $****p < 0.0001$. $###p < 0.001$.

thereby enhancing cell apoptosis, migration, and angiogenesis of hypoxic cells *in vitro* and inducing CNV formation *in vivo*.

It is reported that LCN2 is capable of protecting against ocular inflammation and thus further acts as a promising target for managing ocular diseases such as uveitis and retinal degeneration [20, 21]. LCN2 has been also confirmed as a potential target for AMD treatment [22]. More importantly, the expression of LCN2 is positively correlated with the severity of CNV in AMD [23, 24]. In our study, we proved that LCN2 could prevent viability and induce apoptosis and angiogenesis in ARPE-19 cells after hypoxia.

Additionally, we further predicted the possible target genes of LCN2 by bioinformatics analysis, and we discovered that SOX9 is an underlying regulatory gene of LCN2 in AMD-induced CNV. A promising therapeutic role of SOX9 has been also illustrated in retinal degenerative diseases [25]. Similar to our findings, another study has also observed the downregulation of SOX9 in the dorsal neural retina, which is negatively related to the dorsal choroidal vascular development [26]. In our study, we verified that SOX9 was highly expressed in AMD and hypoxia-induced ARPE-19 cells. And we also proved that SOX9 could upregulate LCN2 in ARPE-19 cells after hypoxia.

SIRT1, a member of the sirtuin gene family, has key roles in the regulation of gene expression, maintenance of chromosome architecture, and cell cycle progression [27]. It has been reported that SIRT1 has various functions, such as antioxidant, antifree radical, antiaging, metabolic regulation, and immune regulation, all of which processes are associated
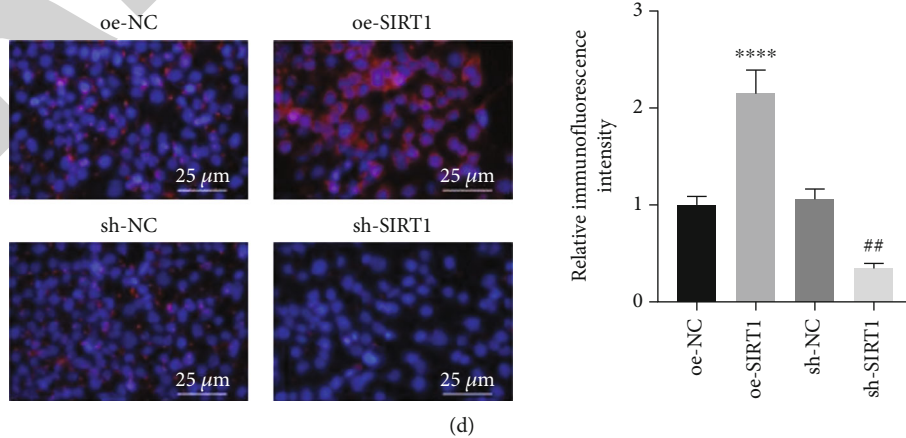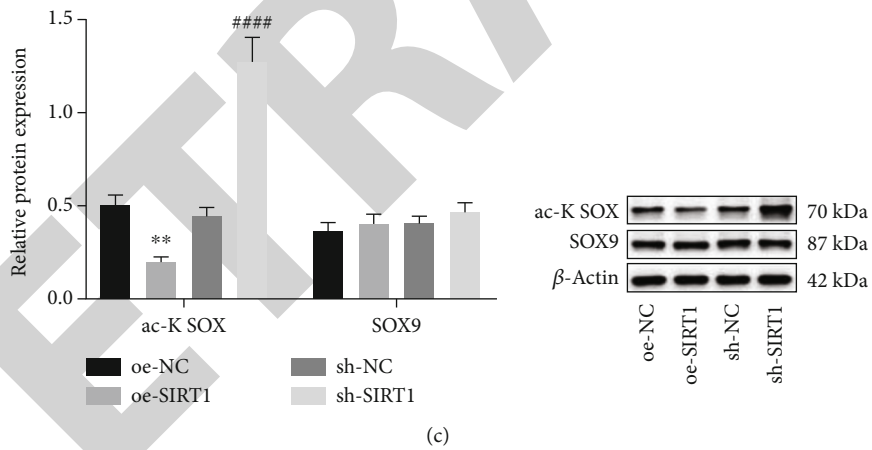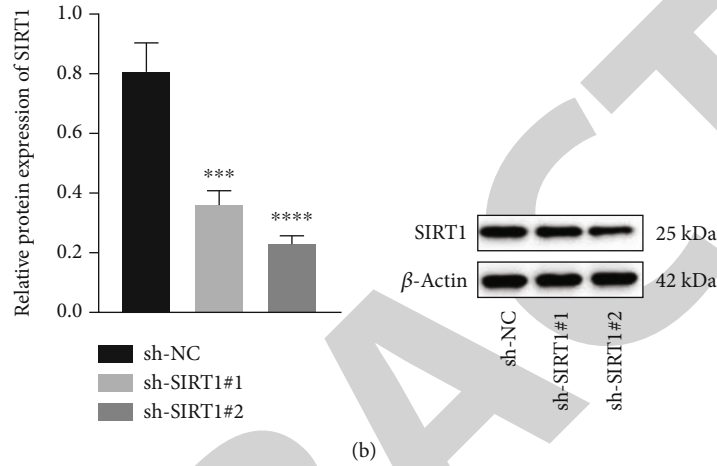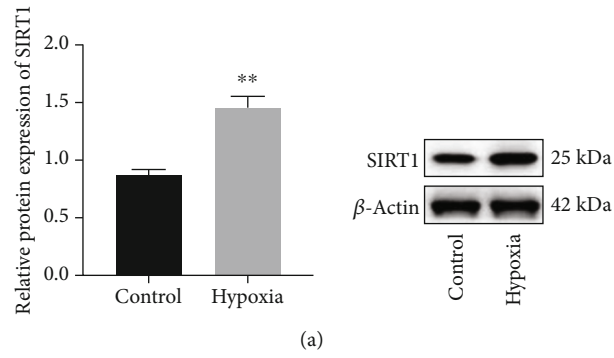
FIGURE 3: Continued.
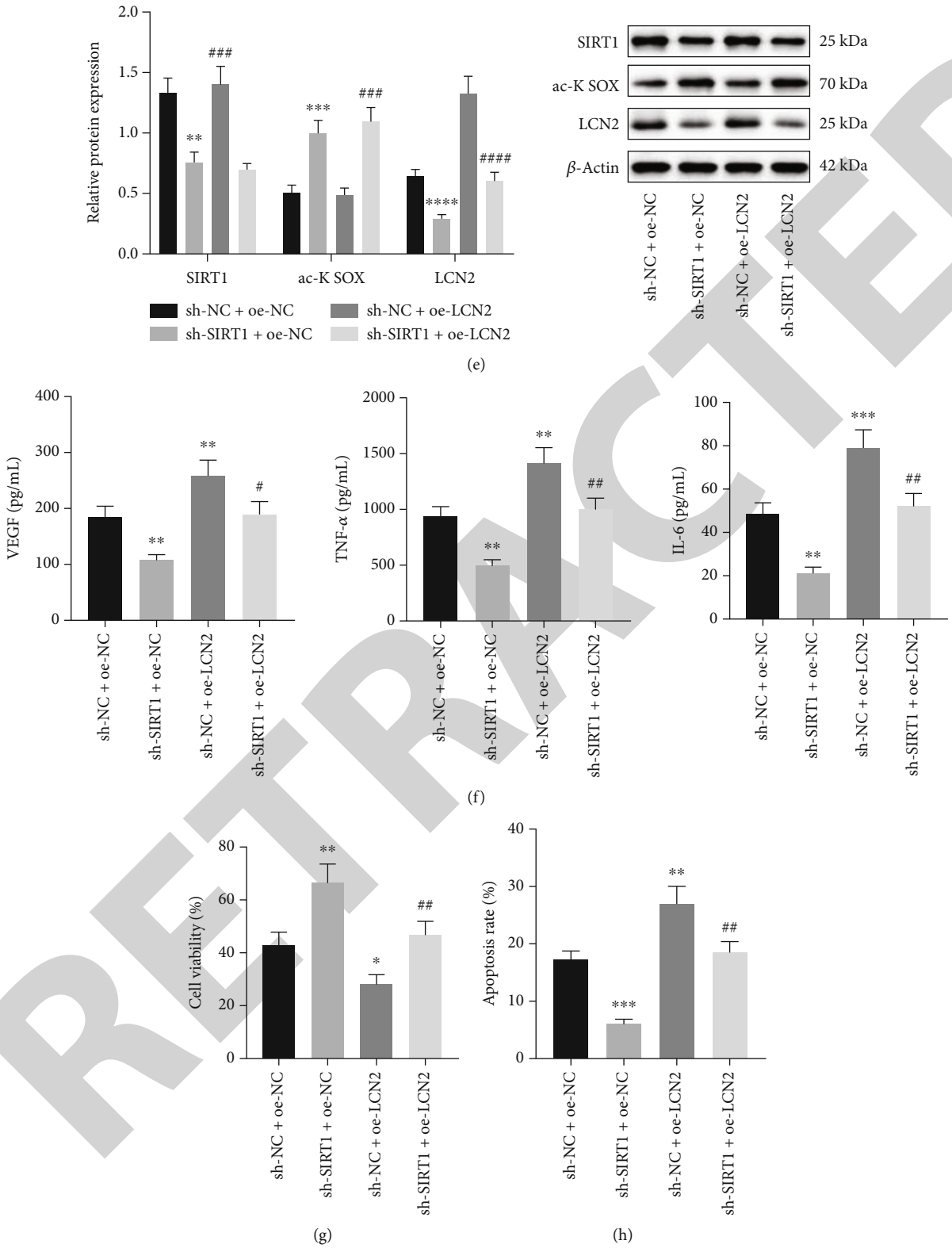
(e)

(f)
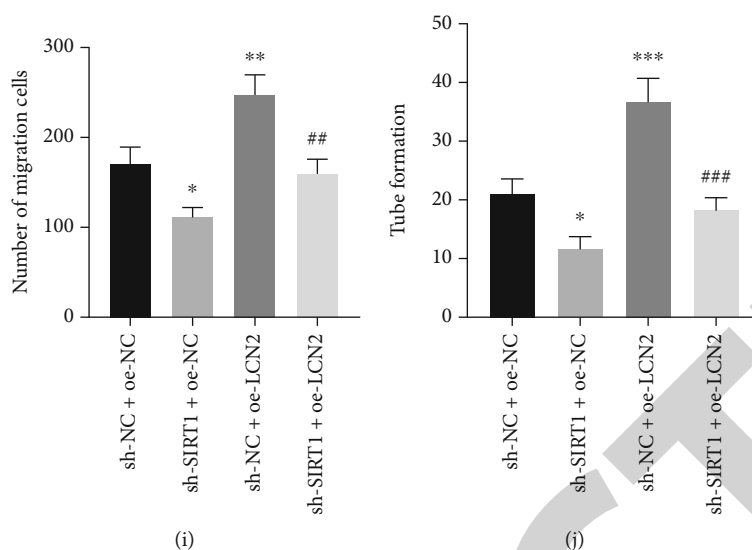

(g)

(h)

Figure 3: Continued.

(i)

(j)

Figure 3: SIRT1 promotes the SOX9 nuclear translocation through the deacetylation of SOX9, thereby increasing the expression of LCN2. (a) The protein expression of SIRT1 in control and hypoxia-exposed ARPE-19 cells determined by Western blot analysis. $^{**}p < 0.01$, compared with control ARPE-19 cells. (b) The protein of SIRT1 in hypoxia-exposed ARPE-19 cells after different transfection determined by Western blot analysis. $^{***}p < 0.001$ and $^{****}p < 0.0001$, compared with hypoxia-exposed ARPE-19 cells transfected with sh-NC. (c) The protein expression of SOX9 and acetylated SOX9 in hypoxia-exposed ARPE-19 cells after different transfection determined by Western blot analysis. $^{**}p < 0.01$, compared with hypoxia-exposed ARPE-19 cells transfected with oe-NC. $^{####}p < 0.0001$, compared with hypoxia-exposed ARPE-19 cells transfected with sh-NC. (d) The nuclear localization of SOX9 in hypoxia-exposed ARPE-19 cells after different transfections determined by immunofluorescence staining (scale bar: 25 μm). (e) The protein expression of SIRT, acetylated SOX9, and LCN2 in the hypoxia-exposed ARPE-19 cells after different transfections determined by Western blot analysis. (f) The content of VEGF, TNF-α, and IL-6 in the conditioned medium of hypoxia-exposed ARPE-19 cells after different transfections determined by ELISA. (g) Hypoxia-exposed ARPE-19 cell viability detected by CCK-8. (h) Hypoxia-exposed ARPE-19 cell apoptosis detected by flow cytometry. (i) HUVEC migration detected by Transwell assay. (j) HUVEC angiogenesis detected by tube formation experiment. In (e)–(h), $^*p < 0.05$, compared with hypoxia-exposed ARPE-19 cells transfected with sh-NC+oe-NC. $^#p < 0.05$, compared with hypoxia-exposed ARPE-19 cells transfected with sh-SIRT1+oe-NC. In (i) and (j), $^*p < 0.05$, compared with HUVECs transfected with sh-NC+oe-NC; $^#p < 0.05$, compared with HUVECs transfected with sh-SIRT1+oe-NC. $^{**}p < 0.01$, $^{***}p < 0.001$, and $^{****}p < 0.0001$. $^{##}p < 0.01$, $^{###}p < 0.001$, and $^{####}p < 0.0001$.

with hypoxia [28]. The study proved that highly expressed SIRT1 is also observed previously in the cornea of mice with diabetic dry eyes [29]. Besides, SIRT1 was also observed to be highly expressed in the anterior capsule and peripheral blood samples of patients with age-related cataract [30]. In our study, we further found that SIRT1 presented abnormally high expression in hypoxic cells.

Furthermore, SIRT1 is a well-recognized deacetylase responsible for SOX9 deacetylation, which further induces SOX9 nuclear localization in retinal pigment epithelial cells [15, 31]. The negative regulation relationship between SIRT1 and SOX9 has been validated in a recent study [10]. To further figure out the function of SIRT1 in AMD, hypoxic cells were transfected with sh-SIRT1, and the results showed that the expression of VEGF, TNF-α, and IL-6 was decreased, cell viability was increased, and the cell migration, apoptosis, and angiogenesis were impaired, indicating that SIRT1 silencing exerted protecting effects on AMD progression. SIRT1 has been reported to prevent the retinal degeneration and inflammation in AMD [32]. Likewise, the therapeutic role of SIRT1 silencing on neovascular AMD has been also highlighted by a prior study [33]. VEGF, TNF-α, and IL-6 are well-established biomarkers for hypoxia, which are increased under the condition of hypoxia [34, 35]. Particu-

larly, the area of laser-induced CNV can be notably decreased by inhibiting VEGF [36]. Additionally, reductions in VEGF, TNF-α, and IL-6 are a hallmark of the retarded formation of CNV in wet AMD [37]. Hence, these findings supported the attenuating function of SIRT1 silencing in the progression of CNV-induced AMD. Further analysis revealed that SIRT1 increased the formation of CNV in mice with AMD by increasing the expression of LCN2 through deacetylation of SOX9. Taken together, the aforementioned indicated the deteriorating role of SIRT1/SOX9/LCN2 in the CNV-induced AMD.

However, studies have shown that SIRT1 has a protective effect against disease, which is not consistent with our current research. For example, miR-138, miR-181a, and miR-181b directly inhibited SIRT1 expression and promoted apoptosis (Wang et al. 2016; [38]). SIRT1 overexpression reversed premature cell death caused by oxidative stress [39]. Activation of SIRT1 maintained retinal barrier integrity while decreasing the expression of inflammatory factors IL-8, IL-6, and MMP-9 [32]. Overall, SIRT1 plays a key role in anti-inflammatory, antiaging, and antioxidant processes, while an additional study also showed that SIRT1 expression was upregulated in AMD samples, which is consistent with our findings. These studies suggest that SIRT1 is not
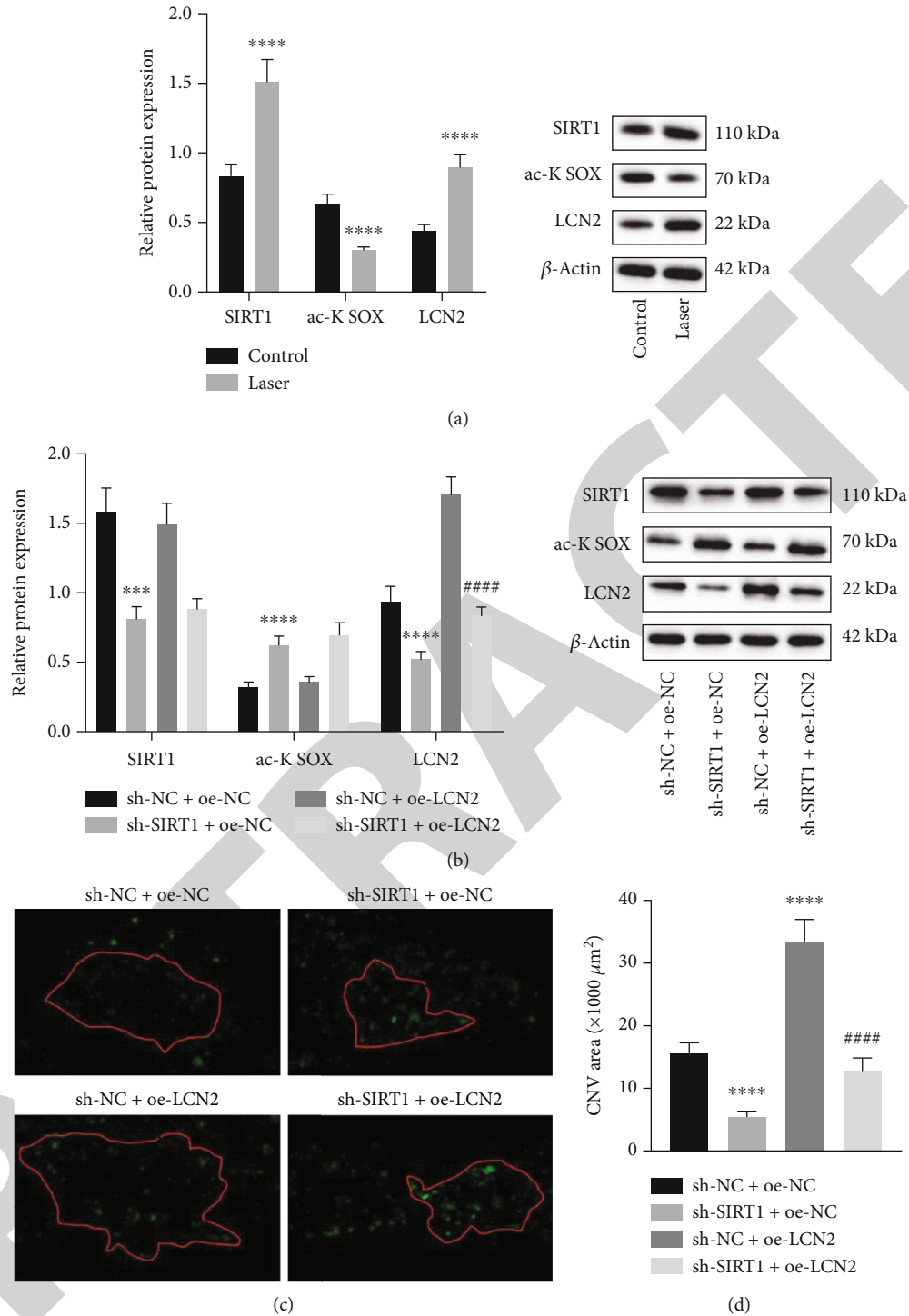
(a)

(b)

(c)

(d)

Figure 4: SIRT1 increases the expression of LCN2 by deacetylating SOX9 to promote the formation of laser-induced CNV in mice. (a) The protein expression of SIRT1, acetylated SOX9, and LCN2 in choroid/RPE tissues of mice determined by Western blot analysis. (b) The protein expression of SIRT1, acetylated SOX9, and LCN2 in choroid/RPE tissues of mice after different treatment determined by Western blot analysis. (c), Immunofluorescence staining analysis of mouse choroid/RPE tissues. Green indicates isolectin B4 and CNV area is within the red line. (d) CNV damage area statistics; scale bar: 50 μm. $^*p < 0.05$, compared with control or mice treated by sh-NC +oe-NC; $^\#p < 0.05$, compared with mice treated by sh-SIRT1+oe-NC. $^{***}p < 0.001$ and $^{****}p < 0.0001$. $^{\#\#\#\#}p < 0.0001$. Measurement data were expressed as the mean ± standard deviation.
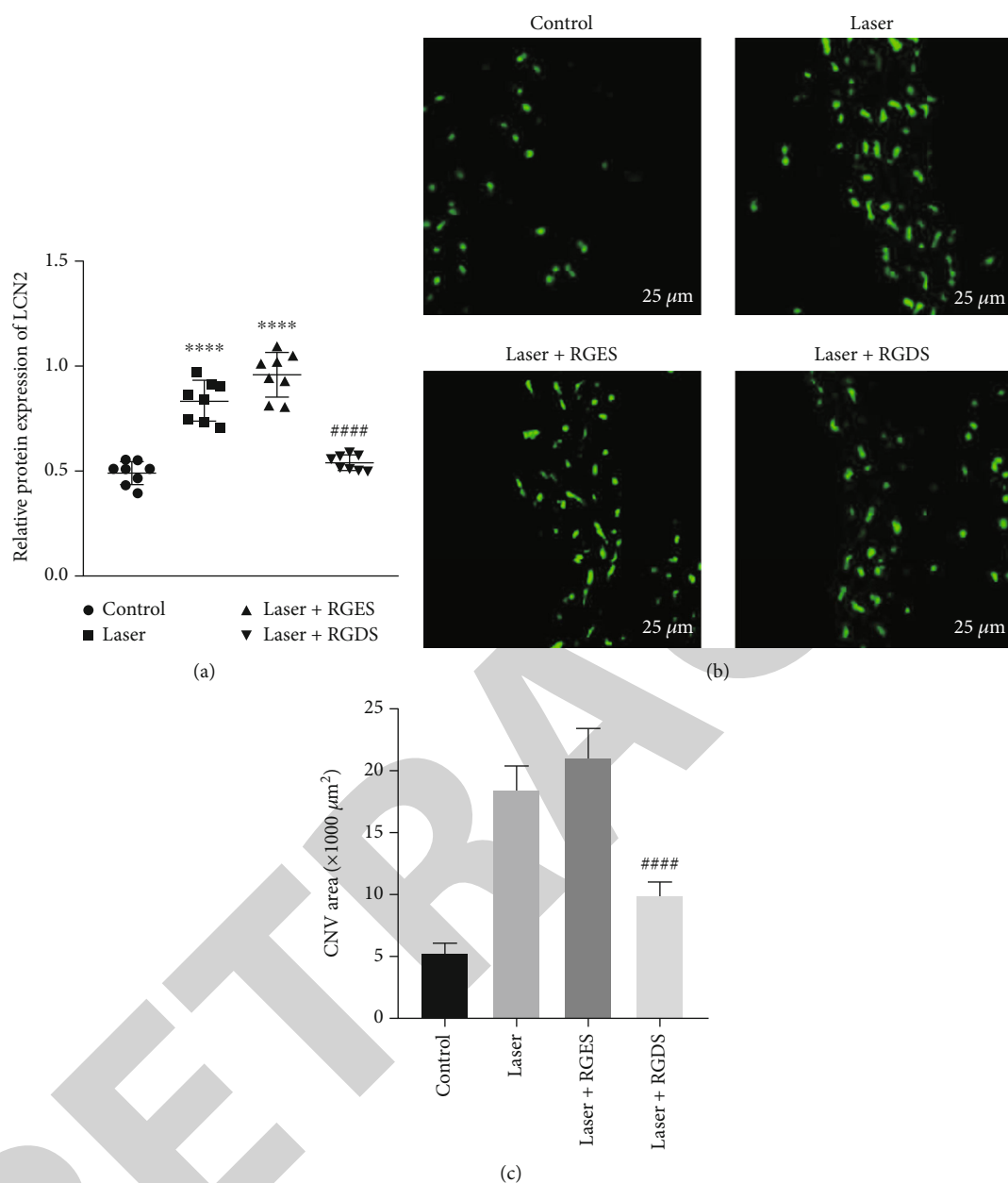
Figure 5: RGDS inhibited the formation of laser-induced CNV in mice. (a) The protein expression of LCN2 in the choroid/RPE tissues of mice determined by Western blot analysis. (b) The expression of isolectin B4 in the choroid/RPE tissues of mice after different treatments determined by immunofluorescence staining; scale bar: 25 μm. (c) Statistics of CNV damage area. ****$p < 0.0001$ compared with control; ####$p < 0.0001$ compared with mice treated by Laser+RGES.

necessarily protective in AMD and is more likely to be two-sided. Previous studies have revealed that SIRT1 acts as a deacetylase with many downstream substrates, such as p65 NF-κB [40], STAT3 [41], and CHK2 [42], SOX9 [43], and plays different roles in various biological processes mainly for deacetylation of histones and nonhistones with different mechanisms of action. Thus, the substrates regulated by SIRT1 deacetylation are all transcription factors, and the regulation of target genes by transcription factors is strongly dependent on the cellular and disease environment. The present study targets one target gene, LCN2, which is indeed

positively regulated by SIRT1/SOX9 during the CNV-induced AMD. Therefore, the different genes (SOX9 and LCN2) regulated by SIRT1 and the different cells and diseases studied are the reasons why the results of SIRT1 studies differ from previous ones.

However, there are certain limitations in the current study. For instance, although we confirmed that SIRT1 deacetylation can exacerbate AMD progression by upregulating SOX9 and increasing LCN2 expression, other signaling pathways also exist in SIRT1 to alleviate AMD progression, which requires further investigation. The effects
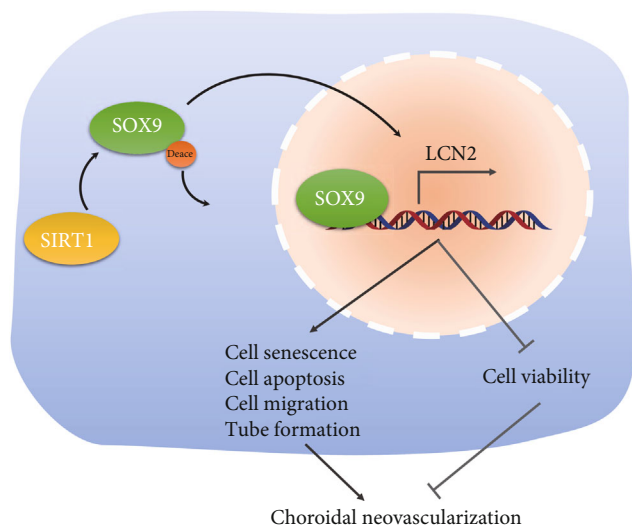
FIGURE 6: Schematic diagram of the mechanism by which SIRT1 influences the formation of CNV caused by AMD. SIRT1 upregulates the expression of LCN2 by deacetylating SOX9 to promote the formation of CNV caused by AMD.

of Oe-SIRT1 or sh-SIRT1 on angiogenesis in animals have not been addressed. The effect of SIRT1/SOX9/LCN2 axis-related inhibitors, such as RGDSv, on angiogenesis in animals needs to be further demonstrated. Exploring whether SIRT1, SOX9, and LCN2 pharmacological inhibitors can improve AMD may have more clinical application. This study validates a shallow mechanism, especially in animal experiments.

5. Conclusion

In summary, our evidence pointed toward that SIRT1 deacetylated SOX9 to promote its nuclear translocation, thereby increasing the expression of LCN2, further inducing the secretion of VEGF and inflammation-related factors, as well as cell apoptosis, migration, and angiogenesis, and ultimately promoting the formation of blood vessels in CNV-induced AMD (Figure 6). Thus, this study helps to deepen the clinical understanding of the pathological process of AMD occurrence and development and provides a scientific basis for the subsequent development of targeted drugs (about SIRT1/SOX9/LCN2 axis) for AMD treatment.

Data Availability

The data used to support the findings of this study are included within the supplementary information file(s).

Additional Points

Data Sharing Statement. The datasets generated/analysed during the current study are available.

Conflicts of Interest

The authors have no conflict of interests to declare.

Authors' Contributions

SZ, ZH, HJ, and JFX designed the study. LYZ, PL, QRL, and YHY collated the data. LY, LL, and HG designed and developed the database, carried out data analyses, and produced the initial draft of the manuscript. SZ and ZH contributed to drafting the manuscript. All authors have read and approved the final submitted manuscript. Su Zhao and Zhi Huang are regarded as co-first authors.

Acknowledgments

Supplementary Materials

Supplementary Materials Fig. S1: Western blot analysis of E-cadherin, N-cadherin, Snail, and Vimentin proteins in ARPE-19 cells exposed to hypoxia. *(Supplementary Materials)*

References

[1] C. Kiel, P. Berber, M. Karlstetter et al., "A circulating microRNA profile in a laser-induced mouse model of choroidal neovascularization," *International Journal of Molecular Sciences*, vol. 21, no. 8, p. 2689, 2020.

[2] P. Mitchell, G. Liew, B. Gopinath, and T. Y. Wong, "Age-related macular degeneration," *Lancet*, vol. 392, no. 10153, pp. 1147–1159, 2018.

[3] S. Mehta, "Age-related macular degeneration," *Age-Related Macular Degeneration. Prim Care*, vol. 42, pp. 377–391, 2015.

[4] F. Ricci, F. Bandello, P. Navarra, G. Staurenghi, M. Stumpp, and M. Zarbin, "Neovascular age-related macular degeneration: therapeutic management and new-upcoming approaches," *International Journal of Molecular Sciences*, vol. 21, no. 21, p. 8242, 2020.

[5] S. Chadha, L. Wang, W. W. Hancock, and U. H. Beier, "Sirtuin-1 in immunotherapy: a Janus-headed target," *Journal of Leukocyte Biology*, vol. 106, no. 2, pp. 337–343, 2019.

[6] J. L. Fry, Y. Shiraishi, R. Turcotte et al., "Vascular smooth muscle Sirtuin-1 protects against aortic dissection during angiotensin II-induced hypertension," *Journal of the American Heart Association*, vol. 4, no. 9, p. e002384, 2015.

[7] J. George, M. Nihal, C. K. Singh, and N. Ahmad, "4'-Bromo-resveratrol, a dual Sirtuin-1 and Sirtuin-3 inhibitor, inhibits melanoma cell growth through mitochondrial metabolic reprogramming," *Molecular Carcinogenesis*, vol. 58, no. 10, pp. 1876–1885, 2019.

[8] K. Kaarniranta, J. Kajdanek, J. Morawiec, E. Pawlowska, and J. Blasiak, "PGC-1alpha protects RPE cells of the aging retina against oxidative stress-induced degeneration through the regulation of senescence and mitochondrial quality control. The significance for AMD pathogenesis," *International Journal of Molecular Sciences*, vol. 19, no. 8, p. 2317, 2018.

[9] H. Zhang, S. He, C. Spee, K. Ishikawa, and D. R. Hinton, "SIRT1 mediated inhibition of VEGF/VEGFR2 signaling by resveratrol and its relevance to choroidal neovascularization," *Cytokine*, vol. 76, no. 2, pp. 549–552, 2015.

[10] D. Feng, X. Kang, R. Wang et al., "Progranulin modulates cartilage-specific gene expression via sirtuin 1-mediated deacetylation of the transcription factors SOX9 and P65," *The Journal of Biological Chemistry*, vol. 295, no. 39, pp. 13640–13650, 2020.

[11] H. Wan, J. Liao, Z. Zhang, X. Zeng, K. Liang, and Y. Wang, "Molecular cloning, characterization, and expression analysis of a sex-biased transcriptional factor *sox9* gene of mud crab *Scylla paramamosain*," *Gene*, vol. 774, p. 145423, 2021.

[12] S. Nakagawa, K. Nishihara, H. Miyata et al., "Molecular markers of tubulointerstitial fibrosis and tubular cell damage in patients with chronic kidney disease," *PLoS One*, vol. 10, no. 8, p. e0136994, 2015.

[13] S. Ghosh, N. Stepicheva, M. Yazdankhah et al., "The role of lipocalin-2 in age-related macular degeneration (AMD)," *Cellular and Molecular Life Sciences*, vol. 77, no. 5, pp. 835–851, 2020.

[14] J. Agbo, A. R. Akinyemi, D. Li et al., "RNA-binding protein hnRNPR reduces neuronal cholesterol levels by binding to and suppressing HMGCR," *Journal of Integrative Neuroscience*, vol. 20, no. 2, pp. 265–276, 2021.

[15] P. Qu, L. Wang, Y. Min, L. McKennett, J. R. Keller, and P. C. Lin, "Vav1 regulates mesenchymal stem cell differentiation decision between adipocyte and chondrocyte via Sirt1," *Stem Cells*, vol. 34, no. 7, pp. 1934–1946, 2016.

[16] S. Hagbi-Levi, M. Abraham, L. Tiosano et al., "Promiscuous chemokine antagonist (BKT130) suppresses laser-induced choroidal neovascularization by inhibition of monocyte recruitment," *Journal of Immunology Research*, vol. 2019, Article ID 8535273, 12 pages, 2019.

[17] S. Jabbehdari and J. T. Handa, "Oxidative stress as a therapeutic target for the prevention and treatment of early age-related macular degeneration," *Survey of Ophthalmology*, vol. 66, no. 3, pp. 423–440, 2021.

[18] M. Yang, K. F. So, W. C. Lam, and A. C. Y. Lo, "Novel programmed cell death as therapeutic targets in age-related macular degeneration," *International Journal of Molecular Sciences*, vol. 21, no. 19, p. 7279, 2020.

[19] M. Zhou, J. Luo, and H. Zhang, "Role of Sirtuin 1 in the pathogenesis of ocular disease (review)," *International Journal of Molecular Medicine*, vol. 42, no. 1, pp. 13–20, 2018.

[20] T. Parmar, V. M. Parmar, L. Perusek et al., "Lipocalin 2 plays an important role in regulating inflammation in retinal degeneration," *Journal of Immunology*, vol. 200, no. 9, pp. 3128–3141, 2018.

[21] W. Tang, J. Ma, R. Gu et al., "Lipocalin 2 suppresses ocular inflammation by inhibiting the activation of NF-$\kappa\beta$ pathway in endotoxin-induced uveitis," *Cellular Physiology and Biochemistry*, vol. 46, no. 1, pp. 375–388, 2018.

[22] S. Ghosh, P. Shang, M. Yazdankhah et al., "Activating the AKT2-nuclear factor-κB-lipocalin-2 axis elicits an inflammatory response in age-related macular degeneration," *The Journal of Pathology*, vol. 241, no. 5, pp. 583–588, 2017.

[23] M. Chen, N. Yang, J. Lechner et al., "Plasma level of lipocalin 2 is increased in neovascular age-related macular degeneration patients, particularly those with macular fibrosis," *Immunity & Ageing*, vol. 17, no. 1, p. 35, 2020.

[24] M. Shen, Y. Tao, Y. Feng, X. Liu, F. Yuan, and H. Zhou, "Quantitative proteomic analysis of mice corneal tissues reveals angiogenesis- related proteins involved in corneal neovascularization," *Biochimica et Biophysica Acta*, vol. 1864, no. 7, pp. 787–793, 2016.

[25] X. Wang, Y. Liu, Y. Ni et al., "Lentivirus vector-mediated knockdown of Sox9 shows neuroprotective effects on light damage in rat retinas," *Molecular Vision*, vol. 25, pp. 703–713, 2019.

[26] S. Goto, A. Onishi, K. Misaki et al., "Neural retina-specific Aldh1a1 controls dorsal choroidal vascular development via Sox9 expression in retinal pigment epithelial cells," *eLife*, vol. 7, p. e32358, 2018.

[27] B. L. Tang, "Sirt1 and the mitochondria," *Molecules and Cells*, vol. 39, no. 2, pp. 87–95, 2016.

[28] X. Meng, J. Tan, M. Li, S. Song, Y. Miao, and Q. Zhang, "Sirt1: role under the condition of ischemia/hypoxia," *Cellular and Molecular Neurobiology*, vol. 37, no. 1, pp. 17–28, 2017.

[29] H. Liu, M. Sheng, Y. Liu et al., "Expression of SIRT1 and oxidative stress in diabetic dry eye," *International Journal of Clinical and Experimental Pathology*, vol. 8, no. 6, pp. 7644–7653, 2015.

[30] N. B. Agaoglu, N. Varol, S. H. Yildiz et al., "Relationship between SIRT1 gene expression level and disease in age-related cataract cases," *Turkish Journal of Medical Sciences*, vol. 49, no. 4, pp. 1068–1072, 2019.

[31] M. Bar Oz, A. Kumar, J. Elayyan et al., "Acetylation reduces SOX9 nuclear entry and ACAN gene transactivation in human chondrocytes," *Aging Cell*, vol. 15, no. 3, pp. 499–508, 2016.

[32] L. Cao, C. Liu, F. Wang, and H. Wang, "SIRT1 negatively regulates amyloid-beta-induced inflammation via the NF-κB pathway," *Brazilian Journal of Medical and Biological Research*, vol. 46, no. 8, pp. 659–669, 2013.

[33] S. C. Maloney, E. Antecka, T. Granner et al., "Expression of SIRT1 in choroidal neovascular membranes," *Retina*, vol. 33, no. 4, pp. 862–866, 2013.

[34] B. Afacan, Z. P. Keles Yucel, C. Pasali, H. Atmaca Ilhan, T. Kose, and G. Emingil, "Effect of non-surgical periodontal treatment on gingival crevicular fluid hypoxia inducible factor-1 alpha, vascular endothelial growth factor and tumor necrosis factor-alpha levels in generalized aggressive periodontitis patients," *Journal of Periodontology*, vol. 91, no. 11, pp. 1495–1502, 2020.

[35] O. Arjamaa, V. Aaltonen, N. Piippo et al., "Hypoxia and inflammation in the release of VEGF and interleukins from human retinal pigment epithelial cells," *Graefe's Archive for Clinical and Experimental Ophthalmology*, vol. 255, no. 9, pp. 1757–1762, 2017.

[36] T. Koo, S. W. Park, D. H. Jo et al., "CRISPR-LbCpf1 prevents choroidal neovascularization in a mouse model of age- related

Hindawi

Retraction

Retracted: Inhibition of Oxidative Stress: An Important Molecular Mechanism of Chinese Herbal Medicine (Astragalus membranaceus, Carthamus tinctorius L., Radix Salvia Miltiorrhizae, etc.) in the Treatment of Ischemic Stroke by Regulating the Antioxidant System

Oxidative Medicine and Cellular Longevity

This article has been retracted by Hindawi, as publisher, following an investigation undertaken by the publisher [1]. This investigation has uncovered evidence of systematic manipulation of the publication and peer-review process. We cannot, therefore, vouch for the reliability or integrity of this article.

Please note that this notice is intended solely to alert readers that the peer-review process of this article has been compromised.

Wiley and Hindawi regret that the usual quality checks did not identify these issues before publication and have since put additional measures in place to safeguard research integrity.

We wish to credit our Research Integrity and Research Publishing teams and anonymous and named external researchers and research integrity experts for contributing to this investigation.

The corresponding author, as the representative of all authors, has been given the opportunity to register their agreement or disagreement to this retraction. We have kept a record of any response received.

References

[1] X. Zhao, Y. He, Y. Zhang, H. Wan, H. Wan, and J. Yang, "Inhibition of Oxidative Stress: An Important Molecular Mechanism of Chinese Herbal Medicine (Astragalus membranaceus, Carthamus tinctorius L., Radix Salvia Miltiorrhizae, etc.) in the Treatment of Ischemic Stroke by Regulating the Antioxidant System," *Oxidative Medicine and Cellular Longevity*, vol. 2022, Article ID 1425369, 10 pages, 2022.

Hindawi

Review Article

Inhibition of Oxidative Stress: An Important Molecular Mechanism of Chinese Herbal Medicine (Astragalus membranaceus, Carthamus tinctorius L., Radix Salvia Miltiorrhizae, etc.) in the Treatment of Ischemic Stroke by Regulating the Antioxidant System

Xixi Zhao [D],[1] **Yu He** [D],[2] **Yangyang Zhang** [D],[1] **Haofang Wan** [D],[3] **Haitong Wan** [D],[4] **and Jiehong Yang** [D][1]

[1]*School of Basic Medical Sciences, Zhejiang Chinese Medical University, Hangzhou 310053, China*
[2]*School of Pharmaceutical Sciences, Zhejiang Chinese Medical University, Hangzhou 310053, China*
[3]*Academy of Chinese Medical Sciences, Zhejiang Chinese Medical University, Hangzhou 310053, China*
[4]*School of Life Sciences, Zhejiang Chinese Medical University, Hangzhou 310053, China*

Correspondence should be addressed to Haitong Wan; whtong@126.com and Jiehong Yang; yjhong@zcmu.edu.cn

Ischemic stroke is a severe cerebrovascular disease with high mortality and morbidity. Traditional Chinese medicine (TCM) has been utilized for thousands of years in China and is becoming increasingly popular all over the world, especially for the treatments of ischemic stroke. More and more evidences have implicated that oxidative stress has been closely related with ischemic stroke. This review will concentrate on the evidence of the action mechanism of Chinese herbal medicine and its active ingredient in preventing ischemic stroke by modulating redox signaling and oxidative stress pathways and providing references for clinical treatment and scientific research applications.

1. Introduction

Cerebrovascular disease is a common neurological disease, which refers to brain dysfunction caused by various vascular diseases [1]. Stroke is the main clinical type of cerebrovascular disease. Among them, atherosclerosis has been well-recognized as one of the main culprits for the rising incidence of stroke-related mortality [2]. Plaque rupture and thrombosis result in the acute clinical complications of stroke. Ischemic stroke accounts for most cases (87%) in stroke and is further subtyped into atherosclerosis, cardioembolic, lacunar, other causes, and cryptogenic strokes [3]. Therefore, atherosclerosis is an important cause of ischemic stroke [4].

Ischemia/reperfusion (I/R) injury refers to a condition in which tissues or organs suffer from ischemia for a period of time and then supplement with oxygen-enriched blood (reperfusion), resulting in aggravated tissue or organ damage. Reperfusion is essential for protecting the injured brain tissue, but it can also lead to reperfusion injury by exacerbating the damage despite restoring the circulation [5]. Cerebral I/R injury further aggravates the pathological damage of cerebral ischemic tissue and the nervous system and even produces irreversible nerve damage and clinical symptoms [6]. Cerebral I/R injury is a very complex cascade of pathophysiological processes involving multiple pathogenic mechanisms, including inflammation, oxidative stress, Ca^{2+} overload, excitatory amino acid toxicity, and

mitochondrial damage, which ultimately lead to neuronal necrosis and apoptosis [7, 8]. Among them, oxidative stress is one of the important pathological mechanisms of the occurrence and development of cerebral I/R injury.

With the continuous deepening of relevant basic research, further exploration of the pathogenesis of ischemic stroke and finding effective drugs are the focus of the current research. Studies have shown that traditional Chinese medicine (TCM) has ameliorating effects on cerebral microcirculation disorders, cerebral damage, and neuronal damage caused by ischemic stroke [9].

In this review, we will first discuss the redox signaling and oxidative stress pathways in ischemic stroke. Simultaneously, we summarize the antioxidant effects of some Chinese herbal medicines, which have inhibition effects on ROS generation and oxidative stress after ischemic stroke. And we have provided a reference basis for clinical treatment and scientific research application.

2. Oxidative Stress and ROS

Oxidative stress is defined as an imbalance between the production of free radicals and the capacity of the antioxidant defense system [10]. This imbalance leads to damage of important biomolecules and organs with potential impact on the whole organism. It is also considered as a critical component of the pathogenesis and progression of brain disease, such as stroke and Alzheimer's and Parkinson's diseases [4, 11–13]. Free radicals can be divided into two categories: reactive oxygen species (ROS) and reactive nitrogen species (RNS). ROS and RNS are well recognized for playing a dual role as both deleterious and beneficial species, since they can be either harmful or beneficial to living systems. Enzymatic antioxidant defenses include superoxide dismutase (SOD), glutathione peroxidase (GSH-Px), and catalase (CAT); nonenzymatic antioxidants are represented by ascorbic acid (vitamin C), α-tocopherol (vitamin E), glutathione, carotenoids, flavonoids, and other antioxidants [14]. Under normal conditions, the free radicals produced by the human body can be eliminated in time by the antioxidant enzymes in the body, so that the generation and elimination of free radicals are in a dynamic balance. This balance is essential for the survival of organisms and their health. When the content of ROS plus RNS in the body exceeds the scavenging ability of its own antioxidant defense system, it can destroy the original redox homeostasis, trigger a variety of damage mechanisms to destroy the antioxidant defense system, and produce oxidative stress [15].

ROS are products of a normal cellular metabolism, including superoxide anion, hydrogen peroxide (H_2O_2), hydroxyl radicals, and singlet oxygen. Most ROS are generated by the mitochondrial respiratory chain in cells [16]. In addition, ROS is also produced by a variety of enzymes, such as NADPH oxidase (NOX), xanthine oxidase, nitric oxide synthase, and other zymogen systems [16]. ROS plays an important role in both physiological and pathological processes. Beneficial effects of ROS occur at low/moderate concentrations and involve physiological roles in cellular responses to anoxia, as for example in the function of a number of cellular signaling systems [17]. But when they are overproduced, it will cause energy depletion and accumulation of toxic substances in the cell, which will eventually lead to cell necrosis [18]. ROS produced during the ischemia and perfusion phases of acute ischemic stroke can lead to brain damage [19].

3. Antioxidative Systems Related to Ischemic Stroke

The state of oxidative stress produced by the destruction of the homeostasis between the body's oxidation and antioxidant systems is the key mechanism underlying ischemic stroke [20]. Oxidative stress can cause inflammation, neuronal apoptosis, excitotoxicity, and damage to the blood-brain barrier, which can aggravate brain damage [21, 22]. Therefore, it is very important to regulate oxidative stress on the biological effects of ischemic stroke and its pathogenesis. Thioredoxin (Trx), glutathione (GSH), and nuclear factor erythroid 2-related factor 2 (Nrf2) systems are three major antioxidant systems responsible for removing overproduced free radicals (Figure 1).

3.1. Nrf2 System. Nrf2, as a key component of endogenous antioxidant defense, and a key transcription factor that maintains cell redox homeostasis, has been demonstrated to protect the brain against stroke-induced injury mostly by alleviating ROS-associated pathological processes [23].

Under basal conditions, Nrf2 is sequestered by cytoplasmic kelch-like ECH associated protein 1 (Keap1) and targeted to proteasomal degradation [24]. Under oxidative stress, Nrf2 dissociates from Keap1 and transfers to the nucleus to promote the transcription of antioxidant response element- (ARE-) dependent genes [25]. These stress conditions lead to the suspension of Keap1–Nrf2 interactions and promote the transcription of a wide variety of antioxidant genes like heme oxygenase-1 (HO-1) and NAD(P)H:quinone oxidoreductase 1 (NQO1), which, in turn, scavenges the cellular oxidative stress [26].

In vivo study has shown that in both peri-infarct and core infarct regions, Nrf2 expression began to increase at 2 h, peaked at 8 h, then decreased at 24 and 72 h of reperfusion in a mouse transient middle cerebral artery occlusion (tMCAO) model [27]. At the same time, it was found that after 24 h of reperfusion, the Nrf2 signaling pathway was obviously activated after drug intervention; the levels of SOD, CAT, Nrf2, HO-1, and NQO-1 increased; and the levels of MDA, 4-hydroxynonenal (4-HNE), 8-hydroxy-2′-deoxyguanosine (8-OHdG), and ROS decreased, in a rat MCAO model [28]. And knockdown of Nrf2 abolished the protective effects of drugs on cell viability and reversed the downregulation of Nrf2 downstream gene levels induced by drugs [28]. In summary, the Nrf2 system plays an important role in regulating the redox steady state.

3.2. GSH System. GSH system comprises NADPH, glutathione reductase (GR), and GSH. GSH is an important nonenzymatic endogenous antioxidant in the human body and is a major endogenous component of the cellular antioxidant defense [29]. It is capable of scavenging various ROS directly
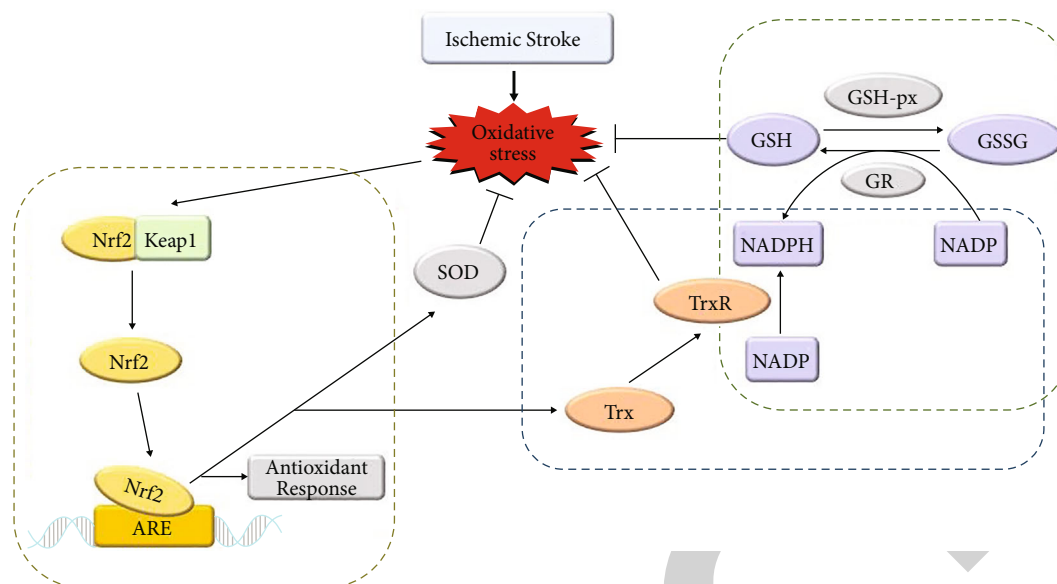
FIGURE 1: The antioxidative systems related to ischemic stroke.

to provide protection from oxidative stress-induced damage. GSH is produced intracellularly from three amino acids—glutamate, cysteine, and glycine—through two consecutive steps catalyzed by γ-glutamyl cysteine ligase (GCL, also known as γ-glutamyl cysteine synthetase) and GSH synthetase (GS) [30]. In the redox reaction, GSH is oxidized and converted into glutathione disulfide (GSSG), which is subsequently reduced to GSH by glutathione reductase [31]. Reduced form glutathione plays key roles in the cellular control of ROS. Thus, the ratio of GSH/GSSG is a good measure of the oxidative stress of an organism [32].

It is reported that the active form of GSH is most abundant in neurons and myelinated axons in a variety of brain regions including hippocampal CA1 neurons, frontal cortex pyramidal neurons, and reticular formation neurons in the unperturbed adult mouse brain [33]. The reduced form of GSH is constitutively synthesized in neurons and readily diffuses into the nucleus to protect DNA from oxidative damage [33]. Researchers found that the GSH levels in mouse CA1 pyramidal neurons were decreased during the first few hours of I/R, accompanied by increased superoxide levels; conversely, the prevention of ischemia/reperfusion-induced increase in superoxide production using an inhibitor of nicotinamide adenine dinucleotide 3-phosphate oxidase, a major source of ROS, was found to suppress the decline in GSH in postischemic neurons [34]. Another literature demonstrated that GSH reduces the brain infarct volume after MCAO injury in the rat brain and attenuates the production of ROS in brain endothelial cells after ischemic injury [35].

These data suggest that abatement of GSH can help reduce the oxidative stress response after I/R injury and relieve the severe brain lesions caused by ischemic stroke. In summary, GSH also plays a vital role in regulating the body's redox homeostasis.

3.3. Trx System. Trx system consists of two types of antioxidant oxidoreductase proteins: Trx and thioredoxin reductase (TrxR) and NADPH as the electron donor [36]. This system operates by transferring electrons from NADPH via TrxR to the active site of Trx [37]. It is widely present in prokaryotic and eukaryotic organisms [38]. Trx is a 12 kDa protein ubiquitously expressed in all living cells, characterized by the highly conserved reduction/oxidation- (redox-) active site sequence Trp-Cys-Gly-Pro-Cys-Lys [39]. The two cysteine residues within the redox-active center of Trx (Cys-32 and Cys-35) are the key for it to regulate redox [37].

Mammalian cells contain two distinct Trxs. Trx1 is localized in the cell cytosol/nucleus, whereas Trx2 is a mitochondrial protein [40]. One literature reported that intracellular Trx1 overexpression has a neuroprotective effect during short duration ischemia and reperfusion [41]. Ischemic neuronal death was attenuated, and superoxide production was decreased after mild focal ischemia in Trx1 transgenic mice [41]. Researchers applied RNA interference targeting Trx1 in a rat model of MCAO-induced focal ischemia. They found that administration of Trx1 siRNA significantly increased mortality, brain infarct size, neurobehavioral deficits, and neuronal cell death in MCAO rat [42]. And in the ischemic brain, administration of antioxidant enzymes peroxiredoxin 3 and Trx2 shows substantial neuroprotective effects by reducing oxidative stress [43].

These data suggest that abatement of Trx may be harmful in cerebral ischemia in the acute phase, and an elevation of Trx could be neuroprotective with respect to brain damage. In short, the Trx system can play a protective role through antioxidant effects to reduce neuronal damage caused by ischemic stroke.

4. Protective Effects of TCM and Its Constituent Compounds on Ischemic Stroke

4.1. Ligusticum chuanxiong. Ligusticum chuanxiong (LC), a crude herbal drug isolated from the dried root or rhizome of *Rhizoma Chuanxiong*, has been widely used in the

treatment of brain and heart diseases. Pharmacological investigations demonstrate that LC possesses antiatherosclerosis, anticancer, antioxidant, antiaging, and antihypertensive properties [44]. Some researchers found that the main active ingredients in LC alcohol extract are ligustrazine, ferulic acid, free phenol, and bound phenol. After the LC alcohol extract is diluted 100 times, the reducing power was equivalent to14.79 μg/mL VC. The clearance rate of 0.9 g/L LC alcohol extract on hydroxy radical was 1.12 times that on superoxide anion, which means the LC alcohol extract has a better scavenging effect on hydroxyl free radicals than superoxide anion [45]. Ligustrazine, also called tetramethylpyrazine, is a main active fraction of the traditional medicine known as LC, which has been proven to regulate the production of oxidative stress and ROS, and is used as clinical medication for cerebral thrombosis, coronary heart disease, and stenocardia recently [46]. Ligustrazine 20 mg/kg increased Nrf2/HO-1 signaling in neutrophils after ischemia [47]. The volatile oil from Chuanxiong can promote the life of cerebral cortex neurons in vitro; decrease cerebral infarction volume; enhance the activities of SOD, GSH-Px, and nitric oxide synthase(NOS); decrease the content of MDA in rats; and alleviate the damages caused by ischemia reperfusion [48].

4.2. Astragalus membranaceus.

Astragalus membranaceus was first recorded in the *Shennong Bencao Jing*, one of the most famous Chinese ancient books in 200 AD, which is nontoxic and has a wide range of therapeutic effects [49, 50]. In China, it is known as "Huangqi." It is used to invigorate the spleen and replenish qi in TCM. Huangqi abounds with polysaccharides, flavonoids, saponins, amino acids, and other compounds [51, 52].

Early literature reported that total flavonoids of *Astragalus membranaceus* had potent antioxidant activity to improve atherosclerosis [53]. As one of the fundamental components in the root of *Astragalus membranaceus*, astragaloside IV (AST IV) exerts protective effects against neurological disorders, such as cerebral I/R injury [54, 55]. Studies have found that AST IV treatment could obviously increase SOD and LDH activities; reduce the production of NOS, MDA, and NO; and downregulate the expression of inducible nitric oxide synthase (iNOS) mRNA to ameliorate the oxidative damage in rats with cerebral I/R injury [56]. What is more, it could alleviate cerebral I/R injury through inhibiting NLRP3 inflammasome-mediated pyroptosis via activating Nrf2 [57]. Meantime, AST IV-tetramethylpyrazine played a pivotal synergistic protective role against focal cerebral ischemic reperfusion damage in a rat experimental model, which could downregulate MDA content and iNOS activity, and upregulate SOD activity [58]. *Astragalus polysaccharides* (APS) are the main active ingredient of *Astragalus membranaceus*, which could also reduce NOS, LDH, NO, and MDA and increase the activities of SOD in the cerebral I/R injury model [59]. Calycosin-7-O-β-D-glucoside is also a representative isoflavone isolated from the root of *Astragalus membranaceus*, which has potential neuroprotective effects [60]. In vitro pharmacological studies indicated that it could alleviate oxygen-glucose deprivation/reoxygenation- (OGD/R-) induced oxidative stress in hippocampal cells by reducing the production of ROS and MDA [61].

4.3. Radix Salvia Miltiorrhizae.

Radix Salvia Miltiorrhizae, as known as "Danshen," a famous Chinese herb medicine, has been widely used in treating stroke. The active ingredients in Danshen are mainly divided into fat-soluble tanshinone compounds and water-soluble salvianolic acids [62]. The water-soluble salvianolic acids include salvianolic acid A, salvianolic acid B, salvianolic acid C, protocatechuic acid, danshensu, and other derivatives [63]. The fat-soluble tanshinone compounds include tanshinone I, tanshinone IIA, dihydrotanshinone, isotanshinone IIA, and isocryptotanshinone [62]. Both of them have significant pharmacological activities, such as antioxidant and anti-inflammatory [63–65]. Salvianolic acid B is the main active ingredient of Danshen, which could increase the level of antioxidant substances and decrease free radicals' production [66]. Experimental studies have shown that salvianolic acid B can significantly raise the activities of SOD, CAT, GSH-Px, and total antioxidant capacity (T-AOC) and reduce the levels of MDA, LDH, and NOS in cerebral ischemia model animals [66, 67]. Danshen polysaccharide is a kind of polysaccharide extracted from the root of Danshen. One literature reported that pretreatment with Danshen polysaccharide for 10 days prior to the blocking bilateral common carotid artery occlusion also significantly increased mitochondria SOD, CAT, and GSH-Px activities and reduced MDA production in cerebral ischemia brain [68]. And tanshinone IIA elicits a neuroprotective effect through attenuating oxidative productions, increasing antioxidant enzyme activity and Nrf2 expression, and inducing Nrf2 nuclear translocation [69].

4.4. Carthamus tinctorius L.

Carthamus tinctorius L., commonly known as safflower in China, was used to promote blood circulation and remove blood stasis, which was recorded as early as in the *Kaibao Bencao* [70]. The chemical constituents of safflower are plentiful and include flavonoids (e.g., quinochalcone C-glycosides), alkaloids, phenolic acids, and fatty acids [71]. Modern pharmacological experiments have demonstrated that safflower has wide-reaching biological activities, including anticoagulation, antioxidation, antihypoxic, anti-inflammation, and protection of cardiovascular and cerebrovascular [72, 73]. Early literature has reported that safflower injection has significant antioxidant activity outside, and its chemical basis may be polyphenols [74]. Both the medium- and high-dose groups of safflower extract can significantly increase the activities of SOD, GSH-Px, and CAT in brain tissue and reduce the content of MDA in acute cerebral ischemic injury in mice [75]. Safflower yellow is the main active ingredient isolated from safflower, including hydroxysafflor yellow A (HSYA) and safflower yellow B (SYB), which are widely used to treat cerebrovascular diseases [76]. It is reported that safflower yellow has obvious protective effects on rats with cerebral I/R injury by decreasing the levels of MDA and NO and increasing the activity of SOD in brain tissue [77]. SYB is a yellow amorphous water-soluble powder and has demonstrated protective effects in neuronal injury models induced by oxidative stress [78]. Wang et al. studied that the antioxidant effects of SYB were driven by an AK046177/miR-134/CREB-dependent mechanism that inhibited this pathway [23]. SYB attenuated the effects of AK046177, inhibited miR-134 expression, and promoted CREB activation, which in turn promoted Nrf2

Table 1: Mechanisms of TCM and its active ingredients to improve oxidative stress.

TCM	Ingredient	Subjects in study	Impact on ROS-related targets	Refs.
Ligusticum chuanxiong	Tetramethylpyrazine	SD rats	↑Nrf2, ↑HO-1	[47]
	Volatile oil	SD rats	↑SOD, ↑GSH-Px, ↓MDA	[48]
Astragalus membranaceus	Astragaloside	SD rats	↑SOD, ↓LDH, ↓NOS, ↓MDA, ↓NO	[56]
	Astragaloside IV	SD rats/SH-5Y5Y cells	↓ROS, ↑Nrf2	[57]
	Astragaloside IV-tetramethylpyrazine	SD rats	↓MDA, ↓iNOS, ↑SOD,	[58]
	Astragalus polysaccharides	SD rats	↑SOD, ↓NOS, ↓MDA, ↓NO, ↓LDH	[59]
	Calycosin-7-O-*B*-D-glucoside	HT22 cells	↓LDH, ↓MDA, ↓ROS, ↑SOD	[61]
Radix Salvia Miltiorrhizae	Salvianolic acid B	Mice	↓MDA, ↑SOD, ↓NOS, ↑T-AOC	[66]
	Salvianolic acid B	SD rats	↑SOD, ↑CAT, ↑GSH-Px, ↓MDA, ↓LDH, ↓NOS	[67]
	Danshen polysaccharide	Wistar rats	↓MDA, ↓ROS, ↑SOD, ↑CAT, ↑GSH-Px,	[68]
	Tanshinone IIA	*Nrf2* knockout mice	↑Nrf2, ↓8-OHdG, ↓MDA, ↑SOD, ↑CAT, ↑GSH-Px, ↑T-AOC	[69]
Carthamus tinctorius L.	Safflower extract	ICR mice	↑SOD, ↑GSH-Px, ↑CAT, ↓MDA	[75]
	Safflower yellow pigment	SD rats	↑SOD, ↓NO, ↓MDA	[77]
	SYB	PC12 cells	↑SOD, ↑GSH-Px, ↓MDA, ↓LDH	[78]
	SYB	SD rats/primary cortical cells	↑Nrf2, ↑SOD, ↓MDA, ↑GSH-Px, ↓NADPH, ↓NOX, ↓ROS	[23]
	HSYA	SD rats	↑SOD, ↑T-AOC, ↓MDA	[79]
	HSYA	PC12 cells	↑SOD, ↓MDA	[80]
Angelica sinensis	*Angelica sinensis* polysaccharides	Rabbits	↑SOD, ↓MDA, ↑CAT, ↑GSH-Px, ↑GSH, ↑GR, ↓NO	[84]
	Angelica sinensis polysaccharides	PC12 cells	↑SOD, ↑GSH-Px, ↓MDA	[85]
	Angelica sinensis polysaccharides	Wistar rats	↑SOD, ↑GSH-Px, ↓MDA	[86]

expression and then increased antioxidant capacities, improved cell respiration, and reduced apoptosis [23]. Wei et al. showed that HSYA might oppose cerebral I/R injury of MCAO rats through attenuating the elevation of the MDA level and decreasing SOD activity in the ipsilateral hemisphere and serum [79]. In an *in vitro* assay, HSYA was shown to block OGD/R-induced PC12 cell apoptosis through the suppression of intracellular oxidative stress [80]. And another study reported that the synergistic protective effect of HSYA and AST IV could increase the activity of SOD, CAT, and GSH-Px; decrease MDA and ROS; and upregulate the expression of Nrf2 in cerebral I/R injury rats [81].

4.5. Angelica sinensis. The dried root of *Angelica sinensis* (Oliv.) Diels, commonly known as Danggui (in Chinese), has been used over thousands of years as well-known Chinese medicines [82]. It has a therapeutic effect on diseases by promoting blood circulation, regulating menstruation, and relieving pain.

With the modernization of TCM, the main components of Danggui have been identified including polysaccharides, organic acids, volatile oils, and flavonoids, as well as vitamins, amino acids, etc. [82, 83]. And modern pharmacological experiments have demonstrated that Danggui could promise neuroprotective effects against ischemic-induced injury by antioxidative stress, antiapoptotic, and anti-inflammatory [82].

The *Angelica sinensis* polysaccharide (ASP) is one of the main extracts from the root of *Angelica sinensis*. One literature reported that pretreatment with ASPs 100 or 300 mg/kg has protective effects for cerebral I/R injury rabbits through increasing the activities of SOD, CAT, GSH-Px, and GR and reducing the production of MDA and NO [84]. In addition, another literature indicated that ASP not only protected PC12 neuronal cells from H_2O_2-induced oxidative and apoptotic injury but also promoted the recovery of MCAO rats from cerebral I/R injury, suggesting that ASP has potential as a neuroprotective agent [85]. It is reported that pretreatment with ASPs 30 or 60 mg/kg could increase the activity of SOD and GSH-Px and decrease MDA in MCAO rats [86].

4.6. Others. The consumption of polyphenol-rich foods has been related to a lower risk of cardiovascular events (cardiovascular mortality, myocardial infarction, and stroke) and cardiovascular risk factors [87]. Curcumin, a polyphenol abundant in the rhizome of the turmeric plant (Curcuma longa), has shown promising neuroprotective effects in animal models of neurodegenerative diseases [88]. Curcumin could prevent mitochondrial dysfunction as it acts by enhancing the action of enzymes of the antioxidant defense system SOD, CAT, and GSH [89]. Besides, in the rat model of ischemia, Mucuna pruriens extract demonstrated antioxidant capacity against brain damage, which indicated the therapeutic potential of this plant in ischemia [90].

5. Conclusion and Prospect

Because the research on ischemic stroke is still in the cognitive stage, most of the mechanisms of action are still unclear, so the diagnosis and treatment methods are still flawed. Therefore, further in-depth study of the mechanism of ische-

mic stroke is of great help in understanding and treating the disease. By arranging the literature, it was found that TCM has a variety of biological activities and antioxidant capacity and can protect against ischemic stroke by regulating oxidative stress, which indicates that TCM has the potential to protect the body from ischemic stroke by antioxidative stress (Table 1). Through the analysis of the existing literature, we found that the antioxidant effect of TCM is the result of multifaceted and multimechanism. TCMs can directly enhance the activity of endogenous antioxidant enzymes (such as SOD, GSH-Px, and CAT) to defend against oxidative stress. In addition, TCMs can modulate signaling pathways related to ROS, such as the Nrf2 pathway (Table 1). And TCMs also can directly reduce the oxidative damage of cellular macromolecules (such as lipids, proteins, and DNA).

Collectively, we first discuss the redox signaling and oxidative stress pathways in ischemic stroke and propose that inhibiting of oxidative stress is a potential target for the treatment and prevention of ischemic stroke. Then, we summarize recent research data and discuss the action mechanism of Chinese herbal medicine and its active ingredients in preventing ischemic stroke by modulating redox signaling and oxidative stress pathways. Due to its antioxidant ingredients, TCM treatment has particular advantages in the treatment of ischemic stroke. But one of the biggest challenges in modernizing TCM is the lack of robust clinical trials. TCM with ischemic stroke treatment effects contain complex and diverse types of active ingredients. Although current studies have found that the active ingredients contained in TCM can play a protective role by regulating oxidative stress to deal with cerebral I/R damage, the mechanism of action is not sufficiently studied, the research scope is relatively limited, and the research indicators are relatively single. It is unclear how these active ingredients work on this target. Thus, aiming at this target, researchers should actively design a plan, through real preclinical research and scientific clinical trials, to explore whether TCM antioxidant treatment can become a breakthrough point in the treatment of ischemic stroke and provide therapeutic strategies and theoretical basis for the clinical treatment of ischemic stroke. By adding more experimental and clinical data to increase the theoretical support of TCM against oxidative stress, we further optimize the active ingredients, dosage, administration time, and administration method of TCM. This will help to facilitate the natural anti-ischemic stroke medicine discovery and development and its bench-to-bedside transformation. And this also will help to apply these TCMs more safely and rationally to avoid adverse events, improve the quality of life of more ischemic stroke patients, and have important application value in clinical practice.

Conflicts of Interest

The authors declared that there was no potential conflict of interest.

Authors' Contributions

XZ, YH, and YZ wrote and revised the manuscript. XZ and HW drew the table and figure. HW and JY carried out

various literature survey studies. All the authors read and approved the final manuscript.

References

[1] X. Hu, T. M. De Silva, J. Chen, and F. M. Faraci, "Cerebral vascular disease and neurovascular injury in ischemic stroke," *Circulation Research*, vol. 120, no. 3, pp. 449–471, 2017.

[2] Y. L. Chow, L. K. Teh, L. H. Chyi, L. F. Lim, C. C. Yee, and L. K. Wei, "Lipid metabolism genes in stroke pathogenesis: the atherosclerosis," *Current Pharmaceutical Design*, vol. 26, no. 34, pp. 4261–4271, 2020.

[3] D. Harpaz, R. C. S. Seet, R. S. Marks, and A. I. Y. Tok, "Blood-based biomarkers are associated with different ischemic stroke mechanisms and enable rapid classification between cardio-embolic and atherosclerosis etiologies," *Diagnostics (Basel)*, vol. 10, no. 10, p. 804, 2020.

[4] Y. C. Cheng, J. M. Sheen, W. L. Hu, and Y. C. Hung, "Polyphenols and oxidative stress in atherosclerosis-related ischemic heart disease and stroke," *Oxidative Medicine and Cellular Longevity*, vol. 2017, 2017.

[5] S. S. Andrabi, S. Parvez, and H. Tabassum, "Ischemic stroke and mitochondria: mechanisms and targets," *Protoplasma*, vol. 257, no. 2, pp. 335–343, 2020.

[6] H. K. Eltzschig and T. Eckle, "Ischemia and reperfusion–from mechanism to translation," *Nature Medicine*, vol. 17, no. 11, pp. 1391–1401, 2011.

[7] Q. Yuan, Y. Yuan, Y. Zheng et al., "Anti-cerebral ischemia reperfusion injury of polysaccharides: a review of the mechanisms," *Biomedicine & Pharmacotherapy*, vol. 137, 2021.

[8] X. Chen, A. Yang, Y. Zhao et al., "Research progress on pathogenesis of ischemic stroke and traditional Chinese medicine commonly used for treatment of ischemic stroke," *China Journal of Chinese Materia Medica*, vol. 44, no. 3, pp. 422–432, 2019.

[9] K. Sun, J. Fan, and J. Han, "Ameliorating effects of traditional Chinese medicine preparation, Chinese Materia Medica and active compounds on ischemia/reperfusion-induced cerebral microcirculatory disturbances and neuron damage," *Acta Pharmaceutica Sinica B*, vol. 5, no. 1, pp. 8–24, 2015.

[10] Z. Ďuračková, "Some current insights into oxidative stress," *Physiological Research*, vol. 59, no. 4, pp. 459–469, 2010.

[11] D. A. Butterfield, "Perspectives on oxidative stress in Alzheimer's disease and predictions of future research emphases," *Journal of Alzheimer's Disease*, vol. 64, no. s1, pp. S469–S479, 2018.

[12] T. Jiang, Q. Sun, and S. Chen, "Oxidative stress: a major pathogenesis and potential therapeutic target of antioxidative agents in parkinson's disease and Alzheimer's disease," *Progress in Neurobiology*, vol. 147, pp. 1–19, 2016.

[13] J. R. Santos, A. M. Gois, D. M. Mendonça, and M. A. Freire, "Nutritional status, oxidative stress and dementia: the role of selenium in Alzheimer's disease," *Frontiers in Aging Neuroscience*, vol. 6, p. 6206, 2014.

[14] M. Valko, D. Leibfritz, J. Moncol, M. T. D. Cronin, M. Mazur, and J. Telser, "Free radicals and antioxidants in normal physiological functions and human disease," *The International Journal of Biochemistry & Cell Biology*, vol. 39, no. 1, pp. 44–84, 2007.

[15] Y. Du, X. Chen, and S. Zhao, "Progress of mechanism of oxidative stress in acute ischemic stroke," *Chinese Journal of Neurotraumatic Surgery*, vol. 7, no. 2, pp. 121–124, 2021.

[16] D. Moris, M. Spartalis, E. Spartalis et al., "The role of reactive oxygen species in the pathophysiology of cardiovascular diseases and the clinical significance of myocardial redox," *Annals of Translational Medicine*, vol. 5, no. 16, p. 326, 2017.

[17] H. Sies and D. P. Jones, "Reactive oxygen species (ROS) as pleiotropic physiological signalling agents," *Nature Reviews. Molecular Cell Biology*, vol. 21, no. 7, pp. 363–383, 2020.

[18] C. A. Juan, J. M. Pérez de la Lastra, F. J. Plou, and E. Pérez-Lebeña, "The chemistry of reactive oxygen species (ROS) revisited: outlining their role in biological macromolecules (DNA, lipids and proteins) and induced pathologies," *International Journal of Molecular Sciences*, vol. 22, no. 9, p. 4642, 2021.

[19] I. Žitňanová, P. Šiarnik, B. Kollár et al., "Oxidative stress markers and their dynamic changes in patients after acute ischemic stroke," *Oxidative Medicine and Cellular Longevity*, vol. 2016, Article ID 9761697, 2016.

[20] C. L. Allen and U. Bayraktutan, "Oxidative stress and its role in the pathogenesis of ischaemic stroke," *International Journal of Stroke*, vol. 4, no. 6, pp. 461–470, 2009.

[21] A. Lau and M. Tymianski, "Glutamate receptors, neurotoxicity and neurodegeneration," *Pflügers Archiv-European Journal of Physiology*, vol. 460, no. 2, pp. 525–542, 2010.

[22] S. Orellana-Urzúa, I. Rojas, L. Líbano, and R. Rodrigo, "Pathophysiology of ischemic stroke: role of oxidative stress," *Current Pharmaceutical Design*, vol. 26, no. 34, pp. 4246–4260, 2020.

[23] C. Wang, H. Wan, Q. Wang et al., "Safflor yellow B attenuates ischemic brain injury via downregulation of long noncoding AK046177 and inhibition of microRNA-134 expression in rats," *Oxidative Medicine and Cellular Longevity*, vol. 2020, Article ID 4586839, 2020.

[24] R. Zhang, M. Xu, Y. Wang, F. Xie, G. Zhang, and X. Qin, "Nrf2—a promising therapeutic target for defensing against oxidative stress in stroke," *Molecular Neurobiology*, vol. 54, no. 8, pp. 6006–6017, 2017.

[25] P. Deshmukh, S. Unni, G. Krishnappa, and B. Padmanabhan, "The keap 1-nrf2 pathway: promising therapeutic target to counteract ROS-mediated damage in cancers and neurodegenerative diseases," *Biophysical Reviews*, vol. 9, no. 1, pp. 41–56, 2017.

[26] S. Jiang, C. Deng, J. Lv et al., "Nrf2 weaves an elaborate network of neuroprotection against stroke," *Molecular Neurobiology*, vol. 54, no. 2, pp. 1440–1455, 2017.

[27] N. Tanaka, Y. Ikeda, Y. Ohta et al., "Expression of keap1-nrf2 system and antioxidative proteins in mouse brain after transient middle cerebral artery occlusion," *Brain Research*, vol. 1370, pp. 246–253, 2011.

[28] F. Zhou, M. Wang, J. Ju et al., "Schizandrin A protects against cerebral ischemia-reperfusion injury by suppressing inflammation and oxidative stress and regulating the AMPK/Nrf2 pathway regulation," *American Journal of Translational Research*, vol. 11, no. 1, pp. 199–209, 2019.

[29] Y. Higashi, T. Aratake, T. Shimizu, S. Shimizu, and M. Saito, "Protective role of glutathione in the hippocampus after brain ischemia," *International Journal of Molecular Sciences*, vol. 22, no. 15, p. 7765, 2021.

[30] K. Aoyama and T. Nakaki, "Impaired glutathione synthesis in neurodegeneration," *International Journal of Molecular Sciences*, vol. 14, no. 10, pp. 21021–21044, 2013.

[31] N. Couto, J. Wood, and J. Barber, "The role of glutathione reductase and related enzymes on cellular redox homoeostasis network," *Free Radical Biology & Medicine*, vol. 95, pp. 27–42, 2016.

[32] Z. Z. Chong, F. Li, and K. Maiese, "Oxidative stress in the brain: novel cellular targets that govern survival during neurodegenerative disease," *Progress in Neurobiology*, vol. 75, no. 3, pp. 207–246, 2005.

[33] V. M. Miller, D. A. Lawrence, T. K. Mondal, and R. F. Seegal, "Reduced glutathione is highly expressed in white matter and neurons in the unperturbed mouse brain – implications for oxidative stress associated with neurodegeneration," *Brain Research*, vol. 1276, pp. 22–30, 2009.

[34] S. J. Won, J. E. Kim, G. F. Cittolin-Santos, and R. A. Swanson, "Assessment at the single-cell level identifies neuronal glutathione depletion as both a cause and effect of ischemia-reperfusion oxidative stress," *The Journal of Neuroscience*, vol. 35, no. 18, pp. 7143–7152, 2015.

[35] J. Song, J. Park, Y. Oh, and J. E. Lee, "Glutathione suppresses cerebral infarct volume and cell death after ischemic injury: involvement of FOXO3 inactivation and Bcl2 expression," *Oxidative Medicine and Cellular Longevity*, vol. 2015, Article ID 426069, 2015.

[36] D. Silva-Adaya, M. E. Gonsebatt, and J. Guevara, "Thioredoxin system regulation in the central nervous system: experimental models and clinical evidence," *Oxidative Medicine and Cellular Longevity*, vol. 2014, Article ID 590808, 2014.

[37] Y. Du, H. Zhang, X. Zhang, J. Lu, and A. Holmgren, "Thioredoxin 1 is inactivated due to oxidation induced by peroxiredoxin under oxidative stress and reactivated by the glutaredoxin system∗," *The Journal of Biological Chemistry*, vol. 288, no. 45, pp. 32241–32247, 2013.

[38] J. Lu and A. Holmgren, "The thioredoxin antioxidant system," *Free Radical Biology & Medicine*, vol. 66, pp. 75–87, 2014.

[39] F. Zhou, P. P. Liu, G. Y. Ying, X. D. Zhu, H. Shen, and G. Chen, "Effects of thioredoxin-1 on neurogenesis after brain ischemia/reperfusion injury," *CNS Neuroscience & Therapeutics*, vol. 19, no. 3, pp. 204-205, 2013.

[40] D. Duan, J. Zhang, J. Yao, Y. Liu, and J. Fang, "Targeting thioredoxin reductase by parthenolide contributes to inducing apoptosis of HeLa cells∗," *The Journal of Biological Chemistry*, vol. 291, no. 19, pp. 10021–10031, 2016.

[41] F. Zhou, M. Gomi, M. Fujimoto et al., "Attenuation of neuronal degeneration in thioredoxin-1 overexpressing mice after mild focal ischemia," *Brain Research*, vol. 1272, pp. 62–70, 2009.

[42] X. Wu, L. Li, L. Zhang et al., "Inhibition of thioredoxin-1 with siRNA exacerbates apoptosis by activating the ASK1-JNK/p38 pathway in brain of a stroke model rats," *Brain Research*, vol. 1599, pp. 20–31, 2015.

[43] I. K. Hwang, K. Y. Yoo, D. W. Kim et al., "Changes in the expression of mitochondrial peroxiredoxin and thioredoxin in neurons and glia and their protective effects in experimental cerebral ischemic damage," *Free Radical Biology & Medicine*, vol. 48, no. 9, pp. 1242–1251, 2010.

[44] J. Shi, R. Li, S. Yang, Y. Phang, C. Zheng, and H. Zhang, "The protective effects and potential mechanisms of ligusticum chuanxiong: focus on anti-inflammatory, antioxidant, and antiapoptotic activities," *Evidence-Based Complementary and Alternative Medicine*, vol. 2020, Article ID 8205983, 2020.

[45] H. Ge, M. Sun, J. Ye, and J. Chen, "Antioxidant activity and resistance to food-borne pathogens from Ligusticum chuanxiong alcohol extract," *Science and Technology of Food Industry*, vol. 40, no. 10, pp. 127–132, 2019.

[46] J. Zou, P. Gao, X. Hao, H. Xu, P. Zhan, and X. Liu, "Recent progress in the structural modification and pharmacological activities of ligustrazine derivatives," *European Journal of Medicinal Chemistry*, vol. 147, pp. 150–162, 2018.

[47] C. Y. Chang, T. K. Kao, W. Y. Chen et al., "Tetramethylpyrazine inhibits neutrophil activation following permanent cerebral ischemia in rats," *Biochemical and Biophysical Research Communications*, vol. 463, no. 3, pp. 421–427, 2015.

[48] Y. M. Sheng, X. L. Meng, Y. Chun, Z. Wang, and Y. Zhang, "Effects of aetherolea from chuanxiong on ischemical reperfusion injury in rats and the survival of cerebral cortex neurons in vitro," *Lishizhen Medicine and Materia Medica Research*, vol. 23, no. 3, pp. 536–538, 2012.

[49] J. Zhang, C. Wu, L. Gao, G. du, and X. Qin, "Astragaloside IV derived from Astragalus membranaceus : a research review on the pharmacological effects," *Advances in Pharmacology*, vol. 87, pp. 89–112, 2020.

[50] C. C. Chen, H. C. Lee, J. H. Chang et al., "Chinese herb astragalus membranaceus enhances recovery of hemorrhagic stroke: double-blind, placebo-controlled, randomized study," *Evidence-Based Complementary and Alternative Medicine*, vol. 2012, Article ID 708452, 2012.

[51] J. Fu, Z. Wang, L. Huang et al., "Review of the botanical characteristics, phytochemistry, and pharmacology of Astragalus membranaceus (huangqi)," *Phytotherapy Research*, vol. 28, no. 9, pp. 1275–1283, 2014.

[52] V. M. Bratkov, A. M. Shkondrov, P. K. Zdraveva, and I. N. Krasteva, "Flavonoids from the genus astragalus: phytochemistry and biological activity," *Pharmacognosy Reviews*, vol. 10, no. 19, pp. 11–32, 2016.

[53] D. Wang, Y. Zhuang, Y. Tian, G. N. Thomas, M. Ying, and B. Tomlinson, "Study of the effects of total flavonoids of astragalus on atherosclerosis formation and potential mechanisms," *Oxidative Medicine and Cellular Longevity*, vol. 2012, Article ID 282383, 2012.

[54] H. L. Wang, Q. H. Zhou, M. B. Xu, X. L. Zhou, and G. Q. Zheng, "Astragaloside iv for experimental focal cerebral ischemia: preclinical evidence and possible mechanisms," *Oxidative Medicine and Cellular Longevity*, vol. 2017, Article ID 8424326, 2017.

[55] I. M. Costa, F. O. V. Lima, L. C. B. Fernandes et al., "Astragaloside iv supplementation promotes a neuroprotective effect in experimental models of neurological disorders: a systematic review," *Current Neuropharmacology*, vol. 17, no. 7, pp. 648–665, 2019.

[56] Y. Yin, W. Li, H. Gong, F. F. Zhu, W. Z. Li, and G. C. Wu, "Protective effect of astragaloside on focal cerebral ischemia/reperfusion injury in rats," *The American Journal of Chinese Medicine*, vol. 38, no. 3, pp. 517–527, 2010.

[57] L. Xiao, Z. Dai, W. Tang, C. Liu, and B. Tang, "Astragaloside IV alleviates cerebral ischemia-reperfusion injury through NLRP3 inflammasome-mediated pyroptosis inhibition via

activating Nrf2," *Oxidative Medicine and Cellular Longevity*, vol. 2021, Article ID 9925561, 2021.

[58] J. Yang, J. Li, J. Lu, Y. Zhang, Z. Zhu, and H. Wan, "Synergistic protective effect of astragaloside IV - tetramethylpyrazine against cerebral ischemic-reperfusion injury induced by transient focal ischemia," *Journal of Ethnopharmacology*, vol. 140, no. 1, pp. 64–72, 2012.

[59] Z. Wang and F. Yang, "Protective effect of astragalus polysaccharide on global cerebral ischemia-reperfusion injury in rats," *Chinese Journal of Gerontology*, vol. 36, no. 5, pp. 1059-1060, 2016.

[60] W. W. Zhang, F. Xu, D. Wang, Y. Jia, and C. Shao-Qing, "Buyang Huanwu Decoction ameliorates ischemic stroke by modulating multiple targets with multiple components: in vitro evidences," *Chinese Journal of Natural Medicines*, vol. 16, no. 3, pp. 194–202, 2018.

[61] X. Yan, A. Yu, H. Zheng, S. Wang, Y. He, and L. Wang, "Calycosin-7-o-β-d-glucoside attenuates OGD/R-induced damage by preventing oxidative stress and neuronal apoptosis via the SIRT1/FOXO1/PGC-1α pathway in HT22 cells," *Neural Plasticity*, vol. 2019, Article ID 8798069, 2019.

[62] Z. Jiang, W. Gao, and L. Huang, "Tanshinones, critical pharmacological components in Salvia miltiorrhiza," *Frontiers in Pharmacology*, vol. 10, 2019.

[63] M. Shi, F. Huang, C. Deng, Y. Wang, and G. Kai, "Bioactivities, biosynthesis and biotechnological production of phenolic acids in Salvia miltiorrhiza," *Critical Reviews in Food Science and Nutrition*, vol. 59, no. 6, pp. 953–964, 2019.

[64] Z. Li, J. Zou, D. Cao, and X. Ma, "Pharmacological basis of tanshinone and new insights into tanshinone as a multitarget natural product for multifaceted diseases," *Biomedicine & Pharmacotherapy*, vol. 130, p. 110599, 2020.

[65] X. Wan, Y. Wang, C. Zhou, H. Guo, S. Ma, and L. Wang, "Research progress on chemical constituents and pharmacological effects of Salvia miltiorrhiza," *Zhong Cao Yao*, vol. 51, no. 3, pp. 788–798, 2020.

[66] Y. F. Jiang, Z. Q. Liu, W. Cui et al., "Antioxidant effect of salvianolic acid b on hippocampal CA1 neurons in mice with cerebral ischemia and reperfusion injury," *Chinese Journal of Integrative Medicine*, vol. 21, no. 7, pp. 516–522, 2015.

[67] G. Wang, L. Zhang, B. Chen, Y. Zhang, L. Kong, and J. Han, "Protective effects of salvianolic acid B on cerebral ischemic reperfusion injury in rats," *Chinese Archives of Traditional Chinese Medicine*, vol. 37, no. 7, pp. 1566–1568, 2019.

[68] Q. Tu, R. Wang, B. Ding, W. Zhong, and H. Cao, "Protective and antioxidant effect of Danshen polysaccharides on cerebral ischemia/reperfusion injury in rats," *International Journal of Biological Macromolecules*, vol. 60, pp. 268–271, 2013.

[69] M. Cai, Y. Guo, S. Wang et al., "Tanshinone IIA elicits neuroprotective effect through activating the nuclear factor erythroid 2-related factor-dependent antioxidant response," *Rejuvenation Research*, vol. 20, no. 4, pp. 286–297, 2017.

[70] P. K. Fu, T. L. Pan, C. Y. Yang, K. C. Jeng, N. Y. Tang, and C. L. Hsieh, "Carthamus tinctorius L. ameliorates brain injury followed by cerebral ischemia-reperfusion in rats by antioxidative and anti-inflammatory mechanisms," *Medical Science*, vol. 19, no. 12, pp. 1368–1375, 2016.

[71] S. Yue, Y. Tang, S. Li, and J. A. Duan, "Chemical and biological properties of quinochalcone C-glycosides from the florets of Carthamus tinctorius," *Molecules*, vol. 18, no. 12, pp. 15220–15254, 2013.

[72] D. Yao, Z. Wang, L. Miao, and L. Wang, "Effects of extracts and isolated compounds from safflower on some index of promoting blood circulation and regulating menstruation," *Journal of Ethnopharmacology*, vol. 191, pp. 264–272, 2016.

[73] X. Zhou, L. Tang, Y. Xu, G. Zhou, and Z. Wang, "Towards a better understanding of medicinal uses of Carthamus tinctorius L. in traditional Chinese medicine: a phytochemical and pharmacological review," *Journal of Ethnopharmacology*, vol. 151, no. 1, pp. 27–43, 2014.

[74] K. Wang, M. Liang, and L. Zhang, "Preliminary study on anticoagulant and antioxidant activity of safflower injection," *Journal of Shanxi University (Natural Science Edition)*, vol. 41, no. 2, pp. 413–418, 2018.

[75] B. Sun, X. Cai, T. Wu, and L. Chen, "Protective effect of Honghua (safflower) extract on cerebral ischemia-reperfusion injury in mice," *Chinese Journal of Traditional Medical Science and Technology*, vol. 25, no. 2, pp. 205–207, 2018.

[76] K. Chen, C. Fu, W. Cong, and Y. Liu, "Chinese expert consensus on clinical application of safflower yellow," *Chinese Journal of Integrated Traditional and Western Medicine*, vol. 37, no. 10, pp. 1167–1173, 2017.

[77] X. Wang, Y. Wang, S. Zhang, X. Chen, and X. Wang, "Protective effect of safflower yellow pigment on cerebral ischemia reperfusion injury in rats," *Journal of Chinese Practical Diagnosis and Therapy*, vol. 28, no. 1, pp. 12–14, 2014.

[78] C. Wang, H. Ma, S. Zhang, Y. Wang, J. Liu, and X. Xiao, "Saflor yellow B suppresses pheochromocytoma cell (PC12) injury induced by oxidative stress via antioxidant system and Bcl-2/Bax pathway," *Naunyn-Schmiedeberg's Archives of Pharmacology*, vol. 380, no. 2, pp. 135–142, 2009.

[79] X. Wei, H. Liu, X. Sun et al., "Hydroxysafflor yellow A protects rat brains against ischemia-reperfusion injury by antioxidant action," *Neuroscience Letters*, vol. 386, no. 1, pp. 58–62, 2005.

[80] L. Fan, X. Dang, Z. Shi, C. Zhang, and K. Wang, "Hydroxysafflor yellow A protects PC12 cells against the apoptosis induced by oxygen and glucose deprivation," *Cellular and Molecular Neurobiology*, vol. 31, no. 8, pp. 1187–1194, 2011.

[81] J. Cao, Z. Chen, Y. Zhu et al., "Huangqi–Honghua combination and its main components ameliorate cerebral infarction with Qi deficiency and blood stasis syndrome by antioxidant action in rats," *Journal of Ethnopharmacology*, vol. 155, no. 2, pp. 1053–1060, 2014.

[82] Y. Han, Y. Chen, Q. Zhang et al., "Overview of therapeutic potentiality of Angelica sinensis for ischemic stroke," *Phytomedicine*, vol. 90, 2021.

[83] W. L. Wei, R. Zeng, C. M. Gu, Y. Qu, and L. F. Huang, "Angelica sinensis in China-a review of botanical profile, ethnopharmacology, phytochemistry and chemical analysis," *Journal of Ethnopharmacology*, vol. 190, pp. 116–141, 2016.

[84] S. Ai, X. Fan, L. Fan et al., "Extraction and chemical characterization of Angelica sinensis polysaccharides and its antioxidant activity," *Carbohydrate Polymers*, vol. 94, no. 2, pp. 731–736, 2013.

[85] T. Lei, H. Li, Z. Fang et al., "Polysaccharides from Angelica sinensis alleviate neuronal cell injury caused by oxidative stress," *Neural Regeneration Research*, vol. 9, no. 3, pp. 260–267, 2014.

[86] A. Yan and Y. Xie, "Effect of Angelicae sinensis radix polysaccharide on oxidative stress level and inflammatory cytokine expression of brain tissues in rats with cerebral ischemia reperfusion injury," *Chinese Journal of Experimental Traditional Medical Formulae*, vol. 24, no. 2, pp. 131–135, 2018.

Retraction

Retracted: Capsaicin Alleviates Vascular Endothelial Dysfunction and Cardiomyopathy via TRPV1/eNOS Pathway in Diabetic Rats

Oxidative Medicine and Cellular Longevity

This article has been retracted by Hindawi, as publisher, following an investigation undertaken by the publisher [1]. This investigation has uncovered evidence of systematic manipulation of the publication and peer-review process. We cannot, therefore, vouch for the reliability or integrity of this article.

Please note that this notice is intended solely to alert readers that the peer-review process of this article has been compromised.

Wiley and Hindawi regret that the usual quality checks did not identify these issues before publication and have since put additional measures in place to safeguard research integrity.

We wish to credit our Research Integrity and Research Publishing teams and anonymous and named external researchers and research integrity experts for contributing to this investigation.

The corresponding author, as the representative of all authors, has been given the opportunity to register their agreement or disagreement to this retraction. We have kept a record of any response received.

References

[1] Q. Wang, C. Zhang, C. Yang, Y. Sun, K. Chen, and Y. Lu, "Capsaicin Alleviates Vascular Endothelial Dysfunction and Cardiomyopathy via TRPV1/eNOS Pathway in Diabetic Rats," *Oxidative Medicine and Cellular Longevity*, vol. 2022, Article ID 6482363, 11 pages, 2022.

Research Article

Capsaicin Alleviates Vascular Endothelial Dysfunction and Cardiomyopathy via TRPV1/eNOS Pathway in Diabetic Rats

Qiuyue Wang,[1] **Caihui Zhang,**[1] **Chen Yang** [ID],[1] **Yue Sun,**[1] **Keyang Chen,**[2] **and Yao Lu** [ID][1,3]

[1]*Department of Anesthesiology, The First Affiliated Hospital of Anhui Medical University, Hefei 230022, China*
[2]*Department of Health Inspection and Quarantine, School of Public Health, Anhui Medical University, Hefei 230032, China*
[3]*Ambulatory Surgery Center, The First Affiliated Hospital of Anhui Medical University, Hefei 230022, China*

Correspondence should be addressed to Chen Yang; yangchen199806@163.com and Yao Lu; luyao-mz@163.com

Background. Endothelial dysfunction and cardiomyopathy are considered to be important vascular complications associated with diabetes. This study was designed to investigate whether capsaicin (CAP), a selective TRPV1 agonist, could prevent diabetes-induced endothelial dysfunction and cardiomyopathy. *Methods.* Male Sprague Dawley rats aged 8 weeks were injected intraperitoneally with streptozotocin (STZ, 50 mg/kg) to establish the diabetes model. The diabetic rats were randomly divided into the untreated diabetes group (DM, 10/group) and diabetes plus CAP treatment group (DM+CAP, 10/group); meanwhile, the nondiabetic healthy rats were used as normal controls (10/group). DM+CAP group were treated with CAP by gavage for 8 weeks. The cultured mouse vascular endothelial cells were exposed to different concentrations of glucose in the presence or absence of CAP treatment. The TRPV1 inhibitor capsazepine (CPZ) and eNOS inhibitor L-NAME were used *in vivo* and *in vitro* experiment. *Results.* CAP treatment significantly decreased the serum total cholesterol (TC) and total triglyceride (TG) and ameliorated the pathogenesis and fibrosis in the heart, while did not significantly improve plasma glucose level and the body weights of diabetic rats. In addition, CAP enhanced the expression of TRPV1 and eNOS in the heart and normalized the vascular permeability under diabetic state. Similarly, CAP treatment also increased nitric oxide and reduced reactive oxygen species. The same results were observed in cultured mouse vascular endothelial cells by CAP treatment. These beneficial effects of CAP were abolished by either CPZ or L-NAME. *Conclusions.* CAP might protect against hyperglycemia-induced endothelial dysfunction and diabetic cardiomyopathy through TRPV1/eNOS pathway.

1. Introduction

Diabetic cardiovascular disease is a major cause of mortality and morbidity in diabetic patients. In fact, diabetes-associated cardiac pathophysiological condition is considered a distinct process referred to as diabetic cardiomyopathy, also leads to poor prognosis [1]. Vascular endothelial dysfunction is thought to play a crucial role in the situation. High blood glucose sabotages the integrity of blood vessels and induces endothelial dysfunction. Reduction in the bioavailability of the nitric oxide (NO) subsequent to the reduction of the endothelial nitric oxide synthase (eNOS) is a characteristic of vascular endothelial dysfunction [2]. eNOS is involved in the regulation of vascular function. In the circulatory system, NO derived from

eNOS is one of the critical signal molecules, functioning as a crux vasoactive factor related to endothelium-dependent relaxation [3]. Physiologically, NO curbs inflammation and vascular hyperplasia. Besides, high-glucose level leads to an increase in reactive oxygen species (ROS) in endothelial cells, which accelerates NO inactivation and decreases NO bioavailability [4, 5]. Oxidative stress is widely believed to play a role in the pathogenesis of diabetes and its complications [6]. Research has proved that appropriate treatments aimed at nitric oxide and oxidative stress have the potential to ameliorate hyperglycemia-induced vascular lesions [7].

Transient receptor potential channels are a diverse group of proteins conserved in many species of mammals and are divided

into 7 subgroups, one of which is the transient receptor potential vanilloid (TRPV) subgroup [8]. TRPV1 exists in many tissues including vascular endothelial cells [9]. Activation of TRPV1 by capsaicin-mediated Ca^{2+} influx in endothelial cells can increase eNOS activity, then stimulates NO production [10]. Therefore, capsaicin is considered to have potential cardiovascular protective effects [11]. Obviously, our previous studies have also confirmed this conclusion [12, 13]. Similarly, there is evidence suggesting that TRPV1 can significantly increase NO production and improve endothelial function through specific targeting of PKA/eNOS phosphorylation [14]. Impairment in capsaicin-mediated vasodilation is associated with downregulation of TRPV1, but whether activated TRPV1 is able to alleviate endothelial cell dysfunction is unclear [15]. Interestingly, in a large Mediterranean population, regular consumption of chili pepper is associated with a lower risk of total and lower death of cardiovascular disease independent of cardiovascular risk factors or adherence to a Mediterranean diet [16]. Capsaicin, as a major component of chili pepper, is a TRPV1 agonist, can improve endothelial function by diet administration in rat model of renovascular hypertension [17]. Consequently, activation of TRPV1 is quite possible to protect noninsulin-dependent diabetes patients. However, in animal experiments, whether oral administration of capsaicin can increase NO and improve vascular endothelial function in T1DM rats is still not clear. Therefore, this study aims at investigating the intervention effects of the high selective agonist capsaicin in T1DM rats and related mechanism.

2. Materials and Methods

The animal study protocol was approved by the Animal Care and Use Committee of Anhui Medical University and the procedures were conducted in accordance with the National Institutes of Health Animal Research Advisory Committee guidelines.

2.1. Animals. Male Sprague–Dawley rats (200-250 g) at 8 weeks old were bought from Anhui Medical Laboratory Animal Center and acclimated for 1 week then were injected intraperitoneally with streptozotocin (STZ, 50 mg/kg body weight) dissolved in 0.1 mol/l citrate buffer (pH 4.5) [18] to establish diabetes model, which was confirmed by fasting plasma glucose level more than 16.7 mmol/l. The diabetic rats were randomly divided into untreated diabetic group (DM) and diabetes plus capsaicin treatment group (DM+CAP); meanwhile, the nondiabetic healthy rats were used as normal controls (NC). The rats in DM+CAP group received oral gavage of CAP at the dose of 0.5 mg/kg/per rat for a duration of 8 weeks, and the rats in the untreated DM group received the vehicle solution, using disposable feeding needle. Diabetic rats were, respectively, gavageded with the combination of capsaicin and the TRPV1 inhibitor capsazepine (CPZ, 5 mg/kg) or the eNOS inhibitor Nnitro-L-arginine methyl ester (L-NAME, 100 mg/kg) in the DM+CAP+CPZ group or DM+CAP+L-NAME group [19]. After the completion of the 8 weeks' treatment, all rats were anesthetized and then sacrificed [20]. Then, the heart and aortic arch were removed and deep frozen until analyzed.

2.2. Detection of Total Cholesterol and Triglycerides. The contents of TC and TG in serum were, respectively, determined by assay kits (Nanjing Jiancheng Bioengineering Research Institute, China).

2.3. In Vivo Permeability Assay. Endothelial permeability in the aortic arch was detected using Evans blue (1%, 30 min). The anesthetized rats were injected with Evans blue dye through the caudal vein, and the aorta was taken out after circulating for half an hour. After the stained aorta was photographed, the dye was extracted with deionized formamide, and the absorbance at 620 nm was measured by microplate reader [21, 22].

2.4. Immunohistochemistry. Rats were anesthetized and then sacrificed by exsanguination; the aortic arch and heart were isolated, dissected, and fixed in 4% paraformaldehyde and embedded in paraffin. After paraffin section, 4 mm sections were stained with hematoxylin and eosin. At the same time, the heart's paraffin sections were stained with Aniline blue and Ponceau S to observe tissue fibrosis. Prepared heart slides were stained with periodic acid Schiff's reagent (PAS) for glycogen and evaluated by light microscopy.′

2.5. Cell Culture. MVECs (catlog# C166 ATCC, Allendale, NJ, USA) were grown in DMEM supplemented with 10% FBS and 1% antibiotics. Cultured cells were maintained at 37°C in a humidified atmosphere of 95% O2, 5% CO_2. The cells were seeded with suitable density and divided into different groups, which included normal-glucose concentration group (NG: 5.5 mmol/l), high-glucose concentration group (HG: 25 mmol/l), and high-glucose concentration plus 1 μmol/l capsaicin group (HG + CAP) [23].

2.6. Western Blot Analysis. Total proteins were separated on a 10% Bis–Tris CriterionTM XT Precast Gel (Bio-Rad, MarneLa-Coquette, France) and transferred to an Immobilon polyvinylidene difuoride (PVDF) membrane (Millipore, Molsheim, France) as described (REF: PMID: 30797815). Antibodies against -TRPV1 (1 : 1000, rabbit) from Abcam (Oakville, Canada) and -eNOS (1/1000, rabbit) were incubated with membranes overnight at 4°C. Membranes were incubated for 1 h at room temperature with a corresponding horseradish peroxidase- (HRP-) conjugated secondary antibody (1/2000, Sigma-Aldrich) and developed using the Luminata™ Forte Western HRP substrate with BeyoECL Plus (Beyotime, Wuhan, China). The relative quantity of the protein of interest compared with the reference protein β-actin (1/5000, mouse, Santa Cruz) was measured with Image J software (NIH, USA).

2.7. Immunofluorescence. The expression of TRPV1 and eNOS in the heart and aorta of rats was detected using immunofluorescence as described (Ref. PMID: 20950828; PMID: 27733157). Concisely, frozen slides were incubated with anti-TRPV1 (1 : 100, NeuroMab, USA) and anti-eNOS (1 : 100, Cell Signaling Technology, USA), followed by corresponding Alexa Fluor-conjugated secondary antibody (1 : 200) before imaging using a fluorescence microscope.

2.8. Nitric Oxide Detection. The rat heart tissue and mouse vascular endothelial cells were used to detect the content of nitric oxide with Griess reagents (Beyotime, Wuhan, China) by the manufacturer's instruction as described (Ref: PMID: 16390827). Also, nitric oxide concentrations of cell culture medium and of rats' serum were tested by the same way [24].

2.9. Hydrogen Peroxide Detection. Preparation of serum samples: 50 mM phosphate buffer was prepared at pH 6.0. The sample was diluted 50 times with 50 mM phosphate buffer. 96 well UV microplate method was used to determine the marker curve. Determination of hydrogen peroxide concentration: the hydrogen peroxide detection reagent was dissolved and kept on ice. 50 μl sample and 100 μl hydrogen peroxide detection reagent were, respectively, added into each well that was shaken gently and mixed thoroughly. The plate was leaved at room temperature (15-30°C) for 30 minutes and then detected at A560 or A540-570 nm immediately. The concentration of hydrogen peroxide in the sample was calculated according to the standard curve [25].

2.10. Detection of Reactive Oxygen Species. After the rats were euthanized and killed, the hearts were removed rapidly. The heart tissues were soaked in paraformaldehyde, dehydrated, embedded, and made into frozen sections, stained with ROS probe. In addition, DCFH-DA ROS fluorescent probe was used to detect the treated cell samples [26]. The results were observed by fluorescence microscope. The relative fluorescence intensities of the samples were measured with Image J software (NIH, USA).

2.11. Permeability Assay. The mixed base glue (Matrigel) was dissolved with coating buffer (0.01 M Tris, pH 8.0 + 0.7% NaCl) to 200-300 μg/ml, 2 ml in total. The solution was placed on ice. The mixed coating solution was injected into 24 chambers (Transwell insert, including filter membrane, pore size 0.4-8 μm) with a sterile syringe at 100 μl/well. The 24-well plate containing 24 chambers was incubated at 37°C for 2 h, then the coating solution in each chamber was removed and 100 μl of mouse vascular endothelial cells at 2-5 × 10^5 was injected into each chamber, which was incubated at 37°C for 1 h to make the cells adhere to the bottom, then 200 μl/well complete medium was added into each chamber. At the same time, 1 ml complete medium was added to each well of the supporting plate. For the treatments, normal-glucose (NC, 5.5 mM) and high-glucose (HG, 25 mM) medium and HG + capsaicin were added to the corresponding chambers and incubated at 37°C for 24 h. All chambers were transferred into a new sterile 24-well supporting plate (each well contained 1 ml fresh complete medium), the old medium in the chambers was removed, and 150 μl FITC dextran solution was gently added into each chamber (final medium concentration, 10 μg/ml), which was placed in dark at room temperature and gently shaken for 20 minutes. 100 μl medium containing FITC from each well of the supporting plate was taken and injected into the corresponding well of the black 96-well plate, which was then placed in the fluorescence reader and measured at the absorption values of 485 and 535 nm, respectively. FITC-dextran flux was valued as a ratio of fluorescence intensities in the lower compartment (20 min) to those in the upper compartment (0 min). The data were expressed as a percentage compared with control [27].

2.12. Annexin V/PI Double Staining. The cell culture medium in wells of the plate was removed and washed it once by PBS. 5 μl annexin V-FITC and 10 μl propidium iodide staining solution were, respectively, added into the wells and gently mixed. The plate was incubated at room temperature (20-25°C) in dark for 20 min and then placed in ice bath. The plate was observed under the fluorescence microscope, annexin V-FITC showed green fluorescence and propidium iodide (PI) showed red fluorescence [28].

2.13. Fluo-4 AM Staining. The cell culture medium in wells of the plate was removed and washed it once by PBS. The 5 μM fluo-4 am probe solution diluted with PBS was added into the wells and gently mixed. After incubated in the dark at 37°C for 30 minutes, the six-well plate was observed under the fluorescence microscope. Fluo-4 showed green fluorescence [29].

2.14. Statistical Analysis. The results are expressed as the means ± SD, and *n* indicated sample size in each group. Statistical analysis was performed using one-way analysis of variance (ANOVA), followed by Tukey's post-hoc analysis to compare the differences among the groups. $p < 0.05$ was considered significant.

3. Results

3.1. Capsaicin Intervention Improved Body Weight, Blood Lipid, and Cardiac Fibrosis of Diabetic Rats. After 2 months' intervention, it is obvious that capsaicin moderately increased the body weights of diabetic rats in the DM+CAP group but did not improve the hyperglycemia caused by diabetes (Figures 1(a) and 1(b)). In addition, diabetes was often accompanied by hyperlipidemia. Similarly, our current data suggested that capsaicin treatment significantly lowered the serum levels of TC and TG (Figures 1(c) and 1(d)). To explore the role of capsaicin in the correction of diabetic cardiomyopathy, myocardial tissue by HE staining was detected. Our current data showed that the overt pathological changes in myocardium were observed in diabetic rats, which was ameliorated by capsaicin treatment (Figure 1(e)). Simultaneously, compared with the NC group, Masson's trichrome, and PAS staining of rat heart sections demonstrated more severe fibrosis in myocardium in DM group, while capsaicin treatment also ameliorated the fibrosis in DM + CAP group (Figure 1(e)). The protective effects of capsaicin on myocardial overt pathological changes and fibrosis in diabetic rats were both abolished by either the inhibitor of TRPV1 (CPZ) or the inhibitor of eNOS (L-NAME) (Figure 1(e)).

3.2. Capsaicin by TRPV1/eNOS Activation Attenuates Heart Oxidative Stress and Increases the Level of NO in Diabetic Rats. To investigate the mechanism underlying the capsaicin function, the immunofluorescence was carried out to detect the signaling-related proteins. Our current results demonstrated that TRPV1 and eNOS expression was sharply decreased in diabetic rats, compared with that in healthy
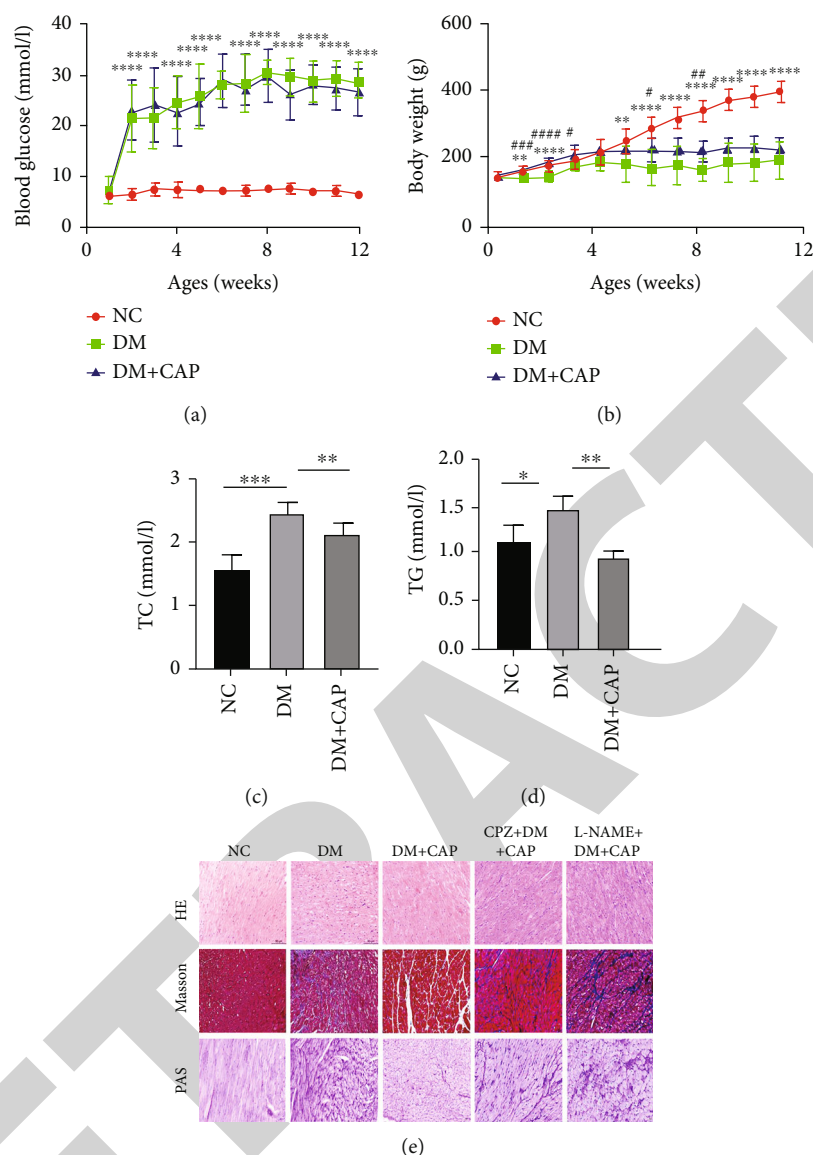
(a)

(b)

(c)

(d)

(e)

Figure 1: Blood glucose, weight, total cholesterol and triglycerides, myocardial pathological injury in rats. (a–b) Body weight is different in the NC, DM, and CAP group. Blood glucose in the DM and CAP group are higher than NC group. (c–d) Total cholesterol and triglycerides. (e) Representative images of H&E-stained, Masson-stained, and PAS-stained heart sections. The scale bar represents $50\,\mu$m. Data are presented as mean $\pm$ SD ($n = 10$ per group). $*** p < 0.001$, $** p < 0.01$, and $* p < 0.05$.

controls (Figure 2(a)). Nevertheless, this decrease caused by diabetes was reversed by capsaicin treatment in DM+CAP group (Figure 2(a)). Consistent with the immunofluorescence data, protein expression in rat heart tissues was also assayed by immunoblots, showing that diabetes markedly lowered the expression of TRPV1 and eNOS, but capsaicin treatment dramatically recovered the expression (Figures 2(b) and 2(c)). Nitric oxide synthase (NOS) is an isoenzyme, which exists in endothelial cells, macrophages, nerve phagocytes, and nerve cells, respectively. In heart tissue, nitric oxide in vascular endothelial cells mainly comes from eNOS. In the present study, we found that the change of nitric oxide content was consistent with eNOS expression in different groups in rat heart tissue (Figure 2(d)). In addition, fluorescent probe for detecting reactive oxygen species indicated that capsaicin treatment reduced ROS production in diabetic rat hearts (Figure 2(e)).

3.3. Capsaicin by TRPV1/eNOS Activation Attenuates Vascular Oxidative Stress and Increases the Level of NO in Diabetic Rats. Vascular HE staining showed that the blood vessel wall of diabetic rat was thicker than that of normal rat, while CAP treatment significantly improved the pathogenic thickness (Figure 3(a)). Immunohistochemical assay indicated that vascular intercellular adhesion molecules (vcam-1) expression was significantly elevated in endothelial and smooth muscle cells from diabetic rats, and that capsaicin treatment overtly mitigated the elevation of vcam-1 in DM+CAP group (Figure 3(b)). For in vivo permeability assay, Miles method was taken to look at the leakage of blood vessels in normal and diabetic rats. Our current data showed the permeability was significantly increased in diabetes compared with normal rats, while capsaicin treatment normalized the vascular permeability under diabetic state
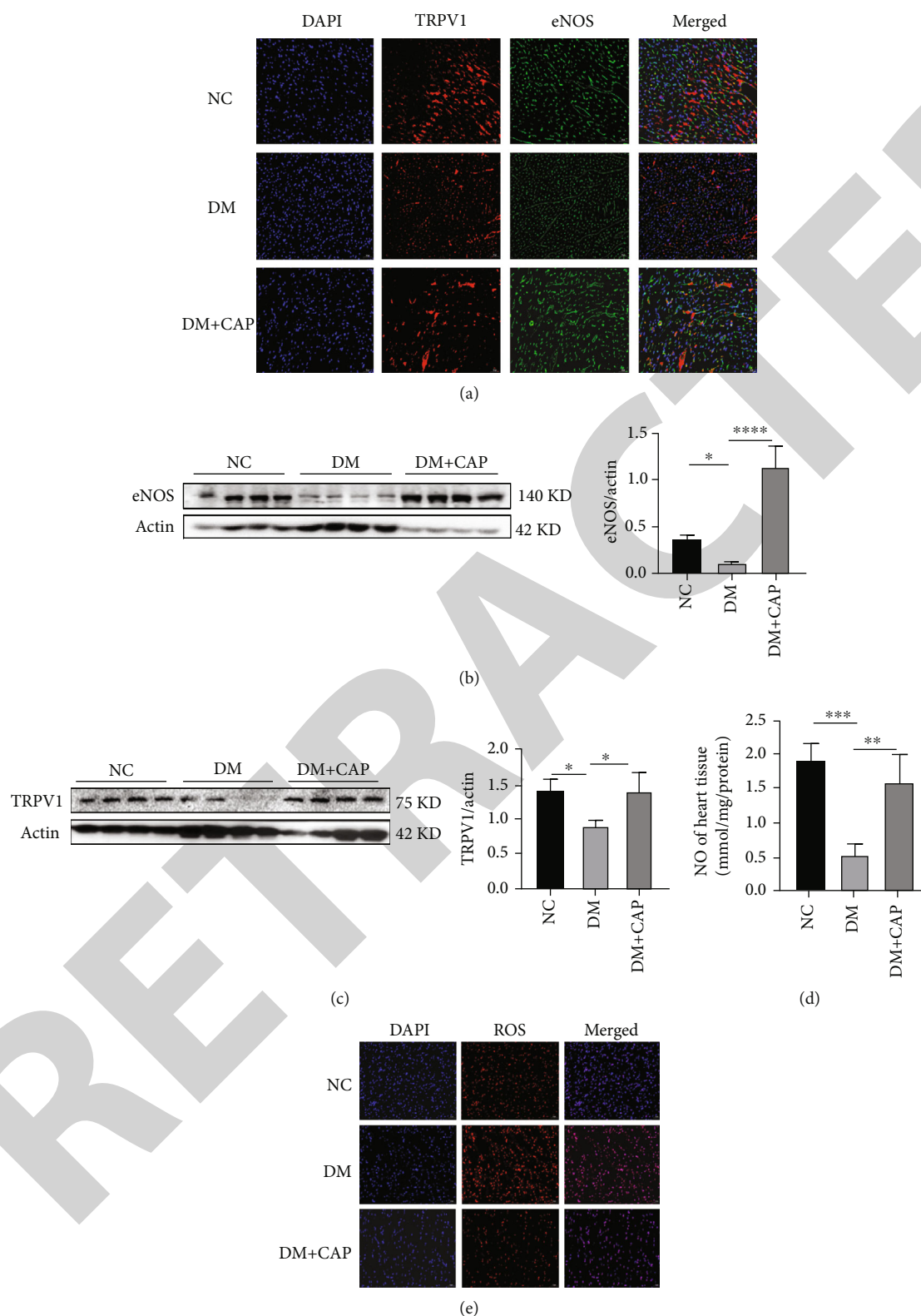
(a)

(b)

(c)

(d)

(e)

Figure 2: TRPV1/eNOS activation by capsaicin attenuates heart oxidative stress and increases the level of NO in diabetic rats. (a) Representative immunofluorescence images showing the coexpression of TRPV1 and eNOS in the heart from the NC, DM, and CAP group (bar denotes $50\,\mu$m). (b–c) The protein expression of TRPV1 and eNOS in the hearts of rat was determined by Western blotting. Quantitative analysis of TRPV1 and eNOS for Western blotting (n =4 per group). (d) The content of nitric oxide in heart tissue. (e) Representative oxidative stress images detected by DAF-2 DA in heart tissue. Data are presented as mean ± SD. $***\ast p < 0.001$, $***\ p <$ 0.001, $\ast\ast p < 0.01$, and $\ast p < 0.05$ represent significant differences in the NC, DM, and CAP group.
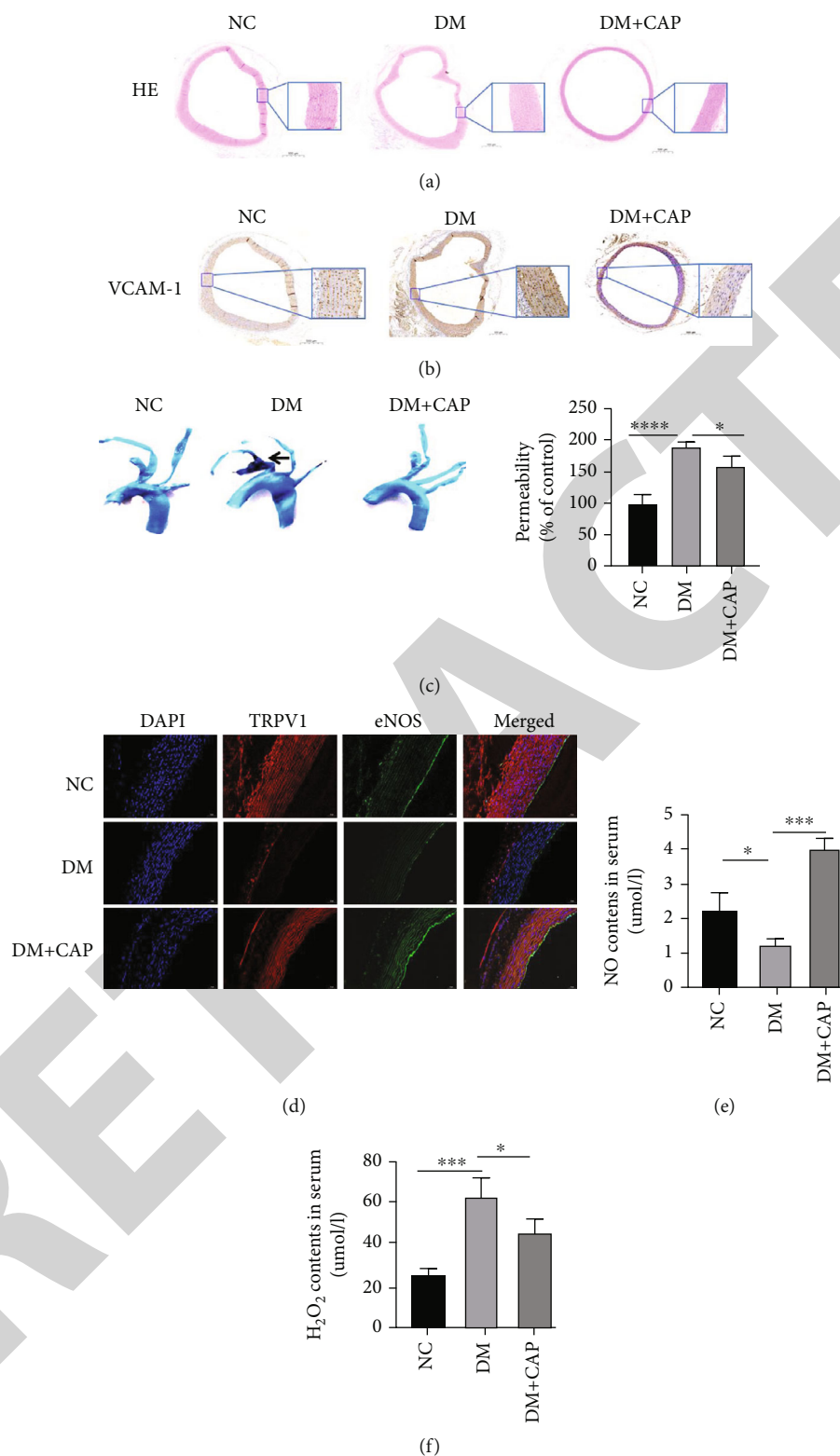
(a)

(b)

(c)

(d)

(e)

(f)

FIGURE 3: TRPV1/eNOS activation by capsaicin attenuates vascular oxidative stress and increases the level of NO in diabetic rats. (a–b) Vascular structure assessed by eosin/hematoxylin coloration, expression of vcam-1 by immunohistochemistry. The scale bar represents $500\,\mu$m and $50\,\mu$m. (c) Vascular permeability assay by Evans blue and the analysis of statistical. (d) Representative immunofluorescence images showing the expression of TRPV1 and eNOS in the blood vessel. (e–f) The content of nitric oxide and hydrogen peroxide in serum. Data are presented as mean ± SD. ∗∗∗ ∗$p < 0.001$, ∗∗∗ $p < 0.001$, and ∗$p < 0.05$ represent significant differences in the NC, DM, and CAP group.
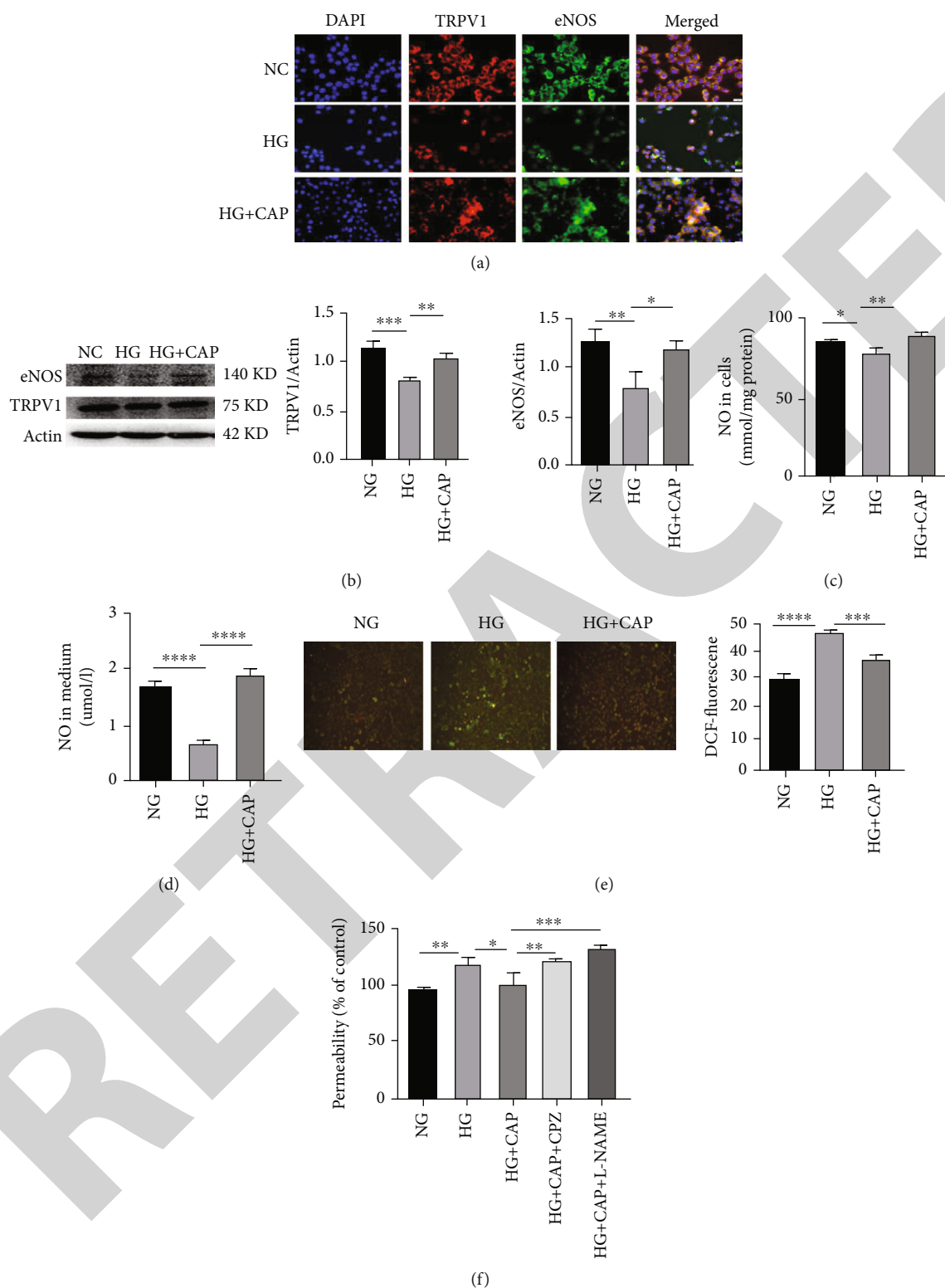
Figure 4: Capsaicin by activation TRPV1/eNOS alleviates oxidative stress and permeability and increases the level of NO in mouse vascular endothelial cells in high-glucose. (a) Representative immunofluorescence staining of TRPV1 and eNOS. The scale bar represents 20 μm. (b) The protein expression of TRPV1 and eNOS was determined by western blotting and quantitative analysis. (c–d) The content of nitric oxide in cell and cell culture medium. (e) Representative images detected by DAF-2 DA and quantitative analysis. (f) Permeability of mouse vascular endothelial cells to FITC- dextran after stimulation with normal-glucose (NG, glucose 5.5 mmol/L), high-glucose (HG, glucose 25 mmol/L), HG+capsaicin (HG+CAP, Cap 1 μmol/L), high-glucose pretreated with CPZ 10 μmol/L 2 hr, then capsaicin 1 μmol/L 24 hr (HG+CAP+CPZ) or high-glucose pretreated with 400 μmol/L NG-nitro-L-arginine methyl ester (L-NAME, an eNOS inhibitor) for 2 hr, then capsaicin for 24 hr (HG+CAP+L-NAME). Data are presented as mean ± SD. $^{****}p < 0.001$, $^{***}p < 0.001$, $^{**}p < 0.01$, and $^{*}p < 0.05$.
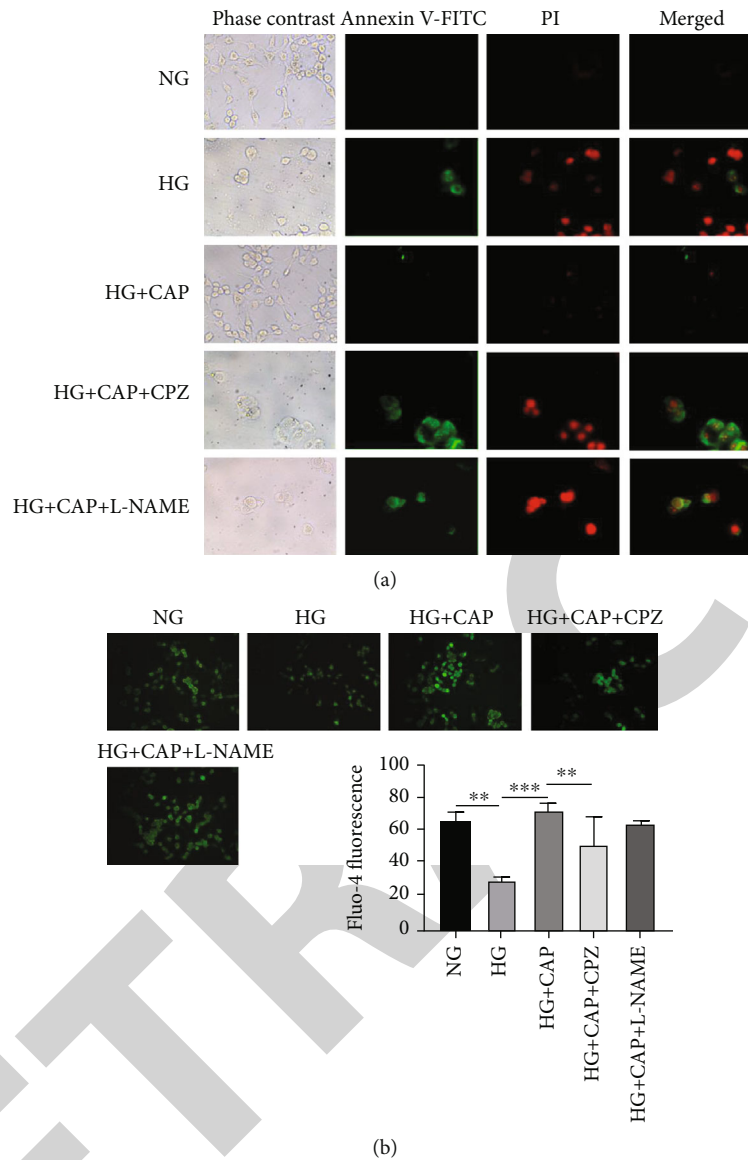
(a)

(b)

FIGURE 5: Capsaicin by activation TRPV1/eNOS prevents endothelial cell apoptosis induced by high glucose. Apoptosis (a) and calcium concentration. (b) of endothelial cells after stimulation with normal-glucose (NG, glucose 5.5mmol/L), high-glucose (HG, glucose 25 mmol/L), HG+capsaicin (HG+CAP, Cap 1 μmol/L), high-glucose pretreated with CPZ 10 μmol/L 2 hr, then capsaicin 1 μmol/L 24 hr (HG+CAP+CPZ) or high-glucose pretreated with 400 μmol/L NG-nitro-L-arginine methyl ester (L-NAME, an eNOS inhibitor) for 2 hr, then capsaicin for 24 hr (HG+CAP+L-NAME).

(Figure 3(c)). The results of vascular immunofluorescence showed the drastic decrease of TRPV1 and eNOS expression in rat blood vessel in untreated diabetic group, which was substantially ameliorated by capsaicin treatment (Figure 3(d)). Concomitantly, capsaicin also greatly reversed the NO production and sharply suppressed the ROS increase in diabetic rats (Figures 3(e) and 3(f)).

3.4. Capsaicin by Activation TRPV1/eNOS Alleviates Oxidative Stress, Permeability, and Cell Apoptosis and Increases the Level of NO in Mouse Vascular Endothelial Cells in High Glucose. To further elucidate the capsaicin function in regulating inter-

cellular permeability, the murine vascular endothelial cells were, respectively, cultured in normal-glucose (NG) and high-glucose (HG) medium, and capsaicin plus HG. The results of these cell immunofluorescence experiments demonstrated that the protein expression levels of TRPV1 and eNOS were significantly downregulated in HG compared with those in NG, however, the capsaicin treatment markedly reversed the decrease in HG +CAP group (Figure 4(a)). Likewise, the WB assay indicated the similar results in the cultured cells by HG or HG + capsaicin (Figure 4(b)). The concentrations of NO produced by eNOS in cultured cells and medium were verified under the different conditions, showing that HG significantly suppressed NO
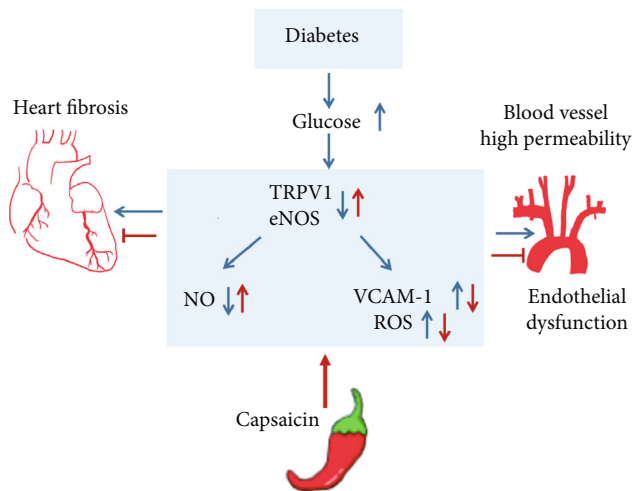
Figure 6: Upregulation of eNOS by TRPV1 activation attenuates hyperglycemia-induced ROS production in endothelial dysfunction. Schematic showing that hyperglycemia triggers endothelial dysfunction by downregulated expression of TRPV1/eNOS, exacerbates oxidative stress, and decreases the level of NO. Capsaicin by activation TRPV1/eNOS alleviates oxidative stress and increases the level of NO in endothelial cells and reduces vascular permeability and ameliorates apoptosis and fibrosis in heart tissue.

production, while capsaicin treatment normalized NO levels compared with the NC (Figures 4(c) and 4(d)). Additionally, oxidative stress is a key factor in the damage of endothelial cells caused by HG. Our current data suggested that ROS levels were sharply elevated by HG, implying the oxidative stress induced by HG. However, capsaicin substantially reduced the oxidative stress (Figure 4(e)). Endothelial cell permeability assay also verified that endothelial cell barrier was destroyed by high-glucose environment and capsaicin treatment improved its function and reduced material leakage, which was invalidated after TRPV1 or eNOS inhibitor treatment (Figure 4(f)). In situ fluorescence detection of annexin V-FITC/PI cell apoptosis, the protective effect of capsaicin on apoptosis impelled by high glucose disappeared after the addition of inhibitor of TRPV1 or eNOS (Figure 5(a)). In situ fluorescence probe was applied for the detection of endothelial cell intracellular calcium; the result showed that the intracellular calcium ion concentration decreased in high-glucose (HG) medium. Then, capsaicin treatment restored intracellular calcium ion concentration in HG medium, which was abolished by the addition of CPZ (TRPV1 inhibitor), but not by the L-NAME (eNOS inhibitor) (Figure 5(b)).

4. Discussion

At present, ointments and patches containing capsaicin are often used for pain treatment [30, 31]. However, as an agonist of TRPV1, the mechanism of capsaicin-mediated improvement in the metabolic diseases is still not completely elucidated. Vascular endothelial dysfunction, as a major hallmark in diabetic cardiomyopathy, may potentially play a role in the development of other diabetic cardiovascular complications like atherosclerosis [32]. When the endothelial cell metabolism is normal, the cells are quiescent and remain in vascular homeostasis. Vascular

barrier composed of endothelial cells is essential for vascular permeability, and vital to maintain vascular function. However, overproduction of AGEs in diabetes increases endothelial cell permeability, inhibits eNOS activity, and activates both NADPH oxidase (NOX) and NF-κB [32]. Another hallmark of endothelial dysfunction is a deficiency in the bioavailability of NO, and diabetes-induced inhibition of nitric oxide is attributable to the inhibition of eNOS, but it is not clear whether it is related to TRPV1. The current study is aimed to explore the relationship between endothelial dysfunction and TRPV1 in diabetes, particularly under capsaicin treatment.

Our present findings reveal that in streptozotocin-induced diabetic rats, the morphological fibrosis caused by diabetes is improved by capsaicin treatment, not only in the heart but also in the blood vessels. As an important factor mediating the adhesion between leukocytes and vascular endothelial cells, vascular intercellular adhesion molecules (vcam-1) play an important role in vascular injury. In normal arteries, it is intermittently expressed in endothelial and smooth muscle cells, and the density is higher where plaques are easy to form [33]. By vascular immunohistochemistry, we found that the upregulation of vcam-1 in diabetes was downregulated after capsaicin treatment. Thereafter, endothelial permeability in the aortic arch was studied using Evans blue to better understand the changes of vascular function. Our current results indicated that capsaicin may truly improve diabetic vascular disorders. In order to reveal the role of TRPV1 in cardiovascular complications of diabetes, we performed immunofluorescence localization and protein quantitative analysis in cardiac tissue and blood vessel. Immunofluorescence allowed us to observe that TRPV1 in blood vessels and heart tissues was downregulated under hyperglycemia and recovered after capsaicin treatment. The double label staining of eNOS and TRPV1 highlighted that eNOS was significantly activated. Quantitative analysis for target protein assayed by Western blotting also verified our conclusions. eNOS relaxes blood vessels through the synthesis of nitric oxide, so we detected the changes of nitric oxide content in the serum and heart to verify that TRPV1 activates eNOS. Excessive release of free radicals damaged vascular function, and eNOS can also reduce the production of reactive oxygen species while releasing nitric oxide. For the changes of reactive oxygen species, we selected fluorescent probes to label heart tissue and endothelial cells in vivo. Our findings revealed that the upregulation of eNOS by capsaicin treatment really suppressed the ROS production. Our in vitro cell experiments confirmed the findings obtained in vivo. Specifically, high glucose reduced the expression of TRPV1/eNOS and NO production, while activation of TRPV1 by capsaicin-mediated Ca^{2+} influx in endothelial cells can increase eNOS activity then stimulate NO production, which implies a novel mechanism underlying capsaicin-mediated amelioration of cardiomyopathy and endothelial dysfunction under diabetes condition.

5. Conclusions

Taken together, our current study suggested that capsaicin intervention may improve the diabetic cardiomyopathy and blood vessel endothelial dysfunction via upregulating TRPV1/

eNOS pathway as illustrated in Figure 6. Our findings in the current study may facilitate clinical trials to extend the application of capsaicin in patients with diabetes, and also might shed a new light into clinical treatment for diabetic complications.

Abbreviations

CAP: Capsaicin
STZ: Streptozotocin
VEGF: Vascular endothelial growth factor
NO: Nitric oxide
eNOS: Endothelial nitric oxide synthase
TC: Total cholesterol
TG: Total triglyceride
ROS: Reactiveoxygen species
TRPV1: Transient receptor potential vanilloid 1
NC: Normal control
DAB: Diaminobenzidine
PVDF: Polyvinylidene fluoride
HRP: Horseradish peroxidase
NOX: NADPH oxidase
Vcam-1: Vascular intercellular adhesion molecules.

Data Availability

The datasets of the current study are available from the corresponding author upon reasonable request.

Ethical Approval

Animal experiments were performed according to the recommendations in the Guide for the Care and Use of Laboratory Animals of the National Institutes of Health (NIH Publication 8th edition, 2011). The experimental procedures and protocols were approved by the Institutional Animal Care and Use Committee of Anhui Medical University.

Consent

All authors gave their consent for publication.

Conflicts of Interest

The authors declare that they have no competing interests.

Authors' Contributions

QW and YL designed the study. QW, CZ, CY, and YS performed experiments and analyzed the data. QW drafted the manuscript. QW, KC, and YL revised the manuscript. KC critically edit/revise the manuscript. All authors read and approved the final manuscript. Qiuyue Wang and Caihui Zhang contributed equally to this study.

Acknowledgments

References

[1] S. Rubler, J. Dlugash, Y. Z. Yuceoglu, T. Kumral, A. W. Branwood, and A. Grishman, "New type of cardiomyopathy associated with diabetic glomerulosclerosis," *The American Journal of Cardiology*, vol. 30, no. 6, pp. 595–602, 1972.

[2] S. B. Williams, J. A. Cusco, M. A. Roddy, M. T. Johnstone, and M. A. Creager, "Impaired nitric oxide-mediated vasodilation in patients with non-insulin- dependent diabetes mellitus," *Journal of the American College of Cardiology*, vol. 27, no. 3, pp. 567–574, 1996.

[3] K. M. Heygate, I. G. Lawrence, M. A. Bennett, and H. Thurston, "Impaired endothelium-dependent relaxation in isolated resistance arteries of spontaneously diabetic rats," *British Journal of Pharmacology*, vol. 116, no. 8, pp. 3251–3259, 1995.

[4] S. Hamed, B. Brenner, A. Aharon, D. Daoud, and A. Roguin, "Nitric oxide and superoxide dismutase modulate endothelial progenitor cell function in type 2 diabetes mellitus," *Cardiovascular Diabetology*, vol. 8, no. 1, p. 56, 2009.

[5] R. M. Mackenzie, I. P. Salt, W. H. Miller, et al., "Mitochondrial reactive oxygen species enhance AMP-activated protein kinase activation in the endothelium of patients with coronary artery disease and diabetes," *Clinical Science*, vol. 124, no. 6, pp. 403–411, 2013.

[6] H. Patel, J. Chen, K. C. Das, and M. Kavdia, "Hyperglycemia induces differential change in oxidative stress at gene expression and functional levels in HUVEC and HMVEC," *Cardiovascular Diabetology*, vol. 12, no. 1, p. 142, 2013.

[7] S. Dal, R. Van der Werf, C. Walter et al., "Treatment of NASH with antioxidant therapy: beneficial effect of red cabbage on type 2 diabetic rats," *Oxidative Medicine and Cellular Longevity*, vol. 2018, Article ID 7019573, 15 pages, 2018.

[8] M. Bishnoi, P. Khare, L. Brown, and S. K. Panchal, "Transient receptor potential (TRP) channels: a metabolic TR (i) P to obesity prevention and therapy," *Obesity Reviews*, vol. 19, no. 9, pp. 1269–1292, 2018.

[9] S. Earley and J. E. Brayden, "Transient receptor potential channels in the vasculature," *Physiological Reviews*, vol. 95, no. 2, pp. 645–690, 2015.

[10] D. Yang, Z. Luo, S. Ma et al., "Activation of TRPV1 by dietary capsaicin improves endothelium-dependent vasorelaxation and prevents hypertension," *Cell Metabolism*, vol. 12, no. 2, pp. 130–141, 2010.

[11] S. Panchal, E. Bliss, and L. Brown, "Capsaicin in metabolic syndrome," *Nutrients*, vol. 10, no. 5, p. 630, 2018.

[12] H. M. Heymann, Y. Wu, Y. Lu, N. Qvit, G. J. Gross, and E. R. Gross, "Transient receptor potential vanilloid 1 inhibitors block laparotomy- and opioid-induced infarct size reduction in rats," *British Journal of Pharmacology*, vol. 174, no. 24, pp. 4826–4835, 2017.

[13] J. Yu, K. Chen, L. Wu, X. Liu, and Y. Lu, "Anesthetic propofol blunts remote preconditioning of trauma-induced cardioprotection _via_ the TRPV1 receptor," *Biomedicine & Pharmacotherapy*, vol. 118, p. 109308, 2019.

[14] L. C. Ching, Y. R. Kou, S. K. Shyue et al., "Molecular mechanisms of activation of endothelial nitric oxide synthase mediated by transient receptor potential vanilloid type 1," *Cardiovascular Research*, vol. 91, no. 3, pp. 492–501, 2011.